THE OPTICAL AND VISUAL PERFORMANCE OF REFRACTIVE AND DIFFRACTIVE BIFOCAL CONTACT LENSES

by

Russell Laurence Woods

A thesis submitted for the degree of

Doctor of Philosophy.

City University, London

Department of Optometry and Visual Science

March, 1992

TABLE OF CONTENTS

TABLE OF CONTENTS 2

LIST OF TABLES AND ILLUSTRATIONS 8

ACKNOWLEDGEMENTS 14

DECLARATION 14

ABSTRACT 15

GLOSSARY 16

1 INTRODUCTION AND AIMS 18

1.1 Age and simultaneous-vision bifocal contact lens wear 19

1.1.1 Anterior eye and age 20

1.1.2 Pupil size and age 22

1.1.3 Spectral transmission and age 24

1.1.4 Chromatic aberration and age 27

1.1.5 Visual acuity and age 27

1.1.6 Contrast sensitivity and age 32

1.2 Bifocal contact lenses 38

1.2.1 Introduction 38

1.2.2 Concentric-design refractive bifocal contact lenses 42

1.2.3 Diffractive bifocal contact lenses 58

1.3 Optical Performance Measurement 76

1.3.1 Introduction 76

1.3.2 The Line Spread Function 77

1.3.3 The Optical Transfer Function 77

1.3.4 The Modulation Transfer Function 79

1.3.5 Bifocal contact lenses 81

1.4 Visual Performance Measurement 82

1.4.1 Introduction 82

1.4.2 Contrast Sensitivity 83

1.4.3 Vistech Charts 84

1.4.4 Letter Charts 85

1.4.5 Australian Vision Charts 86

1.4.6 Pelli-Robson Charts 87

1.4.7 Melbourne Edge Test 90

1.4.8 Visual performance with reduced luminance 90

1.4.9 Distance and near vision testing 91

1.5 Aims and Experimental Design 94

1.5.1 Introduction 94

1.5.2 Physical contact lens measurements 95

1.5.3 Optical performance measurements 95

1.5.4 Visual performance measurements 96

1.5.5 Prediction of visual performance from optical performance measures 97

1.5.6 Rationale and procedures for investigation of refractive bifocal contact lenses 97

1.5.7 Rationale and procedures for investigation of diffractive bifocal contact lenses 99

2 PRELIMINARY EXPERIMENTS ON VISUAL PERFORMANCE 102

2.1 Introduction 102

2.2 A preliminary evaluation of methods of contrast sensitivity presentation 102

2.2.1 Experiment 1 102

2.2.2 Experiment 2 104

2.2.3 Conclusions 109

2.3 A preliminary evaluation of the sensitivity of clinical visual performance measures 110

2.4 Conclusions 120

3 METHODS 122

3.1 Physical measurement of experimental bifocal contact lenses 122

3.1.1 Conventional contact lens assessment 122

3.1.2 Interferometric assessment of surface profile 123

3.2 Optical performance 130

3.2.1 Introduction 130

3.2.2 Modulation Transfer measurement 131

3.2.3 Experimental design 133

3.2.4 Data analysis 136

3.3 Visual Performance 137

3.3.1 Introduction 137

3.3.2 Contrast Sensitivity 138

3.3.3 Letter Charts 139

3.3.4 Australian Vision Chart 139

3.3.5 Pelli-Robson Chart 140

3.3.6 Pupil size 140

3.3.7 Contact Lens location 141

3.4 Longitudinal Chromatic Aberration 141

3.5 Subjects 144

3.5.1 Refractive bifocal contact lenses 145

3.5.2 Diffractive bifocal contact lenses 145

3.5.3 Chromatic aberration 146

3.6 Experimental bifocal contact lenses 146

3.6.1 Rigid refractive bifocal contact lenses 146

3.6.2 Rigid diffractive bifocal contact lenses 147

3.6.3 Soft diffractive bifocal contact lenses 149

3.7 Repeatability coefficients 151

3.8 Multiple Regression Analysis procedures 152

4 RESULTS 154

4.1 Physical Contact Lens Measurement 154

4.1.1 Standard contact lens procedures 154

4.1.2 Diffractive bifocal contact lens surface profile 156

4.2 Optical Performance 163

4.2.1 Introduction 163

4.2.2 System performance 164

4.2.3 Refractive bifocal contact lenses 166

4.2.4 Rigid diffractive bifocal contact lenses 173

4.2.5 Soft diffractive bifocal contact lenses 179

4.3 Visual performance 183

4.3.1 Introduction 183

4.3.2 General Considerations 184

4.3.3 Refractive bifocal contact lenses 186

4.3.4 Rigid diffractive bifocal contact lenses 191

4.3.5 Soft diffractive bifocal contact lenses 196

4.4 Longitudinal Chromatic Aberration of diffractive bifocal contact lenses 200

4.5 Prediction of the optical and visual performance of rigid diffractive bifocal contact lenses from surface profile measurements 201

4.5.1 Optical performance 202

4.5.2 Visual performance 203

4.6 Prediction of visual performance from optical performance 205

4.6.1 Refractive bifocal contact lenses 207

4.6.2 Rigid diffractive bifocal contact lenses 209

4.6.3 Soft diffractive bifocal contact lenses 210

5 DISCUSSION 210

5.1 General considerations 210

5.1.1 Repeatability 211

5.1.2 Luminance 213

5.1.3 Correlation between MTF measures 214

5.1.4 Correlation between visual performance measures 214

5.1.5 The use of pre-presbyopic subjects and artificial pupils 216

5.2 Refractive bifocal contact lenses 217

5.2.1 Bifocal design 218

5.2.2 Pupil size 220

5.2.3 Central optic zone diameter 221

5.2.4 Decentration 224

5.2.5 Optimal central optic zone diameter and pupil size 226

5.2.6 Summary 231

5.3 Rigid diffractive bifocal contact lenses 232

5.3.1 Overall performance 234

5.3.2 Longitudinal Chromatic Aberration 235

5.3.3 Pupil size, wavelength and decentration 236

5.3.4 Assessment of the variability of manufacture 238

5.3.5 Diffractive zone junction height 240

5.3.6 Diamond tool shape 243

5.3.7 The effect of polishing the diffractive surface 245

5.3.8 Summary - Optimising design characteristics 246

5.4 Soft diffractive bifocal contact lenses 247

5.4.1 Assessment of the variability of manufacture 250

5.4.2 Diffractive zone junction height 251

5.4.3 Diamond tool shape 252

5.4.4 Manufacture technique 252

5.4.5 A reverse addition soft diffractive bifocal contact lens 253

5.4.6 Summary - Optimising design characteristics 255

5.5 Predicting visual performance from optical performance 257

5.5.1 Refractive bifocal contact lenses 259

5.5.2 Diffractive bifocal contact lenses 262

5.5.3 Summary - Models of visual performance 264

6 CONCLUSIONS 267

APPENDIX 1 The aging eye and contact lenses - A review of ocular characteristics 269

APPENDIX 2 The aging eye and contact lenses - A review of visual performance 270

APPENDIX 3 A comparison of psychometric methods for measuring the contrast sensitivity of experienced observers 271

APPENDIX 4 Tables relating to the preliminary study 281

APPENDIX 5 Tables relating to optical performance 285

APPENDIX 6 The development of MRA models for optical performance with refractive and diffractive bifocal contact lenses 301

APPENDIX 7 Tables relating to visual performance 303

APPENDIX 8 Tables relating to the prediction of optical and visual performance from surface profile measurements of rigid diffractive bifocal contact lenses 322

APPENDIX 9 Tables relating to the prediction of Visual Performance from Optical Performance measurements 324

REFERENCES AND BIBLIOGRAPHY 330

LIST OF TABLES AND ILLUSTRATIONS

Tables and Figures were numbered according to the Chapter and section within which it is found (i.e. *Table 2.3-1* is the 1^{st} table in the 3^{rd} section of Chapter 2).

Tables

2.3-1 A summary of the preliminary experimental test conditions.

3.1-1 Fringe Appearance Rating Scale.

3.3-1 A summary of the tests of visual performance.

3.6-1 Available experimental rigid diffractive BCL.

3.6-2 Available experimental soft diffractive BCL.

4.2-1 Vergence ratio of nominally identical rigid diffractive BCL.

4.3-1 Repeatability Coefficients determined for the visual performance measures.

4.3-2 Correlation between the visual performance measures.

4.3-3 Pupil size and refractive BCL decentration.

4.3-4 Summary of the ANOVA of visual performance with refractive BCL.

4.3-5 Variability of manufacture of rigid diffractive BCL.

4.3-6 Summary of the ANOVA of visual performance with rigid diffractive BCL.

4.3-7 Summary of the ANOVA of visual performance with rigid diffractive BCL.

4.3-8 The predicted optimal DZJ height for rigid diffractive BCL.

4.3-9 Variability of manufacture of soft diffractive BCL.

4.3-10 DZJ height versus vergence with soft diffractive BCL.

4.3-11 Tool shape versus vergence with soft diffractive BCL.

4.3-12 Manufacture method and DZJ height with soft diffractive BCL.

4.5-1 Visual performance prediction from DZJ height.

4.5-2 The optimal DZJ height predicted with the visual performance measures.

4.6-1 Prediction of visual performance with refractive BCL.

4.6-2 Prediction of visual performance with refractive BCL.

4.6-3 Terms retained in MRA.

4.6-4 Calculated MTF used to predict visual performance.

4.6-5 Prediction of visual performance with rigid diffractive BCL.

4.6-6 Terms retained in MRA.

4.6-7 Prediction of visual performance with soft diffractive BCL.

5.3-1 Relative optical and visual performance with rigid diffractive BCL.

5.3-2 Optimal DZJ height predicted for the three different tool shapes.

Figures

1.1-1 Dark adapted pupil diameter and age.

1.1-2 Light adapted pupil diameter and age.

1.1-3 Spectral transmission change with age.

1.1-4 Spectral energy of diffractive bifocal contact lens foci.

1.1-5 The human relative spectral sensitivity.

1.1-6 Visual acuity with age.

1.1-7 Contrast Sensitivity and age.

1.1-8 Contrast detection and age.

1.1-9 Visual performance with a single vision CL.

1.1-10 Visual performance with BCL.

1.2-1 Image formation with a Centre-Near BCL - distance.

1.2-2 Image formation with a Centre-Near BCL - near.

1.2-3 The optical transfer function for an annular aperture.

1.2-4 The optical transfer function for a circular aperture.

1.2-5 The effect of pupil size and decentration upon refractive BCL.

1.2-6 Image shape with decentred concentric-design refractive BCL.

1.2-7 Central optic zone diameter versus pupil size.

1.2-8 A previous study with soft Centre-Distance refractive BCL.

1.2-9 A previous study with soft Centre-Near refractive BCL.

1.2-10 A simple zone plate.

1.2-11 The development of the kinoform lens.

1.2-12 The spectral energy of a bifocal kinoform lens.

1.2-13 Potential errors in the manufacturing of diffractive BCL.

1.3-1 The measured MTF of the human eye varies with pupil size.

1.4-1 The contrast sensitivity monitor.

1.4-2 A Vistech VCTS 6500 chart.

1.4-3 An Australian Vision Chart.

1.4-4 A Pelli-Robson contrast threshold chart.

1.4-5 A Melbourne Edge Test.

2.2-1 Mean Contrast Sensitivity with five different methods of CS presentation.

2.2-2 The repeatability and duration of five different methods of CS presentation.

2.2-3 Mean Contrast Sensitivity with the reduced APE procedure.

2.3-1 Mean visual performance with a single vision CL.

2.3-2 Mean distance visual performance with a diffractive BCL.

2.3-3 Mean near visual performance with a diffractive BCL.

3.1-1 Angular doubling with a Wollaston prism.

3.1-2 Modified Wollaston prisms, after Nomarski.

3.1-3 A schematic representation of Nomarski interferometry.

3.1-4 The appearance of an interference fringe crossing a DZJ.

3.1-5 The measurements made on diffractive BCL.

3.1-6 An interference micrograph of the surface of a rigid diffractive BCL.

3.1-7 The special attachment devised to hold the BCL on the interferometer.

3.1-8 The Riechert Fe2 Universal microscope with Nomarski Interferometer.

3.2-1 The solid state EROS 200 MTF apparatus.

3.2-2 The optical arrangement for MTF measurement.

3.2-3 Details of the dichroic halogen lamp and the filter.

3.2-4 The relative spectral power distribution of the image.

3.4-1 A diagram of a Badal Optometer incorporating Nagel's principle.

3.4-2 A diagram of the dual channel Badal optometer system which was constructed.

3.6-1 Diagram of the cross-section of the flatted diamond tool.

4.1-1 An interference micrograph of a rigid diffractive BCL.

4.1-2 An interference micrograph of a polished rigid diffractive BCL.

4.1-3 An interference micrograph of an Allergan Echelon soft diffractive BCL.

4.1-4 Measured versus nominal DZJ height of rigid diffractive BCL.

4.1-5 Examples of the measured DZJ height.

4.1-6 Measured versus nominal DZJ height of polished rigid diffractive BCL.

4.1-7 Measured versus nominal DZJ height of soft diffractive BCL.

4.1-8 DZJ width versus DZJ height.

4.1-9 The DZA width of rigid diffractive BCL.

4.1-10 The DZA width of soft diffractive BCL.

4.1-11 The distribution of fringe appearance gradings.

4.1-12 An interference micrograph of the BCL rated grade 4.

4.1-13 Optical performance reduced with increasing surface roughness.

4.2-1 The variation in MTF with aperture for the system.

4.2-2 The variation in MTF with wavelength for the system.

4.2-3 The mean MTF for CN refractive BCL (example).

4.2-4 The mean MTF for rigid diffractive BCL (example).

4.2-5 Five repetitions, on separate days, of MTF measurement.

4.2-6 Test-retest versus average modulation.

4.2-7 MTF repeatability versus spatial frequency.

4.2-8 The variation in MTF with changes in aperture for refractive BCL (example).

4.2-9 The variation in MTF with changes in the COZD of refractive BCL (example).

4.2-10 The average modulation of CN and CD refractive BCL.

4.2-11 Evaluation of the MRA equations for centred refractive BCL.

4.2-12 The predicted optimal COZD of centred refractive BCL.

4.2-13 The measured LSF of a centred refractive BCL.

4.2-14 The measured LSF of a decentred refractive BCL.

4.2-15 The effect of decentration of refractive BCL. (example)

4.2-16 The variation in MTF with decentration of a refractive BCL. (example)

4.2-17 Evaluation of the MRA equations for decentred refractive BCL.

4.2-18 The predicted optimal COZD of decentred refractive BCL.

4.2-19 The variation in the MTF with changes in aperture for diffractive BCL.

4.2-20 The variation in MTF with changes in wavelength for diffractive BCL.

4.2-21 The measured LSF of a centred rigid diffractive BCL.

4.2-22 The measured LSF of a decentred rigid diffractive BCL.

4.2-23 The variation in MTF with decentration of rigid diffractive BCL.

4.2-24 The variation in MTF with DZJ height of rigid diffractive BCL.

4.2-25 The variation in MTF with tool shape of rigid diffractive BCL.

4.2-26 The effect of tool upon optical performance.

4.2-27 The effect of DZJ height upon optical performance.

4.2-28 Vergence ratio varies with tool for rigid diffractive BCL.

4.2-29 Evaluation of the MRA equations for rigid diffractive BCL.

4.2-30 Predicted optimal DZJ height of rigid diffractive BCL.

4.2-31 The effect of polishing rigid diffractive BCL upon optical performance.

4.2-32 Measured DZJ height as a predictor of optical performance.

4.2-33 Variability of manufacture of soft diffractive BCL.

4.2-34 The MTF of soft diffractive BCL lathed with 250 μm tool.

4.2-35 The MTF of soft diffractive BCL lathed with 100 μm tool.

4.2-36 The MTF moulded soft diffractive BCL - 100 μm round tool.

4.2-37 Average modulation versus DZJ height of soft diffractive BCL.

4.2-38 The variation in MTF with tool shape with soft diffractive BCL.

4.2-39 The MTF of a "reverse" add soft diffractive BCL.

4.2-40 The MTF of Allergan Echelon soft diffractive BCL.

4.3-1 The average relative visual performance with refractive BCL (example).

4.3-2 The average relative visual performance with rigid diffractive BCL (example).

4.3-3 Test-retest versus average visual performance.

4.3-4 Repeatability versus relative visual performance.

4.3-5 Visual performance versus pupil size.

4.3-6 Contrast Sensitivity with refractive BCL.

4.3-7 Vision (chart based tests) with refractive BCL.

4.3-8 The average relative visual performance with refractive BCL. (example)

4.3-9 Evaluation of the MRA equations for refractive BCL.

4.3-10 Evaluation of the MRA equations for refractive BCL.

4.3-11 The optimal COZD predicted with MRA.

4.3-12 The optimal COZD predicted with MRA.

4.3-13 Visual performance varies with the DZJ height of rigid diffractive BCL.

4.3-14 Visual performance varies with the DZJ height of rigid diffractive BCL.

4.3-15 The effect of tool shape on the vergence ratio.

4.3-16 The variation in predicted optimal DZJ height with tool shape.

4.3-17 The effect of polishing the diffractive surface.

4.3-18 The effect of polishing the diffractive surface.

4.3-19 Variability of manufacture of soft diffractive BCL.

4.3-20 Visual performance variation with the DZJ height of soft diffractive BCL.

4.3-21 Visual performance variation with the DZJ height of soft diffractive BCL.

4.3-22 "Reverse" add compared to conventional add soft diffractive BCL.

4.3-23 Allergan Echelon compared to an experimental soft diffractive BCL.

4.5-1 Comparison of measured and predicted optical performance.

4.5-2 Comparison of measured and predicted visual performance.

4.5-3 The optimal DZJ height predicted with the visual performance measures.

5.2-1 Optical performance versus aperture size.

5.2-2 Optical performance versus COZD.

5.2-3 Visual performance versus spatial frequency.

5.2-4 COZ pupil coverage variation with pupil size.

5.2-5 Optical performance based prediction of optimal COZD.

5.2-6 Predictions of the optimal COZD with CD and CN refractive BCL.

5.4-1 The spectral energy of a conventional diffractive BCL shown schematically.

5.4-2 The spectral energy of a reverse add diffractive BCL shown schematically.

Acknowledgements

I would like to thank Professor M.H. Freeman, Mr M.J.A. Port, Dr J.E. Saunders and Dr W.D. Thomson for their support, assistance and advice; Mr H. Bennett, Mr C. Brasted, Mr E. Caswell, Mrs C. Gray, and Mr G. Macabbee for their technical assistance, and Mr E. Lancaster for the many hours "below the mast".

This study was funded by Pilkington Plc, with the co-operation of Dr C. Perrott and Dr R. Skipper

Declaration

I grant powers of discretion to the City University Librarian to allow this thesis to be copied in whole or in part without further reference to me. This permission covers only single copies made for study purposes, subject to normal conditions of acknowledgement.

ABSTRACT

The effects of changes in the optical design of simultaneous-vision bifocal contact lenses (BCL) upon optical and visual performance were investigated. In this context, the effects of age upon contact lens wear and theoretical aspects of BCL and previous studies of BCL were reviewed.

The surface profile of both rigid and soft diffractive BCL was investigated with an interferometric technique (Nomarski).

The optical performance (Modulation Transfer Function) was measured with a solid state EROS.

In preliminary studies (a) a range of procedures for the measurement of contrast sensitivity (CS) with a monitor display were determined; and (b) the sensitivity of a monitor-based measure of CS, the Vistech chart, the Pelli-Robson chart the Melbourne Edge Test and low and high contrast visual acuity (VA), all measured at two luminance levels, to changes in the design of rigid diffractive BCL was investigated to determine an optimal routine for the assessment of visual performance.

The main study used the monitor-based CS, the Pelli-Robson chart and low and high contrast VA to measure the visual performance of small groups of subjects wearing the BCL.

The reliability of the optical and the visual performance measures was poor, and related to the poor image quality typical of BCL.

The effect of variations in the central optic zone diameter, pupil size, decentration and BCL design (centre-distance or centre-near) of concentric-design refractive BCL were investigated. The complex relationship between the measured variables and changes with spatial frequency with refractive BCL were demonstrated, leading to predictions for optimal designs.

The effect of changes in wavelength, pupil size, decentration, diffractive zone junction (DZJ) height and DZJ shape of rigid diffractive BCL were investigated. The effect of changes in the manipulated variables, the surface quality and other aspects of manufacture of diffractive BCL were examined, leading to suggestions for improvements in design.

The effect of changes in DZJ height, DZJ shape and manufacture technique (lathe or mould) of soft diffractive BCL were investigated. In addition a "reverse" add soft diffractive BCL was investigated.

The interferometric measurements of the diffractive BCL indicated that small variations in the parameters of interest affect both optical and visual performance.

Changes in visual performance, generally, were matched by similar changes in optical performance. Models to describe visual performance based upon optical performance measures of the same BCL were demonstrated. The utility of these empirically derived equations in the development of future BCLs is discussed.

GLOSSARY

ANOVA ... Analysis of Variance

APE ..... Adaptive Probit Estimation

BCL ..... Bifocal Contact Lens(es)

BOZD .... Back Optic Zone Diameter

CAML .... Continuous, Ascending Methods of Limits

CD ..... Centre Distance (refractive BCL)

cd/m^2 ... candelas per square metre

CDZ ..... Central Diffractive Zone

CDZD .... Central Diffractive Zone Diameter (largest DZD)

CDZR .... Central Diffractive Zone Radius

CL ..... Contact Lens(es)

CN ..... Centre Near (refractive BCL)

COZ ..... Central Optic Zone

COZD .... Central Optic Zone Diameter

COZR .... Central Optic Zone Radius

c.p.d. .. cycles per degree

c.p.mm. . cycles per millimetre

CS ..... Contrast Sensitivity

CS 2 .... Contrast Sensitivity at 2 c.p.d.

CS 4 .... Contrast Sensitivity at 4 c.p.d.

CS 8 .... Contrast Sensitivity at 8 c.p.d.

CS 16 ... Contrast Sensitivity at 16 c.p.d.

CSF ..... Contrast Sensitivity Function

DAML .... Discrete, Ascending Methods of Limits

DZ ..... Diffractive Zone(s)

DZA ..... Diffractive Zone Annulus

DZD ..... Diffractive Zone Diameter(s)

DZJ ..... Diffractive Zone Junction(s)

LCA ..... Longitudinal Chromatic Aberration

logMAR .. Logarithm of the Minimum Angle of Resolution

LSF ..... Line Spread Function

MET ..... Melbourne Edge Test

MOCS .... Method of Constant Stimuli

MTF ..... Modulation Transfer Function

MRA ..... Multiple Regression Analysis

Optimal COZD .... The COZD required to give equal performance at distance and near

Optimal DZJ height .... The DZJ height required to give equal performance at distance and near

OTF ..... Optical Transfer Function

POZ ..... Peripheral Optic Zone

POZD .... Peripheral Optic Zone Diameter

POZR .... Peripheral Optic Zone Radius

PRC ..... Pelli-Robson Contrast threshold chart

PRZ ..... Peripheral Refractive Zone

PRZD .... Peripheral Refractive Zone Diameter

PRZR .... Peripheral Refractive Zone Radius

PSF ..... Point Spread Function

PTF ..... Phase Transfer Function

RZJ ..... Refractive Zone Junction

TD ..... Total Diameter

VA ..... Visual Acuity

VA H .... high contrast Visual Acuity

VA L .... low contrast Visual Acuity

Vergence ratio = $\frac{\text{(distance performance)}}{\text{(distance performance + near performance)}}$

Chapter 1 INTRODUCTION AND AIMS

It was the intention of this study to investigate the effects of variations in the design of various simultaneous-vision bifocal contact lenses (BCL) upon optical and visual performance. Alternating-vision BCL were not examined in this study. In the first chapter the effects of certain age-related changes upon BCL wear; theoretical aspects of BCL and previous studies with BCL; optical performance measures; visual performance measures; and finally the aims and experimental design are discussed. In the second chapter two preliminary studies which were used to establish suitable methods of visual performance measurement are reported. Rigid concentric-design refractive BCL, rigid diffractive BCL and soft diffractive BCL were then examined in a series of studies of the influence of BCL design variations upon optical performance (modulation transfer function) and visual performance (contrast sensitivity, Pelli-Robson contrast thresholds and low and high contrast visual acuity). In addition, physical (interferometric) measurements of the surface profile were made. The experimental methods are detailed in the third chapter and this is followed by experimental results, discussion and conclusions.

This study was the first large scale investigation of the optical performance and visual performance of the same

BCL; the effects of pupil size, central optic zone diameter and BCL decentration upon the optical and visual performance of rigid concentric-design refractive BCL; actual measurements of the diffractive surface of both rigid and soft diffractive BCL; the effect of changes in diffractive BCL lens design upon both optical and visual performance; the effect of surface quality upon optical performance of rigid diffractive BCL; and the first attempt to predict visual performance with BCL from optical performance measures.

1.1 Age and simultaneous-vision bifocal contact lens wear

In this section some of the changes in ocular characteristics and visual performance which occur with increasing age are discussed with particular reference to simultaneous-vision BCL (section 1.2.1). Some of the information contained in this section has been given in more detail in earlier reviews by the author (Woods, 1991c; 1992) and the reader is referred to these articles for more complete references and further information (included as *Appendices 1 and 2*).

Population demographics in all the western nations indicates a trend towards an aging population (OSAC Report, 1990; Papas, 1991). In addition many of the patients fitted with contact lenses (CL) since their

introduction now expect a CL correction of their presbyopic visual problem. Interest in BCL has increased in industry, the ophthalmic professions and amongst the general public as they have become aware of the possibility through the optical and the general media.

1.1.1 ANTERIOR EYE AND AGE

There is a reduction in the volume of the ocular adnexa with age. Changes to the eyelids with age include a reduction in tonus of both upper and lower eyelids, reduced lower eyelid movement and a reduction in palpebral aperture due to a lowering of both the upper and lower eyelids. These changes in the ocular adnexa may influence the location of simultaneous-vision BCL in relation to the pupil and visual axis.

Whilst information is contradictory there appears to be a decrease in tear production with age and an increase in tear retention after the fourth decade due perhaps to changing lid shape and a reduced facility of punctum drainage. As a result there is little change in the tear volume with age, though tear constituents and acidity alter with age. The quality of the tears as measured by the stability of the tear film reduces with age. The incidence of dry eyes increases with age though it is less frequently reported by older subjects. Corneal curvature varies with age and may alter during menopause. Hence BCL may fit and move differently and the pre-

contact lens tear film may be of a lesser quality when compared to the same CL on younger wearers.

The cornea thins with age though corneal thickness may alter during menopause. With age corneal touch sensitivity decreases and corneal fragility increases. Older eyes heal more slowly from experimental insult. The corneal epithelium of cats stressed with CL wear appears to lose adherence to the basement membrane possibly due to changes to Bowman's layer. Clinically there is an increased incidence of kerato-conjunctivitis sicca and epithelial compromise with age especially in the lower cornea. Hence CL wearing older patients are more likely to suffer corneal damage, yet are less likely to be aware of it, and hence are at greater risk of anterior corneal compromise. There are age-related changes in Descemet's membrane and the corneal endothelium while endothelial pump function decreases with age. Long-term wear of hard CL and extended wear CL causes endothelial changes over and above normal age changes. Hence care must still be taken in fitting older long-term hard or extended wear CL patients, and account taken of the increased incidence of endothelial pathology in older patients. Many corneal characteristics also alter in diabetes and after cataract surgery.

Summary

Age-related changes to the ocular adnexa and tear film may effect the location, movement and optical performance

of BCL. The corneal changes discussed may reduce the safety of fitting CL to older patients.

1.1.2 PUPIL SIZE AND AGE

The size of the pupil is dependent upon the retinal illuminance and level of adaptation, accommodation, the state of the entire central nervous system (e.g. fatigue), psychic influences such as fear and pain (e.g. CL induced corneal irritation) and age. Pupil size affected the visual performance with BCL as demonstrated in this study (section 4.3.3).

Dark Adapted

The age-related changes in dark adapted pupil size have been thoroughly described. Summarising the largest study Loewenfeld (1979) stated that "the pupils become larger within the first decade of life. During the second decade the curve rounds a gradual peak, and then a steady decline begins and continues over the remaining life-span". *Figure 1.1-1* shows the change in pupil size with age as found in four studies. There was no dependence of dark adapted pupil size upon sex or iris colour, or skin colour.

The light reflex

The light reflex was maintained with age. For a given pupil size, there was a constant proportional change with luminance independent of age (Kumnick, 1956; Loewenfeld,

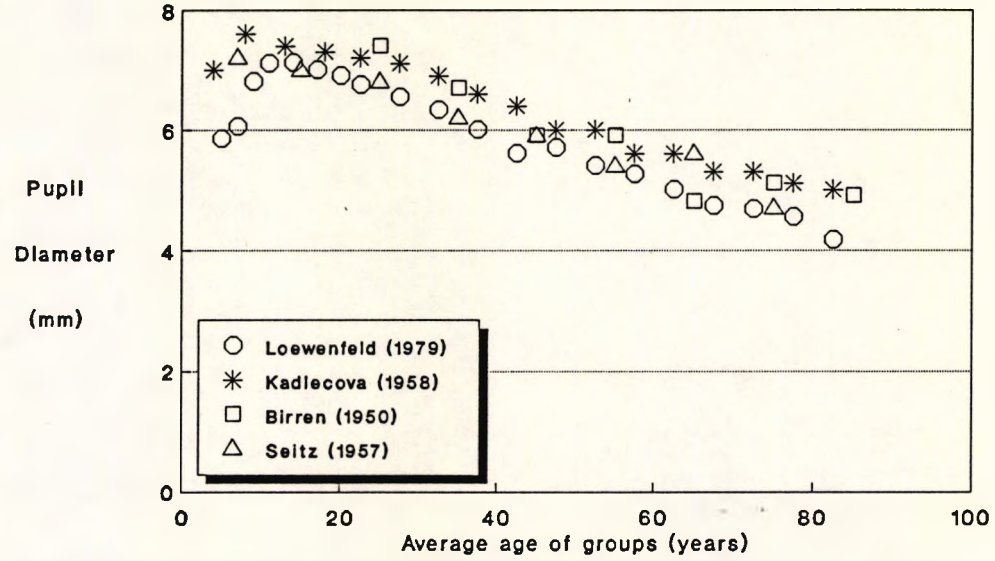

Figure 1.1-1 : The relationship between dark adapted pupil diameter and age. A compilation from four studies (Birren et al, 1950; Kadlecova and Peleska, 1958; Loewenfeld, 1979; Seitz, 1957). The total number of subjects, length of time in the dark and mode of measurement varied between studies.

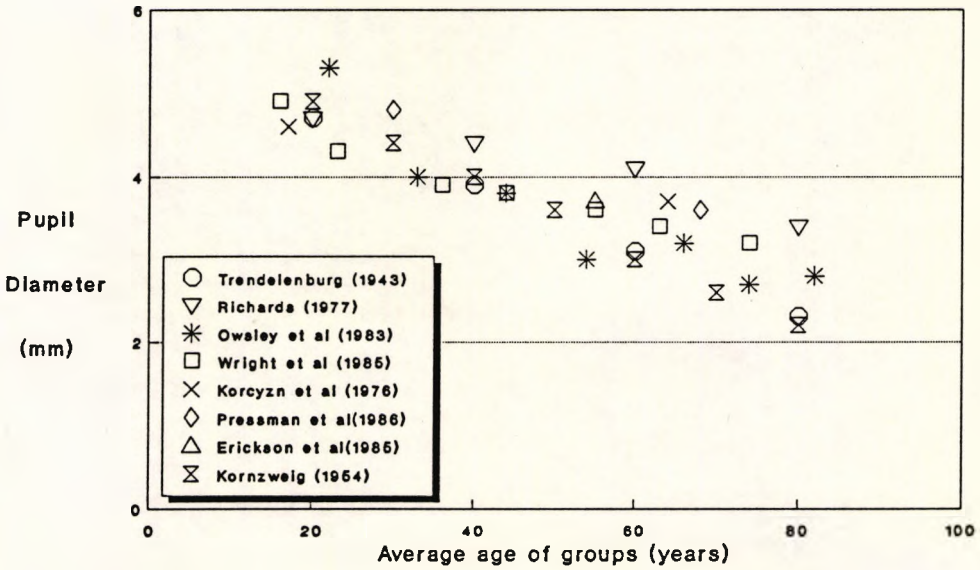

Figure 1.1-2 The relationship between light adapted pupil diameter and age. A compilation of the light adapted pupil diameter as measured in the eight unrelated studies listed. No attempt has been made to compensate for luminance which varied from study to study. The luminance levels quoted were: Erickson and Robboy (1985) 70 cd/m^2; Owsley et al (1983) 103 cd/m^2; Richards (1977) 34 cd/m^2; Wright and Drasdo (1985) 6 cd/m^2.

1979). This was also true of the near reflex. Thus the variation in pupil size with changes in luminance should be predictable from measurement at a single luminance level. For the five subjects reported in this study this was not the case (section 4.2.3)

Light Adapted

Many studies report the light adapted pupil size of their subjects, but with little or no reference to the lighting conditions, psychic state or age of the subjects. To date there have been only limited investigations of the relationship between age and light adapted pupil size under varied stable luminance conditions.

Figure 1.1-2 is a compilation of the results of eight studies which report light adapted pupil size and subject age. The luminance in the quoted studies varied from 6 to 103 cd/m^2. As can be seen in *Figure 1.1-2* the results were quite variable, and appeared not to be related to the luminance levels quoted. This was probably due to the particular experimental conditions and method of measurement, rather than to other factors. In general, under light adapted conditions, the reduced pupil size with age remained. Though not intended as predictive, *Figure 1.1-2* indicates that the average light-adapted pupil size was approximately 5 mm at age 20 years reduced to 3 mm at age 80 years for common levels of luminance.

Summary

Pupil size reduced with age, though the effects of light adaptation have not been well documented. Visual performance with BCL varied with pupil size.

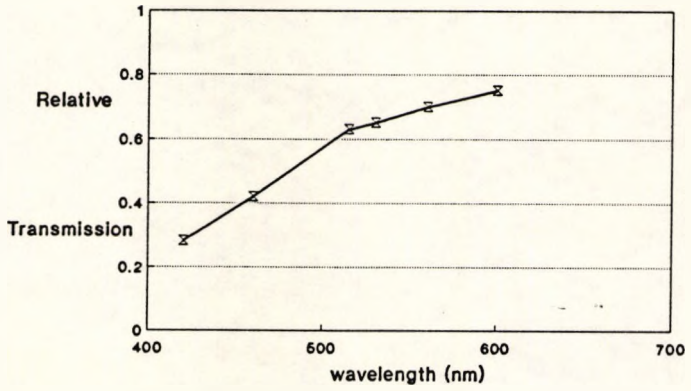

Figure 1.1-3 Spectral transmission change with age. The relative transmission of the entire ocular media is shown as a function of wavelength. Transmission of the ocular media of a 63 year-old observer was compared to a 21 year-old observer, such that the transmission of the younger observer was considered to be unity and that of the older observer relatively reduced. (redrawn from Ruddock, 1965)

1.1.3 SPECTRAL TRANSMISSION AND AGE

There is a wavelength-selective transmission of light through the ocular media of the human eye caused by reflection, absorption and scattering. The relative spectral transmission of an older observer as compared to a younger observer is shown in *Figure 1.1-3*. Total retinal illumination by age sixty was reduced to approximately one-third that at age twenty years through a combination of reduced pupil size and increased attenuation by the ocular media. The major age-related changes in spectral transmission have been attributed to the crystalline

lens, though other tissues of the eye, including the cornea and vitreous, also showed changes in spectral transmittance with age. (review: Woods, 1991c).

Diffractive bifocal contact lenses and spectral transmission

The age-related wavelength selective reduction in transmission may have some unexpected results. Diffractive BCL are wavelength dependent, with the distance image being more "blue" and the near image more "red" (section 1.2.3) as shown in *Figure 1.1-4*.

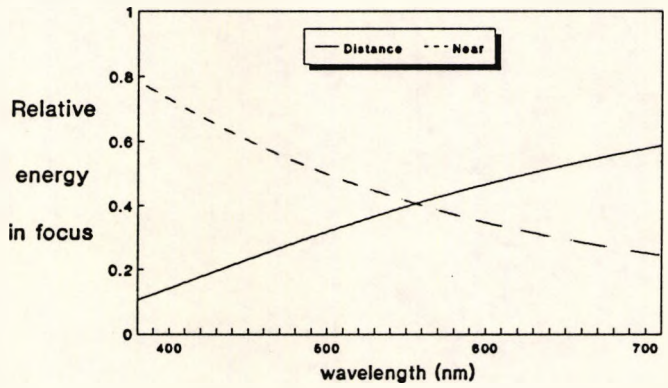

Figure 1.1-4 Spectral energy of diffractive bifocal contact lens foci. Due to the chosen design characteristics, have two major foci (usually zero and first order foci) each containing approximately forty percent of the incident light. When the relative energy is calculated for these two foci the split of the incident light varies with wavelength, with the distance image (zero order focus) being red (long wavelength) dominant and the near image (first order focus) being blue (short wavelength) dominant.

As the older eye is less able to utilise short (blue) wavelengths there is a possibility that some wearers may find the distance image inadequate. This may be further enhanced by the spectral content of the illuminating source. A diffractive lens designed to give a 50 : 50

ratio between distance and near images, given the human spectral sensitivity (Vλ, as shown in *Figure 1.1-5*), in daylight (e.g. D65 in *Figure 1.1-5*) will give a different ratio under a different illuminant. For example, by the author's calculation, when used with tungsten filament lamps (e.g. Standard Illuminant A) which produce most of their energy in the longer (red) wavelengths as shown in *Figure 1.1-5*, the energy in the two images would alter from 50 : 50 to 47 : 53. This may thus further reduce distance vision with diffractive BCL under certain conditions. For example, the current design Pilkington Diffrax rigid diffractive BCL has been reported to be distance vision biased, whilst the Allergan Echelon soft diffractive BCL has been reported to be almost equally balanced between distance and near vision. This balance can be modified with BCL design (section 1.2.3).

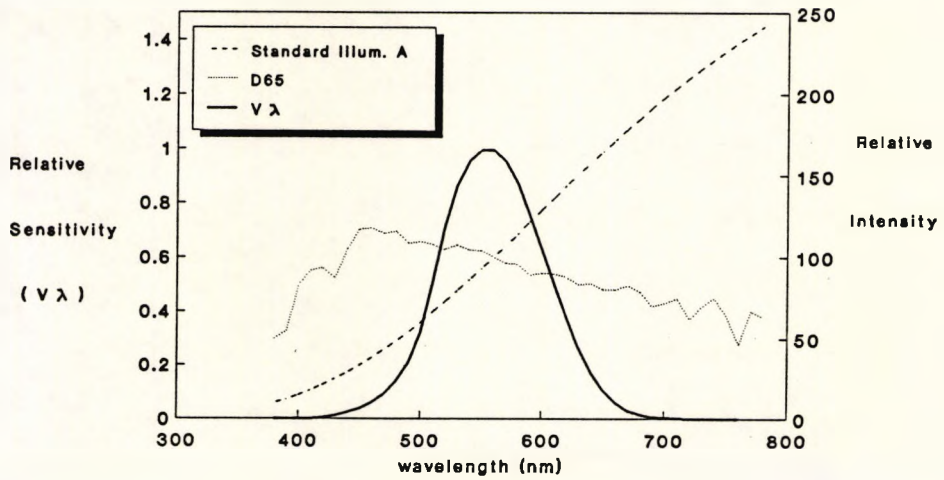

Figure 1.1-5 The human relative spectral sensitivity (Vλ) (solid) and the relative spectral content of two standard light sources: D65 (a daylight equivalent) (dotted) and Standard Illuminant A (tungsten) (dashed) are shown.

Summary

There is a wavelength dependent reduction in spectral transmission with age which may influence visual performance with diffractive BCL.

1.1.4 CHROMATIC ABERRATION AND AGE

The longitudinal chromatic aberration (LCA) of the human eye averages approximately 1.55 Dioptres, for wavelengths between 450 and 650 nm (Bedford and Wyszecki, 1957). Though there have been conflicting reports, the weight of evidence suggests that there are no age-related changes in LCA (review: Woods, 1991c).

As discussed in section 1.2.3, the near focal length of current diffractive BCL is inversely proportional to wavelength, the reverse of the case with refractive LCA such as with spectacle lenses and in the human eye. Theoretical predictions suggest that the LCA of the near (first order) focus of a diffractive BCL would reduce the inherent LCA of the human eye (Charman, 1986; Freeman, 1984). The normal human ocular LCA (between 450 and 650 nm) for near objects would then be reduced from approximately 1.5 to 0.8 Dioptres.

1.1.5 VISUAL ACUITY AND AGE

Visual Acuity (VA) has typically been defined as the ability to identify small objects of high contrast at

relatively high luminance levels. As such, VA is considered a good measure of focus. VA reaches a peak in the third decade of life, after which there is a gradual decline. There is some variability in the published data, much of which can be explained through differences in experimental technique and subject selection criteria. *Figure 1.1-6* shows results from a number of published studies reviewed by Pitts (1982a, b). The reduction in high contrast VA is found to be most pronounced after the fifth decade.

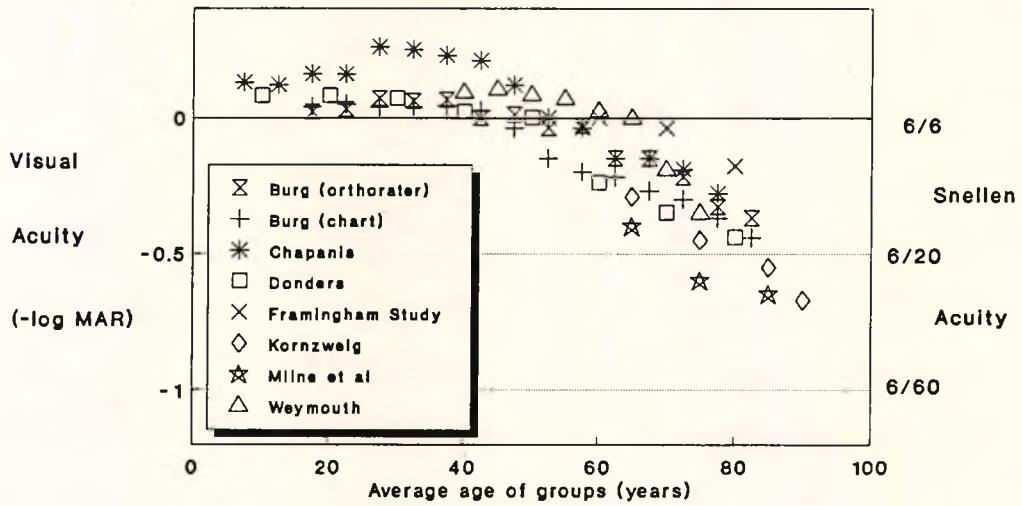

Figure 1.1-6 A compilation of visual acuity changes with age from eight unrelated studies. Visual acuity was reported as the best corrected in either eye which is given in -logMAR units (0 = 6/6, -1 = 6/60). No attempt has been made to compensate for variances in chart type, luminance levels or other factors. (redrawn from Pitts, 1982b)

Luminance

Reduced luminance reduces VA (Campbell and Green, 1965a), and accentuates age-related differences in VA (Richards, 1977). Similar results have been demonstrated with grating acuity and interference fringes (Vola et al,

1983). Increased target luminance greatly improves the VA of older subjects, but not to that of younger subjects (Richards, 1977, Blackwell and Blackwell, 1971). Similarly, the age-related reduction in VA could not be simulated with the use of filters (Weale, 1961). Hence the need for improved lighting for fine or detailed tasks.

Experimental studies have suggested that the sensitivity of VA tests can be improved when performed under low luminance conditions (Adams et al, 1988; Guillon et al, 1988a, b, 1990). The VA of older subjects will reduce significantly more than the VA of younger subjects when luminance is reduced, but the preliminary study reported in section 2.3 did not find increased significance when determining the effect of changes in diffractive BCL design. Despite this result, when fitting BCL, VA under low luminance may determine those patients less likely to succeed with BCL.

Contrast

Whilst there has been much interest in contrast sensitivity there has been limited work with VA charts composed of letters of reduced contrast. Visual acuity (Allen and Vos, 1967, Richards, 1977), threshold detection (Blackwell and Blackwell, 1971) and grating acuity (Woodhouse, 1975) reduced with decreasing target contrast. Experimental studies have led to the recommendation of the use of low contrast VA charts with

a contrast of less than about 15% (Regan and Neima, 1983; Ho and Bilton, 1986; Guillon et al, 1988b; Adams et al, 1988).

Low contrast VA charts were more sensitive to the age-related reduction in VA (review: Woods, 1992). In particular, Richards (1977) noted that, with luminances of greater than 0.3 cd/m^2, the age-related reduction in VA was greater for contrasts of less than 34%. Low contrast VA charts have been shown to be more sensitive than high contrast VA charts to the effects of simultaneous-vision BCL and monovision upon VA (Back et al, 1986, 1987; Papas et al, 1988, 1990). It has been suggested that patients with a reduced low contrast VA may be unsuitable for this form of correction (Freeman and Stone, 1987, Papas et al, 1990).

Pupil size

Theoretical evaluation of the human ocular modulation transfer function (MTF) indicated that the optimal pupil diameter was between 2 and 3 mm, and that higher spatial frequency targets were only severely attenuated for pupil size below 2 mm (van Meeteren, 1974). For young subjects and pupil sizes above 2 mm, VA (97% to 11% contrast) increased with increasing luminance and the optimal pupil diameter reduced from approximately 4 mm at 10 cd/m^2 to 2.5 mm at 1000 cd/m^2 (Campbell and Gregory, 1960; Woodhouse, 1975).

An average (light adapted) pupil of approximately 3 mm was found at about age 70 years, and 5 mm at age 20 years (*Figure 1.1-2*). Thus, at higher light levels, the older pupil was closer to an optimal level than the younger pupil (but visual performance was still reduced). The reverse was true at low light levels. This is complicated by age-related changes in spectral transmission which reduce retinal illuminance.

Pupil size influenced visual performance with most BCL. The choice of an optimal central optic zone diameter (COZD) for a concentric-design BCL is pupil size dependent (Erickson and Robboy, 1985, Jones and Lowther, 1989; Cox, 1986) and complicated by on-eye decentration and lens movement (Woods, 1991a, b). Visual performance and optimal COZD varied with the natural luminance related changes in pupil size. The relatively small (3.5 to 4.2 mm) diameter of the diffractive zone of Allergan Echelon soft diffractive BCL could reduce near VA for some patients with larger pupils and under low luminance conditions. Patients with larger pupils (>= 6 mm) have been reported to be less successful with Echelon BCL (Courtney et al, 1991b).

Summary

With increasing age VA reduced. This reduction was greater for low contrast targets and under low luminance conditions. Neural effects were suggested to explain

these changes which could not be fully explained by a reduction in retinal illuminance.

1.1.6 CONTRAST SENSITIVITY AND AGE

Contrast sensitivity (CS) is a measure of the contrast between object and surround required for detection of the object. Typically both the spatial and temporal characteristics of the object have been varied to investigate CS. CS is considered a measure of certain fundamental aspects of vision which can be used to construct a broader view of visual ability.

Spatial Contrast Sensitivity

Spatial CS (the ability to see faint stripes of varying width) declines with age for intermediate and high spatial frequencies (i.e. above 3 to 5 c.p.d.) but was retained or only slightly reduced for low spatial frequencies (review: Woods, 1992) (e.g. *Figure 1.1-7a*). This has been found over a wide range of test luminances from 2 cd/m^2 (McGrath and Morrison, 1981) to 300 cd/m^2 (Ross et al, 1985). Peak CS shifted to a lower spatial frequency with increasing age. Supra-threshold CS may not show an age-related reduction (Beard et al, 1990; Tulunay-Keesey et al, 1988), though this requires further examination.

Interferometric techniques of CS measurement, which theoretically were not effected by the optical quality of the eye, demonstrated age-related reductions in

(a) monitor based contrast sensitivity

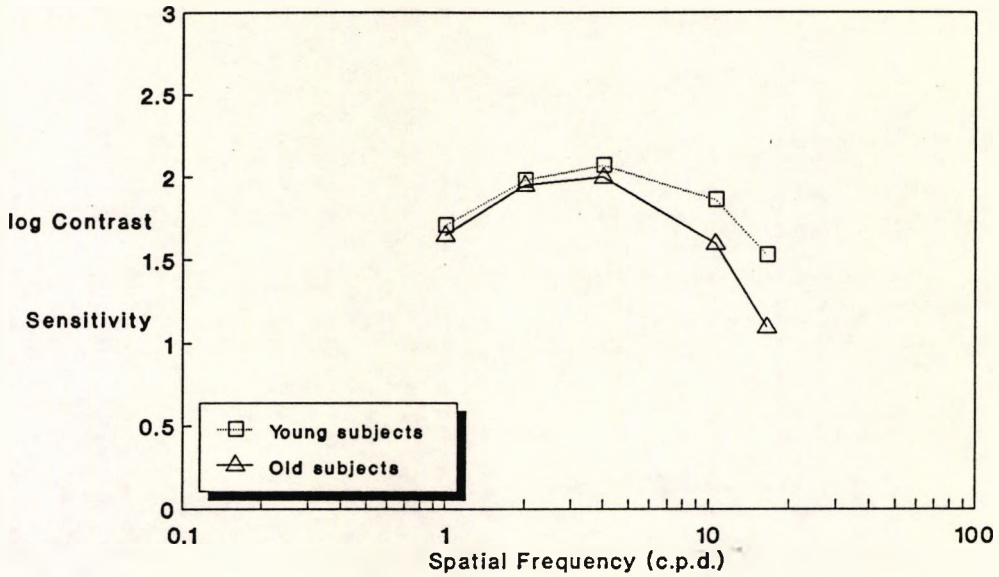

(b) interferometric contrast sensitivity

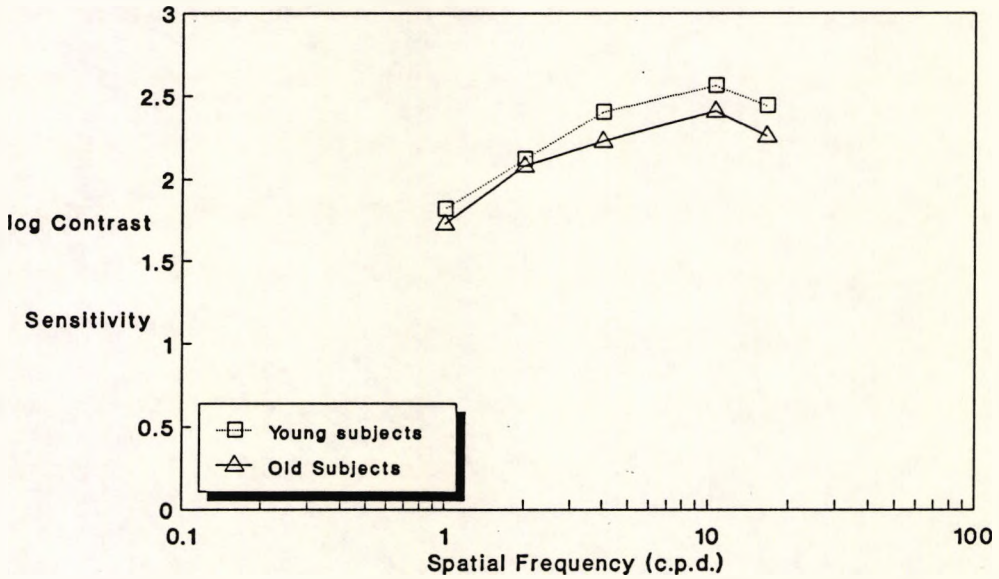

Figure 1.1-7 Contrast Sensitivity (CS) and age. The CS of 16 old (72 ± 4.3 years) and 16 young (21.5 ± 2.7 years) subjects measured with **(a)** a monitor-based computer system and **(b)** a modified Rodenstock retinometer. The latter technique theoretically bypasses the effects of the optical media and assesses the function of the retinal and neural systems. The former assesses the complete visual system with a conventional technique. The older group display significantly lower CS with both tests implying that most of the loss is retinal and neural, with optical factors having only a slight effect at the highest spatial frequency (16.5 c.p.d.) (redrawn from Elliott, 1987)

sensitivity (Morrison and McGrath, 1985; Elliott, 1987). As shown in *Figure 1.1-7b*, optical factors only have an influence on CS at higher spatial frequencies (>11 c.p.d.). There have been some doubts that such interferometric techniques are entirely free of the effects of the ocular media as these procedures have been shown to be poor predictors of visual performance (e.g. Thorpe Davis et al, 1991).

Luminance and spatial contrast sensitivity

With reducing luminance, CS reduced and the peak sensitivity shifted to a lower spatial frequency (van Nes and Bouman, 1967). This simulated the age-related reduction in CS which has been demonstrated across a large range of luminances. The age-related difference in CS was most pronounced at lower luminance levels. Blackwell and Blackwell (1971) calculated the increase in contrast required for detection with luminance of 0.003 to 1710 cd/m^2 (*Figure 1.1-8*). These "contrast multipliers" were found to predict age-related reductions in low contrast VA (Adams et al, 1988).

Pupil size and spatial contrast sensitivity

Senile miosis improved CS, but was not sufficient to counter other changes in the visual system. At higher luminance levels a reduction in pupil size has the effect of improving CS, and shifting the peak CS to a slightly higher spatial frequency (Campbell and Green, 1965a) while the reverse occurs with increasing age as CS

decreased and the peak CS moved to lower spatial frequencies despite reduced pupil size. Smaller pupils were better at the luminance levels used in many studies as the smaller senile pupil appeared to improve CS despite the reduction in retinal illuminance.

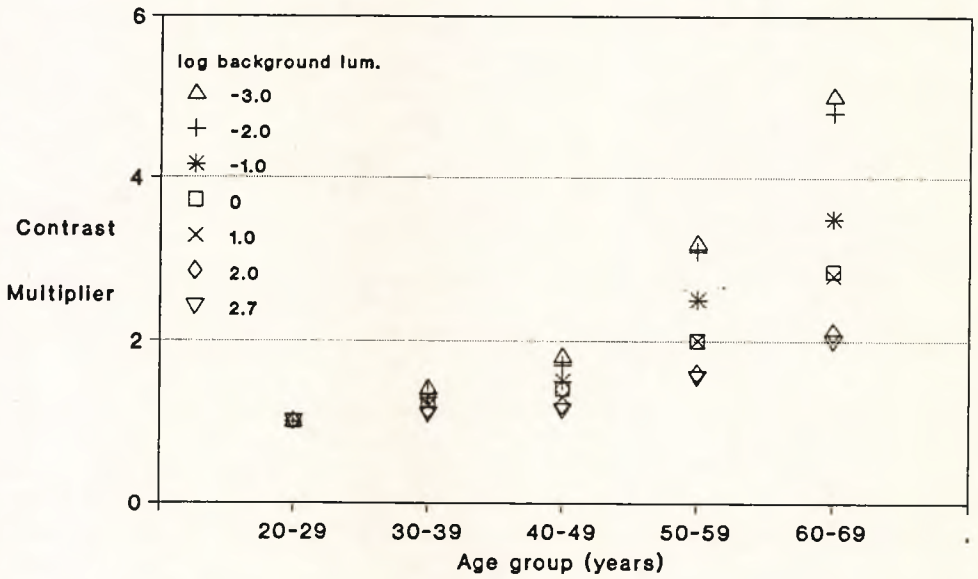

Figure 1.1-8 The relationship between contrast detection, age and luminance level as determined for 156 subjects. The contrast multiplier is the increase in contrast required for each age group to equal the performance of the youngest age group. Hence with decreasing luminance the level of contrast required for equal performance increases with increasing age. (redrawn from Blackwell and Blackwell, 1971)

Variations in CS with pupil size were similar to those previously noted for VA. Reports from this study (Woods, 1991d; Woods et al, 1992a), confirming a previous study (Cox, 1986), have found that the optimal COZD of a concentric-design refractive BCL reduced with increasing spatial frequency content of the test. The significance of this result has been examined more thoroughly in this study (section 4.3.3).

Peak Spatial Contrast Sensitivity and Edge Detection

The contrast between two halves of a target divided by a sharp straight border required for detection is known as the edge detection threshold. It has been suggested that edge detection is mediated by the channel with peak CS (lowest threshold). Edge detection correlated with peak spatial CS (Howell, 1978; Greeves et al, 1987) and correlated with low vision pedestrian mobility (Cunningham et al, 1980). Edge detection, with the Melbourne Edge Test (section 1.4.7), may decline with age (Verbaken and Johnston, 1986; Grey and Yap, 1987). A change would be expected to be consistent with the reduction in peak spatial CS with age.

The Pelli-Robson contrast threshold chart (PRC) measures the detection of large (approximately 3 c.p.d. at 3 metres) letters of reducing contrast (section 1.4.6). This is expected to be a measure of (near) peak CS. An age-related decrease in PRC detection has been demonstrated (Elliott et al, 1990a; Weissgold et al, 1990; Taub and Sturr, 1991) which was greater at a reduced luminance level (Taub and Sturr, 1991).

Temporal Contrast Sensitivity

Temporal CS (the ability to see a object at different rates of flicker) decreased after the fourth decade and this decrease was greatest for higher temporal frequencies (10 to 45 Hz). Differences in retinal illuminance did not fully explain the loss in sensitivity

with increasing age. Peak temporal CS shifted to a lower temporal frequency with increasing age. Temporal CS also varied with spatial frequency, with an age-related loss noted for median but not for very low spatial frequency gratings (Sturr et al, 1988; Elliott et al, 1990c). It is difficult to predict the effect of these changes upon BCL wear. CL movement may reduce the ability to detect objects (Tomlinson and Ridder, 1991) and this may be further reduced by age-related reductions in the temporal CS.

Summary

There was a reduction in peak and higher spatial frequency CS and a reduction in higher temporal frequency CS with age. As with VA, the age-related reduction in CS, which remained at higher levels of illumination, could not be explained by senile miosis, changes to the ocular media transparency, and reduced retinal illuminance. Neural effects have been suggested to explain these changes.

Contact Lens wear

CL wear has been reported to both reduce and enhance VA and CS (review: Woods, 1992). The variability of these findings may have been due to manufacturing effects as the CS with a CL was little different from that without a CL in the more recent studies. BCL of various designs result in a decrease in CS and VA due to the inherent optical compromise of all existing BCL designs (section

1.2.). As an example, typical CSF, PRC and VA results for a single subject from this study with a single vision CL (*Figure 1.1-9*) and with a refractive and a diffractive BCL are shown in *Figure 1.1-10*. The age-related decrease in CS is an additional factor when fitting CL with less than optimal optical performance which has often been neglected. The CL designer, manufacturer and fitter may need to exercise care when offering BCL to older patients due to the possible summation of the BCL induced effects upon age affected visual performance. It has been suggested by Freeman and Stone (1987) "that patients in the lower quartile of 'normal' contrast sensitivity may be contra-indicated for all simultaneous vision lenses".

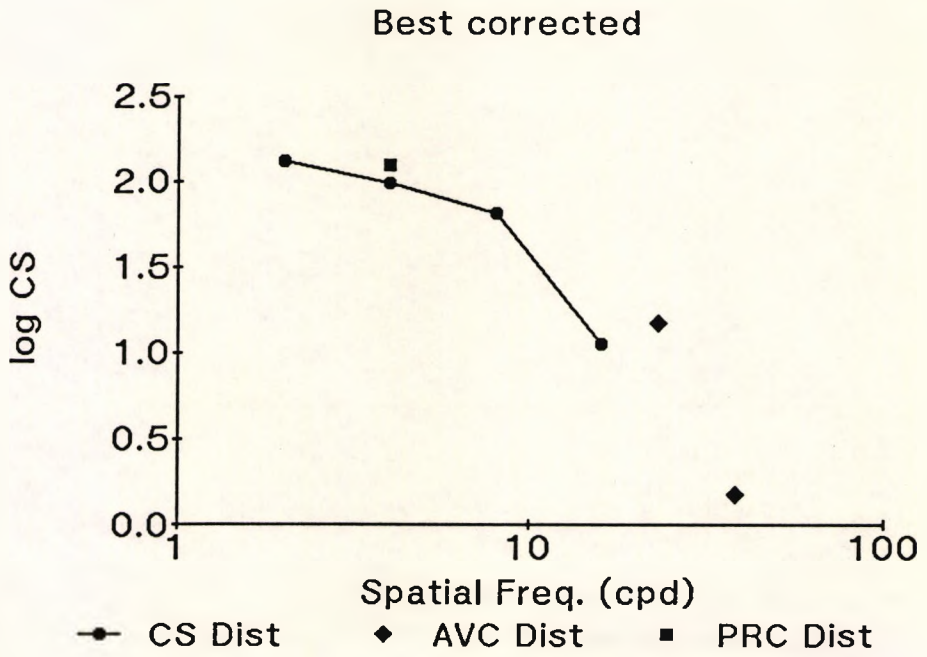

Figure 1.1-9 Visual performance with a single vision contact lens. Contrast sensitivity (CS), Visual Acuity (AVC) and Pelli-Robson contrast thresholds (PRC) for a single subject (#2) (data from this study)

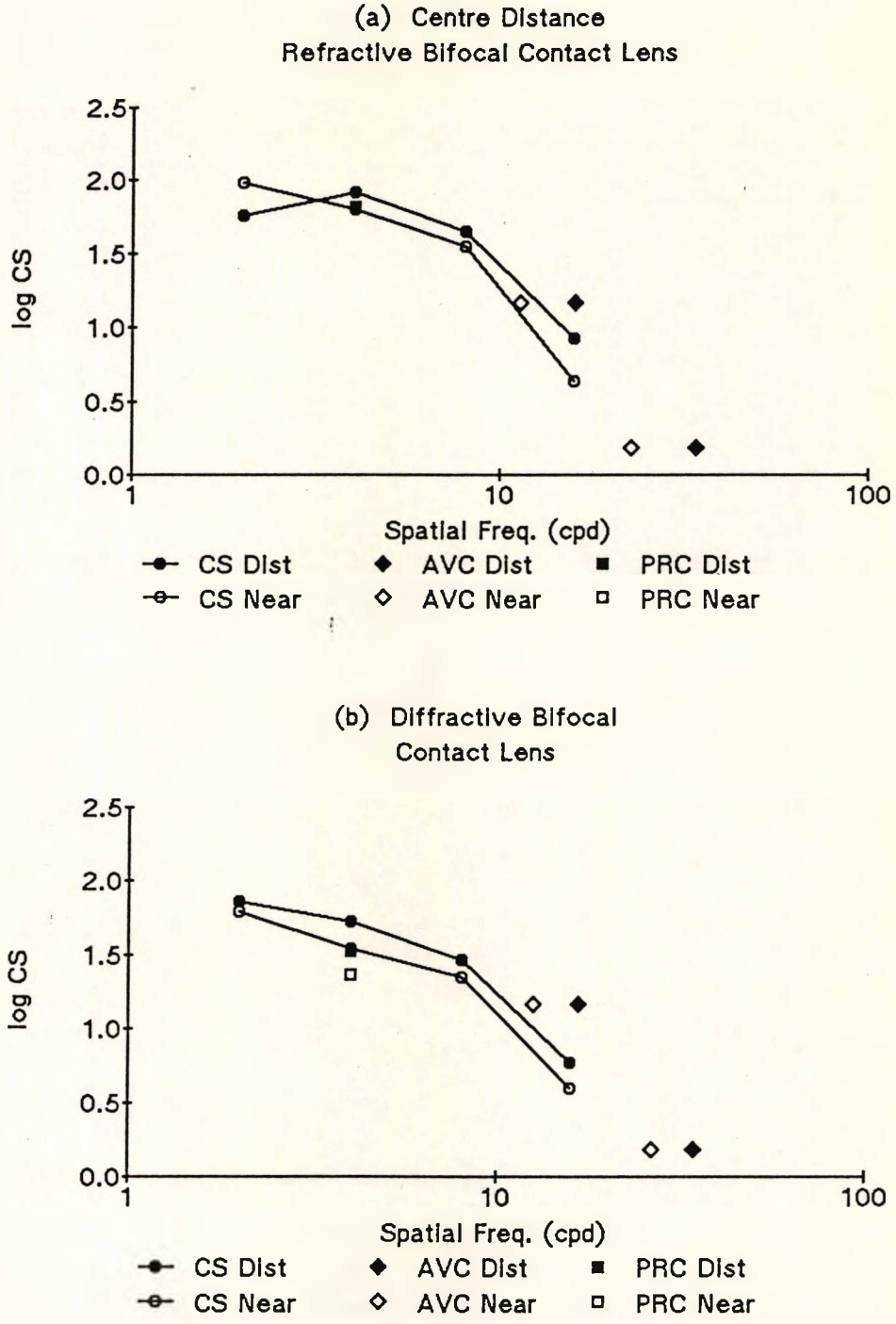

Figure 1.1-10 An example of visual performance with bifocal contact lenses (BCL). Distance and near contrast sensitivity (CS), Visual Acuity (AVC) and Pelli-Robson contrast thresholds (PRC) for a single subject (#2) with **(a)** a near-centre concentric-design BCL (COZD = 2.6 mm); and **(b)** a diffractive BCL (DZJ height 2.0 μm). For comparison the distance visual performance with a single vision contact lens is shown in *Figure 1.1-9*. (data from this study)

Age-related changes are important to the practitioner fitting CL and also to the CL designer, as decisions and priorities may differ for patients of different ages.

1.2 Bifocal Contact Lenses

Section 1.2.1 briefly outlines the contact lens (CL) options available to the presbyope, the various forms of bifocal contact lens (BCL), and the history and current state of BCL fitting. A more lengthy discussion of concentric-design refractive BCL follows, including a review of previous investigations of optical and visual performance with this form of correction (section 1.2.2). The final section (1.2.3) details theoretical aspects of diffractive BCL, the influence of certain changes in BCL design, and discusses previous reports of optical and visual performance with this form of BCL.

1.2.1 INTRODUCTION

As noted in section 1.1, the perception of an enormous potential market for presbyopic CL correction has led to a degree of interest within the CL industry, but only about one percent of CL patients have been fitted with BCL (Holden et al, 1989; Lloyd, 1984; Swarbrick et al, 1985; Sweeney et al, 1991). A slightly larger group have been fitted with the alternative presbyope CL option, monovision (Holden et al, 1989; McGeehon, 1988; Sweeney

et al, 1991). Monovision has been probably the most successful system of presbyopic CL correction, but is considered by many practitioners to be unsatisfactory due to its deleterious effects upon binocular vision (e.g. Harris and Classe, 1988; Josephson, 1989; Lebow and Goldberg, 1975; McMonnies, 1974; Nolan and Nolan, 1984) (review: Josephson et al, 1991).

A large amount of research has been directed towards the development of BCL systems for presbyopia (e.g. Josephson and Caffery, 1986; Lloyd, 1984; Papas, 1991) since BCL were first described by Feinbloom (1938). The first description of a concentric-design BCL has been attributed to Williamson-Noble (1951), and rigid concentric-design BCL have been in use since that time (e.g. Bier, 1967; de Carle, 1957; Hodd, 1969). At present much interest lies in the development of soft and diffractive BCL. Soft BCL have the advantages of greater patient acceptance due to the initial comfort and the ease of fitting for the practitioner. Both large and small CL companies have developed and publicised soft versions of the rigid BCL used by a limited number of experienced practitioners for many years (e.g. Back et al, 1986, 1987; Josephson and Caffery, 1986; Lowther, 1982; Molinari and Caplan, 1986). Diffractive BCL, available in rigid (Churms et al, 1987, Freeman and Stone, 1987) and in soft (Young and Papas, 1987) forms utilise a different optical mechanism to the refractive optics traditionally used to create the BCL effect as

discussed in section 1.2.3. In addition de Carle (1984, 1989a) has proposed multizone refractive BCL which were still under investigation.

Despite much BCL development and promotion, BCL have not received general practitioner acceptance due principally to their reputation for poor patient success. Success rates vary enormously in the literature (e.g. Back et al, 1986, 1987, 1989; Courtney et al, 1991a, b; Maltzman, 1985; Molinari and Caplan, 1986), partly due to BCL design and, as noted by Back et al (1989), partly due to the different classifications of success.

Conventional CL correction of presbyopia may be classified into three major categories : monovision; alternating-vision BCL; and simultaneous-vision BCL (see e.g. Bier and Lowther, 1977; Mandell, 1974; Phillips and Stone, 1989). **Monovision** involves fitting each eye with a single vision CL with the focal powers chosen such that one eye is used for distant vision and the other for near vision. **Alternating-vision** or translating-vision BCL typically have two distinct optical zones and rely upon CL movement with down-gaze to provide near vision. Alternating-vision BCL, due to the design requirements to ensure satisfactory CL movement, often result in a compromise of physiology and comfort. Another disadvantage with alternating-vision BCL is that near vision is only available on down-gaze. Rigid alternating-vision BCL have been fitted by a very small

group of practitioners for at least forty years (e.g. Borish and Soni, 1982; de Carle, 1989b) and more recently there have been some reasonably successful alternating-vision BCL made from gas permeable materials (e.g. Ames et al, 1989; Josephson and Caffery, 1989). Most alternating-vision BCL have been made from rigid materials as it has proven difficult to achieve sufficient CL translation with hydrophilic materials (Borish and Perrigan, 1987; Robboy, 1985; Robboy and Cox, 1988; Robboy and Erickson, 1987). Alternating-vision BCL have not been included in the remainder of this review.

Simultaneous-vision BCL remain stationary over the pupil, with all sections of the BCL forming an image at all times. This may be the two foci of a refractive or diffractive BCL, or the constantly varying focus of a multifocal CL. Such a BCL system forms an image composed of two separate superimposed images. Multifocal CL effectively increase the depth of focus without having discrete foci. This results in an image of reduced optical quality compared to a single vision CL, which has been shown to reduce contrast and cause a visual compromise (Back et al, 1986, 1987; Cox, 1985, 1986; Erickson and Robboy, 1985; McGill et al, 1986, 1987, Papas et al, 1987, 1990), especially under adverse lighting conditions (Guillon and Sayer, 1988; Woods, 1986), an aspect which has been unacceptable to many patients. Both soft and rigid simultaneous-vision BCL have been successfully fitted by a small number of

practitioners. Examples of the reduction in visual performance are shown in *Figure 1.1-10*.

Further development of BCL and the marketing capabilities of the large companies may lead to an increase in the number of presbyopes fitted with BCL. Despite the increased interest, investigation of the available literature indicates that there were a number of fundamental questions regarding BCL design and vision which have not been fully addressed.

1.2.2 CONCENTRIC-DESIGN REFRACTIVE BIFOCAL CONTACT LENSES

Conventional refractive simultaneous-vision designs have typically been radially symmetric with either a near optic surrounding a centre distance (CD) optic or the reverse, a distance optic surrounding a centre near (CN) optic. For this discussion the two optical zones will be referred to as the Central Optical Zone (COZ) and the Peripheral Optical Zone (POZ) (Draft International Contact Lens Standards, 1991).

General considerations

Optical and visual performance have been demonstrated to be influenced by the BCL format (i.e. CN or CD) (Back et al, 1990; Holden, 1986), COZD (Back et al, 1990; Cox, 1986; Erickson and Robboy, 1985; Jones and Lowther, 1989), pupil coverage by the COZ (Charman and Walsh

1986b, 1988; Hodd, 1969) and degree of blending of the refractive zone junction (RZJ) between the COZ and the POZ (Charman and Saunders, 1990; Holden, 1986) or the asphericity of the multifocal designs (Charman, 1983a, 1984; Charman and Saunders, 1990; Charman and Walsh, 1986a, 1986b, 1988; Meier and Lowther, 1983).

Given approximately equal coverage of the pupil by the two zones then one might expect that there would be a balance between distance and near. The COZD required to achieve this is dependent upon pupil size which varies with luminance level and viewing distance. Often it has been assumed that the BCL were centred over the pupil, but CL (particularly rigid CL), are often not centred over the pupil. The pupil is not necessarily centred over the visual axis, nor is it always central with respect to the corneal limbus and with changes in size may alter position in relation to the visual axis (Wilson et al, 1991, 1992). Decentration of a BCL may result in changes in the form of the image which substantially alters optical and visual performance. Image form varies depending whether the light passing through the COZ or the POZ is in focus at the retina. The consequences of these effects are discussed below.

Optical Performance

Concentric-design BCL form images which vary slightly depending upon whether the COZ or the POZ is forming the focus at the retina. For example, with a CN BCL

light from a distant object will be focused on the retina by the POZ (distance power). As shown in *Figure 1.2-1a* light passing through the (near power) COZ (shaded) will form a wide, but low intensity blur. The actual retinal image is composed of the two images. The Line Spread Function (LSF), a cross-section intensity plot of the image of a slit measured on an optical bench (section 1.3.2), demonstrates the effect as shown in *Figure 1.2-1b* ("pedestal" form). The same image form occurs with a CD BCL and a near object. With a more complex object the pedestal form may be expected to reduce spatial detail.

When a near object is viewed by the same BCL type (CN), as shown in *Figure 1.2-2a*, the COZ of the BCL produces a focus at the retina and the (distance power) POZ (shaded) produces a relatively low intensity annular blurred image. The optical bench (LSF) confirms that the final image (*Figure 1.2-2b*) has a different (annular) form. The same image form occurs with a CD BCL and a distant object (Hodd, 1969; Klein and Ho, 1986). With a more complex object the annular form might be expected to reduce overall contrast in the image.

Theoretical considerations

The image shape with concentric-design BCL may be expected to alter resolution and contrast. In an analysis of a new test of resolution, Hotchkiss et al (1951) found that optimal contrast rendition occurred

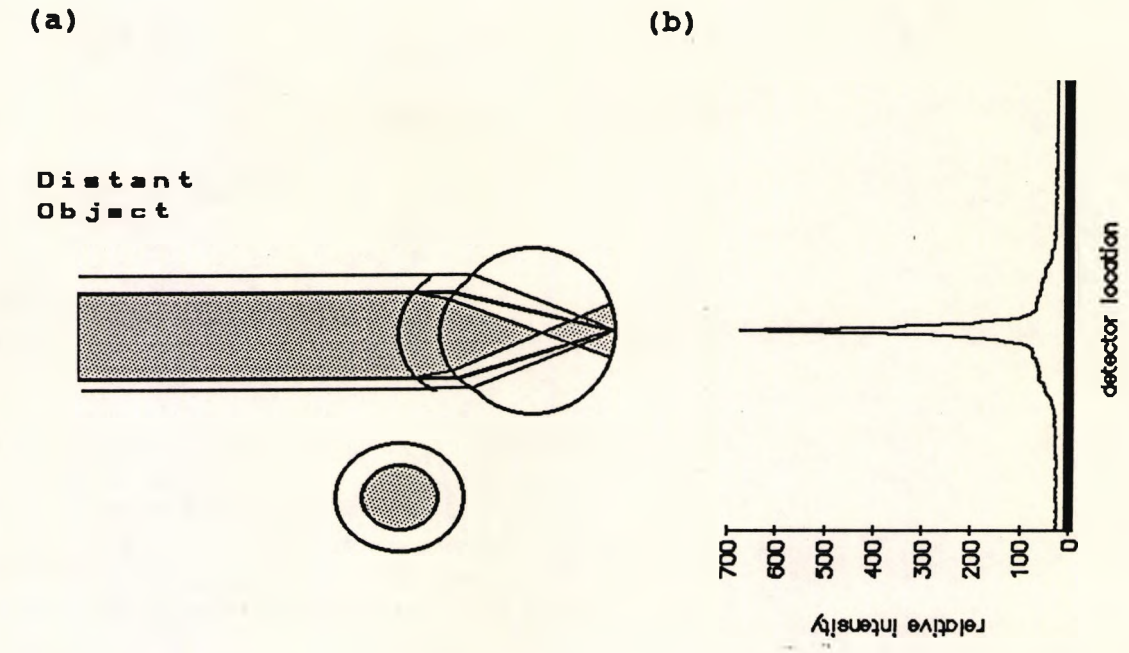

Figure 1.2-1 **(a)** Image formation with a Centre-Near refractive BCL when viewing a distant object. The central optic zone (COZ)(shaded) forms a focus before the retina, creating, at the retina, a blurred image superimposed on the in-focus image formed by the peripheral optic zone (POZ). **(b)** A measured LSF for this arrangement shows the out-of-focus pedestal of light formed by the COZ overlaid on the in-focus image formed by the POZ. (data from this study)

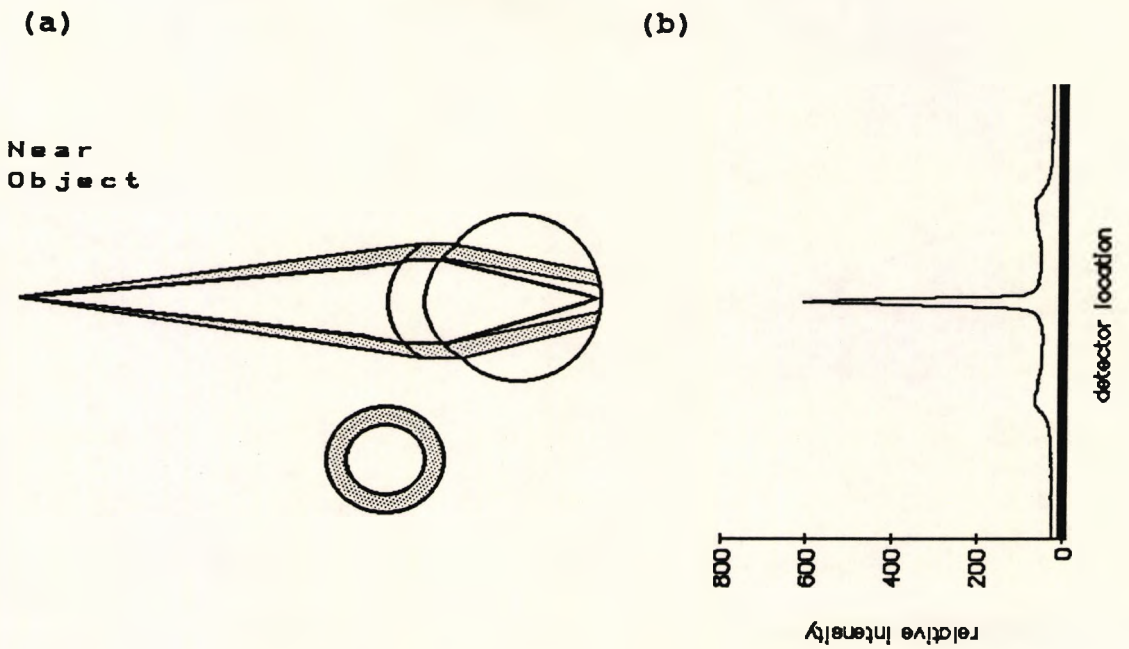

Figure 1.2-2 **(a)** Image formation with a Centre-Near refractive BCL when viewing a near object. The peripheral optic zone (POZ)(shaded) forms a focus beyond the retina hence creating an annular blurred image around the in-focus image formed by the central optic zone (COZ). **(b)** A measured LSF for this arrangement shows the annular out-of-focus image formed by the POZ, overlaid on the in-focus image formed by the COZ. (data from this study)

when the image of a point had a minimum overall size, while best resolution occurred when the image of a point source had the most light concentrated at the centre, even if the overall diameter of the point image was greater. This was reflected in visual performance as Remole (1982) reported that the resolution limit of the human eye was more dependent on the central maximum illuminance than on the total spread of the blur circle.

O'Neill (1956) calculated the optical transfer function (OTF) for an annular aperture and demonstrated that, for a given outer radius, as the inner radius increased the OTF reduced at median spatial frequencies and improved for higher spatial frequencies (*Figure 1.2-3*). This confirmed the earlier report by Steward (1928) that with an annular aperture the central peak narrowed and resolution increased. As the radius of a circular aperture increased the OTF improved (*Figure 1.2-4*) (Hopkins, 1956). If the effect of the out-of-focus image of a concentric-design BCL is disregarded it would be expected that the COZ would give a good median spatial frequency response, with a relatively low cut-off frequency. Conversely the POZ would give a reduced median spatial frequency response, with a higher cut-off frequency and better high spatial frequency response. This should be reflected in changes in visual performance (Remole, 1982).

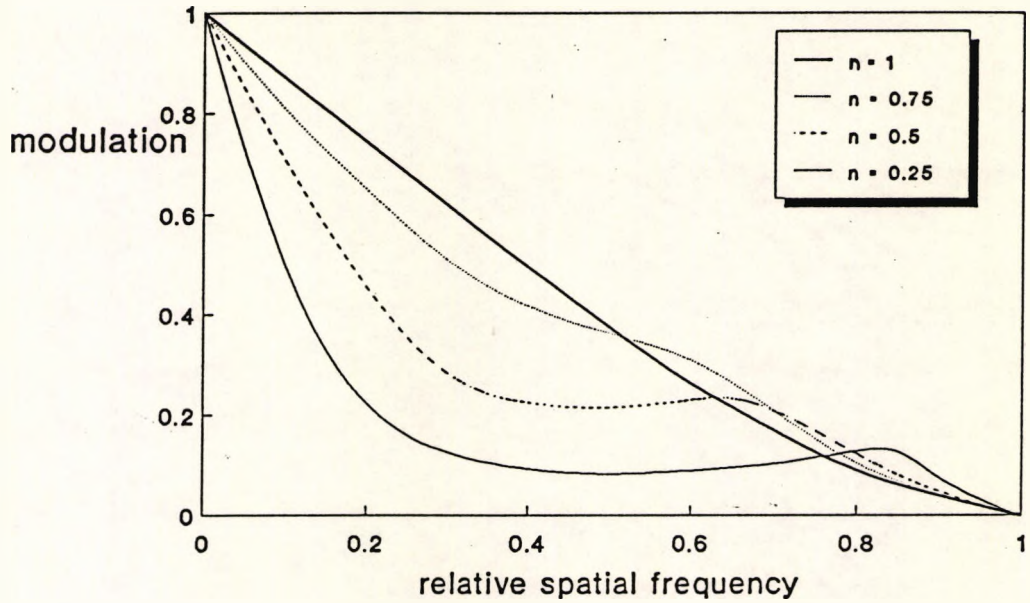

Figure 1.2-3 The modulation transfer function for an annular aperture of varying central radius (r_c) and fixed outer radius (r_o) where $n = (r_o - r_c) / r_o$. (from O'Neill, 1966)

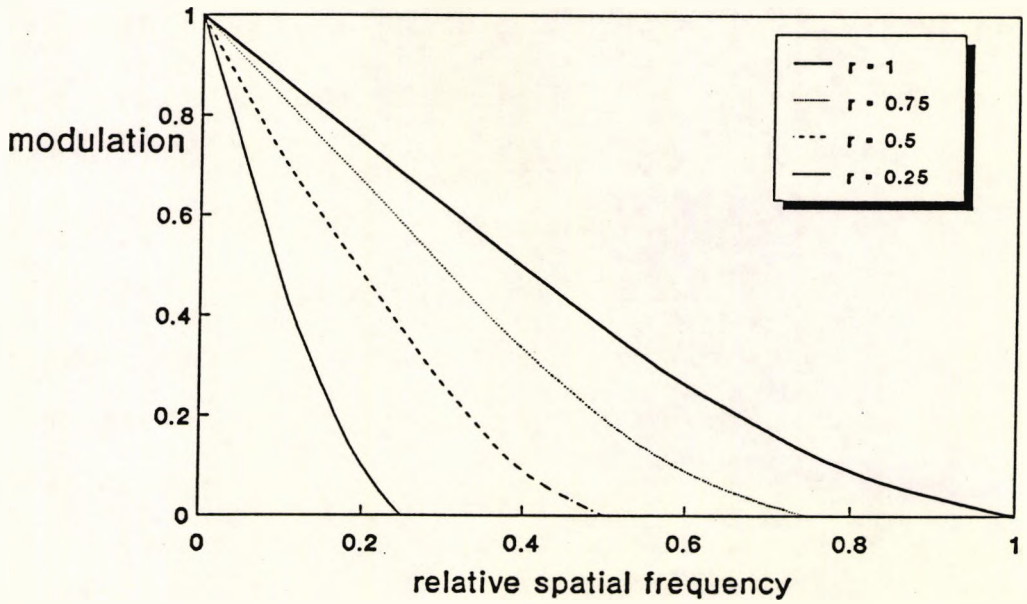

Figure 1.2-4 The modulation transfer function for a circular aperture of varying radius. (redrawn from Hopkins, 1956)

Pupil coverage and contact lens centration

Simultaneous-vision BCL rely upon both optical sections being over the pupil at all times. This will almost always be the case with diffractive BCL and with some of the more exotic designs proposed (e.g. de Carle, 1984, 1989a). Both optical sections of a concentric-design BCL will not necessarily lie over the pupil at all times. Figure 1.2-5a shows a perfectly centred concentric-design BCL where the COZ and the POZ each cover approximately 50% of the pupil area. A simple change in pupil size (due to e.g illuminance or convergence) will lead to a change in the proportion of the pupil covered by the two optic zones as shown in *Figure 1.2-5b*. This change is compounded by CL location and CL movement. It unusual to have a perfectly centred BCL. Decentration of a concentric-design BCL may lead to a variation in the proportion of the pupil covered by the COZ as shown in *Figure 1.2-5c*. Reduction in pupil size may then further reduce the proportion of the pupil covered by the COZ as shown in *Figure 1.2-5d*. Obviously for certain configurations of pupil size, COZD and BCL location the COZ may no longer cover any portion of the pupil. Hence it is imperative in an investigation of concentric-design BCL that the pupil size and BCL location is known during assessment of visual performance. This is confused by variations in pupil size with illuminance, convergence and psychological state.

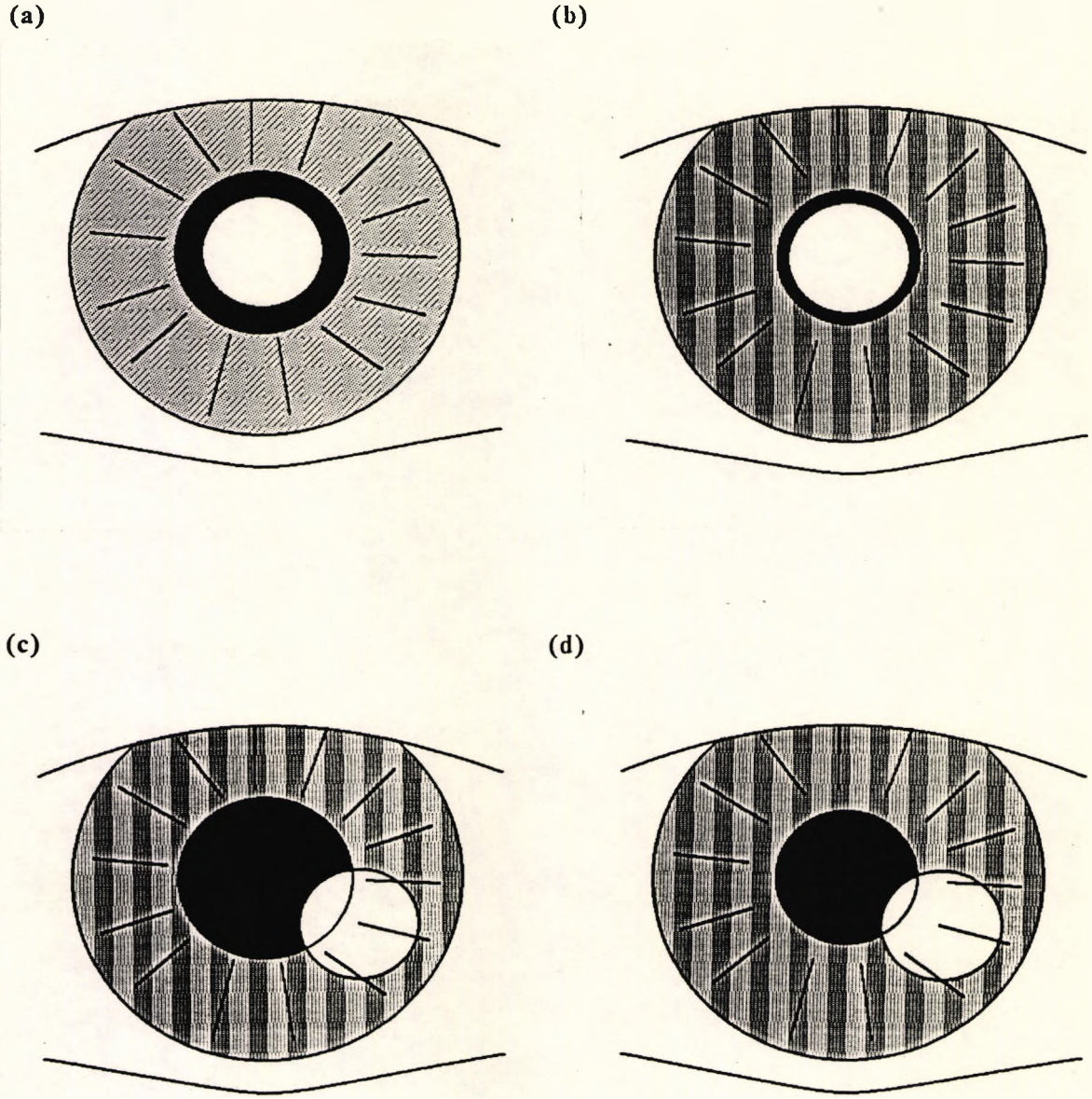

Figure 1.2-5 The effect of pupil size and decentration upon concentric-design refractive BCL. **(a)** A diagrammatic representation of the central optic zone (COZ) (white) of a concentric-design BCL centred over the pupil (black) and iris (shaded). In this instance the COZ of the BCL covers less than 50% of the pupil area, the remainder being covered by the peripheral optic zone (POZ) which has a different optical power to achieve the bifocal effect. **(b)** A reduction in pupil size will lead to a reduction in the area of the pupil covered by the POZ of the BCL. The proportion of the pupil covered by the COZ consequently increases. **(c)** Decentration of a concentric-design BCL will alter the location of the COZ over the pupil and iris. If the COZ remains within the pupil area the proportion of pupil cover by the COZ would remain the same as in (a). As shown, decentration may lead to a change in the area of the pupil which is covered by the COZ. **(d)** A reduction in pupil size may reduce the area of the pupil covered by the COZ of a BCL as compared to (b) and the proportion of the pupil covered by the POZ may increase as compared to (b) and (c).

Theoretical investigations

Three different theoretical approaches have been taken. These have involved simple calculation of relative pupil coverage (Erickson et al, 1988; Robirds, 1988); the calculation of retinal image formation with concentric-design BCL typically by ray tracing techniques (Charman and Walsh 1986b, 1988; Freeman and Stone, 1987; Hodd, 1969; Klein and Ho, 1986; Wesley, 1971); and the calculation of the modulation transfer function (MTF) of the BCL (Charman and Saunders, 1990; Freeman and Stone, 1987; Klein and Ho, 1986).

Erickson et al (1988), in an evaluation of geometrical models and BCL measurements, concluded that COZ location and power distribution were sensitive to pupil size and BCL location. Changes in image form with pupil size and BCL decentration can be simply demonstrated by simple ray tracing (Hodd, 1969). More informatively, spot diagrams based upon computer generated ray tracing calculations which indicate the image intensity have been demonstrated to vary significantly with changes in pupil size (Charman and Walsh 1986b; Freeman and Stone, 1987), changes in COZD (Charman and Walsh 1986b) and with BCL decentration (Wesley, 1971; Charman and Walsh 1986b). Most of these theoretical investigations of the retinal image form are limited as relatively simple aberration free models of the human eye have been used in the calculations.

Calculated MTFs for concentric-design BCL have been produced (Klein and Ho, 1986, Freeman and Stone, 1987, Charman and Saunders, 1990). The calculations by Klein and Ho (1986) appear to suffer from some calculation problem as indicated by their axial intensity plot for the "two zone" BCL on page 29, which bears no resemblance to measured axial intensity (Loshin, 1989). The calculated MTF of concentric-design BCL has been shown to be reduced at all but the lowest spatial frequencies. The MTF appears to vary between the two different foci, though this was difficult to determine as the spatial frequency ranges shown have been relatively restricted. When the COZ forms the focussed image the MTF appears slightly better than when the POZ forms the image. Charman and Saunders (1990) have demonstrated changes in the calculated MTF with pupil size. As would be expected, as the COZD of the CN BCL was increased the near MTF improved and the distance (POZ) MTF reduced and vice versa. Charman and Walsh (1986b, 1988) also demonstrated the dependence of the MTF upon the eccentricity of multifocal CL, pupil size and object vergence.

Optical measurements

Grey and Sheridan (1988) reported the measured MTF of a series of single vision CL. The measured MTFs were all very high and close to the diffraction limit of the measurement system. This was not the case for BCL which have a reduced MTF compared to single vision CL. The

measured MTF of concentric-design BCL was similar to the theoretically calculated MTF and demonstrated the predicted pupil (aperture) dependence (Klein, 1986; Loshin, 1989; Loshin and Hug, 1986; Young et al, 1990). When the COZ formed the focussed image the MTF was depressed in the median spatial frequencies, but appeared to retain fair modulation transfer for higher spatial frequencies, and the MTF reduced with increasing aperture size. Conversely, when the POZ formed the focussed image the MTF improved with increasing aperture size. At 50% pupil coverage by the COZ, at an arbitrarily chosen 12 c.p.d.. the measured modulation of the image formed when light passing through the POZ was in focus was greater than the modulation of the image formed when light passing through the COZ formed the focussed image with both BCL (Young et al, 1990). This did not agree with the calculations of Klein and Ho (1986) which indicated that when the COZ and POZ covered equal areas over the pupil the image formed by the COZ had a better MTF (as noted earlier there was some reason to doubt these calculations). If a higher spatial frequency, for example 30 c.p.d., was examined the COZ was more efficient. This was then in agreement with the changes in modulation with spatial frequency indicated by the calculations of O'Neill (1956). Young et al (1990) used only one COZD of each BCL form (CD and CN) and hence did not investigate the interaction between COZD and aperture size. Other aspects of BCL design were not considered such as the amount of RZJ blending (the CD BCL was

blended, while the CN BCL was not) and placed the aperture at an undefined distance before the BCL as opposed to the on-eye situation. With the optical arrangement used there was a possibility that the magnification of the image introduced by the different focal lengths of the distance and near images may have introduced an erroneous comparison between distance and near (section 1.3.5).

By direct measurement of image contrast with a simulated concentric-design intraocular lens (IOL) and a magnified schematic eye Atebara and Miller (1990) suggested that equal performance was achieved when the COZ covered about 40% of the pupil. This model could be equally applicable to BCL but suffers from a number of problems.

Decentration

When a concentric-design BCL decentres over the aperture (pupil) the image formed by the BCL varies from that shown in *Figures 1.2-1 and 1.2-2*. With some interesting ray tracing diagrams, Hodd (1969) demonstrated the asymmetry of the image shape with decentration. Charman and Walsh (1986b) produced spot diagrams based upon computer generated ray tracing calculations which indicated the image intensity with variations in BCL location and showed that these can alter significantly. The measured LSF, shown in *Figure 1.2-6*, confirmed their calculations. Decentration of the concentric-design BCL produces an orientation dependent OTF. There have been no published

reports of optical measures of decentred simultaneous-vision BCL (except data from this study which has been accepted for publication: Woods, Saunders and Port, 1992). In a discussion of the pupil dependence of alternating-vision BCL Borish (1988) showed the measured MTF of an alternating-vision BCL which demonstrated the effect of the decentred optic in this form of BCL.

Hence it would appear that there has been limited information available about the optical performance of concentric-design BCL. There have been no published reports which directly relate optical performance to visual performance.

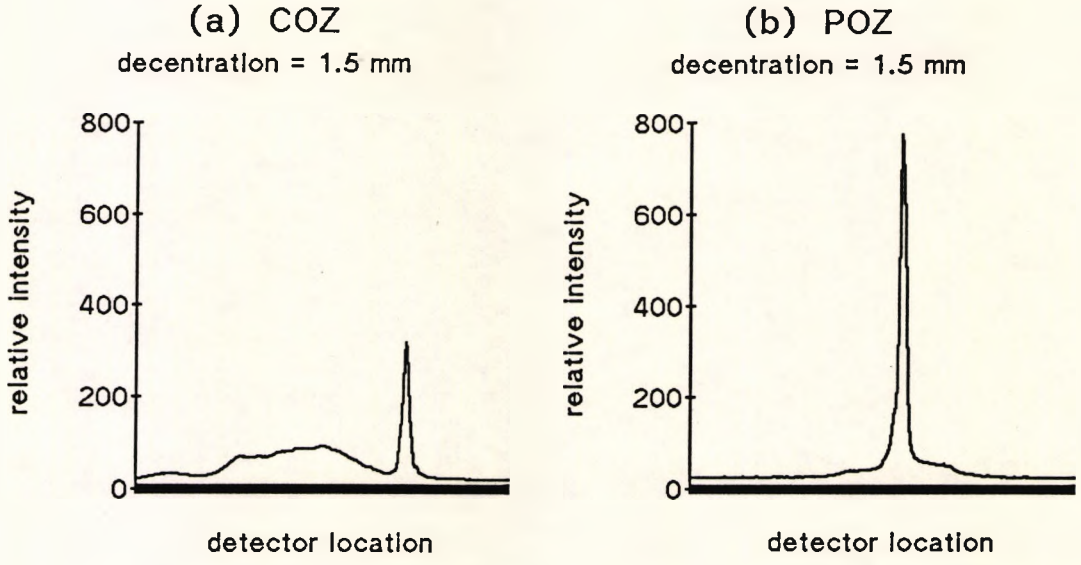

Figure 1.2-6 Image shape with a decentred concentric-design refractive BCL. Line Spread Functions (LSF) measured with the light passing through : **(a)** the central optic zone (COZ) of a 2.6 mm COZD BCL in focus with 1.5 mm decentration over the 4 mm aperture. With increasing decentration there is a dramatic change in image shape and a commensurate reduction in the optical performance (MTF); and **(b)** the peripheral optic zone (POZ) of a 2.6 mm COZD BCL in focus with 1.5 mm decentration over the 4 mm aperture. Increasing decentration has only a small effect upon the image shape. (data from this study)

Visual Performance

The effect of image form

Visual performance varies according to the image form in a predictable way. As noted the resolution limit of the human eye was more dependent on the central maximum illuminance than on the total spread of the blur circle (Remole, 1982). Cox (1985, 1986) demonstrated that the annular blur on the image (*Figure 1.2-2b*) was less detrimental to visual performance than the pedestal form (*Figure 1.2-2a*). Visual performance with light passing through the COZ in focus was similar to a reduction in image contrast, and with the POZ in focus was similar to a reduction in spatial detail (Ho and Bilton, 1986). Effectively, for a given pupil size, the COZ was found to be more efficient than the POZ. For example, with concentric-design BCL, if there was equal pupil coverage by the COZ and POZ of the CN BCL under discussion then the near visual performance would be slightly better than the distance visual performance. From a similar analysis of a CD BCL it can be shown that the reverse occurs. Hence to achieve equal distance and near visual performance the COZ would need to cover less than 50% of the pupil. This does not consider the normal changes in pupil size with convergence.

Many reports of concentric-design BCL have only reported the reductions in high contrast VA and stereoacuity (e.g. Erickson and Robboy, 1985; Jones and Lowther, 1989; Lowther, 1982). Some more recent reports have shown a

reduction in CSF at medium and high spatial frequencies (> 2 c.p.d.), but with no note of centration or pupil coverage by the COZ (Brown et al, 1987; Collins et al, 1989; McGill et al, 1986, 1987; Saunders, 1989, 1990).

Visuomotor tasks and complex task reaction times have been shown to be reduced with BCL (Brown et al, 1987, 1988; Sheedy et al, 1991). Comparison to earlier results with monovision (Sheedy et al, 1988) indicated that the performance reduction was due to reduced visual acuity (image quality) rather than to the reduction in stereoacuity. Stereoacuity has been suggested as predictive of success with concentric-design BCL (Back and Sayer, 1985) and not a reason for vision-related failure (Back et al, 1989).

Pupil coverage

It would be expected that, for a CD BCL, as the proportion of the pupil which was covered by the COZD increased the visual performance for distance would improve and near vision would reduce. The reverse should occur for a CN BCL. As discussed above, this has been demonstrated for optical performance.

Despite the common acceptance of a relationship between pupil size, alterations to BCL design and visual performance very little work has been done to investigate and to quantify this relationship. The two principal investigations of changes in COZD with presbyopic

subjects have been with soft BCL, one with CD (Erickson and Robboy, 1985) and the other with CN (Jones and Lowther, 1989) BCL. The visual performance measure reported in both studies was high contrast VA.

As noted, increasing the COZD would be expected to lead to an improvement in visual performance for the relevant viewing distance, as the image formed would become dominant. Erickson and Robboy (1985) demonstrated that distance vision improved when the (distance) COZD increased, but the expected decrease in near vision did not occur (*Figure 1.2-7*). This study failed to relate the COZD to the actual pupil size, or to give a percentage pupil cover. CL location was recorded, but not related to VA. They concluded that for the average 3.7 mm pupil (range 1.7 to 5.0 mm) a 2.5 mm (distance) COZ (average 46 percent pupil coverage) provided the "best performance for most subjects", though most subjects exhibited a similar performance across two or three zone diameters as assessed with high contrast VA charts.

Jones and Lowther (1989), using a CN BCL, showed that as the (near) COZD increased, the distance vision decreased, but they did not show the expected increase in near vision (*Figure 1.2-8*). They found no correlation between pupil size and COZD. This may have been due to the technique of pupil size estimation, a lack of centration of the BCL, and to the use of high luminance, high contrast VA only (Charman and Saunders, 1990). In

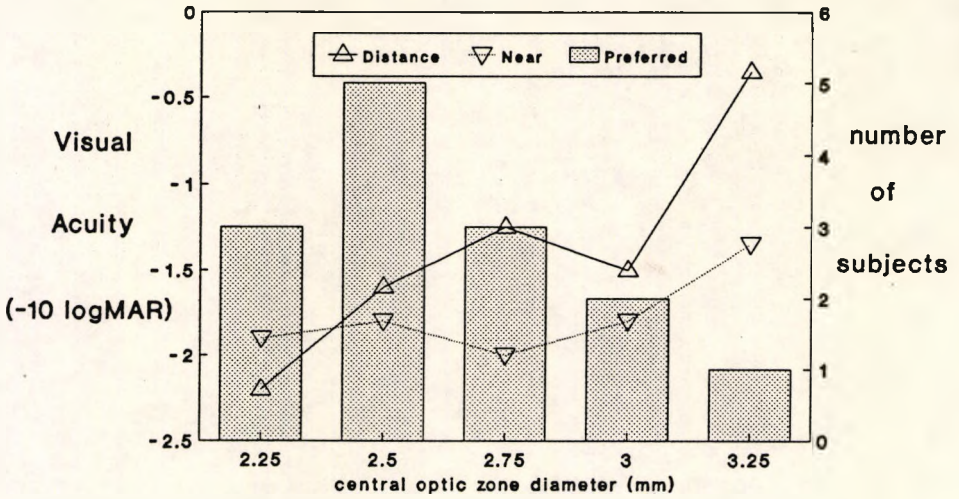

Figure 1.2-7 A previous study with soft Centre-Distance refractive BCL which measured high contrast Visual Acuity at distance and near. As the central optic zone diameter increased distance vision (solid line) was expected to improve, and near vision (dotted line) to deteriorate. (redrawn from Erickson and Robboy, 1985)

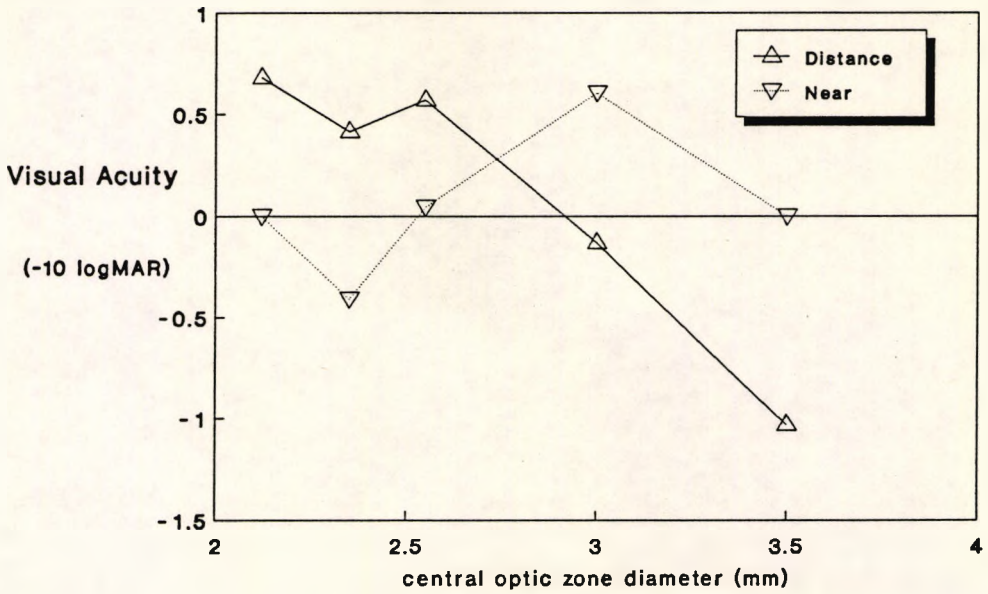

Figure 1.2-8 : A previous study with soft Centre-Near refractive BCL which measured high contrast Visual Acuity at distance and near. As the central optic zone diameter increased near vision (dotted line) was expected to improve, and distance vision (solid line) to deteriorate. (redrawn from Jones and Lowther, 1989)

addition the repeatability of the measure was not tested, and with the small sample size may explain the lack of correlation.

Erickson and Robboy (1985) reported the subjective preference of the subjects for the different COZD as shown in *Figure 1.2-7*. Surprisingly only one subject preferred the largest COZD (3.25 mm) despite the apparently better vision for both distance and near. This was not explained by the authors.

Cox (1985, 1986), with young subjects, investigated power variations across soft CL and demonstrated variations in visual performance with percentage pupil coverage by the COZ with soft CD and CN BCL. Visual performance was assessed with high and low contrast VA and the CSF. The expected trends with changes in COZD were demonstrated with both BCL designs and for all tests. Whilst the diameter of the artificial pupils were stated it was not possible to determine the entrance pupil diameter (pupil size) and thence determine the actual proportion of the pupil covered by the COZ. In an investigation, with presbyopic subjects, of both CD and CN BCL Holden and co-workers (Back et al, 1990; Holden, 1986) found a relationship between COZD and high and low contrast VA which varied with the configuration (i.e. CD or CN). The variation in VA with COZD (Back et al, 1990) was very similar in form to contrast measures in simulation (Atebara and Miller, 1990) and MTF measures (Young et al,

1990). The soft BCL used in both these studies had varying degrees of blending of the RZJ, and which varied systematically between the CD and CN BCL due to the manufacturing technique (cast moulding) (Holden, 1986). Other investigations of the effect of COZD have been performed in the development of commercially available concentric-design BCL, but the results remain unpublished (Carmichael, 1986; Lowther, 1985).

The Stiles-Crawford Effect

Not all light is equal in its effectiveness. Light passing through the centre of the pupil is more effective than light passing through the peripheral pupil (Stiles-Crawford effect). Calculations by the author based upon this effect (data: Crawford, 1972) indicate that the COZ needs to cover less than 50% of the pupil area to be as effective as the POZ. This depends slightly upon pupil size. As shown in *Figure 1.2-9*, for equal relative efficiency between COZ and POZ, the proportion of the pupil covered by the COZ reduces from 43% at 2 mm to 35% at 6 mm.

The human pupil is not fixed in size and for an average 55 year old varies from about 5.5 mm in the dark to about 3.25 mm under normal "room" illumination (Woods, 1991c). As an example, with a 4 mm pupil the COZD must be 2.83 mm to geometrically cover 50% of the pupil, but for the COZ and POZ to be equally effective a 2.55 mm COZD would be required.

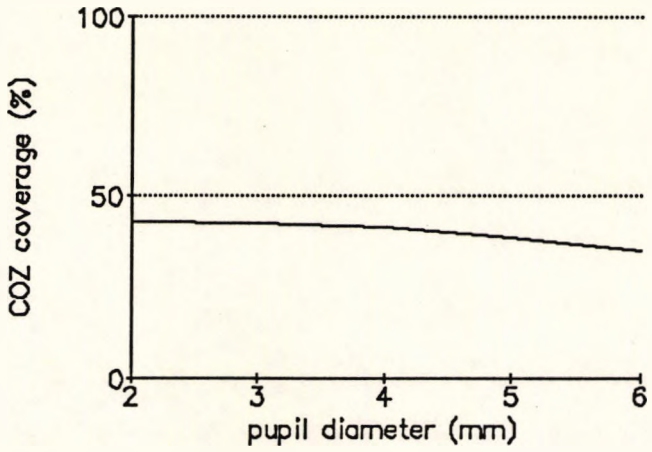

Figure 1.2-9 The Stiles-Crawford effect and central optic zone (COZ) diameter coverage of the pupil. The per cent coverage of the pupil by the COZ of a concentric-design refractive BCL centred over the pupil to achieve equal relative efficiency of the COZ and POZ when the Stiles-Crawford effect is considered.

Decentration

There have been no published studies which relate the amount of decentration of concentric-design BCL to aspects of visual performance. There have been no published studies which relate the form (i.e. degree of blending) of the RZJ to changes in visual performance.

Summary

Hence there is a poorly defined, relationship between pupil size, COZ design, decentration, optical performance and visual performance of concentric-design refractive BCL. Suggestions for COZ coverage of the pupil in the literature have varied from 20% (Breger, 1983) to over 80% (Josephson and Caffery, 1986; Robirds, 1987), though suggestions of 50% pupil coverage have been more common (Bier, 1967, Bier and Lowther, 1977; de Carle, 1989b; Sheedy et al, 1991). There has been some evidence from

studies of concentric-designs (Cox, 1986; Holden, 1986; Klein and Ho, 1986) that 50% may not be optimal.

1.2.3 DIFFRACTIVE BIFOCAL CONTACT LENSES

Diffractive BCL, which utilise the natural interference properties of light to produce the required foci, were the most recent simultaneous-vision innovation. Though the major advantage is the relative independence from the effects of changes in pupil size, the ratio of light in the two images is subject to variation as is discussed below. The diffractive portion of the BCL typically covers the central 3 to 6 mm and is surrounded by a refractive optical zone. For this discussion the two optical zones will be referred to as the Central Diffractive Zone (CDZ) and the Peripheral Refractive Zone (PRZ) (Draft International Contact Lens Standards, 1991).

Theoretical aspects

The development of diffractive BCL is detailed in a historical context and theoretical considerations discussed.

Zone plates

Diffractive BCL were a development from simple zone plates which utilise aspects of the wave nature of light. Fresnel to explain diffraction, utilised Huygen's principle which assumes that each point on a wavefront may be considered as a source of secondary waves or

wavelets. Then, at some given location, *P*, the effect of a wavefront can be considered as the result of a series of wavelets emanating from all points (or for simplicity, small areas) of the original wavefront. The effect at *P* is a result of the summation of the amplitude and relative phase of each wavelet according to the principle of superposition (Ditchburn, 1976). If all the wavelets are in phase resulting in constructive interference then there is an area of increased illumination which is known as a focal point. A special construction, invented by Rayleigh in 1871 (Jenkins and White, 1976), known as a zone plate utilises this principle to form a focus by blocking wavelets from areas which would arrive out of phase.

Only wavelets which are in phase are allowed to reach the focal point F by a typical simple zone plate (*Figure 1.2-10*) which is opaque with a series of clear, narrow, concentric rings with radius r_m according to the equation:

$$r_m = (2 m \lambda f' + (m \lambda)^2)^{\frac{1}{2}}$$

where λ = wavelength of incident light, and f' = distance from plate to F (focal length). As for most purposes the focal length f' is far greater than $(m\lambda)^2$, this may be rewritten:

$$r_m = (2 m \lambda f')^{\frac{1}{2}} \quad ..... \quad \textit{Equation 1.2-1}$$

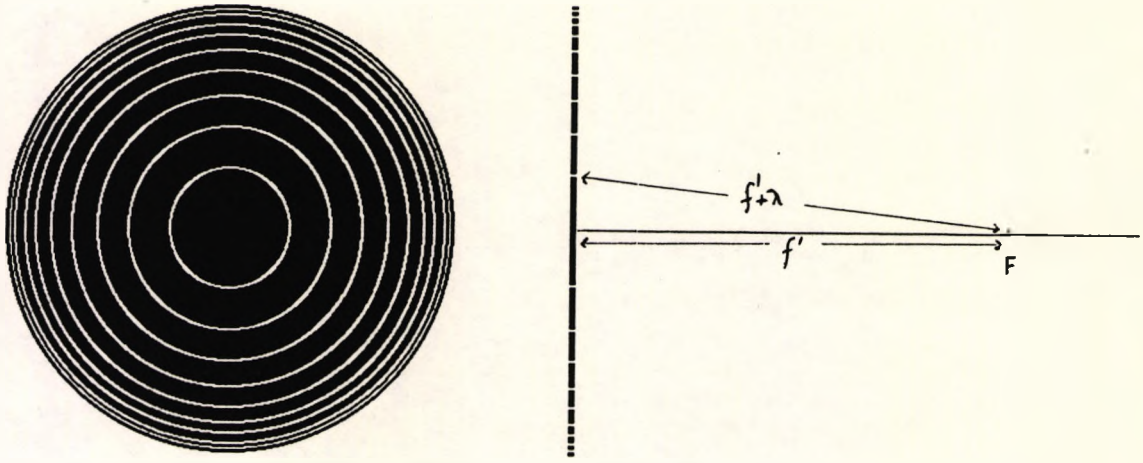

Figure 1.2-10 A simple zone plate. The radii of the clear zones are found according to *Equation 1.2-1*. Then the path length of light incident at the focal length f' from any zone r will be $f' + r\,\lambda$. As all light which is out of phase has been blocked a focus at F will result.

Wavelets passing through these narrow zones will all reach the focal point in phase since the path length from the r^{th} zone will be $f' + r\,\lambda$. It follows from *Equation 1.2-1* and evaluation of the condition of formation of the focal point, the requirement that all wavelets arrive in phase, that the design focus of a zone plate is only one of a series of foci and is termed the first-order focus (Jenkins and White, 1976). Where the outer radius of the m^{th} full-period zone is r_m, the focal length for the k^{th} order focus (f'_k) is given by the equation:

$$f'_k = \tfrac{1}{2}\left\{\frac{r_m^{\,2}}{k\,m\,\lambda}\right\} = \frac{f'}{k} \qquad \ldots\ldots\ldots \quad \textit{Equation 1.2-2}$$

As all the wavelets must arrive at infinity in phase there is a zero-order focus corresponding to no diffractive power. There are effectively no even order foci as the wavelets from alternate zones arrive in opposite phase and hence destructively interfere. Theoretical calculations indicate that the bulk of the energy goes into the zero (35%) and first-order (± 29% each) foci, with decreasing amounts to the higher order foci (Freeman, 1984).

Another problem relates to the polychromatic (white) light of the "real" world. Given fixed zone radii (*Equation 1.2-2*) it can be seen that focal length is inversely proportional to wavelength. This results in substantial chromatic aberration across the visible spectrum and which is the reverse of that found with refractive systems. The implications are discussed below.

The major disadvantage of the zone plate is the low light transmission through the narrow annular zones. For all practical purposes it is not necessary to have the wavelets precisely in phase, and there is little loss of image quality with phase variations of up to π ($\frac{1}{2}\lambda$). This is the classical Fresnel zone plate where the rings are half-period zones (*Figure 1.2-11b*). With this construction approximately half the incident light is absorbed. As a further development to increase the amount of transmitted light Wood (1923) suggested that the opaque sections of the traditional Fresnel zone plate be replaced with a

clear section in which an additional half-phase thickness of optical material is included to bring the wavelets from these segments into phase (*Figure 1.2-11c*). This results in the loss of the zero-order focus as the half-phase reaches infinity out of phase and destructively interferes. The light is then mainly found in the positive and negative first order foci (± 40% each).

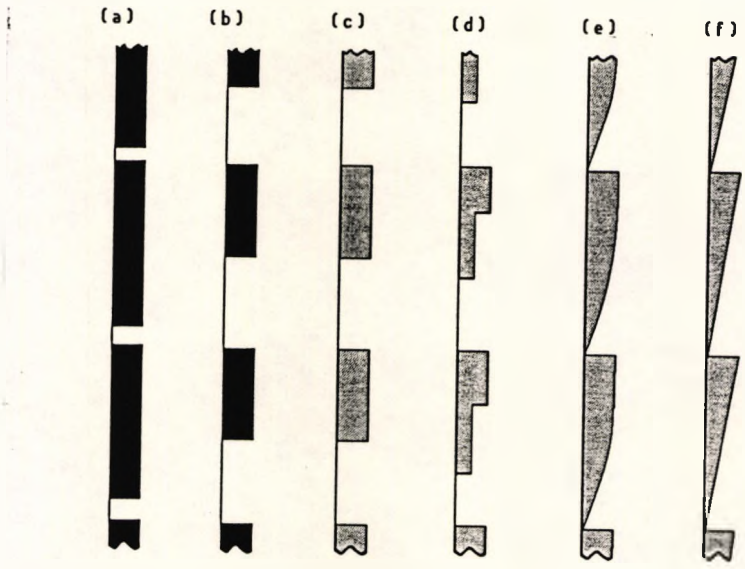

Figure 1.2-11 A schematic representation of the development of the BCL showing the transition from zone plates to a kinoform lens. Cross-sections of two zones (radii according to *Equation 1.2-1*) of **(a)** a simple zone plate; **(b)** a Fresnel zone plate which transmits phase delay of up to $\lambda/2$; **(c)** a half phase (Wood) lens where the light blocked in a Fresnel lens is given an additional $\lambda/2$ delay; **(d)** a lens composed of three sub-zones of $\lambda/3$ phase delay where the area of each annular sub-zone is equal; **(e)** a lens with a continuous asymmetric delay (kinoform) lens (i.e. composed of infinite sub-zones); and **(f)** a lens with triangular sections which approximate an ideal kinoform.

Kinoforms

This construction can be further improved by subdividing each annular zone into more than two steps, producing an asymmetrical staircase of phase delay, to bring the wavelets more closely into phase (Lesem et al, 1969). For example, if the zone is divided into three sub-zones of equal area, such that the phase delay between each stepped sub-zone is $\lambda/3$ (*Figure 1.2-11d*). Further division of the zone into smaller sub-zones will increase the amount of light into the first order focus. With n sub-zones the resulting intensities into the m^{th} order image (I_m) may be found according to:

$$I_m = \left\{ \frac{\sin \pi \left(m - \eta + n^{-1} \right)^2}{\pi \left(m - \eta + n^{-1} \right)} \right\} \quad \ldots \quad \textit{Equation 1.2-3}$$

where $\eta = \lambda_o / \lambda_i$ (λ_o is the design wavelength and λ_i is the wavelength of the imaging light). From *Equation 1.2-3*, for light of the design wavelength ($\eta = 1$), with 3 sub-zones approximately 68% of light is found in the first order focus. This increases to 81% with four sub-zones and 97% with ten sub-zones.

This process can be extended until a smooth asymmetrical transition in phase delay is achieved across each zone (*Figure 1.2-11e*). *Equation 1.2-3* then reduces to:

$$I_m = \left\{ \frac{\sin \pi \left(m - \eta \right)^2}{\pi \left(m - \eta \right)} \right\} \quad \ldots\ldots \quad \textit{Equation 1.2-3a}$$

This kinoform (Lesem et al, 1969) then places 100% of the light (of the design wavelength) into the first order focus (*Equation 1.2-3a*). The ideal form of the transition is parabolic (Lesem et al, 1969; Emerton, 1986), but may be approximated by a triangular section (*Figure 1.2-11f*). Emerton et al (1987) demonstrated the increasing efficiency of triangular sections with increasing number of zones. For example, at the design wavelength the efficiency for 10 triangular zones was approximately 92%. The modification of the kinoform to produce a bifocal effect was first proposed by Freeman (1984).

At this point it is worth discussing the differences between this kinoform design and Fresnel lenses. A Fresnel lens consists of annular facets shaped to bring geometric rays to a common focus. As each facet has the same width and the thickness of the facets (often many thousands of wavelengths) is such that many, uncorrelated phase delays occur with complex amplitude contributions at the focus. Thus, unlike the kinoform lens, a Fresnel lens acts like a single lens, with no systematic constructive interference. The original descriptions by Cohen (1979, 1980, 1982a, 1982b) of an alternative BCL used Fresnel principles. More recently a truly diffractive BCL has been proposed by Cohen (reported by Hemenger and Tomlinson, 1990).

A diffractive bifocal

Returning to diffractive lenses, to achieve the correct phase delay the height (h) of each blaze, step or diffractive zone junction (DZJ) is given by :

$$h = \lambda_o / \delta n \qquad \textit{Equation 1.2-4}$$

where δn is the difference in refractive indices of the material and surrounding media and λ_o the design wavelength. The DZJ height of the diffractive element corresponds with only one particular wavelength, λ_o, and thus only that wavelength is actually in focus. At wavelengths other than the design wavelength (η <> 1) less light is concentrated in the first order focus and appears in other orders of focus (*Equation 1.2-3a*).

For any given design of diffractive BCL, as devised by Freeman (1984, 1986b, 1986c), with correct choice of λ_o, it is possible to place most of the light into the zero and first order foci. By alteration of the λ_o it is then possible to place varying amounts of light in the two (BCL) foci. For example, with a Polycon II diffractive BCL in saline (δn = 1.476 - 1.334), a λ_o = 275 nm will place approximately 40% of the light of 550 nm into each of the zero and first order foci. The split will vary with wavelength as shown in *Figure 1.2-12*, with long (red) wavelengths favouring the zero order (distance) focus and short (blue) wavelengths favouring the first order (near) focus. The remainder of the light goes into the other

orders. This plurality of foci can be seen by careful examination of a diffractive BCL with a focimeter. Unless a wet cell is used, the measured foci will not correspond to those effective on eye as the surrounding media is air not tears altering the phase delay (*Equation 1.2-4*).

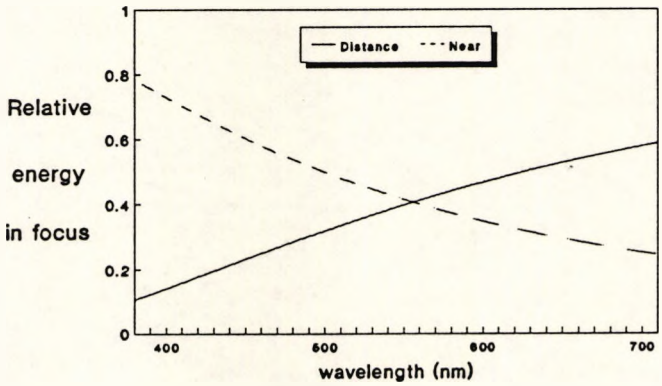

Figure 1.2-12 The spectral energy of the diffractive foci of a kinoform lens used to create a bifocal effect. The bulk of the energy is split between zero and first order foci of an ideal kinoform lens with a design wavelength of 275 nm (from *Equation 1.2-3a*). This places approximately 40% of the light of wavelength 550 nm (approximately the peak of human photopic sensitivity) into each of these foci, with the remainder of the light into the other orders (< 5%). Each of the "bifocal" foci has a distinctly different spectral energy profile.

The annular zones of a diffractive BCL are effectively applied to a normal single vision CL and the normal differences in front and back surface curvature in conjunction with the zero-order diffractive power provide the distance correction. The first-order diffractive power then provides the near correction. A diffractive BCL, like any zone plate, with a focal length f' = 0.5 m and λ = 550 nm requires eleven zones to cover a 5 mm pupil (*Equation 1.2-1*). It is possible to reverse the shape

of the diffractive zones to create a BCL with a negative diffractive focal length. The distance power of a BCL of this "reverse" add BCL would be created by the first order focus, and the near power by the zero order focus. The distance focus would then display the reverse LCA, while the near focus would have only the normal refractive LCA. This may have some advantages as the near focal length may not be as critical.

Chromatic effects

As noted earlier there are some aspects of diffractive BCL image formation which are wavelength dependent. These spectral effects are discussed below.

Chromatic Aberration

The focal length of diffractive optical elements is inversely proportional to wavelength (*Equation 1.2-1*), the reverse of refractive Longitudinal Chromatic Aberration (LCA) such as with spectacle lenses and in the human eye. Theoretical predictions (Freeman, 1984; Charman, 1986) suggest that the LCA of the first order focus (near) of the diffractive BCL would largely negate the inherent axial chromatic aberration of the human eye (approximately 1.5 D between 450 and 650 nm). The LCA of a diffractive focus may be defined by :

$$LCA = \frac{\lambda_{min} - \lambda_{max}}{\lambda_{focus} \times f'} \quad \ldots\ldots\ldots \quad \textit{Equation 1.2-5}$$

where λ_{min} and λ_{max} are the minimum and maximum wavelengths of interest, λ_{focus} is the focus wavelength of the lens and f' the first order focal length. For example, given λ_{max} = 650 nm, λ_{min} = 450 nm, λ_{focus} = 550 nm, and f' = 0.5 m, then the LCA = - 0.73 D.

Though this LCA would be unlikely to cause any effects upon colour perception or visual acuity (Meslin and Obrecht, 1988), it may reduce the depth of focus at near, making the near working distance more critical. The age-related reduction in pupil diameter (section 1.1.2) results in a larger depth of focus for presbyopes than pre-presbyopes and thus the resultant effect of chromatic aberration correction may be minimal.

There have been no reports of investigation of the effects of the LCA of the diffractive focus. Using the example above, with a focus wavelength of 550 nm the focal separation of the zero and first order foci will be 2 D. For 450 nm and 650 nm the separation will be 1.62 D and 2.34 D respectively. It is then feasible to measure the length of the focal separation (distance between the zero and first order foci) at different wavelengths to confirm theoretical calculations.

Spectral transmission

Diffractive BCL are wavelength dependent. As noted earlier, the proportion of light in the zero and first order foci will vary with wavelength as shown in

Figure 1.2-12. Long (red) wavelengths are favoured in the zero order (distance) focus and short (blue) wavelengths are favoured the first order (near) focus. As described in section 1.1.3, the age-related wavelength selective reduction in transmission of shorter wavelengths may reduce intensity of the zero order (distance) image. This effect may be further enhanced by the spectral content of the illuminating source as described in section 1.1.3. As shown, a 50 : 50 ratio between distance and near images in daylight, with Standard Illuminant A (long wavelength dominant) will alter to 47 : 53. This further reduces the intensity of the image of a distant object. As noted below this balance can be modified with BCL design. Difficulties of this sort have not been reported.

Diffractive Zone Junction Height

Variations in phase delay across the visible spectrum introduced by the diffractive zones results in a wavelength dependent spill of light from the first order focus into the zero order (distance) focus. The amount of light in the various foci of a diffractive BCL depends upon the phase delay (as defined by the design wavelength in *Equation 1.2-3a*) and hence the DZJ height (*Figure 1.2-11*). By careful choice of DZJ height it is possible to vary the amount of light in the various foci. As the DZJ height increases the amount of light in the first order focus increases. Hence it is possible to select the ratio of light in the two BCL images. This will alter the image

quality such that variations in DZJ height will lead to variations in the optical and visual performance with DZJ height.

There have been no reports of investigations of the effect of variations in DZJ height of diffractive BCL in the literature.

Other design considerations

As noted above, the ideal cross-sectional form of each zone of a kinoform (diffractive BCL) is parabolic (*Figure 1.2-11e*), though reasonable approximations to the parabolic form (e.g. *Figure 1.2-11f*) will produce diffractive foci with an efficiency which increases as the shape approaches the ideal shape and the number of zones increases (Emerton et al, 1987). The manufacturing technique employed to produce the BCL used in this study created zones of approximately triangular form.

The ideal cross-sectional form also has a sharp DZJ as the phase delay must alter by 2π at this point. Due to physical limitations imposed by manufacturing processes it is not possible to have a sharp DZJ. BCL manufactured with conventional lathes have been limited by the size and shape of the cutting tool. Light will be lost from the desired foci due to the failure to conform to the ideal DZJ shape. This is referred to as the finite tool effect. The loss will depend upon the shape and width of the finite tool effect. A diamond tool with a radius of

250 μm will theoretically produce a finite tool effect 32 μm wide at a 2.0 μm DZJ height. This finite tool effect will occupy a larger proportion of outer zones as the distance between successive zones decreases (*Equation 1.2-1*). For example, the finite tool effect on a BCL with a first-order diffractive focal power of 2.00 D increases from 8% of the first (inner) zone to 28% of the eleventh (outer) zone (approx. 5 mm). This effect has been noted by Charman and Saunders (1990) with Pilkington Diffrax BCL.

Similarly, other failures to conform to the required shape may also result in a reduction in light in the desired foci leading to a reduction in image quality. Some potential manufacturing errors are illustrated in *Figure 1.2-13* (Freeman, 1989).

Manufacturing errors can lead to significant changes in optical performance. For example, from *Equation 1.2-1*, it is possible to demonstrate that a focal length error is proportional to the diffractive zone diameter (DZD). For a BCL with a first-order diffractive focal power of 2.00 D a focal error of 0.125 D will occur if the DZD varies by -3.3% and +3.0%. If 0.125 D is considered the maximum acceptable error in focal power then this translates to a manufacturing tolerances for the first zone of -49 μm / +44 μm, and for the tenth zone of -162 μm / +148 μm.

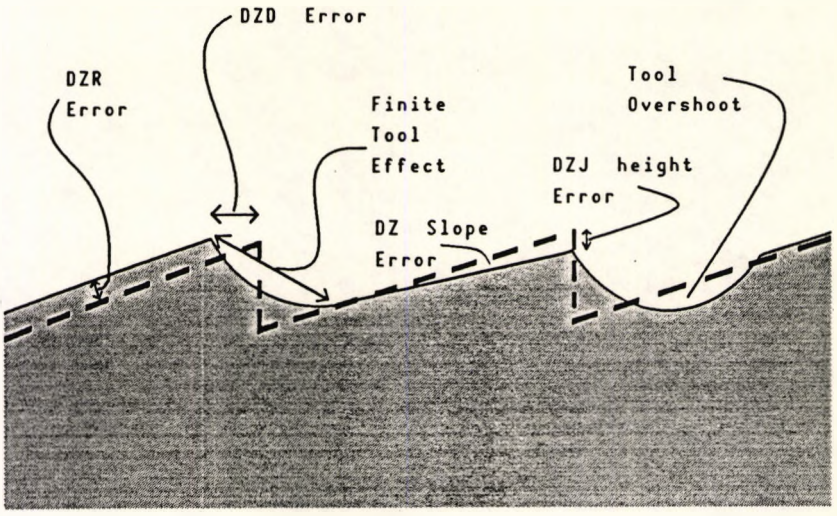

Figure 1.2-13 Potential errors in the manufacturing of diffractive BCL when using a lathe which controls radius and angle. These include a diffractive zone radius (DZR) error, DZ diameter (DZD) error, the finite tool effect, DZ slope error, DZJ height error, and tool overshoot and undershoot. These errors are not mutually exclusive (redrawn from Freeman, 1989).

The influence of these various manufacturing effects have not been reported previously.

Optical Performance

i) Theoretical investigations

Calculations indicate that the MTF of diffractive BCL, like that of concentric-design refractive BCL, shows a characteristic reduction to about forty percent of the single vision MTF (Freeman, 1986c; Freeman and Stone, 1987; Klein and Ho, 1986). The theoretical MTF of diffractive BCL was influenced slightly by pupil diameter giving a change principally in the low spatial frequency response (Edwards and Freeman, 1989). Generally, if an appropriate DZJ height was chosen, the MTF for both distance (zero order) and near (first order) foci were

equal for a particular wavelength (typically about 550 nm). Klein and Ho (1986) demonstrated the effect of DZJ height ("blaze coefficient") on the calculated MTF. As expected, when the effective DZJ height increased the calculated MTF improved at the first order focus and reduced at the zero order focus. The calculated MTF was wavelength dependent as expected (Edwards and Freeman, 1989). Calculation of the polychromatic MTF is very difficult and time consuming. Such calculations indicate that the polychromatic MTF was better than would be expected from consideration of monochromatic MTFs (Edwards and Freeman, 1989; Klein and Ho, 1986).

ii) Optical measurements

Only monochromatic MTF measurements have been reported due to the difficulties introduced by the LCA of the diffractive foci. As the human eye has LCA of about twice the magnitude and in the opposite sense, as previously noted, this is effectively negated in vivo. In addition the human eye was relatively insensitive to chromatic dispersion (Meslin and Obrecht, 1988). The measured MTF of diffractive BCL demonstrates the characteristic reduction suggested by theoretical considerations (Freeman reported in Phillips, 1988; Young et al, 1990). Young et al (1990) demonstrated the changes in optical performance with wavelength discussed earlier. They also noted a degree of pupil dependence of the two commercially available BCL measured, which as they note may be related to the number of diffractive

zones available over the aperture (Emerton et al, 1987) and may also be due to the manufacturing limitations discussed earlier. In addition, when the aperture exceeds the size of the diffractive grating the optical performance will become distance biased as the PRZ has distance power (with current BCL the zero order focus forms the distance focus).

In an assessment of image contrast measured with a CCD camera Lindsay (1990) noted a reduction in image contrast at both foci of two commercially available BCL. The ratio of distance to near image intensity varied significantly between BCL indicating manufacturing difficulties. The technique does not allow any conclusions about the source of the error.

Visual Performance

Clinical information on rigid (Churms et al, 1987; Phillips, 1988; Stone, 1988) and soft (Courtney et al, 1991a, 1991b; Molinari, 1988; Papas et al, 1988, 1989, 1990; Young and Papas, 1987) diffractive BCL suggest a visual compromise in keeping with theoretical considerations. Suggested areas of possible problems with diffractive BCL, including chromatic effects have not been reported as clinical problems. Problems with haloes around small bright light sources have been reported (Churms et al, 1987; Papas et al, 1990) and which it has been suggested may be due to manufacturing effects (Papas et al, 1990). A pupil size dependence of

a soft diffractive BCL has been noted, as patients with small (<3 mm) and large (>6 mm) pupils were found to be less likely to be successful (Courtney et al, 1991b).

Papas and co-workers (Young and Papas, 1987; Papas et al, 1988, 1989, 1990) have demonstrated reductions in VA, CSF, stereoacuity and glare response with a soft diffractive BCL. Low contrast VA was found to be the most sensitive to the effects upon vision. Similarly, Freeman and Mulen (reported in Phillips, 1988) demonstrated that the CSF was depressed over a wide spatial frequency range with a rigid diffractive BCL.

In the only report which has directly related optical performance to visual performance Freeman and Mulen (reported in Phillips, 1988), in a preliminary investigation, noted that the measured reduction in CSF was less than that predicted by measurement of the MTF of the same diffractive BCL. Freeman has proposed an "adaptation" effect to explain the difference. MTF measurement was monochromatic and as noted the polychromatic MTF may be substantially better. This approach may also be too simplistic as the direct prediction of CSF from MTF is not certain as the two optical systems (eye and BCL) are unlikely to be in phase (MTF contains no phase information) (Hopkins, 1988).

There have been no published reports of the effects of changes in diffractive BCL design such as DZJ height or shape upon visual performance.

1.3 Optical Performance Measurement

1.3.1 INTRODUCTION

Numerous methods have been devised to evaluate optical performance of an optical system. These include resolution tests, star tests, image contrast tests, the point spread function, Strehl intensity ratios, the line spread function, edge gradient functions, Foucault's knife edge test, the Schlieren test, shadow tests and interferometric tests. Different tests serve different purposes. It was decided for the optical testing of the BCL under investigation to employ a measure of the spatial frequency response.

The Optical Transfer Function (OTF) and the Modulation Transfer Function (MTF) are measures of the ability of an optical system to transmit optical information. An optical system could constitute a telescope, a camera lens, a contact lens (CL) or even the human eye. For example Campbell and Gubisch (1966) and Walsh and Charman (1985) measured the MTF of the human eye, and Grey and Sheridan (1988) measured the MTF of single vision CL. The MTF has intuitive appeal as it has similarities to

the psychophysical measures employed (Section 1.4) and was chosen to examine the optical performance of the experimental bifocal contact lenses (BCL). In addition, the Line Spread Function (LSF) (from which MTF was calculated) was used to qualitatively examine image formation with the different BCL.

A summary of the theoretical basis of the LSF, OTF and MTF is followed by a brief discussion of the use of the MTF to assess BCL.

1.3.2 THE LINE SPREAD FUNCTION

The LSF is a cross-section of the image of an infinitely narrow slit object, which is effectively a line of point spread functions (PSF). The LSF can be used to qualitatively evaluate changes in image shape and was particularly useful in evaluating the effect of decentration of bifocals upon image formation. Experimentally, the MTF was derived from a measurement of the LSF.

1.3.3 THE OPTICAL TRANSFER FUNCTION

Any optical system, due to aberrations, scattering and diffraction, will reduce the clarity of the image in comparison to the object. Fourier theory suggests that any object (or image) can be described in terms of its spatial frequency content. Assuming that an optical

system imaging incoherent light can be considered linear, the image of a sine wave (object) will have the same frequency, though the amplitude and phase may vary. Similarly, on the assumption of linearity, the transmission of each frequency is not dependent upon the transmission of any other frequency. The OTF gives the response of an optical system to a sinusoidally varying input. Experimentally, the OTF may be determined by measuring the change in contrast (modulation) and the phase shift in the image of a sinusoidal grating, or by calculation from the image of a slit (LSF). The MTF may be described as the ratio between the image contrast and the object contrast. The phase transfer function (PTF) is the variation in phase with frequency. The relationship between the three is described by :

$$(\mathrm{OTF}) = (\mathrm{MTF})\ e^{\,i(\mathrm{PTF})}$$

This allows the mathematical description of the image of any object given the OTF of the imaging system. OTFs are multiplicative, such that the final image formed by a series of optical systems can be found simply by multiplying the OTF of each optical system. The OTF is the Fourier transform of the intensity distribution of the LSF (e.g. Born and Wolf, 1980). As the MTF does not contain phase information MTFs generally are not multiplicative. A detailed discussion of the OTF may be found in Hopkins (1956, 1962) or Born and Wolf (1980).

It was not possible to record the OTF with the available equipment.

1.3.4 THE MODULATION TRANSFER FUNCTION

The MTF is probably the most common measure of optical performance currently in use. Typically the modulation (the ratio of the contrast of the image to the contrast of the original object) is plotted against spatial frequency. The development of techniques of MTF measurement has lead to its common use as a method of describing the quality of an optical system. With current equipment, the MTF of an optical system can be calculated from the LSF by consideration of diffraction theory and involves Gaussian quadrature, Chebyschev polynomials and Bessel functions. Typically an MTF measurement system comprises an illuminated slit which is imaged through the optical system under test. A detector (e.g. photodiode array) is located at the image plane and is oriented perpendicular to the slit image. The MTF can then be calculated from the intensity distribution of the image of the slit.

The Contrast Sensitivity Function (CSF) is a measure of the sensitivity of the visual system to sine wave gratings (section 1.4.2). Retinal image formation is a result of interaction between the OTF of the eye and the OTF of any optical device used. As the eye and BCL are incoherent systems (potential phase differences) and

since there are variable, idiosyncratic ocular aberrations leading to phase differences across the retina (Campbell et al, 1990; Walsh and Charman, 1989) the MTF of the retinal image due to a BCL cannot be theoretically predicted simply from a knowledge of the MTF of the BCL and the optics of the eye. Despite this, it might be expected that the measured CSF and other visual performance measures would reflect the MTF of BCL worn. The CSF is affected by the quality of the retinal image (e.g. Campbell and Green, 1965b) and may be considered in part a correlate of the MTF of the retinal image.

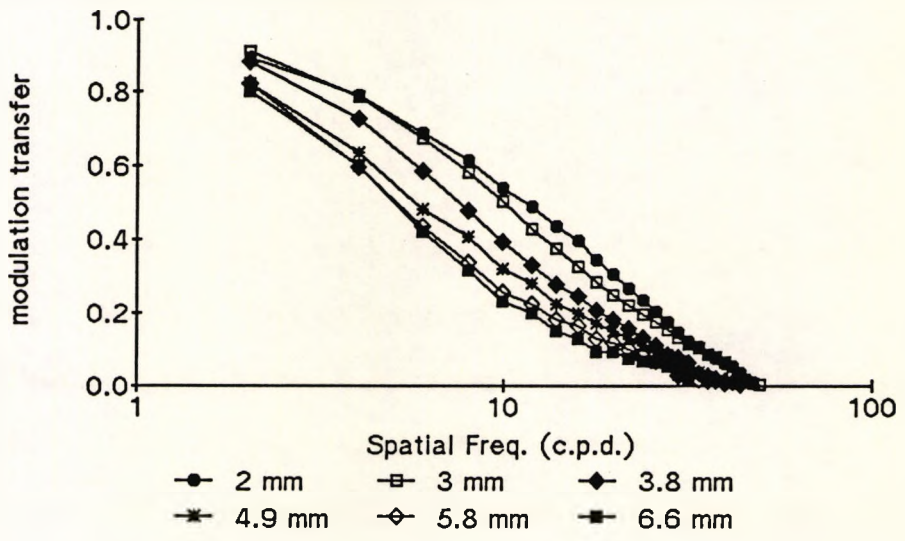

Figure 1.3-1 The measured MTF of the human eye reduces with increasing pupil size. (derived from Campbell and Gubisch, 1966 : figure 7).

A diffraction limited optical system in incoherent illumination has a cut-off frequency (f_c) given approximately by :

$$f_c = (2 \sin \theta) / \lambda \qquad \textit{Equation 1.3-1}$$

Where θ is the acceptance angle of the optical system and λ the wavelength of the incident light (Freeman, 1990). Thus for a diffraction limited system, as shown in *Figure 1.2-4*, as the aperture size increases, f_c increases and the MTF improves (Hopkins, 1956). Conversely, as shown in *Figure 1.3-1*, the MTF of the human eye decreased with increasing pupil size of greater than 2 mm (Campbell and Gubisch, 1966). This was due mainly to the chromatic aberration and (irregular) spherical aberration of the human eye (Freeman, 1990). Hence the significance of MTF results for BCL (particularly those which are more aperture dependent) measured on an optical bench must be treated with some caution as no modification has been made for the various ocular aberrations.

All reports of MTF measurement of diffractive BCL have been performed in monochromatic light due to the problems introduced by the inverse longitudinal chromatic aberration inherent in the diffractive foci. Hence there were further limitations to interpretation of these results.

1.3.5 BIFOCAL CONTACT LENSES

The theoretical MTF and actual measurements of the MTF for both concentric-design refractive BCL (section 1.2.2) and diffractive BCL (section 1.2.3) have been reported

previously. None of these investigations has been as extensive as the present study.

As there were two foci of interest it was important to control for the possible effects of changes in image size at the two foci (magnification is a function of the distances between the object, focussing lenses and the image plane and the acceptance angle of the optical system). This was avoided, as noted in section 3.2.3, by the use of a Badal optometer arrangement during the measurement of the MTF. It was unclear whether previous investigators had taken this precaution.

1.4 Visual Performance Measurement

1.4.1 INTRODUCTION

Visual Acuity (VA) for many years has been the main stay of vision assessment. VA assesses the recognition of small high contrast letters (high spatial frequency), and is thus a measure of the resolution limit of the visual system. It is now recognised that as the resolution of objects of other levels of contrast and spatial frequency is ignored, as a single measure, VA is too simplistic an assessment of visual performance and hence other techniques have been gaining acceptance. The visual performance measures used in this study are described

below. The actual experimental methods are given in sections 2.2, 2.3 and 3.3.

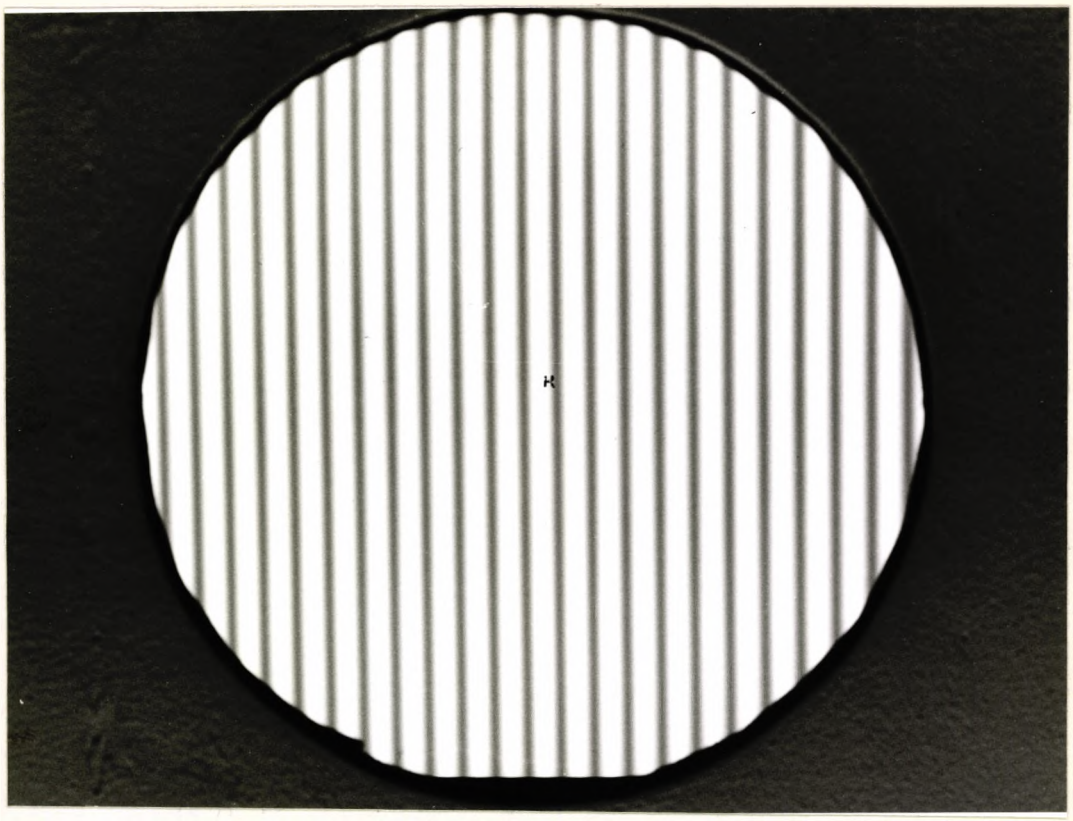

Figure 1.4-1 The contrast sensitivity monitor displaying a low spatial frequency sine wave grating at a high contrast level.

1.4.2 CONTRAST SENSITIVITY

The Contrast Sensitivity Function (CSF) is a measure of the visual threshold for a range of spatial frequencies, and is typically defined as the contrast required to see a grating pattern of varying bar width (spatial frequency) (*Figure 1.4-1*). Visibility of the grating pattern will vary with numerous aspects of the method of presentation including the size and shape of the display, the type of grating (e.g. square or sine wave) and its temporal properties. Traditional methods of CSF measurement with electronically generated grating

patterns have been typically time-consuming and involved sophisticated equipment. A monitor based system was developed for this study (sections 2.2 and 3.3.2).

CS may also be measured with various chart based tests, some of which are described below.

1.4.3 VISTECH CHARTS

Since the first alternative clinical test devised by Arden and Jacobson (1978) there have been a number of clinical chart-based tests of CS. Probably the most commercially successful has been the Vistech VCTS 6500 (Ginsburg, 1984), shown in *Figure 1.4-2*.

The Vistech VCTS 6500 contained five rows of nine discs each containing a sine-wave grating of a fixed average luminance on a higher luminance white background. The spatial frequency varied with each row, increasing from top to bottom. Subjects were required to view a single row and from left to right, and to indicate the orientation of the grating (75, 90 or 105 degrees) in each disc. The contrast reduced from left to right, and the contrast of the last disc correctly identified was recorded as threshold. Significant but low ($r = 0.22$ to $r = 0.48$) correlations with a traditional CRT-CSF procedure (similar to the method of ascending limits with continuous presentation (CAML) procedure described in Section 2.1.2) have been demonstrated (Ginsburg, 1984).

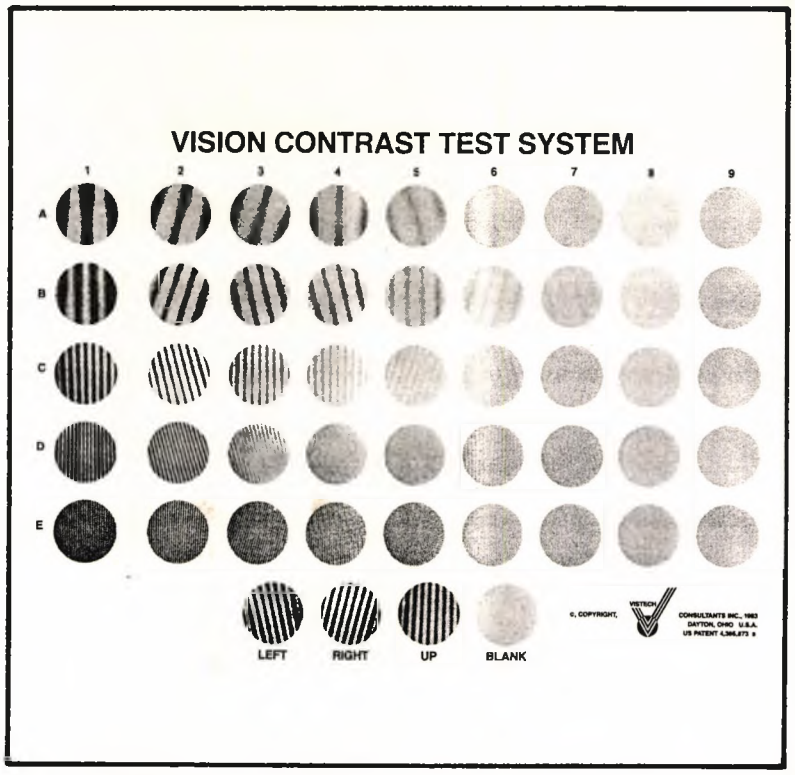

Figure 1.4-2 A Vistech VCTS 6500 chart used for the assessment of contrast sensitivity.

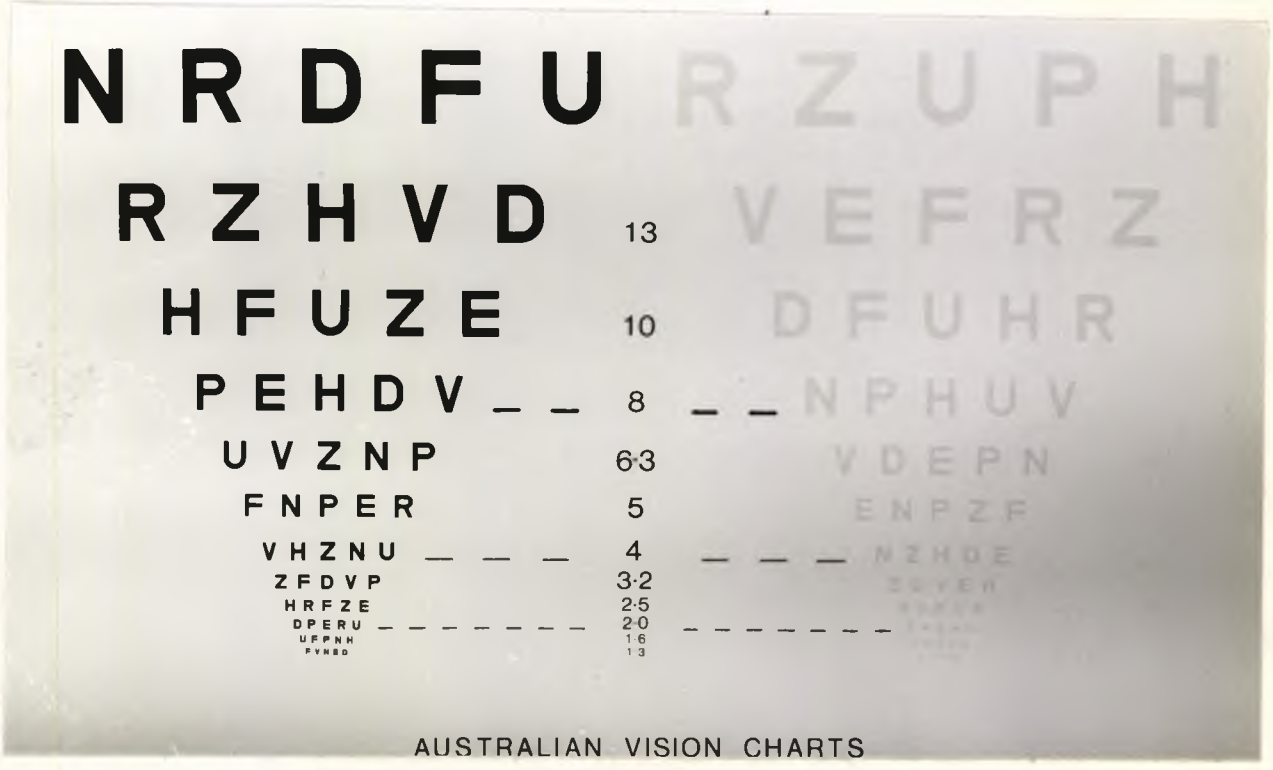

Figure 1.4-3 An Australian Vision Chart used for the assessment of visual acuity at high (90%) and low (10%) contrast.

The large and variable steps between successive discs have been shown to lead to bunched and skewed data (Reeves and Hill, 1987) making estimation of test-retest reliability difficult (Long and Tuck, 1988; Reeves and Hill, 1987). Reliability has been shown to be poor (Reeves et al, 1991; Rubin, 1988) and sensitivity low (Reeves and Hill, 1987). There has been no photometric or other evidence of quality control of the chart production, and the contrast within discs may not have been as stipulated. Though there were a number of problems with this test, many of which have been detailed by Reeves and co-workers, it remains probably the most commonly used chart based CSF measure in clinical practice.

1.4.4 LETTER CHARTS

Despite apparently having been first described by Berry in 1889 (Regan, 1988) only recently have letter recognition tasks with targets of varying contrast been suggested as alternatives to more conventional CSF measures. Some workers (Greeves, Cole and Jacobs, 1987, 1988; Verbaken, 1987a) have suggested that similar information to the CSF can be gained by varying the contrast of letter recognition tasks, which are more familiar to untrained subjects, and an edge detection task. Two different letter charts are described below.

Contrast of letter charts is defined according to the equation :

$$Contrast_L = (Luminance_{max} - Luminance_{min}) / Luminance_{max}$$

which may be converted to the contrast definition used for the monitor-based CS :

$$Contrast_{CS} = \frac{Luminance_{max} - Luminance_{min}}{Luminance_{max} + Luminance_{min}}$$

by the equation :

$$Contrast_{CS} = Contrast_L / (2 - Contrast_L).$$

1.4.5 AUSTRALIAN VISION CHARTS

The Australian Vision Chart (AVC) (Verbaken and Jacobs, 1985; Verbaken, 1987b), measured VA at two contrast levels (10% and 90%) with two different letter sequences as shown in *Figure 1.4-3*.

To overcome many of the shortcomings of the traditional Snellen chart the AVC was designed on the principles set out by Bailey and Lovie (1976). This design used ten letters of approximately equal legibility (BS: 4274, 1968), five to a line, spaced such that the separation between lines and between the individual letters on each line. This avoided the objection to conventional Snellen charts that the task varied at different levels (lines or distances). AVC used a logarithmic progression of letter sizes scored according to the logMAR system (logarithmic Minimum Angle of Resolution: based upon the bar width of the constituent letters) which showed a good

approximation to an equal discriminability scale (Westheimer, 1979).

The test-retest repeatability (95% confidence limit) with normal subjects of similar high contrast VA charts has been reported as between 0.07 and 0.19 logMAR units (Lovie-Kitchin, 1988; Elliott and Sheridan, 1988; Reeves et al, 1991) and as less than 0.10 logMAR units (Greeves et al, 1988) for similar low contrast VA charts. Elliott and Sheridan (1988) reported that subjects with cataract have been reported to have a high contrast VA test-retest repeatability of only slightly worse than normals tested at the same time (0.09 logMAR units), indicating that repeatability was high even under optical degradation.

Charts of varying contrast have been shown to be comparable to electronically generated CSF results (Greeves et al, 1987, 1988), predictive of CSF changes (Regan and Neima, 1983; Greeves et al, 1988) and could differentiate between refractive and diffusive blur (Ho and Bilton, 1986).

1.4.6 PELLI-ROBSON CONTRAST THRESHOLD CHARTS

The Pelli-Robson charts (PRC) (Pelli et al, 1988) were closer to the traditional CS task, the letters being kept at a constant angular size (spatial frequency) while the minimum detectable contrast was determined. PRC, as shown in *Figure 1.4-4*, consisted of eight lines of Snellen

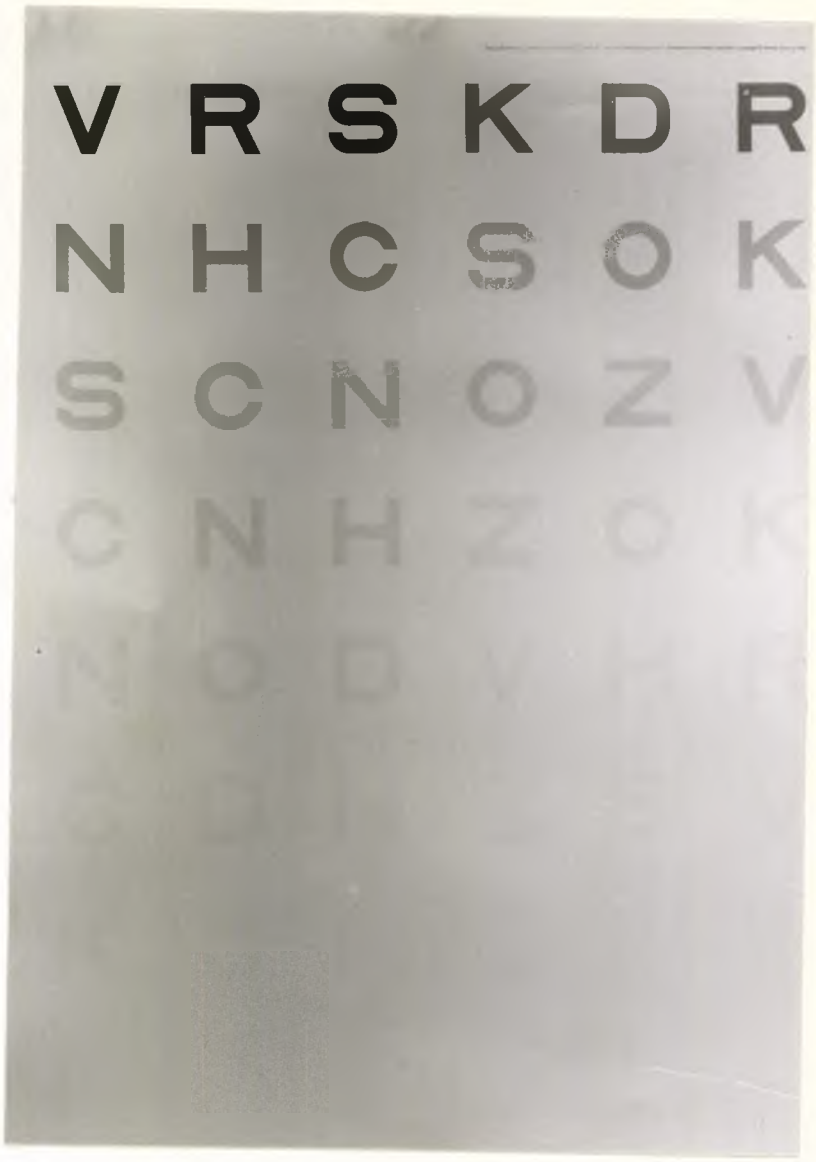

Figure 1.4-4 A Pelli-Robson contrast threshold chart.

optotypes, each line being composed of two groups of three letters. Letters in each group had the same contrast, and the contrast in successive groups reduced by 0.15 log units. At the standard viewing distance of one metre test-retest repeatability (95% confidence) for normals has been reported as less than 0.15 log units (Elliott et al, 1990a).

Pelli et al (1988) suggested that at one metre the letters were equivalent to CSF of between one and two c.p.d., though this has not been confirmed. On the assumption that the angular subtense of the component bars, and hence letter size, related to the principal spatial frequency component, an assessment of visual performance at specified spatial frequencies could be made by varying the angular subtense through variations in viewing distance. There were of course restrictions to this assumption based upon : i) the square wave form of snellen optotypes and consequent higher order spatial frequency content; ii) the complex mixture of the elements composing the letters which introduced a broad range of spatial frequencies; and iii) the letters represented a task which was more complex than the detection of a sine wave in traditional CSF (Bouma, 1971). With these restrictions, PRC contrast detection may be analysed according to the fundamental spatial frequency of the component letters. The average bar width of letters on the Pelli-Robson chart is 9.8 mm (0.56^{o} at 1 m). The fundamental spatial frequency when

viewed from distances of two and four metres was 1.8 and 3.6 c.p.d. respectively.

According to Fourier analysis, a square wave can be analysed as a series of sine waves of increasing frequency and decreasing amplitude. Only the odd harmonics are present. After the first (fundamental), the largest harmonic is the third with an relative amplitude (contrast) of 0.42 ($4/3\pi$) that of the square wave (letter). When the PRC letters were viewed at two and four metres there was a spatial frequency component at 5.3 (1.8 x 3) and 10.7 (3.6 x 3) c.p.d. respectively with a contrast reduced to 0.42 the original. The peak CS of normal observers is typically 3 to 5 c.p.d.. A third harmonic at about 5 c.p.d. may approach the threshold of normal observers but a third harmonic of approximately 11 c.p.d. would be well below the threshold. The amplitude of other harmonics above the peak (3 to 5 c.p.d.) were too small be of interest at these viewing distances at the appropriate spatial frequencies.

Hence at a viewing distance of two metres a spatial frequency component other than the fundamental may have been detected. These other components were consistent for all test conditions and hence would not affect the actual results and the analysis of differences between BCL.

1.4.7 MELBOURNE EDGE TEST

The Melbourne Edge Test (MET) (Verbaken and Johnston, 1986) was a hand held test which consisted of a series of 25 mm discs containing an contrast step of varying orientation on a grey luminance matched background. Each successive disc had a logarithmically reduced contrast to test edge detection (*Figure 1.4-5*).

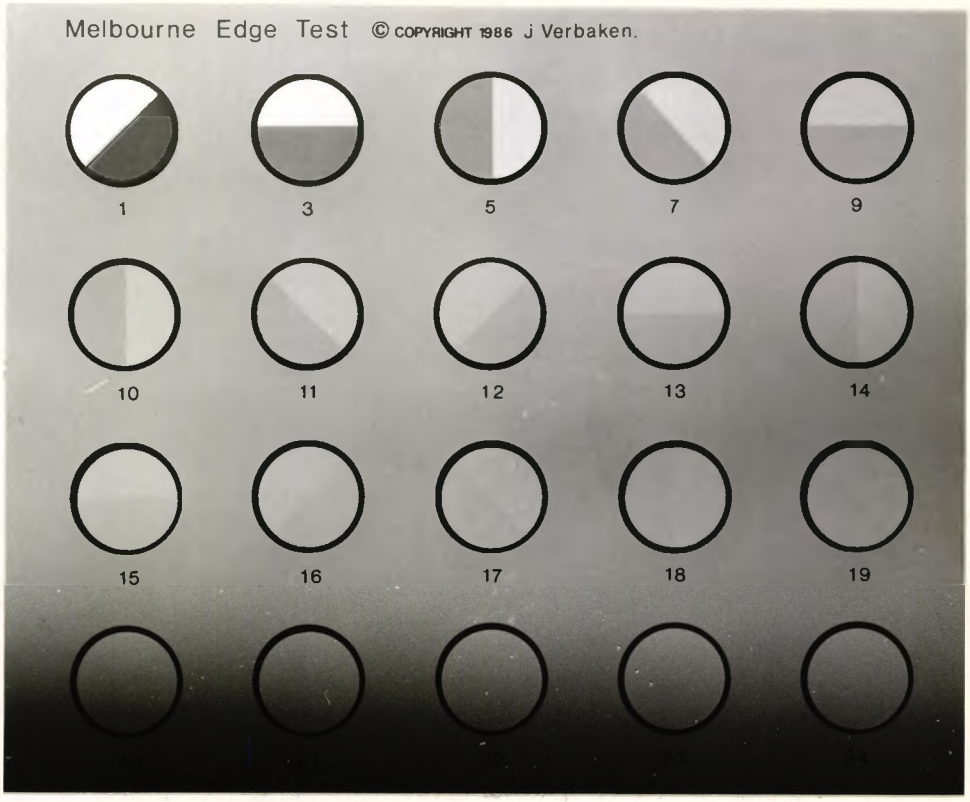

Figure 1.4-4 A Melbourne Edge Test used to assess edge detection, which has been shown to relate to peak contrast sensitivity.

Edge detection has been demonstrated to correlate with the peak spatial CS and to CS at 1 c.p.d. (Cunningham et al, 1980; Greeves et al, 1987), but not to high contrast VA (Greeves et al, 1987). According to Fourier analysis, at an edge all spatial frequencies are present and it has been argued that edge detection would be mediated by the

spatial frequency channel with the lowest threshold. As all spatial frequencies were present, and low spatial frequencies are resistant to optical defocus (Campbell and Green, 1965) the MET was insensitive to reasonable variations in viewing distance (Verbaken and Johnston, 1986). Test-retest repeatability (Standard Error) has been reported as less than 0.075 log units (Greeves et al, 1987).

1.4.8 VISUAL PERFORMANCE WITH REDUCED LUMINANCE

VA and CS have been shown to decrease with reduced luminance (Campbell and Gregory, 1960; Campbell and Robson, 1968). Guillon, Lydon and Solman (1988), on the basis of empirical findings, have suggested that testing at more than one luminance level may demonstrate differences in visual performance which were not evident at traditional high luminance levels. Statistically, this would be indicated by an interaction between luminance and another factor under investigation.

1.4.9 DISTANCE AND NEAR VISION TESTING

The conventional technique for testing near vision has been to have the subject hold a reduced size VA chart in the normal reading position. While this would appear to be the obvious way to test near vision there have been some problems associated with this approach. The major problem has been the difficulty ensuring that the

distance was constant for all subjects, as the normal reading position varied from subject to subject. Varying the distance to the near chart varied the difficulty of the task. This has been overcome by either carefully measuring the distance and converting for the actual distance or by using some means to ensure that the required distance was always used. Another problem has been that conventional near vision charts, commonly contain blocks of text rather than rows of letters, and hence not comparable to the distance vision tests used. Reduced versions of some distance charts have been produced to allow direct comparison of distance and near visual performance, but it has been difficult to ensure good reproduction of charts of the small size required (Verbaken and Jacobs, 1985). In addition it has been very difficult to recreate the same lighting conditions on distance charts at for example 6 m and near charts at 40 cm. Changes in the illuminance could have altered both the visibility of the task and the actual contrast levels of the chart.

As the main interest in this study was the visual performance it was decided to test both distance and near sections of the BCL with the same tests from the same distances, but with an appropriate optical correction. Hence distance vision was considered to be optical infinity and near vision was then measured with an additional (spectacle) lens(es) of appropriate power. For example for a BCL with an add of +2.00 D an

additional lens of power -2.00 D was used to bring the chart into focus with the near section of the BCL. Hence the vergence of the test was varied rather than the test distance. Binocular viewing was a problem with this technique as the convergent stimulus of the object may not match the vergence stimulus, possibly causing diplopia. Hence all investigations were monocular. Another potential problem was the magnification introduced by the additional lenses in a trial frame (vertex distance 12 to 14 mm) however the effects were small. Calculations indicated that the powers involved (<6.00 D) did not introduce magnification sufficient to invalidate the conclusions. Another potential argument against this technique derived from failing to use the subjects preferred distance. As this was not a study investigating wearing patterns or success, and the principal interest was the relative effects upon distance and near visual performance introduced by changes in BCL design this was not a major objection.

The pupil normally reduces in size with near viewing. Convergence related alteration in pupil size did not occur with the experimental design used here and was a disadvantage of this technique. Changes in pupil size alter the proportion of the pupil covered by the COZ and POZ of a concentric-design BCL. This may lead to changes in visual performance and in particular the balance between distance and near. With a knowledge of BCL location and pupil size it was possible to take into

account these variations and to make corrections according to an assumed variation with convergence. Convergence related pupil size variation was assumed to be proportional to the unconverged pupil size (Schafer and Weale, 1970). As changes in pupil size have only a limited effect upon the MTF of diffractive BCL (Young et al, 1990) this was not considered a problem for experiments which involved diffractive BCL. No previous investigation has used this technique, and hence comparisons between distance and near vision have been subject to various restrictions.

1.5 Aims and Experimental Design

1.5.1 INTRODUCTION

A brief outline of the aims of this study and the experimental design follows. The techniques adopted for measurement of BCL parameters, optical performance and visual performance are detailed briefly in sections 1.5.2 to 1.5.4. Sections 1.5.5 and 1.5.6 discuss the rationale and details of the evaluation of the two BCL types - refractive and diffractive - examined in this study.

As noted in section 1.2, descriptions in the literature of the effects of changes in BCL design have been limited. In particular, the visual and the optical performance of the same BCL has not previously been

reported. To address this area, the effect of various changes in BCL design, influencing the optical parameters, of both concentric-design refractive BCL and diffractive BCL upon optical and visual performance were investigated. The optimal BCL design, which was defined as the design which provided equal performance at distance and near, was examined with empirically derived quadratic equations. It was presumed that equal performance at distance and near was the best compromise in BCL design. Prediction of visual performance from optical performance was also investigated. Aspects of the surface of the diffractive BCL were measured and the influence of variations in physical parameters upon optical and visual performance was also investigated.

1.5.2 PHYSICAL CONTACT LENS MEASUREMENTS

All experimental BCL were examined with a range of conventional CL measures (section 3.1.1). In addition the central optic zone diameter (COZD) of refractive BCL and the diffractive zone diameters (DZD) of diffractive BCL were measured. The surface profile of the diffractive BCL including the height and shape of the diffractive zone junctions (DZJ), and the surface quality was assessed with an interferometric technique (section 3.1.2). The influence of the physical measurements upon the optical and visual performance of the BCL were examined (section 4.5). The repeatability of all techniques was examined as described in section 3.7.

1.5.3 OPTICAL PERFORMANCE MEASUREMENTS

As described in sections 1.3 and 3.2, the Modulation Transfer Function was used to examine the optical performance of the experimental BCL, and the Line Spread Function was used to qualitatively evaluate the effect of decentration upon image formation. There have been no previous reports which have examined, simultaneously, as many aspects of refractive BCL design. There have been no previous reports of the effect of changes in design of diffractive BCL upon optical performance.

1.5.4 VISUAL PERFORMANCE MEASUREMENTS

After an investigation to establish an optimal contrast sensitivity (CS) measure (section 2.2), the sensitivity of the visual performance measures discussed in section 1.4 to certain BCL design changes was assessed under two luminance conditions (section 2.3). Following these preliminary evaluations a reduced protocol for the evaluation of visual performance which included the monitor-based CS test, high and low contrast VA and Pelli-Robson charts (PRC) was devised (section 3.3). In addition, the on-eye longitudinal chromatic aberration of a small number of diffractive BCL was examined with a simple psychometric technique (section 3.4).

Visual performance was investigated with a large range of BCL worn by a small group of experienced subjects as opposed to previous studies which have generally used a limited range of BCL on a larger number of subjects. This protocol was expected to more clearly demonstrate the effects of the changes in optical parameters of the experimental BCL upon visual performance.

The limitations of previous reports with refractive BCL have been detailed in section 1.2.2. There have been no reports in the literature of the effect of changes in design of diffractive BCL upon visual performance.

1.5.5 PREDICTION OF VISUAL PERFORMANCE FROM OPTICAL PERFORMANCE MEASURES

The assessment of visual performance is almost invariably time consuming, typically involving a number of both subjects and examiners. During the development of experimental BCL the assessment of the effect of changes in BCL design upon vision is of paramount importance. It would be desirable to be able to reduce or eliminate the requirement for visual testing during the development stage of new BCL designs. It was hoped that by the examination of both the visual and the optical performance of the same BCL it would be possible to predict visual results from optical performance, in which case the lengthy process of visual testing could be reduced. This would, of course, not remove the need to

finally test a new BCL upon experimental subjects, but may reduce the requirement for testing with intermediate or developmental BCL.

There have been no similar reports in the literature.

1.5.6 RATIONALE AND PROCEDURES FOR INVESTIGATION OF REFRACTIVE BIFOCAL CONTACT LENSES

Previous studies have failed to fully demonstrate the expected trends with concentric-design refractive BCL (section 1.2.2). This may have been due to poor control of measurement variance (i.e. few if any repetitions) and testing limited to high contrast VA charts (Erickson and Robboy, 1985; Jones and Lowther, 1989). The only study of refractive BCL to have used more sophisticated visual performance measures was with cyclopleged young subjects (Cox, 1985, 1986).

It was the intention of this study to compare the effects of lens design (centre-distance or centre-near) and COZD upon visual and optical performance. Details of all concentric-design BCL used in this study are given in section 3.6.1. It was expected that optical and visual performance would be dependent upon these BCL design parameters, but would also be influenced by pupil (aperture) size, CL movement and the location of the BCL in relation to the pupil.

For any pupil size and BCL location it was expected that there would be an optimal COZD for a concentric-design BCL which would give equal optical or visual performance between distance and near.

To assess the effect of BCL location upon optical performance measurements were made with varying degrees of decentration of the COZ over the aperture. The actual location of the BCL when worn by the subjects was recorded and the effect upon visual performance investigated. The effect of BCL movement was not investigated in this study.

As noted in section 1.3.4, optical and visual performance vary differently with aperture size, and thus the information from optical measurements may have slightly limited application to visual performance. Despite this objection the effect of variations in aperture size upon optical performance with the range of COZD was investigated.

Optical performance (with the BCL centred over the aperture) was examined with a fully crossed design. The effect of lens location upon optical performance was examined with a reduced cell, incompletely crossed design. The visual performance of five subjects was examined with a fully crossed design.

1.5.6 RATIONALE AND PROCEDURES FOR INVESTIGATION OF DIFFRACTIVE BIFOCAL CONTACT LENSES

As discussed in section 1.2.3, theoretical predictions suggested that the optical performance of diffractive BCL would vary with certain aspects of BCL design. In particular the ratio of light in the two bifocal foci was expected to vary with DZJ height (*Equation 1.2-4*), making a diffractive BCL more or less near-focus biased. The effects upon both optical and visual performance of BCL of different DZJ heights were investigated.

Variations in the DZJ shape, achieved with the use of different diamond lathe tool shapes and diameters, were investigated. Tools with a flatted portion and tools with a smaller diameter (section 3.1) were expected to produce diffractive surfaces which more closely approximated the theoretically correct shape (section 1.2.3). It was presumed that this would alter the ratio between distance and near and possibly improve optical performance, by reducing the amount of light lost from the diffractive foci due to the manufacturing limitations at the DZJ. It was expected that the expected improvement in performance may have been reduced by the increased wear and tear upon flatted diamond tools and upon those with a smaller radius. To investigate the effect of tool quality the shape of the zone junctions and surface quality was examined with interference microscopy (section 3.1).

Details of all diffractive BCL used in this study are given in sections 3.6.2 and 3.6.3.

The influence of these factors upon both optical and visual performance with rigid diffractive BCL, were examined. Multiple Regression Analysis (MRA) was used to predict the optimal DZJ height (equal performance at distance and near) with the different tool shapes. Manufacturing reproducibility was assessed by examining results with BCL with nominally identical parameters.

The range of soft diffractive BCL available, whilst numbering 16, was quite diverse and unfortunately did not lend itself to a well controlled study such as was performed with the rigid BCL. Comparisons of like BCL were made where appropriate. The influence of soft diffractive BCL manufacturing technique (lathe turning versus cast moulding) was examined. A "reverse" add BCL (section 1.2.3) was compared to conventional BCL. The soft BCL were subject to some manufacturing problems and the conclusions that can be drawn from this section may be limited.

Chapter 2 PRELIMINARY EXPERIMENTS ON VISUAL PERFORMANCE

2.1 Introduction

Preliminary experiments were performed to evaluate methods of visual performance assessment. In section 2.2 two experiments examined six methods of monitor-based contrast sensitivity (CS) measurement, from which one method was selected for use in further studies. In section 2.3 the sensitivity, of the chosen CS procedure and various chart-based tests of visual performance, to certain changes in diffractive BCL design was assessed. From these preliminary studies a protocol was devised for use in the main study (section 2.4).

2.2 A Preliminary Evaluation of Methods of Monitor-based Contrast Sensitivity Presentation

2.2.1 CONTRAST SENSITIVITY METHODS: EXPERIMENT 1

A brief summary of this experiment is given here and a full report, which has been submitted for publication, is included as *Appendix 3*.

Contrast Sensitivity Functions (CSF) were determined for ten (10) trained and experienced observers with five

psychometric methods. The psychometric methods investigated ranged from a decision criteria free, but lengthy Method of Constant Stimuli (MOCS) two alternative forced choice procedure through the other procedures which were quicker in application but were subject to increasing levels of observer bias.

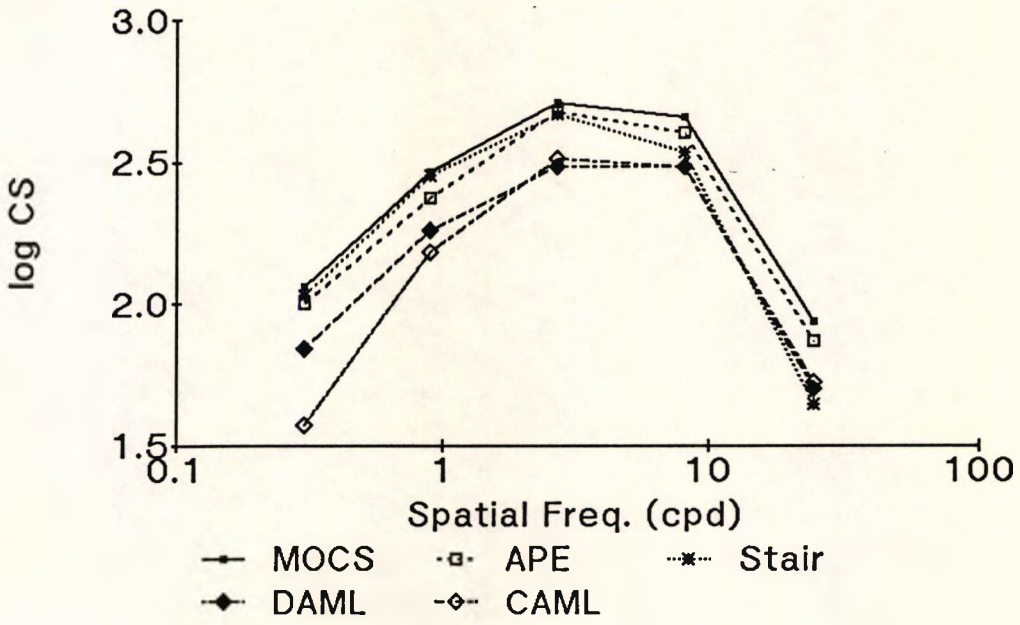

Figure 2.2-1 Mean Contrast Sensitivity (CS) with five different methods of presentation - the Method of Constant Stimuli (MOCS), Adaptive Probit Estimation (APE), single staircase, Discrete Ascending Method of Limits (DAML), and Continuous Ascending Method of Limits (CAML) procedures.

Differences between the five methods were small but characteristic (*Figure 2.2-1*). Whilst all of the procedures were considered to have good test-retest repeatability (small test-retest repeatability coefficient: 2 x standard deviation) , there was an obvious trade off between repeatability and the duration of the procedure (*Figure 2.2-2*), and hence none of the techniques was ideal.

In an attempt to improve this trade off a further method was investigated as reported below.

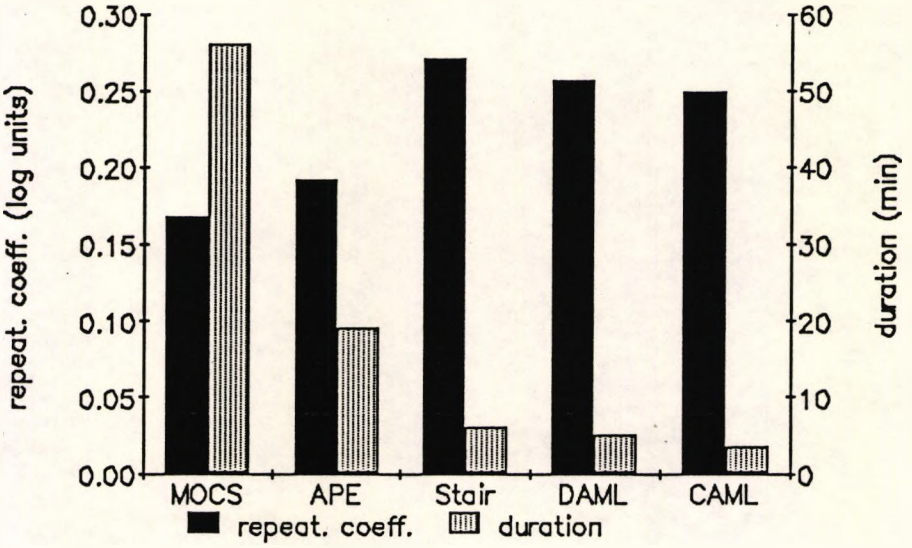

Figure 2.2-2 The repeatability coefficient (1.96 x standard deviation) and duration of five different methods of Contrast Sensitivity presentation - the Method of Constant Stimuli (MOCS), Adaptive Probit Estimation (APE), single staircase, Discrete Ascending Method of Limits (DAML), and Continuous Ascending Method of Limits (CAML) procedures.

2.2.2 CONTRAST SENSITIVITY METHODS: EXPERIMENT 2

Introduction

To evaluate a technique suitable for the major study (relatively short duration, without reducing test-retest repeatability), a reduced version of the Adaptive Probit Estimation (APE) method was devised and tested on the same ten observers used in experiment 1 (section 2.2.1).

Methods

Subjects

Ten colleagues, aged between 22 and 60 years (average 35 years), acted as subjects for the study. The procedure controlling presentation was fully explained to each subject, and each subject attended at least one practice session so that they were completely familiar with the method. Subjects had no known visual dysfunction.

Apparatus

A monitor-based apparatus to measure contrast sensitivity (CS) as described in section 3.3.2 was used. Subjects viewed binocularly with an appropriate optical correction. The total duration of each trial, from the first to the last presentation, was recorded by the computer. Subjects were allowed to rest at any time during the course of the experiment, but this was added to the recorded duration of the trial.

Adaptive Probit Estimation (APE)

APE is a technique designed to estimate the psychometric function with maximum statistical efficiency, based upon the method of constant stimuli (Watt and Andrews, 1981). APE analysed the current response set and accordingly presented stimuli from a predetermined set of stimulus levels for a predetermined total number of presentations.

Each test grating was presented after an appropriate audible cue, and the subject was required to indicate

whether the grating was seen or not seen. The APE program then determined the next stimulus level to be tested, by randomly selecting from a set of levels which bracket the current estimate of the threshold, which was determined by a regular, rapid approximate probit analysis (Finney, 1952) of the data for the most recent set of responses. On completion of the trial a full probit analysis was performed to provide an estimate of the contrast threshold and standard deviation.

Five spatial frequencies of 0.3, 0.9, 2.7, 8.1, and 24.3 c.p.d. were presented in each trial. At the beginning of the trial an appropriate range of contrasts was chosen by presenting gratings of widely differing contrast until a usable range for each spatial frequency was bracketed with ten available contrast levels within the range. At each spatial frequency 16 presentations were made giving a total of 80 presentations. Spatial frequencies were randomly interleaved.

Unfortunately randomly-interleaved spatial frequency presentation has been shown to lead to spatial frequency uncertainty (Cohn and Lasley, 1974; Davis and Graham, 1981) where sensitivity and repeatability were reduced because the subject was not aware of the spatial form of the stimulus. This was probably due to an increased complexity of the task where recognition was required in addition to the normal detection task. The tone which indicated the commencement of the next trial was also

used to indicate the spatial frequency of the next presentation. This was achieved by matching the pitch of the tone to spatial frequency (i.e. low pitch- low spatial frequency, high pitch - high spatial frequency). Pilot studies indicated that this simple procedure enhanced both sensitivity and repeatability.

Results

Mean contrast sensitivity is shown in *Figure 2.2-3* in relation to the earlier results (section 2.2.1). Mean contrast sensitivity with the shortened APE was significantly less ($p < 0.05$) at all spatial frequencies than the MOCS procedure previously reported and did not vary significantly ($p < 0.01$) from the results with the longer APE procedure used previously. Contrast sensitivity was higher at the higher spatial frequencies (8.1, 24.3 c.p.d.) than with the single staircase procedure reported previously ($p < 0.001$). For all spatial frequencies combined, test-retest correlation (Spearman r) was 0.97, the repeatability coefficient 0.182 log units and the duration of testing was 6.26 (± 0.25) minutes. Repeatability coefficients at the five spatial frequencies were 0.19, 0.20, 0.23, 0.08, 0.12 log units for 0.3, 0.9, 2.7, 8.1, and 24.3 c.p.d. respectively.

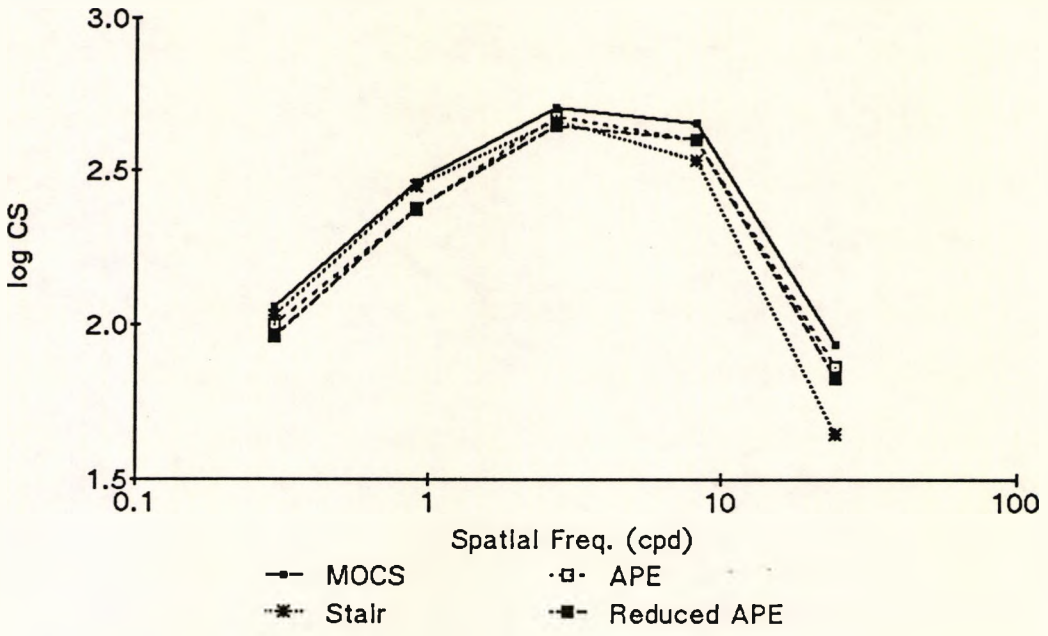

Figure 2.2-3 Mean contrast sensitivity with the reduced APE procedure compared to previous results with MOCS, a longer APE procedure and a similar single staircase procedure.

Discussion

Test-retest correlation and repeatability coefficient with the shortened APE procedure were similar to the full APE procedure previously examined (section 2.2.1). The duration was similar to the single staircase procedure, and much shorter than with MOCS or the full APE procedure.

The randomly interleaved presentation was superficially the same as for the staircase method, but with the actual presentations and stimulus levels controlled by the APE algorithm. Results with the reduced APE did not display the marked, consistent reduction in sensitivity at the high spatial frequencies compared to MOCS found with the single staircase procedure. This may be due to the

theoretical strengths of the APE procedure. It is proposed that observer awareness of the ordered nature of presentation, combined with an altered decision criteria for the higher spatial frequency, has given this result. It is unclear why the decision criteria should alter with spatial frequency. Possibly greater ambiguity was experienced with the higher spatial frequencies. Cornsweet (1962) discussed the theoretical introduction of this type of subject bias which can be avoided with more complex forms of the staircase method. Thus the reduced APE method appears to avoid the problems of the single staircase whilst retaining a good test-retest repeatability and a similar, relatively short duration.

2.2.3 CONCLUSIONS

Test-retest repeatability is a measure of the stability of a particular procedure over time. Care was taken in this study to enhance the repeatability of the psychometric procedure, as demonstrated by the good test-retest repeatability. The modified version of the APE procedure (Experiment 2) was preferred over the other psychometric methods (Experiment 1) due to the theoretical strengths of the underlying procedure, comparable repeatability and reasonable duration. Hence the reduced APE procedure was adopted for the remainder of the study.

2.3 Preliminary Evaluation of the Sensitivity of Clinical Visual Performance Measures

Introduction

A preliminary investigation of the effect of changes in diffractive lens design (diffractive zone junction (DZJ) height) upon visual performance was used to assess the sensitivity of certain clinical vision tests. Also the suggested ability of a reduced luminance condition to increase the sensitivity of any of the vision tests was investigated. This allowed the use of a reduced protocol in the main study.

Variation of the DZJ height (theoretically) alters the ratio of light in the zero and first order foci and hence the ratio between distance and near vision (section 1.2.3).

Methods

Visual performance was evaluated with :

(a) monitor-based measure of CSF (CRT-CSF);

(b) the Vistech VCTS 6500 test charts;

(c) Australian Vision Charts (AVC);

(d) Pelli-Robson contrast threshold charts (PRC); and

(e) an edge detection task, the Melbourne Edge Test (MET).

Visual performance was measured with all tests at two luminance levels. These procedures and tests are discussed in more detail below. As discussed in section

1.4.3 distance and near viewing was achieved by the use of a spectacle correction for the appropriate viewing distance and vergence required. The actual viewing distances and chart luminances are given in *Table 2.3-1*.

Test	Luminance Level (cd/m^2)	Distance (m)	Spatial Frequency (c.p.d.)	Contrast
CRT-CSF	50	1	0.5,1,2,4,8,16	0.25 to 0.001
	0.5	1	0.5,1,2,4,8,16	0.25 to 0.001
Vistech	250	4	2,4,8,16,24	0.25 to 0.005
	2.5	2	1,2,4,8,12	0.25 to 0.005
			approx.	
AVC	250	4	7.5 to 120	0.9, 0.1
	2.5	2	3.75 to 60	0.9, 0.1
			approx.	
PRC	250	2, 4	1.8, 3.6	0.9 to 0.008
	2.5	2, 4	1.8, 3.6	0.9 to 0.008
MET	40	0.4	edge	0.1 to 0.004
	0.4	0.4	edge	0.1 to 0.004

Table 2.3-1 A summary of the luminance levels, test distances, spatial frequencies and contrast levels for the various tests used.

Monitor-based (CRT) Contrast Sensitivity Function

The electronically presented CRT-CSF procedure and equipment was as described in section 3.1.2, except that the reduced Adaptive Probit Estimation (APE) procedure

displayed 6 spatial frequencies of 0.5, 1, 2, 4, 8, and 16 c.p.d.. To determine the CRT-CSF a total of approximately 120 presentations (6 x 20) were made. CRT-CSF at 16 c.p.d. was not included in the final analysis as too few results could be obtained at the low luminance level (0.5 cd/m^2).

Vistech Charts

Vistech VCTS 6500 charts (section 1.4.3) were used at a viewing distance of four metres for the high luminance condition (250 cd/m^2) giving spatial frequencies of 2, 4, 8, 16, and 24 c.p.d.. Due to the reduced visual performance under the low luminance condition (2.5 cd/m^2) a viewing distance of two metres was adopted giving spatial frequencies of 1, 2, 4, 8, and 12 c.p.d.. The size of the Vistech target discs altered with viewing distance which may affect visual performance (Howell and Hess, 1978). Any comparison between the high and low luminance conditions was unfortunately compounded by this effect. Often even the disc with the highest contrast could not be seen at the higher spatial frequency, unfortunately lead to a "ceiling effect" at each luminance level. For this reason only results for 2, 4 and 8 c.p.d. were included in the analysis.

Australian Vision Charts

AVC (section 1.4.5) were used at a viewing distance of four metres for the high luminance condition (250 cd/m^2) and at two metres for the low luminance condition (2.5

cd/m^2) . The viewing distance of the AVC was reduced by half if the second-largest row of letters were not visible. Given appropriate optical correction this will have no effect upon the score of VA charts of this design (Westheimer, 1979).

Pelli-Robson Contrast Threshold Charts

PRC (section 1.4.6) contrast thresholds were determined at both two and four metres for both luminance conditions (250 and 2.5 cd/m^2) .

Melbourne Edge Test

MET (section 1.4.7) contrast thresholds for both luminance conditions (40 and 0.4 cd/m^2) were determined at a viewing distance of approximately forty centimetres in accordance with the manufacturer's instructions.

Viewing Distances

As noted in section 1.4.9, an appropriate optical correction to place the test at optical infinity for the assessment of distance vision was worn for each viewing distance. An additional negative lens was worn for near vision assessment to negate the BCL addition (i.e. to place the target optically at the near viewing distance).

Luminance and Illumination Conditions

The CRT-CSF had a mean luminance of 50 cd/m^2. The Vistech, AVC and PRC were all mounted on a matt white board with an average luminance of 250 cd/m^2, and with

less than 10% variance in illuminance across the charts. The MET was illuminated by general room lighting supplemented by an angle-poise lamp to provide an average illuminance of 250 lux and a background luminance of 40 cd/m^2.

The reduced luminance condition was obtained with goggles with the original lenses replaced by neutral density filters of 2.0. This effectively reduced luminance by a factor of 100. The low luminance condition was always tested after a suitable period of adaptation. High and low luminance sessions were randomly interspersed. This is summarised in *Table 2.3-1*.

Experimental Design

Tests were presented in a pseudo-random order. BCL were used in a random order. All results were recorded and scored by a computer program according to the APE procedure (CRT-CSF), the manufacturers' instructions (Vistech, PRC, MET), or Bailey and Lovie (1976) for the AVC. To reduce memory effects, all chart tests were available in at least two versions, each with a different sequence. Two versions of each chart test were presented for each condition and the results averaged.

Subject

As this was essentially a pilot study to determine which visual tests to use in the main study the right eye of a single young subject (the author) was used. Cycloplegia

was induced with 0.5% cyclopentolate to simulate the reduced accommodative range of presbyopes. The accommodative range was assessed regularly, and testing discontinued if the accommodative range exceeded 1 dioptre. An ocular anaesthetic was also used where necessary to reduce the effects of excessive lacrimation. The best refractive correction for the relevant distance and BCL was worn in a trial frame with an artificial pupil of 3.5 mm for all experiments. This diameter pupil was chosen as it represents an average pupil diameter for presbyopes (Woods, 1991c).

Experimental Bifocal Contact Lenses

Preform rigid diffractive BCL were lathed in Polycon II material with a 250 μm diamond tool by Pilkington VisionCare. Tricurve rigid BCL were produced from the preforms at the Department of Optometry and Visual Science, City University. The nominal DZJ heights were 3.0, 2.6, 2.2, 2.0, 1.8 and 1.4 μm (details in section 3.6.2).

Results

CS results with both the CRT-CSF and the Vistech charts were of the conventional form. Results for all visual performance measures with BCL were reduced compared with single vision CL (*Figure 2.3-1*), in line with previous reports (Phillips, 1988; Papas et al, 1988, Saunders and Charman, 1989).

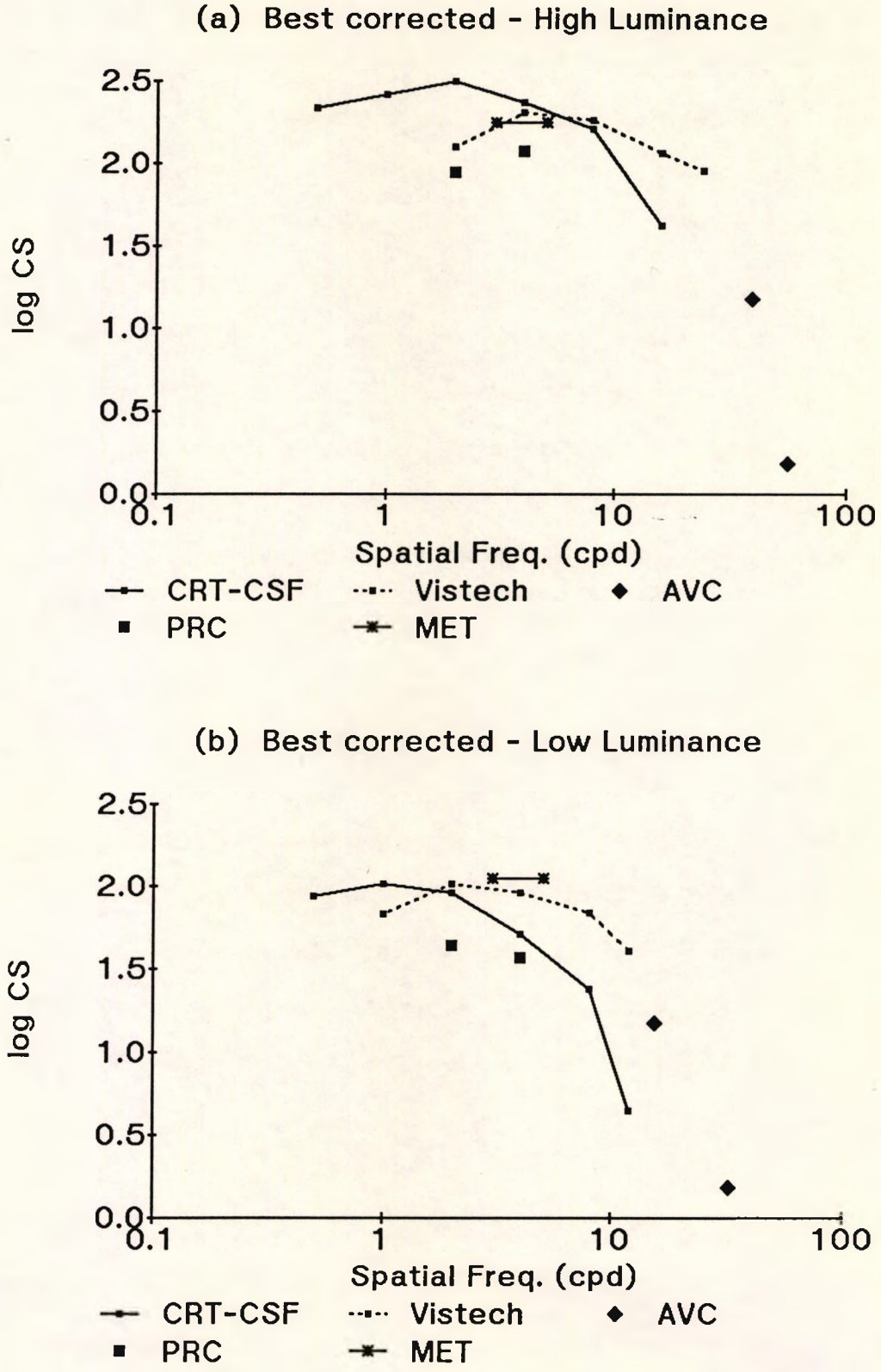

Figure 2.3-1 Mean visual performance with a single vision CL at (a) high and (b) low luminance. CRT-CSF (solid curve), Vistech (dotted), AVC (diamonds), PRC (squares) and MET (solid horizontal bar) results are shown.

As an example, the mean results for a BCL with a DZJ height of 2.2 μm are shown in *Figures 2.3-2* and *2.3-3*. To aid in the interpretation of VA, PRC and MET results in relation to the CSF measures a procedure to graphically represent the results was used following the method of Greeves et al (1988). AVC logMAR scores were compared to spatial frequency results on the assumption that logMAR can be related to the log threshold contrast of a grating of equal angular subtense. PRC were plotted according to the fundamental frequency of the letters (section 1.4.6). The MET was plotted as a short bar at approximately 3 to 5 c.p.d. which represents a common value for the peak of the CSF.

On the assumption that letters comprise square wave gratings, the expected CS would be higher than for the equivalent CSF measure which comprises sine wave gratings (Campbell and Robson, 1964, 1968). Ginsburg (1981), reviewing the prediction of V.A. from CSF, noted that VA includes a number of other factors apart from simple detection, which include recognition, the varying visibility of different letters and interaction effects between successive lines, which all lead to a reduced sensitivity. Effectively the AVC provide the high spatial frequency end of the CSF curve. The contrast thresholds indicated by the PRC charts were generally below those measured with the CRT-CSF and the Vistech charts, despite the correction for contrast formulae noted in section 1.4.6. This suggested that the

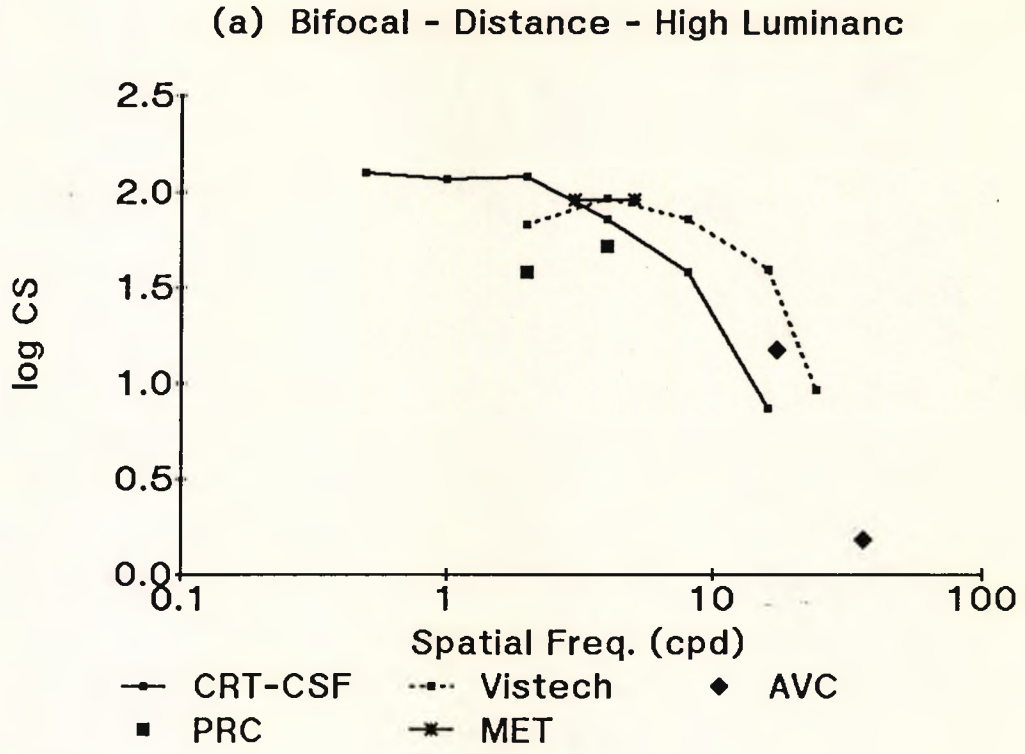

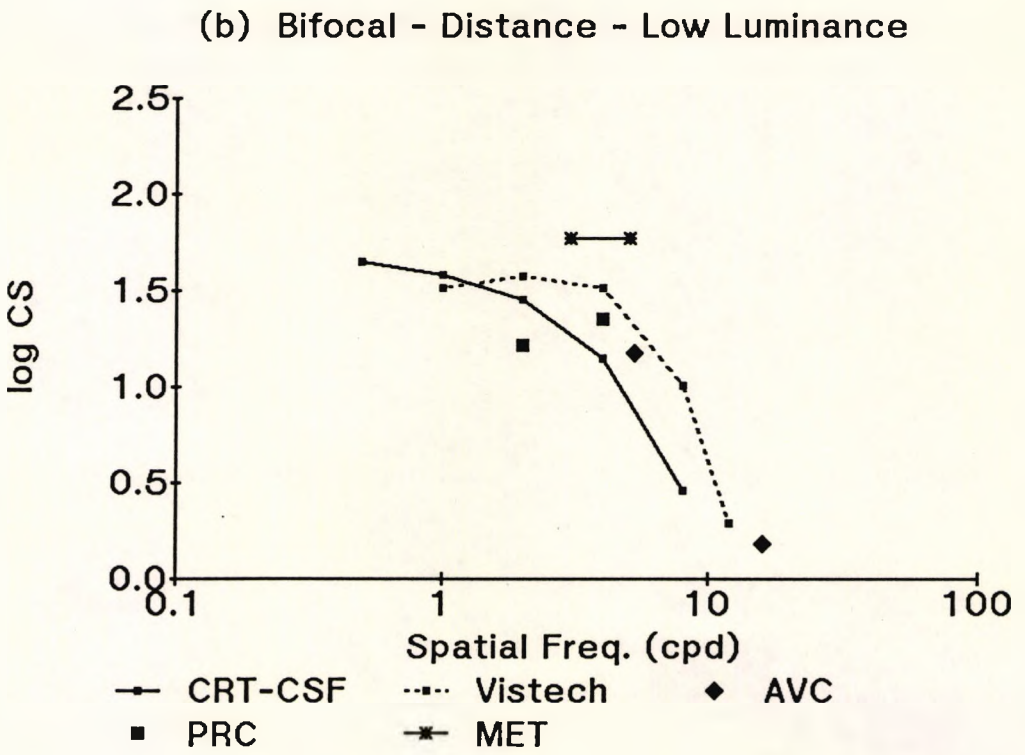

Figure 2.3-2 Mean distance visual performance with a diffractive BCL with a DZJ height of 2.2 μm at **(a)** high and **(b)** low luminance. CRT-CSF (solid curve), Vistech (dotted), AVC (diamonds), PRC (squares) and MET (solid horizontal bar) results are shown.

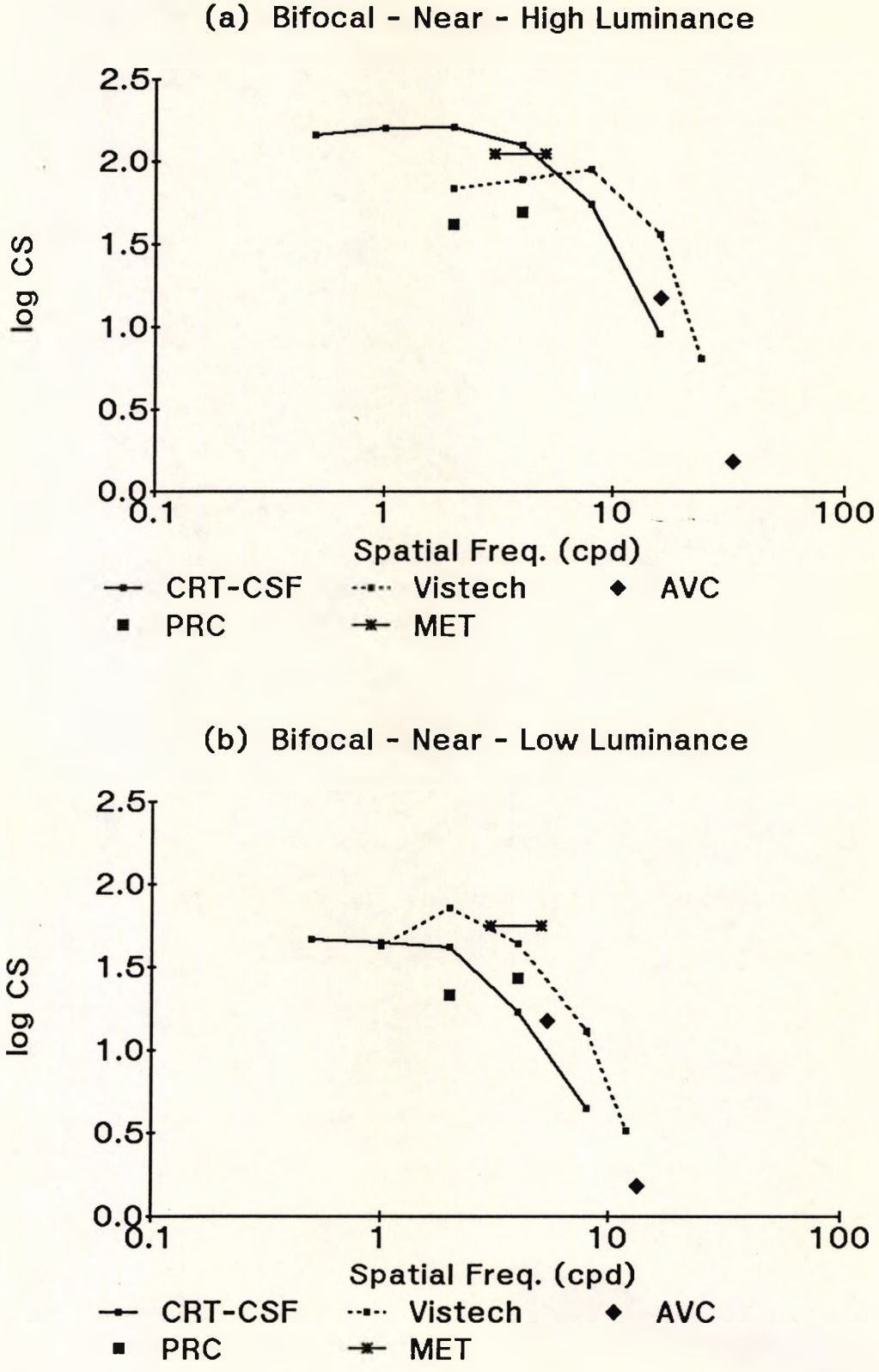

Figure 2.3-3 Mean near visual performance with a diffractive BCL with a DZJ height of 2.2 μm at **(a)** high and **(b)** low luminance. CRT-CSF (solid curve), Vistech (dotted), AVC (diamonds), PRC (squares) and MET (solid horizontal bar) results are shown.

assumptions about the concordance between the conventional CS task and PRC may not be correct. Similar results have been reported recently (Weissgold et al, 1991).

An analysis of variance (ANOVA) was performed for each visual performance measure with DZJ height (H), luminance level (L) and vergence (V) as factors. ANOVAs for one, two and three repetitions (also four repetitions for CRT-CSF) were examined to investigate the sensitivity of the different visual performance measures to the effects of interest. In particular an interaction between DZJ height and vergence (H x V) was expected as this would indicate that the theoretical calculations which predict a variation in the ratio of light in the two bifocal images were correct. In addition it was of interest to see any higher order interactions between luminance and the other factors. The results have been summarised in *Appendix 4* which shows, for each of the visual performance measures, the F-ratio and the significance level. The F-ratio may be considered as an indication of the size of an effect (i.e. a larger F-ratio indicates a larger effect).

The major trend was that, as expected, there was an increased significance of the effects of interest with increasing numbers of repetitions. With both CRT-CSF and Vistech charts there was an increasing level of significance with increasing spatial frequency. As

expected there was a large effect of luminance, but this was not of interest. There were no significant interactions between luminance and the other factors except with the PRC charts.

The major effect of interest was the interaction between DZJ height and vergence (H x V). CRT-CSF measures showed no significance with a single repetition, some significance at 4 and 8 c.p.d. was noted with two repetitions ($p < 0.05$), significance increased for 1, 2, 4 and 8 c.p.d. with three repetitions, though this was only at the 0.05 level for the 1 and 2 c.p.d.. All spatial frequencies reached significance after four repetitions. Vistech charts similarly showed significance at 8 c.p.d. ($p < 0.05$) after a single repetition, after two repetitions significance was noted for both 2 and 8 c.p.d., but not for 4 c.p.d., which only reached the 0.05 level of significance after 3 repetitions. PRC charts at both viewing distances (spatial frequencies), after only one repetition, showed significance which increased with the number of repetitions. The AVC charts required two repetitions for significance and there was no increase in the level of significance after the third repetition. No significant effect for the interaction was noted for the MET.

Discussion

The aim of this study was to determine which of the range of tests chosen could detect differences in the visual

performance with a range of diffractive BCL, by investigating the relative sensitivity of the various tests and the change in luminance level.

As there were no consistent interactions between luminance and the other factors it would appear that there was no increase in information or sensitivity gained by including this procedure. Hence this procedure (luminance variation) was discontinued thereby reducing test time by half.

The sensitivity of the various tests for the purposes of this pilot study may be defined as the level at which significance was achieved for the important interaction between DZJ height and vergence (H x V). On this basis CRT-CSF required more than four repetitions for all five spatial frequencies. If only the three higher spatial frequencies were considered, two or three repetitions were required for significance. Similarly, with the Vistech charts two or three repetitions were required, while with AVC and PRC only two repetitions were required. The interaction was not found with the MET.

Low spatial frequencies were generally little affected by defocus, as confirmed by the difficulty in achieving significance with the lower spatial frequencies and the MET. This was not the case with the PRC at 2 metres. This suggests that, at this distance, spatial frequencies other than the fundamental frequency may be influencing

threshold detection. There seemed little benefit in examining the effects of interest with these tests.

2.4 Conclusions

These results indicate that changes in visual performance due to the BCL were limited for spatial frequencies below 2 c.p.d. and hence for the remainder of this study it was decided to concentrate on the mid and high spatial frequencies. Testing with reduced luminance showed a reduction in visual performance on all tests as expected but did not increase sensitivity to the effects of interest. Hence tests at reduced luminance were not included in the main study.

Due to the reservations about the Vistech test noted in section 1.4.3, and as it appeared to offer no significant benefit over CRT-CSF it was decided to retain the CRT-CSF for the main study, using 2, 4, 8 and 16 c.p.d.. Both the AVC and PRC were sensitive to the effects of interest. It was decided that the information from the PRC test at 2 metres may be suspect and possibly redundant and thus was not included in the main study. The MET was not sensitive to the effects of interest and not included in the main study.

In conclusion, the tests to be used in the main study were :

(a) CRT-CSF (2, 4, 8 and 16 c.p.d.) at 1 metre;

(b) PRC at 4 metre; and

(c) AVC (high and low contrast) at 4 metre.

These are detailed in section 3.3.

Chapter 3 METHODS

3.1 Physical measurement of experimental bifocal contact lenses

3.1.1 STANDARD CONTACT LENS PROCEDURES

All experimental BCL were checked for quality and physical characteristics. Where appropriate the British Standard Institution (BS 5562, 1978) tolerances were adopted. The following parameters of the BCL were checked with traditional rigid CL verification procedures (e.g. Stone and Phillips, 1989) : refractive powers (in saline and in air), total diameter (TD), optical quality (with a form of Foucault's knife test), centre thickness (t_c), edge thickness (t_e) and edge shape. For the concentric-design refractive BCL central optic zone radius (COZR), central optic zone diameter (COZD), peripheral optic zone radius (POZR) and peripheral optic zone diameter (POZD) were measured with traditional techniques. For diffractive BCL, the diameters of the diffractive rings (here called diffractive zone diameter: DZD) were measured with a projection magnifier, and the apparent radius of the central diffractive zone (CDZR) and the peripheral refractive zone radius (PRZR) was measured with a conventional radiuscope.

3.1.2 INTERFEROMETRIC ASSESSMENT OF SURFACE PROFILE

A surface reflectance microscopic procedure (Riechert Fe2 Universal microscope with Nomarski Interferometer) was employed to examine the surface structure of the experimental BCL. A review of the optical principles is followed by a description of the experimental apparatus and methodology adopted.

Nomarski interferometry

A Wollaston prism is typically composed of two calcite prisms with the same angle θ combined to form a plane parallel plate, with the optical axes crossed and parallel to the outer surfaces (*Figure 3.1-1*). At the junction between the prisms there is shearing (lateral displacement) of the incident beam into ordinary and extraordinary wavefronts (*Figure 3.1-1*). The two resultant polarised beams produce an inclined localisation plane.

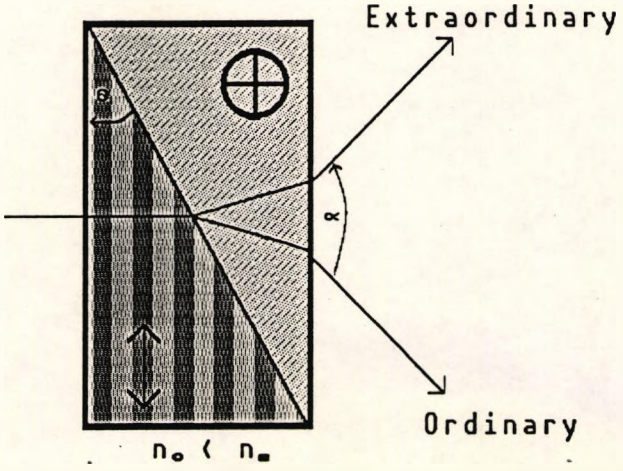

Figure 3.1-1 Angular doubling with a Wollaston prism. Where $\alpha = 2 (n_o - n_e) \tan \theta$, and the plane of localisation is inclined to the face of the prism. The arrow and arrow head (cross) represent the alignment of the calcite prisms.

Nomarski proposed the use of two Wollaston prisms separated by a half-wave plate (*Figure 3.1-2a*) to produce a plane of localisation parallel to the face of the Wollaston prism. In a second proposal Nomarski suggested the use of a specially modified Wollaston prism in which one of the axes of the calcite is inclined to the outer face (*Figure 3.1-2b*). This technique has been especially useful for interferometers in microscopy (Francon, 1966).

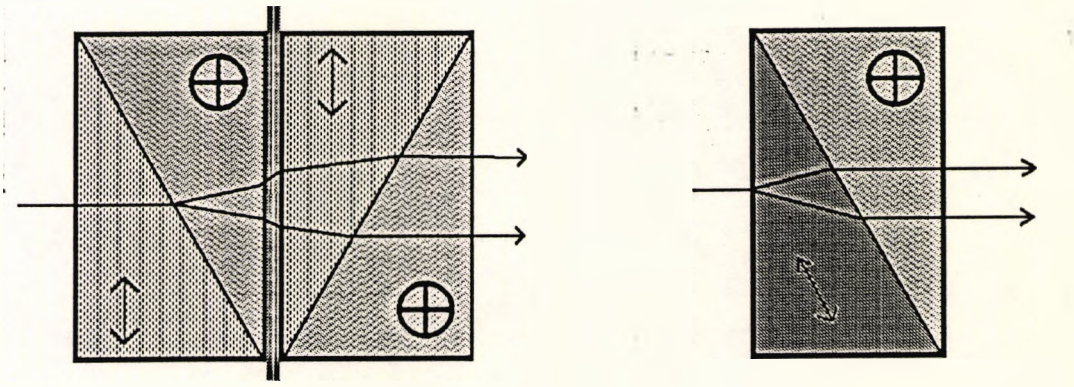

Figure 3.1-2 Modified Wollaston prisms, after Nomarski, which produce a plane of localisation parallel to the face of the prism. The arrows and arrow heads (crosses) represent the alignment of the calcite prisms.

Image interpretation

This type of double-refracting system with angular shear produced two wavefronts from the incident beam. The slight displacement and tilt of the two images resulted in interference fringes due to path (phase) differences. In effect the wavefront became its own reference. The fringes were lines of constant phase and are like contour lines showing changes in relative position of the two images. Considering a surface consisting of a simple step, in *Figure 3.1-3* the two images of the surface WS_o and

WS_e have both a lateral displacement and a phase shift. A resultant single interference fringe (K_1K_2) is shown changing direction as the relative phase (shown as the distance between the two surfaces) varies from t_o to t_s. The depth of the step could then be measured as the displacement of the fringe (d). When the surface above and below the step were parallel then the interference fringe would be continuous as shown. Though the surface of the BCL examined was curved (radius of curvature 7300 to 7900 μm), across the very small field of view of the Reichert interference microscope (350 μm) there was a sag of only 2 μm and the surface was considered to be flat as the fringes were parallel.

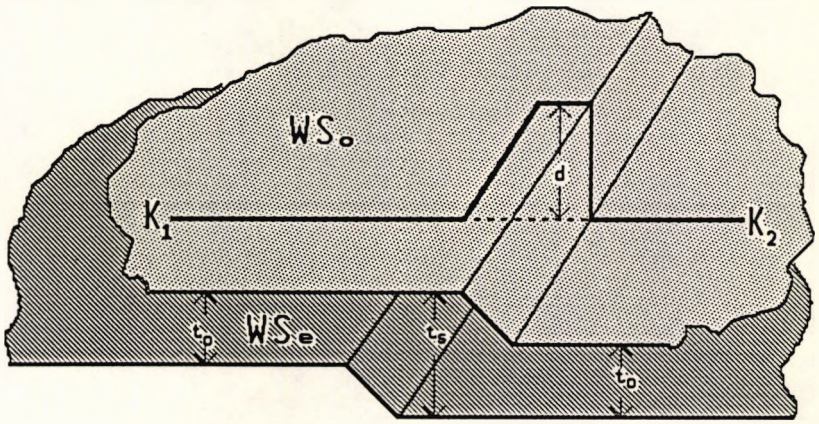

Figure 3.1-3 A schematic representation of Nomarski interferometry. A single interference fringe is shown diagrammatically in angular shear. The two wavefronts WS_0 and WS_e from a surface with a small step are shown with a lateral displacement and a phase shift (represented as a vertical displacement). The resulting interference fringe (K_1K_2) is displaced laterally according to the relative phase (distance) between the wavefronts (t_o to t_s) effectively creating a contour line. The displacement, d, of the interference fringe by the step is proportional to the height of the step.

Due to the optical arrangement of the equipment used the fringes were diagonal in the field of view. In addition the diffractive zone junction (DZJ) of the actual BCL was curved, and the DZJ examined, often had small distortions

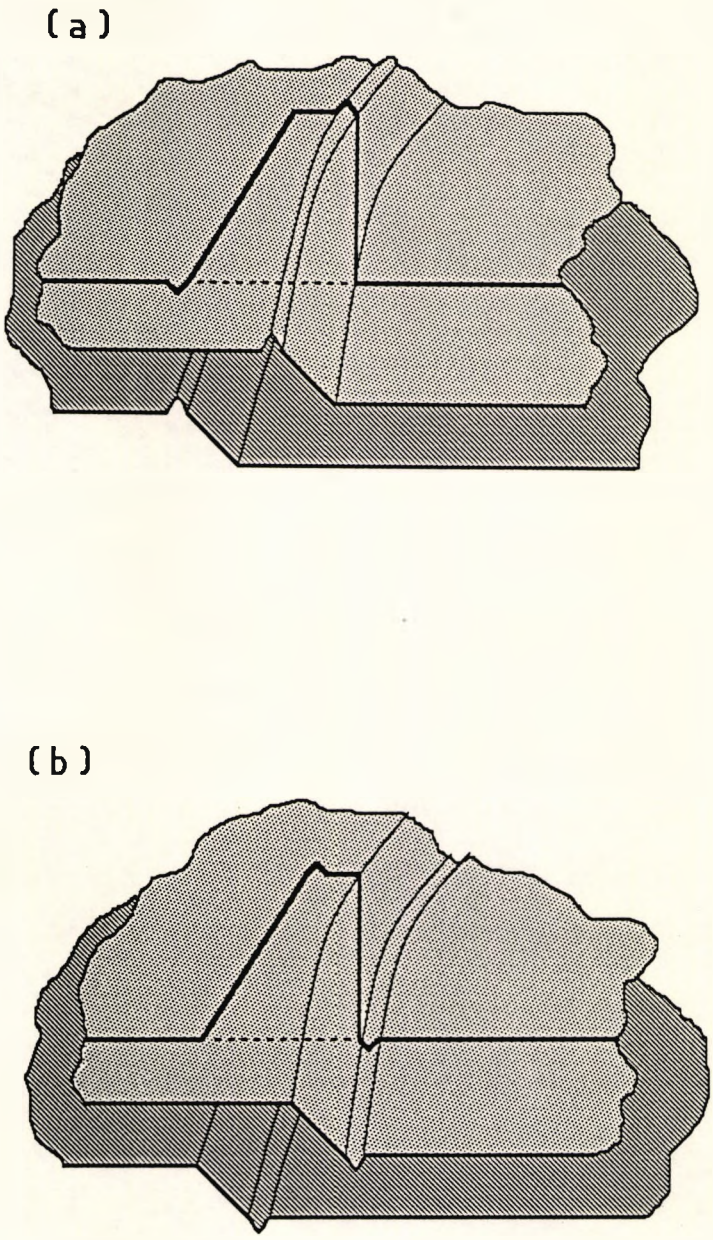

Figure 3.1-4 A diagrammatic representation of the appearance of an interference fringe crossing a DZJ with (**a**) a ridge at the upper edge of the step; and (**b**) a groove below the step.

as shown in *Figure 3.1-4* which appear as shown in *Figure 3.1-5*. Unlike the single fringe shown in *Figure 3.1-5*, the field of view was full of fringes (*Figure 3.1-6*).

Measurement procedure

To enhance the accuracy and ease of performance a thin reflective coating was applied to some of the early BCL examined. The surfaces to be examined were sputter coated with a microscopic layer of gold. The total thickness of this layer was less than 60 nm, and as sputter coating is known to provide an even layer of material (hence its use in electron microscopic procedures) the layer should make no difference to the parameters of interest (1000 to 4000 nm depth). However, sufficient reflectance could be obtained from the untreated surface, and though the image was more difficult to work with the majority of BCL were examined without the aid of gold coating. This also allowed the examination of hydrated soft diffractive BCL which were not suitable for gold coating.

The BCL was mounted on a specially constructed, pivoted bracket designed to place the BCL surface centre of curvature at the centre of rotation of the bracket and thus maintain the BCL surface perpendicular to the incident illumination for all orientations (*Figure 3.1-7*). This ensured maximal light intensity and image quality of the interference fringes. The bracket was then mounted

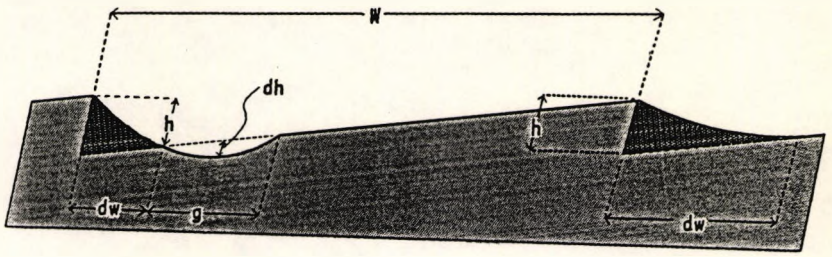

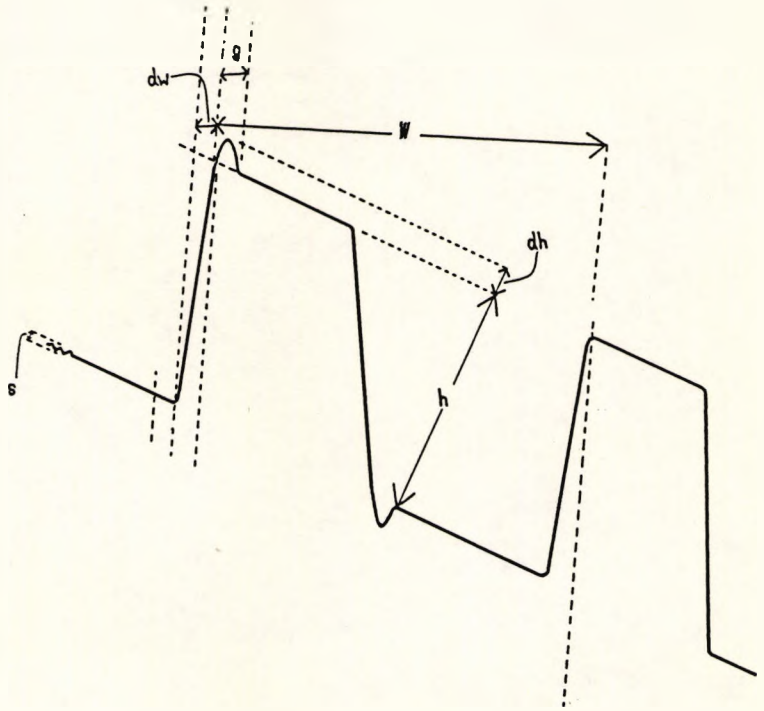

Figure 3.1-5 The measurements made on diffractive BCL. A diagrammatic representation of (**a**) a cross-section of a portion of a diffractive BCL, where the darker shading represents the failure to produce the "ideal" DZJ shape due to the finite size of the tool; and (**b**) the resultant fringe appearance. The various measurements, **h** the DZJ height, **dh** the overshoot by the tool, **w** the annular zone width, **dw** the width of the DZJ (tool size), and **g** the width of the tool overshoot are shown.

Figure 3.1-6 An interference micrograph of the surface of a rigid diffractive BCL. Everything is doubled by the Wollaston prism, including the dust particles (e.g. the two dark oval shaped spots in the bottom left corner). Two complete DZJ (each seen as the two curved, vertical lines, labelled Y and Z) are shown. As shown diagrammatically in *Figure 3.1-5* the interference fringes (diagonal stripes) are displaced vertically (up) by the DZJ at e.g. Y_1 (first wavefront in *Figure 3.1-3*) and then return at e.g. Y_2 (down, at the DZJ of the second wavefront) to lie as a continuation of the original position of the fringe. The relative displacement of the fringe represents the height of the surface feature, in this case the DZJ.

on a Reichert Fe2 Universal Microscope with Nomarski Interferometer (*Figure 3.1-8*).

A series of photographs were taken across the BCL surface such that each diffractive zone junction (DZJ) was in at least two different photographs, and at two different locations on the DZJ. A series of measurements (at least three of each zone in each photograph) were then made from the photographic plates. Some early photographic records were taken with Polaroid type 611 CRT image recording black and white Land film. The Land camera proved satisfactory but the film was expensive. The majority of photographs were taken with a standard 35 mm format using panchromatic black and white Polaroid T-Max 100 ASA or Kodak Technical Pan 25 ASA film (which proved to have better contrast definition, consequently improving resolution of the interference fringes). Measurements were made on high contrast monochromatic 7 x 5 inch prints. As expected, there was no significant difference in fringe measurements from the two systems.

With monochromatic light of wavelength λ the height of any surface discontinuity could be measured in terms of the displacement of the interference fringes. A Mercury Green source with wavelength of 546 nm was used for all interferometric measurements. As each fringe represents a half wavelength phase difference (π) the height of the surface discontinuity (∂) can be measured by counting the

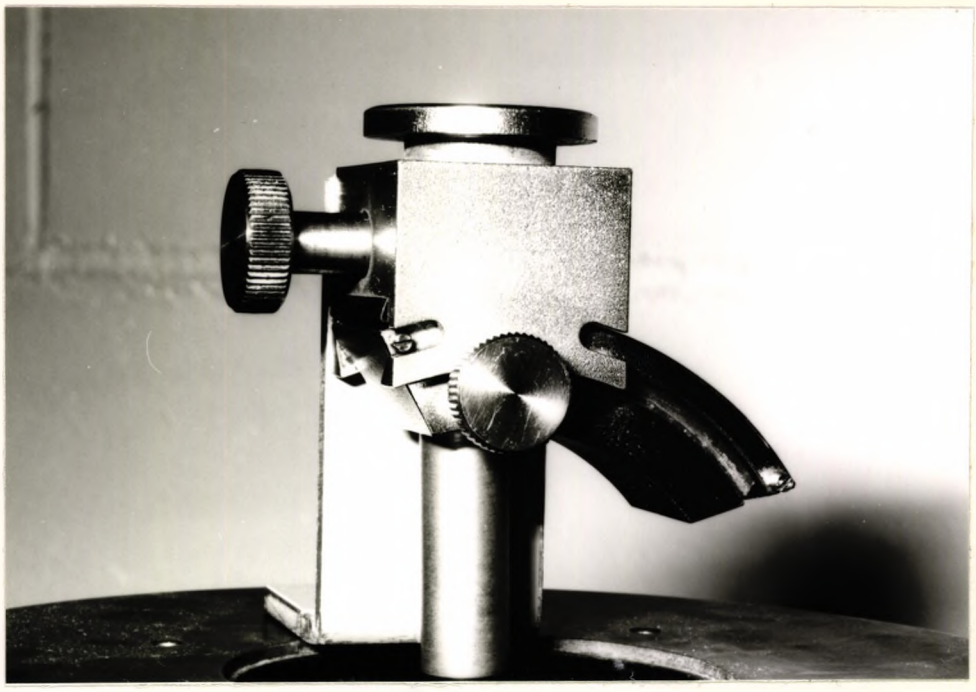

Figure 3.1-7 The special attachment devised to hold the contact lens, ensuring that the contact lens surface is perpendicular to the incident light.

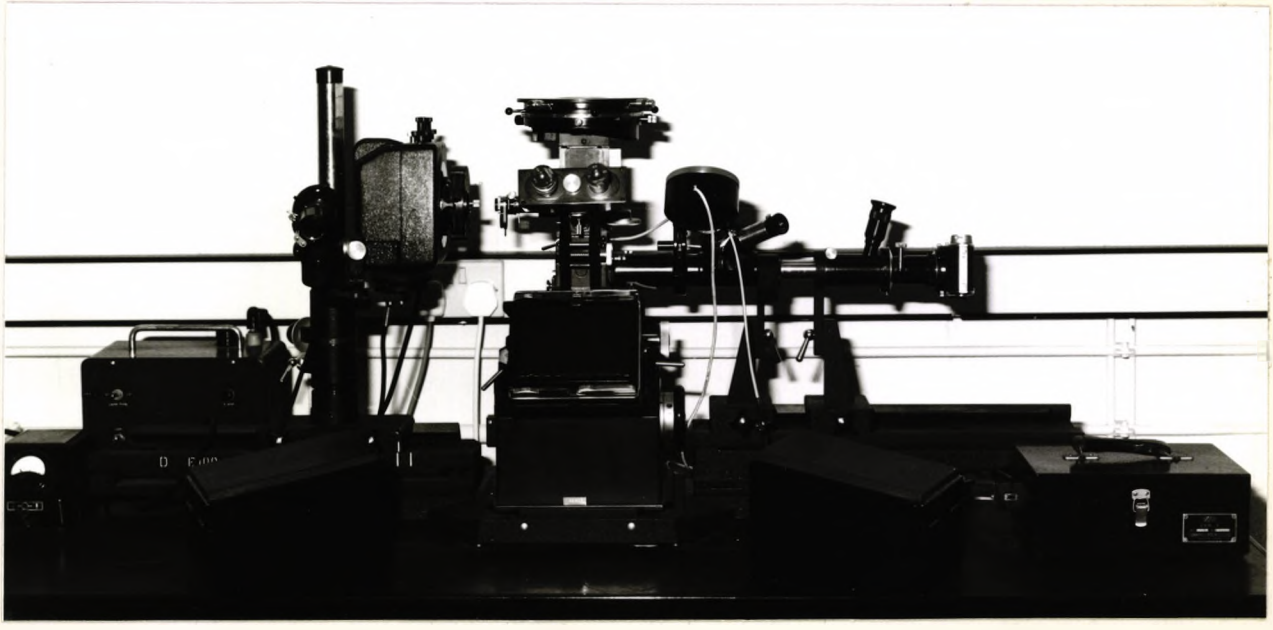

Figure 3.1-8 The Riechert Fe2 Universal microscope with Nomarski Interferometer.

numbers of fringes (n) which were displaced (Ditchburn, 1976). Hence :

$$\partial = \tfrac{1}{2} n \lambda \qquad \textit{Equation 3.1}$$

The maximal or worst case error for this measurement was considered to be one eighth of an interference fringe (0.07 μm). Repeated measurement of the height of a number of DZJ on different occasions and with the two different photographic systems indicated a repeatability (95% confidence limit) of better than ± 0.04 μm (i.e. 2% error for a step height of 2 μm).

Photographs of a Riechert graticule allowed establishment of a scale for horizontal displacement of other elements viewed under the same conditions. The maximal or worst case error was considered to be 2 μm (0.5 mm on the photographic plate), and by repeated measurement of the annular zone width the 95% confidence limit was found to be less than 2 μm (e.g. 0.6% error for the first annular zone).

A number of measurements were made on each diffractive zone representing different aspects of the surface shape (*Figure 3.1-5*). The first aspect of interest was the height of the DZJ (step height or blaze height). The DZJ height (h) determined the proportion of light in the various foci (section 1.2.3). The annular zone width (w), the displacement between successive DZJ, was measured as the

distance between equivalent points at the beginning of successive DZJ. This is effectively a measure of DZD which determined the focal length of the diffractive foci.

During the course of measurement a great degree of variability was noted in both the quality of the fringe appearance and the shape of the DZJ. The fringe appearance indicated the quality of the machined BCL surface. A subjective rating scale, given in Table 3.1-1, was developed to assess fringe appearance. Ratings were related to the apparent displacement of the interference fringes due to the quality of the lathed surface of the BCL.

0	smooth	
1	just noticeable	< 0.25 fringe width
2	noticeable	0.25 to 0.5 fringe width
3	interfering	0.5 to 1.0 fringe width
4	severe	> 1.0 fringe width

Table 3.1-1 Fringe Appearance Rating Scale based upon visual assessment of the interference micrographs.

The Rayleigh criteria suggests that deviations in an optical surface (e.g. telescope lens) of a quarter wavelength is acceptable (i.e. up to grade 2 in the Rating scale used). The Rayleigh criteria was devised

with reference to deviations over relatively large areas of a lens, it was uncertain whether this criterion of acceptability was useful for numerous variations over relatively small lens areas as seen on the BCL.

The irregularity at the DZJ represented a failure to produce the required surface shape, as discussed in section 1.2.3. Due to manufacturing limitations the actual shape of the DZJ was distorted by the finite size and shape of the lathe tool and any manufacturing errors. The width of the DZJ was often composed of two portions, firstly the finite tool effect and secondly a portion due to a manufacturing error, where the lathe apparently overshot forming a small groove at the DZJ. These aspects of the DZJ shape were measured as the width of the finite tool effect (dw), and the height (dh) and the width (g) of any manufacturing overshoot (*Figure 3.1-5*).

3.2 Optical performance

3.2.1 INTRODUCTION

The aim was to investigate the optical performance of concentric-design refractive BCL and diffractive BCL with different optical characteristics. In particular to investigate the effect of aperture size (pupil), COZD and the location over the aperture of refractive BCL. Similarly to investigate the effect of wavelength,

aperture size, DZJ height, DZJ shape and location over the aperture of diffractive BCL. The Modulation Transfer Function (MTF) and Line Spread Function (LSF), as discussed in Section 1.3, were used to evaluate optical performance.

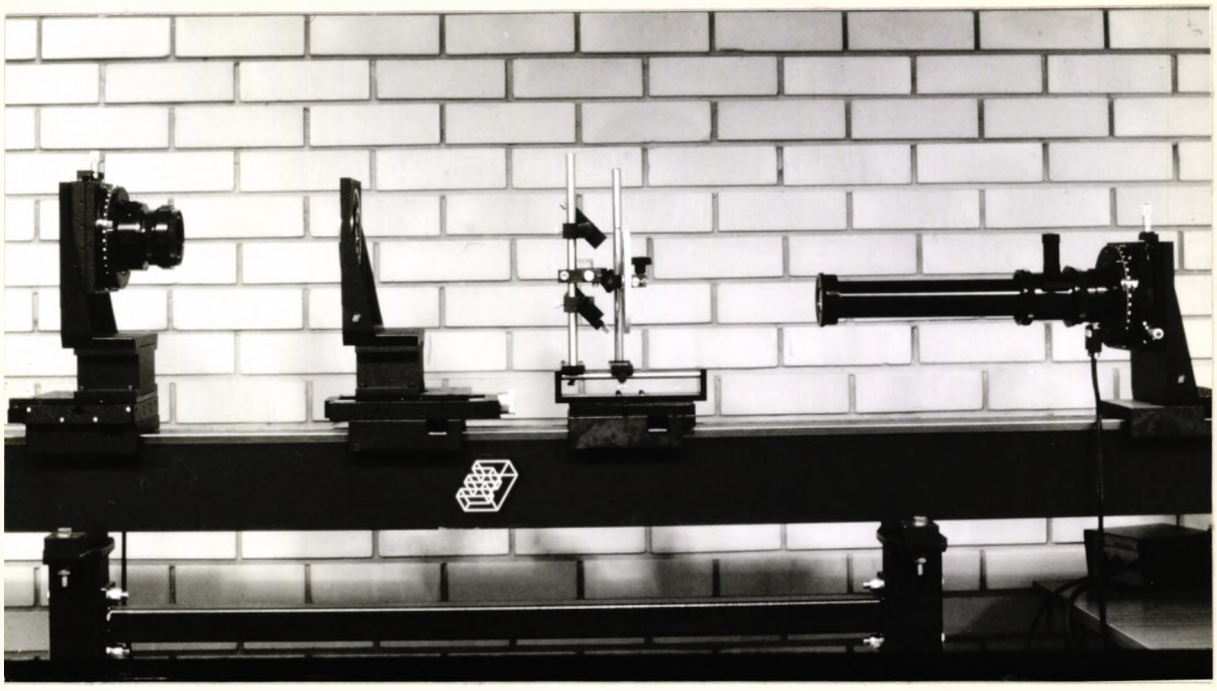

Figure 3.2-1 The Ealing Electro-Optics (Watford, U.K.) solid state EROS 200 MTF apparatus used to measure the MTF.

3.2.2 MODULATION TRANSFER MEASUREMENT

An Ealing Electro-Optics (Watford, U.K.) solid state EROS 200 MTF apparatus was used to measure the MTF of the experimental BCL (*Figure 3.2-1*). The solid state photodiode array comprised 256 diodes at a spacing of 25 μm which provided an array length of 6.4 mm. The output of the photodiode array was electronically captured, stored, and analysed by an Amstrad 1512 (IBM PC clone) computer. The

speed of capture was dependent upon the image intensity, but was as short as 20 ms, which allowed (almost) real-time viewing of the LSF or MTF on the computer monitor. This allowed very accurate alignment and focusing of the test system. An accuracy of less than 5% was claimed by the manufacturers. A few modifications were made to the conventional arrangement of the equipment to allow testing of BCL (*Figure 3.2-2*).

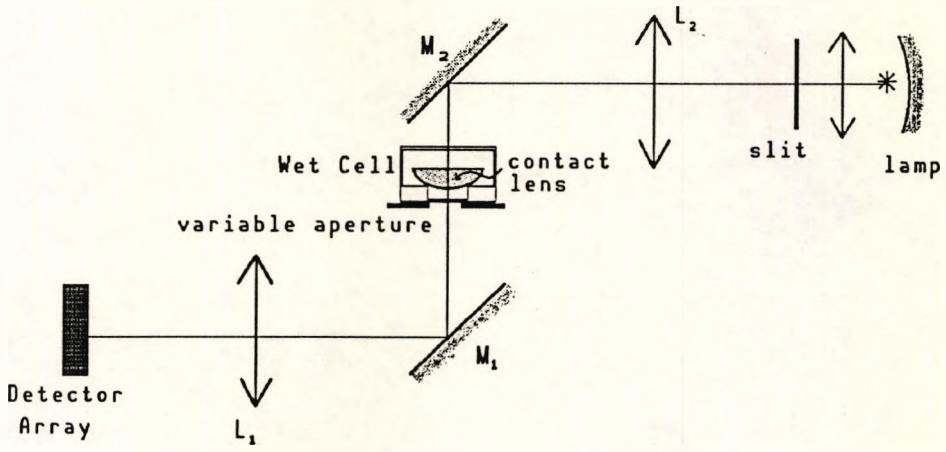

Figure 3.2-2 The optical arrangement for Modulation Transfer Function measurement with a solid state EROS 200 shown schematically. The lamp is used to form a slit object which is imaged through the system onto the detector array. The two objective lenses (L_1, L_2) were placed at their respective focal lengths from the test contact lens in the saline filled wet cell to form a Badal optometer with unit magnification. A variable aperture was placed 3 mm from the BCL. To allow the contact lens to remain horizontal a periscope arrangement was constructed with two mirrors (M_1, M_2). (Not to scale).

The near diffractive and the refractive COZ optical power of the BCL were designed for use in the ocular tear layer, and hence the BCL were held in a saline filled wet cell. To allow the BCL under test to lie horizontally, and hence unstressed, the optical path was altered with

mirrors (M_1, M_2) to form a periscope arrangement (*Figure 3.2-2*). A variable aperture was placed 3 mm below the test BCL. The two objective lenses (L_1, L_2) were fixed at their respective focal lengths (381 mm) from the test BCL in a Badal optometer arrangement which was then a unit magnification system. The distance of the slit object was varied to form a best focus image at the detector array. Hence the image formed by the two different focal powers of each BCL were of equal size.

Normally the extent of the image which was analysed was limited by the EROS program to reduce the effects of straylight. This software feature had a tendency to occasionally treat outer portions of a poor BCL image as straylight. Hence, due to the width of the image formed by a BCL, the conventional software potentially may have overestimated the quality of the image. Ealing Electro-Optics provided a modified version of the controlling software (version: Eros451p) which did not limit the extent of the image.

Atmospheric and other conditions in the test laboratory conformed to the U.K. Instrument Industry Standards Committee (BS 4779: 1971).

3.2.3 EXPERIMENTAL DESIGN

BCL were selected in a random order. Aperture diameters were randomly selected and the object vergence (distance

or near) presented in a pseudo-random order for each BCL. With the BCL located centrally within the saline filled wet cell, the wet cell was placed in the appropriate position above the aperture. When required, to test the effect of decentration of the BCL over the aperture, the BCL was moved in relation to the aperture, which remained centred on the optical bench. Decentration of the BCL (and wet cell) was introduced with engineering thickness gauges (Matrix M-79, Coventry Gauge & Tool Co. Ltd., U.K.). All results were recorded for a range from 0 to 10 cycles per millimetre (0 to 66.3 c.p.d.).

MTF measurements were taken at both distance and near focal lengths of each BCL. LSF for various BCL, aperture, decentration configurations were also recorded to illustrate the changes in image shape.

Refractive bifocal contact lenses

All measurements were done with the white light from a dichroic halogen capsule lamp and filter with a spectral output and transmission curves shown in *Figure 3.2-3*. The resultant spectral power distribution of the image (*Figure 3.2-4*) was similar to the human photopic sensitivity (*Figure 1.1-5*).

To investigate the relationship between BCL design, COZD and aperture size, MTF measurements were taken for a variety of aperture sizes (6, 5, 4, 3.5, 3, 2 mm) with at least two BCL of each design (CD or CN) and each COZD.

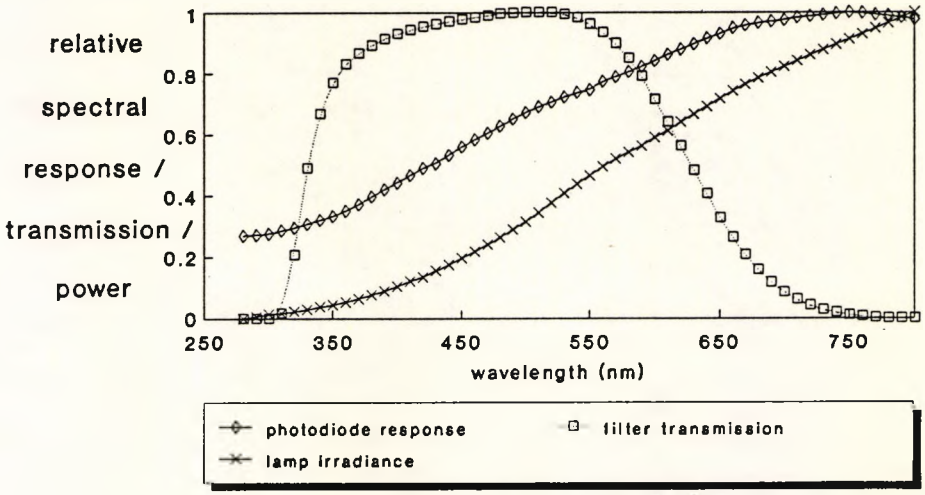

Figure 3.2-3 Spectral irradiance of the dichroic halogen lamp and spectral transmission of the filter to reduce infra-red output used in the optical measurement of the refractive bifocal contact lenses.

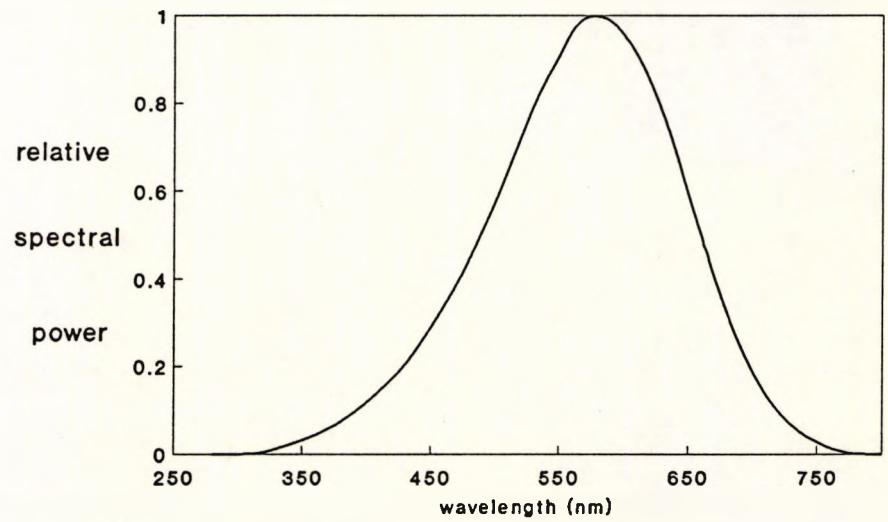

Figure 3.2-4 The relative spectral power distribution of the image used in the optical measurement of the refractive bifocal contact lenses. This was derived from the spectral irradiance of the lamp and the spectral transmission of the filter, as shown in *Figure 3.2-3*.

To investigate the effect of decentration, MTF measurements using decentrations of the BCL from the optic axis of 0.25, 0.5, 0.75, 1.0, 1.25, 1.5 and 2.0 mm were taken with two BCL of each design.

Diffractive bifocal contact lenses

All measurements were done with near monochromatic light by inserting interference filters with a half-height bandwidth of 10 nm (Balzer) into the beam. Measurement in "white" light was not possible due to the large longitudinal chromatic aberration of the first order diffractive focus.

To investigate the effect of variation in wavelength a small number of BCL were measured with a range of interference filters with peak wavelengths of 450, 499, 548, 573, 599 and 667 nm. The effect of changes in aperture was investigated for aperture sizes of 6, 5, 4, 3.5, 3, and 2 mm. To investigate the effects of the changes in BCL design MTF measurements were made with interference filters with peak wavelengths at 548 and 573 nm. These two wavelengths were chosen as the former is close to the peak of the human photopic spectral sensitivity (*Figure 1.1-5*) of 555 nm and the latter, it was thought may have been a better predictor of visual performance for older subjects (due to age-related changes in ocular spectral transmission as discussed in Sections 1.1.3 and 1.2.3). To investigate the effect of decentration, MTF measurements were taken with

decentrations of the BCL from the optic axis of 0.5, 1.0, 1.5 and 2.0 mm over a 4 mm aperture.

3.2.4 DATA ANALYSIS

For the majority of the data analysis all spatial frequencies were considered. Occasionally, in an attempt to simplify the analysis of optical performance, the MTF data was treated in one of two ways. Firstly the area under the MTF curve (this is equivalent to the average of the MTF). This area may be considered as a figure of merit for the overall optical performance, and might be expected to relate to the general form of the CSF with a particular BCL. Secondly the spatial frequency at which the modulation fell below 0.1 (range 1.0 to 0) was recorded. It was felt that this parameter may equate to subjective visual acuity (in such tasks the contrast of the target, a dark letter on a light background, is maintained and the spatial frequency (letter size) reduced until the subjective visual threshold is reached). These two indices of optical performance were arbitrarily chosen from any number of other possibilities but might be expected to correlate with measures of visual performance.

3.3 Visual Performance

3.3.1 INTRODUCTION

The effect of alterations in the design of BCL upon visual performance was evaluated with :

(a) a traditional monitor presented measure of CS;

(b) Australian Vision Charts (AVC); and

(c) Pelli-Robson contrast threshold charts (PRC).

The viewing distance, luminance level, spatial frequencies and contrast levels of each test are shown in *Table 3.3-1* and are discussed below.

Test	Luminance Level (cd/m^2)	Distance (m)	Spatial Frequency (c.p.d.)	Contrast
CRT-CSF	50	1	2,4,8,16	0.25 to 0.001
AVC	250	4	approx. 7.5 to 120	0.9, 0.1
PRC	250	4	approx. 3.6	0.9 to 0.008

Table 3.3-1 A summary of the luminance levels, test distances, spatial frequencies and contrast levels for the various tests of visual performance.

As discussed in section 1.4.9, an optical correction was used to place each test at optical infinity for "distance" testing and appropriate lenses were introduced to produce a 2 Dioptre vergence for "near" viewing (and best vision found by subjective refraction).

3.3.2 CONTRAST SENSITIVITY

Sinusoidal gratings were presented on a high resolution monochrome monitor (Manitron model VLR 1593/80) with a P4 (white) phosphor, producing 800 non-interlaced vertical scan lines at a field scan frequency of 100 Hz. The monitor was driven by a pattern generator (Millipede Prisma VR1000) interfaced to an IBM AT personal computer. The pattern generator provided 10 bit control of screen luminance and allowed between-field presentation of gratings. The monitor is shown in *Figure 1.4-1*

The monitor was calibrated with a Lichtmesstechnik (LMT L1003) light meter. Potential error in contrast produced by changes in screen luminance over time, was reduced to less than 0.006 log contrast units. This was achieved by displaying a blank screen at the mean luminance used during the experiment (50 cd/m^2), for two hours prior to the commencement of each session.

The monitor screen was masked to give a circular field subtending a visual angle of 11.5 degrees from the viewing distance of 1 metre. The luminance and colour of the surround were matched approximately to the screen. Head movements were restrained by a chin and forehead rest and subjects were instructed to fixate a small target at the centre of the screen.

The presentation procedure was a randomised Adaptive Probit Estimation (APE) technique (Watt and Andrews, 1981). Approximately 20 presentations of each of four spatial frequencies (2, 4, 8, and 16 c.p.d.) were randomly interleaved, with contrast levels determined by the APE procedure (section 2.2) to maximise the efficiency of the threshold determination. Spatial frequency was indicated to the subject by a "matched" auditory tone to reduce spatial frequency uncertainty (Davis and Graham, 1981). This technique was chosen as the best compromise between accuracy and speed after the preliminary studies described in section 2.2.

3.3.3 LETTER CHARTS - VIEWING DISTANCE AND LUMINANCE

The AVC and PRC were mounted on a large matt white board, and viewed from 4 metres. The average illuminance was 1050 lux and the luminance of the white surrounds and letter charts was 250 cd/m^2 with less than 10% variance in luminance across the charts (LMT L1003 light meter). Further details are given below.

3.3.4 AUSTRALIAN VISION CHARTS

As described in section 1.4.5, each AVC (*Figure 1.4-2*) consisted of two letter series of different contrast (10% and 90%) each with a different letter sequence. Four AVC were available, and were interchanged to reduce the effects of memory. Two charts were presented at each

trial and the results averaged. A viewing distance of four metres was used normally for the AVC. If the second-largest row of letters were not visible the viewing distance was reduced to 2 metres. Given appropriate optical correction this had no effect upon the AVC score (Westheimer, 1979).

3.3.5 PELLI-ROBSON CONTRAST THRESHOLD CHARTS

As described in section 1.4.6, at four metres the fundamental spatial frequency of the PRC letters (*Figure 1.4-3*) was 3.6 c.p.d. (Campbell and Robson, 1968). There were, of course, restrictions to this assumption (Bouma, 1971). Only two PRC letter sequences were available. To reduce the effects of memory another PRC chart was cut into vertical strips which could then be overlaid on the PRC thereby increasing the number of letter sequences. The results for the two PRC charts were averaged at each trial. As suggested by Elliott et al (1990b), to improve reliability, a call of "C" for "O" or "O" for "C" was scored as correct.

3.3.6 PUPIL SIZE

To allow an accurate determination of pupil size under the given test conditions pupil size was measured, whilst the subject viewed a blank white field at a range of luminances from 0.001 to 320 cd/m^2, with an infra-red pupillometer which had a potential accuracy of 0.01 mm

(Barbur et al, 1987). Repeated measures indicated that the absolute pupil size varied on retest by as much as 0.5 mm. Each subject was measured with the range of screen luminances at least twice. A quadratic regression analysis was performed to determine a line of best fit and the pupil size at the two test luminances (50 and 250 cd/m^2) interpolated.

3.3.7 CONTACT LENS LOCATION

The fit of each refractive BCL and the location of the COZ in relation to the pupil was determined for each refractive BCL for each subject with a slit-lamp biomicroscope fitted with a graticule eyepiece by the same investigator. The decentration in relation to the pupil centre could then be determined (worst case ± 0.35 mm). The measured decentration was an estimate by the author of the average position of the BCL on the eye. The repeatability (95% confidence limit) of this assessment was estimated by repeated measures as ± 0.11 mm. Pupil coverage by the COZ could then be determined for each of the two test luminances and the pupil sizes as calculated.

3.4 Longitudinal Chromatic Aberration

The on-eye longitudinal chromatic aberration (LCA) was measured with BCL by a psychometric method described

below to confirm theoretical calculations which suggest that the first order (near) focus of a diffractive BCL has a LCA of an order reverse to that found in refractive optical systems and the human eye (section 1.2.3).

Apparatus

An instrument to measure chromatic aberration was devised and built. Constructed on the Badal Optometer principle (Bennett and Rabbetts, 1984) the ocular focal length was determined for two narrow bandwidth (10 nm) interference filters with central wavelengths of 450 and 650 nm (Balzer). A Badal optometer (*Figure 3.4-1*), incorporating Nagel's principle (Emsley, 1944), by placing the second focal point of the optical system coincident with the nodal point of the observer's eye, allows movement of the target without significant retinal image size variation (Jenkins, 1963; Wittenberg, 1988).

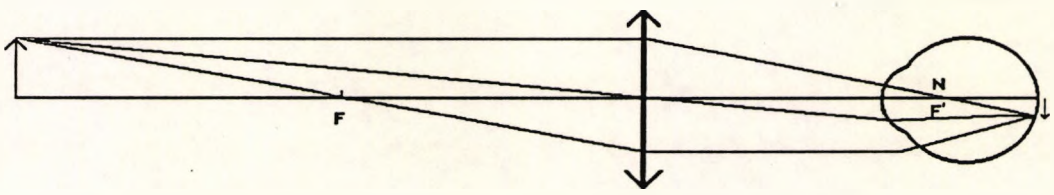

Figure 3.4-1 A diagram of a Badal Optometer incorporating Nagel's principle. As the second focal point of the lens is coincident with the nodal point of the observer's eye, there is no significant variation in image size with target movement (Emsley, 1944)

As dioptric vergence varied linearly with object location according to the Newtonian relationship, LCA was then determined by the equation :

$$LCA = F^2 \times (d_{max} - d_{min}) \qquad \textit{Equation 3.4-1}$$

where F is the power of the imaging lens and d_{max} and d_{min} the distances from the lens with the respective filters.

A dual channel Badal optometer system was constructed as shown in *Figure 3.4.2*. Each channel contained identical but inverted targets consisting of a central square wave grating of a moderately high spatial frequency and peripheral elements. Ideally, high spatial frequency targets should be used for critical determinations of focus. This compromise was necessary due to the reduced resolution with BCL and the low transmission of the interference filters.

Procedure

The white, luminance matched target viewed through the left channel was adjusted for zero accommodative demand and acted as an accommodative-lock. The experimental target was viewed through the right channel which contained the experimental interference filters. The two experimental interference filters were presented in a pseudo-random order. Both targets were visible to the subject at all times. The subject, restrained with chin and forehead rests and a dental bite and an artificial pupil immediately in front of the eye, manually adjusted the position of the experimental target via a rotating knurled knob (method of adjustment), whilst ensuring that

other target (accommodative-lock) remained clear. The subject was asked to adjust the position of the experimental target for maximum clarity, and if a range of settings were encompassed by this criterion, then the subject was required to adjust for the midpoint of the range. An average of ten results with each filter were recorded and analysed with an interfaced BBC microcomputer.

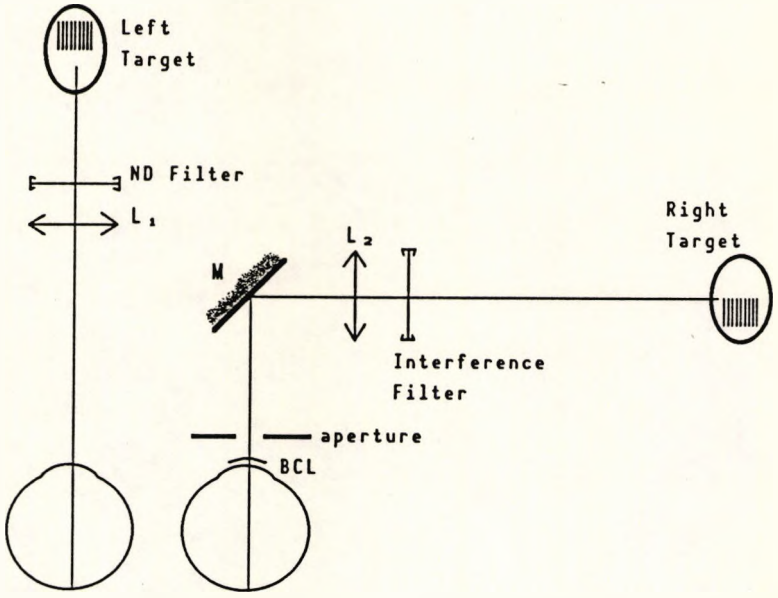

Figure 3.4-2 A diagram of the dual channel Badal optometer system which was constructed. Identical but inverted targets consisting of a central square wave grating and a peripheral elements were viewed with each eye. The left eye acted as an accommodative-lock. The experimental target was viewed with interference filters by the right eye which wore the experimental BCL. The focal length was determined for each filter by altering the distance between lens L_2 and the right target.

3.5 Subjects

Subjects wore a BCL in one eye for visual assessment. A topical ocular anaesthetic was also used when requested to reduce the effects of excessive lacrimation. The best

refractive correction (including any astigmatic correction) for the relevant viewing distance and BCL was worn in a trial frame. Each BCL was worn for no longer than 45 minutes. All subjects received training with the various vision tests to reduce learning effects and to acquaint them with BCL vision.

3.5.1 REFRACTIVE BIFOCAL CONTACT LENSES

Five presbyopic subjects, recruited through advertisement in the Optometry Clinic, with ages from 57 to 65 years, wore ten refractive BCL as detailed in section 3.6.1 for at least two replications. Since the pupil size and location of the BCL in relation to the pupil were expected to influence visual performance these aspects were measured for all subjects with each refractive BCL (sections 3.3.4 and 3.3.5).

3.5.2 DIFFRACTIVE BIFOCAL CONTACT LENSES

Two presbyopic subjects (colleagues) with ages of 49 and 61 years and one pre-presbyopic subject (the author: 32 years) wore a range of rigid and soft diffractive BCL as detailed in sections 3.6.2 and 3.6.3.

All visual assessment of the pre-presbyopic subject was made under cycloplegia. A regular check was made during CL wear to ensure that there was no significant corneal oedema and that the subject's accommodation was less than

1 dioptre. An artificial pupil of 3.5 mm was worn in a trial frame. This size pupil was chosen as it represented an average pupil diameter for presbyopes (Woods, 1991c). The limitations of using an artificial pupil are considered in section 5.1.

3.5.3 LONGITUDINAL CHROMATIC ABERRATION

A pre-presbyopic subject (the author: 32 years) wore a small range of refractive and diffractive BCL. The BCL was worn in the cyclopleged right eye and a 3.5 mm artificial pupil was used.

3.6 Experimental bifocal contact lenses

Except where noted the BCL described here were not available on a commercial basis.

3.6.1 RIGID REFRACTIVE BIFOCAL CONTACT LENSES

The rigid refractive BCL used were made by Pilkington VisionCare. Some CL finishing was performed at City University. The BCL were a PMMA back-surface concentric-design with central optic zone diameters (COZD) of 3.4, 3.0, 2.6, 2.2, and 1.8 mm. The peripheral optic zone diameter (POZD) was fixed at 7.5 mm. BCL were available in both a centre-distance (CD) and a centre-near (CN) format with a near addition of 2.00 Dioptres in vivo.

All BCL were a conventional tri-curve (C3) design with an effective BOZD of 7.5 mm and a calculated axial edge lift of 0.15 mm at the overall diameter of 9.5 mm. Care was taken to ensure that there were no bubbles under the BCL when worn by the subjects (de Carle, 1989).

3.6.2 RIGID DIFFRACTIVE BIFOCAL CONTACT LENSES

The rigid diffractive BCL used were made by Pilkington VisionCare. Some CL finishing was performed at City University. All BCL were lathed in Polycon II with a central diffractive zone diameter (CDZD) of 5 mm and had a near addition of 2.00 Dioptres in vivo. The peripheral refractive zone diameter (PRZD) was fixed at 7.5 mm. Apart from some production Pilkington Diffrax BCL, all rigid diffractive BCL were a conventional tri-curve (C3) design with an effective BOZD of 7.5 mm and a calculated edge lift of 0.15 mm at the overall diameter of 9.5 mm.

Diffractive Zone Junction height

Alteration of the DZJ height, as noted in section 1.2.3, should alter the proportion of light in the various diffractive foci. Rigid diffractive BCL with nominal DZJ heights of 1.4 to 5.0 μm were investigated.

Tool shape

Alteration of the diamond tool used to manufacture the diffractive zone surface should alter the shape of the

DZJ. As noted in section 1.2.3, this was expected to alter the optical performance of the diffractive BCL. Diamond tools of 250, 100 and 50 μm diameter and a 250 μm diameter tool with a flatted section as shown in *Figure 3.6-1* were investigated. Combinations of DZJ height and diamond tool which were available are indicated in Table 3.6-1.

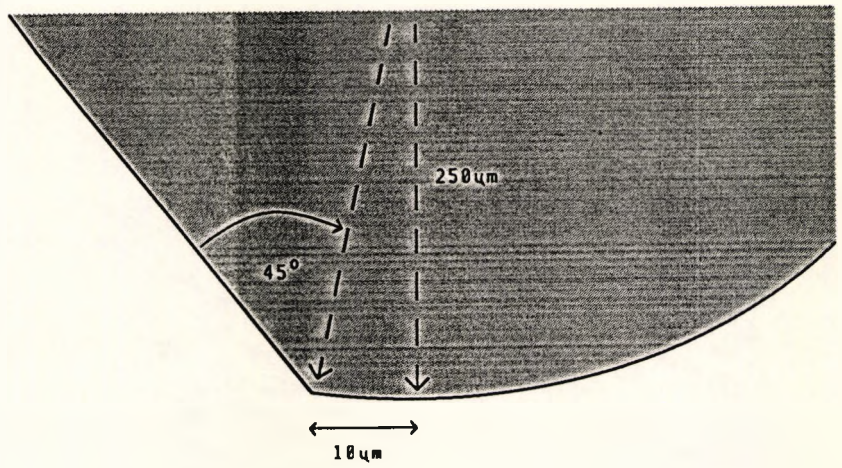

Figure 3.6-1 Diagram of a cross-section of the flatted diamond tool used in manufacture of certain experimental diffractive BCL.

Polish

In the process of manufacturing some diffractive BCL received an unintentional light polish of the diffractive zone surface. As a result the DZJ height and shape were not as specified. These "polished" BCL were mixed with the "unpolished" BCL and had to be examined separately. The polishing was uncontrolled and of varying degree as indicated by interferometric examination.

Nominal DZJ height (μm)	Tool shape			
	250 μm round	100 μm round	50 μm round	250 μm flatted
1.4	1, P			
1.8	1, P	1		1
2.0	1, D, P	2	1	1
2.2	2, P	1		1
2.5	1	1		1
2.6	2, P	1		1
3.0	2, P	1	1	1
4.0	1	1	1	1
5.0		1		

Table 3.6-1 Available experimental rigid diffractive BCL. The number represents the number of repeated production runs. "P" indicates that some BCL of these nominal parameters received an unintentional polish of the diffractive surface. "D" indicates that Pilkington Diffrax BCL were available.

3.6.3 SOFT DIFFRACTIVE BIFOCAL CONTACT LENSES

The soft diffractive BCL used were made by Pilkington VisionCare. All soft BCL were HEMA with a CDZD of 5 mm and had a near addition of either 2.00 or 2.50 Dioptre in vitro.

Diffractive Zone Junction height

Soft diffractive BCL with nominal "dry" DZJ heights of 2.6 to 4.0 μm were investigated.

Tool shape

Diamond tools of 250 and 100 μm diameter and a 250 μm diameter tool with a flatted section as shown in *Figure 3.6-1* were investigated.

Manufacture technique

Soft diffractive BCL were either made by conventional lathing of a HEMA button or by a (Pilkington Visioncare proprietary) moulding technique.

A limited range of combinations of DZJ height, diamond tool and manufacture technique were available as indicated in *Table 3.6-2*.

Nominal "dry" DZJ height (μm)	Tool shape and Manufacture Technique			
	250 μm round Lathed	250 μm Flatted Lathed	100 μm round Lathed	100 μm round Moulded
2.5				1
2.6				1
2.7	1			
3.0	1		1	2 R
3.3		1	1	1
3.6			1	
4.0	1		1	
4.4				1

Table 3.6-2 Available experimental soft diffractive BCL. The number represents the number of repeated production runs. "R" indicates available with a "reverse" addition

Reverse addition

Three soft diffractive BCL with a "reverse" addition (utilises the zero order (near) and minus one order (distance) images) were examined.

Commercially available bifocal contact lens

In addition Allergan Echelon soft diffractive BCL were examined by the same procedures.

3.7 Repeatability coefficients

In accordance with the suggestions of Bland and Altman (1986) the repeatability of both the optical performance measure (MTF) and the visual performance measures (CS, PRC and AVC) was assessed in terms of the variance of the distribution of differences between two measures made on separate occasions (i.e. test-retest). The repeatability coefficient was defined for this study, as recommended by the British Standard Institution (BS 5479 : part 1, 1979), as 1.96 times the standard deviation of the test-retest differences (Bland and Altman, 1986). This is effectively a 95% confidence limit expressed in terms of the units of measurement. In recent years the repeatability coefficient has become the preferred method of assessing the reliability of clinical tests (e.g. Elliott and Sheridan, 1988; Reeves et al, 1991; Wood et al, 1988)

3.8 Multiple Regression Analysis procedures

Multiple Regression Analysis (MRA) was used to model a single dependent variable (e.g. MTF or visual acuity) in terms of both (manipulated) independent variables (e.g. BCL design or DZJ height) and covariates (e.g. pupil size). This allowed an assessment of the influence of the variables and any interaction terms, but more importantly the development of predictive models. To facilitate the selection of appropriate models a two stage procedure was adopted. Initially all terms were forced into the equation in a standard MRA procedure, then a stepwise MRA procedure was used to remove those terms which were statistically redundant. MRA could have lead to over optimistic estimates of predictive power where the independent variables were highly correlated and where the number of terms included in the final equation was large in relation to the sample size (Tabachnick and Fidell, 1983; Winer, 1971). Problems due to multicollinearity (excessive correlation between the independent variables) were reduced by limiting the tolerance and the use of the stepwise procedure (Tabachnick and Fidell, 1983). A range of models was investigated for each analysis, and each model presented in Chapter 4 was considered to be the most appropriate and most useful. All models were examined for a range of possible errors with standard procedures, and in particular the model was devised to obtain an even spread of residuals. This proved particularly important in

section 4.2. The reported multiple correlation (R^2) was adjusted for the number of terms and sample size (Winer, 1971).

Chapter 4 RESULTS

Introduction

Physical measurements of the bifocal contact lenses (BCL) are reported in section 4.1. Subsequent sections examine the optical performance (section 4.2) and visual performance (section 4.3) of both forms of BCL; the measurement of the on-eye longitudinal chromatic aberration with diffractive BCL (section 4.4); and, finally, the development of empirical models to describe visual and optical performance in terms of the physical measures (section 4.5) and visual performance in terms of the optical performance measure (section 4.6).

4.1 Physical Contact Lens Measurements

BCL quality, evaluated by a range of standard procedures is reported in section 4.1.1. The surface profile of the experimental diffractive BCL is reported in section 4.1.2, and includes the first report of measurements of the surface profile of soft diffractive BCL known to the author.

4.1.1 STANDARD CONTACT LENS PROCEDURES

Standard CL measures, as described in section 3.1.1, were used to verify the optical and dimensional quality of the

experimental BCL. The parameters of all experimental BCL were found to be within the British Standard CL tolerances (BSI 5562: 1978). There was no apparent systematic bias in production. The Central Optic Zone (COZ) junction of the refractive BCL was distinct (<5 μm), with no blending for both types (CD or CN) and COZD did not vary from the nominal diameter by more than 0.05 mm. Nominal rather than the measured Central Optic Zone Diameter (COZD) was used for the purposes of the analysis in later sections.

Examination, with a radiuscope, of the rigid diffractive BCL showed two different measurements of Back Optic Zone Radius (BOZR) over the Central Diffractive Zone (CDZ). The weaker image in the radiuscope represented the conventional BOZR, and the brighter image the effective radius of the CDZ and will be referred to as the Central Diffractive Zone Radius (CDZR). This represented the "flatter" curve used to create the diffractive surface. As noted in section 1.2.3, this represented a compromise resulting in a substantial deviation from the theoretical surface profile. This allowed a method of predicting the Diffractive Zone Junction (DZJ) height as DZJ height is a function of CDZR, BOZR and (first order) diffractive focal length (section 1.2.3).

Multiple regression analysis (MRA) indicated that nominal DZJ height was a function of CDZR and BOZR given by the following equation:

DZJ height = 0.629 + 2.552 (CDZR - BOZR) + 0.679 (CDZR - BOZR)^2

(Adjusted R^2 = 0.903; $p < 0.0001$)

The squared term was included for theoretical reasons, but the relationship was equally well described by:

DZJ height = 0.304 + 3.534 (CDZR - BOZR)

(Adjusted R^2 = 0.901; $p < 0.0001$)

These equations are only applicable for BCL with a +2.00 Dioptre addition.

4.1.2 DIFFRACTIVE BIFOCAL CONTACT LENS SURFACE PROFILE

Due to time constraints, only 38 rigid diffractive (27 non-polished and 11 polished) and 4 soft diffractive (3 hydrated and 1 dry) BCL were examined by interferometry. The various measures compared well with the calculated or expected values indicating no systematic errors in the interferometric technique. Aspects of the surface profile are detailed below.

Diffractive Zone Shape

Rigid Diffractive BCL

The interference micrographs, an example of which is shown in *Figure 4.1-1a*, confirmed the shape of the diffractive zones (DZ), which is shown diagrammatically

(a)

(b)

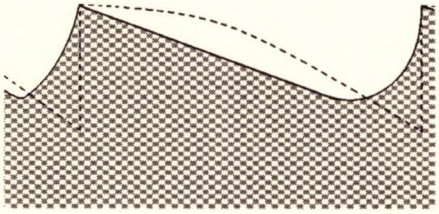

Figure 4.1-1 **(a)** An interference micrograph of a rigid diffractive BCL - 2.2 μm DZJ height, lathed with a 250 μm diamond tool. The second, third and fourth DZJ are shown. There is a broad (approx. 25 μm), shallow (approx. 0.1 μm) tool overshoot at the third DZJ (represented by the third and fourth curved and approximately vertical lines - everything is doubled). There is some variation in the BCL surface shown by the "tremor" in the fringe (grade 1). **(b)** A schematic representation of a cross-section of a diffractive zone of a rigid diffractive BCL. The dotted line represents the ideal shape.

(a)

(b)

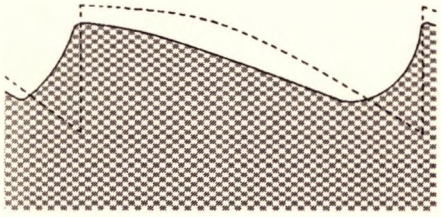

Figure 4.1-2 **(a)** An interference micrograph of a polished rigid diffractive BCL - 2.6 μm DZJ height, lathed with a 250 μm diamond tool. The third, fourth and fifth DZJ are shown. **(b)** A schematic representation of a cross-section of a diffractive zone of a polished rigid diffractive BCL. The dotted line represents the ideal shape.

(a)

(b)

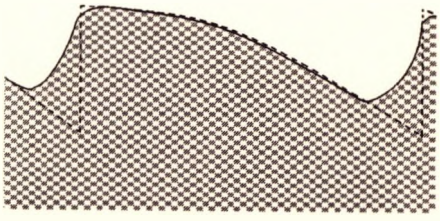

Figure 4.1-3 **(a)** An interference micrograph of an Allergan Echelon soft diffractive BCL. The third, fourth and fifth DZJ are shown. **(b)** A schematic representation of a cross-section of a diffractive zone of an Allergan Echelon soft diffractive BCL. The dotted line represents the ideal shape. The shape was determined empirically and may not match the theoretical shape as closely as implied in this diagram.

in *Figure 4.1-1b*. The experimental soft diffractive BCL had the same DZ shape.

Polished Rigid Diffractive BCL

As shown in *Figure 4.1-2* the shape of the DZ was modified by the unintentional polishing (section 3.6.2) of the diffractive section of the BCL back surface. The profile became slightly rounded at the higher sections of the DZ, and became effectively more like the theoretically ideal shape.

The Echelon Soft Diffractive BCL

The Allergan Echelon soft diffractive BCL have a DZ with a different profile as shown in *Figure 4.1-3*. This was matched empirically, and was closer to the ideal parabolic form of the DZ (Lesem et al, 1969; Emerton et al, 1987), though the highest point of the DZ has been distinctly rounded.

Diffractive Zone Junction Height

Rigid Diffractive BCL

It was possible to differentiate between rigid diffractive BCL of different DZJ heights, and, as shown in *Figure 4.1-4*, the measured DZJ height varied with the nominal DZJ height. Averages of the measured DZJ height from all BCL of the same nominal value BCL were found to be significantly different ($p < 0.0001$) from each other.

The measured DZJ height of all BCL was found to vary between DZJs (i.e. DZJ height was not consistent across a BCL). As shown in *Figure 4.1-5*, there was no consistent

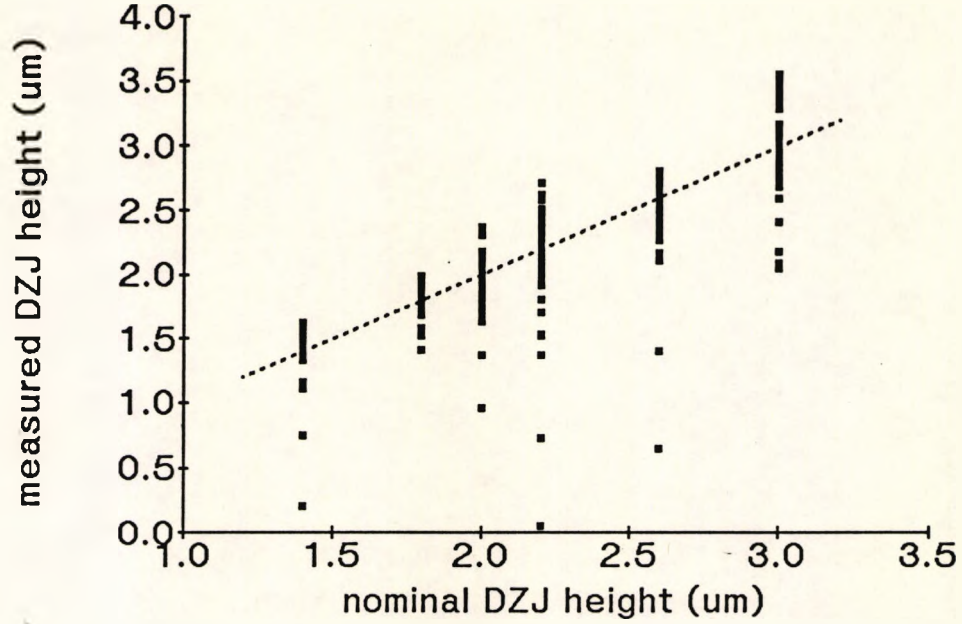

Figure 4.1-4 Measured DZJ height varied with nominal DZJ height of rigid diffractive BCL. There was considerable variability on certain BCL, in particular the first DZJ, which were almost all well below the dotted line which represents the expected DZJ height. Regression analysis r^2 = 0.64 and the slope did not vary significantly from 1.

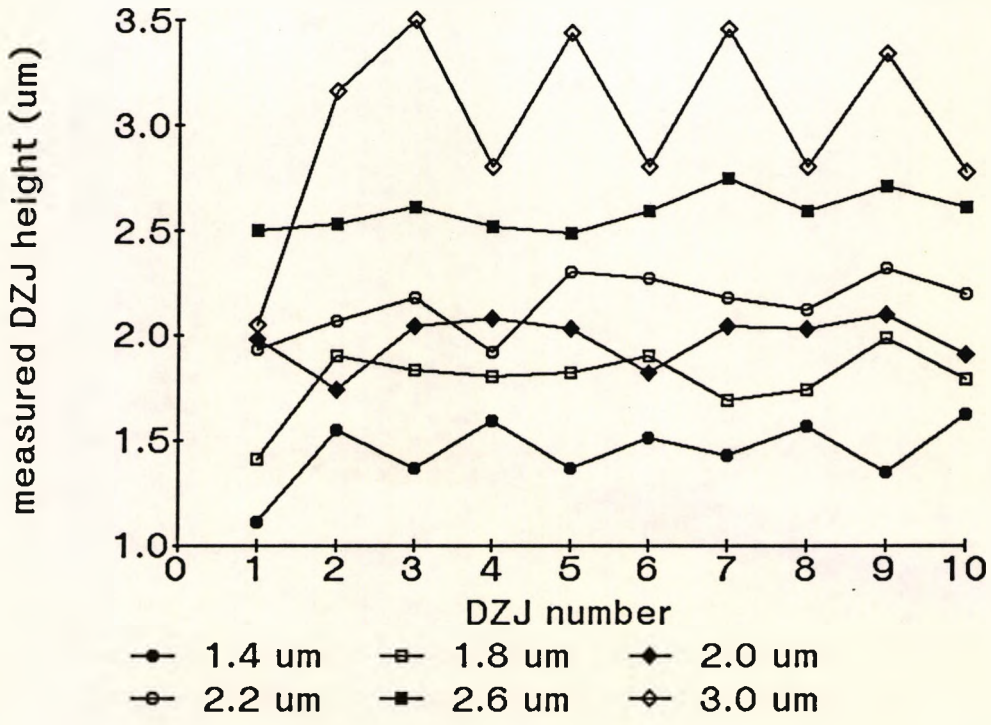

Figure 4.1-5 Examples of the measured DZJ height of six arbitrarily chosen rigid diffractive BCL of nominal DZJ heights as shown.

trend to the variation except that the first DZJ was significantly smaller than the other DZJs. Though there was no trend, certain BCL were found to be very consistent in the measured DZJ height, whilst other BCL had large variations between DZs. There was no common pattern to this variation.

As the average measured DZJ height was highly correlated with the nominal DZJ height (r^2 = 0.64), for the purposes of later analyses nominal DZJ height was considered.

Polished rigid diffractive BCL

The unintentional polishing of certain rigid diffractive BCL, as shown in *Figure 4.1-6*, reduced the DZJ height by an average 0.44 μm as compared to the nominal DZJ height.

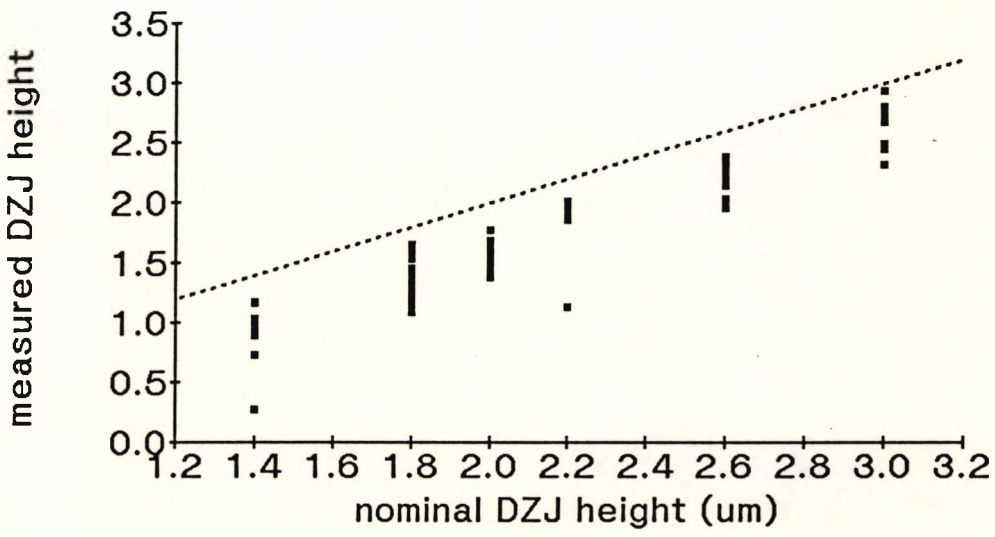

Figure 4.1-6 Measured DZJ height varied with nominal DZJ height of polished rigid diffractive BCL and was less than expected (dotted line). The variability between zones was less than noted with the non-polished BCL, but the first DZJ remained typically smaller than the other DZJ. Regression analysis r^2 = 0.91 and the slope did not vary significantly from 1.

Soft Diffractive BCL

As shown in *Figure 4.1-7*, as expected, the measured DZJ height of the dry (unhydrated) soft diffractive BCL was the same as the nominal DZJ height, and the DZJ heights of the two measured hydrated soft diffractive BCL were larger than the nominal DZJ height.

The effect of variations in DZJ height

The effect of the irregularities in DZJ height is uncertain, but incorrect DZJ heights may create unwanted half phase variations placing light into other orders, or spreading light between the two bifocal foci. Edwards and Freeman (1989) calculated that significant reductions in the height of the first DZJ markedly reduced optical performance (modulation transfer function) of diffractive BCL.

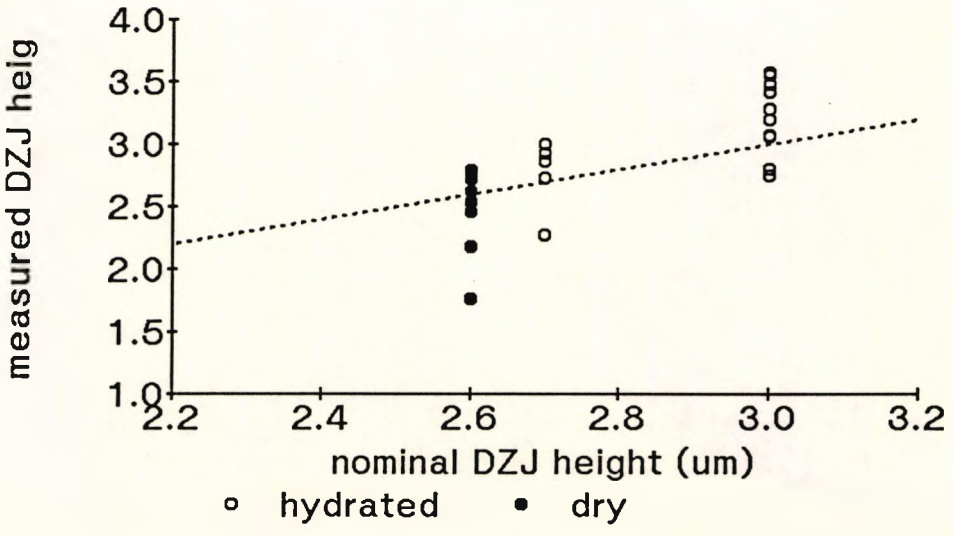

Figure 4.1-7 Measured DZJ height varied with nominal DZJ height of soft diffractive BCL. As expected the DZJ height of the hydrated soft BCL were greater than the nominal DZJ height.

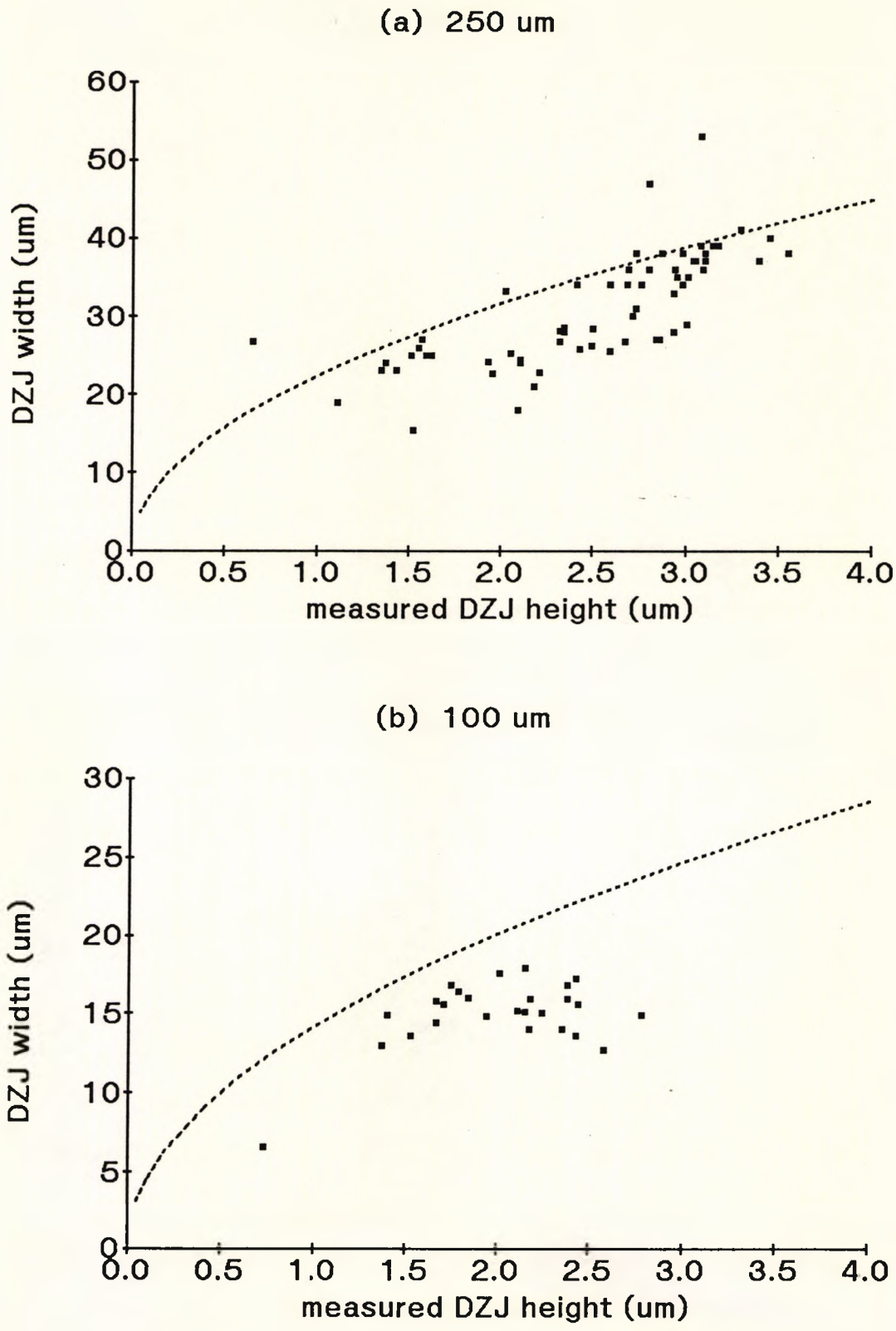

Figure 4.1-8 DZJ width versus DZJ height. The DZJ width is a measure of the finite tool effect, which was expected to vary with DZJ height and tool shape (dotted line). This is shown for rigid diffractive BCL manufactured with **(a)** 250 μm; and **(b)** 100 μm round diamond tool. Note the difference in scale.

Diffractive Zone Junction Width

The width of the DZJ represents the "finite tool effect" (section 1.2.3). As shown in *Figure 4.1-8*, this varied with tool shape and DZJ height as expected by calculation. There was an apparent tendency to underestimate the DZJ width (compared to the calculated value), which was most probably due to the difficulty in determining the precise location of the commencement and conclusion of the DZJ.

Diffractive Zone Annulus Width

Rigid Diffractive BCL

Figure 4.1-9 shows that the measured DZA width was as expected (*Equation 1.2-1*). There was no consistent variation between BCL. As the maximum error in the optical power of the diffractive foci (*Equation 1.2-1*) expected from the measured DZA widths was less than 0.125 Dioptre, the BCL were considered acceptable. Polishing had no effect upon DZA width.

Soft Diffractive BCL

The three measured soft diffractive BCL had a 2.5 Dioptre Add and hence the DZA widths were expected to differ from the rigid diffractive BCL which all had a 2.00 Dioptre Add. As shown in *Figure 4.1-10*, as expected, the DZA widths of the hydrated soft BCL were larger than the dry soft BCL.

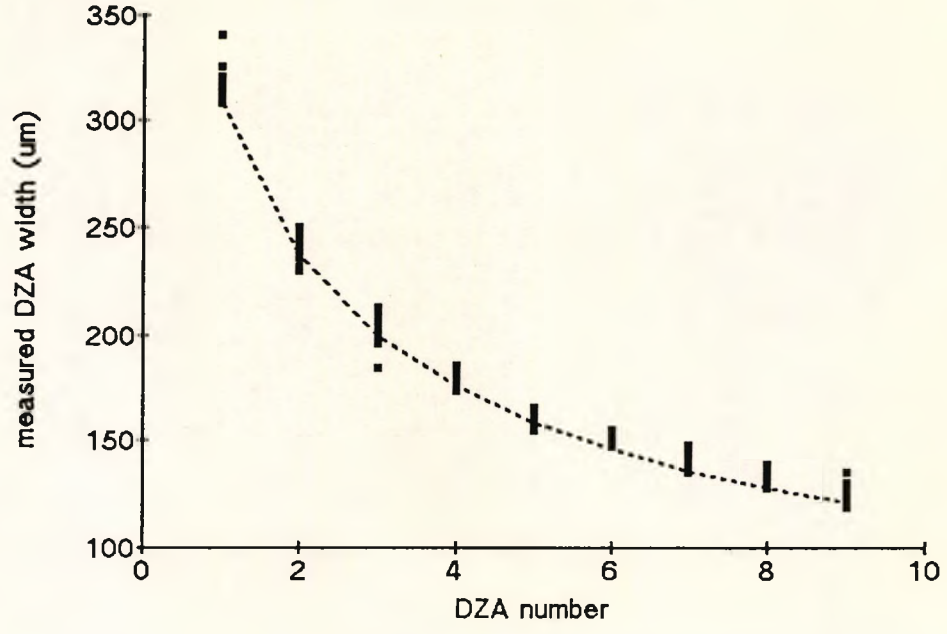

Figure 4.1-9 The measured diffractive zone annulus (DZA) width of rigid diffractive BCL was similar to the expected values (dotted line).

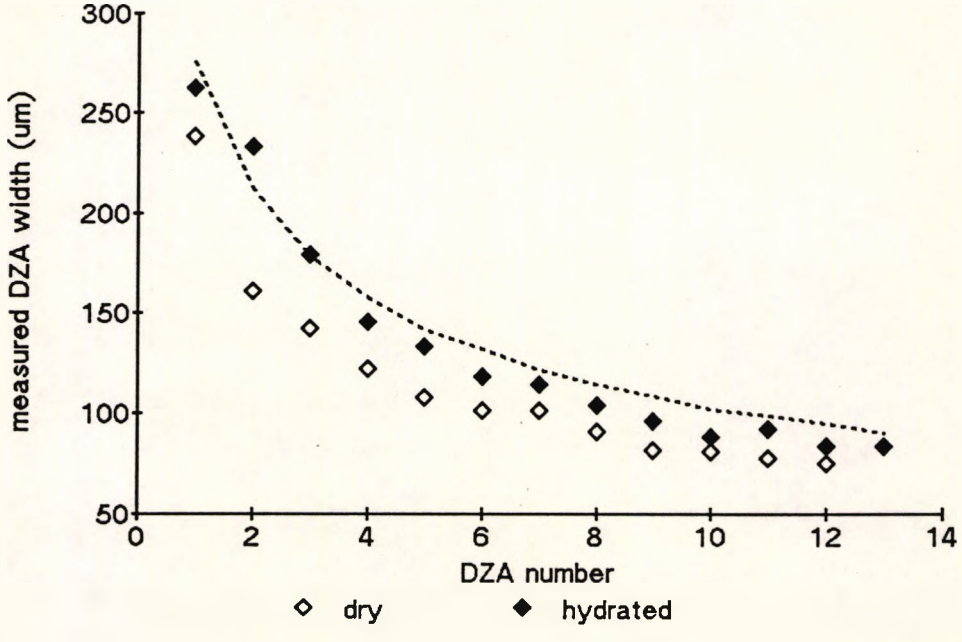

Figure 4.1-10 The measured diffractive zone annulus (DZA) width of soft diffractive BCL was similar to the expected values (dotted line) for the hydrated BCL, but, as expected, the DZA widths of the dry soft BCL were smaller.

Surface Effects

Fringe Appearance Grading Scale

The distribution of fringe appearance grades (section 3.1.2) is shown in *Figure 4.1-11* for the different diffractive BCL types and tools. The majority of BCL were grade 1 or 2 (<0.07 μm or 0.07 to 0.14 μm). Only one rigid BCL with each of the 50 μm round and 250 μm flatted tools was examined, but both of these were rated as grade 3 (0.15 to 0.27 μm). Virtually all the polished rigid BCL were rated as grade 0. *Figure 4.1-12* shows an interference micrograph of the BCL rated grade 4 (variations >0.27 μm i.e. 1 fringe width).

The fringe appearance indicated the quality of the machined BCL surface which could be affected by the shape of the diamond tool, damage or wear to the tool, speed of lathe rotation, material qualities and movements (e.g. vibration) in the lathe. As the material and the lathe were the same for all BCL, the changes in surface quality noted probably relate to the diamond tool.

Changes in surface quality of up to a quarter wavelength (grade 2) fall within the Rayleigh criteria. This theoretical consideration of a quarter wavelength was contrived with regards large scale but small deviations from the required surface in e.g. a telescope lens. A surface with numerous small changes in relative position may result in increased scatter. It was expected that increased scatter would not be detected by MTF

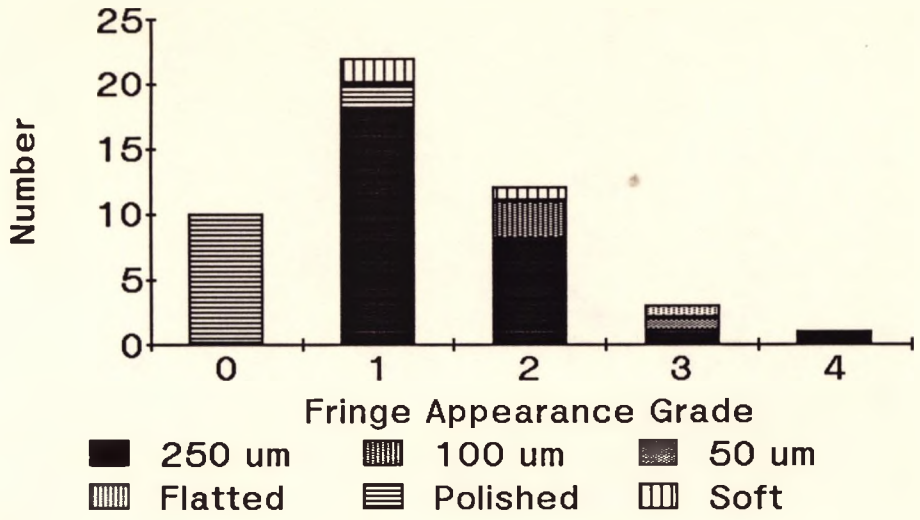

Figure 4.1-11 The distribution of fringe appearance grade (*Table 3.1-1*) for the different diffractive BCL types and tools.

Figure 4.1-12 An interference micrograph of the BCL rated grade 4 (variations >0.27 μm i.e. 1 fringe width).

measurements due to certain assumptions made in the calculation of MTF, but might result in a reduced visual performance.

A significant ($p < 0.001$) reduction in the optical performance (average MTF) with worsening fringe appearance, as shown in *Figure 4.1-13*, was found. This was apparent at all spatial frequencies. Visual performance measures did not demonstrate this trend. The reduction in optical performance may have been due to other characteristics of the BCL which were uncontrolled (e.g. average DZJ height varied between the groups).

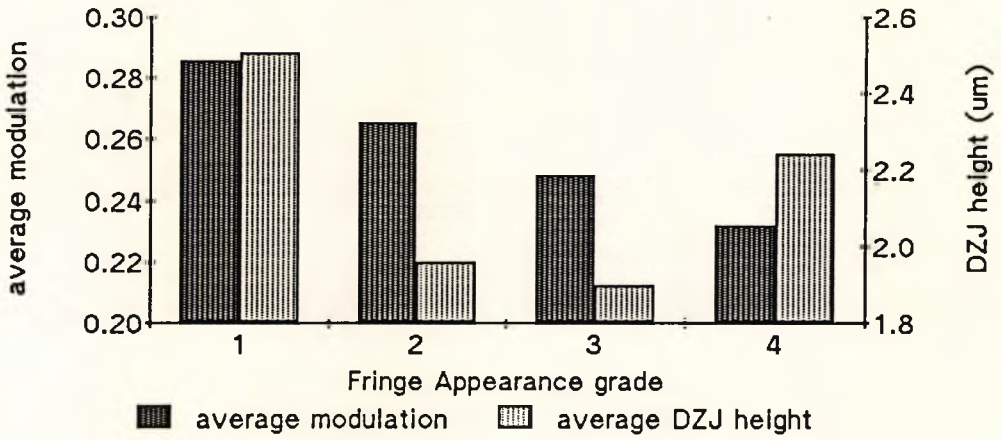

Figure 4.1-13 Optical performance (average MTF) reduced with increasing surface roughness (fringe appearance grade). Other aspects of BCL design were not equal between the groups, and as an example, the average DZJ height varied between the groups.

Irregularities at the Diffractive Zone Junction

The shape of the DZJ varied between BCL, with some BCL having a consistently well formed DZJ, whilst the DZJ shape of other BCL varied between DZJ. Irregular DZJ shape was most common and largest for the first DZJ.

Typically the irregularity at the DZJ would vary at different points around the circumference of the DZJ.

The DZJ irregularity was created as the lathe altered location to produce the DZJ. Inaccurate relocation of the BCL surface laterally could result in a "ridge" if the position of the tool when it commenced the new zone was slightly beyond the point from which it was withdrawn (*Figure 3.1-4a*). A failure to accurately relocate the BCL surface vertically could result in a variation in DZJ height from that required, but if only momentary could result in a "groove" (*Figure 3.1-4b*). The "groove" at the lower edge of the DZJ was most common.

No consistent effect of the DZJ irregularity upon optical or visual performance was noted. This may be related to the limited field of view of the interferometric technique, such that the measurement at a single point may not represent the overall effect at a particular DZJ.

4.2 Optical Performance

4.2.1 INTRODUCTION

This section considers the performance of the Modulation Transfer Function (MTF) measurement equipment (section 4.2.2), the optical performance (measured in terms of the Line Spread Function (LSF), MTF and Critical Frequency

(CF : section 3.2) of the experimental rigid refractive (section 4.2.3), rigid diffractive (section 4.2.4) and soft diffractive (section 4.2.5) BCL, and two commercially available diffractive BCL (sections 4.2.4 and 4.2.5). More than 1800 separate MTF measurements were made, each at 16 spatial frequencies. Hence it was not possible to present all the data, and, where appropriate, examples, typically of averaged data, have been used to illustrate important aspects of the data. Analysis of Variance (ANOVA) was used to investigate the influence of the manipulated variables. Multiple Regression Analysis (MRA) was used to further investigate the often complex relationships. Empirical models, expressed as polynomial equations were developed to allow the prediction of optimal BCL designs.

4.2.2 SYSTEM PERFORMANCE

Aperture Size and Wavelength

Figure 4.2-1 shows the MTF measured with no experimental CL in situ for apertures from 2 to 6 mm at 548 nm. Similar variations with aperture were found with the other filters. The improvement in MTF with increasing aperture was expected (Freeman, 1990). *Figure 4.2-2* shows the slight variation in MTF with wavelength. These results show the optical limits of the experimental apparatus and proved to be virtually indistinguishable from the calculated diffraction limit of the system. Results with single

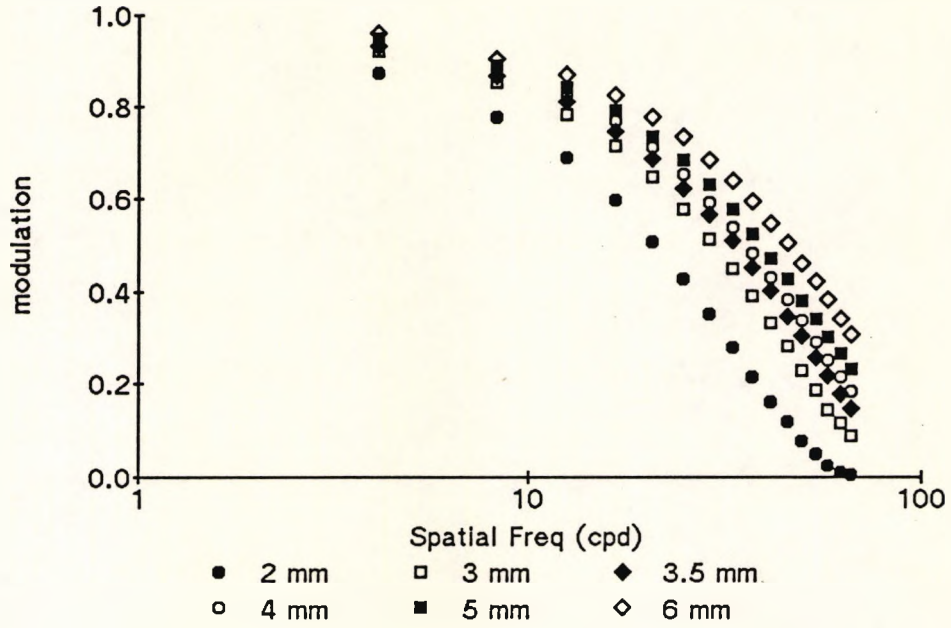

Figure 4.2-1 The variation in MTF with aperture for the system including the wet cell and the 548 nm interference filter but no experimental BCL.

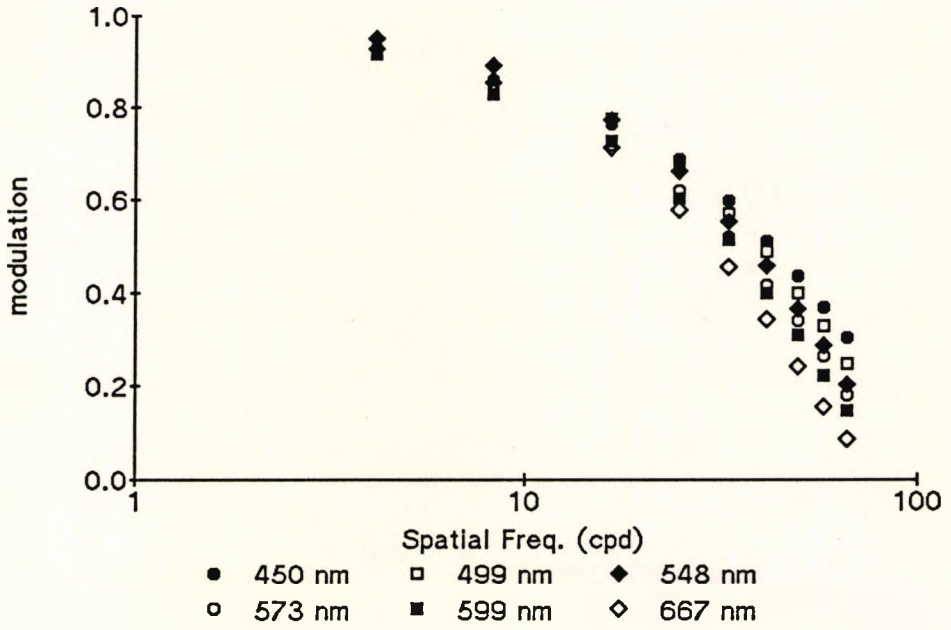

Figure 4.2-2 The variation in MTF with wavelength for the system and the experimental interference filters (3.2 mm aperture).

vision CL were not significantly different (Gray and Sheridan, 1988).

Bifocal Contact Lenses

The MTF measured with centre near (CN) refractive BCL is shown in *Figure 4.2-3* and with diffractive BCL in *Figure 4.2-4*. As described previously (section 1.2) the MTF was reduced compared to a single vision CL.

Repeatability

A typical example of five repetitions of the MTF measurement is shown in *Figure 4.2-5*. To assess the overall repeatability, 75 different rigid diffractive BCL, were measured, at 548 nm, at distance and near, twice on separate occasions (at least days apart). *Figure 4.2-6* shows that the difference in modulation between test and retest was greater at higher average modulation and lower spatial frequency. The test-retest repeatability coefficients (section 3.7) are shown in *Figure 4.2-7*. The manufacturer quoted an error of 1% (equivalent to a repeatability coefficient of 0.01 modulation) for MTF measurement. Thus with BCL, a degraded optical image, the repeatability was worse than expected with all spatial frequencies examined.

The repeatability coefficient of CF was found to be ±12.8 c.p.d. (n = 150), and there was a slight tendency for greater variance at larger values of CF.

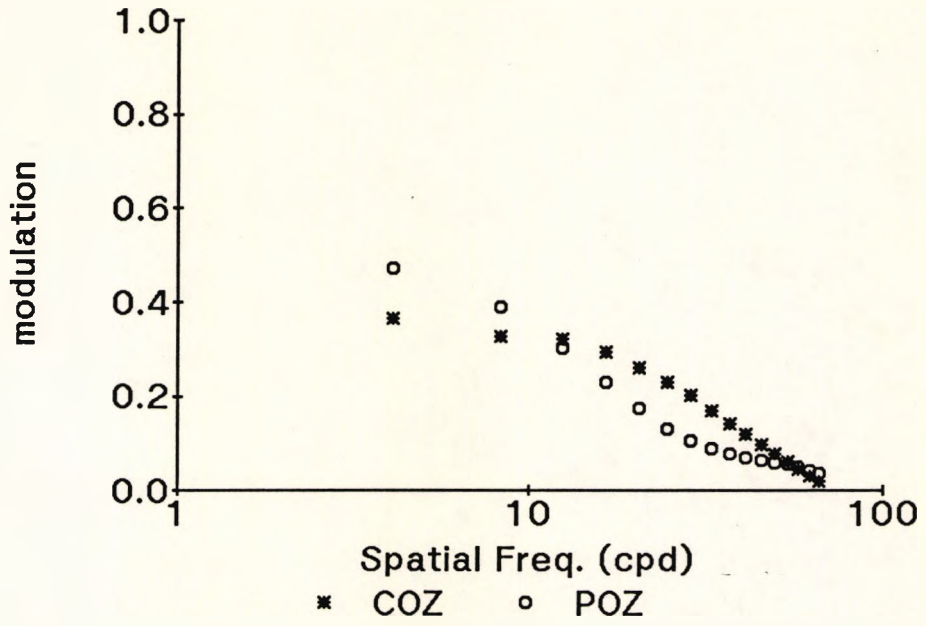

Figure 4.2-3 The mean MTF for centre near refractive BCL (2.6 mm COZD) over a 4 mm aperture (s.d. reduces from 0.041 at 4 c.p.d. to 0.004 at 66 c.p.d.; n = 6).

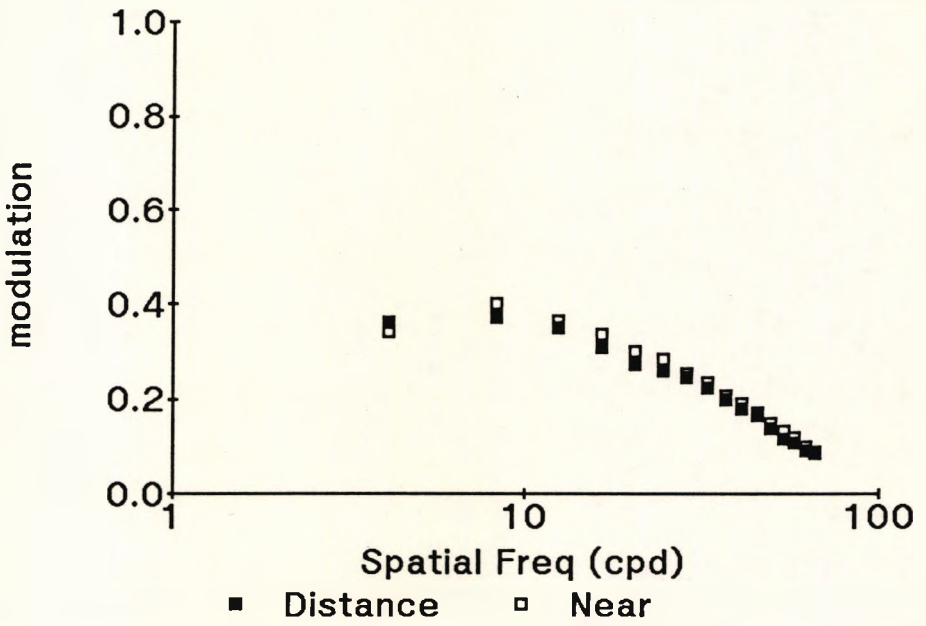

Figure 4.2-4 The mean MTF for rigid diffractive BCL (2.0 μm DZJ height; 250 μm tool) over a 3.5 mm aperture with the 548 nm interference filter (s.d. reduces from 0.063 at 4 c.p.d. to 0.016 at 66 c.p.d.; n = 18).

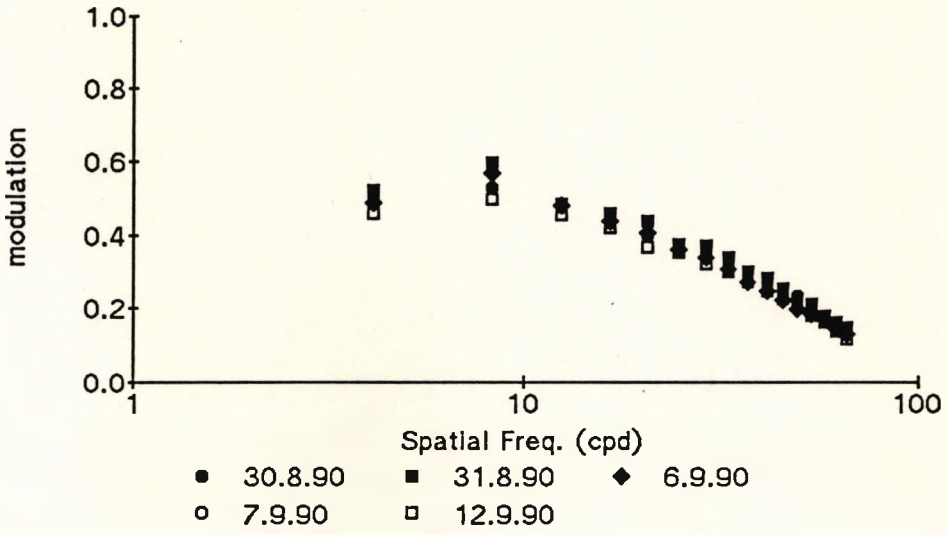

Figure 4.2-5 Five repetitions, on separate days, of MTF measurement of the distance focus of a rigid diffractive BCL (2.6 μm DZJ height, 250 μm tool).

Correlation between spatial frequencies

The correlation (R^2), for all MTF measurements with BCL (n = 1802), between each of the 16 spatial frequencies was very high (range : R^2 = 0.996 between adjacent spatial frequencies, to R^2 = 0.680 between the most distant spatial frequencies). Principal component analysis indicated that the measured modulation could be represented by a single component (i.e. the measured MTF did not contain separate spatial frequency components).

4.2.3 REFRACTIVE BIFOCAL CONTACT LENSES

The optical performance with refractive BCL was firstly examined with the BCL centred over the aperture (pupil); and secondly with the BCL decentred over the aperture. Data with centred refractive BCL were analysed with ANOVA. Since not all combinations of COZD, aperture and

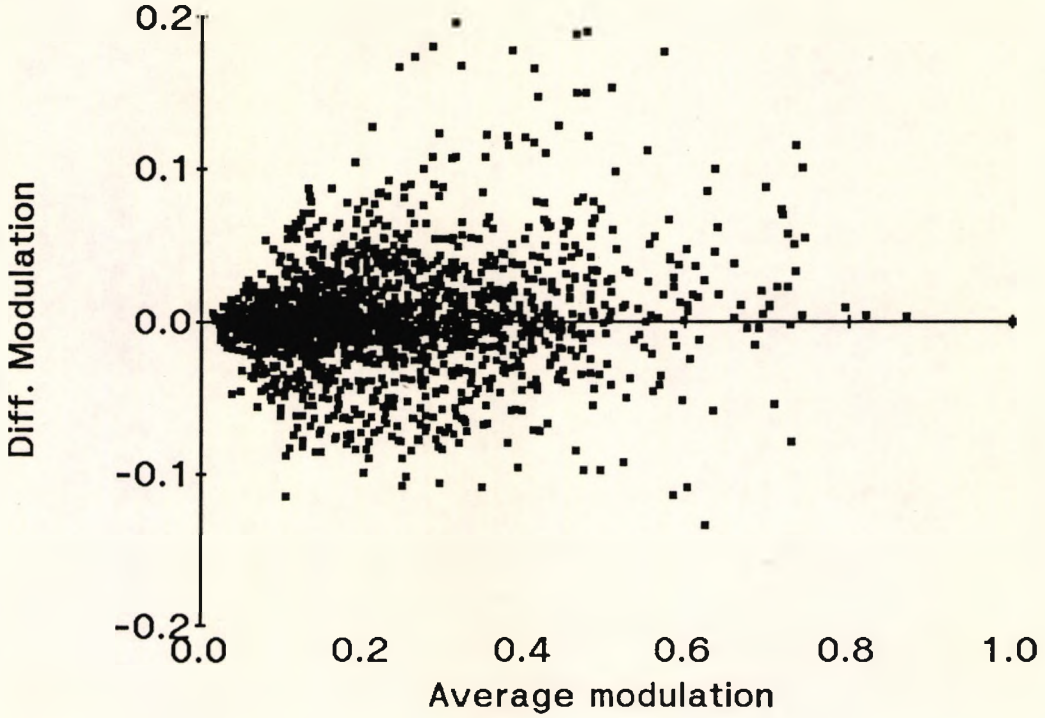

Figure 4.2-6 Test-retest versus average modulation. The spread of the test-retest difference increased with average modulation (distance and near at 16 spatial frequencies) for 75 different rigid diffractive BCL (n = 75 x 2 x 16).

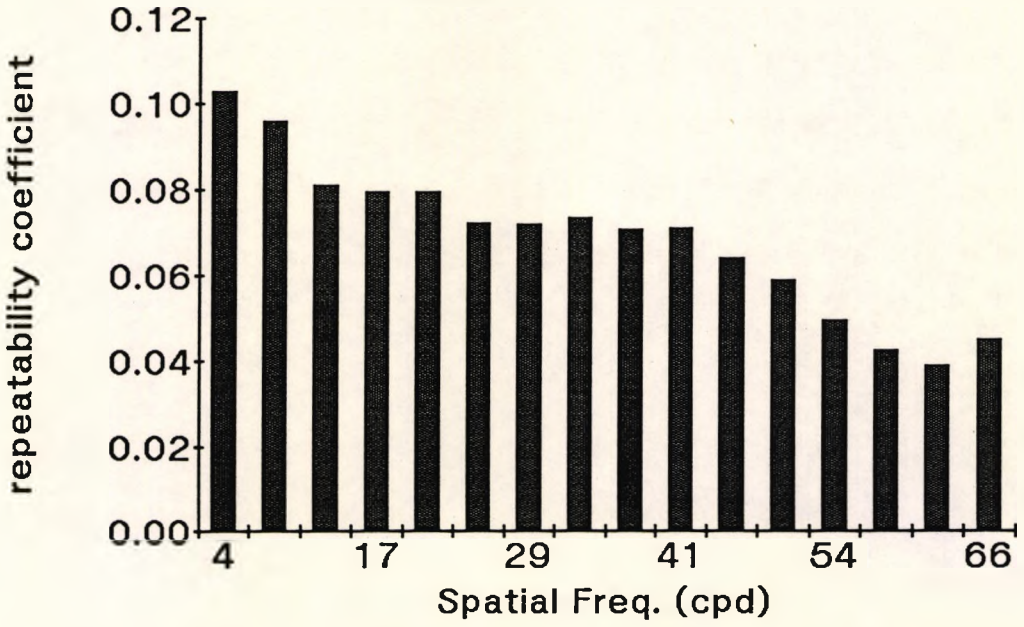

Figure 4.2-7 The variation in the repeatability coefficient (2 x standard deviation) with spatial frequency.

decentration were studied, ANOVA of restricted data was used as a preliminary step prior to MRA. The MRA equations allowed the prediction of the optimal COZD for a given aperture, decentration and spatial frequency. The equations were also used to predict visual performance by incorporating the measured pupil size and on-eye BCL decentration in section 4.6.1.

Centred Refractive Bifocal Contact Lenses : Aperture Size and Central Optic Zone Diameter

The MTF and CF varied with aperture size and with COZD at both distance and near. As examples, this is shown in *Figure 4.2-8* for the 2.6 mm COZD, and in *Figure 4.2-9* for the 4 mm aperture.

The relationship between lens design (CD or CN), vergence (distance or near), COZD (D), aperture (P) and spatial frequency (F) was initially examined with ANOVA. This indicated that there was a significant difference ($p < 0.001$) between CD and CN lens optical performance if the COZ and POZ were considered (i.e. the distance focal performance with a CD lens was the same as the near focal performance with a CN lens). The CD BCL were significantly better with both COZ and POZ forming the focus as shown in *Figure 4.2-10* ($p < 0.001$). Whilst the standard errors were very small, allowing significant differences to be demonstrated between the BCL types, the standard deviations were larger than the actual values of the average modulation. In addition, there were no

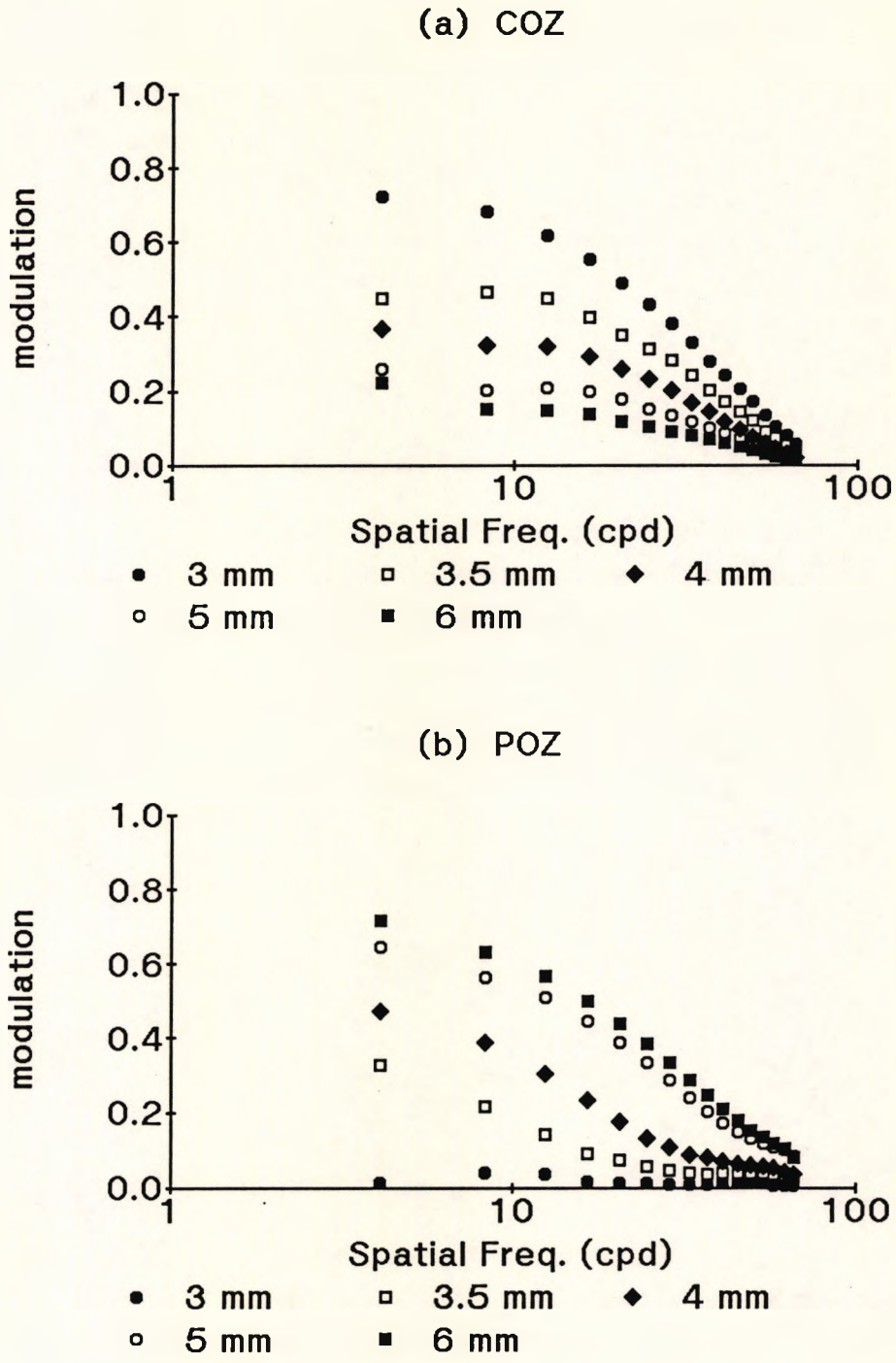

Figure 4.2-8 The variation in MTF with changes in aperture for refractive BCL with a 2.6 COZD and **(a)** the COZ forming the focus or **(b)** the POZ forming the focus.

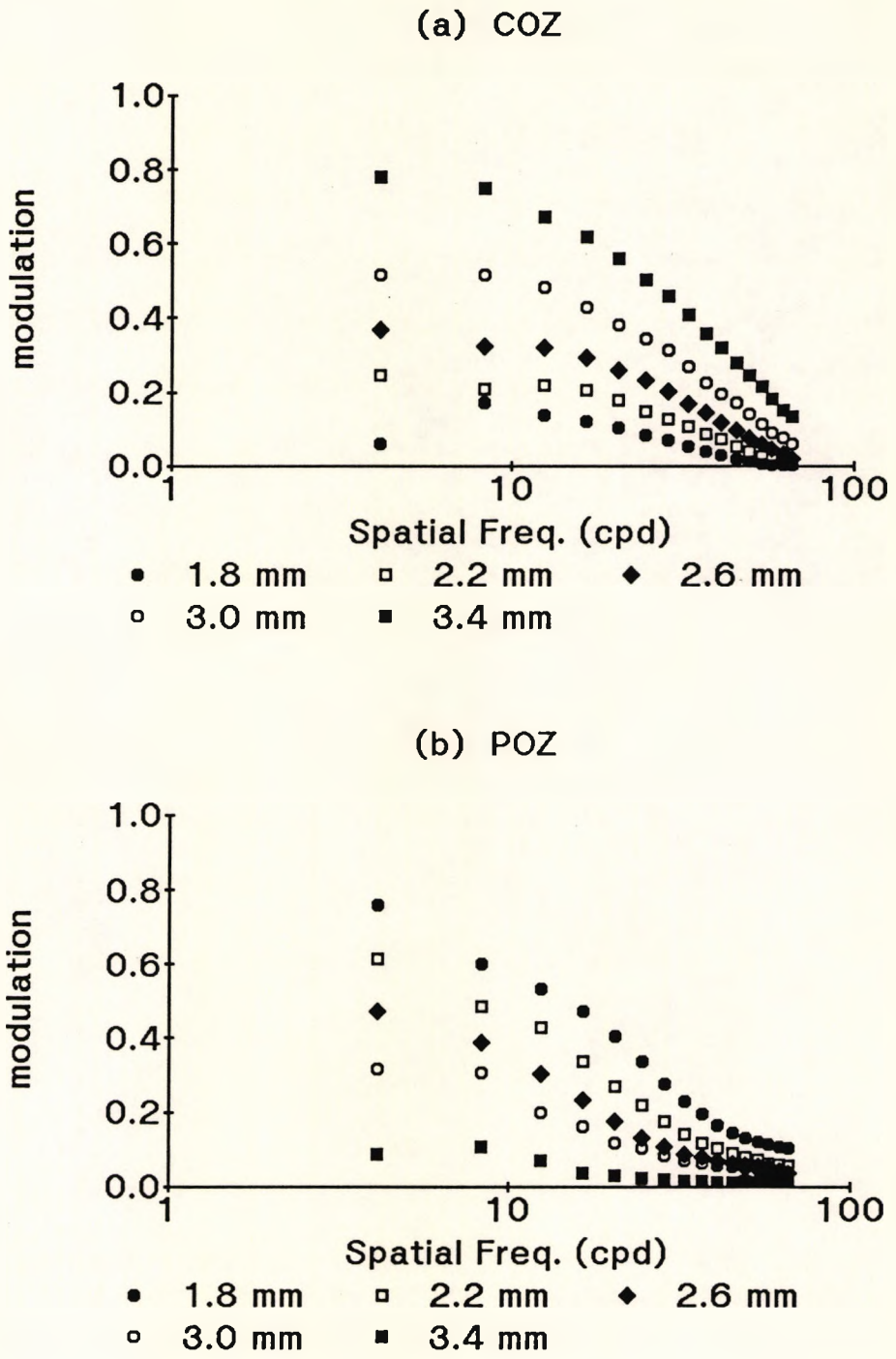

Figure 4.2-9 The variation in MTF with changes in the COZD of refractive BCL over a 4 mm aperture and **(a)** the COZ forming the focus or **(b)** the POZ forming the focus.

significant higher order interactions which included these two factors (lens design and vergence). Hence, for the purposes of this analysis the effect was not considered important. Removal of these interactions from the ANOVA significantly reduced the complexity of the analysis. Thus it was satisfactory to only consider the optic of the lens which is in-focus by combining the factors lens design and vergence to form the factor Optic (O), which was crossed with the other factors. Results of the ANOVA are given in *Appendix 5 (A5-1)*.

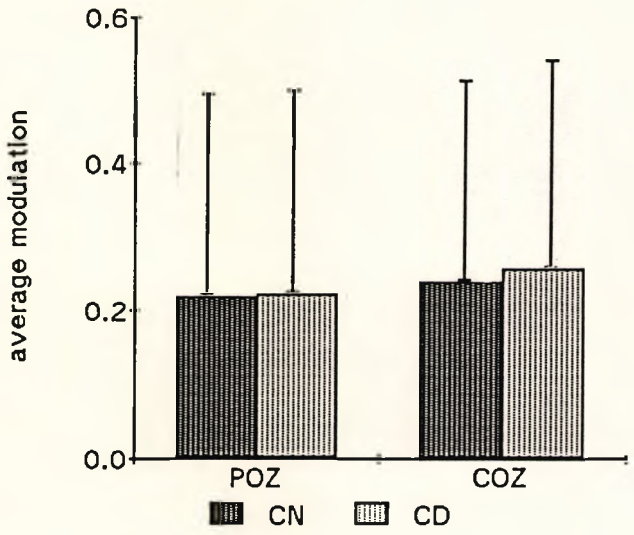

Figure 4.2-10 The average modulation of all centre near (CN) and all centre distance (CD) refractive BCL with the peripheral optic zone (POZ) and the central optic zone (COZ) forming the focus. The differences shown were significant ($p < 0.001$; standard error varied from 0.007 to 0.008 as $n = 1148$ to 1561). Error bars represent standard deviation.

All factors and interactions were highly significant ($p < 0.001$). As expected, the interaction O x D confirmed that as COZD increased the MTF of the image formed with the COZ in-focus improved while the MTF formed with the POZ in-focus reduced and vice-versa (*Figure 4.2-9*).

Similarly the interaction O x P confirmed the effect of the changes in aperture shown in *Figure 4.2-8*. The interaction O x D x P indicated that the changes in COZD varied with aperture. Changes in MTF with spatial frequency (interactions O x F; O x D x F; O x P x F) are also illustrated in *Figures 4.2-3, 4.2-8 and 4.2-9*, where at lower spatial frequencies the MTF with POZ forming the focus were better, whilst this was reversed at higher spatial frequencies.

Centred Refractive Bifocal Contact Lenses : A model for changes in MTF

An empirical model for changes in MTF was developed, using MRA, to allow the prediction of the MTF with a given COZD, aperture and spatial frequency. This would then allow prediction of an optimal COZD (equal distance and near optical performance) which can be compared to the visual performance measures. The development of the model is given in *Appendix 6*.

The final MRA model of optical performance included variations in the MTF with all five available COZD over apertures from 2 mm to 6 mm. The equations were :

<u>for central optic zone :</u>

$$\begin{aligned} mod = {} & 1 - 0.2\,sf + 0.01\,sf^{2} - 0.7\,sf^{-1} + 0.1\,sf^{-3} \\ & + aperture \times (0.06\,sf + 0.002\,sf^{2} - 0.3\,sf^{-1} - 0.3\,sf^{-2} - 0.006\,sf^{-3}) \\ & + COZD \times (0.03\,sf - 0.003\,sf^{2} + 0.2\,sf^{-1} + 0.4\,sf^{-2} - 0.2\,sf^{-3}) \\ & + COZD \times aperture \times (0.005\,sf - 0.0005\,sf^{2}) \end{aligned}$$

<u>for peripheral optic zone :</u>

$$\begin{aligned} mod = {} & 1 - 0.3\,sf + 0.03\,sf^{2} - 0.9\,sf^{-1} + 0.3\,sf^{-3} \\ & + aperture \times (0.05\,sf - 0.004\,sf^{2} + 0.2\,sf^{-1} - 0.06\,sf^{-3}) \\ & + COZD \times (0.05\,sf - 0.004\,sf^{2} - 0.6\,sf^{-1} + 0.7\,sf^{-2} - 0.2\,sf^{-3}) \\ & + COZD \times aperture \times (-0.01\,sf + 0.001\,sf^{2}) \end{aligned}$$

(adjusted $R^2 = 0.949$; s.e. = 0.062; n = 5449; $p < 0.0001$).

Where the modulation (mod) is given in terms of the spatial frequency (sf). Full details of the MRA have been included in *Appendix 5 (A5-2)*. Such complex equations were required due to the shape of the MTF (the sf terms give an even spread of residuals) and the interactions between COZD, aperture and spatial frequency (ANOVA). Though simpler MRA equations were possible, as the equations were to be used for prediction of optical performance, the large number of terms was retained.

The MRA equations were tested by comparing the actual data and predicted MTF for arbitrarily chosen combinations of COZD and aperture. Examples are given in *Figure 4.2-11*. The MRA prediction of the MTF for the 1.8 mm COZD over a 2 mm aperture was less convincing than the other two examples. This example was at the very limits of the range of COZD and aperture combinations, and further examination indicated that other combinations were generally better.

The solution of these equations for equal modulation with focus by the COZ and by the POZ (equal distance and near) showed a variation in the optimal COZD with aperture and spatial frequency which is demonstrated in *Figure 4.2-12*. As suggested by examination of *Figure 4.2-3* and earlier reports (O'Neill, 1956) the predicted optimal COZD was smaller for median than low or high spatial frequencies.

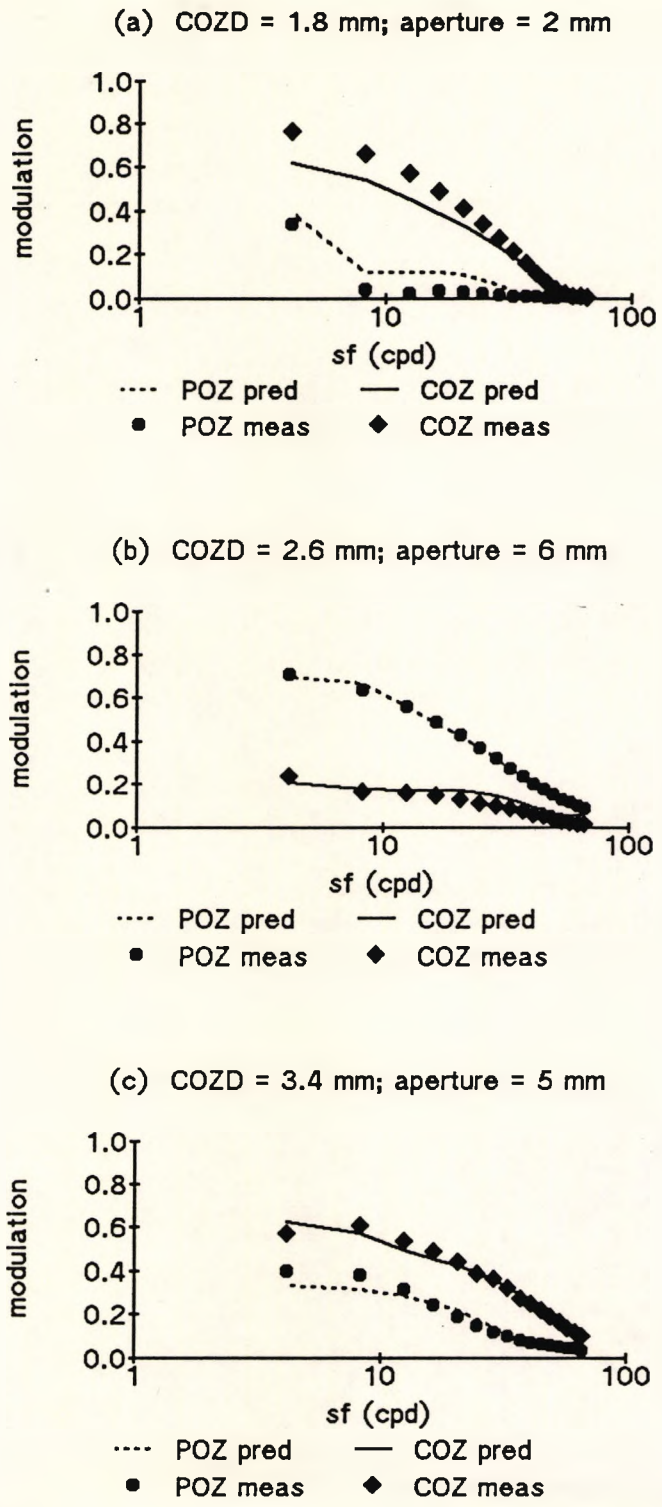

Figure 4.2-11 Evaluation of the MRA equations for centred refractive BCL. Predicted MTF (open) versus measured MTF (filled) with the COZ (diamond) or the POZ (circle) forming the focus for arbitrarily chosen combinations of COZD and aperture **(a)** COZD = 1.8 mm, aperture = 2 mm; **(b)** COZD = 2.6 mm, aperture = 6 mm; and **(c)** COZD = 3.4 mm, aperture = 5 mm.

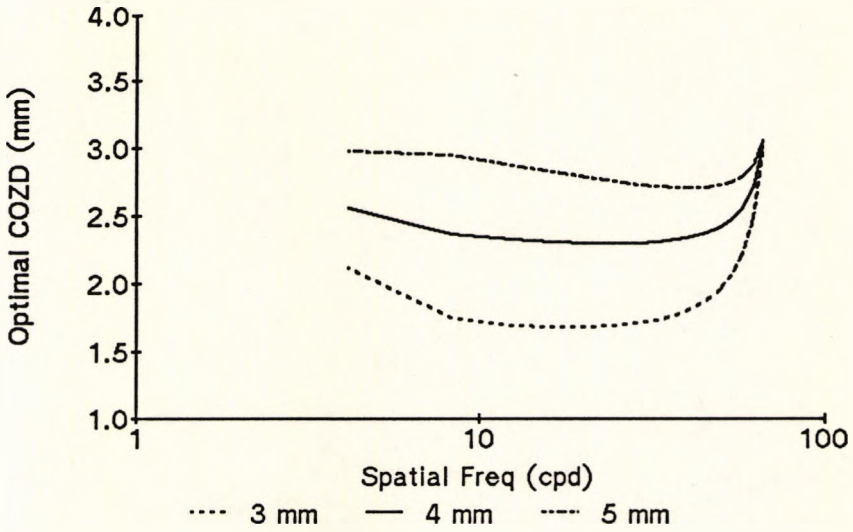

Figure 4.2-12 The optimal COZD (equal distance and near) of refractive BCL over different apertures which is predicted by the MRA equations varies slightly with spatial frequency. (s.e. = 0.087)

Decentred Refractive Bifocal Contact Lenses: Aperture size, COZD and decentration

Each of four 2.6 mm COZD BCL were progressively decentred across 3, 4 and 5 mm apertures, and four 1.8 mm COZD and four 3.4 mm COZD BCL were decentred over a 4 mm aperture. An example of the effect of decentration upon the measured LSF is shown in *Figures 4.2-13* and *4.2-14*. With increasing decentration, as shown in *Figure 4.2-15*, there was little change in CF for the POZ, and a reduction for the COZ. As shown in *Figure 4.2-16*, the MTF also varied with decentration, and similarly the reduction was greater for the COZ than for the POZ. The effect of decentration varied with COZD and with aperture size and was greatest with smaller apertures. The effect became more marked once the COZ was no longer fully within the aperture, and

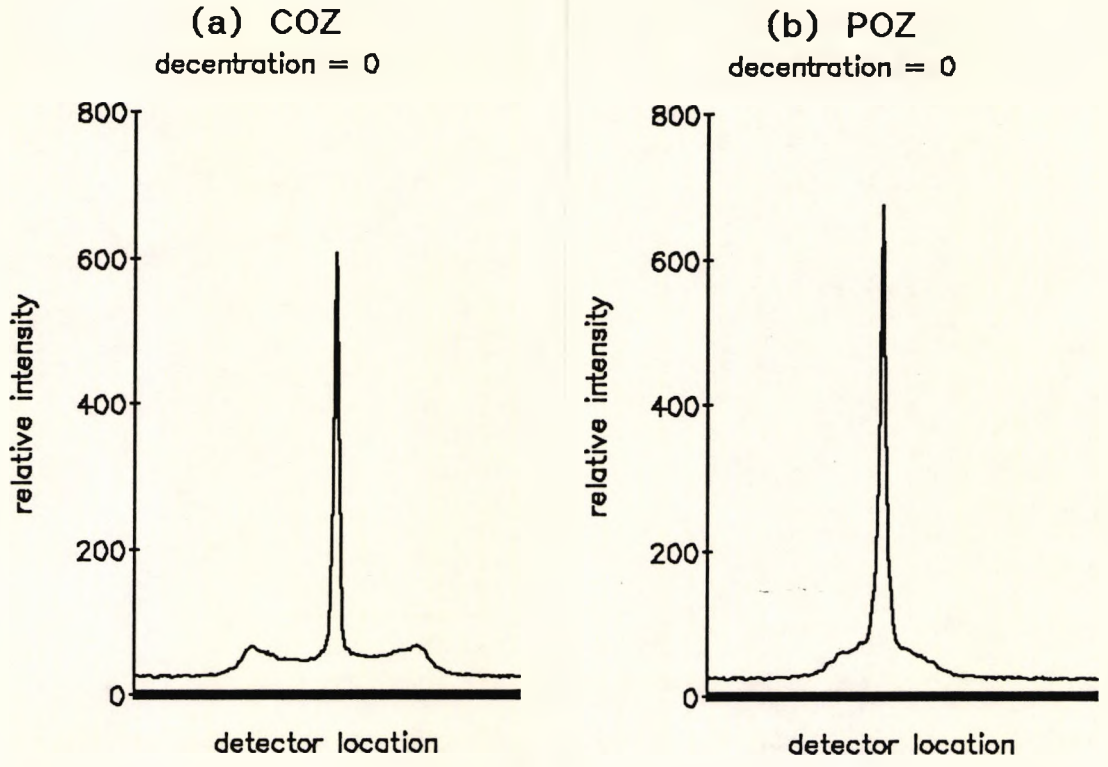

Figure 4.2-13 The measured LSF of a refractive BCL with a 2.6 mm COZD centred over a 4 mm aperture with **(a)** the COZ forming the focus or **(b)** the POZ forming the focus.

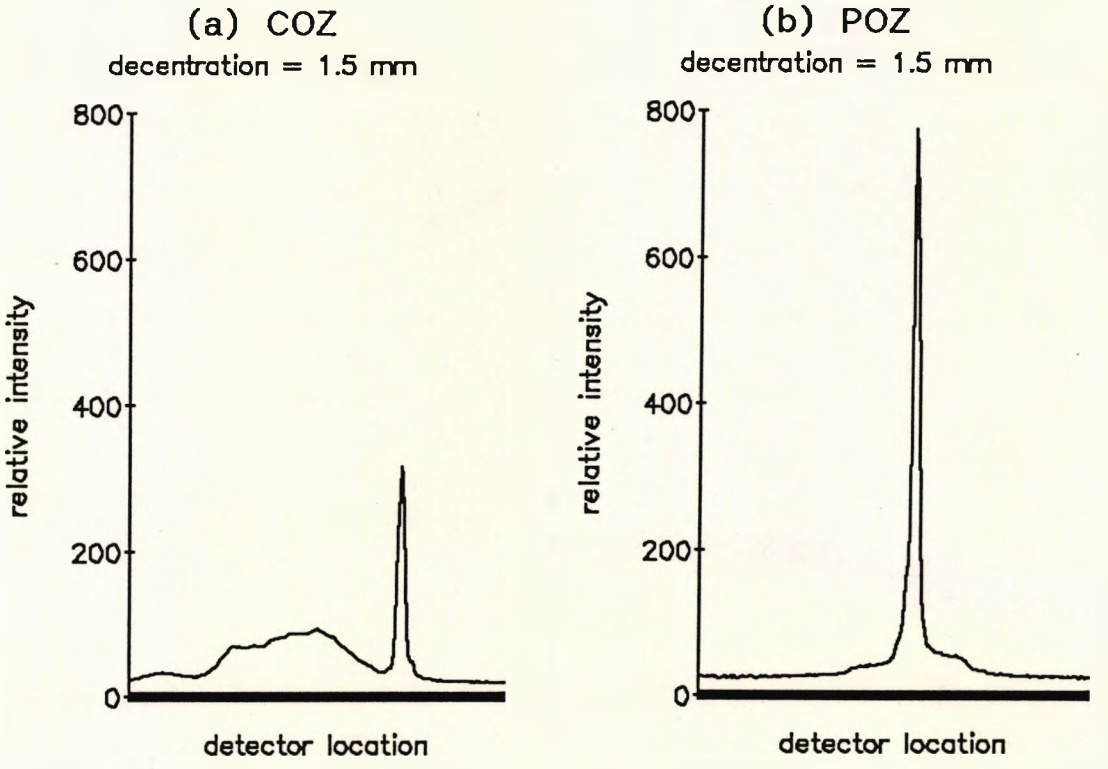

Figure 4.2-14 The measured LSF of a refractive BCL with a 2.6 mm COZD decentred 1.5 mm over a 4 mm aperture with **(a)** the COZ forming the focus or **(b)** the POZ forming the focus.

hence the proportion of the aperture covered by the COZ decreased (*Figure 4.2-15*).

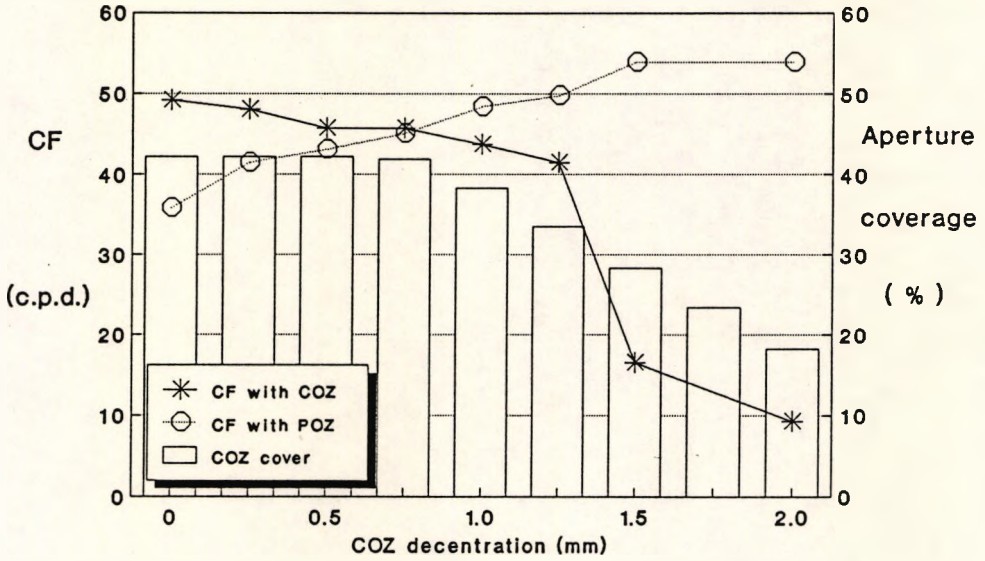

Figure 4.2-15 The effect of decentration of refractive BCL. Critical frequency (CF) and coverage of the aperture by the COZ varied with decentration of a 2.6 mm COZD refractive BCL over a 4 mm aperture.

Decentred Refractive Bifocal Contact Lenses : A model for changes in MTF

As a preliminary analysis two separate ANOVA were performed to investigate the effect of decentration upon MTF (*Appendix 5 (A5-3)*). On the basis of the ANOVA, an empirical model for MTF variation with decentration was developed using MRA. The equations were :

<u>for central optic zone :</u>

$$\begin{aligned} mod = {} & 0.9 - 0.2\,sf + 0.007\,sf^{2} - 1.1\,sf^{-1} + 1.8\,sf^{-2} - 0.8\,sf^{-3} \\ & + aperture \times (-0.02 - 0.02\,sf + 0.002\,sf^{2} - 0.2\,sf^{-1} - 0.3\,sf^{-2} + 0.2\,sf^{-3}) \\ & + decentration\,(-0.06 - 0.06\,sf + 0.008\,sf^{2} - 1.1\,sf^{-1} + 0.3\,sf^{-2} + 0.1\,sf^{-3}) \\ & + COZD \times (0.09 + 0.03\,sf - 0.003\,sf^{2} + 0.2\,sf^{-1} + 0.08\,sf^{-2} - 0.09\,sf^{-3}) \\ & + aperture \times decentration \times (0.07 - 0.02\,COZD + 0.01\,sf - 0.002\,sf^{2} \\ & \qquad + 0.1\,sf^{-1} + 0.09\,sf^{-2} - 0.1\,sf^{-3}) \end{aligned}$$

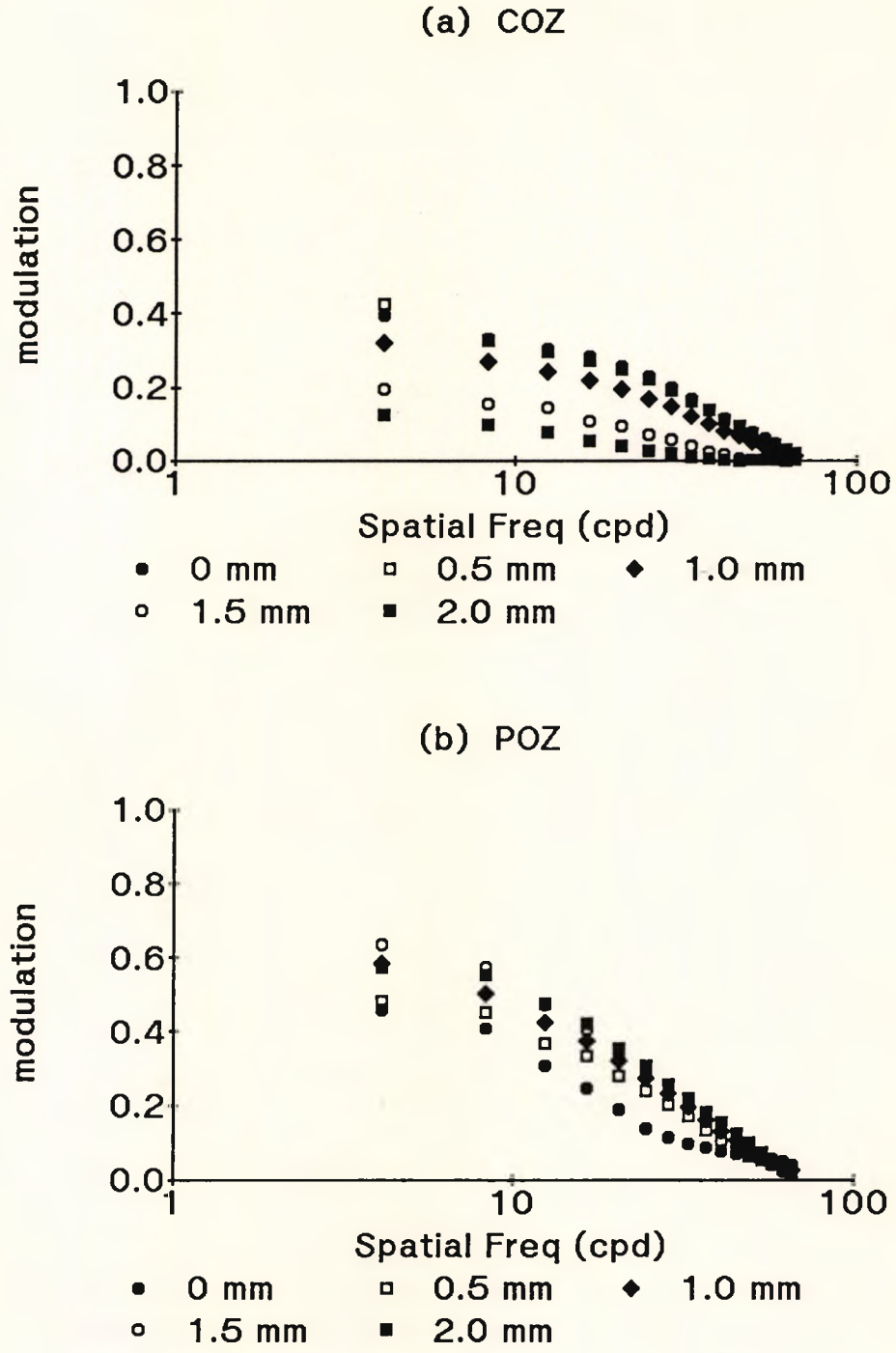

Figure 4.2-16 The variation in MTF with decentration of a refractive BCL with a 2.6 mm COZD over a 4 mm aperture and **(a)** the COZ forming the focus; or **(b)** the POZ forming the focus.

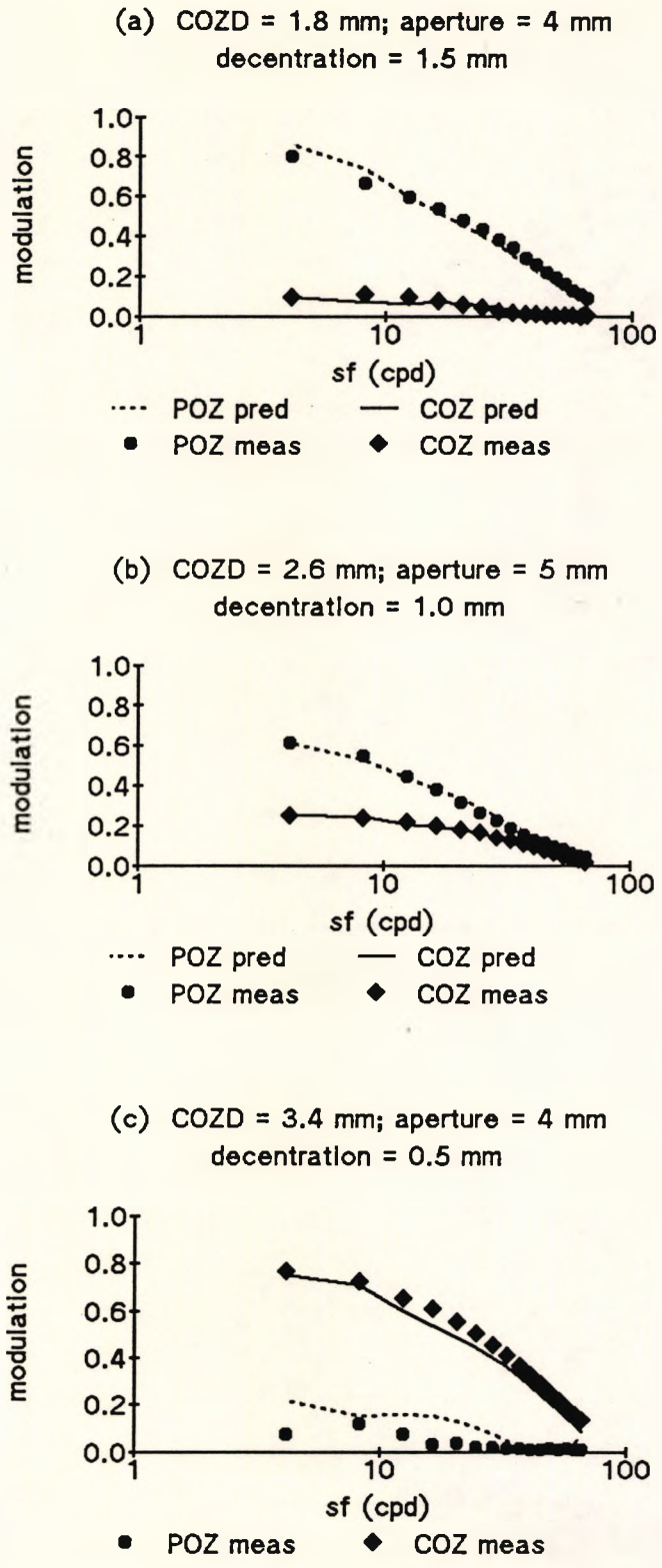

Figure 4.2-17 Evaluation of the MRA equations for decentred refractive BCL. Predicted MTF versus measured MTF with the COZ (diamond) or the POZ (circle) forming the focus for arbitrarily chosen combinations of COZD, aperture and decentration and aperture **(a)** COZD = 1.8 mm, aperture = 4 mm, decentration = 1.5; **(b)** COZD = 2.6 mm, aperture = 5 mm, decentration = 1.0 mm; and **(c)** COZD = 3.4 mm, aperture = 4 mm, decentration = 0.5 mm.

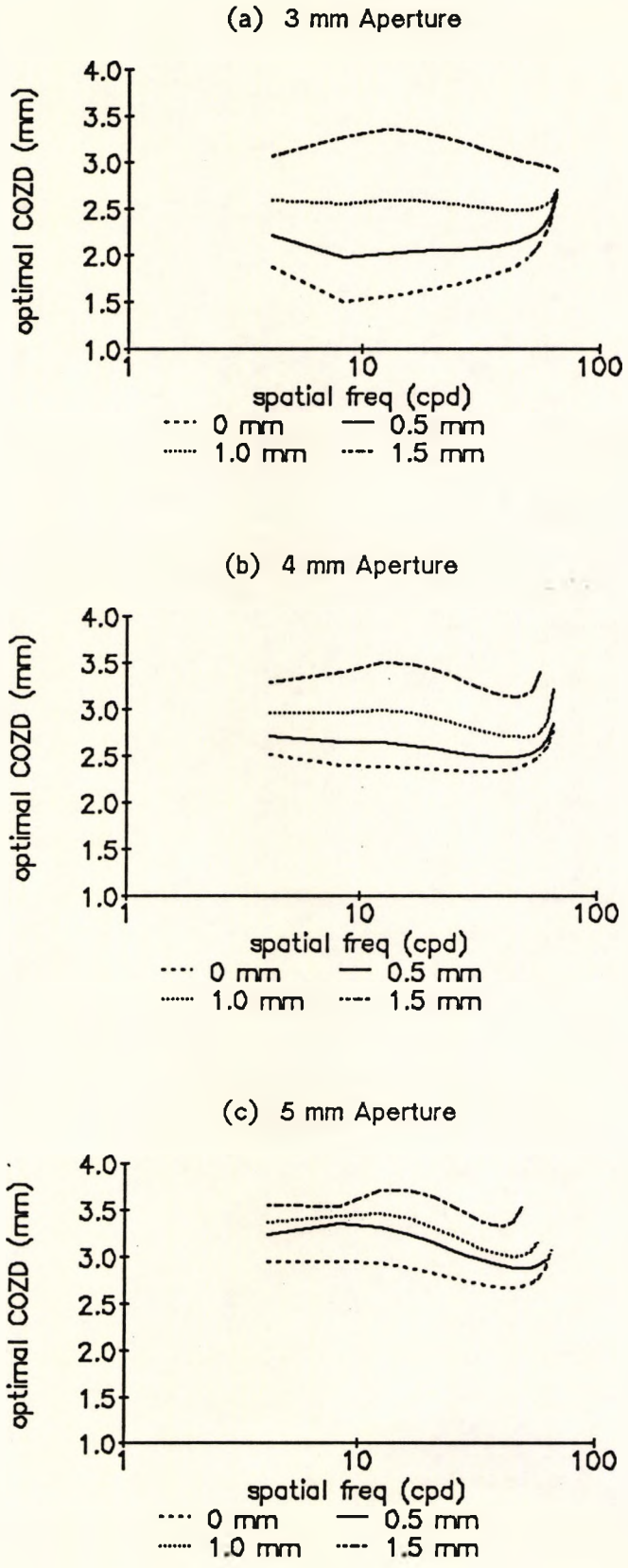

Figure 4.2-18 The predicted optimal COZD of decentred refractive BCL. The optimal COZD (equal distance and near), was predicted by MRA equations, for **(a)** 3 mm; **(b)** 4 mm; and **(c)** 5 mm apertures with the COZ decentred 0 mm, 0.5 mm, 1.0 mm or 1.5 mm over the aperture. (s.e. = 0.052)

for peripheral optic zone :

$$\text{mod} = 1.1 - 0.2\,sf + 0.01\,sf^{2} - 2.7\,sf^{-1} + 1.8\,sf^{-2} - 0.3\,sf^{-3}$$
$$+ \text{aperture} \times (0.02\,sf - 0.002\,sf^{2} + 0.6\,sf^{-1} - 0.3\,sf^{-2})$$
$$+ \text{decentration} \times (0.07\,sf - 0.009\,sf^{2} + 1.2\,sf^{-1} + 0.3\,sf^{-2} - 0.5\,sf^{-3})$$
$$+ \text{COZD} \times (-0.05 - 0.03\,sf + 0.003\,sf^{2} - 0.3\,sf^{-1} + 0.04\,sf^{-3})$$
$$+ \text{aperture} \times \text{decentration} \times (-0.03 + 0.01\,\text{COZD} - 0.01\,sf + 0.002\,sf^{2} - 0.3\,sf^{-1} + 0.08\,sf^{-3})$$

(adjusted multiple $R^2 = 0.955$; s.e. = 0.056; n = 8441, $p < 0.0001$)

The full details of the MRA have been included in *Appendix 5 (A5-4)*. The MRA equations were tested by comparing the actual data and predicted MTF for arbitrarily chosen combinations of COZD, aperture and decentration. Examples are given in *Figure 4.2-17*.

The solution of these equations for equal modulation with focus by the COZ and with the POZ is shown in *Figure 4.2-18*. The variation in the predicted optimal COZD with spatial frequency altered with decentration, due to changes in the relative shape of the MTF (COZ v POZ) with decentration which can be seen in *Figure 4.2-16*, and which were a result of changes in the image shape demonstrated in *Figures 4.2-13 and 4.2-14*. Hence the choice of an optimal COZD was dependent upon the aperture size, any decentration and the spatial frequency of interest.

4.2.4 RIGID DIFFRACTIVE BIFOCAL CONTACT LENSES

The effects of aperture size, wavelength and decentration upon optical performance with rigid diffractive BCL were demonstrated, and changes in optical performance were used to demonstrate the variability of manufacture. The major investigation examined the effect of variations in

Diffractive Zone Junction (DZJ) height and tool shape upon optical performance with ANOVA and MRA. The MRA equations were used to develop an empirical model which allowed a prediction of the optimal DZJ height (equal distance and near performance).

Aperture size

As shown in *Figure 4.2-19*, the MTF of rigid diffractive BCL varied slightly with aperture size at both distance and near, but only the near MTF with a 6 mm aperture was significantly different ($p < 0.001$). The optical performance of the diffractive BCL would appear to be resistant to changes in aperture up to the 5 mm size of the central diffractive zone. Conversely, the system, as shown in *Figure 4.2-1*, was aperture dependent, as were the refractive BCL (*Figure 4.2-8*).

Wavelength

As shown in *Figure 4.2-20*, and as theoretically predicted (*Equation 1.2-3*), with increasing wavelength, the MTF of the distance focus increased and the MTF of the near focus decreased.

Decentration

An example of the effect of decentration upon the measured LSF is shown in *Figures 4.2-21* and *4.2-22*. The MTF varied with decentration at both distance and near as shown in *Figure 4.2-23*. The reduction in optical performance was greater at near than at distance, and was greater

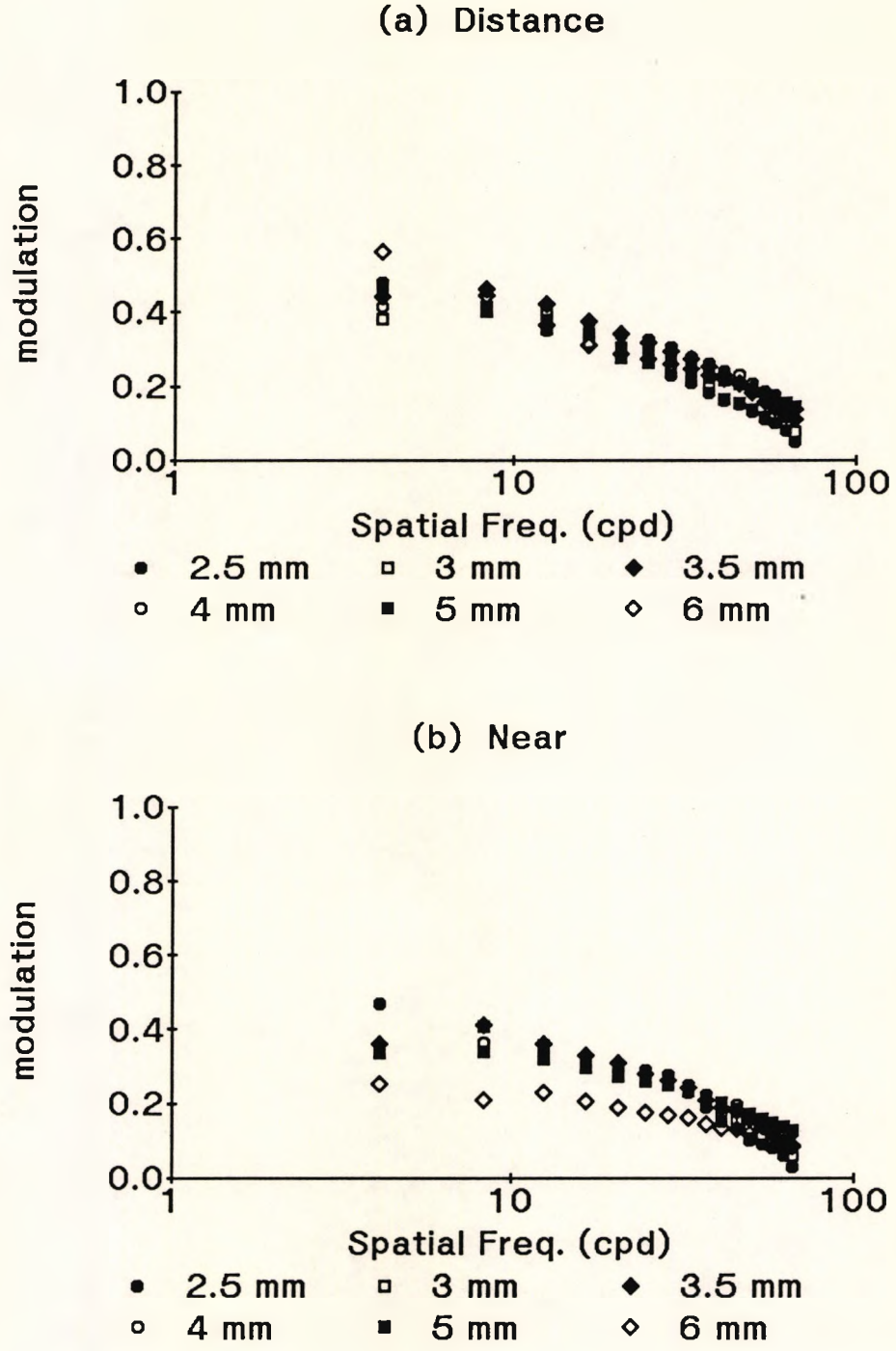

Figure 4.2-19 The effect of changes in aperture upon the MTF with a rigid diffractive BCL - 2.0 μm DZJ height, 250 μm tool - at **(a)** distance; and **(b)** near.

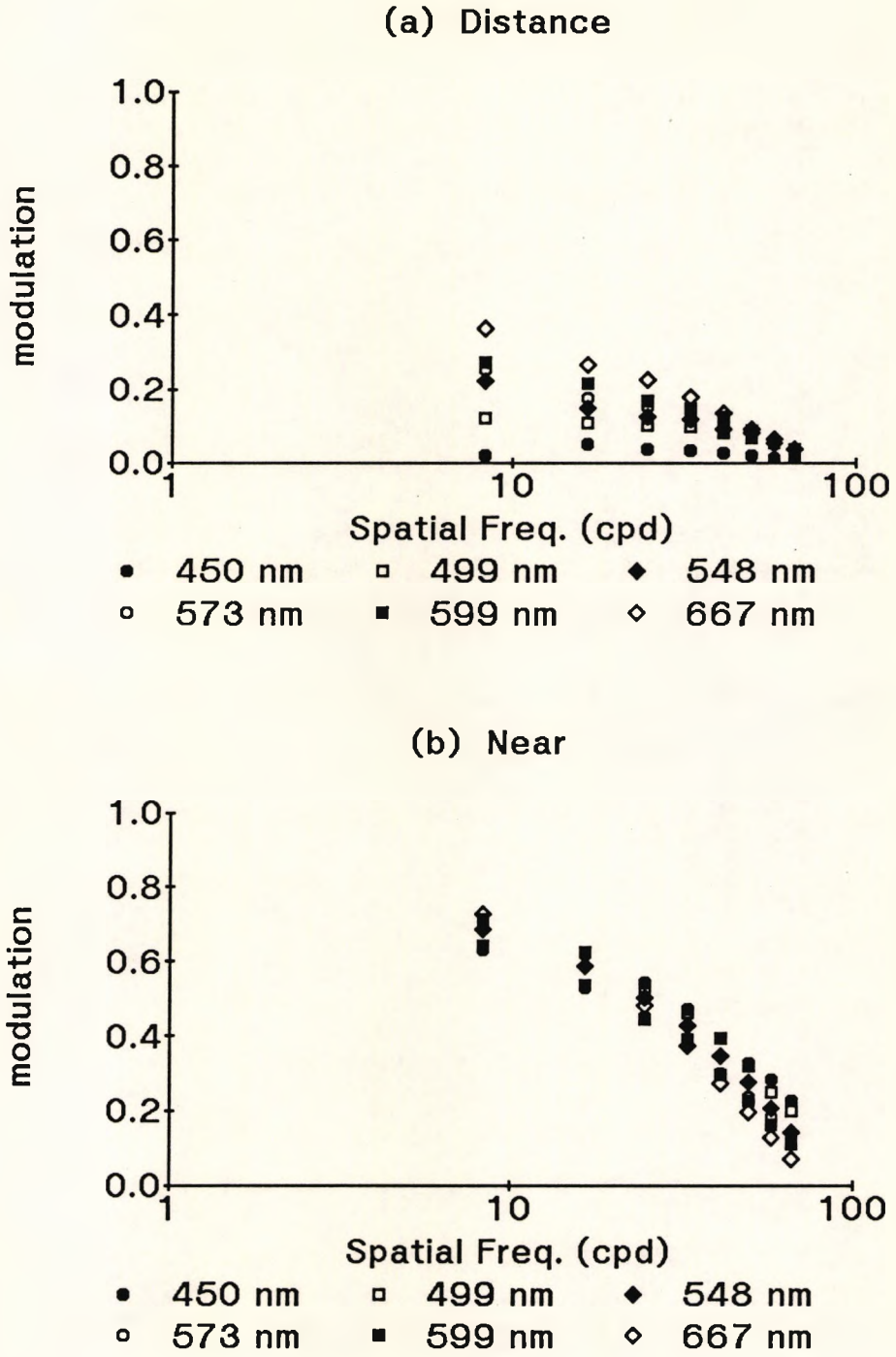

Figure 4.2-20 The variation in MTF with changes in wavelength for a rigid diffractive BCL - 2.6 μm DZJ height, 250 μm tool - at **(a)** distance; and **(b)** near.

with larger apertures. It is interesting to note the change in the shape of the distance MTF with decentration, as there was a more pronounced reduction between about 20 and 30 c.p.d. which is approximated to 6/6 VA. This was related to the shape of the image (*Figure 4.2-22a*).

Variability of manufacture

As the significance of the changes in optical design under investigation in this study were limited by the variability of the manufacture process, this was examined firstly by comparing two batches (production runs separated by about six months) of nominally identical BCL (DZJ height 2.2 and 2.6 μm; 250 μm round diamond tool). ANOVA (*Appendix 5 (A5-5)*) indicated a significant difference between the two batches ($p < 0.001$) and a significant interaction between the batch, DZJ height and vergence ($p = 0.008$) indicating a variation in the ratio between distance and near between batches.

In addition the experimental BCL with a 2.0 μm DZJ height manufactured with the 250 μm round diamond tool were compared to Pilkington Diffrax BCL (which were nominally identical). ANOVA (*Appendix 5 (A5-6)*) indicated a significant difference between the two BCL types ($p < 0.001$), and a significant interaction between the BCL type and vergence ($p < 0.001$). *Table 4.2-1* shows the variability in the vergence ratio (defined as = distance / distance + near; with MTF averaged for all spatial

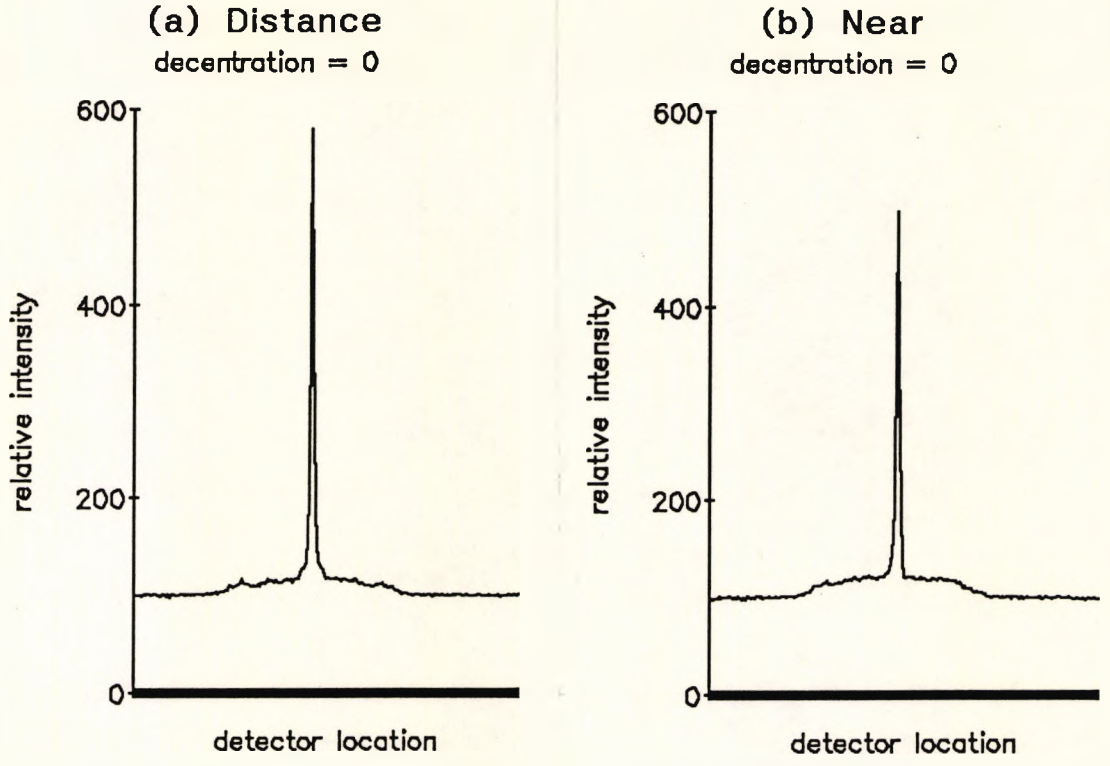

Figure 4.2-21 The measured LSF of a rigid diffractive BCL - 2.0 μm DZJ height, 250 μm tool - centred over a 4 mm aperture at **(a)** distance and **(b)** near.

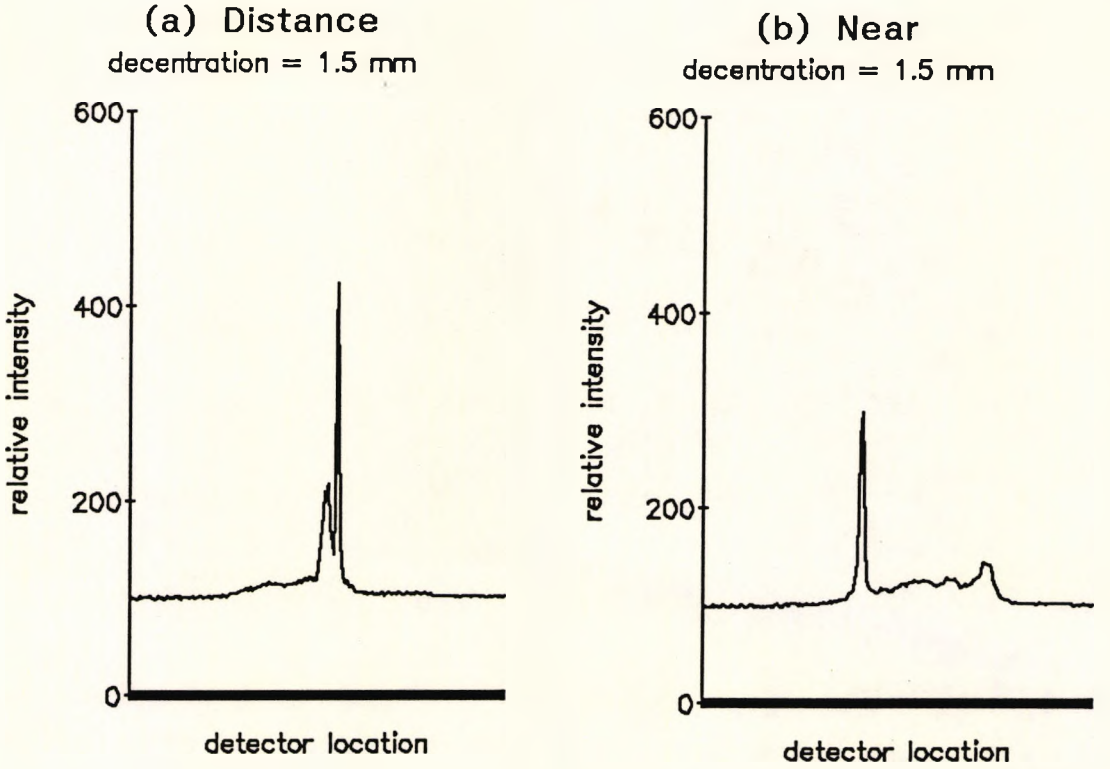

Figure 4.2-22 The measured LSF of a rigid diffractive BCL - 2.0 μm DZJ height , 250 μm tool - decentred 1.5 mm over a 4 mm aperture at **(a)** distance and **(b)** near.

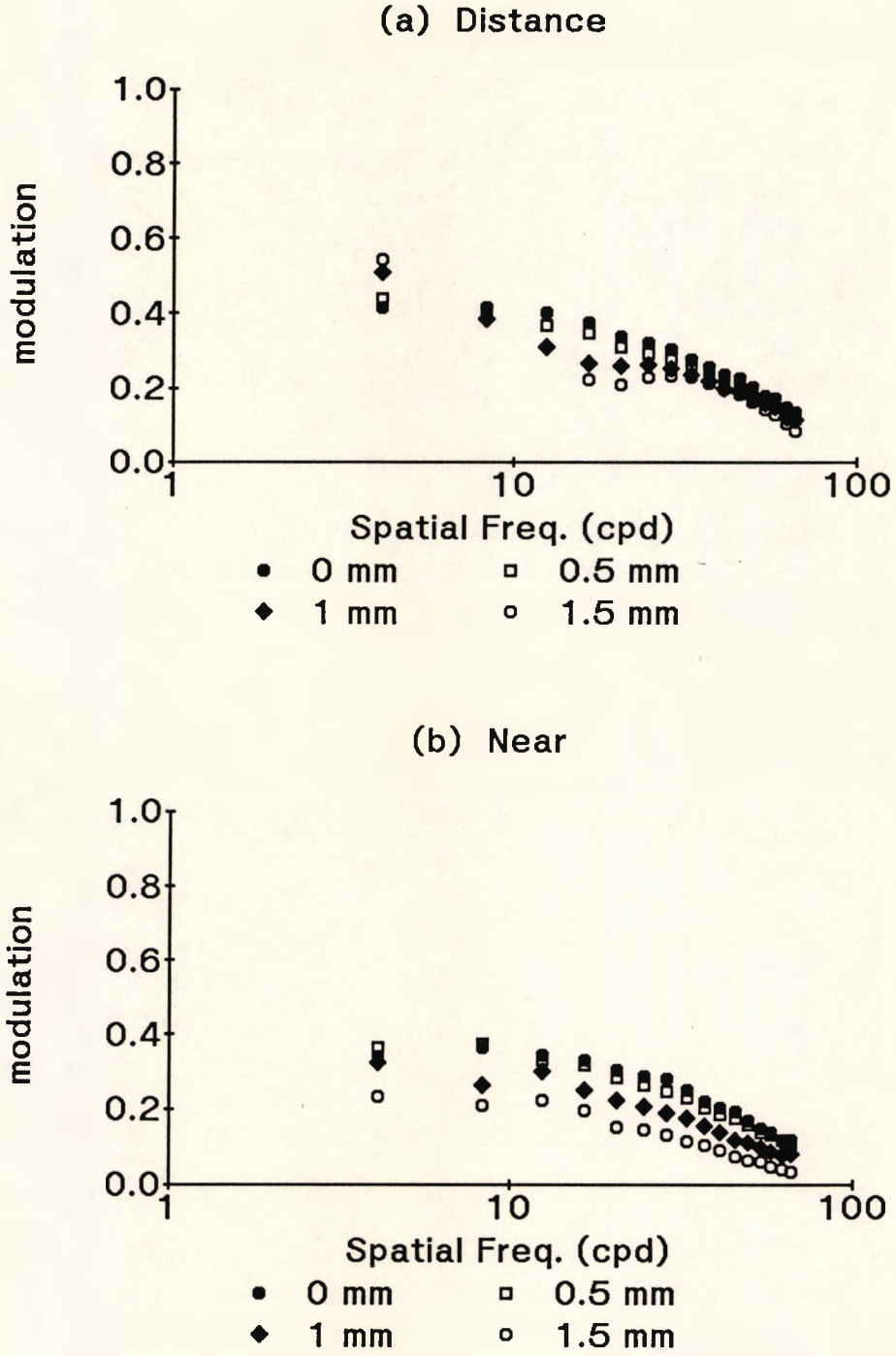

Figure 4.2-23 The variation in MTF with decentration of a rigid diffractive BCL 2.0 μm DZJ height, 250 μm tool, over a 4 mm aperture at **(a)** distance; and **(b)** near.

frequencies) between individual BCL. The vergence ratio varies from 0 to 1, and if greater than 0.5 indicates a bias to distance.

	Experimental BCL			Pilkington Diffrax	
code	Vergence Ratio (D/D+N)	s.e.	code	Vergence Ratio (D/D+N)	s.e.
B1	0.49	0.06	DX1	0.54	0.08
B2	0.59	0.09	DX2	0.48	0.06
B3	0.44	0.05	DX3	0.53	0.08
B4	0.45	0.05	DX4	0.55	0.08
B5	0.51	0.07	DX5	0.55	0.08
B6	0.52	0.07	DX6	0.59	0.10

Table 4.2-1 Vergence ratio of nominally identical rigid diffractive BCL. Ratio between the average MTF (n = 2 x 16) at distance and near for rigid diffractive BCL with nominally identical diffractive zones indicates the distance or near biased of each BCL. A vergence ratio greater than 0.5 indicates a bias to distance. The vergence ratio of the experimental BCL was slightly different to the Pilkington Diffrax (p = 0.02).

Diffractive Zone Junction Height and Diamond Tool Shape

The MTF varied with DZJ height at both distance and near as shown, for example, in *Figure 4.2-24* for BCL made with the flatted tool. As shown in *Figure 4.2-25* differences in the MTF due to tool shape were small.

The relationship between DZJ height (H), tool shape (T), vergence (V) and spatial frequency (F) was examined with ANOVA. MTF results at two wavelengths (548 nm and 573 nm) were considered. ANOVA results are included in *Appendix 5 (A5-7)*.

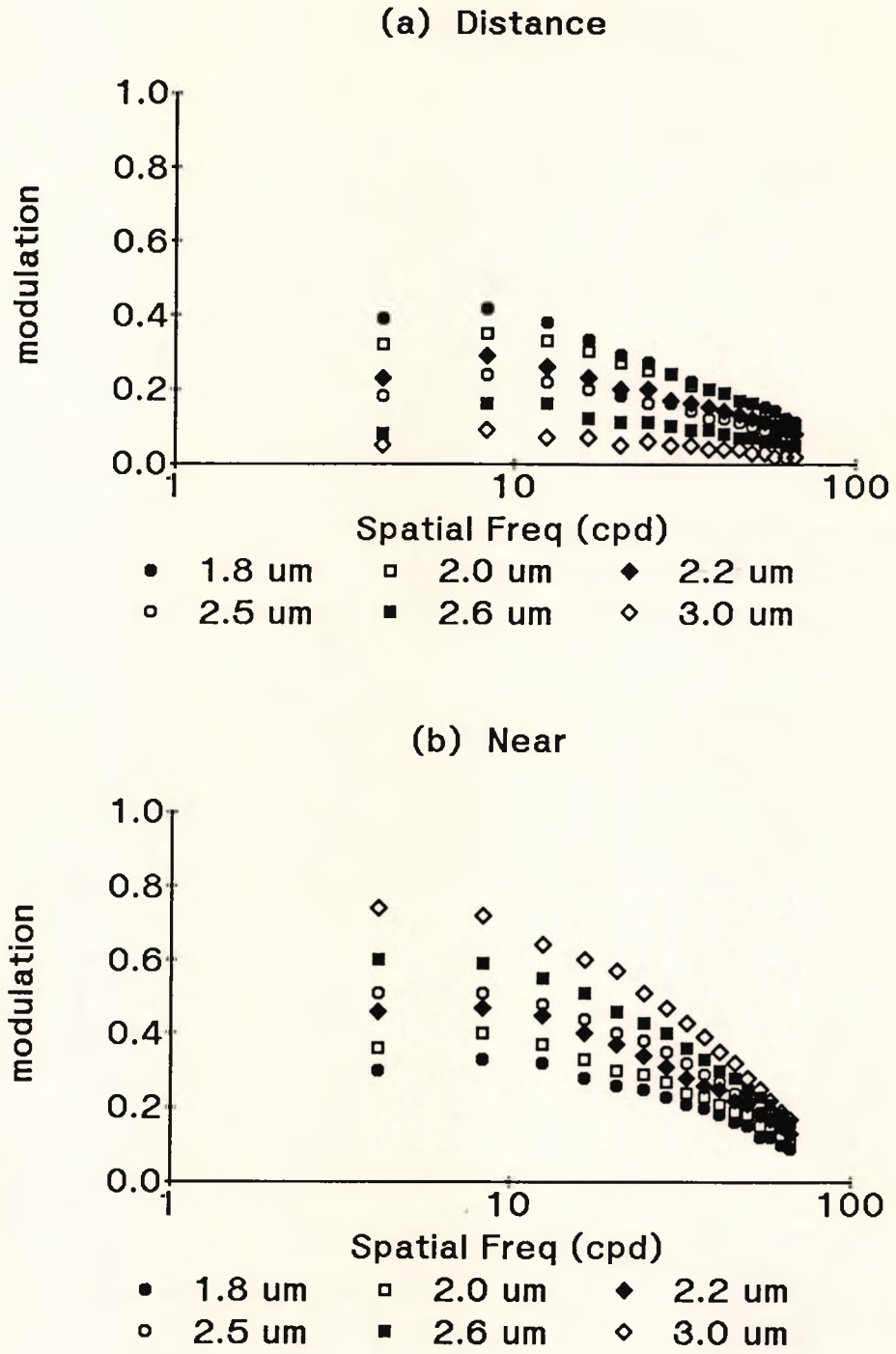

Figure 4.2-24 The variation in MTF with DZJ height of rigid diffractive BCL manufactured with the flatted tool at **(a)** distance; and **(b)** near.

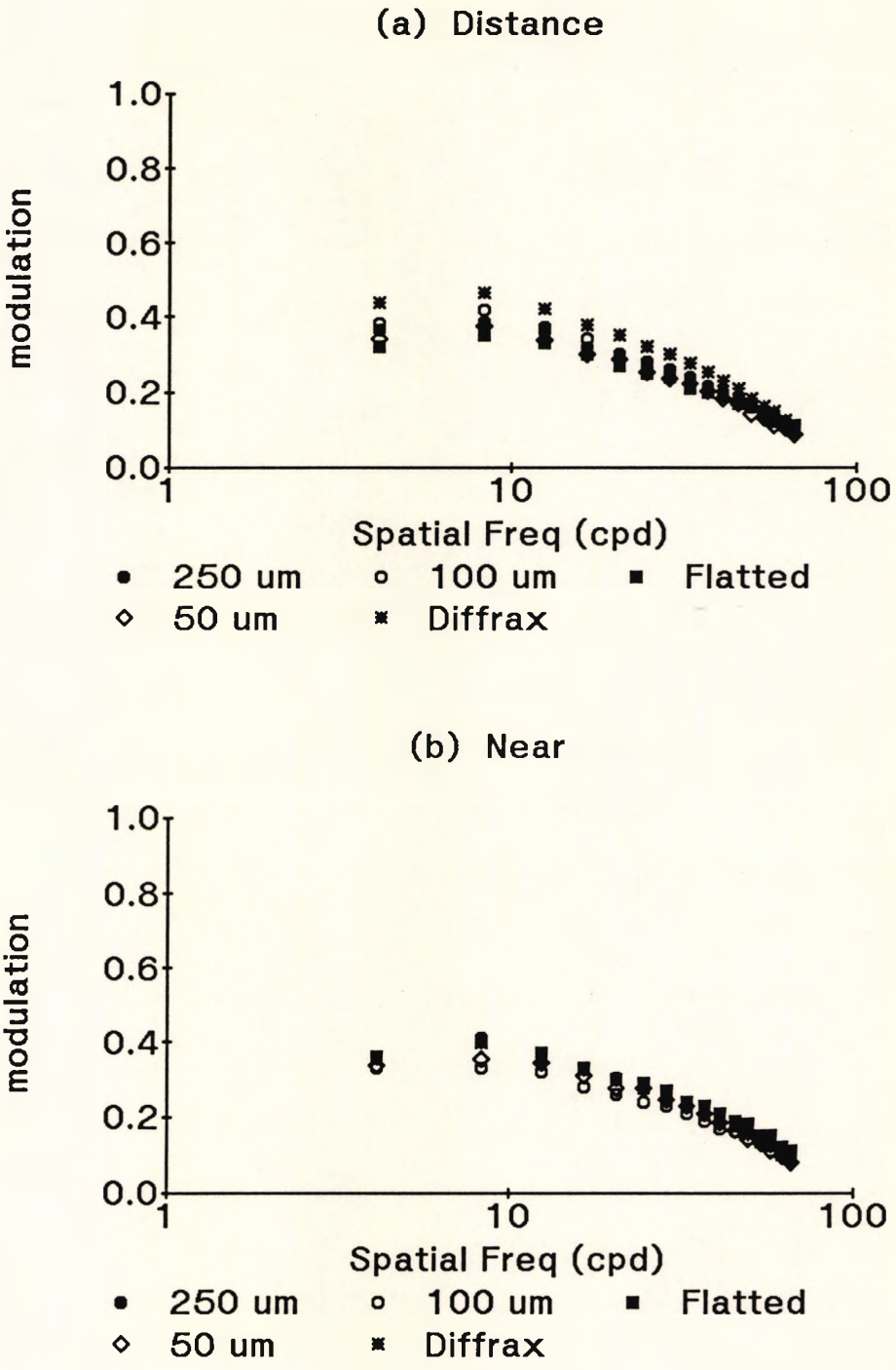

Figure 4.2-25 The variation in MTF with tool shape of rigid diffractive BCL of 2.0 μm DZJ height at **(a)** distance; and **(b)** near.

As expected, the strong interaction between DZJ height and vergence (H x V; $p < 0.001$) confirmed that, with increasing DZJ height, average modulation increased for the near focus and reduced for the distance focus. This effect varied with spatial frequency (H x V x F; $p < 0.001$), as illustrated in *Figure 4.2-24*. The interaction between tool shape and vergence (T x V; $p < 0.001$) confirmed that, as shown in *Figure 4.2-26*, the BCL made with the 250 μm flatted tool were more near biased over the range of DZJ heights chosen compared to the other two tool shapes. *Figure 4.2-27* shows the increase in the average modulation for the near focus and reduction for the distance focus with increasing DZJ height which varied between the three different tool shapes as demonstrated by the interaction H x T x V ($p < 0.001$). The shape of the MTF did not vary between the different tool shapes across the range of DZJ heights (H x T x F; $p = 1$) at distance or near (H x T x V x F; $p = 1$).

A further ANOVA (*Appendix 5 (A5-8)*), for rigid diffractive BCL with a DZJ height of 2.0 μm, indicated that there was a significant difference between the four tools ($p < 0.001$) and a difference in the balance between distance and near (T x V: $p < 0.001$). *Figure 4.2-28* shows that the vergence ratio altered only slightly with the different tools as suggested by *Figure 4.2-25*.

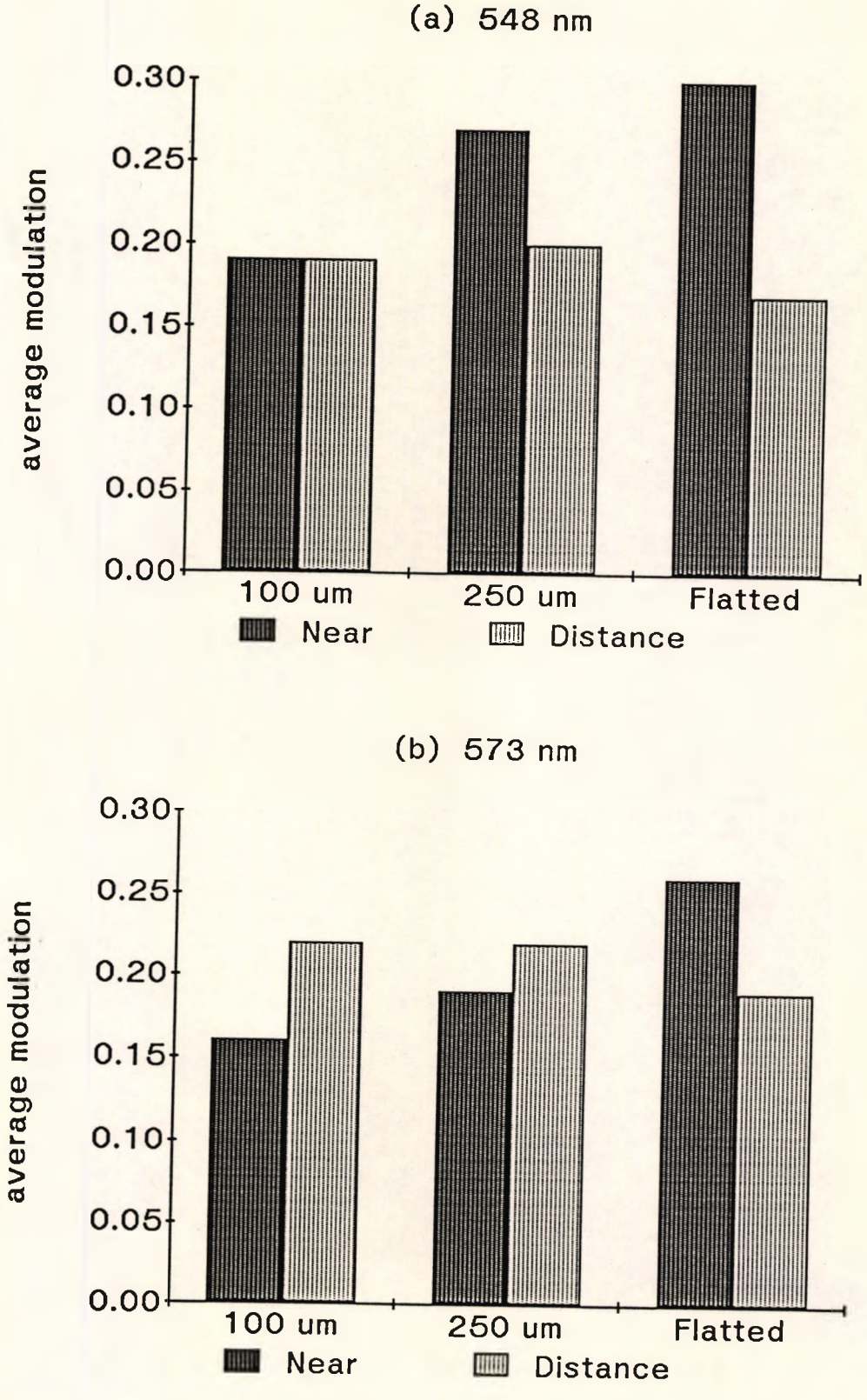

Figure 4.2-26 The effect of tool upon optical performance. The average modulation of rigid diffractive BCL manufactured with the three tool shapes at near (dark) and distance (light) at (a) 548 nm; and (b) 573 nm.

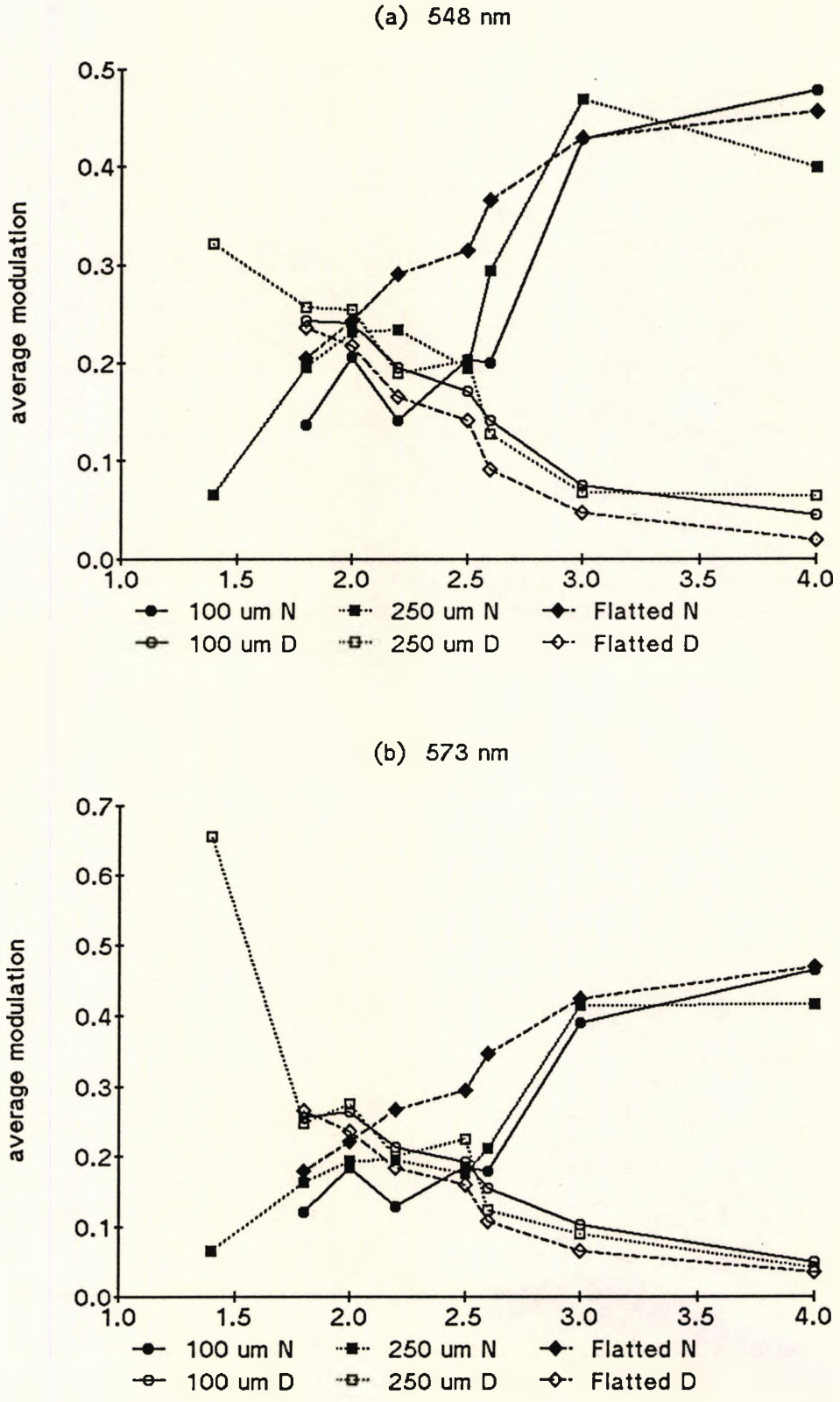

Figure 4.2-27 The effect of DZJ height upon optical performance. The average modulation of rigid diffractive BCL manufactured with the three tool shapes (100 μm - round; 250 μm - square; flatted - diamond) varied with DZJ height at near (filled) and distance (open) at **(a)** 548 nm; and **(b)** 573 nm.

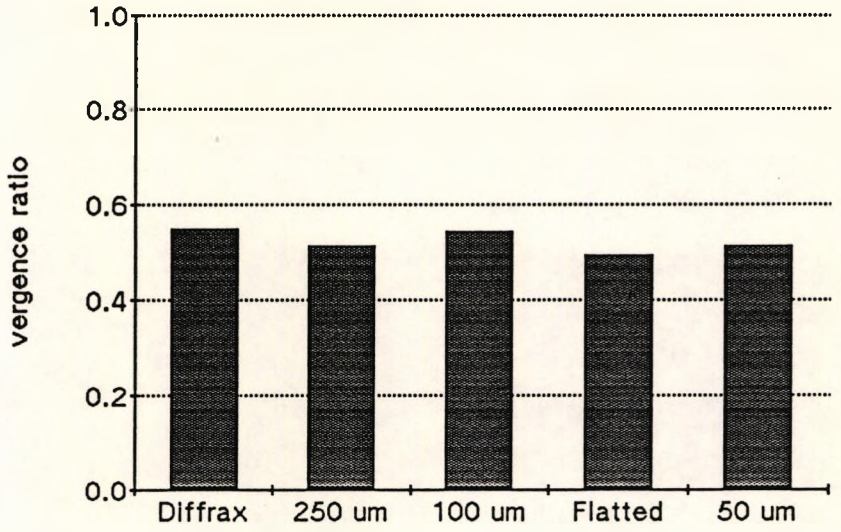

Figure 4.2-28 Vergence ratio varied with tool. The vergence ratio between the average MTF at distance and near for rigid diffractive BCL with 2.0 μm DZJ height indicated the distance or near bias of different tools. A vergence ratio greater than 0.5 indicated a bias to distance.

Rigid Diffractive BCL: A model of changes in MTF

Using MRA, an empirical model for changes in MTF was developed to allow the prediction of the MTF with a given DZJ height, tool shape and spatial frequency. This allowed prediction of an optimal DZJ height (equal distance and near optical performance) for each tool shape and the two wavelengths (548 nm and 573 nm), and comparison to the visual performance measures (section 4.3.4).

Details of the development of the model are given in *Appendix 6*. As an example, the equation for the 250 μm tool measured at 548 nm was :

<u>for distance :</u>

$$\text{mod} = 1.0 - 0.1\ sf + 0.006\ sf^{2} - 0.8\ sf^{-1} + 2.4\ sf^{-2} - 1.2\ sf^{-3} + \text{DZJ height} \times (-0.005\ sf - 0.5\ sf^{-1} - 0.08\ sf^{-2} + 0.2\ sf^{-3})$$

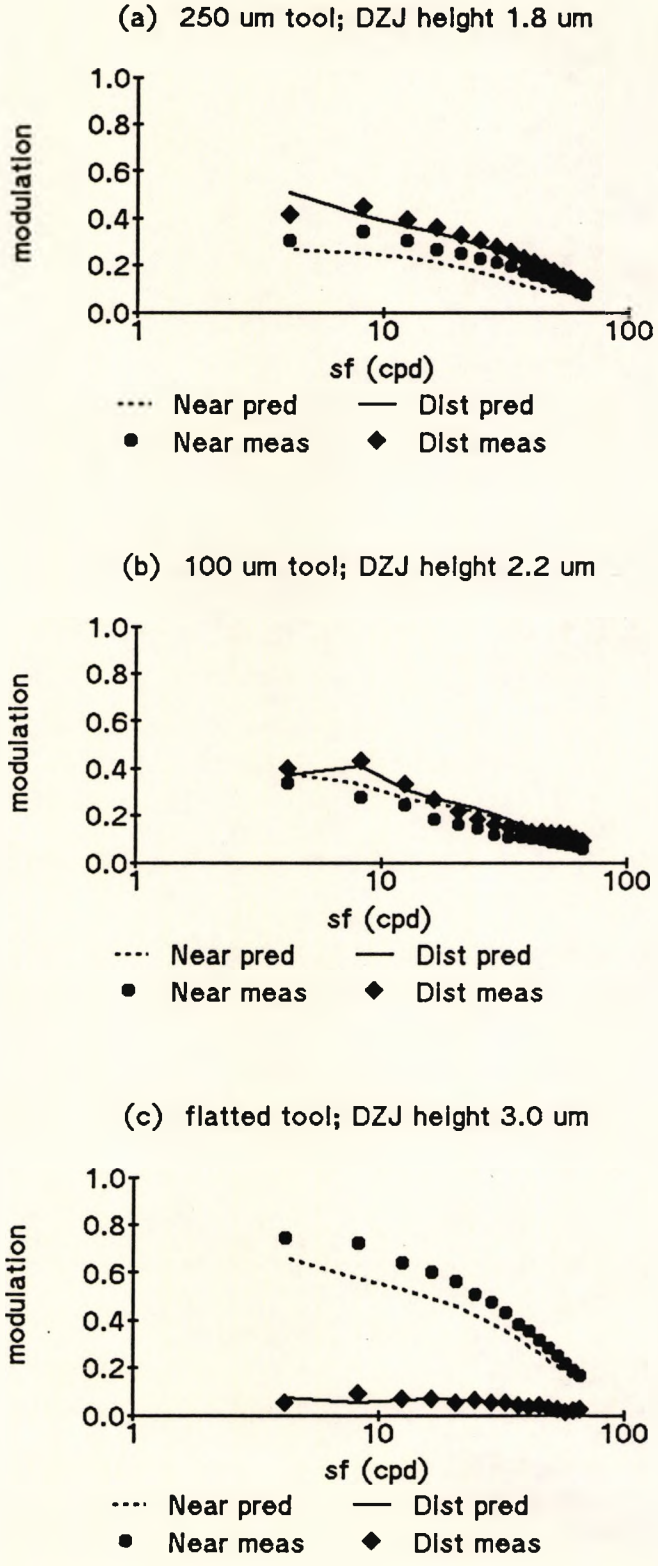

Figure 4.2-29 Evaluation of the MRA equations for rigid diffractive BCL. Predicted MTF at near (dashed line) and distance (solid line) versus measured MTF at near (circle) and distance (diamond) for arbitrarily chosen combinations of DZJ height and tool shape at 548 nm **(a)** 250 μm tool, 1.8 μm DZJ height; **(b)** 100 μm tool, 2.2 μm DZJ height; and **(c)** flatted tool, 3.0 μm DZJ height.

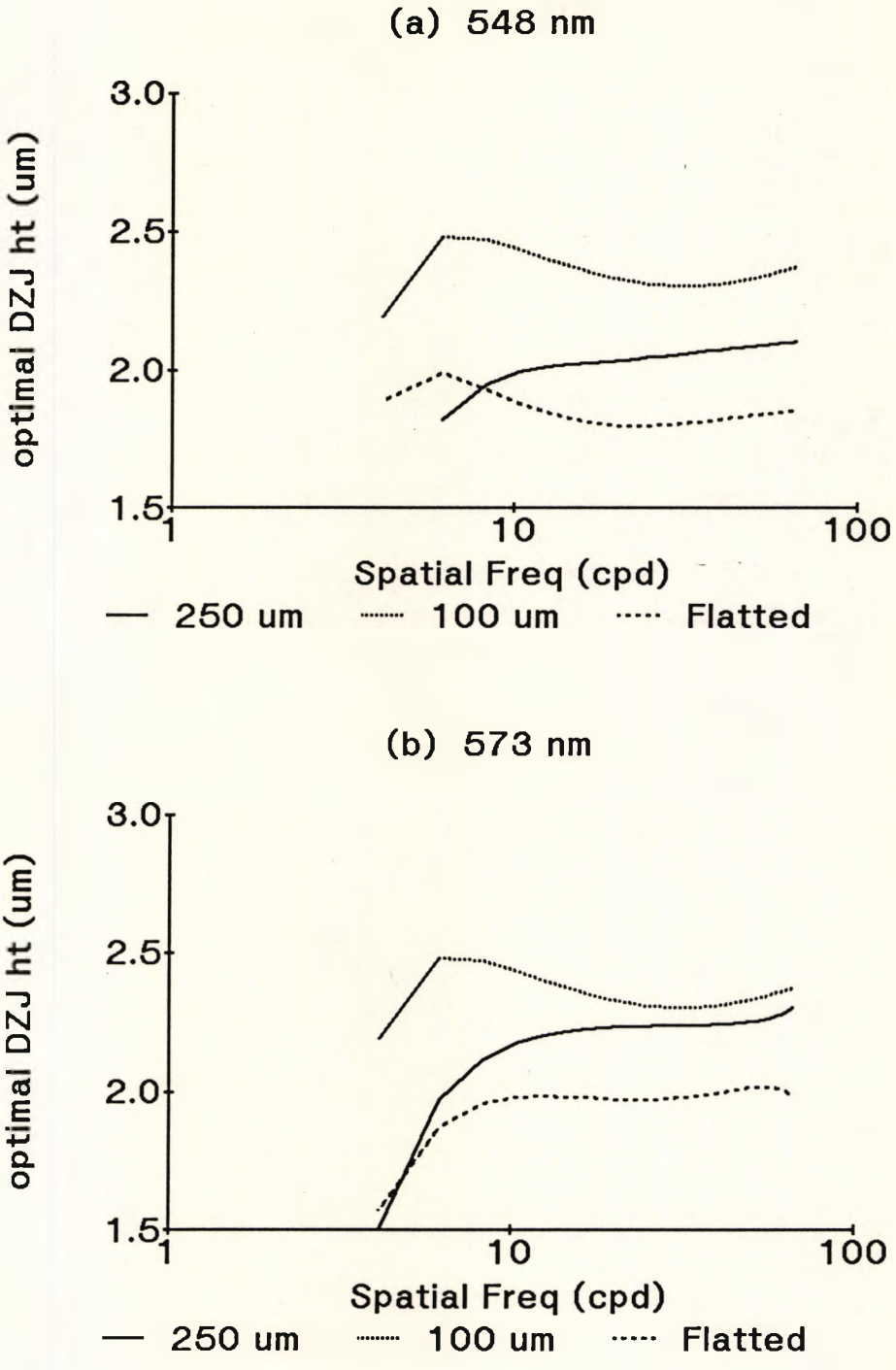

Figure 4.2-30 Predicted optimal DZJ height (equal distance and near) of rigid diffractive BCL with the three different tool shapes predicted by the MRA equations with the **(a)** 548 nm; and **(b)** 573 nm interference filters, was shown to vary between the tools and with spatial frequency.

for near :

$$\text{mod} = 1.0 - 0.1\,sf + 0.006\,sf^{2} - 3.6\,sf^{-1} + 3.6\,sf^{-2} - 1.2\,sf^{-3} + \text{DZJ height} \times (\,sf^{-1} - 0.9\,sf^{-2} + 0.3\,sf^{-3}$$

($R^2 = 0.915$; s.e. = 0.068; n = 3969; $p < 0.0001$)

Details of the MRA equations for each tool shape with the two wavelengths are given in *Appendix 5 (A5-9)*. The equations were tested by comparing the actual data and predicted MTF for arbitrarily chosen combinations of DZJ height, tool shape and wavelength. Examples are shown in *Figure 4.2-29*.

The MRA equations were then used to determine the optimal DZJ height (equal distance and near optical performance) for each tool shape. The optimal DZJ height varied with wavelength, tool shape and with spatial frequency (*Figure 4.2-30*).

The effect of back surface polishing of rigid diffractive bifocal contact lenses

As expected, the polished BCL were more distance biased than the non-polished BCL of the same nominal DZJ height and tool shape (*Figure 4.2-31*). When the measured DZJ height (section 4.1) of the polished BCL was considered, optical performance was similar to the non-polished BCL (*Figure 4.2-32*). Apart from the 1.4 μm DZJ height BCL, polishing did not reduce optical performance, merely altering the bias between distance and near.

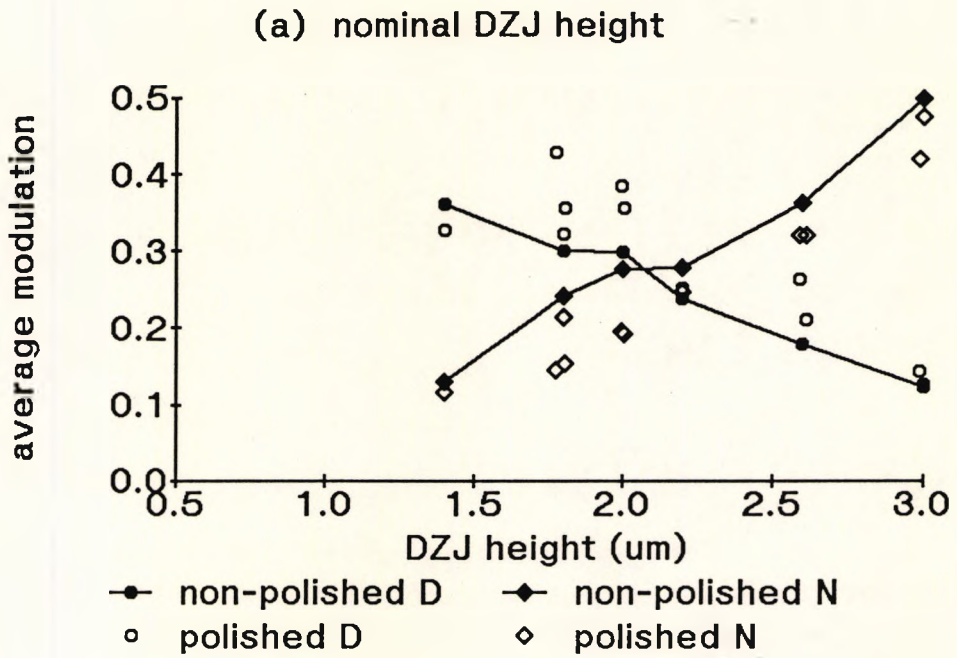

Figure 4.2-31 The effect of polishing rigid diffractive BCL upon optical performance. The average MTF versus the nominal DZJ height of polished (open) compared to nominally identical non-polished (filled) rigid diffractive BCL lathed with 250 μm round tool at distance (circle) and near (diamond).

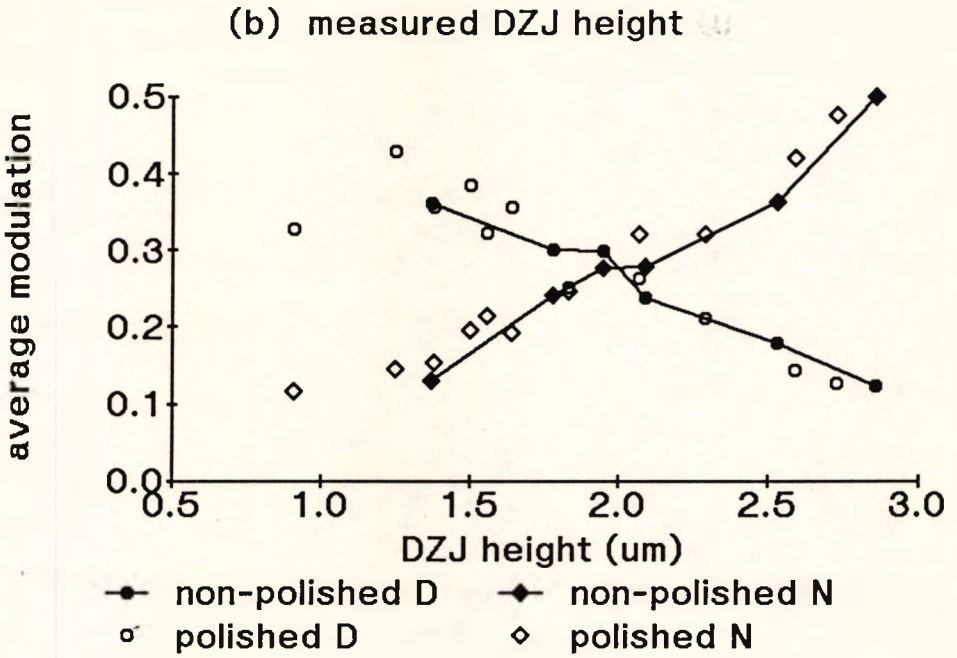

Figure 4.2-32 Measured DZJ height as a predictor of optical performance. The average MTF versus the measured DZJ height of polished (open) and nominally identical non-polished (filled) rigid diffractive BCL at distance (circle) and near (diamond).

4.2.5 SOFT DIFFRACTIVE BIFOCAL CONTACT LENSES

The available soft diffractive BCL were a heterogeneous group, and, where possible, comparisons between different design characteristics have been made. All data reported in this section was recorded at 548 nm.

Average optical performance

The average MTF (distance and near) averaged for all soft diffractive BCL was significantly less than for all the rigid diffractive BCL ($p < 0.001$), indicating a relatively reduced optical performance. The reduced optical quality limited the ability to demonstrate some of the effects of interest.

Variability of manufacture

The variability of the manufacture process was investigated by comparing three batches of nominally identical BCL (DZJ height 3.0 μm; 100 μm tool; moulded). Two of the batches were from the same production run. As shown in *Figure 4.2-33*, ANOVA (*Appendix 5 (A5-10)*) indicated a significant difference between the batches ($p < 0.001$) and a significant interaction between the batch and vergence ($p < 0.001$) indicating a variation in the ratio between distance and near between batches. Variations from the nominal parameters reduced the ability to demonstrate some of the effects of interest.

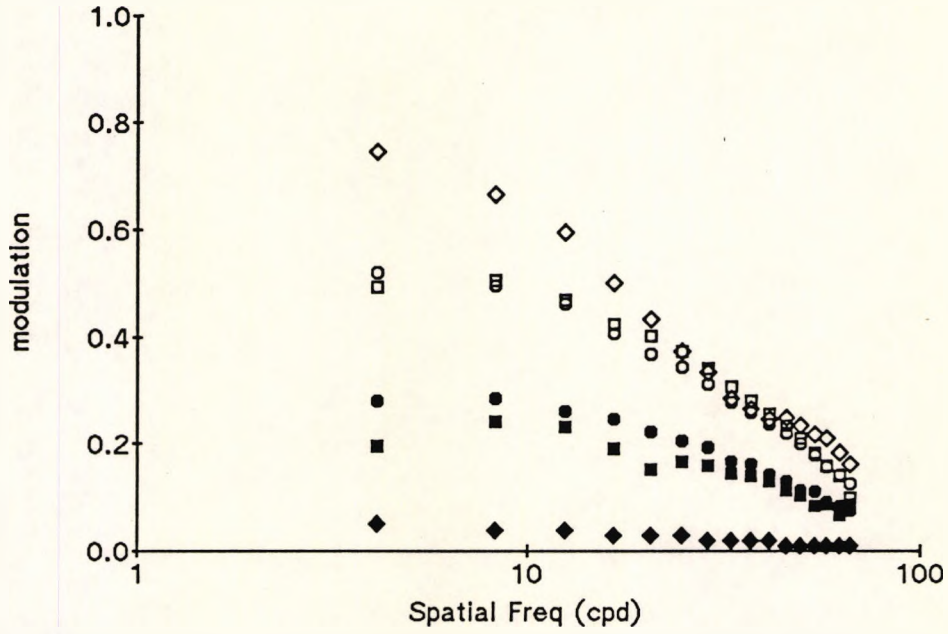

Figure 4.2-33 Variability of manufacture of soft diffractive BCL. The MTF at distance (filled) and near (open) of three nominally identical soft diffractive BCL (3.0 μm DZJ height; 100 μm tool; moulded)

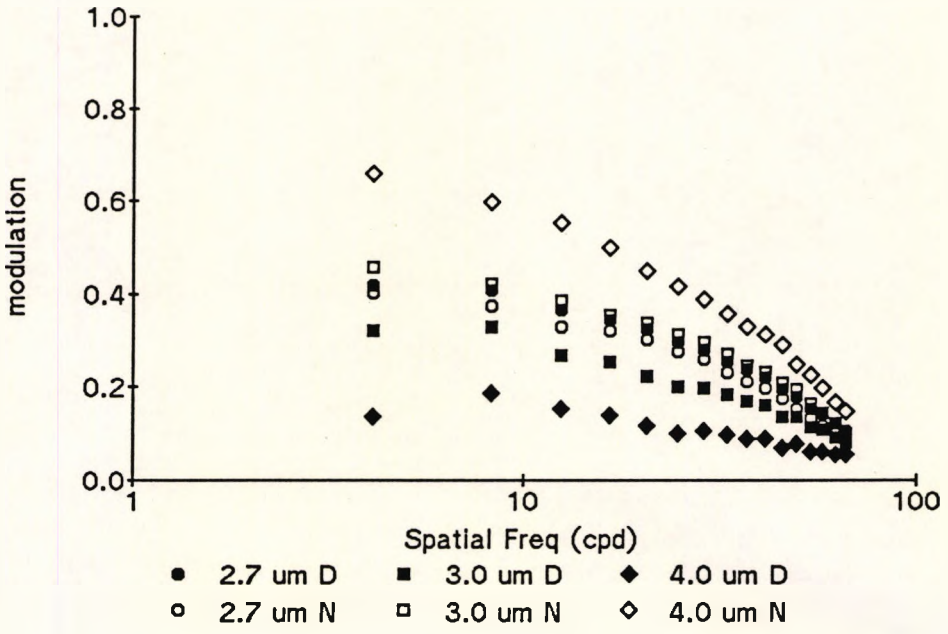

Figure 4.2-34 The variation in MTF with DZJ height at distance (filled) and near (open) of soft diffractive BCL lathed with 250 μm tool.

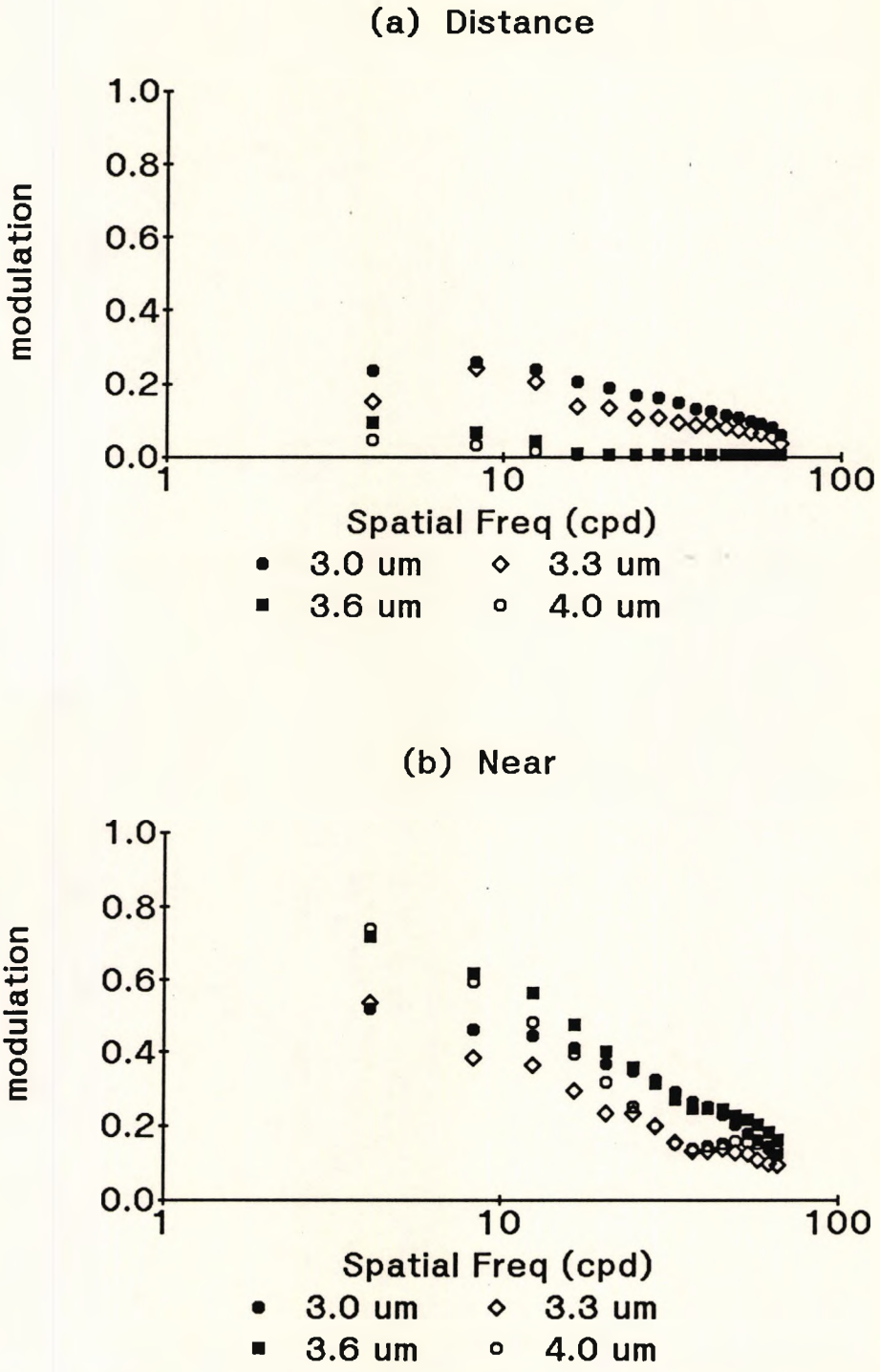

Figure 4.2-35 The variation in MTF with DZJ height at **(a)** distance and **(b)** near of soft diffractive BCL lathed with 100 μm tool.

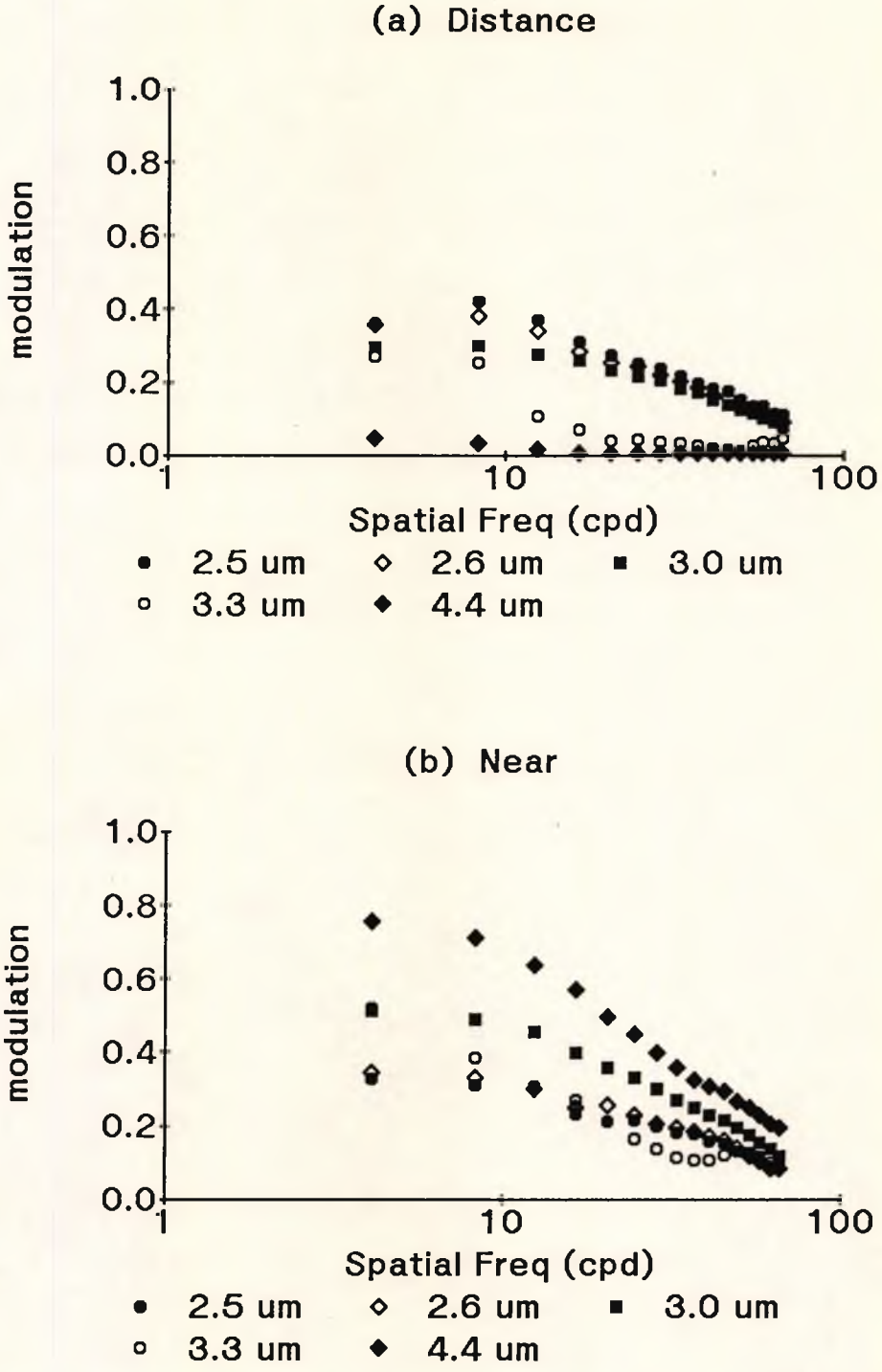

Figure 4.2-36 The variation in MTF with DZJ height at **(a)** distance and **(b)** near of moulded soft diffractive BCL, the brass mould lathed with a 100 μm round tool.

Diffractive Zone Junction Height

As expected, and confirmed by the ANOVA (*Appendix 5 (A5-11)*) interaction between DZJ height and vergence ($p < 0.001$), the near MTF improved and the distance MTF reduced with increasing DZJ height for the 250 μm tool, lathed BCL (*Figure 4.2-34*); the 100 μm tool, lathed BCL (*Figure 4.2-35*); and the 100 μm tool, moulded BCL (*Figure 4.2-36*). There was a significant variation in the shape of the MTF at distance and near with both 100 μm and 250 μm tool, lathed soft diffractive BCL ($p < 0.001$) but not with the moulded BCL ($p = 0.55$).

As a summary, *Figure 4.2-37* shows the expected increase in average modulation with increasing DZJ height for the near focus (open symbols) and reduction for the distance focus (filled symbols).

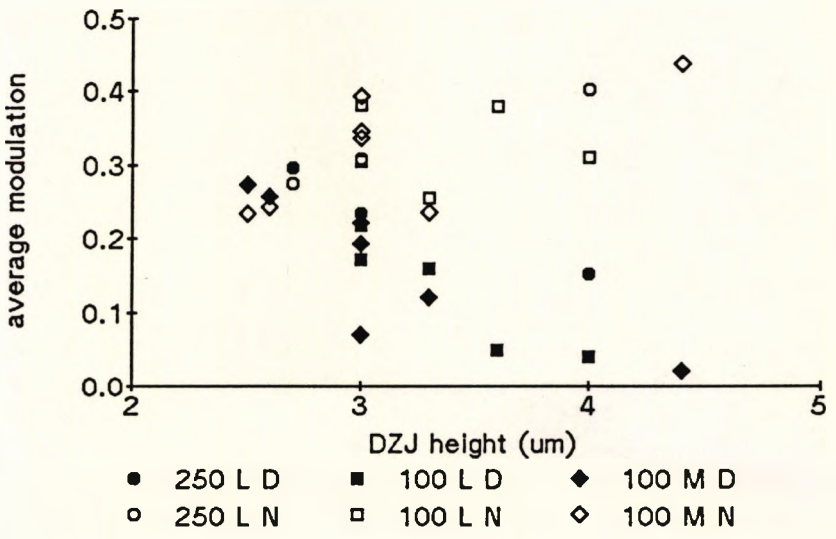

Figure 4.2-37 Average modulation versus DZJ height of soft diffractive BCL. Average modulation increased for the near focus (open) and decreased for the distance focus (filled) with increasing DZJ height for the lathed (L) 250 μm tool (circle), 100 μm tool (square) and moulded (M) 100 μm (diamond) soft diffractive BCL. There was no apparent difference between tool shapes or methods of manufacture.

Diamond Tool Shape

As shown in *Figure 4.2-38*, tool shape did not have a consistent effect upon the optical performance of lathed BCL with DZJ heights of 3.0 μm, 3.3 μm and 4.0 μm. The most pronounced difference was the MTF of the 3.3 μm, flatted tool BCL, which was far more near biased than the other two 3.3 DZJ height BCL (*Figure 4.2-38b*).

Figure 4.2-37 summarises the variation in average MTF with DZJ height for the different tool shapes, and indicates that there was no clear difference between the tools.

Manufacture technique

The method of manufacture (lathe cutting or moulding) was compared for soft diffractive BCL with nominal DZJ heights of 3.0 and 3.3 μm using an ANOVA (*Appendix 5 (A5-12)*). There was no overall difference between the two manufacture techniques ($p = 0.15$). The interaction between manufacture and DZJ height ($p < 0.001$) and the weak interaction between manufacture, DZJ height and vergence ($p = 0.09$) shown in *Figures 4.2-38 and 4.2-37*, indicates that the 3.0 μm BCL were better, at both distance and near with both manufacture techniques, than the 3.3 μm BCL. This implies manufacturing problems as the 3.3 μm BCL were expected to be better at near than the 3.0 μm BCL.

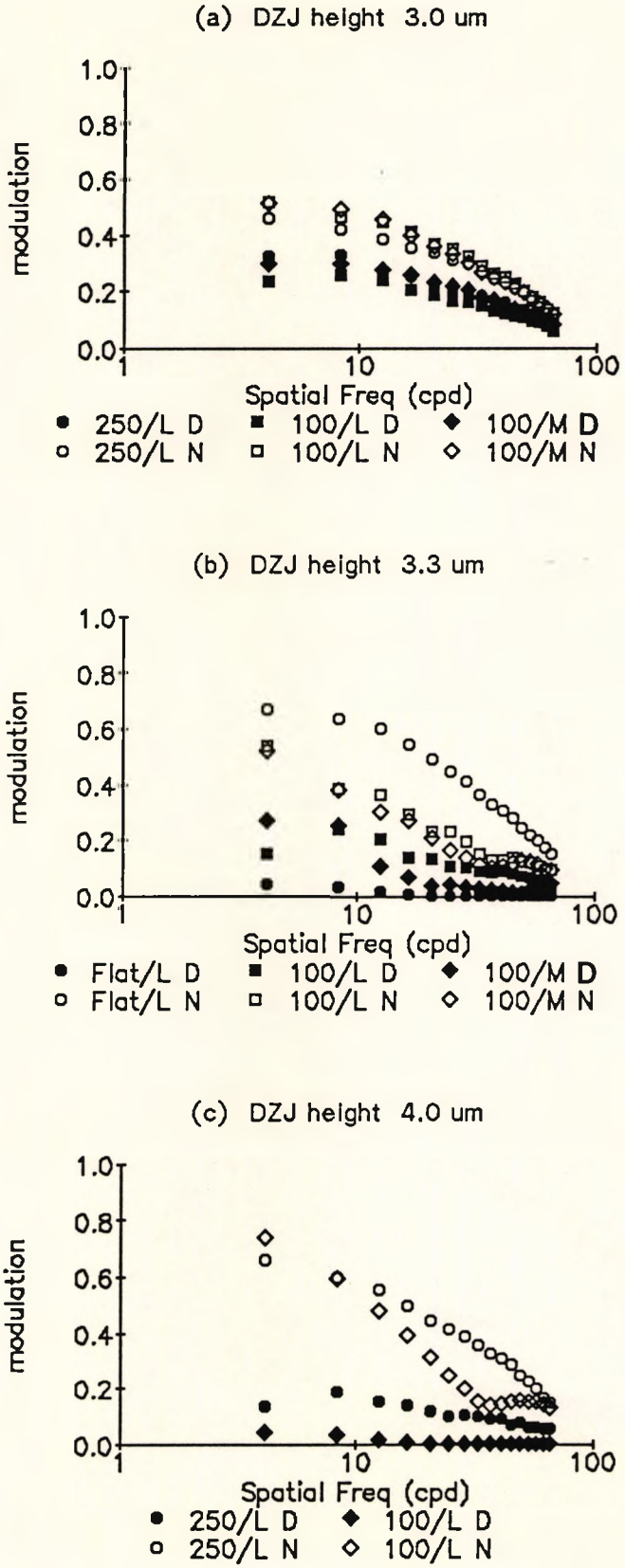

Figure 4.2-38 The variation in MTF with tool shape for **(a)** 3.0 μm; **(b)** 3.3 μm; and **(c)** 4.0 μm DZJ height, lathed (L) and moulded (M) soft diffractive BCL at distance (filled) and near (open).

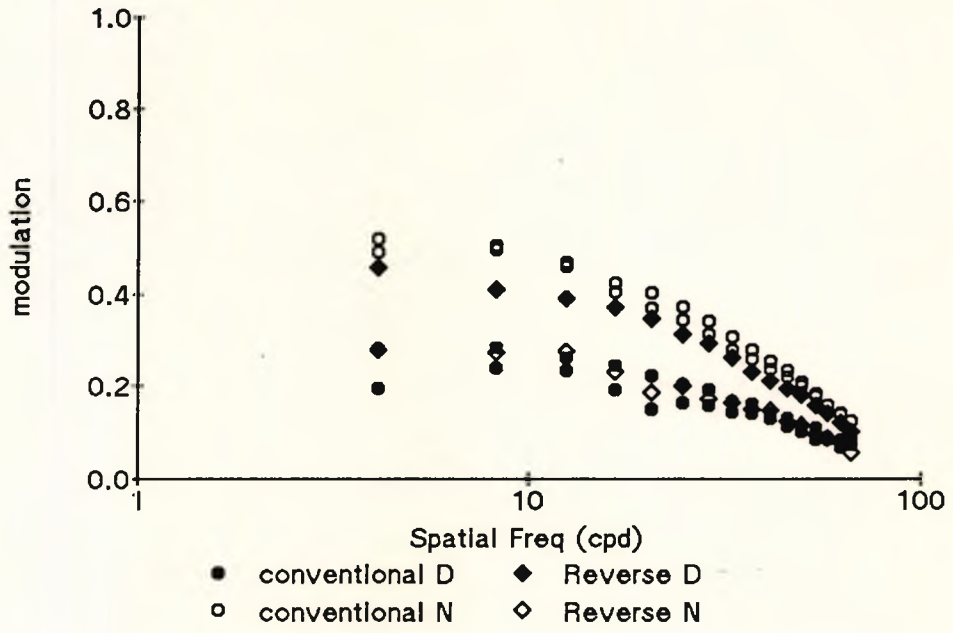

Figure 4.2-39 The MTF of a "reverse" add soft diffractive BCL 3.0 μm DZJ height, 100 μm tool, moulded (diamond) was found to differ from conventional soft diffractive BCL of the same nominal parameters (circle). The "reverse" add BCL was distance (filled) biased, whilst the conventional BCL were near (open) biased.

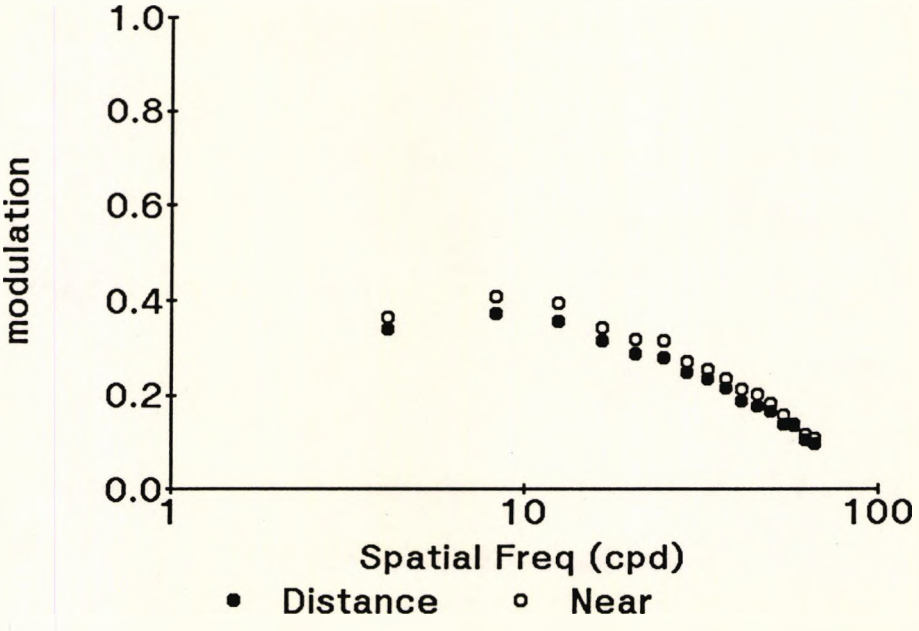

Figure 4.2-40 The average MTF of three Allergan Echelon soft diffractive BCL was found to be better than any of the soft diffractive BCL available for this study.

"Reverse" add soft diffractive bifocal contact lens

A "reverse" add BCL utilises the negative first order diffractive focus to form the distance image and the zero order focus to form the near image (section 1.2.3). Hence the image formation varied from the other diffractive BCL used in this study. As shown in *Figure 4.2-39* the MTF of a "reverse" add BCL was different from a "conventional" BCL (zero order focus forms distance image, positive first order focus forms near image) of the same nominal DZJ height. This was consistent with the ANOVA (*Appendix 5 (A5-13)*) interactions between addition type and vergence ($p < 0.001$) and between addition type, vergence and spatial frequency ($p < 0.001$)

A commercially available soft diffractive bifocal contact lens

The MTF of the Allergan Echelon soft diffractive BCL is shown in *Figure 4.2-40*. The overall optical performance was better than any of the soft diffractive BCL available for this study.

4.3 Visual Performance

4.3.1 INTRODUCTION

The repeatability of the visual performance measures and the correlation between the measures is described in section 4.3.2. Subsequent sections examine visual

performance with the refractive (section 4.3.3), rigid diffractive (section 4.3.4) and soft diffractive (section 4.3.5) BCL. Results have been compared to the two commercially available diffractive BCL (sections 4.3.4 and 4.3.5). Almost 1400 separate measurements with BCL were made, each with the 7 visual performance measures (section 3.3). Hence it was not possible to present all the data, and, where appropriate, examples, typically of averaged data, have been used to illustrate important aspects of the data. Analysis of Variance (ANOVA) was used to investigate the effect of manipulated variables, and Multiple Regression Analysis (MRA) was used to include uncontrolled variables in the analysis, to investigate trends within the data and to develop empirical models to allow the prediction of optimal BCL design.

4.3.2 GENERAL CONSIDERATIONS

Relative visual performance

All visual performance measures have been converted to a relative measure to remove the effects of different absolute visual performance levels by individual subjects. Data is presented in the form of the relative visual performance where :

$$\text{rel. visual performance} = \log \left\{ \frac{\text{Visual performance with BCL}}{\text{Visual performance without BCL}} \right\}$$

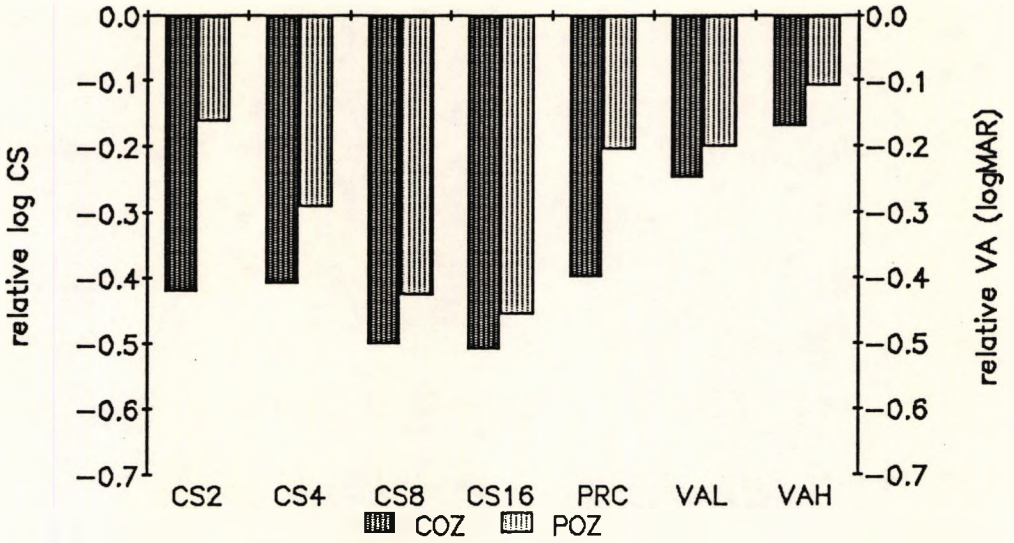

Figure 4.3-1 An example of the visual performance with refractive BCL. The average relative visual performance (reduction due to BCL) with refractive BCL with a 2.6 mm COZD (n = 26). Contrast Sensitivity at 2, 4, 8 and 16 c.p.d. (CS 2, CS 4, CS 8, CS 16), Pelli-Robson contrast threshold (PRC), and Visual Acuity at low and high contrast (VA L, VA H). Note that the greatest difference in CS between focus with the COZ and the POZ is at the low spatial frequencies (2 and 4 c.p.d.) See also *Figure 4.3-8*.

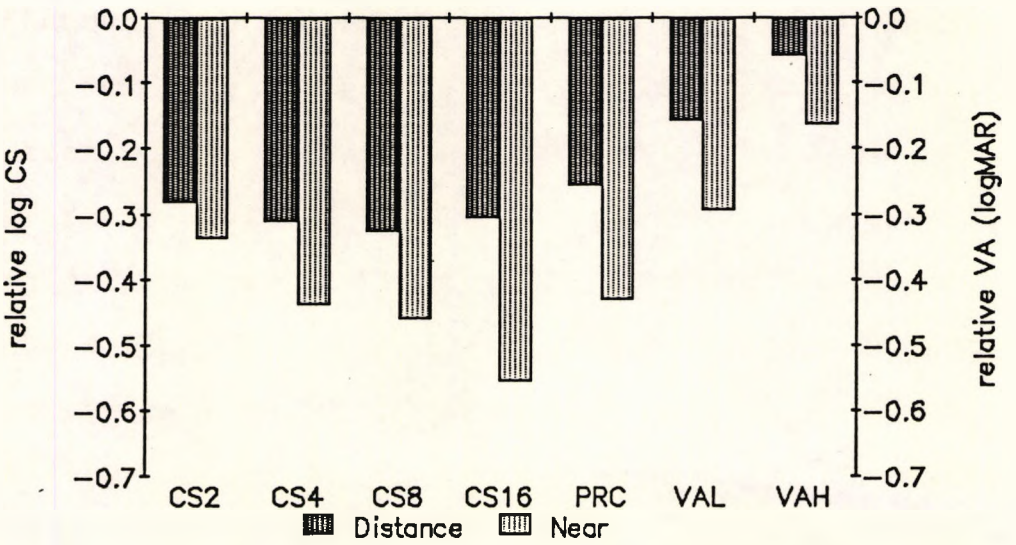

Figure 4.3-2 An example of the visual performance with rigid diffractive BCL. The average relative visual performance (reduction due to BCL) with rigid diffractive BCL (2.0 μm DZJ height; 250 μm tool) (n = 34). Contrast Sensitivity at 2, 4, 8 and 16 c.p.d. (CS 2, CS 4, CS 8, CS 16), Pelli-Robson contrast threshold (PRC), and Visual Acuity at low and high contrast (VA L, VA H). Note that the greatest difference in CS between distance and near is at higher spatial frequencies (8 and 16 c.p.d.).

Hence data was not presented in this section in the form of the conventional CSF plot.

Bifocal Contact Lenses

It was not possible to present data for all 1391 measures of visual performance with BCL. Reductions in visual performance were similar to those previously reported (for discussion see section 1.2.3). As an example, visual performance, presented in the form of conventional CSF plots, are shown in *Figures 1.1-10, 2.3-2* and *2.3-3*. As further examples, relative visual performance averaged for all subjects, with a centre near (CN) refractive BCL is shown in *Figure 4.3-1* and with a diffractive BCL in *Figure 4.3-2*.

Repeatability

Repeatability Coefficients of the visual performance measures (*Table 4.3-1*) were assessed by examining the test-retest repeatability of the five subjects wearing refractive BCL (n = 94) and the three subjects wearing rigid diffractive BCL (n = 213) and soft diffractive BCL (n = 120). The variability of test-retest did not alter with average visual performance, as shown in *Figure 4.3-3*, as an example, for CS at 4 c.p.d. and low contrast VA with rigid diffractive BCL.

Repeatability coefficients increased with increasing spatial frequency and with decreasing AVC contrast. The

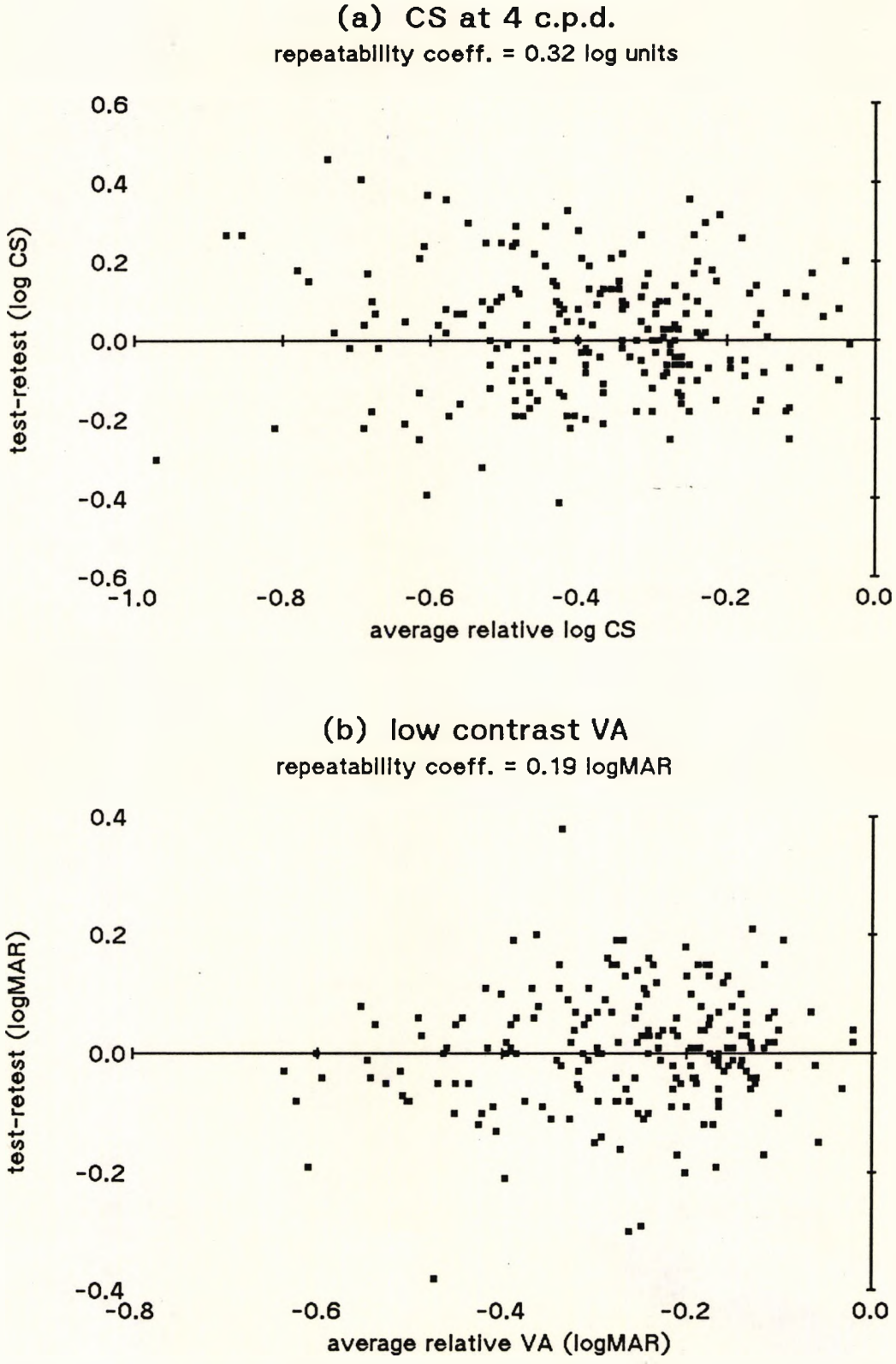

Figure 4.3-3 An example of the variability of test-retest with visual performance. Test-retest versus average visual performance shown for (a) contrast sensitivity at 4 c.p.d.; and (b) low contrast visual acuity with rigid diffractive BCL (n = 213). There was no trend for increased variability with reduced relative visual performance.

repeatability coefficients were larger for the soft diffractive BCL than the rigid diffractive BCL.

As shown in *Figure 4.3-4* the repeatability coefficients increased significantly with decreased relative visual performance (R^2 = 0.85; $p < 0.0001$). The repeatability coefficients represented 68% to 96% of the average relative visual performance, except for high contrast VA, which had repeatability coefficients larger than the average relative visual performance.

	Rigid Diffractive n = 213	Soft Diffractive n = 120	Refractive n = 94
		(log contrast units)	
CS at 2 c.p.d.	0.266	0.279	0.272
CS at 4 c.p.d.	0.317	0.411	0.332
CS at 8 c.p.d.	0.366	0.461	0.422
CS at 16 c.p.d.	0.436	0.499	0.452
PRC at 4 m	0.243	0.362	0.222
		(logMAR units)	
AVC Low contrast	0.193	0.344	0.183
AVC High contrast	0.182	0.266	0.172

Table 4.3-1 Repeatability coefficients (section 3.7) determined for the visual performance measures. This was a measure of the reliability (i.e. 95% confidence limit) of an individual result.

Correlation between visual performance measures

As shown for all BCL worn by all subjects (n = 1391) in *Table 4.3-2*, all the visual performance measures were significantly correlated with each other. Correlation was higher between visual performance measures with similar spatial frequency content. Principal component

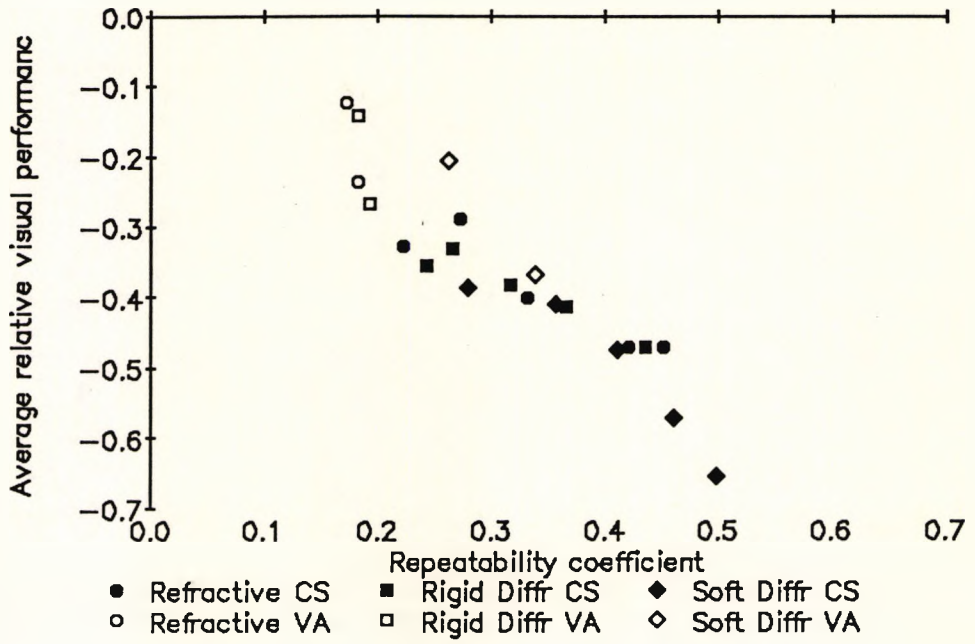

Figure 4.3-4 Repeatability versus relative visual performance. The repeatability coefficient was highly correlated (r^2 = 0.85; p < 0.001) with the average reduction in CS (filled) and VA (open) with the refractive (circle), rigid (square) and soft (diamond) diffractive BCL.

	CS 2	CS 4	CS 8	CS 16	PRC	VA L
CS 4	0.59					
CS 8	0.55	0.74				
CS 16	0.54	0.68	0.79			
PRC	0.53	0.61	0.55	0.51		
VA L	0.44	0.66	0.62	0.65	0.75	
VA H	0.27	0.52	0.51	0.55	0.60	0.84

Table 4.3-2 Correlation (Pearson r) between the visual performance measures (n = 1391) with all BCL worn by all subjects. All correlations were highly significant (p <= 0.001). The low correlations suggest the importance of measurement of visual performance at a range of spatial frequencies.

analysis indicated that the measured visual performance could be represented by a single component (i.e. the measured visual performance did not contain separate spatial frequency components).

4.3.3 REFRACTIVE BIFOCAL CONTACT LENSES

Visual performance with refractive BCL was firstly analysed with an ANOVA. MRA was then employed to further investigate the effects of pupil size and BCL decentration. The MRA equations allowed the prediction of the optimal COZD for a given pupil size, decentration and visual performance measure.

Subject	Pupil size		BCL Decentration	
	Monitor (mm)	Charts (mm)	CD (mm)	CN (mm)
1	3.6	3.0	1.11 (0.4 to 1.3)	0.98
2	3.5	2.8	0.87 (0.3 to 1.6)	0.75
3	2.7	2.4	0.80 (0.2 to 1.7)	1.32
4	2.6	2.1	1.90 (0.4 to 2.4)	1.59
5	2.9	2.6	1.44 (0.4 to 1.9)	0.81

Table 4.3-3 Pupil size and refractive BCL decentration. Calculated pupil size at the two experimental luminance levels (max s.e. = 0.3 mm) and mean measured BCL decentration of centre distance (CD) and centre near (CN) refractive BCL for each of the five subjects (the range of the measured decentration is shown in brackets).

Measured pupil size and decentration

Table 4.3-3 shows, for all subjects, the calculated pupil sizes for the test luminances and the BCL decentration with both centre distance (CD) and centre near (CN) BCL. CD lenses tended to decentre slightly more (1.18 mm) than CN lenses (1.07 mm) ($p = 0.12$), but there was a great degree of variability. The proportion of the pupil covered by the COZD varied between the BCL types at both luminance levels (monitor (50 cd/m^2): 42% v 50%, $p = 0.017$; charts (250 cd/m^2): 41% v 49%, $p = 0.007$).

Aperture Size and Central Optic Zone Diameter

BCL design (L), COZD (D) and vergence (V) were included as ANOVA factors and the decentration of the COZ over the pupil and the size of the pupil were included as a covariates in an ANOVA of visual performance results. CS results were analysed with spatial frequency considered as a factor (F). Similarly VA chart contrast level was considered as a factor (C). The ANOVA tables are given in *Appendix 7 (A7-1)* and the more important aspects summarised in *Table 4.3-4*.

As shown in *Figure 4.3-5*, and confirmed by the covariate pupil size, relative visual performance reduced with increasing pupil size. Decentration had a significant effect upon CS and a weak effect upon VA.

As expected, and confirmed by the interaction L x D x V, *Figures 4.3-6 and 4.3-7* show that vision with all visual

	CS	PRC	AVC
decentration	<0.001	0.8	0.016
pupil size	<0.001	<0.001	<0.001
COZD (D)	0.04	0.11	0.3
Lens Design (L)	0.003	0.6	0.002
D x L x V	<0.001	<0.001	<0.001
L x V x F	<0.001		
L x V x C			<0.001
D x L x V x F	0.12		
D x L x V x C			0.003

Table 4.3-4 Summary of the ANOVA of visual performance with refractive BCL. The levels of significance of selected covariates (decentration, pupil size), factors (COZD (D), Lens design (L)) and interactions (including factors vergence (V), spatial frequency (F) and contrast (C), as detailed in text) for the ANOVAs of visual performance with refractive BCL. Full details of the ANOVAs are given in *Appendix 6 (A6-1)*.

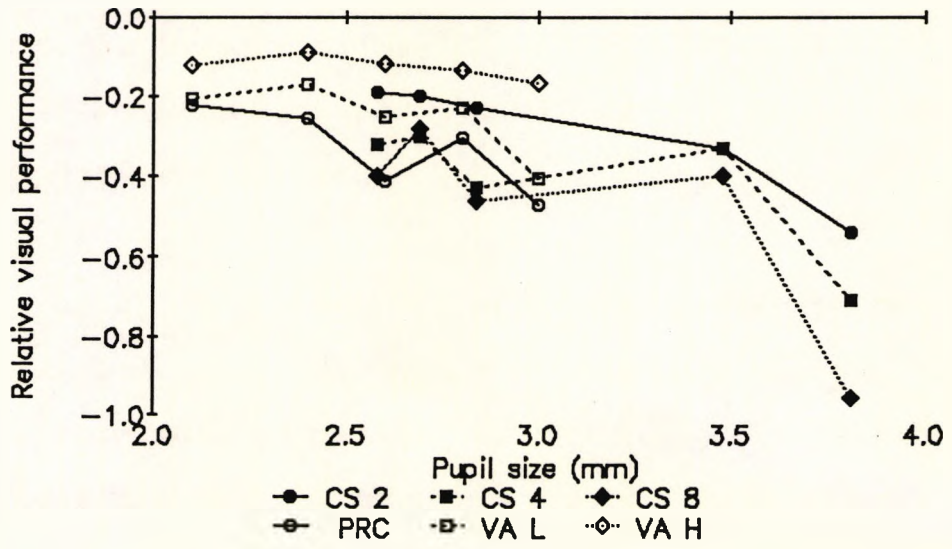

Figure 4.3-5 Visual performance versus pupil size. The relative visual performance (reduction with refractive BCL) reduced with increasing measured pupil size of the five subjects.

performance measures improved as the COZD increased when the COZ formed the focus (CD distance, CN near) and reduced when the POZ formed the focus (CD near, CN distance). The COZD at which the COZ and the POZ performed equally appears to vary slightly with the spatial frequency content of the visual performance measure. The interaction L x D x V x F suggests that this was not significant with CS, though there was a significant interaction (L x D x V x C) between the two contrast levels of the AVC. As shown in *Figures 4.3-6* and *4.3-7*, and confirmed by the interactions L x V x F and L x V x C, the relative visual performance varies between COZ and POZ at different spatial frequencies and AVC contrasts. *Figures 4.3-1 and 4.3-8* show that when the POZ formed the focus the reduction in CS was smaller at low (2 and 4 c.p.d.) than at higher (8 and 16 c.p.d.) spatial frequencies across the range of COZD. The variation of optical performance with spatial frequency shown in *Figure 4.2-3* indicated the optical basis for this difference in visual performance.

A model for changes in visual performance

MRA was used to develop empirical models of visual performance in terms of COZD, pupil size and BCL location. The models were used to predict an optimal COZD (equal distance and near). To simplify the analysis, as noted in the optical evaluation of the same BCL (section 4.2.3), the interaction between lens design and vergence (L x V) could be reduced to a single factor - the optic

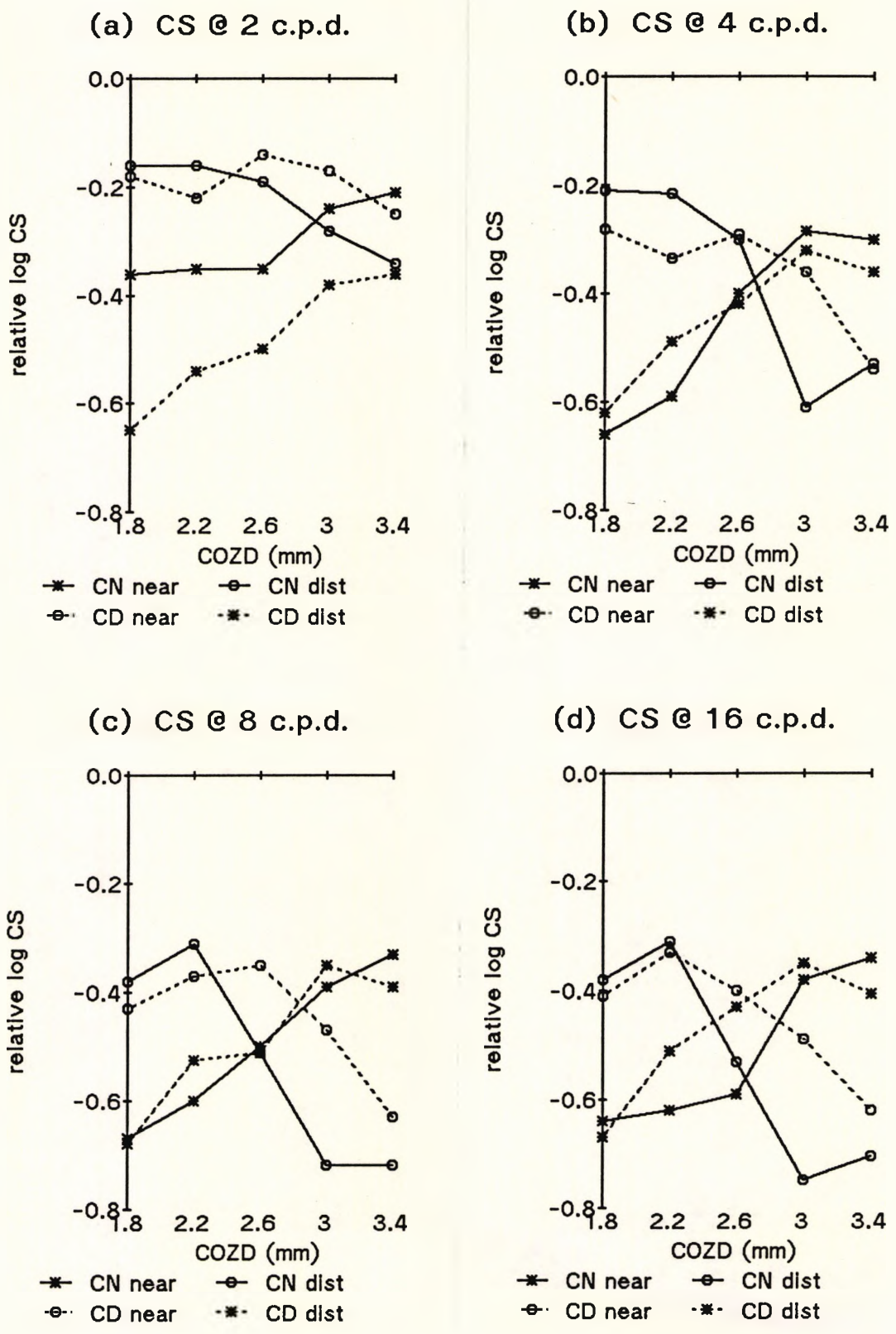

Figure 4.3-6 Contrast Sensitivity (CS) with refractive BCL. As COZD increases visual performance improves with the COZ forming the focus (asterisk) and reduces with the POZ forming the focus (circle) with both centre near (CN: solid line) and centre distance (CD: dotted line) refractive BCL for CS at **(a)** 2 c.p.d.; **(b)** 4 c.p.d.; **(c)** 8 c.p.d.; and **(d)** 16 c.p.d.

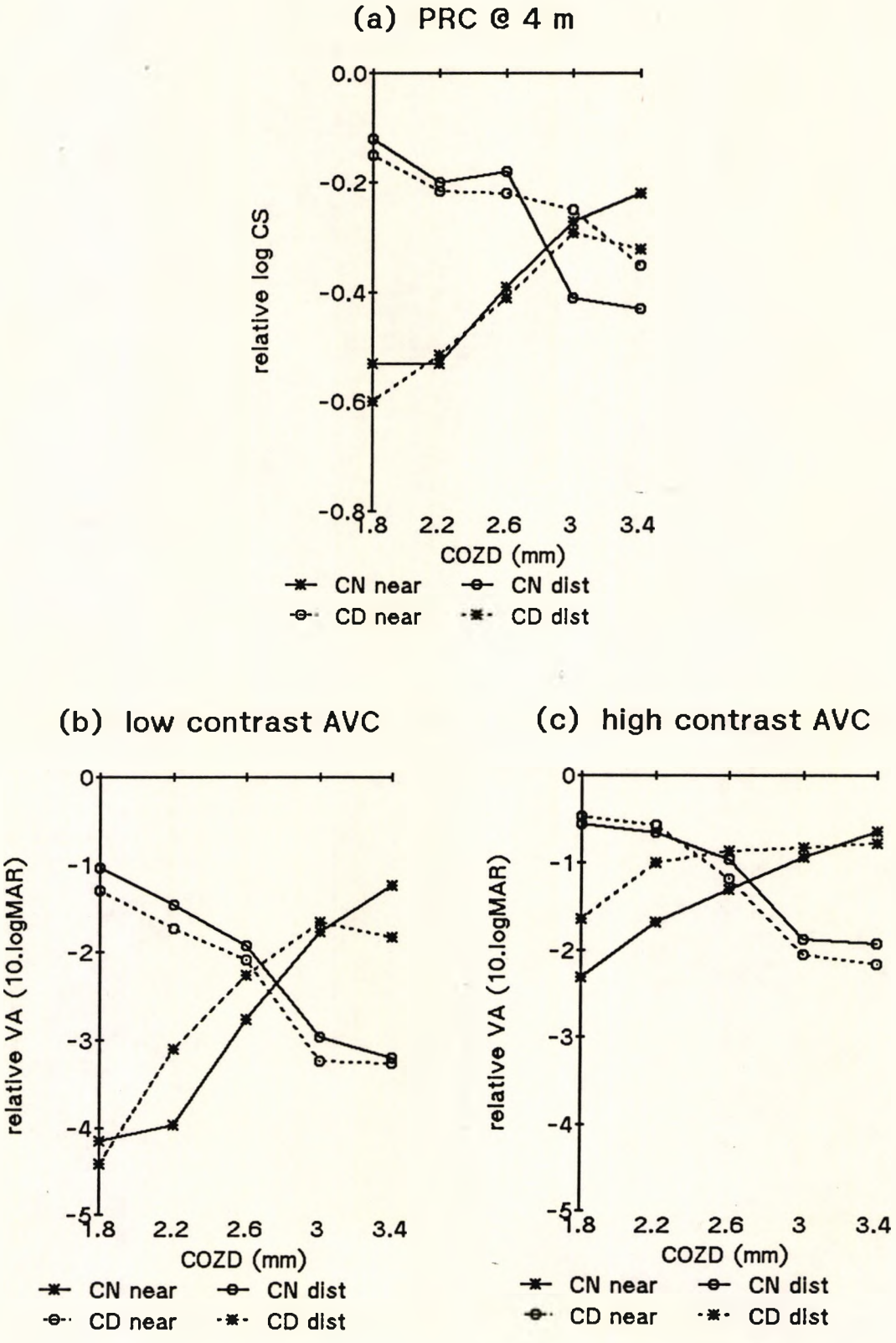

Figure 4.3-7 Vision (chart based tests) with refractive BCL. As COZD increases visual performance improves with the COZ forming the focus (asterisk) and reduces with the POZ forming the focus (circle) with both centre near (CN: solid line) and centre distance (CD: dotted line) refractive BCL for **(a)** PRC at 4 m ; **(b)** low contrast AVC; and **(c)** high contrast AVC.

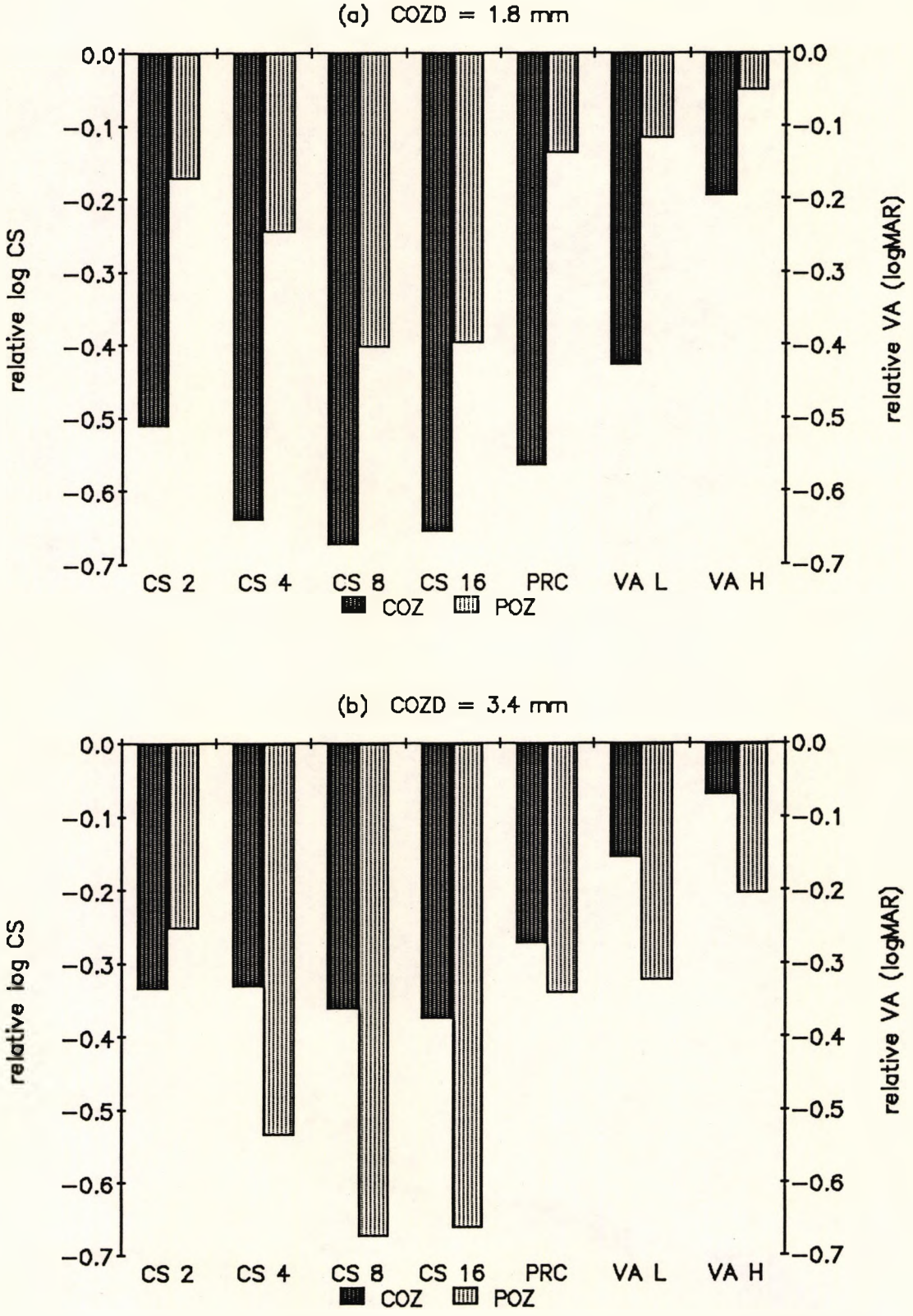

Figure 4.3-8 The average relative visual performance (difference from without BCL) with refractive BCL **(a)** 1.8 mm COZD (n = 28); and **(b)** 3.4 mm COZD (n = 25). Contrast Sensitivity at 2, 4, 8 and 16 c.p.d. (CS 2, CS 4, CS 8, CS 16), Pelli- Robson contrast threshold (PRC), and Visual Acuity at low and high contrast (VA L, VA H). When the POZ forms the focus the loss in CS is least at the low spatial frequencies (2 and 4 c.p.d.) whilst the loss is almost equal at all spatial frequencies when the COZ forms the focus. Also *Figure 4.3-1* with 2.6 mm COZD.

zone of the BCL which was in focus (i.e. the COZ or the POZ). As shown in *Figures 4.3-6 and 4.3-7*, this was confirmed by the ANOVA interaction between lens design and optic zone for the AVC ($p = 0.97$) and PRC ($p = 0.18$) but not for CS ($p = 0.002$). A range of potential MRA equations was investigated. All MRA equations obtained were significant ($p < 0.0001$) with adjusted R^2 values which varied between 0.30 and 0.55. As an example, the equations derived for PRC are shown below. One equation describes the visual performance when viewing with the COZ forming the focus and the other when viewing with the POZ forming the focus.

<u>with COZ forming the focus</u>
relative PRC = - 0.35 - 0.063 pupil + 0.10 COZD
+ decentration x (- 0.13 pupil + 0.10 COZD)

<u>with POZ forming the focus</u>
relative PRC = 0.39 - 0.26 COZD + decentration x (- 0.076 pupil + 0.10 COZD)

(adjusted $R^2 = 0.551$, s.e. = 0.134, n = 256)

Details of MRA of all visual performance measures are given in *Appendix 7 (A7-2)*. The stepwise MRA procedure removed terms which had low significance and hence not all terms were included in all (7 x 2) equations. There were no consistent trends for the terms which were retained, and the only terms included in all equations describing visual performance were the two terms for COZD (with COZ and with POZ).

To evaluate the MRA equations the predictions were compared to raw data. For example, as shown in *Figures 4.3-9 and 4.3-10* for CS at 16 c.p.d. and low contrast VA, the

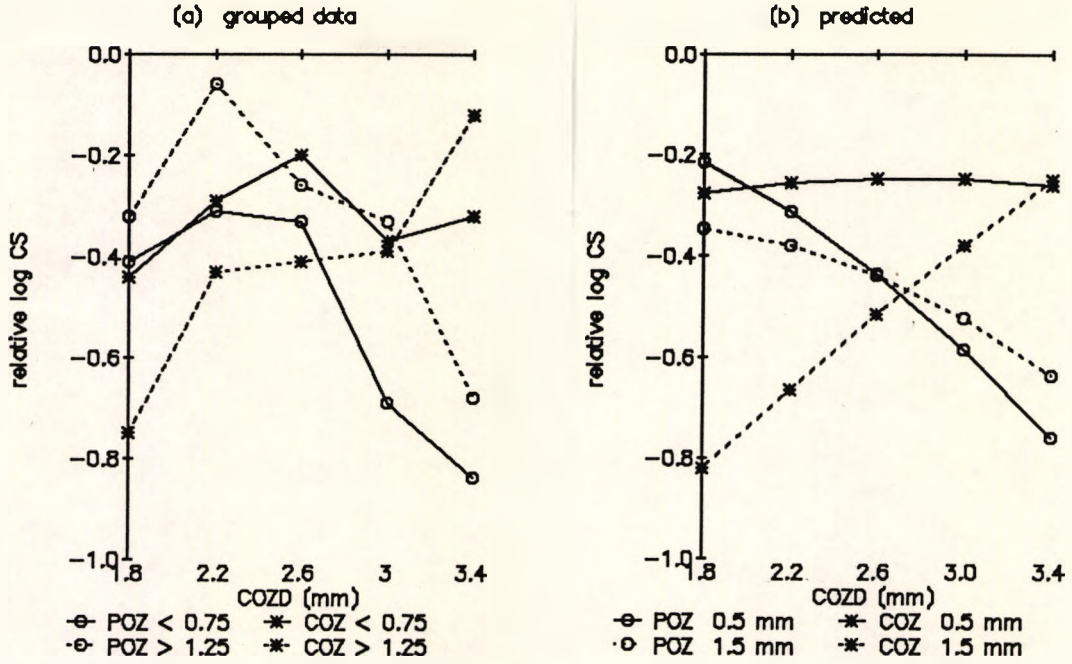

Figure 4.3-9 Evaluation of the MRA equations describing visual performance with refractive BCL - example for CS at 16 c.p.d.. The MRA prediction was compared to grouped data using the COZ (asterisk) and the POZ (circle). **(a)** Actual data for BCL with decentrations of less than 0.75 mm (solid lines) and greater than 1.25 mm (dotted lines) were compared to **(b)** the predicted values for decentrations of 0.5 mm (solid lines) and 1.5 mm (dotted lines) (the approximate means of the raw data), with an average pupil size (3.0 mm).

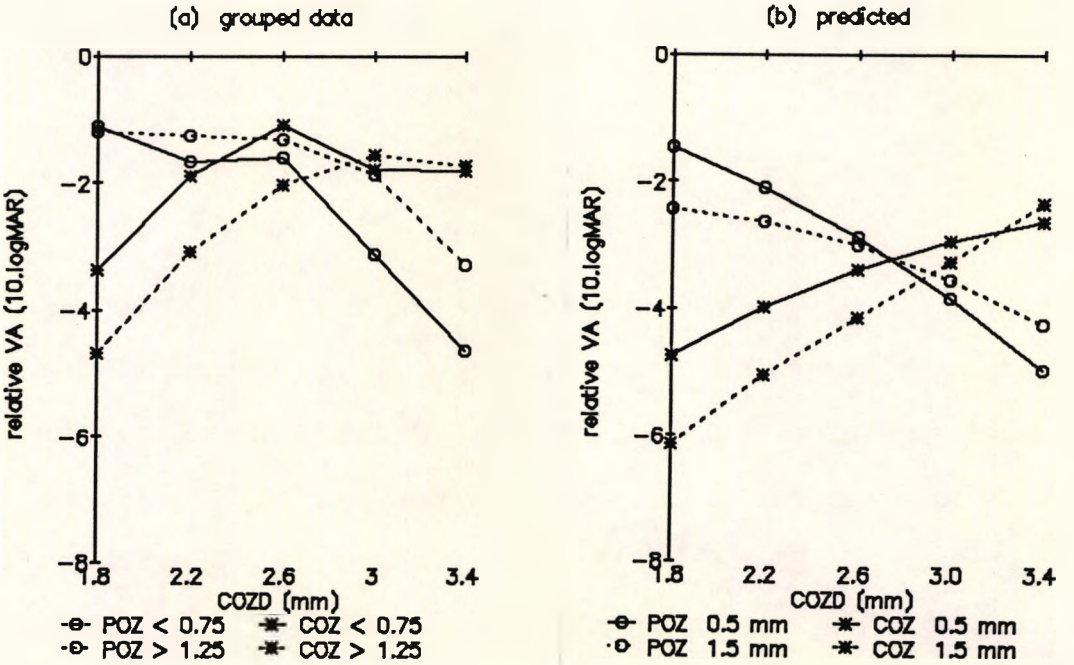

Figure 4.3-10 Evaluation of the MRA equations describing visual performance with refractive BCL - example for low contrast VA . The MRA prediction was compared to grouped data with COZ (asterisk) and POZ (circle). **(a)** Actual data for BCL with decentrations of less than 0.75 mm (solid lines) and greater than 1.25 mm (dotted lines) were compared to **(b)** the predicted values for decentrations of 0.5 mm (solid lines) and 1.5 mm (dotted lines) (the approximate means of the raw data), with an average pupil size (3.0 mm).

actual data for decentrations of less than 0.75 mm and greater than 1.25 mm were compared to the predicted values for decentrations of 0.5 mm and 1.5 mm (the approximate means of the raw data), with an average pupil size (3.0 mm). As the raw data was grouped, and only 30 to 55% of the variation was explained by the MRA equations, the conformity of the predicted data to the actual data was not as convincing as with optical performance (section 4.2.3).

The MRA equations were solved for equal visual performance between COZ and POZ. As shown in *Figures 4.3-11 and 4.3-12*, the optimal COZD varied with pupil size, decentration, and the different visual performance measure. This was consistent with the optical performance predictions given in section 4.2.3.

4.3.4 RIGID DIFFRACTIVE BIFOCAL CONTACT LENSES

Changes in visual performance were used to investigate the variability of manufacture. The major investigation examined the effect of variations in Diffractive Zone Junction (DZJ) height and tool shape upon visual performance with ANOVA and MRA. For the purposes of the ANOVA, CS results were analysed with spatial frequency considered as a factor (F), and similarly AVC contrast level was considered as a factor (C). The MRA equations were used to develop an empirical model which allowed a

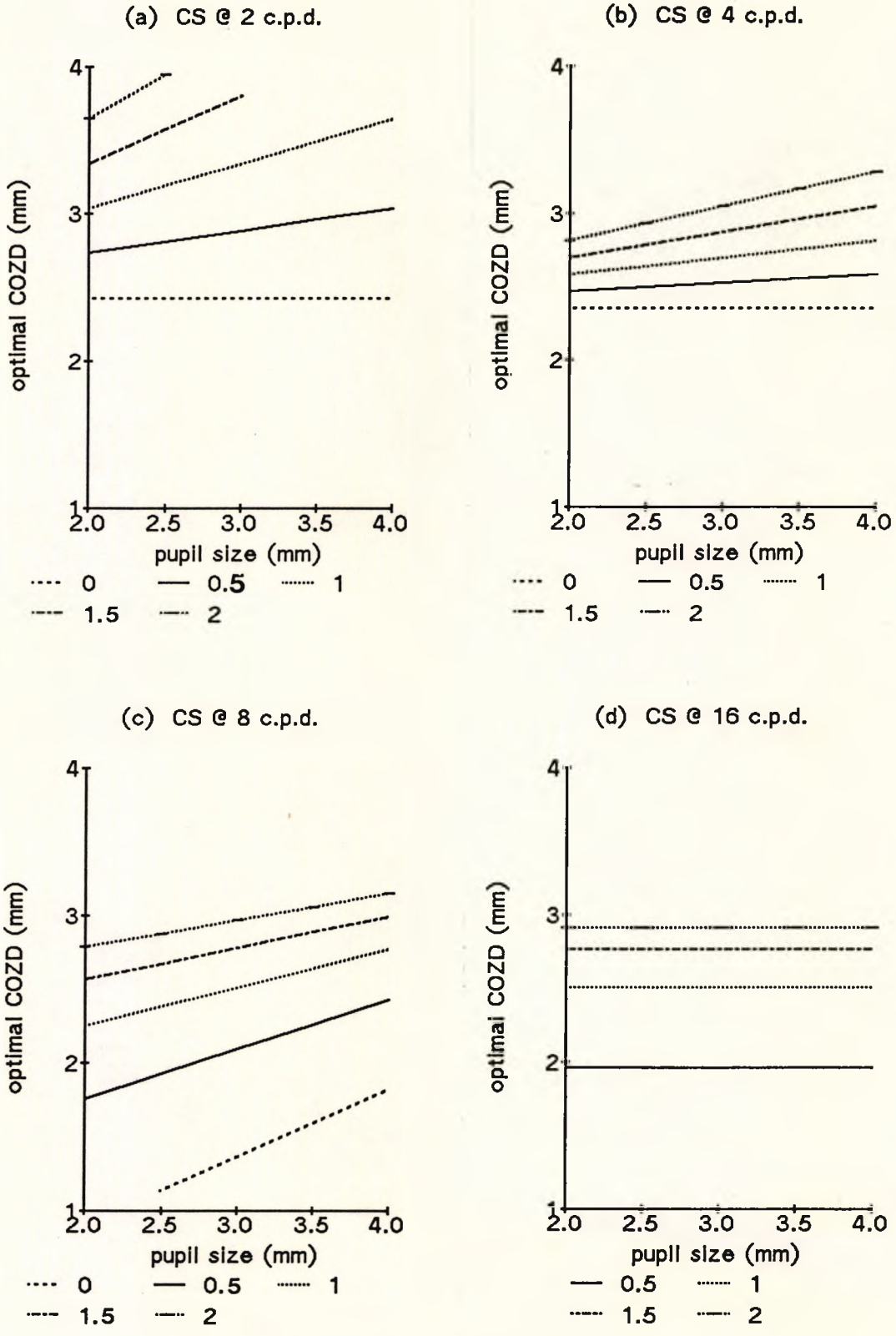

Figure 4.3-11 The optimal COZD predicted with MRA. The optimal COZD for refractive BCL with the COZ decentred 0 to 2 mm over pupils of 2 to 4 mm for CS at **(a)** 2 c.p.d.; **(b)** 4 c.p.d.; **(c)** 8 c.p.d.; and **(d)** 16 c.p.d. predicted by the MRA equations.

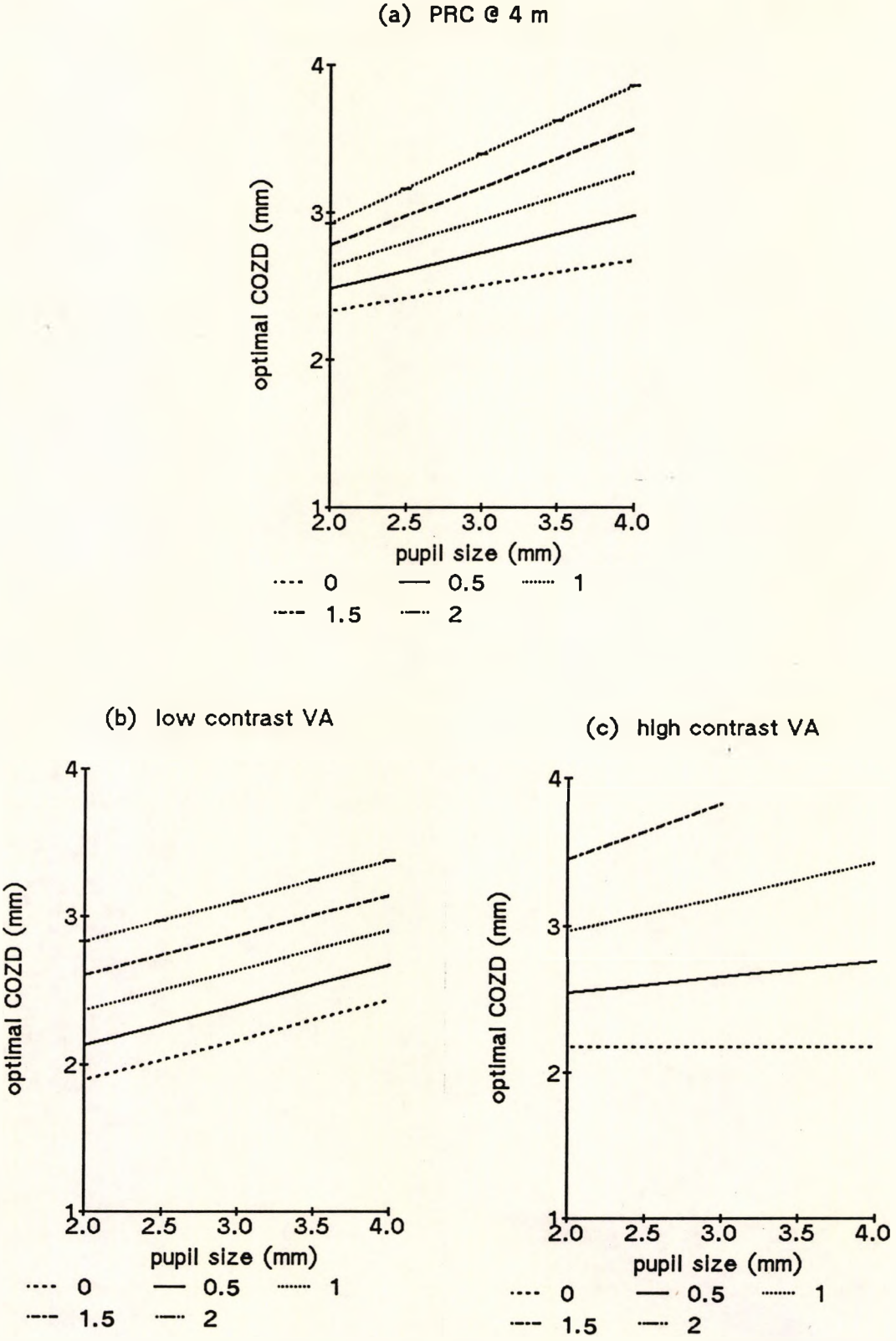

Figure 4.3-12 The optimal COZD predicted with MRA. The optimal COZD for refractive BCL with the COZ decentred 0 to 2 mm over pupils of 2 to 4 mm for **(a)** PRC at 4 m ; **(b)** low contrast AVC; and **(c)** high contrast AVC predicted by the MRA equations.

prediction of the optimal DZJ height (equal distance and near) for each of the visual performance measures.

A preliminary investigation of the data indicated that, when the relative visual performance with BCL was considered, there were no consistent differences between the results for the two presbyopic subjects and the young cyclopleged subject, and hence data were combined.

Variability of manufacture

The variability of the manufacture process was investigated by comparing two batches (production runs separated by about six months) of nominally identical BCL (DZJ height 2.2 and 2.6 μm; 250 μm round diamond tool). ANOVA (*Appendix 7 (A7-3)*) indicated a significant difference between the two batches with PRC ($p = 0.01$) but not with CS and AVC (($p = 0.65$; $p = 0.84$ respectively); and no significant interaction between the batch, DZJ height and vergence ($p = 0.09$; $p = 0.69$; $p = 0.49$) with CS, PRC and AVC (respectively). Conversely, as noted in section 4.2.4, there was a significant difference in optical performance.

In addition, experimental BCL with a 2.0 μm DZJ height manufactured with the 250 μm round diamond tool were compared to Pilkington Diffrax BCL (which were nominally identical). ANOVA (*Appendix 7 (A7-4)*) indicated no significant difference between the two BCL types with CS, PRC or AVC ($p = 0.37$; $p = 0.61$; $p = 0.45$) and a

Experimental BCL			Pilkington Diffrax		
code	Vergence Ratio	s.e.	code	Vergence Ratio	s.e.
CS at 8 c.p.d.					
B1	0.42	0.16	DX1	0.71	0.26
B2	0.59	0.20	DX2	0.72	0.38
B3	0.36	0.44	DX3	0.63	0.57
B4	0.46	0.50	DX4	0.59	0.31
B5	0.49	0.44	DX5	0.58	0.29
B6	0.49	0.50	DX6	0.63	0.45
High Contrast VA					
B1	0.66	0.06	DX1	0.63	0.11
B2	0.76	1.17	DX2	0.79	0.58
B3	0.60	0.28	DX3	0.86	0.81
B4	0.38	0.34	DX4	0.99	1.52
B5	0.92	0.11	DX5	0.87	0.60
B6	0.62	0.92	DX6	0.81	0.60

Table 4.3-5 Variability of manufacture of rigid diffractive BCL. The vergence ratio (distance/distance+near) of the average CS at 8 c.p.d. and high contrast VA with rigid diffractive BCL of nominally identical DZJ height indicates the distance or near bias of each BCL. A ratio greater than 0.5 indicates a bias to distance. The large standard errors (s.e.), due to the small number of repetitions with each BCL (n = 2 to 4) make the interpretation of differences between individual BCL difficult. The vergence ratio of the experimental BCL was significantly different from Pilkington Diffrax with CS at 8 c.p.d. (p = 0.001) but not with high contrast VA (p = 0.09).

	CS	**PRC**	**AVC**
Tool (T)	0.001	0.001	0.32
H x V	<0.001	<0.001	<0.001
H x T x V	<0.001	0.028	<0.001
H x V x F	<0.001		
H x V x C			<0.001

Table 4.3-6 Summary of the ANOVA of visual performance with rigid diffractive BCL. The levels of significance of selected factors (Tool (T)) and interactions (including factors DZJ Height (H) Vergence (V) Spatial Frequency (F) and contrast (C), as detailed in text) for the ANOVAs of visual performance with rigid diffractive BCL. Full details of the ANOVAs are given in *Appendix 6 (A6-5)*.

significant interaction between the BCL type and vergence with CS ($p < 0.001$) but not with PRC and AVC ($p = 0.22$; $p = 0.16$). Conversely, as noted in section 4.2.4, there was a significant difference in optical performance.

The relative visual performance between distance and near was expressed as the vergence ratio (distance / distance + near) which varied between 0 and 1, and if greater than 0.5 then the BCL was distance vision biased. *Table 4.3-5* shows the variability in the vergence ratio of nominally identical BCL with, for example, two of the visual performance measures, which can be compared to the variation in optical performance shown in *Table 4.2-1.*

Diffractive Zone Junction Height and Tool Shape

DZJ heights (H) of 1.8 to 3.0 μm, Tool shapes (T) 250 μm, 100 μm and flatted, and Vergences (V) of distance and near, were investigated with ANOVA and the results given in *Appendix 7 (A7-5)* are summarised in *Table 4.3-6*.

As expected, with all tool shapes as shown in *Figures 4.3-13 and 4.3-14*, and confirmed by the interaction H x V, as the DZJ height increased near visual performance improved and distance visual performance reduced. The variation in distance and near visual performance with DZJ height varied with the tool shape, as confirmed by the interaction H x T x V. The ratio between distance and near CS at different DZJ heights varied with spatial frequency, confirmed by the interaction H x V x F and

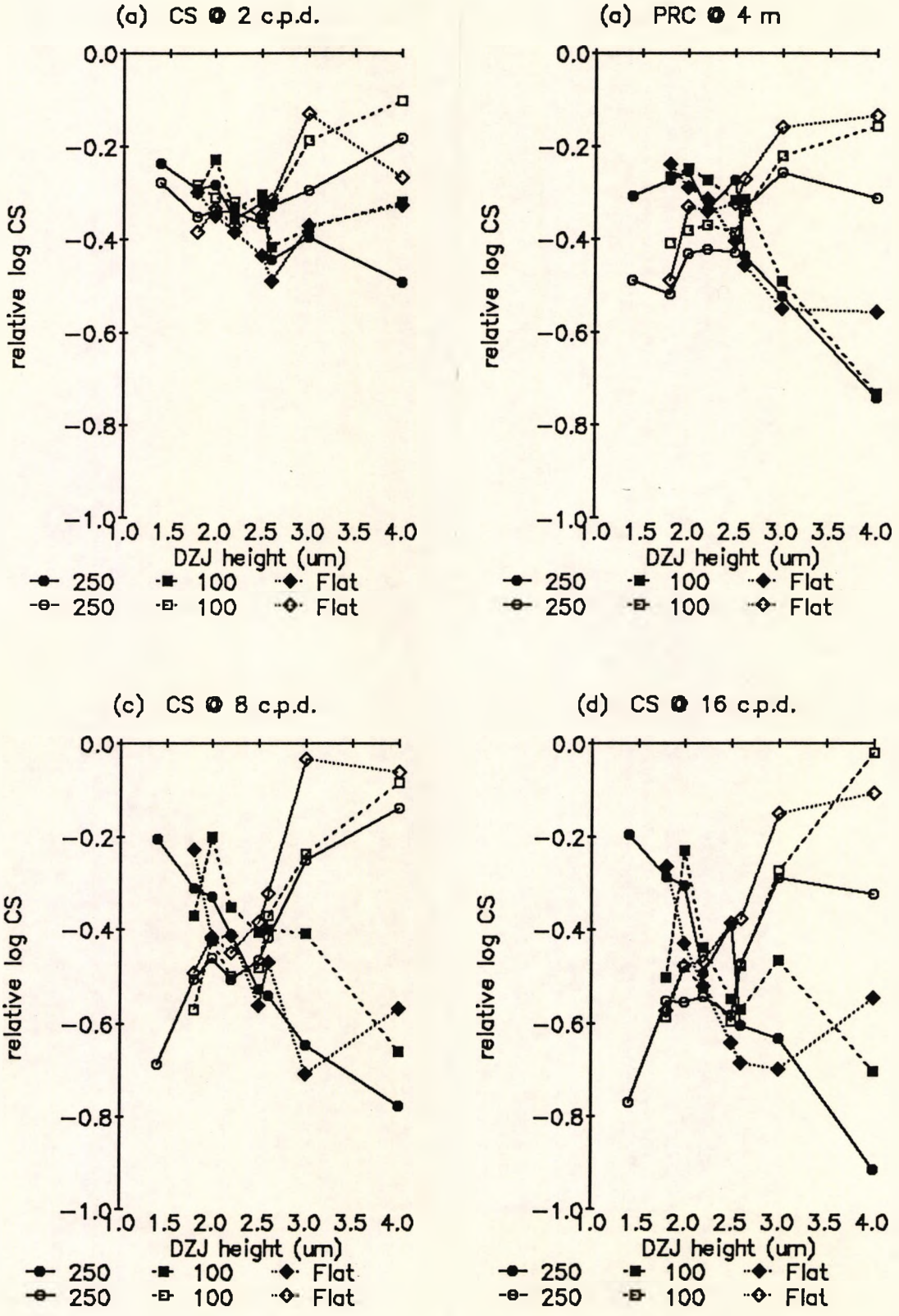

Figure 4.3-13 Visual performance variation with the DZJ height of rigid diffractive BCL. As DZJ height increases visual performance at near (open) improves and reduces at distance (filled) for rigid diffractive BCL manufactured with the 250 μm (circle, solid line), 100 μm (square, dashed line) and the flatted (diamond, dotted line) tool for CS at **(a)** 2 c.p.d.; **(b)** 4 c.p.d.; **(c)** 8 c.p.d.; and **(d)** 16 c.p.d.

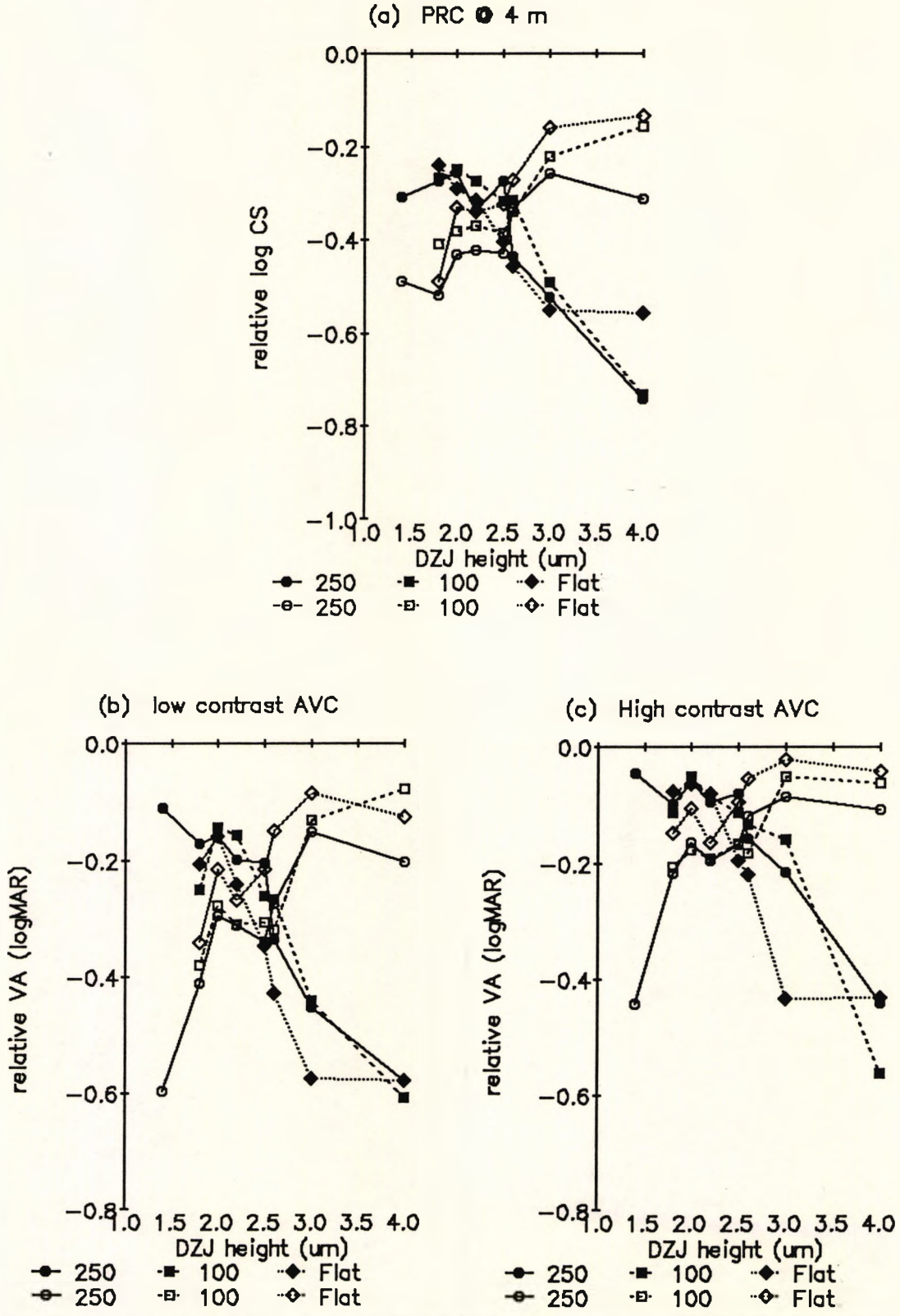

Figure 4.3-14 Visual performance variation with the DZJ height of rigid diffractive BCL. As DZJ height increases visual performance at near (open) improves and reduces at distance (filled) for rigid diffractive BCL manufactured with the 250 μm (circle, solid line), 100 μm (square, dashed line) and the flatted (diamond, dotted line) tool for **(a)** PRC at 4 m ; **(b)** low contrast AVC; and **(c)** high contrast AVC.

similarly VA varied with contrast as confirmed by the interaction H x V x C.

A further ANOVA (*Appendix 7 (A7-6)*), summarised in *Table 4.3-7*, examined the tool shapes 250 μm, 100 μm, 50 μm and flatted, all with a 2.0 μm DZJ height. The average relative CS with the 50 μm and 100 μm tools was better than with the other tools. Differences between the tools were less evident with the AVC. As shown in *Figure 4.3-15*, there was a difference in the ratio between distance and near for the different tools confirmed by the interaction T x V.

	CS	PRC	AVC
Tool (T)	0.001	0.001	0.025
T x V	<0.001	<0.001	0.005

Table 4.3-7 Summary of the ANOVA of visual performance with rigid diffractive BCL. The levels of significance of the factor, Tool, and the interaction between Tool and Vergence (T x V), as detailed in text, for the ANOVAs of visual performance with rigid diffractive BCL with a 2.0 μm DZJ height. Full details of the ANOVAs are given in *Appendix 7 (A7-6)*.

The effect of DZJ height and tool shape upon visual performance was further investigated with MRA.

A model of changes in visual performance

Using MRA, an empirical model for changes in visual performance was developed to allow the prediction of the visual performance with a given DZJ height and tool

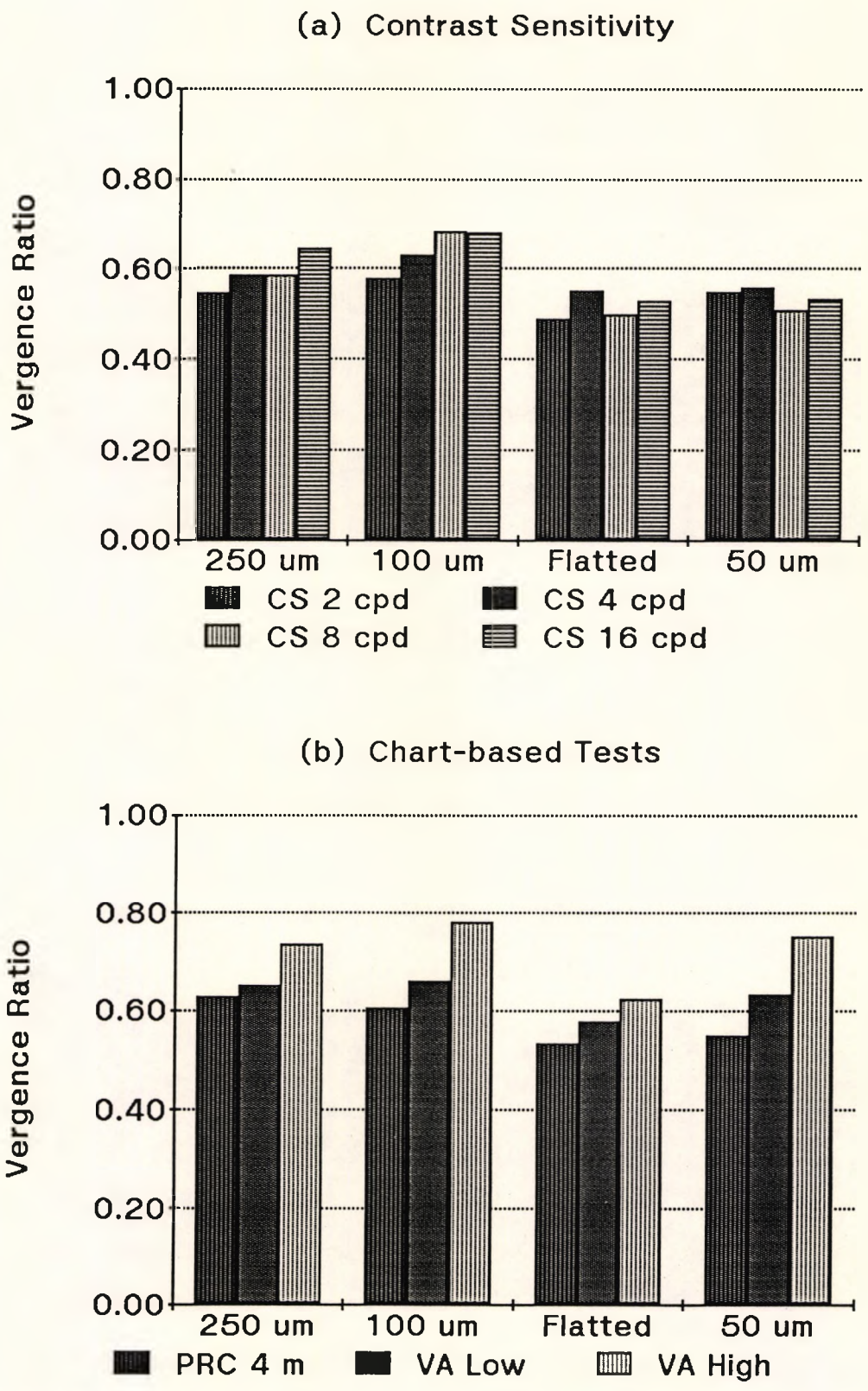

Figure 4.3-15 The effect of tool shape on the vergence ratio. The vergence ratio (distance / distance + near), with all visual performance measures, varied significantly between BCL with a DZJ height of 2.0 μm made with different tools. This vergence ratio is shown for (a) CS ; and (b) the chart-based tests. A vergence ratio greater than 0.5 indicates a bias to distance vision. Differences between tools was most obvious with CS and PRC.

shape. This then allowed prediction of an optimal DZJ height (equal distance and near visual performance) for each tool shape. The prediction was compared to the optical performance measures in section 4.2.4.

All MRA equations obtained, given in *Appendix 7 (A7-7)*, were significant ($p < 0.0001$) though the adjusted R^2 varied from only 0.04 to 0.46. As an example, the equations derived for PRC with the 100 μm tool are shown below.

at distance
relative PRC = 0.16 - 0.20 DZJ height

at near
relative PRC = - 0.62 + 0.11 DZJ height

(adjusted R^2 = 0.380, s.e. = 0.102, n = 148)

The optimal DZJ height for equal visual performance, as derived from the MRA equations (*Figure 4.3-16* and *Table 4.3-8*), varied with tool shape ($p < 0.001$) and between the visual performance measures ($p < 0.001$). As noted previously, the relatively large standard errors associated with this assessment were a result of the variability of the visual data (Taylor, 1982).

The effect of back surface polishing of rigid diffractive bifocal contact lenses

As expected back surface polishing altered the ratio between distance and near as compared to the nominally equivalent (non-polished) BCL for all visual performance measures. This is demonstrated, for example, with CS at 16 c.p.d. in *Figure 4.3-17a* and low contrast VA in *Figure 4.3-18a.*

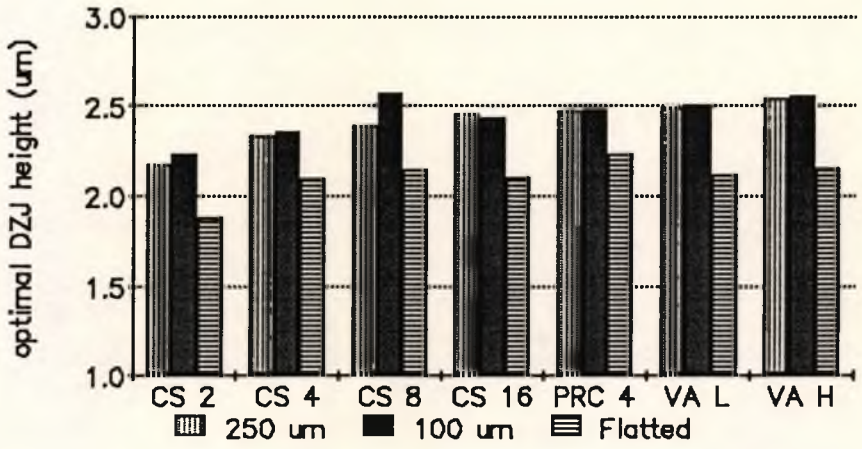

Figure 4.3-16 The variation in predicted optimal DZJ height with tool shape. The optimal DZJ height (equal distance and near) predicted by MRA equations for each of the three tools and each of the visual performance measures. Values and standard errors are given in *Table 4.3-8*.

	optimal DZJ height (μm)	s.e.	n
250 μm Tool			
CS 2	2.17	0.29	278
CS 4	2.33	0.14	278
CS 8	2.39	0.15	278
CS 16	2.45	0.15	278
PRC	2.47	0.12	270
VA L	2.49	0.10	270
VA H	2.54	0.11	270
100 μm Tool			
CS 2	2.23	0.48	149
CS 4	2.35	0.18	149
CS 8	2.56	0.22	149
CS 16	2.43	0.25	149
PRC	2.48	0.14	147
VA L	2.51	0.16	147
VA H	2.55	0.17	147
Flatted Tool			
CS 2	1.88	0.60	131
CS 4	2.10	0.17	131
CS 8	2.14	0.25	131
CS 16	2.10	0.24	131
PRC	2.23	0.18	131
VA L	2.12	0.17	131
VA H	2.15	0.19	131

Table 4.3-8 The predicted optimal DZJ height for rigid diffractive BCL. The optimal DZJ height (equal distance and near) was predicted by MRA equations for each of the three tools and each of the visual performance measures. The ratios and standard errors (s.e.) relate to *Figure 4.3-16*.

When the measured DZJ height (section 4.1) of the polished BCL was considered, optical performance was similar to the non-polished BCL (*Figures 4.3-17b and 4.3-18b*). Apart from the 1.4 μm nominal DZJ height BCL, polishing did not reduce visual performance, merely altering the bias between distance and near.

4.3.5 SOFT DIFFRACTIVE BIFOCAL CONTACT LENSES

The available soft diffractive BCL were a heterogeneous group, and, where possible, comparisons between different design characteristics have been made.

The poor optical quality compared to the rigid diffractive BCL reported in section 4.2.5 was reflected in greater reductions in visual performance and larger repeatability coefficients (section 4.3.2).

Variability of manufacture

The variability of the manufacture process was investigated by comparing three batches of nominally identical BCL (DZJ height 3.0 μm; 100 μm tool; moulded). Two of the batches were from the same production run. As shown in *Figure 4.3-19* and summarised in *Table 4.3-9*, ANOVA indicated a significant difference between the batches with CS and AVC but not with PRC. A significant interaction between the batch and vergence noted with CS indicates a variation in the ratio between distance and near between batches with CS.

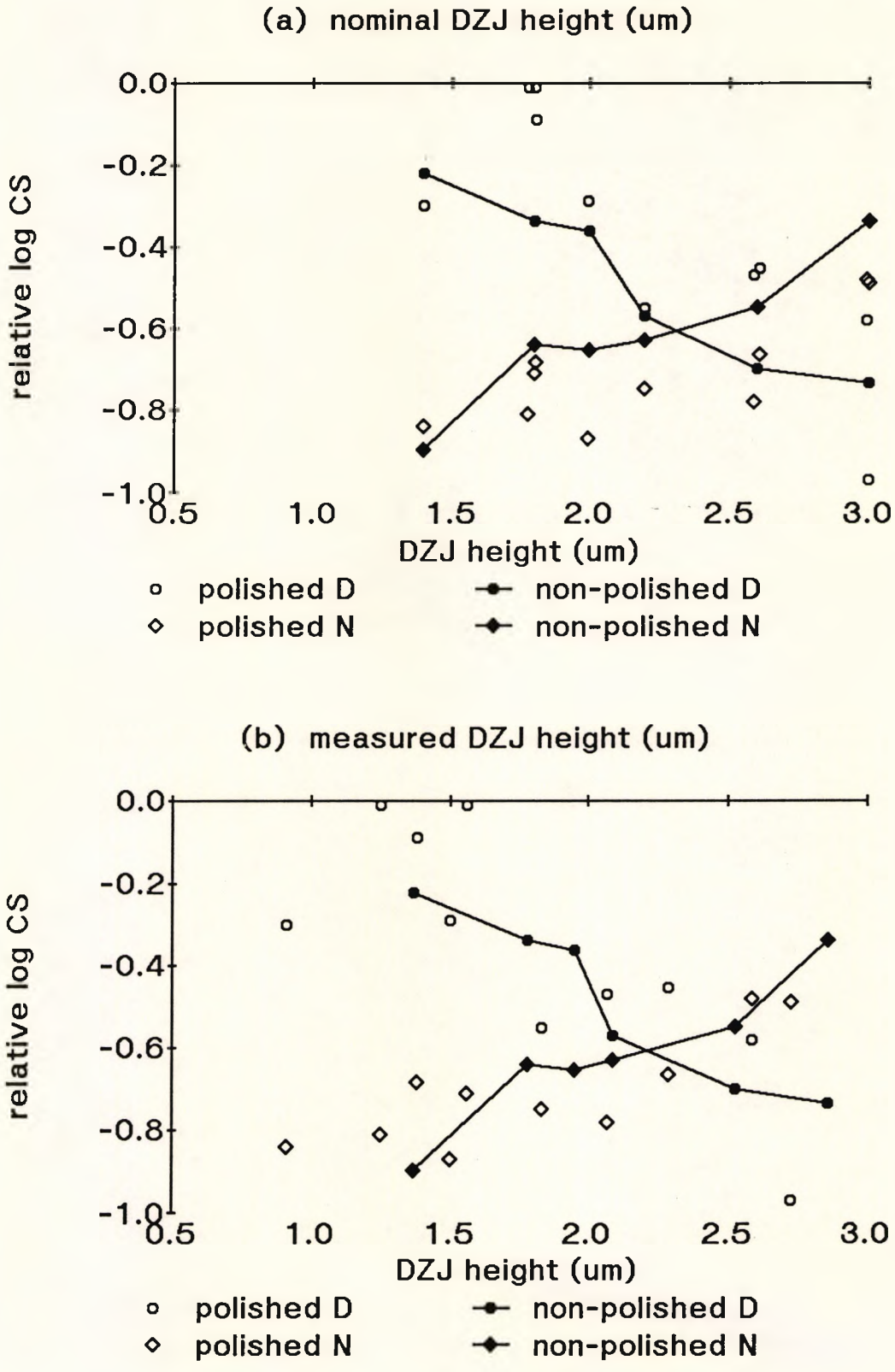

Figure 4.3-17 The effect of polishing the diffractive surface. The variation in CS at 16 c.p.d. with **(a)** nominal DZJ height; and **(b)** measured DZJ height is shown for polished (open) and non-polished (filled) rigid diffractive BCL at distance (circles) and near (diamonds). The visual performance of the polished BCL was similar to the non-polished BCL when the measured DZJ height was considered.

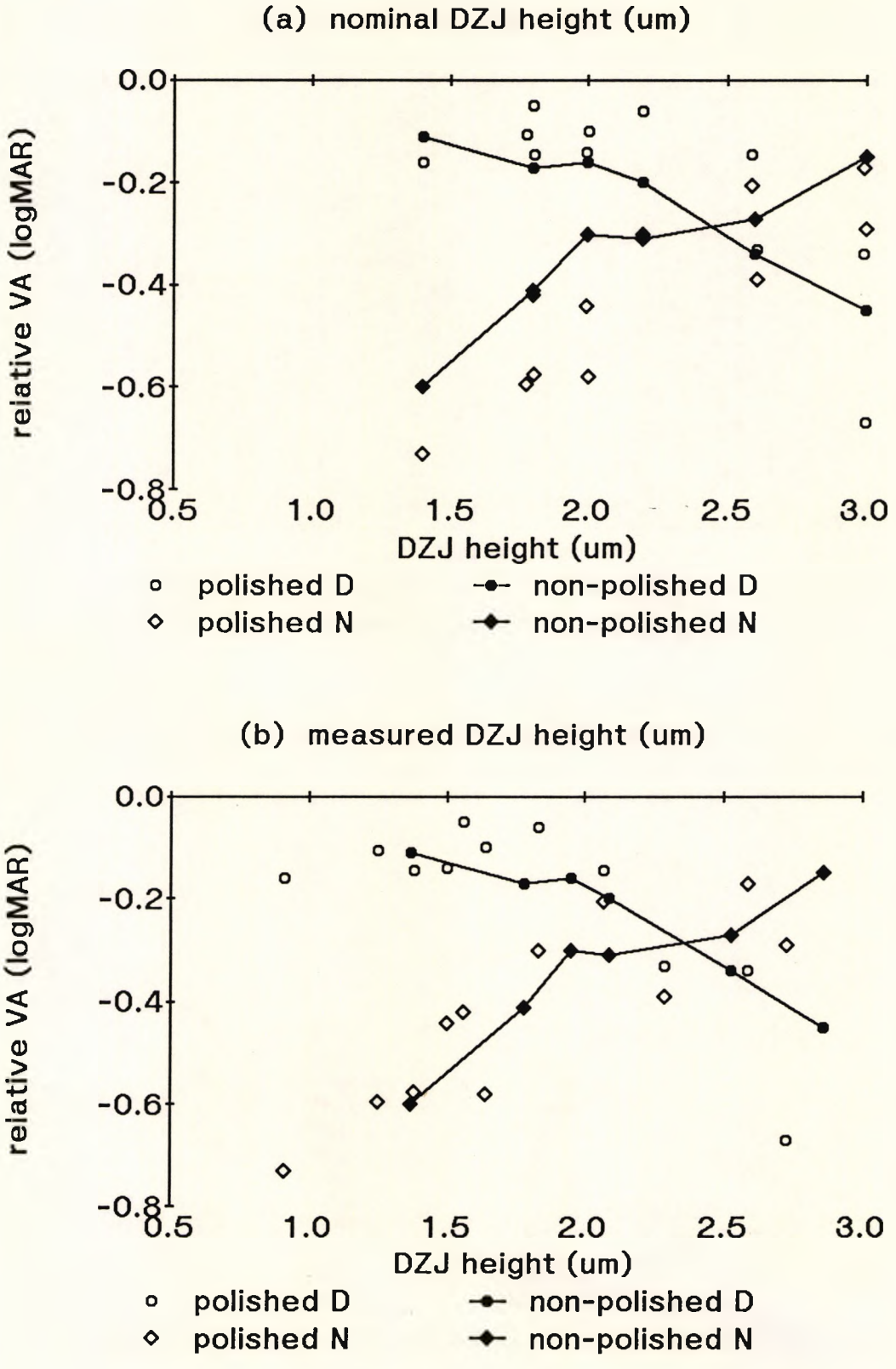

Figure 4.3-18 The effect of polishing the diffractive surface. The variation in low contrast VA with **(a)** nominal DZJ height; and **(b)** measured DZJ height is shown for polished (open) and non-polished (filled) rigid diffractive BCL at distance (circles) and near (diamonds). The visual performance of the polished BCL was similar to the non-polished BCL when the measured DZJ height was considered.

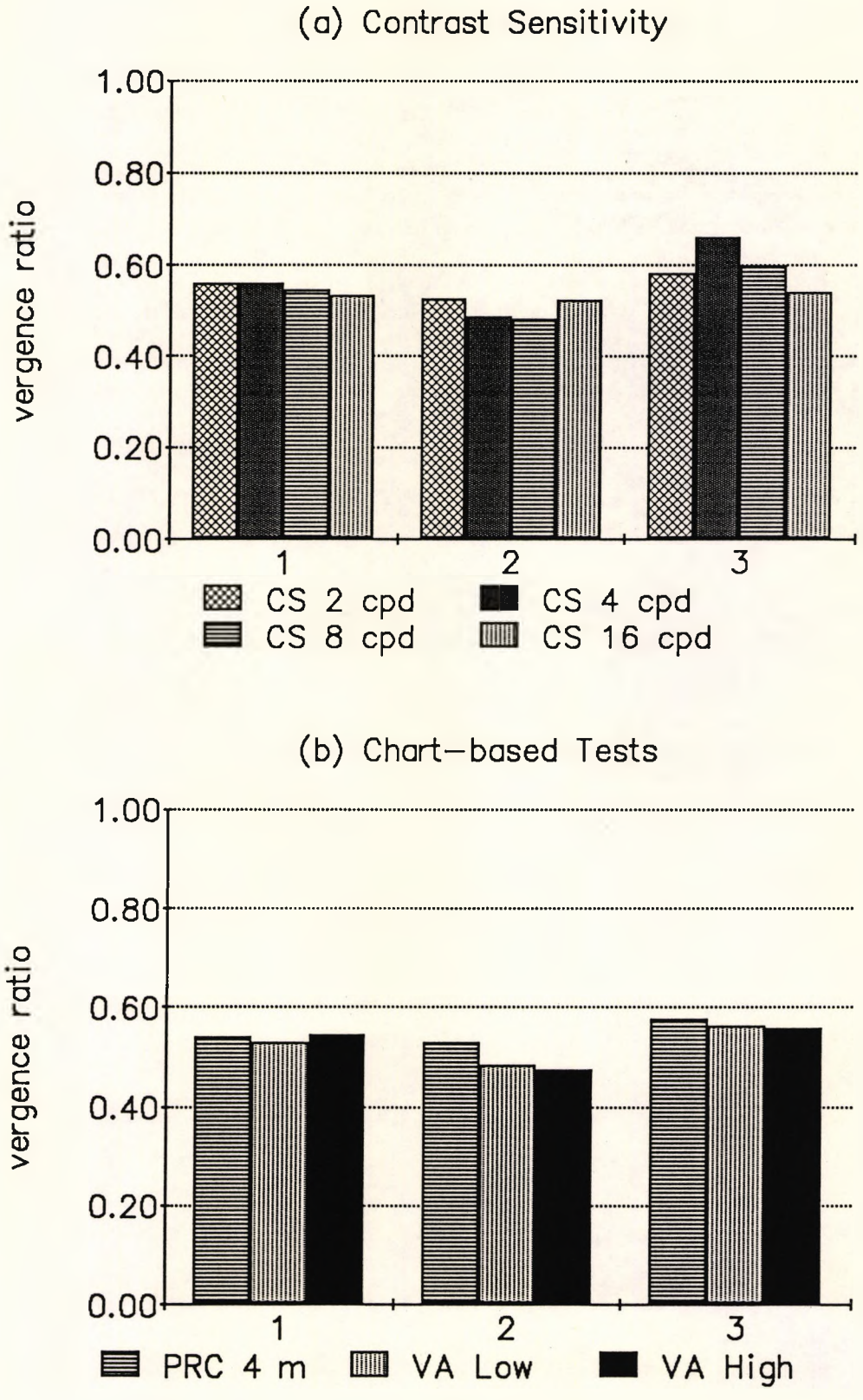

Figure 4.3-19 Variability of manufacture of soft diffractive BCL. The vergence ratio with **(a)** contrast sensitivity; and **(b)** the chart-based test of three nominally identical soft diffractive BCL (3.0 μm DZJ height; 100 μm tool; moulded). A ratio of greater than 0.5 indicates a distance bias. The vergence ratio varied significantly between the BCL with CS but not the chart based tests. A significant difference was found in the average CS and average VA between the BCL.

Effect	CS	PRC	AVC
Batch (B)	< 0.001	0.14	< 0.001
B x V	0.001	0.70	0.36

Table 4.3-9 Variability of manufacture of soft diffractive BCL. Summary of ANOVA of visual performance measures investigating differences between three nominally identical batches of moulded 3.0 μm DZJ height 100 μm tool soft diffractive BCL. The significance of the Batch and the interaction between Batch and Vergence (B x V) is given.

Tool	Manufacture	CS	PRC	AVC
250 μm	Lathed	< 0.001	0.085	0.005
100 μm	Lathed	< 0.001	0.026	0.001
100 μm	Moulded	1.0	0.42	0.40

Table 4.3-10 DZJ height versus vergence with soft diffractive BCL. Summary of ANOVA of visual performance measures investigating differences between DZJ height with 250 μm and 100 μm tool lathed BCL and 100 μm moulded soft diffractive BCL. The significance of the interaction between DZJ height and Vergence is given.

DZJ height	Effect	CS	PRC	AVC
3.0 μm	Tool (T)	0.89	0.09	0.95
	T x V	0.84	0.01	< 0.001
3.3 μm	Tool (T)	0.50	0.85	0.27
	T x V	0.86	0.42	0.87
4.0 μm	Tool (T)	< 0.001	0.002	< 0.001
	T x V	< 0.001	0.026	< 0.001

Table 4.3-11 Tool shape versus vergence with soft diffractive BCL. Summary of ANOVA of visual performance measures investigating differences between tools with lathed soft diffractive BCL of three different DZJ heights (3.0, 3.3, 4.0 μm). The significance of the factor Tool and the interaction between Tool and Vergence (T x V) is given.

Diffractive Zone Junction Height

The variation with DZJ height was less than expected, and less than the variation in optical performance (section 4.2.5). In general, the near visual performance improved and the distance visual performance reduced with increasing DZJ height as shown in *Figures 4.3-20* and *4.3-21*. *Table 4.3-10* shows the significance of this interaction for CS and AVC but not for PRC with the 250 μm tool, and 100 μm tool, lathed BCL. Conversely, no significant interaction between DZJ height and vergence was noted with the 100 μm tool, moulded BCL. Optical performance indicated a significant interaction with all three groups of BCL described above as shown in *Figure 4.2-37*.

Diamond Tool Shape

As shown in *Figures 4.3-20* and *4.3-21*, tool shape did not have a consistent effect upon visual performance. *Table 4.3-11* summarises the results of ANOVAs which investigated the effect of tool with lathed BCL with three different DZJ heights. A significant difference between the 4.0 μm DZJ height lathed BCL made with the 250 μm and 100 μm tools and an interaction between tool and vergence was noted. A weak interaction between tool and vergence was noted with 3.0 μm DZJ height lathed BCL made with the 250 μm and 100 μm tools. No significant difference was noted between the 3.3 μm DZJ height lathed BCL made with the 100 μm and flatted tools. The most pronounced difference in optical performance due to tool was the MTF of the

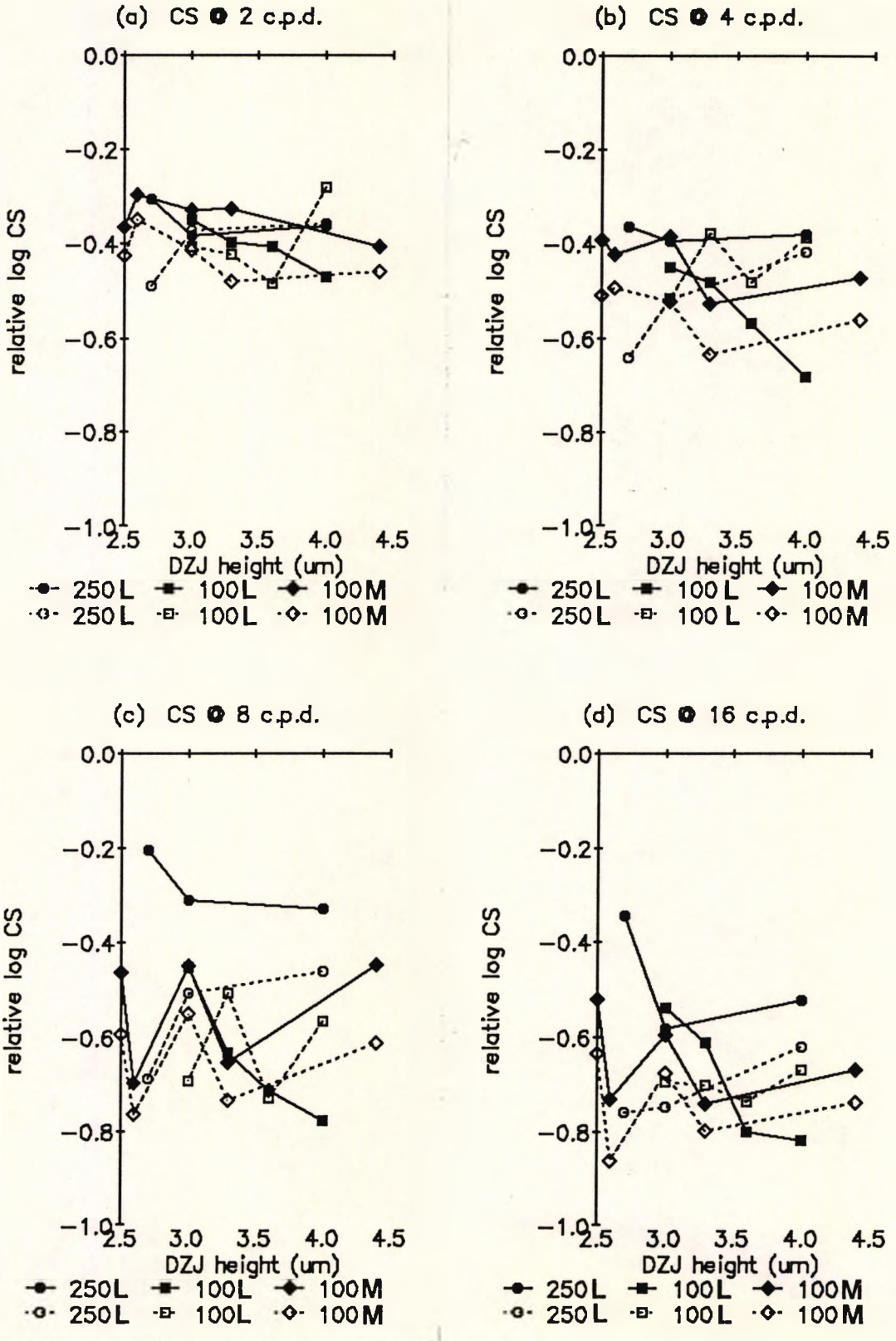

Figure 4.3-20 Visual performance variation with the DZJ height of soft diffractive BCL. As DZJ height increases visual performance at near (open symbols, dashed lines) was expected to improve and to reduce at distance (filled symbols, solid lines) for CS at **(a)** 2 c.p.d.; **(b)** 4 c.p.d.; **(c)** 8 c.p.d.; and **(d)** 16 c.p.d.. This was apparent for lathed (L) soft diffractive BCL manufactured with the 250 μm tool (circles) and 100 μm tool (square) but not for the moulded (M) 100 μm tool BCL (diamond).

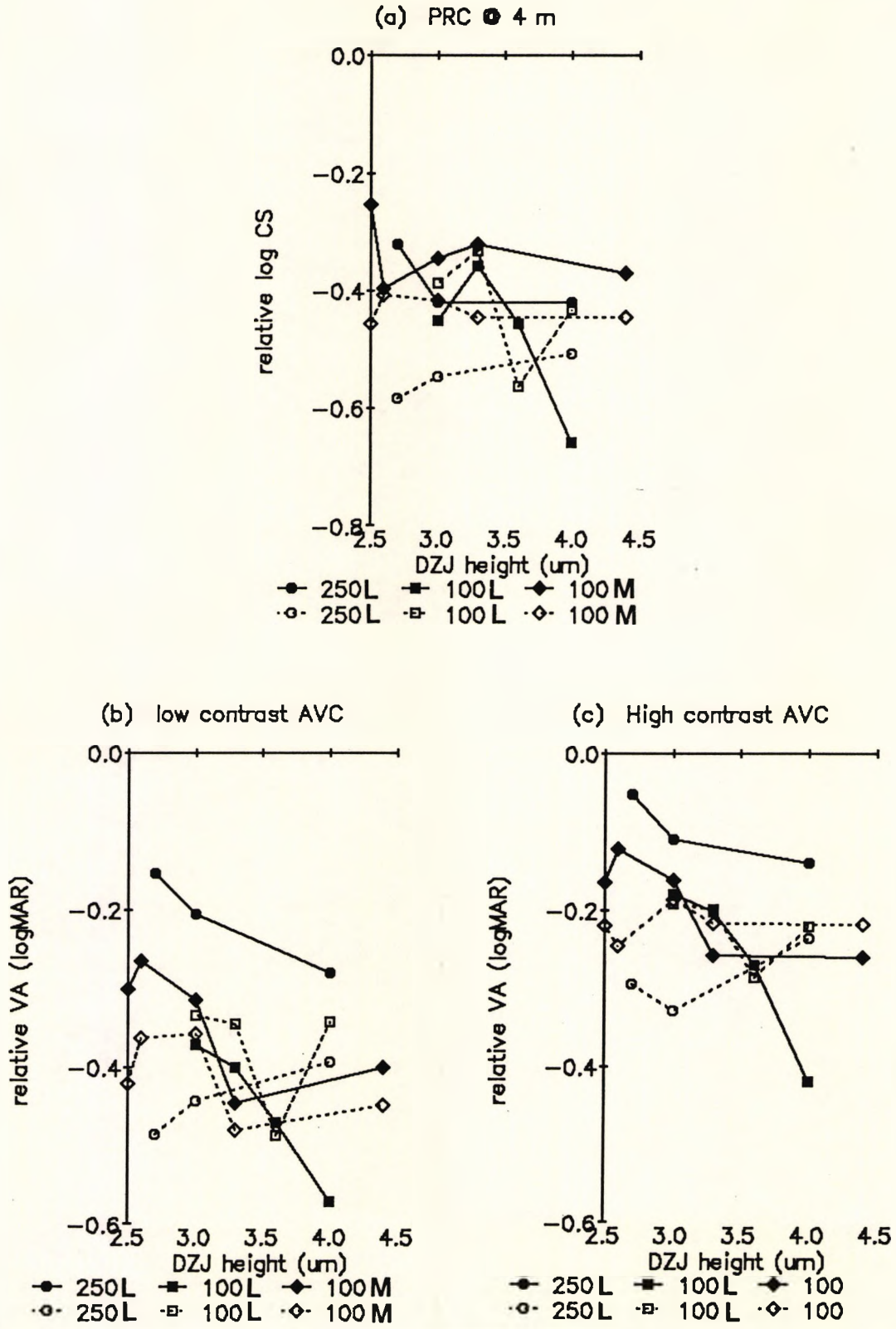

Figure 4.3-21 Visual performance variation with the DZJ height of soft diffractive BCL. As DZJ height increases visual performance at near (open symbols, dashed lines) was expected to improve and to reduce at distance (filled symbols, solid lines) for CS at **(a)** PRC at 4 m ; **(b)** low contrast AVC; and **(c)** high contrast AVC.. This was apparent for lathed (L) soft diffractive BCL manufactured with the 250 μm tool (circles) and 100 μm tool (square) but not for the moulded (M) 100 μm tool BCL (diamond).

3.3 μm, flatted tool BCL, which was far more near biased than the other 3.3 DZJ height BCL (*Figure 4.2-37b*).

Manufacture technique

The method of manufacture (lathe cutting or moulding) was compared for soft diffractive BCL with nominal DZJ heights of 3.0 and 3.3 μm using an ANOVA and the significance of the effects of interest are given in *Table 4.3-12*. There was no overall difference between the two manufacture techniques and an interaction between manufacture and DZJ height noted with CS. The average visual performances with the 3.0 μm BCL were better, with both manufacture techniques than the 3.3 μm BCL, and the 3.3 μm BCL was more highly biased to distance than the 3.0 μm BCL, which implied manufacturing problems.

Effect	CS	PRC	AVC
Manufacture (M)	0.70	0.47	0.74
DZJ height (H)	0.005	0.28	0.003
M x H	0.007	0.21	0.06
M x H x V	0.071	0.91	0.70

Table 4.3-12 Manufacture method and DZJ height versus vergence with soft diffractive BCL. Summary of ANOVA of visual performance measures investigating differences between lathed and moulded soft diffractive BCL of two DZJ heights (3.0, 3.3 μm). The significance of the factors Manufacture and DZJ height and the interactions between Manufacture and DZJ height (M x H) and between Manufacture, DZJ height and Vergence (M x H x V) is given.

"Reverse" add soft diffractive bifocal contact lens

A "reverse" add BCL utilises the negative first order diffractive focus to form the distance image and the zero order focus to form the near image (section 1.2.3). Hence the image formation varies from the other diffractive BCL used in this study. As shown in *Figure 4.3-22* the vergence ratio of a "reverse" add BCL was different from "conventional" BCL (zero order focus forms distance image, positive first order focus forms near image) of the same nominal DZJ height. This was consistent with the ANOVA (*Appendix 7 (A7-8)*) interactions between addition type and vergence with CS, PRC and AVC ($p < 0.001$; $p < 0.001$; $p = 0.02$). The bias in visual performance was the reverse of that found for optical performance at 548 nm and 573 nm (*Figure 4.2-38*).

A commercially available soft diffractive bifocal contact lens

The relative visual performance of the Allergan Echelon soft diffractive BCL is shown in *Figure 4.3-23*. The overall optical performance was better than any of the soft diffractive BCL available for this study.

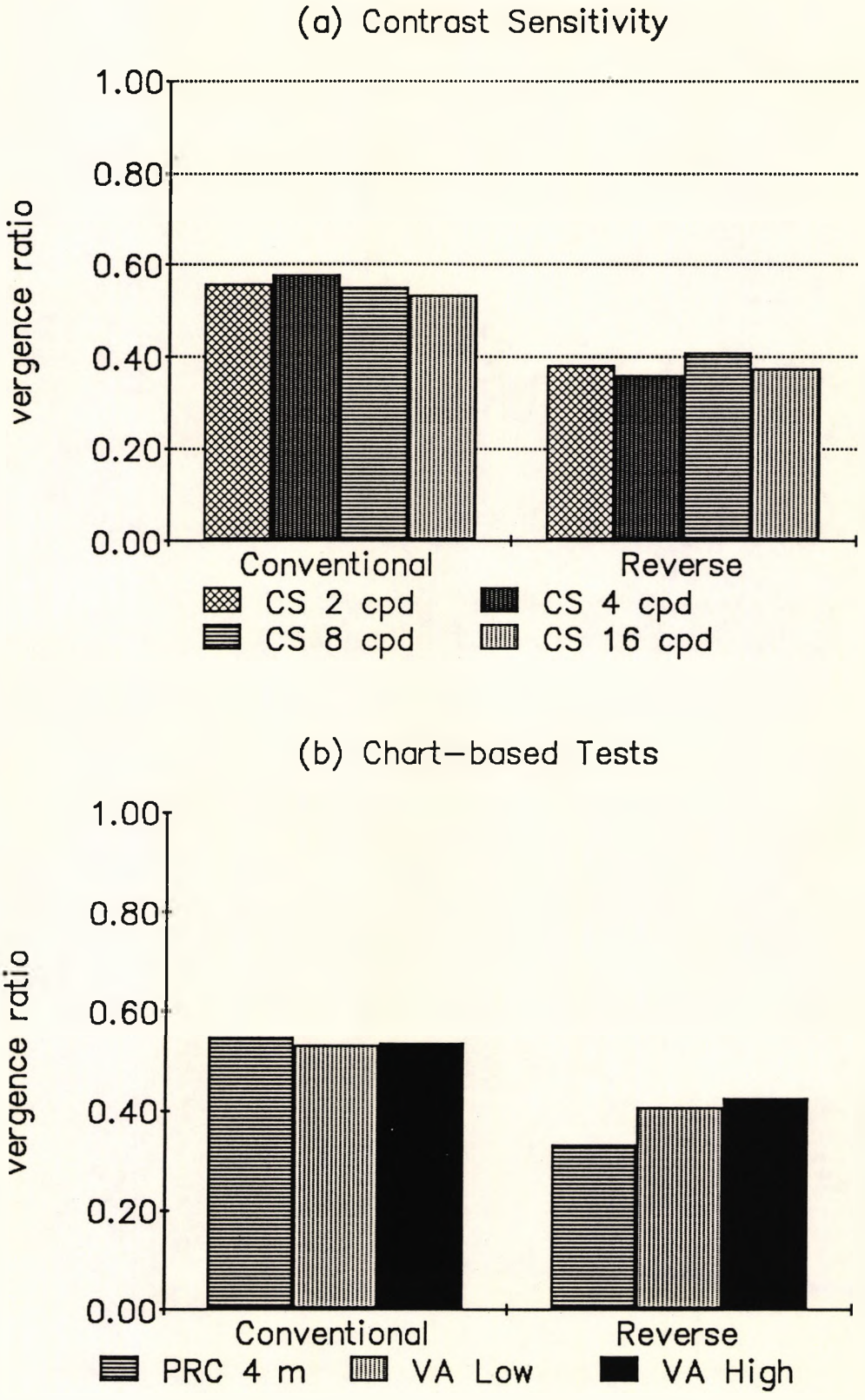

Figure 4.3-22 "Reverse" add compared to conventional add soft diffractive BCL. The vergence ratio of a "reverse" add 3.0 μm DZJ height, 100 μm tool, moulded soft diffractive BCL was found to differ from conventional soft diffractive BCL of the same nominal parameters. The "reverse" add BCL was near biased, whilst the conventional BCL were distance biased.

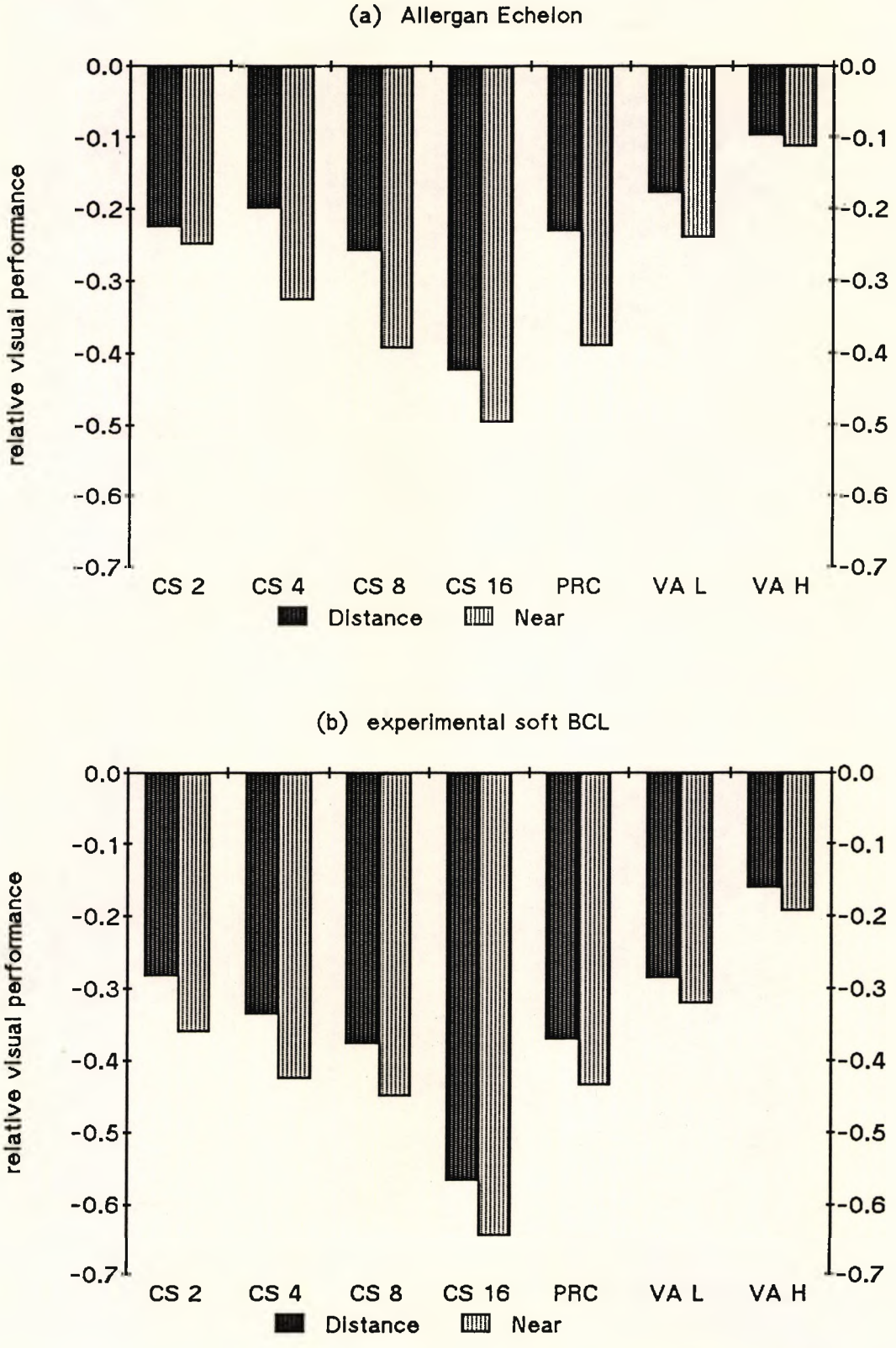

Figure 4.3-23 Allergan Echelon compared to an experimental soft diffractive BCL. **(a)** The average relative visual performance of Allergan Echelon soft diffractive BCL was found to be better than any of the soft diffractive BCL available for this study. **(b)** An example of the average relative visual performance with the best soft diffractive BCL used in this study.

4.4 Longitudinal Chromatic Aberration of diffractive bifocal contact lenses

The Longitudinal Chromatic Aberration (LCA) of four rigid diffractive BCL (2.0 μm DZJ height; 250 μm rounded tool) was measured as described in section 3.4. This was then compared to the LCA of two refractive BCL (2.6 mm COZD).

Repeatability

Test-retest repeatability (section 3.7) for repeated (n = 12) measures with both BCL types was found to be ±0.42 Dioptres (D). Thus this technique demonstrated poor repeatability compared to the size of the effects of interest.

Bifocal contact lenses

For diffractive BCL, the average LCA of the distance image (1.43 ± 0.23 D) was greater than the average LCA of the near image (0.76 ± 0.34 D) (student T = 2.83; n = 4; $p < 0.05$). For refractive BCL, the average LCA of the distance image (1.38 ± 0.33 D) was not different from the average LCA of the near image (1.26 ± 0.35 D) (student T = 0.25; n = 2; $p > 0.1$).

Summary

As suggested by *Equation 1.2-1* the LCA of the diffractive near focus was smaller than the LCA of the distance focus. As expected there was no difference with refractive BCL.

4.5 Prediction of the Optical and Visual Performance of Rigid Diffractive Bifocal Contact Lenses from surface profile measurements

A stepwise Multiple Regression Analysis (MRA) procedure (section 3.8) was used to investigate the relationship between measured diffractive zone junction (DZJ) height of rigid diffractive BCL made with the 250 μm diamond tool (section 4.1) and

(a) the optical performance (section 4.2); and

(b) the visual performance (section 4.3);

measured at distance and near. Empirical models describing optical performance are given in section 4.5.1 and describing visual performance in section 4.5.2. These models allowed the prediction of optimal DZJ heights (equal performance at distance and near), which were compared to the models developed using nominal DZJ height in sections 4.2.4 and 4.3.4.

4.5.1 OPTICAL PERFORMANCE

The measured DZJ height at each DZJ was highly correlated with the measured DZJ height at other DZJs (section 4.1.2). The third and eighth DZJs were the most highly correlated with the average MTF.

The variation in averaged MTF could be described by equations using the measured height of the third DZJ

(with adjusted R^2 = 0.784 at 548 nm, and R^2 =0.751 at 573 nm). Details of the MRA are given in *Appendix 8 (A8-1a)*.

Average MTF was slightly better described by MRA equations in terms of the average DZJ height (adjusted R^2 = 0.807 at 548 nm, and R^2 = 0.782 at 573 nm). Details of the MRA are given in *Appendix 8 (A8-1b)*. *Figure 4.5-1* shows that measured average modulation was well predicted by these MRA equations.

Optimal DZJ height

By solving the equations which used the average DZJ height for equal performance at distance and near, the predicted optimal DZJ height for the rigid diffractive BCL made with the 250 μm tool was found to be 1.99 μm at 548 nm and 2.07 μm at 573 nm. This compares well with, but was systematically smaller than the predicted optimal DZJ height found in section 4.2.4 using nominal DZJ heights (averaged for all spatial frequencies - 2.03 (range 1.6 to 2.1) μm at 548 nm and 2.20 (range 1.6 to 2.3) μm at 573 nm) (*Figure 4.2-30*).

4.5.2 VISUAL PERFORMANCE

The measured height of the inner DZJs (i.e. 2, 3, 4, 5) were the most highly correlated with the visual performance measures.

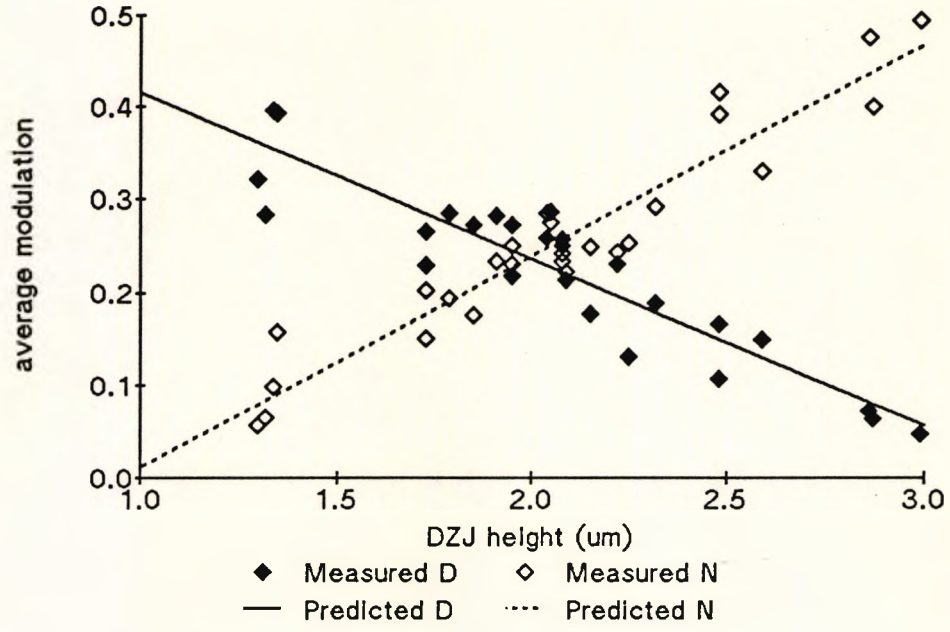

Figure 4.5-1 Comparison of measured and predicted optical performance. Average modulation measured at 548 nm at distance (filled) and near (open) compared to the average predicted modulation at distance (solid line) and near (dotted line) derived from MRA of the measured DZJ height. (adjusted R^2 = 0.807; $p < 0.0001$)

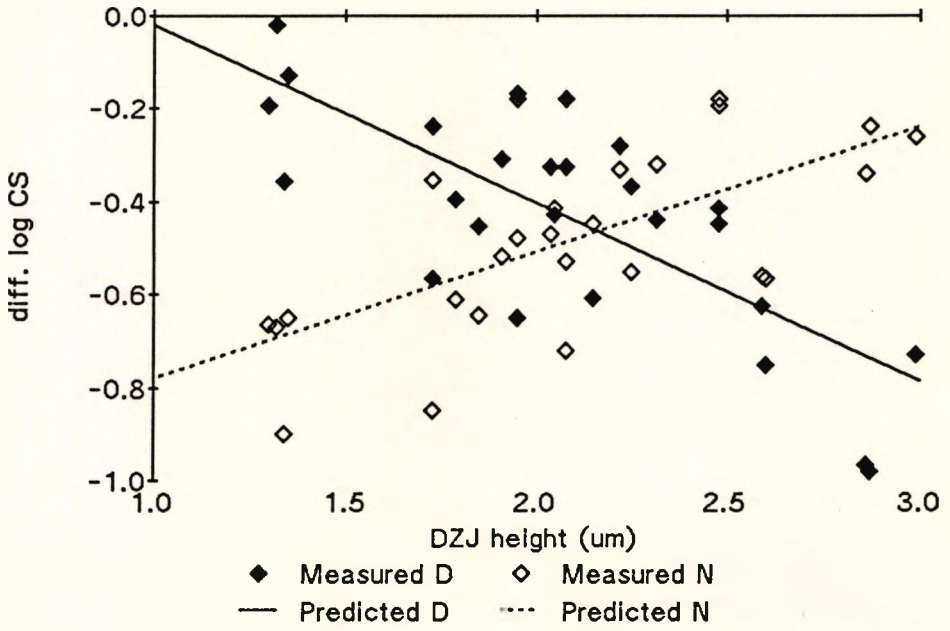

Figure 4.5-2 Comparison of measured and predicted visual performance. As an example the average measured CS at 8 c.p.d. at distance (filled) and near (open) compared to that predicted, at distance (solid line) and near (dotted line), from MRA of the measured DZJ height (adjusted R^2 = 0.414; $p < 0.0001$). Similar results were found with the other visual performance measures (*Table 4.5-1*).

The averaged visual performance was described in terms of the averaged DZJ height. The MRA equations are given in *Appendix 8 (A8-2)*, and the adjusted R^2 values are shown in *Table 4.5-1*. Interestingly, the stepwise MRA procedure removed the term for DZJ height from the equation describing near visual performance for CS at 2 and 4 c.p.d..

visual performance	DZJ height measured	nominal
CS 2 cpd	0.406	0.108
CS 4 cpd	0.425	0.272
CS 8 cpd	0.414	0.250
CS 16 cpd	0.438	0.264
PRC 4 m	0.517	0.383
VA low	0.635	0.464
VA high	0.559	0.410

Table 4.5-1 Visual performance prediction from DZJ height. The adjusted R^2 of MRA which describe the average visual performance with rigid diffractive BCL (250 μm tool) in terms of the average measured DZJ height and the nominal DZJ height (from section 4.3.4). All MRA were highly significant (measured: $n = 48$, $p < 0.0001$; nominal: $n = 271$, $p < 0.0001$).

Measured DZJ height was a better predictor of visual performance than the nominal DZJ height (section 4.3.4) as shown in *Table 4.5-1*. As an example of the MRA equations, *Figure 4.5-2* shows the measured reduction in visual performance with CS at 8 c.p.d. compared to that

	optimal DZJ height (μm)	s.e.	n
CS 2	2.01	0.25	48
CS 4	2.08	0.24	48
CS 8	2.17	0.25	48
CS 16	2.27	0.25	48
PRC	2.22	0.21	48
VA L	2.23	0.16	48
VA H	2.35	0.21	48

Table 4.5-2 The predicted optimal DZJ height with the different visual performance measures. The optimal DZJ height (equal distance and near) predicted by MRA equations derived using the measured DZJ height of rigid diffractive BCL made with the 250 μm tool for each of the visual performance measures. The optimal DZJ height was smaller than predicted by the MRA in section 4.3.4 which used the nominal DZJ height.

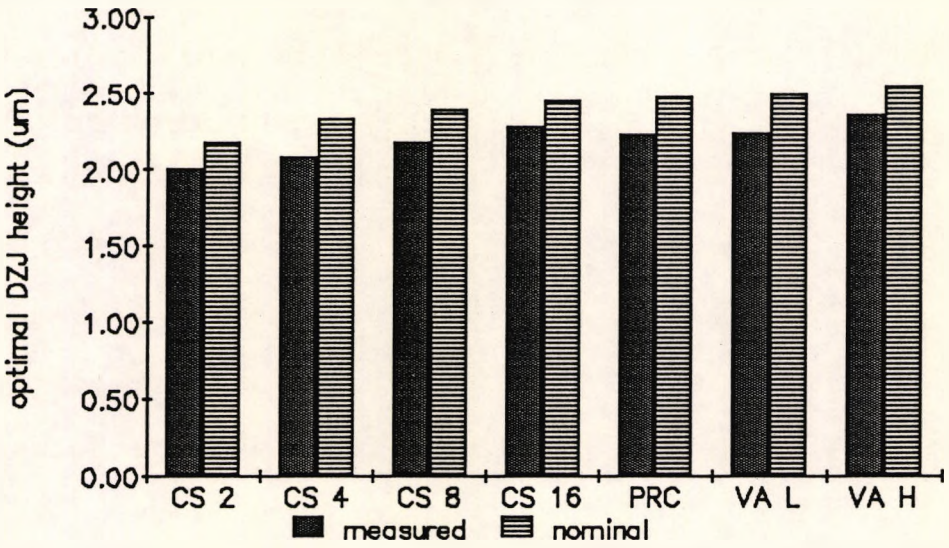

Figure 4.5-3 The predicted optimal DZJ height with the different visual performance measures. Optimal DZJ height (equal distance and near) was predicted by MRA equations derived using the measured DZJ height of rigid diffractive BCL made with the 250 μm tool for each of the visual performance measures and were smaller than the optimal DZJ height predicted by the MRA in section 4.3.4 which used the nominal DZJ height. There was a consistent trend for a larger optimal DZJ height with increasing spatial frequency content of the visual performance measure.

predicted by the MRA equation. Similar results were found with the other visual performance measures.

Optimal DZJ height

The predicted optimal DZJ heights for each of the visual performance measures with rigid diffractive BCL made with the 250 μm tool, found by solving the above MRA equations for equal performance at distance and near, are given in *Table 4.5-2*. *Figure 4.5-3* shows that, as noted in section 4.5.1 for optical performance, the optimal DZJ heights predicted using measured DZJ height were comparable to, but slightly smaller than those found in section 4.3.4 using nominal DZJ height (*Table 4.3-8* and *Figure 4.3-16*).

4.6 Prediction of Visual Performance from Optical Performance measures

Empirical models of visual performance in terms of the measured optical performance were derived using multiple regression analysis (MRA). The models of visual performance with refractive BCL are described in section 4.6.1, and with rigid and soft diffractive BCL in sections 4.6.2 and 4.6.3 respectively.

Preliminary investigation

As noted in section 4.2.2, principal component analysis indicated only a single factor describing the measured modulation at each of the 16 spatial frequencies (i.e. no

spatial frequency related components were present). Further analysis indicated that there were weak and inconsistent relationships between the spatial frequency content of the optical performance measures (i.e. the modulation at the 16 spatial frequencies) and that of the visual performance measures as indicated by the correlations between the measured modulation and the visual performance measures. The high correlations between the measured modulation at the different spatial frequencies increased the risk of over-optimistic estimation of the predictive power of any derived models.

Numerous data reductions were investigated and the models presented here were derived with the number of terms in the subsequent MRA restricted to the measured modulation at four spatial frequencies (4, 12, 25, and 66 c.p.d.). A stepwise MRA procedure (section 3.8) was then used to develop equations, in terms of the modulation at the four spatial frequencies, to describe each visual performance measure. No *a priori* assumptions were made about the spatial frequency content of the optical or visual performance measures. As noted in section 3.8, terms which were judged to be statistically redundant were removed from the MRA equations by the stepwise procedure.

Relative optical performance

As with the visual performance measures (section 4.3.2), the MTF could be described in terms of the relative

optical performance. Data was converted to the form of the relative optical performance where :

$$\text{rel. optical performance} = \log \left\{ \frac{\text{modulation with BCL}}{\text{modulation without BCL}} \right\}$$

Equations were derived using both the measured modulation and the relative optical performance.

4.6.1 REFRACTIVE BIFOCAL CONTACT LENSES

Initially, a series of empirical MRA models was derived using the measured MTF of centred refractive BCL to predict the different visual performance measures. In a second analysis the MTF predicted by the equation empirically derived in section 4.2.3 to describe the MTF of decentred refractive BCL was used to predict visual performance.

Models using measured MTF of refractive Bifocal Contact Lenses with different apertures

MTF measurements made with each refractive BCL centred over apertures of 3 to 5 mm were averaged separately for each aperture stop and each spatial frequency. The averaged, measured modulations were then used in a stepwise MRA (section 3.8) to predict visual performance measures which had been averaged for all subjects.

The average measured pupil size of the five subjects was 3.1 mm when viewing the CS test and 2.6 mm when viewing

the chart-based tests (*Table 4.3-2*). A preliminary visual examination of the data indicated that the optical performance with BCL centred over the 4 mm aperture stop most closely matched the changes in visual performance noted. As shown in *Table 4.6-1*, as had been expected, most visual performance measures were slightly better predicted using the MTF measured with the 4 mm aperture.

In section 4.3.3, visual performance was described, in terms of the COZD, pupil size and the decentration of the BCL, by a set of equations derived with MRA. As shown in *Table 4.6-2*, optical performance was generally a better predictor of visual performance.

As shown in *Table 4.6-3* for the 4 mm aperture, the MRA equations, given in *Appendix 9 (A9-1)*, provided limited support for the hypothesis that the lower spatial frequency visual performance measures (CS at 2 and 4 c.p.d.) would have been best predicted by the modulation measured at lower spatial frequencies, while the visual performance measures with a higher spatial frequency content (VA) would have been best predicted by the modulation measured at higher spatial frequencies.

Models using predicted MTF of decentred refractive Bifocal Contact Lenses

In the second analysis, the model developed in section 4.2.3 to describe the MTF with decentred refractive BCL was used to predict the modulation at each of the same 4

Visual Performance	adjusted R^2 with aperture stop 3 mm	3.5 mm	4 mm	5 mm
CS at 2 c.p.d.	0.394	0.371*	0.469	0.365
CS at 4 c.p.d.	0.737	0.569	0.778	0.751
CS at 8 c.p.d.	0.518	0.366	0.554	0.505
CS at 16 c.p.d.	0.446	0.329*	0.461	0.415
PRC at 4 m	0.610	0.540	0.802	0.792
low contrast VA	0.643	0.721	0.755	0.797
high contrast VA	0.511	0.543	0.469	0.501

* $p < 0.0005$ (all others p 0.0001)

Table 4.6-1 Prediction of visual performance with refractive BCL. The adjusted R^2 for the MRA which used the MTF measured with refractive BCL (n = 36) over different apertures to predict the average visual performance with the same BCL. All MRA $p < 0.0001$ except as shown.

Visual Performance	Adjusted R^2
CS at 2 c.p.d.	0.490
CS at 4 c.p.d.	0.436
CS at 8 c.p.d.	0.443
CS at 16 c.p.d.	0.441
PRC at 4 m	0.551
low contrast VA	0.521
high contrast VA	0.300

Table 4.6-2 Prediction of visual performance with refractive BCL. The adjusted R^2 for MRA equations derived in section 4.3.3 to describe visual performance with refractive BCL in terms of COZD, pupil size and decentration. All equations $p < 0.0001$; n = 255.

Spatial Freq. (c.p.d)	Standardised Regression Coefficients (βeta) Visual Performance Measure CS 2 c.p.d.	CS 4 c.p.d.	CS 8 c.p.d.	CS 16 c.p.d.	PRC	VA Low contrast	VA High contrast
4			1.86	2.18			
12	5.57	7.54	3.32	3.12	10.5	6.75	1.84
25	5.10	5.38	2.33	2.14	8.85	4.71	
66							2.02

Table 4.6-3 Terms retained in MRA illustrated the weak relationship between the spatial frequency of MTF and visual performance measures in MRA equations for refractive BCL. The standardised regression coefficients (βeta) of the modulation measured at the spatial frequencies shown for the MRA which attempted to describe visual performance (CS at 2, 4, 8, and 16 c.p.d., PRC at 4 m and low and high contrast VA). There was a weak trend, as might have been expected, for the higher spatial frequency modulation terms to be retained by the stepwise MRA procedure in the equations which described visual performance measures with a higher spatial frequency content (and vice versa). In this example, MTF was measured with the BCL over a 4 mm aperture, and similar results were found with the other apertures. Details of all MRA equations are included in *Appendix 9*.

Visual Performance	Adjusted R^2
CS at 2 c.p.d.	0.364
CS at 4 c.p.d.	0.355
CS at 8 c.p.d.	0.272
CS at 16 c.p.d.	0.247
PRC at 4 m	0.587
low contrast VA	0.564
high contrast VA	0.317

Table 4.6-4 Calculated MTF used to predict visual performance of refractive BCL. The adjusted R^2 for MRA equations which described visual performance in terms of the modulation calculated with the MRA equation for decentred refractive BCL derived in section 4.2.3 which incorporated the measured COZD, pupil size and decentration. (all equations $p < 0.0001$; $n = 129$)

spatial frequencies for the given configuration of measured pupil size, measured BCL decentration and COZD for each subject with each BCL. The calculated modulation was then subject to a stepwise MRA and models developed to predict visual performance.

As indicated by the adjusted R^2 values given in *Table 4.6-4*, the predicted MTF was less successful at predicting visual performance than the measured MTF of centred refractive BCL (*Table 4.6-1*), and no better than knowledge of the COZD, pupil size and decentration, as shown in *Table 4.6-2*.

4.6.2 RIGID DIFFRACTIVE BIFOCAL CONTACT LENSES

All nominally identical (i.e. the same tool shape and DZJ height) rigid diffractive BCL were grouped and the average MTF used in a stepwise MRA to predict average visual performance. As shown in *Table 4.6-5*, the MTF measured at 573 nm was a better predictor than data measured at 548 nm.

As a comparison, visual performance was predicted in section 4.3.4 by empirically derived MRA equations, given in *Appendix 7 (A7-7)*, in terms of the nominal DZJ height, with an adjusted R^2 which varied from only 0.04 to 0.46 ($p < 0.0001$). In section 4.5.2 visual performance was predicted by empirically derived MRA equations, given in *Appendix 8 (A8-2)*, in terms of the measured DZJ height, with

Visual Performance	adjusted R^2 Interference Filter 548 nm	573 nm
CS at 2 c.p.d.	0.478	0.402
CS at 4 c.p.d.	0.785	0.819
CS at 8 c.p.d.	0.695	0.731
CS at 16 c.p.d.	0.598	0.684
PRC at 4 m	0.691	0.801
low contrast VA	0.773	0.880
high contrast VA	0.695	0.765

Table 4.6-5 Prediction of visual performance with rigid diffractive BCL. The adjusted R^2 for MRA equations which describe the visual performance averaged for groups of nominally identical rigid diffractive BCL in terms of the measured modulation at 4 spatial frequencies. All equations $p < 0.0001$; $n = 46$.

Spatial Freq. (c.p.d)	Standardised Regression Coefficients (βeta) Visual Performance Measure CS 2 c.p.d.	CS 4 c.p.d.	CS 8 c.p.d.	CS 16 c.p.d.	PRC	VA Low contrast	VA High contrast
4							
12	0.65	0.91	0.86		0.75	0.44	
25				0.83	0.88		
66					1.01	0.51	0.88

Table 4.6-6 The relationship between the spatial frequency of MTF and visual performance measures in MRA equations for rigid diffractive BCL. The standardised regression coefficients (βeta) of the modulation measured at the spatial frequencies shown for the MRA which attempted to describe visual performance (CS at 2, 4, 8, and 16 c.p.d., PRC at 4 m and with low and high contrast VA). There was a weak trend, as might have been expected, for the higher spatial frequency modulation terms to be retained by the stepwise MRA procedure in the equations which described visual performance measures with a higher spatial frequency content (and vice versa). In this example, MTF was measured at 573 nm, and similar results were found at 548 nm. Details of all MRA equations are included in *Appendix 9*.

an adjusted R^2 which varied from 0.41 to 0.64 ($p < 0.0001$).

The MRA equations (*Appendix 9 (A9-2)*), as shown for example in *Table 4.6-6* for the equations derived from the MTF measured at 573 nm again provided limited support for the hypothesis that the spatial frequency content of the visual performance measure would be related to the spatial frequency of the measured modulation terms retained by the stepwise MRA procedure.

4.6.3 SOFT DIFFRACTIVE BIFOCAL CONTACT LENSES

A series of empirical MRA models were derived using the MTF measured at 4 spatial frequencies for each soft diffractive BCL to predict the different visual performance measures.

The MRA equations derived by this technique were all significant ($p < 0.025$), though the adjusted R^2 values, as shown in *Table 4.6-7* varied from only 0.07 to 0.23. As with the refractive and rigid diffractive BCL, there was a weak relationship between the spatial frequency of the terms used in the final MRA equations (measured modulation) and the spatial frequency of the visual performance measure.

Visual Performance	Adjusted R^2
CS at 2 c.p.d.	0.071*
CS at 4 c.p.d.	0.102*
CS at 8 c.p.d.	0.113*
CS at 16 c.p.d.	0.131**
PRC at 4 m	0.172**
low contrast VA	0.231***
high contrast VA	0.197***

* $p < 0.025$; ** $p < 0.01$; *** $p < 0.001$

Table 4.6-7 Prediction of visual performance with soft diffractive BCL. The adjusted R^2 for MRA equations which describe visual performance with soft diffractive BCL in terms of the measured MTF (modulation) at 16 spatial frequencies at 548 nm. (n = 61).

Chapter 5 DISCUSSION

Introduction

The general concordance between optical and visual performance results was high, indicating that the Modulation Transfer Function (MTF) was a useful index for investigating the effects of changes in BCL design upon visual performance. This chapter discusses similarities and considers differences between results with the optical and visual performance measures of rigid refractive (section 5.2), rigid diffractive (section 5.3) and soft diffractive (section 5.4) bifocal contact lenses (BCL). In section 5.1 some general aspects of the results are considered, and in section 5.5 the use of optical performance measures to predict visual performance is discussed.

5.1 General considerations

The following general conclusions, which relate to the general interpretation of the results, are discussed :

a) Repeatability of both optical and visual performance measures was worse than previously reported, and was related to image quality (section 5.1.1);

b) Luminance changes were found not to improve the sensitivity of the visual performance measures to changes in BCL design (section 5.1.2);

c) The measured modulation at the different spatial frequencies were highly correlated (section 5.1.3);

d) The visual performance measures were all significantly correlated (section 5.1.4);

e) There was no difference in the visual performance (with diffractive BCL) between the cyclopeged pre-presbyopic subject and the presbyopic subjects (section 5.1.5)

5.1.1 REPEATABILITY

The repeatability coefficients, the 95% confidence limit of the test-retest distribution (section 3.7), were larger than previously reported. The repeatability coefficients for the MTF measurement of the present study (*Figure 4.2-7*), represented approximately 25% of the potential measurement range, as compared to the 1% claimed by the manufacturer, and may reflect the image quality of BCL. Though not examined experimentally, it was the author's impression that the inherent variability of the system (between measurement variations) was at least 5%, making the 1% standard deviation reported by Gray and Sheridan (1988) for single vision CL rather surprising. It is worth noting that, in that study, only three measurements were averaged in each "experiment". The poor repeatability with BCL suggests that, if the MTF is to be used for testing or development of BCL, a number of repetitions would be required to improve reliability.

The repeatability coefficients for the visual performance measures of the present study (*Table 4.3-1*), varied from approximately 20% to 63% of the potential measurement range, varied with the spatial frequency of contrast sensitivity (CS) and the contrast of visual acuity (VA) chart, and were larger (by 1.5 to 4 times) than reported previously with optimally corrected normal subjects (e.g. section 2.2; Elliott et al, 1990a; Greeves et al, 1988; Lovie-Kitchin, 1988; Reeves et al, 1991). As shown in *Figure 4.3-4*, the repeatability coefficients were significantly correlated with the average reduction in visual performance which indicated that the reduction in repeatability was due to the poor quality of vision with BCL making accurate repeated measure more difficult. Though this might have been expected, the variation with spatial frequency and with optical quality has not been reported previously. Increased variability has been reported for subjects suffering from ophthalmic diseases and may increase with deteriorating visual performance (Elliott and Sheridan, 1988; Ross et al, 1984; Wood et al, 1988). The variation with spatial frequency may be partly explained by the relative resistance of lower spatial frequencies to optical degradation (Campbell and Green, 1965a; Green and Campbell, 1965; Kay and Morrison, 1987). The poor repeatability of visual performance measures with BCL reduces the ability to detect differences and changes, both in experimental and clinical work. The clinician fitting BCL must therefore

be aware that comparatively large apparent fluctuations in vision with BCL are "normal".

5.1.2 LUMINANCE

The failure to find an increased sensitivity to the effects of variations in diffractive BCL design with reduced luminance reported in section 2.3 was in contradiction to the results of Guillon et al (1988, 1991) and Guillon and Sayer (1988). The control of pupil size (fixed for both luminance levels) in the present study may explain this discrepancy. As Guillon and co-workers allowed natural variations in pupil size to occur with variations in luminance, the effect of luminance was confounded with the effect of pupil size. Hence what has been reported as an increased sensitivity under reduced luminance conditions was probably due to the increased pupil size and the inherent changes in optical performance of the human eye (e.g. spherical aberration) as shown in *Figure 1.3-1*. The variations between CL reported by Guillon and co-workers thus may have been related to the ability of different CL to correct the aberrations of a more dilated pupil rather than an increased sensitivity of VA measurement with reduced luminance. This does not reduce the significance of their results, and it is possible that testing under reduced luminance conditions, with natural pupils, may elicit differences between BCL which affect the ability of a patient to wear a particular BCL.

5.1.3 CORRELATION BETWEEN MTF MEASURES

The very high correlations between the modulation of the MTF at the different spatial frequencies and the failure to find, with principal component analysis, factors loaded for different spatial frequencies (section 4.2.2) were not surprising as the MTF is a mathematical function which was calculated from the measured Line Spread Function (LSF). As a result, measurement at a limited number of spatial frequencies could be expected to adequately describe variations in the MTF, and this was demonstrated in section 4.6.

5.1.4 CORRELATION BETWEEN VISUAL PERFORMANCE MEASURES

The significant correlations between the visual performance measures (*Table 4.3-2*) and failure to find more than a single factor with principal component analysis indicated that all of the visual performance measures used in the present study were affected similarly by BCL wear. The difference from the report of Sekuler et al (1984) who described 3 factors in the CS measured over a similar range of spatial frequencies may have been due to the different experimental conditions. In the present study the CS during optical degradation (due to BCL wear) of a small group of subjects (n = 8) was measured as compared to the best corrected CS of 91 subjects with a wide age range measured by Sekuler et al (1984). The

contention that CS at spatial frequencies, separated by a factor of 4, are independent (Sekuler and Mulvanney, 1983) also was not confirmed by the present study. The present study was in agreement with other studies (Brown and Lovie-Kitchin, 1989; Owsley et al, 1983) over a similar spatial frequency range. Despite this, as noted in sections 5.2 and 5.3, some aspects of visual performance with the BCL were spatial frequency dependent. Consequently, the lower correlations between visual performance measures with a low spatial frequency content (e.g. CS at 2 c.p.d.) and those with a high spatial frequency content (e.g. VA) would suggest that tests of visual performance should include a low to median spatial frequency test, since some aspect of vision was not assessed with the other tests of visual performance utilised here. The relevance of changes in visual performance at low spatial frequencies to the ability to successfully wear BCL has not been demonstrated.

A relationship between the fundamental frequency of the Pelli-Robson contrast thresholds (PRC) and CS measures has not been previously reported. PRC (calculated fundamental frequency 3.6 c.p.d. at 4 m) was correlated with CS at 4 c.p.d. ($r = 0.61$) better than any of the other CS measures (2, 8, 16 c.p.d.). In addition, correlation was high with low contrast ($r = 0.75$) and high contrast ($r = 0.60$) VA. Also, as noted in section 2.3, there were systematic differences in the absolute

values, and differences in the effect of reduced luminance between the PRC and CS results, confirming the report of Waiss and Cohen (1991). This suggests that the analysis of the PRC in terms of its fundamental frequency, as discussed in section 1.4, was adequate, but that at 4 metres there was significant higher spatial frequency information (Bouma, 1971). It would be interesting to extend this analysis to a wider range of applications and other measurement distances.

5.1.5 THE USE OF PRE-PRESBYOPIC SUBJECTS AND ARTIFICIAL PUPILS

The use of an artificial pupil, whilst having a long history in visual science, does not represent the real situation as the artificial pupil (worn during the investigation of diffractive BCL by one subject) limited the incoming beam and hence the area of the diffractive element of the BCL which was active, whereas the natural pupil limited the beam after the light had passed through the diffractive element.

There was no consistent nor significant difference in the results obtained with rigid and soft diffractive BCL worn by (a) a pre-presbyopic subject (cyclopleged and using an artificial pupil); and (b) the two presbyopic subjects (natural pupils). Hence, the data could be combined for the analysis. The use of cyclopleged pre-presbyopes to investigate the effects of changes in diffractive BCL

design upon visual performance would appear to be a viable alternative for the assessment of visual performance with diffractive BCL, but was unsuccessful when attempted by the author with rigid refractive BCL due to the significant effects of decentration and movement discussed in section 5.2. Cox (1985, 1986) reported results with cyclopleged pre-presbyopes wearing soft concentric-design BCL, using artificial pupils and taking care to ensure centration, which were generally confirmed by the present study, except for the estimates for pupil coverage by the central optical zone (COZ) (based upon the artificial pupil diameter rather than the effective diameter at the BCL).

5.2 Refractive concentric-design bifocal contact lenses

The complexity of the relationship between the various factors investigated has been demonstrated by the present study. The following major findings are discussed in this section :

a) A significant but trivial difference between the Centre-Distance (CD) and Centre-Near (CN) concentric-designs (section 5.2.1);

b) Optical performance improved with increasing aperture size, while relative visual performance reduced with increasing pupil size (section 5.2.2);

c) The ratio between distance and near performance varied with pupil size (section 5.2.2);

d) The ratio between distance and near varied with central optic zone diameter (COZD) (section 5.2.3);
e) Both optical and visual performance varied with spatial frequency with changes in COZD (section 5.2.3)
f) Optical and visual performance were shown to alter with decentration of the BCL (section 5.2.4);
g) Both optical and visual performance varied with spatial frequency with changes in decentration (section 5.2.4)
h) A model developed using Multiple Regression Analysis (MRA) of the optical and the visual performance measures has been used to show how the optimal COZD varied with pupil size, decentration and spatial frequency (section 5.2.5).
i) Optimal cover of the pupil by the COZ was shown to vary with pupil size and spatial frequency.

In general there was good agreement between the optical and the visual performance measures and the MTF was shown to be a useful indicator of visual performance. The importance of the findings and in particular differences between optical and visual performance are discussed.

5.2.1 BIFOCAL DESIGN

The results of section 4.3.3 showed that CS at 8 and 16 c.p.d. and VA were better with the CD BCL, but conversely CS at 2 and 4 c.p.d. and PRC were better with the CN BCL. A variation with spatial frequency was not noted with

optical performance, as CD BCL were found to provide better optical performance at both distance and near than CN BCL at all spatial frequencies (section 4.2.3).

Apart from the COZ, the lens design was the same for CD and CN lenses. The CD BCL had a steeper COZR (back surface) and may have been more stable, though they tended to decentre more on-eye. The steeper COZR may be expected to trap bubbles, but care was taken to ensure that this did not happen. It was most likely that the differences in the curvature of the optical surfaces required to produce back-surface refractive BCL resulted in differences in the optical aberrations which affected optical and hence visual performance. Spherical aberration would have reduced the effective separation of the two foci of the CN design compared to the CD design, thereby comparatively restricting the spread of the out-of-focus image, which would have had a more detrimental effect upon higher spatial frequencies. The additional effect of ocular spherical aberration may explain the difference between the optical and visual performance measures.

The differences between the two BCL designs were considered to be trivial as the differences were very small. In the present study, during visual performance measurement, the pupil size was effectively fixed. The consequences of natural variations in pupil size are discussed in section 5.2.6.

5.2.2 PUPIL SIZE

The MTF of the optical performance measurement apparatus (*Figure 4.2-1*) increased with increasing aperture as expected (*Figure 1.2-4*; Hopkins, 1956). Conversely, as shown in *Figure 1.3-1*, the measured MTF of the human eye has previously been shown to reduce with increasing pupil size (Campbell and Gubisch, 1966). Hence it was expected that there would be some differences between results with optical and visual performance.

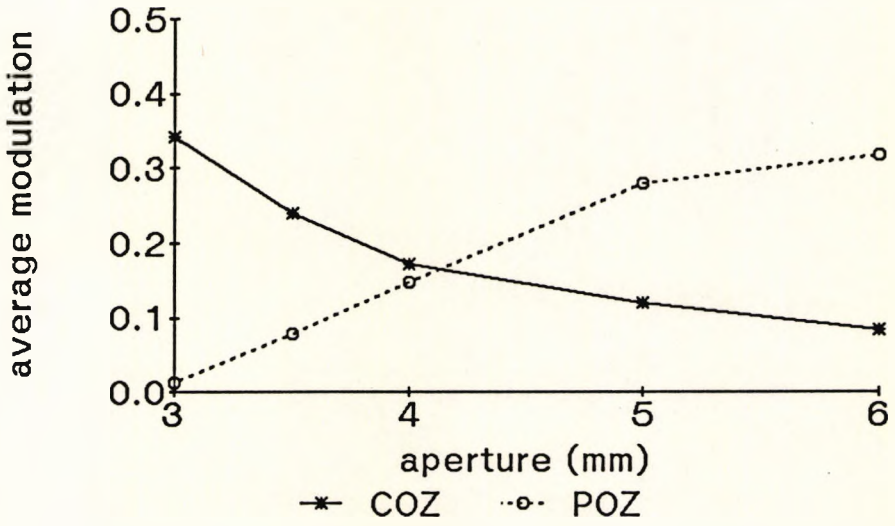

Figure 5.2-1 Optical performance versus aperture size. The variation in the average modulation for 2.6 mm COZD refractive BCL over apertures from 3 to 6 mm.

As a summary of the effect of changes in optical performance with aperture, *Figure 5.2-1* shows the variation in the average modulation for 2.6 mm COZD refractive BCL (taken from the complete MTFs of *Figure 4.2-8*). As expected from a consideration of the geometric area of the COZ over the pupil, with increasing pupil size, both optical

performance and visual performance reduced with the COZ (CD distance, CN near) forming the focus, and improved with the peripheral optic zone (POZ) (CD near, CN distance). Whilst the average modulation with the COZ and the POZ was different, the increase in the overall optical performance (averaged for COZ and POZ) with aperture was significant, but considered trivial. Conversely, it was interesting that the relative visual performance reduced with increasing pupil size (*Figure 4.3-5*), an effect not previously demonstrated, and which suggests that a large pupil size may be a disadvantage when fitting concentric-design BCL.

5.2.3 CENTRAL OPTIC ZONE DIAMETER

The present study was able to clearly demonstrate the expected effects of changes in COZD. *Figure 5.2-2* shows a summary of the effect of changes in optical performance with COZD (taken from the MTFs of *Figure 4.2-9*). Very similar changes in visual performance were noted for the same BCL (*Figures 4.3-6* and *4.3-7*).

Most previous studies of visual performance have failed to conclusively show, for soft refractive BCL worn by presbyopic subjects (Erickson and Robboy, 1985; Jones and Lowther, 1989), the expected changes with vergence (distance or near) and COZD. The present study, with presbyopic subjects and natural pupils, may have been more successful, despite the large amounts of on-eye BCL

decentration (average 1.1 mm in the present study) and the greater movement of rigid CL, due to the number of repetitions and range of visual performance measures. These results were in agreement with Cox (1986) who carefully controlled extraneous factors, including decentration, in a study using pre-presbyopic subjects, cycloplegia and artificial pupils.

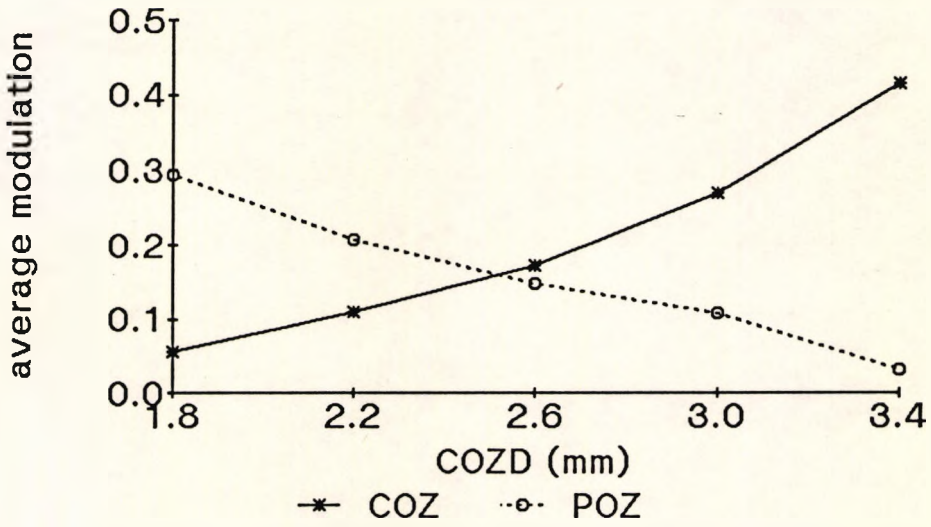

Figure 5.2-2 Optical performance versus COZD. As a summary, the variation in the average modulation with COZD of refractive BCL over a 4 mm aperture with either the COZ or the POZ forming the focus.

Both optical and visual performance varied with spatial frequency. The shape of the MTF for the image formed with the COZ in focus was different to that with the POZ in focus (*Figure 4.2-3*) confirming the theoretical calculations of O'Neill (1956) and in agreement with the MTF measurements of Young et al (1990). This variation was complicated by variations with aperture size (*Figure 4.2-8*) and with COZD (*Figure 4.2-9*). Thus the balance between COZ and POZ (or distance and near) was dependent upon

COZD, aperture and the spatial frequency of interest. A similar variation with spatial frequency was noted with the visual performance measures as shown in *Figures 4.3-1* and *4.3-8*. The reduction in CS was almost equal with all spatial frequencies with the COZ forming the focus, but increased with increasing spatial frequency with the POZ forming the focus. This is shown diagrammatically in *Figure 5.2-3*. Similar variations in CS with spatial frequency were apparent in the only other report of CS measures with concentric-design BCL (Cox, 1985, 1986). The effect of the differences with spatial frequency upon the optimal COZD predicted by MRA is discussed in section 5.2.5.

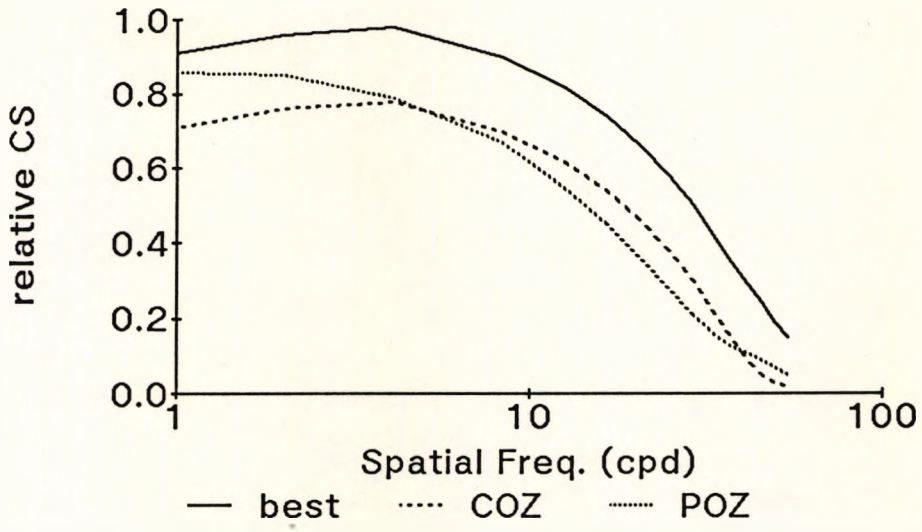

Figure 5.2-3 Visual performance versus spatial frequency. A schematic representation of the best-corrected CSF (solid line) and the CSF with the COZ (dashed) and POZ (dotted) of a refractive BCL forming the focus. The greater reduction in CS with increasing spatial frequency with the POZ, but not with the COZ reflects the optical performance measurements.

The largest COZD gave best overall (distance + near) optical performance with all apertures (2 to 6 mm),

while, conversely, no significant variation in the overall visual performance with COZD was noted. This was not in agreement with previous studies which appear to have shown that the overall visual performance (high contrast VA) varied with COZD (*Figure 1.2-7*; Erickson and Robboy, 1985 and *Figure 1.2-8*; Jones and Lowther, 1989). As there was no reason to expect a change in the overall visual performance, neither study presented a statistical analysis of the difference, and since the present study used a range of visual performance measures and was more carefully controlled, the difference in visual performance with COZD noted in the two studies mentioned was probably an artifact.

5.2.4 DECENTRATION

The average measured on-eye decentration of the refractive BCL was 1.1 mm (range 0.2 to 2.1 mm) over pupils which averaged 2.8 mm (range 2.1 to 3.6 mm). The significance of decentration upon optical performance and visual performance and the interactions between decentration, COZD and pupil size were demonstrated with MRA (section 4.2.3 and 4.3.3 respectively).

When a refractive BCL was decentred across the aperture (pupil) the image (LSF) became markedly asymmetric, altering the balance of the image (*Figure 4.2-14*). With increased decentration the optical performance was slightly improved with the POZ forming the focus and

dramatically reduced with the COZ forming the focus as shown in *Figures 4.2-15* and *4.2-16*. As shown in *Figures 4.3-9* and *4.3-10*, similar changes in visual performance with decentration were noted. Previously, the effects of decentration have only been discussed (Erickson et al, 1988) or diagrams based upon theoretical calculations presented (Hodd, 1969; Charman and Walsh, 1986b), or mentioned, but the relationship to the measured VA apparently not investigated (Erickson and Robboy, 1985).

The measure of on-eye decentration used in the present study was based upon measurement with a slit-lamp biomicroscope of the pupil size and the average location of the BCL during primary gaze. This measure was chosen for use as it represented a technique available to the clinician. The technique was limited by the presumption that the pupil would alter size with changes in illuminance about a common centre, which has been shown to be incorrect (Wilson et al, 1991, 1992) and in addition it failed to take into account differences between the optic axis, visual axis and pupil centre. Conversely, for the measurement of the MTF upon an optical bench, the aperture (pupil) and detector (equivalent to the visual axis) were centred on the optic axis. In addition on-eye movement of the BCL, which was not measured, would affect decentration and has been demonstrated to have a transitory effect upon vision (Tomlinson and Ridder, 1992). Further work could investigate the effect of the movement and location of

the BCL and the effect of pupil decentration from the visual and optical axes of the eye upon visual performance with, for example, "real time" video monitoring of BCL location. Despite these limitations the measurement of decentration was found to be useful in the prediction of visual performance (MRA) and could be usefully employed by the clinician.

5.2.5 OPTIMAL CENTRAL OPTIC ZONE DIAMETER AND PUPIL SIZE

The empirically based MRA equations in sections 4.2.3 and 4.3.3 which describe the optical and the visual performance with refractive BCL were solved for equal modulation or equal visual performance with focus by the COZ and the POZ. This was considered to be an optimal COZD (i.e. equal distance and near performance).

Centred Refractive Bifocal Contact Lenses

The optimal COZD predicted from MTF measurement showed a variation with aperture size and with spatial frequency which is demonstrated in *Figure 4.2-12*. As suggested by the theoretical calculations of O'Neill (1956), the predicted optimal COZD was smaller for median spatial frequencies than at low and high spatial frequencies. The optimal COZD suggested by this analysis, averaged for all measured spatial frequencies, reduced from 42% of a 3 mm aperture to 32% of a 5 mm aperture. This was very similar to the prediction from the calculations made in

section 1.2.2 (*Figure 1.2-7*), based upon the Stiles-Crawford effect (relative directional sensitivity of the human eye), which suggested that the optimal COZD should reduce from 43% of a 2 mm to 35% of a 6 mm pupil. This confirmed the measurement of the image contrast of an enlarged model eye by Atebara and Miller (1990), which suggested that the COZ of an optimal concentric-design bifocal intraocular lens should cover approximately 40% of a 3 mm pupil. Other authors have suggested that the COZ of a concentric-design BCL should cover as much as 90% (3.8 mm on 4 mm pupil) (Robirds, 1987) and as little as 20% (Breger, 1983) .

Visual performance was more difficult to assess as none of the experimental refractive BCL centred perfectly on-eye, and thus the use of the MRA equations derived from measured visual performance to predict the optimal COZD of centred refractive BCL involved an extrapolation. With this reservation, the predicted optimal per cent cover by the COZ is shown in *Figure 5.2-4* to reduce with pupil size and to vary between the visual performance measures. For example, the predicted optimal per cent cover was between 50 and 80% of a 3 mm pupil. This variation in the per cent pupil cover was much greater than predicted from the MTF measures.

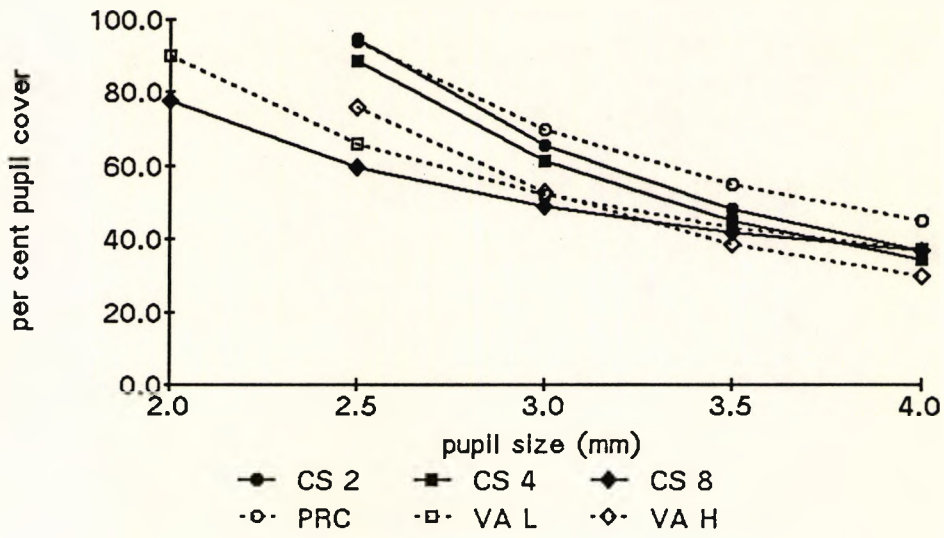

Figure 5.2-4 COZ pupil coverage variation with pupil size. Optimal percentage pupil cover by the COZ of refractive BCL with no decentration predicted by MRA of measured visual performance.

Optimal pupil coverage was difficult to determine from previous studies, but, given some assumptions, the Erickson and Robboy (1985) study of CD soft BCL (*Figure 1.2-7*) using high contrast VA, suggested that the median preferred COZ (2.5 mm) covered 46% of the reported average 3.7 mm pupil. Conversely optimal pupil coverage for the Jones and Lowther (1989) study with CN soft BCL (*Figure 1.2-8*) measured using high contrast VA was about 87% with the reported average 3 mm pupil. Neither of these studies ensured centration. A re-examination of the study by Cox (1986), which investigated the effects of spherical aberration using CD and CN BCL as a model, indicated a trend to smaller optimal pupil coverage with higher spatial frequency tests for pre-presbyopic subjects wearing well centred soft concentric-design BCL with artificial pupils of 4 to 6 mm. The optimal pupil

coverage varied with the spatial frequency of the CS measure from 47% at 0.7 c.p.d. to 22% at 30 c.p.d. and reduced from 40% with low (10%) contrast VA to 15% with high (85%) contrast VA. The artificial pupil sizes were used to determine the optimal pupil coverage and may not represent the actual entrance pupil size.

Differences between predictions from the optical and the visual measures may result from the spherical and other aberrations of the human eye, which increase with increasing pupil size (Campbell and Gubisch, 1966), while the MTF improved with increasing aperture. The POZ would be expected to produce a comparatively worse retinal image with increasing pupil size, and would need to cover more of the pupil to provide visual performance equal to the COZ. The clinician fitting concentric-design BCL should be aware of the reduction in the optimal pupil cover by the COZ with increasing pupil size and the differences between tests which measure visual performance at different spatial frequencies.

Decentred Refractive Bifocal Contact Lenses

Suggestions that the COZ of a concentric-design refractive BCL should cover 50% of the pupil (e.g. Bier, 1967) have presumed centration. BCL decentration, which changed the shape of the MTF (*Figure 4.2-16*), altered the optimal COZD predicted from optical performance (*Figure 4.2-18*). With larger decentration the predicted optimal COZD was larger for median spatial frequencies than for

low and high spatial frequencies, the reverse of the prediction with centred BCL. The optimal COZD predicted by the MRA at 4 and 30 c.p.d. with varying decentration is shown in *Figure 5.2-5* not to vary dramatically with spatial frequency.

As noted in section 5.2.3, the optimal COZD predicted from MRA of the visual performance measures (*Figures 4.3-11* and *4.3-12*) was expected to vary with the spatial frequency of the visual performance measure, and with decentration. There was a slight trend for a smaller predicted optimal COZD with visual performance measures with a higher spatial frequency content. As expected, in general, the predicted optimal COZD increased with increasing pupil size and increasing decentration. The optimal COZD predicted from optical performance shown in *Figure 5.2-5* was very similar.

Only 30 to 55% of the variability of the visual performance data was explained by the MRA. This may be partly due to the poor repeatability of the visual performance measures (section 4.3.2), but suggests that some other factors, such as the movement of the BCL (Tomlinson and Ridder, 1992), may have been important. As noted in section 5.2.4, understanding of the complex relationship may be improved by a study which compares the visual performance to the location of the COZ in relation to both the pupil and the visual axis.

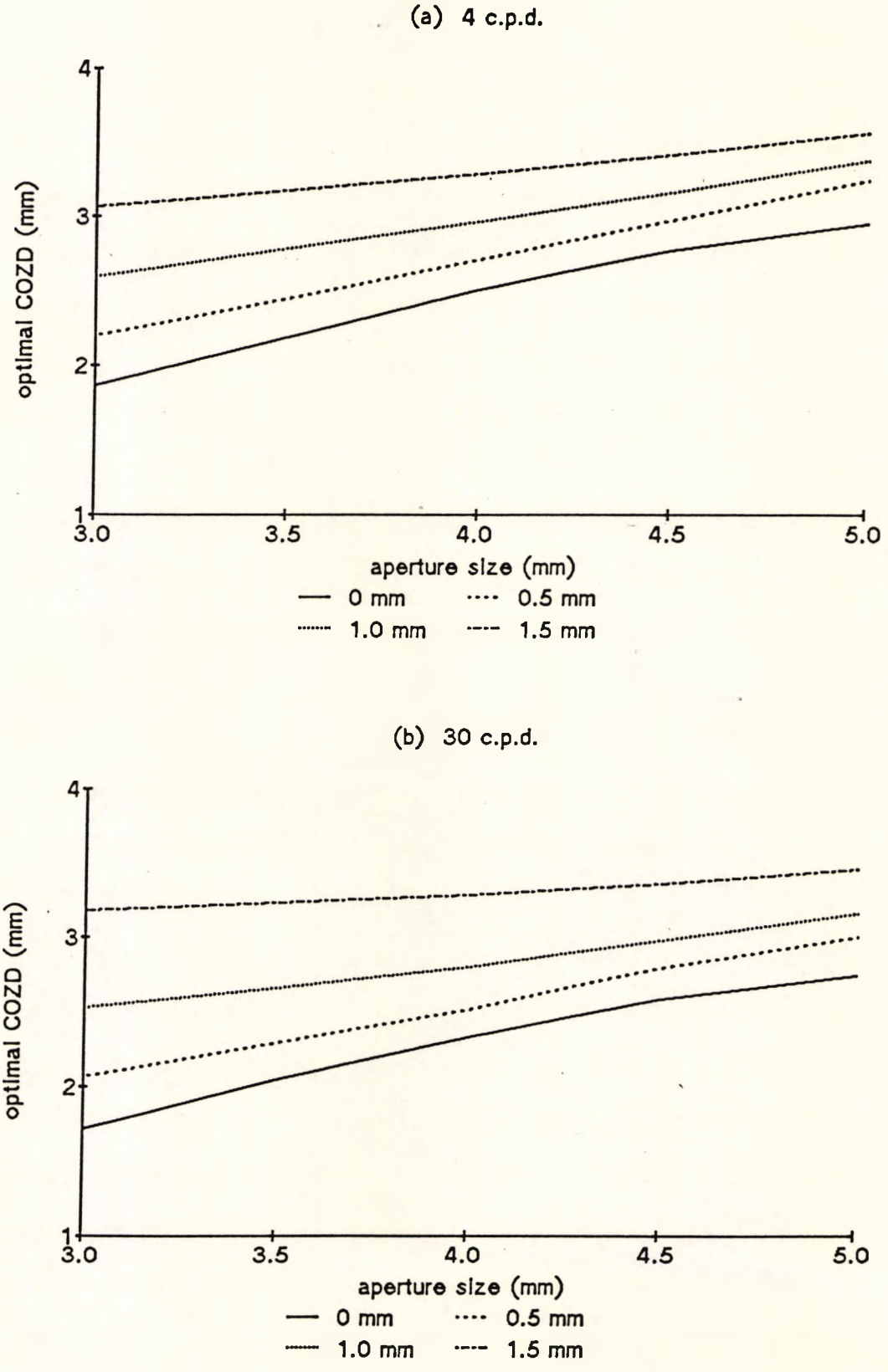

Figure 5.2-5 Optical performance based prediction of optimal COZD. The optimal COZD (equal distance and near) was predicted by MRA (section 4.2.3) of the optical performance (MTF) at **(a)** 4 c.p.d.; and **(b)** 30 c.p.d. with decentration of 0 to 1.5 mm.

The present study has confirmed the importance of fit and centration. Where decentration cannot be avoided despite fit modifications (e.g. increased total diameter or modification of base curves), the COZD and possibly the design (CD or CN) should be modified after consideration of the effects of variations in pupil size.

5.2.6 SUMMARY

The complicated relationship between COZD, pupil size, BCL decentration and spatial frequency has been demonstrated. As optical and visual performance alters with decentration and pupil size, a concentric-design refractive BCL which, for example, may have been COZ biased when centred over the pupil, with decentration or reduced luminance may become POZ biased.

The human pupil is not fixed in size and for an average 55 year old varies from about 5.5 mm in the dark to about 3.25 mm under normal "room" illumination (Woods, 1991c). Hence, on-eye, a COZD which was optimal for one luminance condition may not be optimal for another luminance level. The converged pupil size of presbyopes has been reported by Schafer and Weale (1970) to be about 85% of the unconverged pupil size with a 50 cm (2 Dioptre) stimulus and to be relatively independent of dark adapted pupil size and level of adaptation. This obviously will alter the pupil coverage by the COZ. For example, the COZ of a centred BCL which covers 40% of the pupil at distance,

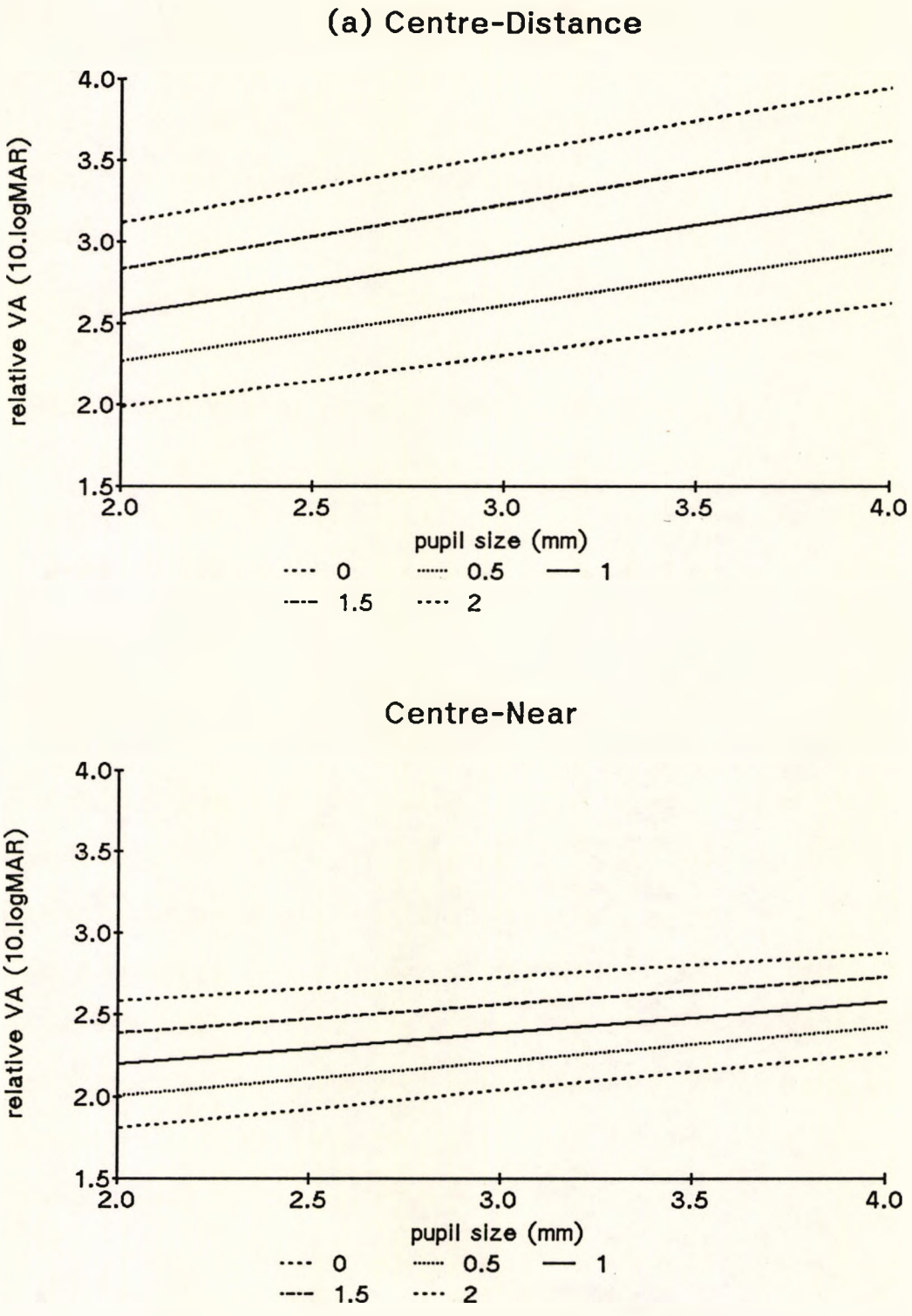

Figure 5.2-6 Predictions for the optimal COZD with **(a)** centre-distance; and **(b)** centre-near refractive BCL. As an example, the different predictions for the optimal COZD for CD and CN BCL based upon the measured low contrast VA and a convergence stimulus of 2 Dioptres resulting in near vision pupillary constriction to 0.85 the size of the pupil at distance viewing (Schafer and Weale, 1970). This may be compared to *Figure 4.3-12* which shows the prediction without the correction for convergence related pupillary constriction.

with 2 Dioptres convergence, will cover 55% of the pupil. If centred, a CN BCL would benefit from convergence related pupillary constriction, though this may be more complicated with decentration (*Figure 1.2-5*). *Figure 5.2-6* shows, that when convergence related pupillary constriction was considered the optimal COZD predicted for CD BCL was larger than for CN BCL . As noted by Baude and Miege (1992), most critical near vision tasks are performed with reasonably high levels of illuminance, which would further increase pupillary constriction, and increase the difference demonstrated in *Figure 5.2-6*.

Hence the clinician fitting concentric-design BCL must consider potential changes in pupil size and the decentration of the BCL. The examination of visual performance under different illumination levels (to naturally vary pupil size) with BCL of different COZD may be necessary for a full assessment of visual performance. Low contrast VA and the higher spatial frequency CS, were the most sensitive of the visual performance measures used to the effects of BCL wear, though this was offset by a lower repeatability.

5.3 Rigid diffractive bifocal contact lenses

Most findings supported theoretical considerations and are considered with regards to current production

techniques. The following major findings are discussed in this section :

a) The relative reduction in optical performance was similar to the relative reduction in visual performance (section 5.3.1);

b) Longitudinal Chromatic Aberration (LCA) was reduced for the near (diffractive) focus (section 5.3.2);

c) Optical performance was resistant to variations in aperture sizes between 2.5 and 5 mm (section 5.3.3);

d) The expected changes in optical performance with wavelength were demonstrated (section 5.3.3);

e) The effect of decentration upon optical performance was demonstrated, and shown to vary with spatial frequency (section 5.3.3);

f) Optical performance was shown to be more sensitive to the variability of manufacture than the visual performance measures (section 5.3.4);

g) Diffractive Zone Junction (DZJ) height was shown to alter the ratio between distance and near of both optical and visual performance measures (section 5.3.5);

g) DZJ shape, as defined by the shape of the diamond tool, was shown to influence both optical and visual performance (section 5.3.6);

h) Light polishing of the diffractive was shown to alter the DZJ height, the shape of the DZ and the ratio between distance and near performance, though overall performance was not affected (section 5.3.7);

i) MRA predictions of the optimal DZJ height (equal distance and near) based upon the optical and visual performance measures were similar, but systematically different (section 5.3.8).

In general there was good concordance between optical performance and visual performance measures and the MTF was shown to be a useful indicator of visual performance. The importance of the findings and in particular differences between optical and visual performance are discussed.

5.3.1 OVERALL PERFORMANCE

The overall (distance + near) reduction in visual performance (CS) was similar or slightly larger than the overall reduction in optical performance (*Table 5.3-1*). Conversely, Freeman and Mulen (reported by Phillips, 1988) suggested that the reduction in visual performance (CS) was less than that predicted by optical performance (MTF) and suggested an "adaptation" effect (n = 4). The present study used similar techniques, was more extensive (n = 129) and included numerous repetitions.

Though, as discussed in section 1.4, visual performance is based upon a combination of the OTF of the BCL, the OTF of the eye, intraocular scatter and neural processes, it was interesting that the reduction in visual performance was closely matched by the reduction in the

MTF of the BCL. The prediction of visual performance from the MTF measurements is discussed in section 5.5.

Optical			Visual	
s.f. (c.p.d.)	log relative modulation 548 nm	573 nm	s.f. (c.p.d.)	log relative C.S.
8	-0.35	-0.33	2	-0.34
17	-0.39	-0.37	4	-0.40
25	-0.41	-0.40	8	-0.42
33	-0.41	-0.38	16	-0.48
41	-0.41	-0.38		

Table 5.3-1 Relative optical and visual performance averaged for all rigid diffractive BCL and all subjects. The relative reduction in the MTF (compared to the system MTF *Figure 4.2-1*) was similar to the average relative visual performance (CS).

5.3.2 LONGITUDINAL CHROMATIC ABERRATION

The focal length of the near (first order) focus of diffractive BCL is inversely proportional to wavelength (*Equation 1.2-1*) and the reverse of refractive LCA such as with spectacle lenses and in the human eye (Charman, 1986; Freeman, 1984). As discussed in section 1.2.3, the LCA of the first order focus (near) of the diffractive BCL was predicted to reduce the inherent LCA of the human eye from approximately 1.5 D to 0.75 D (between 450 and 650 nm), whilst there should be no difference with refractive BCL. This was confirmed by measurement on an

optical bench by the author (unfortunately no data was collected) and on-eye in a limited study (section 4.4).

As expected, the average on-eye LCA with the rigid diffractive BCL was shorter with the near than the distance image, whilst there was no difference in LCA with the refractive BCL. There have been no previously published reports of the LCA measured on-eye with BCL.

The procedure proved difficult for the subject due principally to the poor image quality with the BCL and the low luminance of the targets with the narrow band interference filters. Although attempts were made to improve clarity through various changes in the target, increased luminance of the targets and the introduction of a bite bar. Inevitably, repeatability was low.

Clinical experience suggests that the reduced LCA with diffractive BCL presents no major clinical advantages nor disadvantages.

5.3.3 PUPIL SIZE, WAVELENGTH AND DECENTRATION

As shown in *Figure 4.2-19*, the optical performance of the diffractive BCL was virtually independent of the aperture size, for apertures of 2.5 to 5 mm, the size of the central diffractive zone (CDZ) for the experimental BCL. This was in agreement with theoretical calculations (Freeman, 1984; Klein and Ho, 1986) and with a previous

measure of diffractive BCL (Young et al, 1990). In a clinical study, Courtney et al (1991b) reported reduced success with Allergan Echelon soft diffractive BCL for subjects with large (>6 mm) pupils.

As expected from consideration of *Equation 1.2-3a*, with longer wavelengths, the MTF of the distance (zero order) image improved, whilst the MTF with the near (first order) image reduced (*Figure 4.2-20*). This confirmed previous reports (Young et al, 1990).

There have been no published reports of the effect of decentration upon optical performance. The reduction in near MTF with increased decentration was expected, as the diffractive zone covered less of the pupil. Slightly surprising was the wavelength selective change in distance optical performance with increased decentration (*Figure 4.2-23*). Effectively the MTF at median to high spatial frequencies (10 to 30 c.p.d.) reduced while the MTF at lower spatial frequencies improved. An explanation lies in *Figure 4.2-22* which shows the comparatively strong and discrete out-of-focus (near) image in the LSF of the distance image of the decentred diffractive BCL. This out-of-focus image would be expected to disrupt the image contrast of relatively high spatial frequencies as seen in the MTF. This suggested that centration is important when fitting diffractive BCL, and that tests such as VA (at low and high contrast) would be most affected by decentration.

The effect of decentration upon visual performance with diffractive BCL was not investigated in the present study. Courtney et al (1991b) noted, but did not quantify, clinical effects of poor soft diffractive BCL centration. It is uncertain how the differences between the pupil centre, optic axis and visual axis would influence this result. Bradley et al (1991a) recently described an entoptic phenomenon which allowed the subjective alignment of the diffractive element over the visual axis which would allow further investigation of the effect of decentration. The present study confirmed the importance of fit and centration when fitting diffractive BCL.

5.3.4 ASSESSMENT OF THE VARIABILITY OF MANUFACTURE

The investigation of the variability of manufacture in sections 4.2.4 and 4.3.4, showed that optical performance was more sensitive than the visual performance measures to differences between diffractive BCL.

Lindsay (1990) reported a variation in the ratio between distance and near image intensity which it was suggested indicated manufacturing variability. Similar variation in the vergence ratio (defined as = distance / (distance + near)) was found in the present study with both optical and visual performance measures. The vergence ratio given in *Table 4.2-1* for optical performance was only weakly correlated with the vergence ratio found for the visual

performance measures given in *Table 4.3-5* (R^2 = 0.32 to 0.38; p = 0.05). This weak correlation may have been due to (a) the low number of repetitions with each of the BCL, leaving each a poor estimate of the true ratio; and (b) the averaging of all spatial frequencies to obtain the estimate for optical performance, which may have been better with a limited range of spatial frequencies.

Measured DZJ height was more highly correlated with optical and visual performance measures, than was the nominal DZJ height (section 4.5), suggesting that the DZJ height of many of the BCL were not as specified, and that relatively minor variations in DZJ height influenced optical and visual performance.

The present study did not investigate the effects of the various irregularities at the DZJ which were identified and the effects of the relatively consistently small DZJ height of the first DZJ (section 4.1.2). As the area of the DZ covered by these irregularities (shown diagrammatically in *Figures 3.1-4* and *3.1-5*) was often as large as the finite tool effect discussed in section 5.3.6 an effect upon visual performance would be expected. Edwards and Freeman (1989) have calculated that a reduction in the height of the first DZJ would have a significant effect upon the MTF, due to a reduction in the quality of the near (first order diffractive) image.

5.3.5 DIFFRACTIVE ZONE JUNCTION HEIGHT

Optical performance measurement (MTF) confirmed theoretical predictions (Freeman, 1984; Klein and Ho, 1986), as shown in *Figures 4.2-24* and *4.2-27*, that as DZJ height increased the near image improved and the distance image reduced. Similarly, as shown in *Figures 4.3-13* and *4.3-14* visual performance improved at near and reduced at distance with increasing DZJ height. There have been no previously published reports of the effect of DZJ height upon optical or visual performance.

As can be seen in *Figures 4.2-27, 4.3-13* and *4.3-14*, there was some variability apparent in this assessment which relied upon the nominal DZJ height. Though nominal DZJ height was highly correlated with the measured DZJ height (section 4.1.2), in section 4.5 it was shown that both the optical and the visual performance could be better predicted by the measured than the nominal DZJ height. Unfortunately it was not practical to measure all 189 rigid diffractive BCL, and many of the conclusions drawn from the present study have been based upon the nominal DZJ height. As noted in section 4.5, it would have been sufficient to measure the DZJ height at one or two DZJs rather than at every DZJ, as was done in the present study, to provide a reasonable estimate of the real DZJ height.

The empirically derived MRA equations given in sections 4.2.4 and 4.3.4 to describe the optical and the visual

performance with rigid diffractive BCL were solved for equal modulation or equal visual performance with distance and near. The optimal DZJ height predicted from optical performance was similar to that predicted from visual performance. As summarised in *Table 5.3-2*, the optimal DZJ height predicted from both optical (*Figure 4.2-30*) and visual (*Table 4.3-5*) performance was found to increase slightly with spatial frequency and to vary with tool shape.

Tool	Interference Filter 548 nm	573 nm	CS 2 c.p.d.	VA high contrast
250 μm	2.03	2.20	2.17	2.54
100 μm	2.33	2.33	2.23	2.55
Flatted	1.84	1.98	1.88	2.15

Table 5.3-2 Optimal DZJ height predicted for the three different tool shapes. The optimal DZJ height, shown in *Figure 4.2-30*, predicted from optical performance measurement (MTF) at each wavelength was averaged for all spatial frequencies (4 to 66 c.p.d.). The predicted optimal DZJ height was generally greater for all visual performance measures and increased with the spatial frequency of the measure as shown in *Figure 4.3-16* and *Table 4.3-8*. As an example of the range, CS at 2 c.p.d and high contrast VA are shown.

Differences between the predictions are now discussed. The optimal DZJ height predicted by the visual performance measures was systematically greater than that predicted by optical performance measurement at either wavelength. This suggested that the optimal interference filter for use in measurement of the MTF would have a longer peak wavelength than those used here. This was

confirmed by the better prediction of visual performance at 573 nm than at 548 nm as noted below, and by the change in vergence ratio with the "reverse" add soft diffractive BCL (section 5.4.5).

The optimal DZJ height predicted from the average measured DZJ height (section 4.5) was found to be smaller than that predicted from the nominal DZJ height. The inclusion of first DZJ, which was typically smaller than all other measured DZJs, in the average DZJ height may have introduced a systematic bias. As an alternative, the use of one DZJ (e.g. the third DZJ) or an average of a small group of the inner DZJs (which did not include the first DZJ) may be preferred as a technique for a quicker estimation of DZJ height.

Optical performance measurement proved to be a good predictor of the variation in visual performance with DZJ height, though as noted previously, if the MTF were to be used to assess the effect of changes in BCL design a number of repetitions would be required to improve reliability (section 5.1.1). As interferometric measurement of the surface profile was not as good a predictor of visual performance, and the technique was laborious, this procedure would only be recommended for the purposes of calibration (of the manufacture process) and fundamental examination of diffractive surfaces.

5.3.6 DIAMOND TOOL SHAPE

As discussed in section 1.2.3, due to manufacturing limitations, the diffractive surface profile did not conform to the ideal shape. In particular, the finite size of the diamond tool used to lathe the diffractive surface restricted conformity to the theoretical shape of the DZJ as shown in *Figure 1.2-13*. Diamond tools with a flatted portion and tools with a smaller diameter were expected to produce diffractive surfaces which more closely approximated the theoretically correct shape and it was expected that this would (a) improve the optical performance by reducing the amount of light lost from the diffractive foci; and (b) alter the ratio between distance and near by allowing more light to reach the first diffractive focus. There have been no previously published reports of similar investigations.

The results partly confirmed the predictions. The different tool shapes produced measurably different DZJ shapes as expected (section 4.1.2). The overall optical performance (averaged for distance and near) of the rigid diffractive BCL made with the 100 μm tool was worse than with the 250 μm tool which was worse than the flatted tool. Conversely, visual performance was worst with the 250 μm tool. The difference between the optical and visual results may have been due to unequal numbers of repetitions in the groups compared (e.g. a BCL may have been measured once optically but more than once in visual

performance) which could have distorted the averages presented. The expected improvement in optical performance with "better" DZJ shape may not have been demonstrated due to increased wear and tear upon flatted diamond and smaller radius tools and the sensitivity of the MTF to changes in the surface quality noted in section 4.1.2 (fringe appearance grading), though, due to time constraints, insufficient BCL were examined to substantiate this possible explanation.

The finite tool effect was expected to spill light from the near (first order) focus, thereby making the BCL more distance biased. The difference in DZJ shape was significant in altering the balance between distance and near of both optical and visual performance, though this was not immediately apparent from examination of *Figures 4.2-27*, *4.3-13* and *4.3-14*. As shown in *Table 5.3-1* the difference between the tools in the predicted optimal DZJ height was similar for both optical and visual performance measures, though, as noted above, the absolute values differed. It had been expected that BCL made with both the 100 μm and flatted diamond tools would have a smaller optimal DZJ height than BCL made with the 250 μm tool. This was the case for BCL made with the flatted tool but not for BCL made with the 100 μm tool, which optical performance would even suggest required a larger DZJ height for equal distance and near performance.

Whilst differences in optical and visual performance with the different DZJ shapes were demonstrated in the present study, the differences were generally much smaller than the repeatability of the measurement and sufficiently small to be considered clinically insignificant. It is possible, that with more careful manufacture, that the differences between the DZJ shapes would have been greater. Given the current production procedures there would appear to be no benefit from a change from the standard 250 μm tool.

5.3.7 THE EFFECT OF POLISHING THE DIFFRACTIVE SURFACE

Not surprisingly, the unintentional polishing of the diffractive surface which occurred during the processing of a small number of the rigid diffractive BCL altered the balance between distance and near. The optical performance (*Figure 4.2-32*) and visual performance (*Figure 4.3-17*) could be quite well predicted by the measured DZJ height. The overall optical and visual performance was not reduced compared to the non-polished BCL.

Interferometric examination reported in section 4.1.2 (*Figure 4.1-2*) showed that the surface profile of polished BCL came slightly closer to the theoretically correct shape than the non-polished BCL (*Figure 4.1-1*). The surface quality of polished BCL was much better (fringe appearance grading), which may be expected to slightly

improve optical quality, though it was not possible to test this.

This would suggest that a carefully controlled degree of polishing of the diffractive surface may have slight advantages, though this would probably be outweighed by the increased cost of manufacture and the difficulty of ensuring equal levels of polishing of all BCL. Polishing could possibly reduce the variability of manufacture noted earlier.

5.3.8 SUMMARY - OPTIMISING DESIGN CHARACTERISTICS

The optical performance measure (MTF) was more sensitive to differences in quality of the diffractive surface and due to variability in manufacture than the visual performance measures, and thus these differences were not considered to have been clinically significant.

Decentration altered the MTF at distance (*Figure 4.2-23*) particularly at the moderate to high spatial frequencies (10 to 30 c.p.d.), and clinicians fitting diffractive BCL would be advised to enhance BCL centration where possible.

There was no apparent advantage to any of the tool shapes used in the present study. As has been noted in section 5.3.6, the DZJ height in conjunction with a selected tool shape influenced the ratio between distance and near in a

characteristic way. It was unclear why the optimal DZJ found in the present study (*Table 4.3-5*) for the 250 μm tool, at between 2.2 and 2.5 μm, was larger than suggested by theoretical calculation (1.95 μm) and larger than used in the current rigid diffractive BCL (2.0 μm). One potential explanation which could be investigated was the relatively consistent incorrect (small) height of the first DZJ noted in section 4.1.2, which would be expected to bias the performance to distance (Edwards and Freeman, 1989).

The specification of the optimal DZJ height as meaning equal distance and near performance has not been tested on a clinical basis. Possibly BCL wearers may have different visual requirements. For example, a slight bias to distance may be preferred to facilitate driving. In addition the relevance of the variation in the optimal DZJ height with the spatial frequency of the visual performance measure remains to be tested.

5.4 Soft diffractive bifocal contact lenses

Most conclusions were restricted by the limited range of soft BCL available for use in the study. The following major findings are discussed in this section :

a) The optical quality of the experimental soft diffractive BCL was poor;

b) Results with Allergan Echelon soft diffractive BCL were similar to a previous study;

c) Optical performance was shown to be more sensitive to the variability of manufacture than the visual performance measures (section 5.4.1);

c) Diffractive Zone Junction (DZJ) height was shown to alter the ratio between distance and near of the MTF but not the visual performance measures (section 5.4.2);

d) No consistent differences due to changes in DZJ shape, as defined by the shape of the diamond tool, were shown (section 5.4.3);

e) No consistent differences due to changes in the manufacture process (lathe or moulding) were shown (section 5.4.4);

f) A "reverse" add soft diffractive was demonstrated to provide an effective bifocal effect (section 5.4.5);

g) An interference filter of a longer peak wavelength than those used was shown to be required to simulate the changes in visual performance (section 5.4.5);

In general there was a poor concordance between optical performance and visual performance measures with the soft diffractive BCL. Many of the effects found for optical performance measurement were not found for measurement of visual performance with the same soft diffractive BCL. The optical quality of the experimental soft diffractive BCL was poor compared to the rigid diffractive BCL as reported in section 4.2.5 and was reflected in greater

reductions in visual performance (section 4.3.2), and in the poor repeatability of the visual performance measures with the soft diffractive BCL (*Table 4.3-1*). In addition, the general quality of some of the soft diffractive BCL was poor, such that some of the lathed soft BCL caused discomfort when worn. Hence any conclusions from this section may be limited. The available soft diffractive BCL were a heterogeneous group, and the comparisons between different design characteristics which were possible are discussed.

Previous Reports

The results of the present study were similar to previous measurement of MTF (Young et al, 1990) and visual performance (Papas et al, 1988, 1989, 1990; Young et al, 1987) with Allergan Echelon soft diffractive BCL. The MTF measured by Young et al (1990) was slightly better than that found in the present study, but showed a similar slight bias to the distance image with a similar aperture size (*Figure 4.2-40*). In a series of complementary visual studies, Papas and co-workers measured distance and near vision, but the method of vision measurement at near did not allow a direct comparison between distance and near. At distance, the relative high contrast VA was similar, but a greater reduction in low contrast VA was noted in the present study (*Figure 4.3-23*). Similar charts and luminance levels were used. The BCL used by Young et al, (1990) and Papas et al (1990) were obviously from a different production lot, which may have had slightly

better optical quality than those used in the present study.

The ability to reproduce the results of Papas et al (1990) and Young et al (1990) indicated that the procedures used were satisfactory, and that the difficulty in demonstrating differences between the experimental soft diffractive BCL was, as suggested above, due to the poor optical quality of the available BCL.

5.4.1 ASSESSMENT OF THE VARIABILITY OF MANUFACTURE

Significant differences in overall performance and in the ratio between distance and near were found in both optical and visual performance between the three batches of soft diffractive BCL (section 4.2.5 and 4.3.5). Further examination showed that the same batch was found to vary from the other two with all tests. This batch was part of the same production run as one of the other two batches, highlighting the variability in the moulding process.

Whilst it was not possible to make direct comparisons between other soft diffractive BCL, examination of the results indicates that there was a large degree of variability between BCL which should have been similar (e.g. *Figures 4.2-37, 4.2-38, 4.3-20* and *4.3-21*). This suggests a failure to produce BCL of the nominal parameters. As

noted above the poor quality of the soft diffractive BCL, and the failure to produce BCL of the nominal parameters may be considered as a cause for the failure to display some of the effects of interest.

It was not possible to determine the cause of the variability from the results of the present study as, due to time constraints, it was not possible to examine the surface profile of all of the soft diffractive BCL.

5.4.2 DIFFRACTIVE ZONE JUNCTION HEIGHT

As discussed in section 5.3.5, as DZJ height increased the near image was expected to improve and the distance image was expected to reduce, with commensurate changes in visual performance. Optical performance with the soft diffractive BCL did vary with the nominal DZJ height almost as expected (*Figures 4.2-34* to *4.2-37*), but the same trends were not apparent as changes in visual performance (*Figures 4.3-20* and *4.3-21*), especially at low spatial frequency.

There were some unexpected variations in the shape of the MTF for the near focus of certain BCL (e.g. 4.0 μm DZJ height in *Figure 4.2-35b* and 3.3 μm DZJ height in *Figure 4.2-36b*) which were reminiscent of the changes with decentration shown for rigid diffractive BCL in section 4.2.4. In particular there was an apparent reduction in the MTF at median to high spatial frequencies (10 to 30 c.p.d.). This was thought to have been due to a poorly constructed

central diffractive zone, as it was very unlikely that the BCL were actually decentred when measured, as each MTF shown was an average of at least four separate measurements, and the placement of the BCL over the aperture, though done manually, was a hyperacuity task (rings within a circle) and subject to only minor random errors.

Unfortunately, due to time constraints, it was not possible to examine the surface profile of each of the experimental soft diffractive BCL to determine the reasons for the failure to show the expected trends as clearly as was possible with the rigid diffractive BCL.

5.4.3 DIAMOND TOOL SHAPE

There was no obvious effect of tool shape on optical performance (*Figures 4.2-37* and *4.2-38*) nor on visual performance (*Figures 4.3-20* and *4.3-21*), except perhaps an increased bias to near optical and visual performance with the flatted tool. Any real differences due to the tool shape may have been masked by the poor optical quality of the available soft diffractive BCL.

5.4.4 MANUFACTURE TECHNIQUE

There was no obvious effect of using lathe cutting or moulding on optical performance (*Figures 4.2-37* and *4.2-38*) nor on visual performance (*Figures 4.3-20* and *4.3-21*). Any real

differences due to the manufacture technique may have been masked by the poor optical quality of the available soft diffractive BCL.

5.4.5 A REVERSE ADDITION SOFT DIFFRACTIVE BIFOCAL CONTACT LENS

A "reverse" add diffractive BCL utilises the negative first order diffractive focus to form the distance image, and uses the zero order focus (refractive) to form the near image (section 1.2.3). Hence the optical arrangement is the reverse of that used in a "conventional" diffractive BCL, which use the zero order image for distance, and the positive first order image for near. There have been no previous reports of "reverse" add diffractive BCL.

The optical (*Figure 4.2-39*) and the visual (*Figure 4.3-22*) performance indicated that this form of diffractive BCL works as effectively as the conventional diffractive BCL. As expected the vergence ratio was reversed compared to the conventional BCL, such that visual performance was distance biased with the conventional BCL and near biased with the "reverse" add BCL (*Figure 4.3-22*). Optical performance, when measured at both 548 nm and 573 nm, of the conventional BCL was near biased, whilst the "reverse" add was distance biased. Hence the vergence ratio was the opposite of that found with the visual performance measures.

The difference in the optical and visual performance results may be explained by consideration of the differences between the bifocal foci with wavelength. As discussed in section 1.2.3, the spectral energy of each diffractive foci varies with wavelength (*Equation 1.2-3a*). As shown in *Figure 1.2-12*, for conventional diffractive BCL, the distance image is long wavelength biased, and the near image short wavelength biased. This is reversed for a "reverse" add diffractive BCL. As the spectral energy increases there is a commensurate improvement in the MTF (Emerton, 1986) which has been demonstrated by the present study to correlate with improved visual performance. *Figures 5.4-1* and *5.4-2* show diagrammatically the spectral energy in the distance (solid line) and near (dashed line) foci of a conventional and a "reverse" add diffractive BCL respectively, while the solid arrows represent the positions at which the optical measurements where taken. Hence, as shown, optical performance with the conventional BCL was near biased and with the "reverse" add distance biased. The vergence ratio was closer to 0.5 (equal distance and near) at 573 nm than at 548 nm. The open arrows shown in *Figures 5.41* and *5.4-2* represent the wavelength at which optical measurements would be required to reverse the measured vergence ratio, and hence to replicate the visual performance results. As noted in section 5.3.5, it was unclear why the visual performance would be equivalent to optical performance measurement at a long wavelength (> 573 nm) when visual performance would be expected to be best at approximately

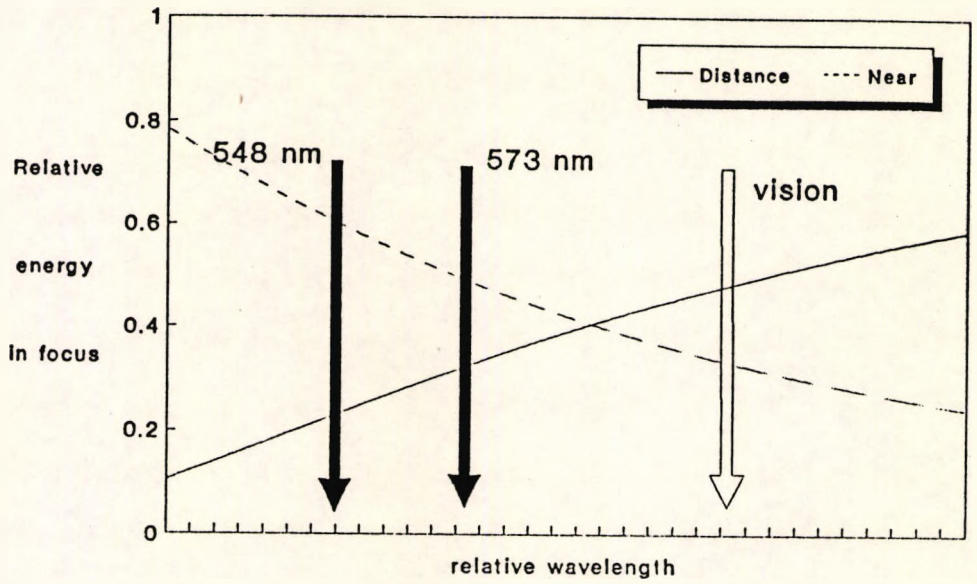

Figure 5.41 The spectral energy of a conventional diffractive BCL shown schematically. The distance focus is long wavelength biased and the near focus short wavelength biased (*Equation 1.2.3a*). Image quality and the MTF improve with increasing spectral energy. The solid arrows represent the positions at which optical performance measures were made, as indicated by the vergence ratio (distance / distance + near). To explain the difference in the measured vergence ratio found with the visual performance measures compared to the optical performance measures, the equivalent wavelength would be longer than 573 nm (open arrow).

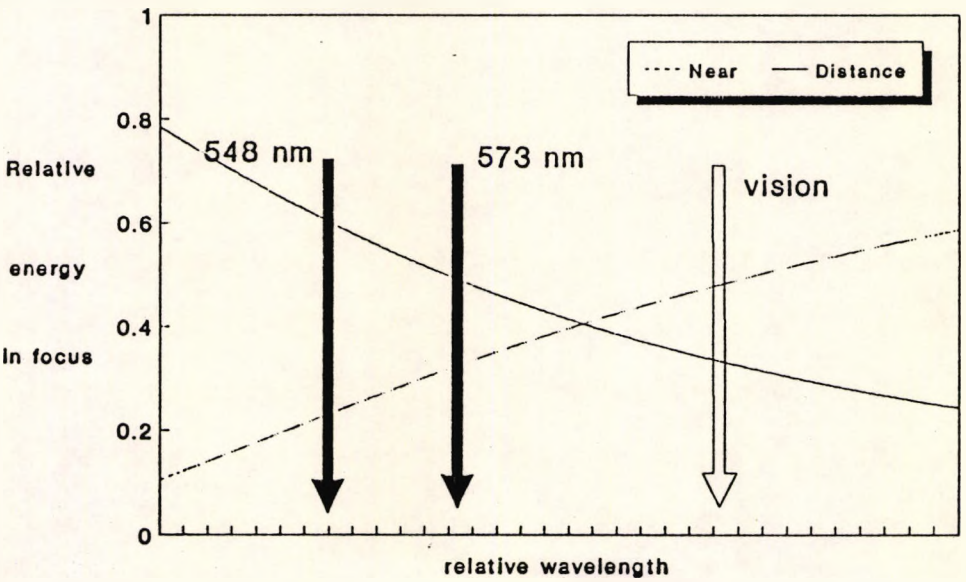

Figure 5.4-2 The spectral energy of a reverse add diffractive BCL shown schematically. The distance focus is short wavelength biased and the near focus long wavelength biased (*Equation 1.2.3a*). Image quality and the MTF improve with increasing spectral energy. The solid arrows represent the positions at which optical performance measures were made as indicated by the vergence ratio (distance / distance + near). To explain the difference in the measured vergence ratio found with the visual performance measures compared to the optical performance measures, the equivalent wavelength would be longer than 573 nm (open arrow).

550 nm (e.g. Vλ in *Figure 1.1-4*). The VA and PRC charts were illuminated with tungsten halide spot lamps which are slightly long wavelength biased, while the monitor used to measure CS used a P4 phosphor which was slightly short wavelength biased. Hence the wavelength at which the visual performance measures were made would not appear to be the cause of the discrepancy. A difference between the refractive indices of the fluids surrounding the BCL used during optical (saline) and visual (tears) performance measurement could explain the discrepancy, but the size of the difference would have to have been greater than would normally be attributed to these fluids (section 5.5.2). Alternatively there may be wavelength dependent differences in the refractive index of the BCL materials and the surrounding media which have not been reported.

A "reverse" add diffractive BCL has been demonstrated, and has been shown to differ, as expected, from a conventional diffractive BCL. Further investigation would be required to determine whether the differences in the design, and particularly the reduced LCA at the distance focus, was a clinical benefit.

5.4.6 SUMMARY - OPTIMISING DESIGN CHARACTERISTICS

Due to the heterogeneity of the available experimental soft diffractive BCL, the poor optical quality (see sections 4.2.5 and 4.3.5 for comparisons to a

commercially available soft diffractive BCL) and the variability of manufacture there were few conclusions which could be drawn from this section of the study. The production problems which were evident during the present study must be overcome before a successful soft diffractive BCL can be made with the equipment which was used to produce the experimental soft diffractive BCL. It was not the aim of the present study to identify particular problems in production.

In general the lathed BCL were better than the moulded BCL which were available. As noted in section 5.3.5, a carefully controlled degree of polishing of the diffractive surface may have slight advantages, though these would probably be outweighed by the increased cost of manufacture and the difficulty of ensuring equal levels of polishing of all BCL. Whilst controlled polishing may then prove too difficult to institute with rigid diffractive BCL production, where currently each BCL is individually lathed, there could be advantages in the production of moulded soft diffractive BCL. Here a small number of (typically) brass masters are lathed for use in the moulding process, producing numerous moulded BCL. Polishing of the brass masters could be controlled and even measured. This would need further investigation.

Though the optical quality was no better than the other experimental BCL, the "reverse" add BCL proved to be a

viable option. Further work would be required to investigate any potential advantages of this design. The major difference which would require investigation is the reduced LCA of the distance (first order diffractive) focus.

5.5 Predicting visual performance from optical performance

MRA models were empirically derived to describe visual performance (CS, PRC, and VA) from optical performance (MTF) in section 4.6 and the following major findings are discussed in this section:

a) visual performance with refractive BCL was predicted from the MTF calculated from measured pupil size, decentration and COZD (Adjusted R^2 range 0.25 to 0.58) (section 5.5.1);

b) visual performance with refractive BCL was predicted from the measured MTF with a range of aperture sizes (3 to 5 mm) (Adjusted R^2 range 0.37 to 0.80). The 4 mm aperture was found generally to give the best prediction (section 5.5.1);

c) visual performance with rigid diffractive BCL was predicted from the MTF measured at 548 and 573 nm (Adjusted R^2 range 0.40 to 0.88). Prediction was slightly better at 573 nm (section 5.5.2);

d) visual performance with soft diffractive BCL was predicted from the MTF measured at 548 nm (Adjusted R^2 range 0.07 to 0.23); and

e) The spatial frequency of the MTF measurement was only weakly related to the spatial frequency content of the visual performance measures.

The ability to predict visual performance from optical performance was demonstrated. The amount of the variance explained by the derived equations (i.e. the adjusted R^2) varied between the BCL types and the visual performance measures. The relevance of these results are discussed.

A previous study

The only previous attempt to evaluate the optical and visual performance of the same BCL, was a preliminary investigation by Freeman and Mulen (reported in Phillips, 1988). This was limited to reporting that the overall reduction in visual performance was less than predicted by the measured optical performance. This was not supported by the present study (section 5.3.1).

The Multiple Regression Models

The empirical models relating optical and visual performance derived in section 4.6 were based upon the MTF data measured at 4 spatial frequencies. The 4 spatial frequencies were chosen to cover the full range of spatial frequencies studied, after a preliminary examination of the correlations between visual performance and the modulation measured at each of the

original 16 spatial frequencies. As shown in *Tables 4.6-3* and *4.6-6*, there was a weak relationship between the spatial frequency content of the visual performance measure and that of the MTF terms retained in the stepwise MRA. This was due to the high correlations between MTF data at the different spatial frequencies (section 5.1.3) and the correlations between the visual performance measures (section 5.1.4). The BCL were shown to have, in general, similar effects at all spatial frequencies of the measured MTF and with all visual performance measures. Hence visual performance was correlated almost equally well with measured MTF data at all the spatial frequencies. The stepwise MRA procedure retained those spatial frequencies with the greatest ability to explain the variations in visual performance, and as noted, there was often very little difference between the different spatial frequencies. Various averaging procedures and other constrictions of the data were investigated, and the MRA models given were judged to be the most useful.

5.5.1 REFRACTIVE BIFOCAL CONTACT LENSES

Two different approaches to the prediction of visual performance with refractive BCL were made in the present study. The first was based upon the calculated MTF derived from MTF measurements of decentred BCL, while the second was based upon the actual measured MTF of centred BCL.

Calculated optical performance

Aperture size and BCL decentration were shown to influence, and could be used to predict optical performance (section 4.2.3). As there were differences in the size of the pupil and BCL decentration between subjects, it was expected that these factors would influence the visual performance in a predictable way. Thus, it was expected that visual performance would have been best predicted by optical performance which had been calculated from the measured COZD, pupil size and BCL decentration. As shown in section 4.6.1 (*Table 4.6-4*), visual performance could be predicted using this approach.

Unfortunately, the MRA model derived from the calculated optical performance was no better than the MRA model derived in section 4.3.3 which used COZD, pupil size and decentration to predict visual performance. Perhaps this was not surprising considering that essentially the same information was used in each MRA model, and an extra step was required to derive the calculated optical performance. In addition, as discussed in section 5.2.4, the on-eye situation was not entirely analogous to the optical measurement, as the optic axis, visual axis and pupil centre of the eye are rarely concentric, and the decentration measurement was an average, whereas the BCL on-eye was constantly moving, altering the optical performance.

Measured optical performance

As shown in section 4.6.1 (*Table 4.6-1*), the measured optical performance of centred refractive BCL provided a better prediction of visual performance than the model discussed above. The average pupil size was 2.8 mm, and it might have been expected that measurements of optical performance with the 3 mm aperture may have been the best predictor of visual performance. Examination of the trends in the data suggested that the visual performance data may have been best matched by optical performance with the 4 mm aperture. As can be seen in *Table 4.6-1* the MTF measured with the 4 mm aperture size was slightly better than the others (range 3 to 5 mm) in the prediction of visual performance. This was not surprising as the variation in optical performance with COZD and vergence changed significantly with aperture.

Differences between the on-eye situation and the BCL during MTF measurement may explain the better prediction of visual performance with an aperture larger than the measured pupil. In the optical apparatus used to measure the MTF, the aperture stop was 3 mm behind the BCL, and light leaving the BCL, due to Badal optometer arrangement, was parallel, being focussed by a subsequent lens onto the detector array (*Figure 3.2-2*). Conversely, when on-eye, the effective size of COZ at the pupil (aperture stop) would have been effectively reduced to approximately 0.85 of the measured diameter by the power of the cornea (Gullstrand-Emsley schematic eye: Bennett

and Rabbetts, 1984), whereas the COZD effective at the aperture stop on the optical bench would not have reduced. Hence, considering the area of the COZD and the aperture stop, a measured 2.8 mm pupil would be represented by a 3.9 mm aperture stop on the optical bench (2.8×0.85^{-2}).

5.5.2 DIFFRACTIVE BIFOCAL CONTACT LENSES

Rigid diffractive BCL

Visual performance with rigid diffractive BCL was predicted from the measured optical performance with MRA equations with good adjusted R^2 values (*Table 4.6-5*). These equations better predicted visual performance than equations based upon the nominal DZJ height (section 4.3.4), or the measured DZJ height (section 4.5.2). Hence the MTF was demonstrated to be a useful method for the prediction of visual performance with rigid diffractive BCL.

Soft diffractive BCL

Visual performance with soft diffractive BCL was predicted from the measured optical performance (section 4.6.3) with low adjusted R^2 values (*Table 4.6-7*) and comparatively low significance ($p < 0.025$). This was probably due to the poor optical quality of the soft diffractive BCL which reduced the repeatability of visual performance measurement (section 4.3.2). It was also not surprising, as the trends demonstrated with optical

performance (*Figures 4.2-34, 4.2-35* and *4.2-36*) were not demonstrated with the visual performance measures (*Figures 4.3-20* and *4.3-21*).

Choice of interference filter for MTF measurement

As noted in section 5.4.5, the interference filters used for measurement of optical performance of rigid diffractive BCL would appear not to have been ideal (note refractive BCL were measured in "white" light). The optimal DZJ height predicted from measurements at both 548 nm and 573 nm was consistently under estimated (*Table 5.3-2*). An interference filter with a longer peak wavelength than those used in the present study would be required to predict a similar optimal DZJ height to that found with visual performance.

It was uncertain why the predicted optimal DZJ height found from MRA of the optical performance measures should have differed systematically from that based upon the visual performance measures. Some of the difference may have been due to a difference between the refractive index of the surrounding medium when measuring optical performance (saline) as compared to when measuring visual performance (tears). This would alter the effective design wavelength (*Equations 1.2-3a* and *1.2-4*), thereby altering the ratio between distance and near. Calculations, which did not take into account the variation in refractive index with wavelength, indicated that a 5% change in the difference between the refractive index of the BCL and

the surrounding medium (i.e. a change in refractive index of the surrounding medium from 1.334 to 1.340) would alter the optimal DZJ height by approximately 0.1 μm. This difference would appear to be greater than normally quoted for tears and saline (e.g. Phillips and Stone, 1989). Differences in the variation of refractive index with wavelength could also be investigated.

It was not possible to simply measure the MTF of diffractive BCL in "white" light since the longitudinal chromatic aberration of the diffractive focus which is an advantage on-eye dramatically reduced the image quality on an optical bench. As noted in section 1.2.3, calculations of the polychromatic MTF suggested a better optical performance than found with the monochromatic MTF (Klein and Ho, 1986; Edwards and Freeman, 1989). Given the number of BCL involved in the present study it was not possible to measure all BCL at a full range of wavelengths as would have been required. The polychromatic MTF could be the subject of further studies, though from a practical viewpoint, a single measure will always be preferred if the technique is to be used regularly for the evaluation of BCL.

5.5.3 SUMMARY - MODELS OF VISUAL PERFORMANCE

This study measured the image quality of the same BCL optically and visually and attempted to develop models to explain the visual performance from the measured optical

performance. Image quality and aspects of CL wear lead to poor repeatability of the visual performance measures, which in turn reduced the ability of the models to predict changes in visual performance. Despite this, the relationship between the optical performance and certain visual performance measures was demonstrated, with the result that reasonable models were developed for the prediction of visual performance with rigid refractive and diffractive BCL. These models should be tested with another group of subjects to assess the durability of the models. In addition, the relevance of the different visual performance measures used in the present study has not been demonstrated in the "real world".

One important aspect which has not been considered in the current study which may have influenced visual performance was the optical quality of the eyes of the individual subjects. Individual variations in pupil location with changes in pupil size (Walsh, 1988; Wilson et al, 1991, 1992) and differences in the location of the pupil in relation to the visual and optical axes may be important in BCL wear and require investigation (Campbell et al, 1990).

Future work investigating the performance of BCL could usefully involve measurement of the quality of the actual retinal image with the BCL in situ, either objectively or subjectively with available techniques which could be adapted (e.g. Campbell et al, 1990; Howland and Howland,

1976, 1977; Santamaria et al, 1987; Walsh and Charman, 1985, 1989). Physical measurement of the retinal image by any double-pass procedure (e.g. Campbell and Gubisch, 1966; Santamaria et al, 1987; Walsh and Charman, 1985, 1989) would be very difficult computationally, particularly for diffractive BCL where the image on emerging from the eye would comprise three major foci (the two at the retina would be doubled again on exiting the eye by the diffractive BCL, and two of the four images would coincide: Freeman, 1992). Objective procedures which involve the location of aspects of the retinal image may be required rather than attempting to reconstruct the retinal image.

Another area which the present study was not designed to investigate, but which may improve the understanding of vision with rigid BCL, would involve a study of the effects of rigid BCL movement and location in relation to both the pupil and to the visual axis. The short term fluctuations (<100 ms) in visual performance which have been demonstrated after the blink (Tomlinson and Ridder, 1992) would be expected to be more pronounced and probably of longer duration with BCL compared to single vision CL. In particular a technique to monitor variations in visual performance whilst simultaneously tracking the BCL on-eye would assist in better understanding the requirements for rigid BCL design.

Chapter 6 CONCLUSIONS

The effects of changes in the optical design of refractive and diffractive bifocal contact lenses (BCL) upon the optical and visual performance have been demonstrated. The major findings were :

a) Optical performance measurements were in good agreement with the visual performance measures, and possible explanations for the minor differences have been discussed;

b) Concentric-design refractive BCL were affected by central optic zone diameter (COZD), the BCL configuration (Centre-Distance or Centre-Near), pupil size, decentration and spatial frequency. The optimal COZD has been shown to vary with each of these variables;

c) Changes in diffractive BCL design - diffractive zone junction (DZJ) height and DZJ shape - influenced both optical and visual performance. The effects of surface quality, DZJ irregularities, pupil size, wavelength and decentration have been considered. Suggestions have been made for improvements in diffractive BCL design and manufacture;

d) An interferometric technique (Nomarski) has been used to make a variety of measurements of both rigid and soft diffractive BCL, which were related to optical and

visual performance. Problems in the manufacture of the central diffractive zone have been identified;

e) A "reverse" add soft diffractive BCL has been demonstrated to provide an effective bifocal effect;

f) low contrast VA has been shown to be sensitive to the effects of BCL and has been recommended as an addition to conventional clinical tests;

g) both optical performance and visual performance measures showed comparatively poor repeatability, which has been shown to be related to the optical quality of the BCL and to vary with spatial frequency;

h) The concordance between visual and optical performance measures with diffractive BCL may be improved by the use of a longer wavelength for the optical performance measurement than employed in this study; and

i) The ability to predict visual performance from measured optical performance of BCL has been demonstrated. This was influenced by the optical quality of the BCL.

The majority of the effects described were expected from theoretical considerations. The relationship between the measured MTF and a range of visual performance measures has been shown for the first time, demonstrating the MTF as a useful tool for the assessment of the effect of changes in BCL design. Models have been developed which may assist in the development of future BCL.

APPENDIX 1

Reprinted from:

The Journal of the
BRITISH CONTACT LENS
ASSOCIATION

Journal of the British Contact Lens Association, Vol. 14, No. 3, pp 115–127, 1991
Printed in Great Britain

THE AGING EYE AND CONTACT LENSES – A REVIEW OF OCULAR CHARACTERISTICS

*Russell L. Woods**

(Received 18th March 1991, in revised form 20th May 1991)

Abstract — *Most contact lens practitioners are dealing with an increasing number of otherwise healthy 'older' (presbyopic) patients. Examination of the literature indicates a persistent theme of age-related change, which generally becomes significant after the fourth decade. This review documents changes that are reported in the ocular adnexa, tear film, cornea, pupil, intraocular pressure, refractive state, spectral transmission, and chromatic aberration. The effects of these various changes on the fitting and wear of contact lenses by older patients are discussed.*

KEY WORDS: Age, aging, review, tear film, cornea, pupil, ocular media, spectral transmission, chromatic aberration, intraocular pressure.

Introduction

THE NATURE of contact lens fitting is likely to alter slowly as population demographics in all the western nations indicate a trend towards an aging population. This change to the classical population pyramid is enhanced by the post-war 'baby boomers', who are now entering the presbyopic age bracket. In addition, many of the patients fitted with contact lenses since their introduction are now entering this group and expecting a contact lens correction of their presbyopic visual problem.

Ocular changes that are acknowledged to occur with age and that may influence contact lens wear include decreased tonus of both upper[1,2], and lower eyelids[3], a reduced palpebral aperture[4,5], decreased lacrimal secretion[6,7], reduced tear stability[8,9] changes to the cornea and ocular media, decreased pupil diameter[4,10,11], and the effects of the increased intake of systemic drugs.[12,13] Weale[14,15] has given a very comprehensive review of ocular age-related changes. Aspects of such changes to ocular characteristics with regard to lens wear are discussed in this article. Visual performance changes with age include the decrease in visual acuity[16] (which is greater under reduced levels of illumination[17]), the reduction in contrast sensitivity for high and intermediate spatial frequencies[18–20], reduced stereoacuity[21,22], and increased glare sensitivity.[23,24] All of these factors are of importance when fitting contact lenses to the aging eye. Physiological considerations may be different and visual performance generally reduced. Particular care must then be taken with contact lens modalities that compromise aspects of vision, for example, monovision and bifocal contact lenses.

The older contact lens patient can present special problems to the practitioner, in addition to presbyopia. Older patients may require fitting of aphakic or therapeutic contact lenses. This will often involve the use of extended-wear contact lenses, as older patients will often experience handling difficulties. Most advanced contact lens texts provide information about non-routine contact lens fitting requirements for older patients. Phillips[25], for example, has produced a useful review.

Interest in bifocal contact lenses is increasing within the industry and the optical professions, and amongst the general public as they become aware of the option through the general and optical media. Contact lens companies are developing and publicising hydrophilic versions of the rigid bifocal contact lenses, as used by a limited number of experienced practitioners for many years, and new diffractive bifocal contact lenses are becoming available. Further development of bifocal contact lenses, the marketing capabilities of the large companies, and increased acceptance of contact lenses as a potential modality may lead to an increase in the number of presbyopes fitted with contact lenses. Despite this enormous potential market, surveys of contact lens fitting patterns[26–28] indicate that only 1% of contact lens patients are fitted with bifocal lenses. A slightly larger group are fitted with the alternative presbyopic contact lens option (monovision), the most successful system[26], but considered by many practitioners to be unsatisfactory due to its deleterious effects upon binocular vision.[29–31]

The proportion of contact lens patients who are presbyopic and the proportion of presbyopes who wear contact lenses are uncertain, but are generally assumed to be small. Despite this, as mentioned above, practitioners are likely to encounter an increasing number and proportion of presbyopic contact lens patients. With this in mind, some of the special ocular problems that may influence contact lens fitting and wear are reviewed herein.

Ocular Adnexa

There are marked alterations with age to the tissues of the ocular adnexa, due to a 'progressive loss of tone and bulk'.[32] Changes with age to the eyelids, including a loss of tonus, reduced movement, and the reduction

* BOptom (Hons) MBCO

sleep, thereby increasing overnight swelling and possibly reducing tolerance to contact lens wear.

Pyron *et al.*[37] reported a selective adherence of certain bacteria to the human bulbar conjunctiva, which appeared to vary with age. This implies that there may be a differential susceptibility of individuals to infection with specific bacteria, which needs further investigation.

Lawrenson[38], investigating the limbal touch threshold, has found an age-related decrease in sensitivity that is most pronounced after the fourth decade.

Pingueculae become more common with age and, if near the limbus, may lift the lids away from the surrounding conjunctiva and cornea, causing a local area of drying as the tear layer is not restored with blinking. Rigid lenses may cause irritation of pingueculae and increase the dessication and associated vascularisation. Soft contact lenses may fail to centre properly.

The lids may swell during the menopause and the resultant hormonal changes may cause increased water retention.[13] Xerosis of the conjunctiva may also occur during the menopause.[13]

Tear Film

The literature demonstrates a controversy that exists regarding the relationships between tear flow, tear volume, and age. Early descriptions of a decrease in tear volume with age generally relied upon results obtained with the Schirmer test (e.g., Norn[39]), which are acknowledged to induce reflex lacrimal secretion (i.e., the tear flow due to discomfort associated with the test, and measured as the difference in tear flow with and without local anaesthetic). Lamberts *et al.*[40] investigated reflex lacrimation and reported no age-related reduction in the Schirmer test results after the instillation of a topical anaesthetic. This was due to a negative correlation between age and reflex lacrimation. Corneal sensitivity decreases with age[41] and would account for the decrease in reflex lacrimation and the earlier reports of age changes. Contradictory reports of a (subjective) fluorescein colorimetric matching procedure[6,12] imply a possible age-related reduction in tear flow. A reduction in lacrimal secretion with age was demonstrated by Furukawa and Polse[6], who measured tear-turnover rate (subjects aged 15–63 years) with a fluorophotometer. Earlier, Mishima *et al.*[42] reported no tear flow–age relationship as assessed with colorimetric matching and fluorophotometry, with a smaller sample and no subjects over the age of 50 years. Hamano *et al.*[7] measured tear volume with a phenol-red impregnated cotton thread which, due to its quick application (approximately 15s), is claimed to estimate the inferior conjunctival tear volume (but probably includes some basal secretion). Hamano *et al.*[7] reported that the percentage of eyes with less than 15mm wet length increased significantly with increasing age. The percentage with a wet length of less than 10mm was greatest in the 30–39 year age group, as shown in *Figure 3*. It is interesting to speculate that

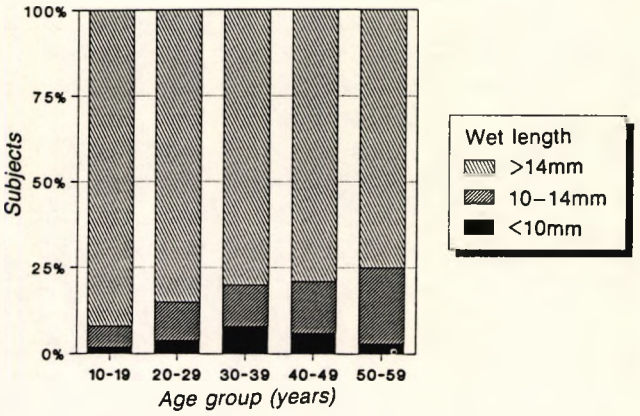

Figure 3. *The relationship between age and the wet length of a phenol-red impregnated cotton thread. The wet length is assumed to relate to the inferior tear volume (redrawn from Hamano* et al.[7]*).*

there may be two factors at work: the first, a real decrease in tear production with age, and the second, an increase in tear retention after the fourth decade due, perhaps, to changing lid shape and a reduced facility of punctum drainage. In addition, the constituents of the tears may alter with age.

The pre-corneal tear film, composed of lipids, proteins, mucus, salts, and water from many glands, is not solely dependent upon volume or flow rates. Changes with age in five tear protein concentrations have been demonstrated by McGill *et al.*[43], but the significance of each of the numerous constituents has yet to be determined. McGill *et al.*[43] suggest the diagnostic use of lysozyme and lactoferrin assays, as these proteins have been demonstrated to be at reduced levels in dry eyes. Some elderly patients will have reduced tear flow due to disease, such as rheumatoid arthiritis [e.g., keratoconjunctivitis sicca (KCS) in Sjogren's syndrome]. KCS is an age-related aqueous deficiency syndrome, which affects more females than males, and commonly appears between the fifth and sixth decades. Rose bengal and lysozyme assay are diagnostic of KCS.[33] Special care must be exercised if any patients with a reduced lysozyme tear content are to be fitted with contact lenses, as this may increase susceptibility to infection.

Koetting and Andrews[44] reported an age-related reduction in tear pH (more acidic). This may affect the fitting characteristics of certain high water-content soft contact lenses.

All of these techniques are intrusive to varying degrees, so some non-intrusive techniques are now discussed. The inferior tear prism has been estimated to contain over 80% of the tear volume. Using a non-invasive technique, Port and Asaria[45] measured the inferior tear prism with a modified optical pachometer and noted no age-related difference between two small population samples.

Clinical measures of tear stability are often used as diagnostic tests in contact lens practice. Andres *et al.*[46] reported a significant reduction in fluorescein tear break-up time (BUT) with increasing age and found it

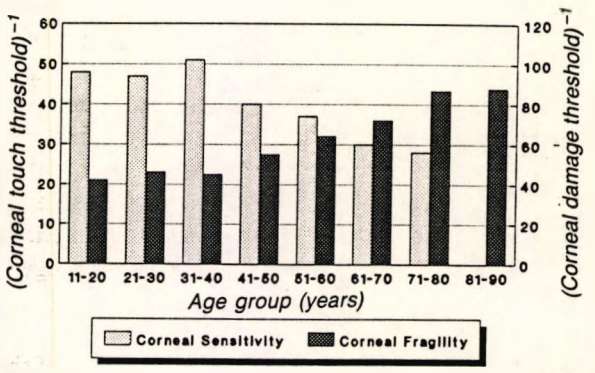

Figure 4. *Corneal sensitivity (corneal touch threshold^{-1}) and corneal fragility (corneal damage threshold^{-1}) as a function of age. The means for each age group are shown. Corneal sensitivity decreases with age[41], while corneal fragility increases with age[71] after about the fourth decade of life.*

Corneal fragility (corneal damage threshold^{-1}) appears to increase with age. Millodot and Owens[71] found a progressive increase in fragility with age from 11 to 80 years, corresponding to the decrease in sensitivity, as shown in *Figure 4*. Millodot and Owens[71] also noted that younger eyes healed more quickly from the experimental insult, confirming animal studies by Marre[72], who noted a significantly reduced rate of corneal wound closure in older rabbits. Similarly, cat corneal epithelium stressed with contact lens wear appears to lose adherence to the basement membrane.[73] Changes with age to Bowman's layer, the corneal epithelial basement membrane, were reported by Alvarado *et al.*[74] and may explain the increased fragility, through changes in membrane thickness and type, that may result in a weakened attachment of the epithelium to the underlying basement membrane. Clinically, there is an increased incidence of sicca and epithelial compromise (as indicated by rose bengal and fluorescein staining) with age, especially in the lower cornea.[75] Also, there is an age-related increase in the degree of corneal fluorescein staining, which is normally found in about 20% of non-contact lens wearers.[76] Hence, older patients who wear contact lenses are more likely to suffer corneal damage, yet are less likely to be aware of it, and hence are at greater risk of corneal compromise.

Descemet's membrane increases in thickness with age.[77,78] The regularity of the young human corneal endothelial cellular mosaic is progressively lost with increasing age. Endothelial cell density decreases as the mean cell area increases with age.[79,80] Also, there is an increase in cellular polymegethism and cellular pleomorphism as the cell numbers decrease with age.[67,81] Measures of cellular polymegethism and pleomorphism appear to be more sensitive measures of endothelial compromise than are cell density measures.[81]

Wigham and Hodson[82] report a diminished endothelial pump capability with age. It is possible that this is partially compensated by an increased barrier function and decreased ionic permeability, and they note 'should last for a couple of centuries'. Contact lens induced oedema was used by O'Neal and Polse[83] to demonstrate a correlation between endothelial cell area variation and recovery rate, as a measure of endothelial pump efficiency. Their data suggests that the endothelial pump function decreases by approximately 10% between the third and seventh decades. Sweeney and Holden[67] demonstrated a relationship between induced corneal oedema and epithelial thickness and polymegethism. Wilson and Roper-Hall[84] argue that, as in the clinically normal cornea it is so unusual to detect a pathologically low endothelial cell count, there is little to worry about. Long-term wear of hard contact lenses[85] and extended-wear contact lenses[86,87] causes endothelial changes over and above normal age-related changes in control subjects. Considering this, and the preliminary data of Wigham and Hodson[82], the endothelium is probably not the primary source of concern with corneal decompensation, until stressed by a contact lens. There is a large individual variation in corneal ability to deal with anoxic stress, and patients should be assessed on an individual basis. Care must still be taken with regard to older long-term hard or extended-wear contact lens patients, and account taken of the increased incidence of endothelial pathology in older patients.

Cataract surgery may cause flattening of the cornea, a lower corneal apex, and increase in corneal toricity (steeper horizontal), thereby imposing difficulties in fitting rigid contact lenses.[88] Epithelial thickness is slightly reduced[25]; corneal innervation is reduced by half and hence sensitivity is reduced[89]; the basal metabolic rate and oxygen demand are lower, resulting in greater tolerance to hypoxia[90]; and endothelial cell density is reduced.

Diabetes, which becomes more common with advancing age, is known to retard corneal epithelial healing, increase the risk of corneal neovascularization[91], reduce corneal sensitivity, and increase corneal fragility.[92] Diabetes has also been reported to lead to an increased susceptibility to infection[93], to increase the incidence of recurrent epithelial erosions[94], and to cause endothelial morphological changes.[95] Finally, with increasing age there is an increased incidence of various corneal conditions.[96]

Contact lens fitting for older patients is thus fraught with greater dangers than that for the typical younger patient. Practitioners must be aware of the decreased corneal sensitivity, increased corneal fragility, reduced rate of epithelial healing, reduced tear flow, increased incidence of corneal age-related disorders, and the greater possibility of corneal decompensation through contact lens induced stress.

Pupil Size

The size of the pupil is dependent upon the retinal luminance and state of adaptation, the state of the entire

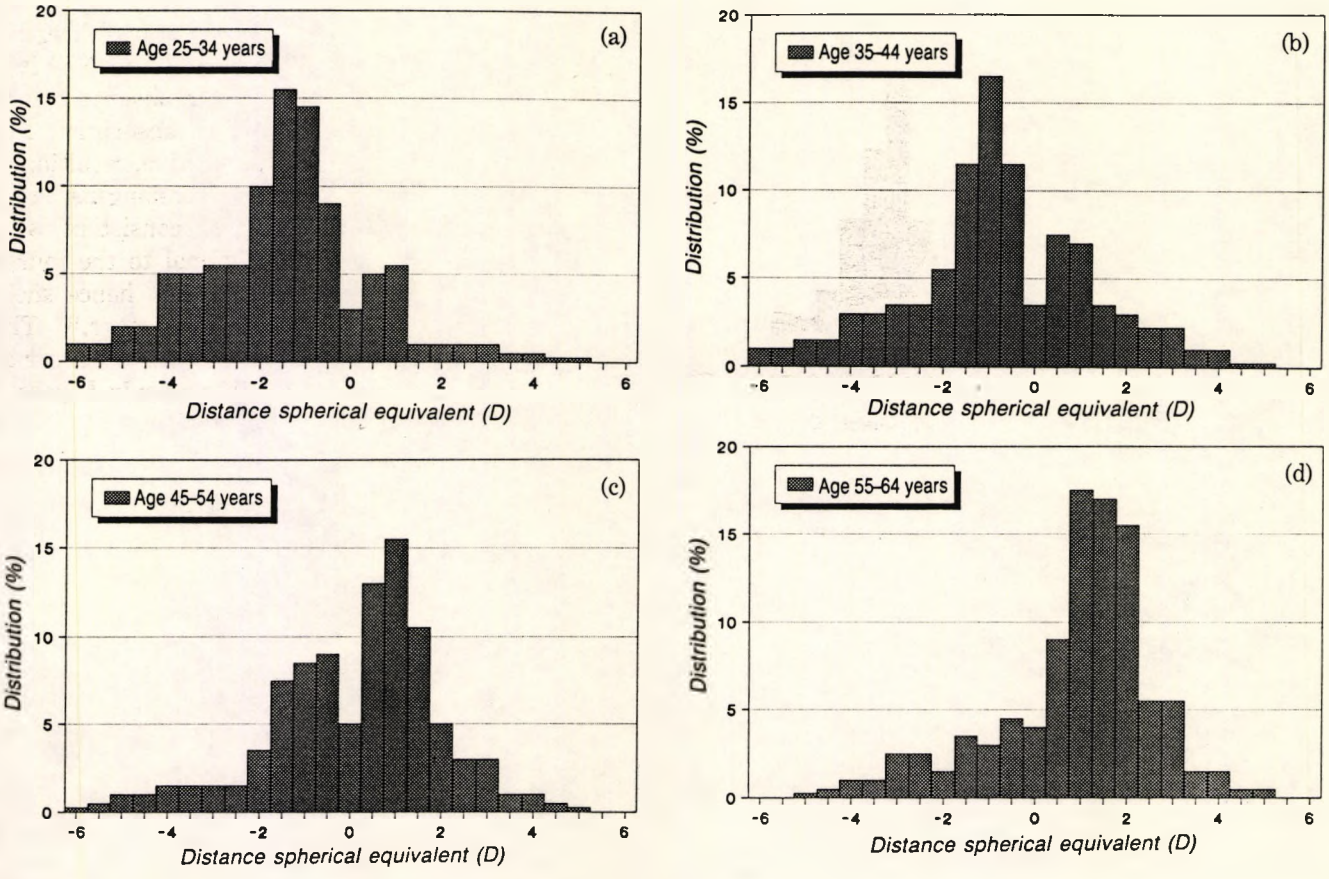

Figure 7. *The refractive profile, shown as the distance spherical equivalent correction, changes with increasing age. The distribution percentage (in half dioptre steps), is shown for: (a) age 25–34 years; (b) age 35–44 years; (c) age 45–54 years; (d) 55–64 years; and (e) age 65–74 years. With increasing age the proportion of the age group who require optical correction shifts from predominantly myopic to predominantly hypermetropic. The data is derived from US government information (quoted in Friant and Miller[117]).*

significant change in contrast sensitivity for pupil diameters <4mm. This was for one subject (herself) with clear (young) ocular media.

De Groot and Gebhard[112] analysed the data from eight studies that investigated the relationship between pupil size and luminance of large adapting fields. The weighted compiled results were described with the curve:

$$\log D = 0.8558 - 4.01 \times 10^{-4}(\log B + 8.1)^3$$

where D is the diameter (mm) of the natural pupil and B is the luminance (mL) of the adapting field. The difficulty is that the age of the subjects in the majority of the studies used was not available, and the known alteration in pupil size with age was not considered.

Intraocular pressure

Intraocular pressure (IOP) does not change significantly until the fifth decade, after which it increases with age in Caucasians.[113,114] Conversely, with an Oriental population, Shiose[115] reported a consistent tendency of IOP to decrease with age. Contact lens wear reduces oxygen supply to the cornea and may lead to decompensation of a cornea already stressed by a raised IOP.[25] Phillips[25] suggests that even mild cases of ocular hypertension should be fitted with extended wear contact lenses only with great care.

Refractive state

There is a shift in the distribution of refractive corrections with age, such that the proportion of hypermetropes increases with increasing age, as shown in *Figures 7(a)–7(e).* Refractive index changes in the crystalline lens are associated with nuclear cataracts. The age-related increased incidence of nuclear cataract can cause an apparent myopic shift for age groups older than those shown. Phelps-Brown[116] suggests that those who do not suffer nuclear cataractous changes maintain the hypermetropic shift, implying that older populations become (at least) bimodal.

Friant and Miller[117] reported that the distribution of distance powers of dispensed Alges bifocal contact

Allen and Vos[63] reported an increased back-scatter of light by the cornea with age. Vos and Boogard[128] estimated that 25–30% of intraocular scatter is due to the cornea. Much of the attenuation is attributed to scatter that occurs principally in the stroma.[64] Visual symptoms with corneal oedema have traditionally been explained as changes in the stromal matrix. Cox and Holden[129] have demonstrated that epithelial oedema induced by hypotonic saline produces haloes and reduced contrast sensitivity, while anoxia-induced stromal oedema results in no measurable visual loss. This implies that reduction in visual function is not a good predictor of physiological corneal oedema.

Aqueous

The aqueous has a high transmittance through the visible spectrum. No age-related changes in spectral transmission[62,130] or the refractive index[131] of the aqueous have been noted.

Crystalline Lens

The crystalline lens is responsible for the majority of the intraocular attenuation of light transmission[132] through absorption, probably related to pigmentation, and scatter. Said and Weale[125] reported a progressive increase in the optical density of the lens with increasing age, particularly for short wavelengths, as shown in *Figure 10.* Boettner and Wolter[62] demonstrated similar age-related changes *in vitro.* Millodot[133] reported a reduction in ocular chromatic aberration of approximately one-third between phakic (normal) and aphakic, age-matched eyes, inferring that the remaining chromatic aberration is due to the other ocular tissues. Millodot and Newton[127] reported an age-related change in the refractive index of the crystalline lens. Back-scatter by the lens also increases with age.[23,63] Siew *et al.*[134], through analysis of light scatter of thin sections of crystalline lens, infer that the major age change is syneresis, a gradual reduction of water of hydration from the protein aggregates. This was confirmed by measures of lenticular water content by Lahm *et al.*[135] These ultrastructural changes result in an increase with age in the light scatter. The crystalline lens is the principal u.v. filter in the human eye, and thus the aphakic eye is prone to damage from this short wavelength radiation. Aphakic patients should be routinely fitted with contact lenses that incorporate a u.v. filter.

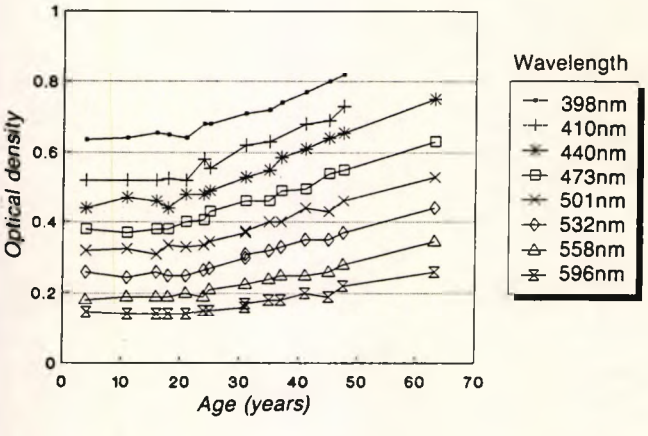

Figure 10. *The variation in optical density of the human lens with age at various wavelengths. The change is greatest after about 25 years of age and greater with shorter wavelengths (redrawn from Said and Weale[125]).*

Vitreous

There is some back-scatter within the vitreous[23,118] and an age-related reduction in transmission of about 10%.[62] The refractive index does not alter with age.[137]

The Retina and Colour Discrimination

Forward scatter by the retina also reduces the light available to the receptors by an estimated 30%.[136] Macular pigmentation is subject to large individual variations[122,123] and will selectively attenuate the light transmitted to the photoreceptors, influencing colour perception. Human retinae examined by high performance liquid chromatography demonstrated no dependence upon age for the quantities of the two major macular pigments (zeaxanthin and lutein), for donors aged 3–95 years.[137] With colorimetric examination, Kelly[138] and Ruddock[121,122] have demonstrated no age-related effect of macular pigmentation upon colour discrimination.

In a variety of colorimetric experiments, Ruddock[122] demonstrated a correlation between age and spectral transmission for wavelengths 420–600nm and ages 16–61 years, and a greater decrease in transmission for shorter wavelengths. Despite large individual variations, Werner[123] has demonstrated an increased attenuation of short, but not medium or long, wavelengths with increasing age, from 4.5 months to 66 years (400–650nm), as measured with visually evoked responses.

Diffractive Bifocal Contact Lenses and Spectral Transmission

The age-related wavelength-selective reduction in transmission may have some unexpected results. Diffractive bifocal contact lenses are wavelength dependent, with the distance image being more 'blue' and the near image more 'red'[139,140], as shown in *Figure 11.* As the older eye is less able to utilise short (blue) wavelengths, there is a possibility that some wearers may find the distance image inadequate. This may be further enhanced by the spectral content of the illuminating source. A diffractive lens designed to give a 50:50 ratio between distance and near images, given the human spectral sensitivity ($V\lambda$, as shown in *Figure 12)* in daylight (e.g., D65 in *Figure 12*), will give a different ratio under a different illuminant. For example, when used with tungsten filament lamps (e.g., Standard Illuminant A), which produce most of their energy in the longer (red) wavelengths, as shown in *Figure 12,* the energy in the two images would alter from 50:50 to 47:53. This may thus further reduce

Address for Correspondence
Russell L. Woods, Department of Optometry and Visual Science, City University, 311–321 Goswell Road, London EC1V 7DD.

Postscript. Estimates of the variance of data (e.g., standard deviation) have not been included in the figures in an attempt to improve clarity and to retain a consistent style. Interested readers are advised to consult the original source as indicated.

REFERENCES

[1] Hill, J.C. Analysis of senile changes in the palpebral fissure. *Trans. Ophthalmol. Soc. UK*, **95**(1), 49–53 (1975).
[2] Vihlen, F.S. and Wilson, G. The relation between eyelid tension, corneal toricity, and age. *Invest. Ophthalmol. Vis. Sci.*, **24**(10), 1367–1373 (1983).
[3] Shore, J.W. Changes in lower eyelid resting position, movement, and tone with age. *Am. J. Ophthalmol.*, **99**, 415–423 (1985).
[4] Loewenfeld, I.E. Pupillary changes related to age, in *Topics in Neuro-Ophthalmology*, Williams & Wilkins, Baltimore, pp 124–150 (1979).
[5] Sanke, R.F. Relationship of senile ptosis to age. *Ann. Ophthalmol.*, **16**(10), 928–931 (1984).
[6] Furukawa, R.E. and Polse, K.A. Changes in tear flow accompanying aging. *Am. J. Optom. Physiol. Optics*, **55**(2), 69–74 (1978).
[7] Hamano, T., Mitsunaga, S., Kotani, S., Hamano, T., Hamano, K., Hamano, H., Sakamoto, R., and Tamura, H. Tear volume in relation to contact lens wear and age. *Contact Lens Assoc. Ophthalmol. J.*, **16**(1), 57–61 (1990).
[8] Guillon, J.P. and Guillon, M. *Predicting the Marginal Dry Eye Contact Lens Patient*, presented at the British Contact Lens Association Annual Conference, May, 1988.
[9] Patel, S. and Farrell, J.C. Age-related changes in precorneal tear film stability. *Am. J. Optom. Physiol. Opt.*, **66**(3), 175–178 (1988).
[10] Birren, J.E., Casperson, R.C., and Botwinick, J. Age changes in pupil size. *J. Gerontol.*, **5**, 216–225 (1950).
[11] Kadlecova, V., Peleska, M., and Vasko, A. Dependence on age of the diameter of the pupil in the dark. *Nature*, **182**, 1520–1521 (1958).
[12] Luppelli, L. A review of lacrimal function tests in relation to CL practice. *Contact Lens J.*, **14**(8), 4–17 (1986).
[13] Stone, J. Assessment of patient suitability for contact lenses, in *Contact Lenses*, 3rd edn, Phillips, A.J. and Stone, J. (Eds), Butterworths, London, pp 270–298 (1989).
[14] Weale, R.A. *The Aging Eye*, H.K. Lewis, London (1963).
[15] Weale, R.A. *A Biography of the Eye*, H.K. Lewis, London (1982).
[16] Pitts, D.G. Visual acuity as a function of age. *J. Am. Optom. Assoc.*, **53**(2), 117–124 (1982). See also, Pitts, D. G. The effects of aging on selected visual functions: dark adaptation, visual acuity, stereopsis, and brightness contrast, in *Aging and Human Visual Function*, Liss, New York, pp 131–159 (1982).
[17] Richards, O.W. Effects of luminance and contrast on visual acuity, ages 16 to 90 years. *Am. J. Optom. Physiol. Optics*, **54**(3), 178–184 (1977).
[18] Owsley, C., Sekuler, R., and Siemsen, D. Contrast sensitivity throughout adulthood. *Vision Res.*, **23**(7), 689–699 (1983).
[19] Wright, C.E. and Drasdo, N. The influence of age on the spatial and temporal contrast sensitivity function. *Doc. Ophthalmol.*, **59**, 385–395 (1985).
[20] Elliott, D.B. Contrast sensitivity decline with ageing: a neural or optical phenomenon? *Ophthal. Physiol. Opt.*, **7**(4), 415–419 (1987).
[21] Jani, S.N. The age factor in stereopsis screening. *Am. J. Optom. Arch. Am. Acad. Optom.*, **43**(9), 653–657 (1966).
[22] Woods, R.L. Stereopsis with monovision and two concentric bifocal contact lens systems, presented at the Society of Experimental Optometry, July, 1986.
[23] Wolf, E. Glare and age. *Arch. Ophthalmol.*, **64**, 502–514 (1960).
[24] Reading, V.M. Disability glare and age. *Vision Res.*, **8**, 207–214 (1968).
[25] Phillips, A.J. Contact lenses and the elderly patient, in *Vision and Ageing*, Rosenbloom, A. A. and Morgan, M. W. (Eds), Professional Press, New York, pp 267–300 (1986).
[26] Lloyd, M. Presbyopic contact lens correction – old and new. *J. Br. Contact Lens Assoc.*, **7**(3), 131–136 (1984).
[27] Swarbrick, H., Pye, D., and Holden, B.A. Current Australian contact lens practice. *Aust. J. Optom.*, **68**(1), 2–7 (1985).
[28] McGeehon, M. Survey: Practitioners unhappy with current bifocal lenses. *Contact Lens Forum*, **13**(6), 22–25 (1988).
[29] McMonnies, C.W. Monocular fogging in contact lens practice. *Aust. J. Optom.*, **57**(1), 28–32 (1974).
[30] Lebow, K.A. and Goldberg, J.B. Characteristics of binocular vision for presbyopic patients wearing single vision contact lenses. *J. Am. Optom. Assoc.*, **46**(11), 1116–1123 (1975).
[31] Nolan, J.A. and Nolan, J.J. Driving with monovision. *Optom. Monthly*, **August**, 308–313 (1984).
[32] Tyers, A.G. Aging and the ocular adnexa: a review. *J. Royal Soc. Med.*, **75**, 900–902 (1982).
[33] Kanski, J.J. *The Eye in Systemic Disease*, Butterworths, London (1986).
[34] Miller, S.J.H. *Parson's Diseases of the Eye*, 16th edn, Churchill Livingstone, Edinburgh (1978).
[35] Borish, I.M. and Perrigan, D. Relative movement of lower lid and line of sight from distant to near fixation. *Am. J. Optom. Physiol. Opt.*, **64**(12), 881–887 (1987).
[36] Isenberg, S.J. and Green, B.F. Changes in conjunctival oxygen tension in advancing age. *Critical Care Med.*, **13**(8), 683–685 (1985).
[37] Pyron, M., Wilhelmus, K., and Osato, M. The effect of age on bacterial adherence to human conjunctiva. *ARVO Annual Conference*, **2212–41**, 450 (1990).
[38] Lawrenson, J. personal communication (1991).
[39] Norn, M.S. Tear secretion in normal eyes. *Acta Ophthalmol.*, **43**, 224–231 (1965).
[40] Lamberts, D.W., Foster, C.S., and Perry, H.D. Schirmer test after topical anesthesia and the tear meniscus height in normal eyes. *Arch. Ophthalmol.*, **97**, 1082–1085 (1979).
[41] Millodot, M. The influence of age on the sensitivity of the cornea. *Invest. Ophthalmol. Vis. Sci.*, **16**(3), 240–242 (1977).
[42] Mishima, S., Grasset, A., Klyce, S.D., and Baum, J.L. Determination of tear volume and tear flow. *Invest. Ophthalmol.*, **5**(3), 264–275 (1966).
[43] McGill, J.I., Liakos, G.M., Goulding, N., and Seal, D.V. Normal tear protein profiles and age-related changes. *Br. J. Ophthalmol.*, **68**, 316–320 (1984).
[44] Koetting, R.A. and Andrews, C.E. The relationship of age, keratometry and miscellaneous physiological factors in hydrogel lens wear. *Am. J. Optom.*, **56**(10), 642 (1979).
[45] Port, M.J.A. and Asaria, T.S. The assessment of human tear volume. *J. Br. Contact Lens Assoc.*, **13**(1), 76–82 (1990).
[46] Andres, S., Henriquez, A., Garcia, M.L., Valero, J., and Valls, O. Factors of the precorneal tear film break-up time (BUT) and tolerance of contact lenses. *Int. Contact Lens Clin.*, **14**(3), 103–107 (1987).
[47] Vanley, G.T., Leopold, I.H., and Gregg, T. H. Interpretation of tear film break-up. *Arch. Ophthalmol.*, **95**, 445–448 (1977).
[48] Mengher, L.S., Bron, A.J., Tonge, S. R., and Gilbert, D.J. Effect of fluoroscein instillation on the pre-corneal tear film stability. *Curr. Eye Res.*, **4**(1), 9–12, (1985).
[49] Guillon, J.-P., *Tear Film Structure of the Contact Lens Wearer*, PhD. Thesis, The City University, London (1989).
[50] Mengher, L.S., Bron, A.J., Tonge, S.R., and Gilbert, D.J. A non-invasive instrument for clinical assessment of the pre-corneal tear film stability. *Curr. Eye Res.*, **4**(1), 1–7 (1985).
[51] Guillon, J.-P. Tear film structure and contact lenses, in *The Pre-ocular Tear Film: in Health, Disease and Contact Lens Wear*, Holly F.J. (Ed.), International Tear Film Symposium, Lubbock, Texas, November 1984, Chapter 8 (1986).
[52] Hirji, N., Patel, S., and Callander, M. Human tear film pre-rupture phase time (TP-RPT) – A non-invasive technique for evaluating the pre-corneal tear film using a novel keratometer mire, *Ophthal. Physiol. Opt.*, **9**(2), 139–142 (1989).
[53] Norn, M. Expressibility of meibomian secretion. Relation to age, lipid precorneal film, scales, foam, hair and pigmentation. *Acta Ophthalmol.*, **65**(2), 137–142 (1987).
[54] Norn, M. Meibomian orifices and Marx's line studied by triple vital staining. *Acta Ophthalmol.*, **63**, 698–700 (1985).

[118] Weale, R.A. Notes on the photometric significance of the human crystalline lens. *Vision Res.*, **1**, 183–191 (1961).

[119] Charman, W.N. The retinal image in the human eye, in *Progress in Retinal Research*, Osborne, N and Chader, G. (Eds), pp 1–49 (1983).

[120] Ijspeert, J.K., de Waard, P.W.T., van den Berg, T.J.T.P., and de Jong, P.T.V.M. The intraocular straylight function in 129 healthy volunteers; dependence on angle, age and pigmentation. *Vision Res.*, **30**(5), 699–707 (1990).

[121] Ruddock, K.H. The effect of age upon colour vision: I Response in the receptoral system of the human eye. *Vision Res.*, **5**, 37–45 (1965).

[122] Ruddock, K.H. The effect of age upon colour vision: II Changes with age in light transmission of the ocular media. *Vision Res.*, **5**, 47–58 (1965).

[123] Werner, J.S. Development of scotopic sensitivity and the absorption spectrum of the human ocular media. *J. Opt. Soc. Am.*, **72**(2), 247–258 (1982).

[124] Ruddock, K.H. Light transmission through the ocular media and macular pigment and its significance for psychophysical investigation, in *Handbook of Sensory Physiology, vol. VII (4)*, Jameson, D. and Hurvich, L.M. (Eds), pp 455–469 (1972).

[125] Said, F.S. and Weale, R.A. The variation with age of the spectral transmissivity of the living human crystalline lens. *Gerontologia*, **3**, 213–231 (1959).

[126] Lerman, S. Biophysical aspects of corneal and lenticular transparency. *Curr. Eye Res.*, **3**(1), 3–14 (1984).

[127] Millodot, M. and Newton, I.A. A possible change of refractive index with age and its relevance to chromatic aberration. *Albrecht v. Graefes Arch. klin. exp. Ophthalmol.*, **201**, 159–167 (1976).

[128] Vos, J.J. and Boogard, J. Contribution of the cornea to entoptic scatter. *J. Opt. Soc. Am.*, **53**, 869–873 (1963).

[129] Cox, I. and Holden, B.A. Can vision loss be used as a quantitative assessment of corneal edema. *Int. Contact Lens Clin.*, **17**, 176–180 (1990).

[130] Wolf, E. and Gardiner, J.S. Studies on the scatter of light in the dioptric media of the eye as a basis of visual glare. *Arch. Ophthalmol.*, **74**, 338–345 (1965).

[131] Benefield, D., Stonecipher, K.G., Gordon, R., Morriss, R., Tee, H., and Celdwell, D. Age related changes of refractive index of the human crystalline lens. *ARVO Annual Conference*, **784–24**, 158 (1990).

[132] Weale, R.A. Retinal illumination and age. *Trans. Illum. Eng. Soc. (London)*, **26**(2), 95–100 (1961).

[133] Millodot, M. The influence of age on the chromatic aberration of the eye. *Albrecht v. Graefes Arch. klin. exp. Ophthalmol.*, **198**, 235–243 (1976).

[134] Siew, E.L., Opalecky, D., and Bettelheim, F.A. Light scattering of normal human lens: II Age dependence of the light scattering parameters. *Exp. Eye Res.*, **33**, 603–614 (1981).

[135] Lahm, D., Lee, L.K., and Bettelheim, F.A. Age dependence of freezable and nonfreezable water content of normal human lenses. *Invest. Ophthalmol. Vis. Sci.*, **26**, 1162–1165 (1985).

[136] Vos, J.J. and Bouman, M.A. Contribution of the retina to entoptic scatter. *J. Opt. Soc. Am.*, **54**, 95–100 (1964).

[137] Bone, R.A., Landrum, J.T., Fernandez, L., and Tarsis, S.L. Analysis of the macular pigment by HPLC: Retinal distribution and age study. *Invest. Ophthalmol. Vis. Sci.*, **29**(6), 843–849 (1988).

[138] Kelly, K.L. Observer differences in color-mixture functions studied by means of a pair of metameric grays. *J. Res. Nat. Bur. Stand. (Wash.)*, **60**, 97–103 (1958).

[139] Klein, S.A. and Ho, Z.Y. Multizone bifocal contact lens design, *Current Developments in Optical Engineering and Diffraction Phenomena*, SPIE Vol. 679, pp 25–35 (1986).

[140] Young, G., Grey, C.P., and Papas, E.B. Simultaneous vision bifocal contact lenses: A comparative assessment of the *in vitro* optical performance. *Optom. Vision Sci.*, **67**(5), 339–345 (1990).

[141] Jenkins, T.C.A. Aberrations of the eye and their effects on vision: Part II. *Br. J. Physiol. Opt.*, **20**, 161–201 (1963).

[142] Mordi, J.A. and Adrian, W.K. The influence of age on chromatic aberration of the human eye. *Am. J. Optom. Physiol. Optics*, **62**(12), 864–869 (1985).

[143] Ware, C. Human axial chromatic aberration found not to decline with age. *Graefe's Arch. Clin. Exp. Ophthalmol.*, **218**, 39–41 (1982).

[144] Pease, P.L. and Cooper, D.P. Longitudinal chromatic aberration and age. *Am. J. Optom. Physiol. Opt.*, **63**, 106P (1986).

[145] Howarth, P.A., Zhang, X.X., Bradley, A., Still, D.L., and Thibos, L.N. Does the chromatic aberration of the eye vary with age? *J. Opt. Soc. Am.*, **5**(12), 2087–2092 (1988).

[146] Charman, W.N. The path to presbyopia: straight or crooked? *Ophthal. Physiol. Opt.*, **9**(4), 424–430 (1989).

APPENDIX 2

Reprinted from:

The Journal of the
BRITISH CONTACT LENS
ASSOCIATION

Journal of the British Contact Lens Association, Vol. 15, No. 1, pp 31-43, 1992
Printed in Great Britain

THE AGING EYE AND CONTACT LENSES - A REVIEW OF VISUAL PERFORMANCE

*Russell L. Woods**

(Received 18th March 1991, in revised form 1st July 1991)

Abstract - *Most contact lens practitioners are dealing with an increasing number of otherwise healthy older (presbyopic) patients. Examination of the literature indicates a persistent theme of age-related change which generally becomes significant after the fourth decade. This review, the second of two parts, documents reported age-related changes in visual acuity, contrast sensitivity, stereoacuity, hyperacuity, colour vision, and visual fields. The effects of these various changes on the fitting and wear of contact lenses by older patients are discussed.*

KEY WORDS: Age, aging, review, visual performance, colour vision, visual acuity, contrast sensitivity, hyperacuity, stereopsis, visual fields.

Introduction

AS DISCUSSED in Part 1[1], contact lens fitting is likely to alter slowly, since population demographics in all the western nations indicate a trend towards an aging population. Ocular changes acknowledged to occur with age that may influence contact lens wear include decreased pupil diameter[2-4], decreased tonus of both upper[5,6] and lower eyelids[7], changes to the palpebral aperture[4,5,8], decreased lacrimal secretion[9,10], reduced tear stability[11,12], reduced corneal sensitivity[13,14], increased corneal fragility[15], changes to the ocular media[16-18], and the effects of the increased intake of systemic drugs.[19,20] These aspects have been discussed in the first part of this review.[1] In this, the second part, age-related changes in visual acuity[21] (and the effects of luminance level[22]), contrast sensitivity[23-25], stereoacuity[26,27], glare sensitivity[28,29], colour vision[30-33], and visual field[34] are discussed. All of these factors are of importance when fitting the aging eye. With increased age, physiological considerations alter and visual performance is generally reduced. Particular care must then be taken with contact lens modalities which compromise aspects of visual performance, for example bifocal and monovision contact lenses.

Interest in bifocal contact lenses is increasing in industry, the optical professions, and amongst the public as they become aware of the option through the general and optical media. Contact lens companies are developing and publicising hydrophilic versions of the rigid bifocal contact lenses used by a limited number of experienced practitioners for many years and, recently, diffractive bifocal contact lenses have become available.[35,36] Most contact lens practitioners are wary of fitting bifocal contact lenses because of a general perception of poor success rates and prolonged chair time. Some of these difficulties may be due to a lack of understanding of the differences between younger and older patients, which this article attempts to address.

Further development of bifocal contact lenses, the marketing capabilities of the large companies, and an increased acceptance of contact lenses as a potential modality may lead to an increase in the number of presbyopes fitted with contact lenses. Despite this enormous potential market, recent contact lens surveys[37-39] indicate that only 1% of contact lens patients are fitted with bifocal lenses (consider this against the 'bread-and-butter' presbyopic spectacle provision in an average practice). Slightly more patients are fitted with the alternative presbyopic contact lens option (monovision), the most successful system[37], but considered by many practitioners to be unsatisfactory because of its deleterious effects upon binocular vision.[40-43]

The proportions of contact lens patients who are presbyopic and of presbyopes who wear contact lenses are uncertain, but generally assumed to be small. Despite this, as mentioned above, practitioners are likely to encounter an increasing number and proportion of presbyopic contact lens patients. With this in mind, some of the special visual problems which may influence contact lens fitting and wear are reviewed herein.

Visual Acuity

Visual acuity (VA) at birth is approximately 6/250, improving to 6/6 within the first year and reaching a peak in the third decade, after which there is a gradual decline.[21,44] There is some variability in the published data, much of which can be explained through differences in experimental techniques and subject selection criteria. *Figure 1* contains results from a number of published studies reviewed by Pitts.[21] The reduction in high contrast VA is found to be most pronounced after the fifth decade.

* *BOptom (Hons) MBCO.*

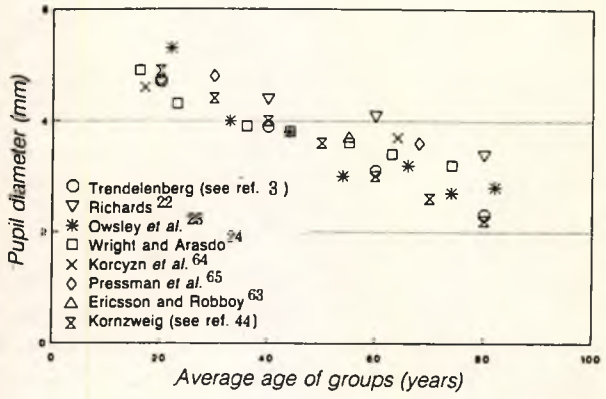

Figure 2. *A compilation of light-adapted pupil diameters, as measured in eight unrelated studies. No attempt has been made to compensate for the illuminance of the eye, which varied from study to study. Luminance levels quoted varied from 6-103cd/m².*

5mm at 20 years of age (*Figure 2*). Thus, at higher light levels, the older pupil is closer to an optimal level than the younger pupil (but visual performance is still reduced). The reverse is true at low light levels. This is complicated by changes which reduce retinal illuminance approximately threefold.[48]

Pupil size influences visual performance with most bifocal lenses. The choice of optimal size for a concentric design bifocal contact lens is pupil size dependent[63,66] and is complicated by on-eye decentration.[67] Calculations which incorporate the Stiles-Crawford effect[51], optical performance measures[67], and high and low contrast VA[51] indicate that the optimal (equal distance and near) pupil coverage by the segment is about 40%. Visual peformance and optimal segment size will vary with the natural luminance-related changes in pupil size. Aspheric or multifocal lenses (e.g., PS45, CALS, PA1) are also pupil size dependent[68,69], such that the effective addition will be governed by the patient's pupil size. The relatively small (3.5mm) diameter of the diffractive zone of Echelon soft bifocal contact lenses could reduce near VA for some patients with larger pupils and under low luminance conditions.

Visual performance with alternating-vision bifocal contact lenses, when fitted well, can be excellent, but is influenced by aspects of the fitting parameters[70,71], and will also vary with pupil size. With increased pupil size a larger section of the near segment will intrude upon the pupil zone during distance viewing. Also, for near viewing with a larger pupil, more lens movement will be necessary to obtain full coverage of the pupil by the near segment. Hodd[72] and Charman and Walsh[73] have demonstrated diagrammatically the image form of certain alternating-vision and simultaneous-vision bifocals.

Summary

With increasing age VA reduces. This reduction is greater for low contrast targets and under low luminance conditions. Neural effects have been suggested to explain these changes, which cannot be fully explained by a reduction in retinal illuminance.[48]

Contrast Sensitivity

Spatial Contrast Sensitivity

A common complaint amongst the elderly is that, though the VA is good, they experience difficulties of reduced illumination and contrast in real life situations. An explanation can be found in the age-related changes in contrast sensitivity (the ability to see faint stripes of varying width). Contrast sensitivity (CS) declines with age for intermediate and high spatial frequencies (i.e., above 3-5cpd) but is retained or only slightly reduced for low spatial frequencies[23-25,74-80] (e.g., *Figure 3a*). This is found over a wide range of test luminances, from 2cd/m² (McGrath and Morrison[75]) to 300cd/m² (Ross *et al.*[80]). Peak CS shifts to a lower spatial frequency with increasing age[23,80,81], as shown in *Figure 3a*. Supra-threshold CS may not

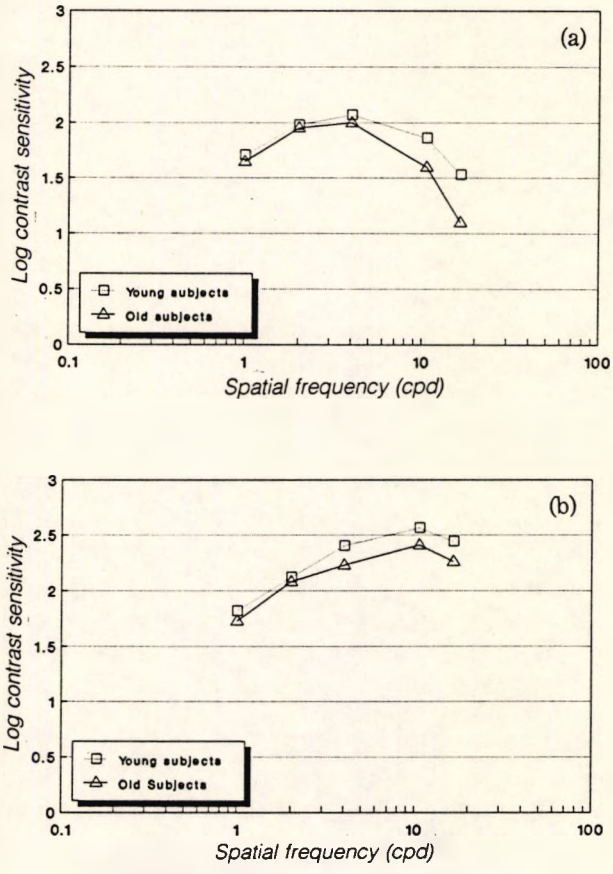

Figure 3. *The contrast sensitivity of 16 old (72 ± 4.3 years) and 16 young (21.5 ± 2.7 years) subjects measured with* (a) *a monitor-based computer system and* (b) *a modified Rodenstock retinometer. The latter technique theoretically bypasses the effects of the optical media and assesses the function of the retinal and neural systems. The former assesses the complete visual system with a conventional technique. The older group displays significantly lower contrast sensitivity, with both tests implying that most of the loss is retinal and neural, with optical factors having only a slight effect at the highest spatial frequency (16.5cpd) (redrawn from Elliott[25]).*

Temporal Contrast Sensitivity

Foveal flicker sensitivity decreases after the fourth decade and this decrease is greatest for higher temporal frequencies (10-45Hz). Differences in retinal illuminance do not[100,101] or only partly[24] explain the loss in sensitivity with increasing age. Temporal sensitivity also varies with spatial frequency, with an age-related loss noted for median but not for very low spatial frequency gratings.[102] Peak temporal sensitivity shifts to a lower temporal frequency with increasing age.[81,103] A reduction in motion enhancement (sensitivity improvement to a moving low spatial frequency grating) for older subjects[23] may be partly explained by the reduction in sensitivity to peripheral objects with reduced pupil size.[104]

Summary

There is a reduction in peak and higher spatial frequency sensitivity and a reduction in higher temporal frequency sensitivity with age. As with VA, the age-related reduction in CS, which remains at higher levels of illumination, cannot be accounted for by senile miosis, changes to the ocular media transparency, and reduced retinal illuminance.[18,25] There may be a neural basis to much of the loss of CS with age.

Contact lens wear is reported both to reduce[105-113] and enhance[49,114] VA and CS. The variability of these findings may be due to manufacturing effects, as the more recent studies show that CS with a contact lens is little different from that without a contact lens. Tinted contact lenses may slightly reduce CS.[115,116] Bifocal contact lenses of various designs result in a decrease in CS and VA[51,56,57,66,117-121], due to the inherent optical compromise of all existing bifocal designs. Typical CS functions for a single subject with a concentric design and with a diffractive bifocal contact lens are shown in *Figures 5a* and *5b*, respectively, and compared to a single vision lens (unpublished data). The age-related decrease in CS is an additional factor often neglected when fitting contact lenses with less than optimal optical performance. The contact lens designer, manufacturer, and fitter may need to exercise care when offering contact lenses to older patients, due to the possible summation of the contact lens induced effects upon age-affected visual performance. It has been suggested by Freeman and Stone[58] that 'patients in the lower quartile of "normal" contrast sensitivy may be contraindicated for all simultaneous vision lenses.' A clinical measure of CS is recommended prior to fitting, as those older patients with reduced CS are likely to be unduly affected by the poor optical performance of simultaneous-vision bifocal contact lenses.

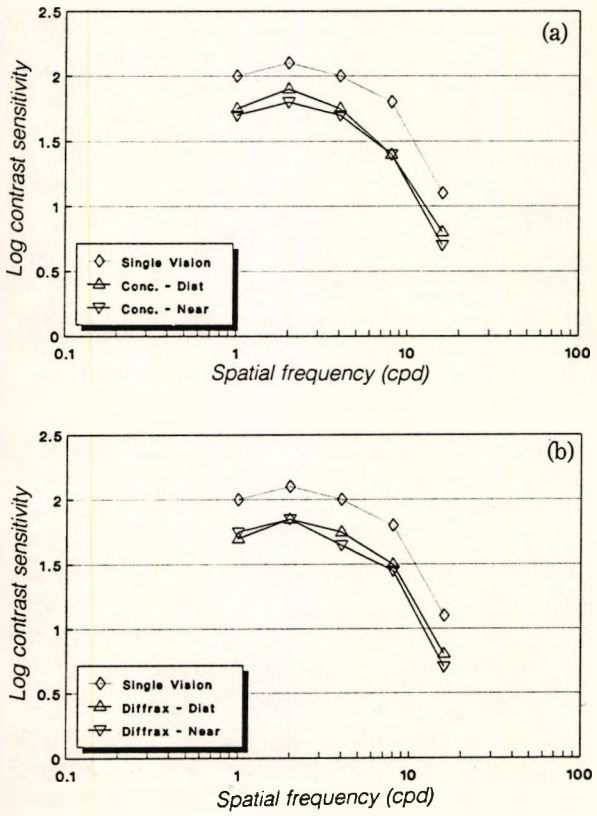

Figure 5. *Distance and near contrast sensitivity functions with* (a) *a near-distance concentric-design bifocal contact lens, and* (b) *a diffractive bifocal contact lens. For comparison the contrast sensitivity function for distance with a single vision contact lens is shown (unpublished data).*

Stereopsis

The human stereoscopic threshold is generally between 2-5 seconds of arc.[122] This varies with exposure duration, implying that the neural processes require about 100msec to operate optimally.[44] There are no conclusive studies of the relationship between stereoacuity and age. Stereoscopic acuity appears to develop during the first decade, though there are difficulties in applying steroacuity tests (or any test) to young children.[123]

Emmes[124] found a reduced mean near stereoacuity (Wirt polaroid vectogram) for presbyopic (over 40 years old) compared to pre-presbyopic subjects. The most comprehensive examination is that of Jani[26], who examined the percentage of failures of (screened) volunteers at an optometric screening with the Diastereo test. Jani reported a slight decrease in the number of failures after the first decade, a relatively constant number (about 5%) up to the fifth decade, after which there was a marked increase in the number of failures. This is shown in *Figure 6*. Bell *et al.*[125], using the Verhoeff stereopter, found a decrease in stereoacuity after 40 years of age in healthy subjects. Conversely, for subjects aged 8-46 years, Hofstetter and Bertsch[126], using the Diastereo test, failed to demonstrate a relationship with age. This is probably due to the restricted age range and the strict selection criteria.

Hoffman *et al.*[127] found a reduced distance stereoacuity, with a Howard-Dohlmann apparatus, for older subjects (mean age 64 years) compared to younger

It is advisable that, upon initial fitting, the patient be made aware of the potential reduction in stereoacuity, and be asked to at least make the first trip in a motor vehicle as a passenger and to take particular care when parking. The effect of reduced stereoperception upon driving ability remains untested in law.[139]

Hyperacuity

Due to concurrent optical changes, it is difficult to determine whether neural processes are involved in the age-related changes in visual function. A number of recent articles have investigated certain hyperacuity tasks[140] that are relatively independent of visual optics[141-143] in an attempt to answer this question. The very resistance of certain hyperacuity tasks to optical degradation implies the involvement of neural mechanisms that are different from those subserving VA, high spatial frequency CS, and stereoacuity.

Oscillatory movement displacement thresholds (detection of movement of vertical bars) increase with increasing age.[144,145]

Odom *et al.*[146] investigated vernier acuity (precision with which an observer can locate one line relative to another) and vernier bias (repeatability of the observer's alignment). They demonstrated no change in vernier thresholds, and an increased vernier bias with age. They suggest that changes in vernier bias may be due to distortion of the retinal substrate. This may relate to the phase differences noted by Walsh and Charman.[147,148] The change in vernier bias was step-like between the fourth and fifth decades, unlike a (progressive) neural degeneration, and Odom *et al.* conclude that this may relate to the onset of presbyopia (though they do not say why this should be so).

The resistance to optical degradation of hyperacuity tasks suggests that the reduction in image quality inherent with simultaneous-vision bifocal contact lenses and with monovision would have no additional effect upon the ability of older patients to perform hyperacuity tasks. Needless to say, if the object is sufficiently blurred then the task will not be performed adequately.

Visual Performance: A Neural Origin?

Evidence for a neural basis for the age changes, rather than the effect being due to deterioration of the optical media and reduced pupil size that induces attenuation of light transmission, comes from a variety of sources. Owsley *et al.*[78] demonstrated that the loss of intermediate and high spatial frequencies was comparable for similarly aged subjects with normal, clear crystalline lenses and those with intraocular lens implants, and both were worse than young adults. This makes the implicit assumption that the modulation transfer function, for higher spatial frequencies, of the intraocular lens is better than that of the aged human crystalline lens, and this has not been tested, as the authors note, though in a different context). The age-related increase in pre-retinal ocular absorption and scatter is principally within the crystalline lens, which undergoes the greatest age-related changes in transparency.[16] The effect of glare, whilst age-related, is not related to spatial frequency, implying that the age-related changes in CS are not related to changes in the optical media.[25,149] The reduction in performance cannot be entirely simulated with filters[79], which produce the estimated reduction in transmission.[48,150] Changes in light transmission of the ocular media and senile miosis are therefore not sufficient to explain the reduction in CS and VA with age.

Interferometric evaluation of grating detection, which bypasses the ocular media, also indicates that the reduction in sensitivity is partly due to neural changes which occur with increasing age.[25,79] This almost certainly relates to the reported displacement and distortion of cell nuclei in the outer nuclear layer, to reduction in density of macular photoreceptors[151,152], and to reduced retinal rod density.[153,154] Retinal ganglion cell axons are also distorted[155] and reduced in number[156,157] with age. This must affect the function and resolution of the visual system. Slightly surprisingly, spatial summation areas under both photopic and scotopic viewing conditions are not reduced with age.[158] Further anatomical changes include a substantial reduction in cortical (macular projection area) cell density found with age.[159] There is obviously a large degree of redundancy in the visual system as, for example, more than half the ganglion cell axons in the optic nerve are damaged before a clinical reduction in visual field occurs.[160] Most visual functions are probably reduced with age, but the ability to detect them is limited by the resolution of the test procedure and other confounding factors (e.g., retinal illuminance).

Thus, a common mechanism almost certainly underlies the age-related changes in visual function, including VA, CS, and stereoacuity.[81] Though reduced retinal illuminance explains some of the decrease, it appears that there is probably also a neural loss with age that accounts for the reduction in VA in apparently healthy older subjects. Weale[150] suggested (with some very broad assumptions) that the decrease in VA is due to neural loss at all levels of the visual system, with a suggested 0.29% loss of cells per year. More recent anatomical studies report higher rates of cell loss.[152,156,159]

The optical performance of modern single-vision lenses[161] will not detrimentally affect the visual performance of older patients. On the other hand, bifocal contact lenses reduce CS, VA, and stereoacuity; hence a clinical measure of CS or low contrast VA is recommended prior to fitting. Stereoacuity (e.g., polaroid vectograms) may be predictive of success with simultaneous-vision bifocal contact lenses. Monovision appears to have only a slight effect upon CS

as a veiling glare. Photopic stress, such as produced by a camera flash, temporarily alters retinal sensitivity and is known as scotomatic glare. There is an increase in both veiling and scotomatic glare sensitivity with age.[28,29]

The ability to identify a target in the presence of veiling glare is greatest in the third decade, and then decreases with age.[28] Wolf[28] noted that the two aphakic eyes measured showed an improvement in target detection over the mean for the age group, but not to levels achieved in younger subjects. The back-scatter from the crystalline lens and vitreous is weakly correlated with age and veiling glare sensitivity.[17] Allen and Vos[18] demonstrated increased light scatter in both the cornea and lens with increasing age, and a reduction in variable contrast VA with increasing age. They felt that back-scatter in the anterior ocular media could not account for the decrease in visual performance. Back-scatter may not be a a measure of the forward-scatter by the anterior ocular media, which actually impairs visual performance. Increased glare with a greater degree of incipient cataract suggests that changes to the lens with age cause much of the glare sensitivity increase with age[28], but there are other contributory factors.

Paulsson and Sjosstrand[149] and Elliott[25] demonstrated that the sensitivity to veiling glare of older subjects was greater than that for younger subjects by a factor of two. Glare sensitivity was greater for lower spatial frequencies for all ages. This correlation with spatial frequency suggests that the age-related changes in CS are not due to increased light scatter by the optical media. Evidence is limited in this area, but this would imply that there is not a neural element in increased glare sensitivity.

Increased sensitivity to veiling glare with age may be due to a variety of factors, which include increased light scatter and absorption by the ocular media (including the retina) and neurological impairment. Senile miosis would be expected to reduce glare through a reduction in oblique rays, but as all the light must pass through the thicker, central portion of the lens, light scatter may increase. The cornea and vitreous alter in absorption and scatter with age and may contribute to glare.[28] Wavelength-dependent Rayleigh scatter, particularly in the crystalline lens, is thought to account for much of the alteration in ocular media absorption with age[175], and may be the cause of increased glare sensitivity with age. Carter[176,177] suggests that veiling glare may be further increased with age by the increased fluorescence of the aging lens, though this has not been demonstrated.

Simultaneous-vision bifocal contact lenses are known to reduce image quality[68] by effectively splitting the light into two separate foci. At least one of these foci will be out of focus for any particular object of regard, and will thus act as a type of glare source, diffusing light across a relatively broad area of the retina. This may then increase the sensitivity to veiling glare of these patients. Some wearers of diffractive bifocal lenses have reported glare associated with monochromatic (e.g., sodium) lights used in many built-up areas and on motorways, and which has lead some wearers to avoid their use for night driving.[35] Edge flare associated with multicurve rigid contact lenses might be expected to be a greater problem for older wearers, but, thankfully, pupils are typically smaller with increasing age. Under conditions of decreased luminance, the near portion of an alternating-vision bifocal contact lenses will cover more of the pupil and may cause increased veiling glare.

Scotomatic glare sensitivity has been shown to increase after the fourth[28], fifth[178], or sixth[179] decade. Reading[29] found that increases in readaptation time can be accounted for partially by the decrease in retinal illumination with age.[48] In a well-controlled study, Elliott and Whitaker[180] found that, even when changes in retinal illuminance were taken into account, scotomatic glare recovery time increased throughout adulthood.

Older patients are more susceptible to glare and, as noted, this can be influenced by certain forms of contact lens. Contact lens practitioners should be aware of these changes, but should be careful that problems with glare are not simply dismissed without an adequate check for potential causes, such as lenticular changes or corneal oedema. Veiling glare due to corneal oedema might be expected to be have a greater effect upon older patients, though they may be less likely to report it if glare is considered normal. Tinted contact lenses prescribed to alleviate photophobia, which may be due to increased glare, could reduce transmission to an extent which may significantly effect visual function under low luminance.[22,47,50,62,98] Glare may be worse in the mornings and evenings, as corneal oedema is often greater then, and the sun is lower in the sky.

Visual Field

Like the other psychophysical functions examined here, age-related changes occur in the visual field. There is a general, continuous shrinkage of the visual field with age, traditionally described as a depression of isopters.[34] The older 'hill of vision' becomes depressed and steeper due to a greater reduction in sensitivity in the periphery than the centre.[181] This may result from senile miosis[104], the increased absorption of the ocular media[48], the location of the upper eyelid[5,8], neuroretinal delays and the decrease in reaction times with age[29], and may be simulated by reducing the oxygen tension of the gas mixtures inspired by younger subjects.[182] As would then be expected, VA reduction in the peripheral visual field is greater for older subjects.[183]

In the simplest evaluation of the extent of the visual field, Burg[184], after screening 17,479 subjects

[27] Woods, R.L. *Stereopsis with Monovision and Two Concentric Bifocal Contact Lens Systems*, presented at the Society of Experimental Optometry, July, 1986.

[28] Wolf, E. Glare and age. *Arch. Ophthalmol.*, **64**, 502-514 (1960).

[29] Reading, V.M. Disability glare and age. *Vision Res.*, **8**, 207-214 (1968).

[30] Lakowski, R. Age and colour vision. *Advance Sci.*, **15**, 231-236 (1958).

[31] Verriest, G., Valdevyvere, R., and Vanderdonck, R. Nouvelles recerches se rapportant a l'influence du sexe et de l'age sue la discrimination chromatique, ainsi qu'a la signification pratique des resultats du test 100 hue de Farnsworth–Munsell. *Rev. Opt. Theor. Instr.*, **42**, 499 (1962).

[32] Verriest, G. Further studies on acquired deficiency of colour vision. *J. Opt. Soc. Am.*, **53**(1), 185-195 (1963).

[33] Ruddock, K.H. The effect of age upon colour vision - I. Response in the receptoral system of the human eye. *Vision Res.*, **5**, 37-45 (1965).

[34] Harrington, D.O. *The Visual Fields*, 4th edn, C.V. Mosby, St Louis, 1976.

[35] Churms, P.W., Freeman, M.H., Melling, V., Stone, J., and Walker, P.J.C. The development and clinical performance of a new diffractive bifocal contact lens. *Optom. Today*, **27**(22), 721-724 (1987).

[36] Young, G. and Papas, E. *Clinical Evaluation of a Soft Diffractive Bifocal Contact Lens*, presented at the American Academy of Optometry Annual Conference, December, 1987.

[37] Lloyd, M., Presbyopic contact lens correction - old and new. *J. Br. Contact Lens Assoc.*, **7**(3), 131-136 (1984).

[38] Swarbrick, H., Pye, D., and Holden, B.A. Current Australian contact lens practice. *Aust. J. Optom.*, **68**(1), 2-7 (1985).

[39] McGeehon, M. Survey: Practitioners unhappy with current bifocal lenses. *Contact Lens Forum*, **13**(6), 22-25 (1988).

[40] McMonnies, C.W. Monocular fogging in contact lens practice. *Aust. J. Optom.*, **57**(1), 28-32 (1974).

[41] Lebow, K.A. and Goldberg, J.B. Characteristics of binocular vision for presbyopic patients wearing single vision contact lenses. *J. Am. Optom. Assoc.*, **46**(11), 1116-1123 (1975).

[42] Nolan, J.A. and Nolan, J.J. Driving with monovision. *Optom. Monthly*, 308-313, August (1984).

[43] Josephson, J.E. The monovision controversy. *J. Br. Contact Lens Assoc.*, **6**(4), 60-65 (1983).

[44] Pitts, D.G. The effects of aging on selected visual functions: dark adaptation, visual acuity, stereopsis, and brightness contrast, in *Aging and Human Visual Function*, Liss, New York, pp 131-159 (1982).

[45] Campbell, F.W. and Green, D.G. Optical and retinal factors affecting visual resolution. *J. Physiol.*, **181**, 576-593 (1965).

[46] Vola, J.L., Cornu, L., Carruel, C., Gastaud, P., and Leid, J. High and low luminance visual acuity in relation to age. *J. Fr. Ophthalmol.*, **6**(5), 473-479 (1983).

[47] Blackwell, O.M. and Blackwell, H.R. Visual performance data for 156 normal observers of various ages. *J. Illum. Eng. Soc.*, **1**, 3-13 (1971).

[48] Weale, R.A. Notes on the photometric significance of the human crystalline lens. *Vision Res.*, **1**, 183-191 (1961).

[49] Guillon, M., Lydon, D.P.M., and Solman, R.T. Effect of target contrast and luminance on soft contact lens and spectacle visual performance. *Curr. Eye Res.*, **7**(7), 635-647 (1988).

[50] Adams, A.J., Wong, L.S., Wong, L., and Gould, B. Visual acuity changes with age: some new perspectives. *Am. J. Optom. Physiol. Opt.*, **65**(5), 403-406 (1988).

[51] Woods, R.L., Port, M.J.A., and Saunders, J.E. Concentric-design bifocal contact lenses: Visual performance. Submitted to *J. Br. Contact Lens Assoc.*

[52] Woodhouse, J.M. The effect of pupil size on grating detection at various contrast levels. *Vision Res.*, **15**, 645-648 (1975).

[53] Regan, D. and Neima, D. Low-contrast lettter charts as a test of visual function. *Opthalmol.*, **90**(10), 1192-1200 (1983).

[54] Holden, B.A. Personal communication (1986).

[55] Brown, B. and Lovie-Kitchin, J. High and low contrast acuity and clinical contrast sensitivity tested in a normal population. *Optom. Visual Sci.*, **66**(7), 467-473 (1989).

[56] Papas, E., Young, G., and Grey, C. *Visual Performance with Soft Diffractive Bifocal Contact Lenses*, presented at the British Contact Lens Association Annual Conference, May, 1988.

[57] Back, A.P., Woods, R.L., and Holden, B.A. The comparative visual performance of monovision and various concentric bifocals. *J. Br. Contact Lens Assoc.*, **10**, 46-47 (1987).

[58] Freeman, M.H. and Stone, J. A new diffractive bifocal contact lens. *J. Br. Contact Lens Assoc.*, **10**,, 15-22 (1987).

[59] Van Meeteren, A. Calculations on the optical modulation transfer function of the human eye for white light. *Optica Acta*, **21**(5), 395-412 (1974).

[60] Campbell, F.W. and Gregory, A.H. Effect of pupil size on visual acuity. *Nature*, **187**, 1121-1123 (1960).

[61] Woodhouse, J.M. and Campbell, F.W. The role of the pupil light reflex in aiding adaptation to the dark. *Vision Res.*, **15**, 649-653 (1975).

[62] Fletcher, R.J. and Nisted, M. A study of coloured contact lenses and their performance. *Ophthal. Optician*, **3**, 1151-1154, 1161-1163, 1203-1206, 1212-1213 (1963).

[63] Erickson, P. and Robboy, M. Performance of a hydrophilic concentric bifocal contact lens. *Am. J. Optom. Physiol. Opt.*, **62**(10), 702-708 (1985).

[64] Korczyn, A.D., Laor, N., and Nemet, P. Sympathetic pupillary tone in old age. *Arch. Ophthalmol.*, **94**, 1905-1906 (1976).

[65] Pressman, M.R., DiPhillipo, M.A., and Fry, J.M. Senile miosis: The possible contribution of disordered sleep and daytime sleepiness. *J. Gerontol.*, **41**(5), 629-634 (1986).

[66] Jones, B. and Lowther, G.E. The effect of near zone size of a center-near zone hydrogel contact lens bifocal on visual acuity. *Int. Contact Lens Clin.*, **16**(3), 87-93 (1989).

[67] Woods, R.L., Saunders, J.E., and Port, M.J.A. Concentric-design bifocal contact lenses - Optical performance. Submitted to *J. Br. Contact Lens Assoc.*

[68] Young, G., Grey, C.P., and Papas, E.B. Simultaneous vision bifocal contact lenses: A comparative assessment of the *in vitro* optical performance. *Optometry Vision Sci.*, **67**(5), 339-345 (1990).

[69] Charman, W.N. and Saunders, B. Theoretical and practical factors influencing the optical performance of contact lenses for the presbyope. *J. Br. Contact Lens. Assoc.*, **13**, 67-75 (1990).

[70] Robboy, M. and Erickson, P. Performance comparison of current hydrophilic alternating vision bifocal contact lenses. *Int. Contact Lens Clin.*, **14**(6), 237-243 (1987).

[71] Ames, K.S., Erickson, P., Godio, L., and Medici, L. Factors influencing vision with rigid gas permeable bifocals. *Optom. Vis. Sci.*, **66**, 92-97 (1989).

[72] Hodd, F.A.B. A design study of bifocal contact lenses. *Ophthal. Optician*, **9**(9), 450-469; **9**(11), 588-600; **9**(12), 644-653; **9**(13), 700-702 (1969).

[73] Charman, W.N. and Walsh, G. Retinal image quality with different designs of bifocal contact lens. *J. Br. Contact Lens Assoc.*, **9**, 13-19 (1986).

[74] Derefeldt, G., Lennerstrand, G., and Lundh, B. Age variations in normal human contrast sensitivity. *Acta Ophthalmol.*, **57**, 679-690 (1979).

[75] McGrath, C. and Morrison, J.D. The effects of age on spatial frequency perception in human subjects. *Q. J. Exp. Physiol.*, **66**, 253-261 (1981).

[76] Kline, D.W., Schieber, F., Abusamra, L.C., and Coyne, A.C. Age, the eye, and the visual channels: Contrast sensitivity and response speed. *J. Gerontol.*, **38**(2), 211-216 (1983).

[77] Ginsburg, A.P. A new contrast sensitivity vision test chart. *Am. J. Optom. Physiol. Optics*, **61**(6), 403-407 (1984).

[78] Owsley, C., Gardner, T., Sekuler, R., and Lieberman, H. Role of the crystalline lens in the spatial vision loss of the elderly. *Invest. Opthalmol. Visual Sci.*, **26**, 1165-1170 (1985).

[79] Morrison, J.D. and McGrath, C. Assessment of the optical contributions to the age-related deterioration in vision. *J. Exp. Physiol.*, **70**, 249-269 (1985).

[80] Ross, J.E., Clarke, D.D., and Bron, A.J. Effect of age on contrast sensitivity function: uniocular and binocular findings. *Br. J. Ophthalmol.*, **69**(1), 51-56 (1985).

[81] Greene, H.A. and Madden, D.J. Adult age differences in visual acuity, stereopsis, and contrast sensitivity. *Am. J. Optom. Physiol. Optics*, **64**(10), 749-753 (1987).

[82] Tulunay-Keesey, U., Ver Hoeve, J.N., and Terkla-McGrane, C. Threshold and suprathreshold spatiotemporal response throughout adulthood. *J. Opt. Soc. Am. A*, **5**(12), 2191-2219 (1988).

[83] Beard, B.L., Neufeld, S., and Yager, D. Age-related reductions in sensitivity are not evident at suprathreshold contrast levels. *ARVO Annual Conference*, 51-23 (1990).

[84] Van Nes, F.L. and Bouman, M.A. Spatial modulation transfer in the human eye. *J. Opt. Soc. Am.*, **57**(3), 401-406 (1967).

141 Stigmar, G. Blurred visual stimuli: II. The effect of blurred visual stimuli on vernier and stereoacuity. *Acta Ophthalmol.*, **49**, 364 (1971).

142 Williams, R.A., Enoch, J.M., and Essock, E.A. The resistance of selected hyperacuity configuration of retinal image degradation. *Invest. Ophthalmol. Visual Sci.*, **25**, 389 (1984).

143 Whitaker, D. and Buckingham, T. Theory and evidence for a clincial hyperacuity test. *Ophthal. Physiol. Opt.*, **7**(4), 431-435 (1987).

144 Buckingham, T., Whitaker, D., and Banford, D. Movement in decline? Oscillatory movement displacement thresholds increase with ageing. *Ophthal. Physiol. Opt.*, **7**(4), 411-413 (1987).

145 Scheiber, F., Hiris, E., White, J., Williams, M., and Brannan, J. Assessing age-differences in motion perception using simple oscillatory displacement versus random dot cinematography. *ARVO Annual Conference*, **1746-9**, 355 (1990).

146 Odom, J.V., Vasquez, R.J., Schwartz, T.L., and Linberg, J.V. Adult vernier thresholds do not increase with age; Vernier bias does. *Invest. Ophthalmol. Visual Sci.*, **30**(5), 1004-1008 (1989).

147 Walsh, G. and Charman, W.N. Measurement of the axial wavefront aberration of the human eye. *Ophthal. Physiol. Opt.*, **5**(1), 23-31 (1985).

148 Walsh, G. and Charman, W.N. The effect of defocus on the contrast and phase of the retinal image of a sinusoidal grating. *Ophthal. Physiol. Opt.*, **9**(4), 398-404 (1989).

149 Paulsson, L.-E. and Sjostrand, J. Contrast sensitivity in the presence of a glare source. *Invest. Ophthalmol. Visual Sci.*, **19**(4), 401-406 (1980).

150 Weale, R.A. Senile changes in visual acuity. *Trans. Ophthalmol. Soc. UK*, **95**, 36-38 (1975).

151 Marshall, J., Grindle, J., Ansell, P.L., and Borwein, B. Convolution in human rods: an ageing process. *Br. J. Ophthalmol.*, **63**, 181-187 (1979).

152 Gartner, S. and Henkind, P., Aging and degeneration of the human macula. 1. Outer nuclear layer and photoreceptors. *Br. J. Ophthalmol.*, **65**, 23-28 (1981).

153 Curcio, C.A., Allen, K.A., and Kalina, R.E. Reorganization of the human photoreceptor mosaic following age-related rod loss. *ARVO Annual Conference*, **189-12**, 38 (1990).

154 Gao, H., Rayborn, M.E., Myers, K.E., and Hollyfield, J.G. Differential loss of neurons during aging of human retina. *ARVO Annual Conference*, **1754-17**, 357 (1990).

155 Vrabec, F. Senile changes in the ganglion cells of the human retina. *Br. J. Ophthalmol.*, **49**, 561-572 (1965).

156 Dolman, C.L., McCormick, A.Q., and Drance, S.M. Aging of the optic nerve. *Arch. Ophthalmol.*, **98**, 2052-2058 (1980).

157 Balazsi, A.G., Rootman, J., Drance, S.M., Schulzer, M., and Douglas, G.R. The effect of age on the nerve fibre population of the human optic nerve. *Am. J. Ophthalmol.*, **97**, 760-766 (1984).

158 Brown, B., Peterken, K.J., Bowman, K.J., and Crassini, B. Spatial summation in young and elderly observers. *Ophthal. Physiol. Opt.*, **9**(3), 310-313 (1989).

159 Devaney, K.O. and Johnson, H.A. Neuron loss in the aging visual cortex of man. *J. Gerontol.*, **35**(6), 836-841 (1980).

160 Quigley, H.A., Addicks, E.M., and Green, W.R. Optic nerve damage in human glaucoma. III. Quantitative correlation of nerve fiber loss and visual field defect in glaucoma, ischemic neuropathy, papilledema, and toxic neuropathy. *Arch. Ophthalmol.*, **100**, 135-146 (1982).

161 Grey, C.P. and Sheridan, M. The modulation transfer function of contact lenses. *J. Br. Contact Lens Assoc.*, **11**(1), 9-17 (1988).

162 Wright, W.D. *Researches in Normal and Defective Colour Vision*, Henry Kimpton, London (1946).

163 Ruddock, K.H. The effect of age upon colour vision - II. Changes with age in light transmission of the ocular media, *Vision Res.*, **5**, 47-58 (1965).

164 Pinckers, A. Colour vision and age. *Ophthalmologica*, **181**, 23-30 (1980).

165 Knoblauch, K., Saunders, F., Kusuda, M., Hynes, R., Podgor, M., Higgins, K.E., and deMonasterio, F.M. Age and luminance effects in the Farnsworth-Munsell 100-hue test. *Appl. Opt.*, **26**, 1441-1448 (1987).

166 Helve, J. and Krause, U. The influence of age on performance in the panel D-15 colour vision test. *Acta Ophthalmol.*, **50**(6), 896-900 (1972).

167 Werner, J.S., Peterzell, D.H., and Scheetz, A.J. Light, vision and aging. *Optom. Vision Sci.*, **67**(3), 214-229 (1990).

168 Said, F.S. and Weale, R.A. The variation with age of the spectral transmission of the living human crystalline lens. *Gerontologica*, **3**, 213-231 (1959).

169 Weale, R.A. Aging and vision. *Vision Res.*, **26**(9), 1507-1512 (1986).

170 Birch, J., Chisolm, I.A., Kinnear, P., Marre, M., Pinckers, A.J.L.G., Pokorny, J., Smith, V.C., and Verriest, G. Acquired color vision defects. In *Congenital and Acquired Color Vision Defects*. Pokorny, J., Smith, V.C., Verriest, G., and Pinckers, A.J.L.G. (eds), Grune & Stratton, pp 243-339 (1979).

171 Jurkus, J.M., Lee, D.Y., Bordwell, W., and Ruggerio, R. The effect of tinted soft lenses on colour discrimination. *Int. Eyecare*, **1**(5), 371-375 (1985).

172 La Bissoniere, P.E. The x-chrom lens. *Int. Contact Lens Clin.*, **1**(4), 48-55 (1974).

173 Stone J. Special types of contact lenses and their uses, in *Contact Lenses*, 3rd edn, Phillips, A.J. and Stone, J. (eds), Butterworths, London, pp 870-901 (1989).

174 Bell, L., Troland, L.T., and Verhoeff, F.H. Report of the subcommittee on glare of the research committee. *Trans. Illum. Engin. Soc.*, **17**, 734ff (1922).

175 Ruddock, K.H. Light transmission through the ocular media and macular pigment and its significance for psychophysical investigation. *Handbook of Sensory Physiology*, Jameson, D. and Hurvich, L.M. (eds), pp 455-469 (1972).

176 Carter, J.H. The effects of aging on selected visual functions: colour vision, glare sensitivity, field of vision, and accommodation. In *Aging and Human Visual Function*, Liss, New York, pp 121-130 (1982).

177 Carter, J.H. Predictable visual responses to increasing age. *J. Am. Optom. Assoc.*, **53**(1), 31-36 (1982).

178 Forsius, H., Krause, U., and Erickson, A.W. Dazzling test in central serous retinopathy. *Acta Ophthalmol.*, **41**, 25-32 (1963).

179 Collins, M. The onset of prolonged glare recovery with age. *Ophthal. Physiol. Opt.*, **9**(4), 368-371 (1989).

180 Elliott, D.B. and Whitaker, D. Decline in retinal function with age. *ARVO Annual Conference*, **1755-18**, 357 (1990).

181 Collin, H.B., Han, C., and Khor, P.C. Age changes in the visual field using the Hunphrey visual field analyser. *Clin. Exp. Optom.*, **71**(6), 174-178 (1988).

182 Wolf, E. and Nadroski, A.S. Extent of the visual field. Changes with age and oxygen tension. *Arch Ophthalmol*, **86**, 637-642 (1971).

183 Collins, M.J. Peripheral visual acuity and age. *Ophthal. Physiol. Opt.*, **9**(3), 314-316 (1989).

184 Burg, A. Lateral visual field as related to age and sex, *J. App. Psychol.*, **52**(1), 10-15 (1968).

185 Drance, S.M., Berry, V., and Hughes, A. Studies on the effects of age on the central and peripheral isopters of the visual field in normal subjects. *Am. J. Ophthalmol.*, **63**, 1667-1672 (1967).

186 Williams, T.D. Aging and the central visual field area. *Am. J. Optom. Physiol. Opt.*, **60**(11), 888-891 (1983).

187 Haas, A., Flammer, J. and Schneider, U. Influence of age on the visual fields of normal subjects. *Am. J. Ophthalmol.*, **101**, 199-203 (1986).

188 Jaffe, G.J., Alvarado, J.A. and Juster, R.P. Age-related changes of the visual field. *Arch. Ophthalmol.*, **104**, 1021-1025 (1986).

189 Ball, K.K., Beard, B.L., Roenker, D.L., Miller, R.L. and Griggs, D.S. Age and visual search: expanding the useful field of view. *J. Opt. Soc. Am. A*, **5**(12), 2210-2219 (1988).

190 Atchison, D.A. Effect of defocus on visual field measurement. *Ophthal. Physiol. Opt.*, **7**(3), 259-266 (1988).

191 Collins, M.J., Brown, B., Verney, S.J., Makras, M. and Bowman, K.J. Peripheral visual acuity with monovision and other contact lens corrections for presbyopia. *Optom. Vis. Sci.*, **66**, 370-374 (1989).

APPENDIX 3

Article submitted to *Clinical Vision Sciences.*

A COMPARISON OF PSYCHOMETRIC METHODS FOR MEASURING THE CONTRAST SENSITIVITY OF EXPERIENCED OBSERVERS

by

Russell L. Woods and W. David Thomson

SUMMARY

(1) Contrast sensitivity functions were obtained for ten healthy, trained and experienced observers using five different psychometric methods, on two occasions. The methods included the method of constant stimuli, adaptive probit estimation, single staircase, and two implementations of the ascending method of limits.
(2) The absolute values and the shape of the contrast sensitivity functions were found to be strongly influenced by psychometric method.
(3) Inter and intra-subject variances were similar for each method.
(4) These results suggest that there may be little advantage to be gained by using complex (and often time consuming) psychometric methods in situations where inter and intra-subject differences are of principal interest.
(5) Caution is required in extending these conclusions to situations where inexperienced observers are to be tested.

INTRODUCTION

Measurements of contrast sensitivity are being used increasingly in vision research and for the clinical assessment of visual function. This has led to a proliferation of instrumentation and techniques for measuring contrast sensitivity.

The choice of a psychometric method for measuring contrast sensitivity will depend on a number of factors (footnote a). In a clinical setting the duration of the test and the repeatability may be most important. In a research environment other factors such as the inferred validity may be the overriding consideration. The difficulty of the task and the dependence of the method on the subject's decision criteria must be taken into account. In some cases there may be some flexibility in the psychometric method selected, in others, the choice of method may be constrained by the hardware, software or nature of the test.

Many early investigations of contrast sensitivity employed the method of adjustment (e.g. Westheimer, 1960; Campbell and Green, 1965; Campbell and Robson, 1968). In these studies the subjects were typically given direct control of the grating contrast and instructed to adjust the contrast until the grating was seen / not seen. The mean of several such settings was taken as the contrast sensitivity. This method has the advantages of being simple and fast and it appeared to produce reliable results with practiced observers. However, thresholds obtained in this way are prone to variability introduced by differences between the criteria for detection adopted by the subjects and differences in the adjustment strategy. Furthermore, differences between strategies adopted by subjects to determine the threshold may lead to different levels of adaptation to the stimulus.

The method of limits has proved quite popular in both the clinical and laboratory setting (Arden and Jacobson, 1978; Ginsburg and Cannon, 1983; Cox, 1986). The

grating contrast is first increased from below threshold with subjects instructed to respond when the grating is detected, then decreased from above threshold until the grating is no longer detected. The method is often restricted to an ascending limit (increasing contrast) to avoid spatial frequency adaptation effects (Kelly, 1972) and after images produced by the supra-threshold stimuli (Ginsburg and Cannon, 1983). This technique has the advantage of being quick and simple and the procedure is claimed to be suitable for use with inexperienced observers (Arden and Jacobson, 1978; Ginsburg and Cannon, 1983) and experienced observers (Cox, 1986). However, measurements obtained by this method are strongly affected by the criteria for detection adopted by the subject (Vaegan and Halliday, 1982; Reeves et al, 1988) and may be influenced by the examiner (Reeves et al, 1988).

The staircase method in its various forms (Dixon and Mood, 1948; Cornsweet, 1962), has been used extensively for the measurement of contrast sensitivity (Kelly and Savoie, 1973; Higgins et al, 1984). In its simplest form, each discrete stimulus presentation is determined by the response to the preceding presentation with the stimulus level incremented or decremented according to a negative or positive response respectively. Many adaptations of the basic staircase procedure have been described including interweaved staircases (Cornsweet, 1962), various algorithms governing the response requirements for a reversal (Rose et al, 1970) and the application of Two Alternative Forced Choice responses (Kelly and Savoie, 1973; Higgins et al, 1984).

Conventional constant stimuli procedures involve the presentation of a fixed number of randomly-ordered stimuli of pre-determined contrast levels (Guilford, 1954). Multiple presentations at each contrast level allow the construction of a "Probability of seeing" curve for a particular spatial frequency which can be analysed in a variety of ways to provide an estimate of the threshold and the variance of the responses. Phenomenal reporting (i.e. Yes/No) or true forced choice responses may be employed. The method of constant stimuli in its various forms is widely regarded as having greatest inferred validity (footnote b) and to be the most repeatable psychometric method (Blackwell, 1952; Guilford, 1954) but the large number of responses required makes the procedure very time-consuming.

In general, there is a trade-off between repeatability and speed, with the experimenter making a form of cost-benefit analysis of various psychometric techniques. Relative weightings given to these factors may vary according to the experimental requirements, and are almost certainly different in the clinical situation.

The introduction of adaptive procedures which are claimed by their designers to provide results comparable to conventional constant stimuli procedures but requiring fewer presentations, provide an attractive alternative. These methods include "Parameter Estimation by Sequential Testing" (PEST: Taylor and Creelman, 1967), a Bayesian method (QUEST: Watson and Pelli, 1983), Adaptive Probit Estimation (APE: Watt and Andrews, 1981) and a Maximum Liklihood approach (Hall, 1981)

Psychometric method has been demonstrated to have an influence on measurements of contrast sensitivity with experienced observers (Kelly and Savoie, 1973) and inexperienced observers (Vaegan and Halliday, 1982; Ginsburg and Cannon, 1983; Higgins et al, 1984; Long and Tuck, 1988). In earlier comparative studies results with the method of adjustment have been shown to be more repeatable and to have a lower inter-subject variance than results obtained with the von Bekesy procedure (Ginsburg and Cannon, 1983; Long and Tuck, 1988); various methods of limits have proved better than the method of adjustment (Vaegan and Halliday, 1982; Ginsburg and Cannon, 1983; Corwin and Richman, 1986); and a clinical application of a forced choice procedure has proved superior to a method of limits (Vaegan and Halliday, 1982). Both Kelly and Savoie (1973) with experienced observers and Higgins et al (1984) with inexperienced observers reported significant shifts in decision criteria with a method of adjustment but not with a forced choice staircase procedure. In both studies results with the forced choice staircase procedure were more repeatable and the inter-subject variance was smaller than results obtained by the method of adjustment. Contrast sensitivity measurements have also been demonstrated to be subject to variable practice effects (Vaegan and Halliday, 1982; Kelly and Tomlinson, 1987; Long and Penn, 1987); to vary with the test (Vaegan and Halliday, 1982; Corwin and Richman, 1986; Long and Tuck, 1988). Clinical investigations of contrast sensitivity have reported larger intra-subject and inter-subject variance of

measurements with non-normal observers (Vaegan and Halliday, 1982; Reeves et al, 1987, Wood et al, 1988).

The aim of this study was to investigate the effect of psychometric method on contrast sensitivity measurements. This may assist with the selection of the most suitable psychometric method for particular situations, and aid the comparison of data obtained using different methods.

The five psychophysical methods investigated represent a purposefully selected cross-section of psychometric methods which have been used commonly in studies of contrast sensitivity. These were:

1) Method Of Constant Stimuli (MOCS) with Two Alternative Forced Choice (2AFC) responses
2) Adaptive Probit Estimation (APE) (Watt and Andrews, 1981)
3) Single Staircase (e.g. Cornsweet, 1962)
4) Discrete Ascending Method of Limits (DAML)
5) Continuous Ascending Method of Limits (CAML) (e.g. Ginsburg and Cannon, 1983)

Problems with this approach are firstly, the exact rules governing the psychometric procedures referred to in the literature are seldom made explicit and secondly, there are wide variations in the implementation of procedures between studies. It was beyond the scope of the present study to investigate the effects of these differences in implementation of individual procedures, and the approach that has been adopted has been to use a "typical" method for each procedure. Extrapolation of this data for a variation in the implementation of a procedure requires caution.

METHODS

Subjects

Ten colleagues, aged between 22 and 60 years (average 35 years), acted as subjects for the study. All subjects were experienced at making psychophysical judgements. The procedures controlling presentation for each psychometric method were fully explained to each subject, and each subject attended at least one practice session prior to the main study so that they were completely familiar with each method. Subjects had no known visual dysfunction.

Apparatus

Sinusoidal gratings were presented on a high resolution monochrome monitor (Manitron model VLR 1593/80) with a P4 (white) phosphor, producing 800 non-interlaced vertical scan lines at a field scan frequency of 100Hz. The monitor was driven by a pattern generator (Millipede Prisma VR1000) interfaced to an IBM AT personal computer. The pattern generator provided 10 bit control of screen luminance and allowed between-field presentation of gratings.

The monitor was calibrated with a Lichtmesstechnik (LMT L1003) light meter. Potential error in contrast produced by changes in screen luminance over time, was reduced to less than 0.006 log contrast units. This was achieved by displaying a blank screen at the mean luminance used during the experiment (50 cd/m^2), for two hours prior to the commencement of each session.

The monitor screen was masked to give a circular field subtending a visual angle of 11.5 degrees from the viewing distance of 1 metre. The mean luminance of the display was 50 cd/m^2 and the luminance and colour of the surround were matched approximately to the screen. Head movements were restrained by a chin and forehead rest and subjects were instructed to fixate a small target at the centre of the screen. Tests were carried out binocularly and appropriate refractive corrections were provided where necessary.

According to the procedures detailed below, subjects were required to respond to the sinusoidal gratings presented by pressing one of two buttons. The total duration of each trial, from the first to the last presentation, was recorded by the computer.

Psychometric Methods

The temporal envelope for the presentation of the grating contrast has been shown to affect contrast sensitivity measurements particularly for low spatial frequency gratings (Kelly, 1971; Green, 1981). Various temporal envelopes including ramps, Gaussians, pulses and continuous presentation have been employed in studies described in the literature (Kelly, 1971, 1972; Tulunay-Keesey and Bennis, 1979). To some extent the choice of temporal envelope depends on the aspect of visual function under investigation. However, in some cases the temporal envelope is constrained by the hardware, software, methodology or a combination thereof.

For procedures 1 to 4, the contrast of the grating was pulsed for one second (i.e. stepped from zero to the test contrast). For procedure 5 (DAML) the contrast was slowly ramped in logarithmic increments from below the contrast threshold. Other aspects of the various procedures are detailed below, and summarised in *Table 1.*

1) Method of constant stimuli (MOCS)
This procedure was implemented in five blocks with a single spatial frequency tested in each block (in accordance with the recommendations of Blackwell (1952) for optimizing inferred validity and repeatability) (footnote c). Theoretically, the repeatability of the procedure increases with the number of contrast levels tested and the number of presentations at each contrast. However, a series of pilot studies indicated that, in practice, an excessive number of presentations resulted in observer fatigue which actually reduced repeatability. The optimum number of presentations within a block was found to be approximately one hundred. Therefore, five contrast levels, distributed in equal logarithmic steps about the predicted contrast sensitivity, were selected, and gratings at each contrast level were presented twenty times making a total of 100 presentations per spatial frequency. After a suitable rest period the next spatial frequency was tested. The entire procedure therefore involved a total of five hundred presentations. To minimise order effects, a Latin square was used to allocate the order of spatial frequency presentation for each subject.

In each case the test grating was presented in one of two temporal intervals indicated by appropriate audible cues. The subject was required to indicate which interval the grating was most likely to have occurred. Feedback provided in the form of an audible tone indicated if the response was correct (Blackwell, 1952). This "Two-alternative- forced-choice" procedure is theoretically criteria-free as no decision is made by the subject about the visibility or otherwise of the grating.

The data in the form of a proportion correct was corrected for "guessing" by the equation:

$$p = (p' - c) \; / \; (1 - c)$$

where p = corrected proportion, p' = raw proportion, and c = proportion of chance (0.5). Contrast sensitivities and standard deviations, were extracted from the psychometric function by Probit Analysis (Finney, 1952).

2) Adaptive Probit Estimation (APE)
Adaptive Probit Estimation is based on an algorithm which controls stimulus magnitude (contrast) and aims to estimate the psychometric function with maximum statistical efficiency (Watt and Andrews, 1981). The algorithm was arranged to make a total of 50 presentations for each spatial frequency and to use 10 contrast levels distributed in equal logarithmic steps about the estimated contrast sensitivity.

In this implementation, each test grating was presented after an audible cue, and the subject was required to indicate whether the grating was seen or not seen. The APE algorithm performed a rapid approximate probit analysis of the most recent set of responses and used this information to obtain a running estimate of the contrast sensitivity. The next stimulus contrast to be tested was randomly selected from the set of contrasts which bracketed the current estimate of contrast sensitivity. On completion of the trial a full probit analysis was performed to provide an estimate of the contrast sensitivity and the associated standard deviation.

Contrast sensitivity at each spatial frequency was measured in five separate blocks, and the order of presentation of the spatial frequencies was determined by another Latin square.

PSYCHOMETRIC METHOD	RESPONSE	STIMULUS PRESENTATION			ANALYSIS
MOCS	temporal 2 a.f.c.	dual discrete	block	500	Probit
APE	Yes / No	discrete	block	250	Probit
Staircase	Yes / No	discrete	random	70 -100	average
DAML	visible	discrete	random	20	average
CAML	visible	ramped	random	20	average

Table 1 : A summary of the experimental psychometric methods and modes of data analysis employed in this study.

3) Single Staircase
The staircase procedure is a method of serial exploration where the magnitude of the stimulus (contrast) is varied according to the response(s) to preceding stimulus level(s).

In this implementation, the five spatial frequencies were presented in a random interleaved staircase procedure. Commencing at a random contrast level, contrast was decremented or incremented depending on whether the preceding presentation at that spatial frequency was seen or not seen respectively. Contrast was incremented or decremented in logarithmic steps and the stepsize was reduced each time a reversal in response was recorded (i.e. a change from "seen" to "not seen" or vice versa). This procedure was repeated until a predetermined minimum stepsize (0.1 log contrast units) was reached. Thereafter, the stepsize was maintained constant and the contrast sensitivity was taken as the mean of the contrasts at the next four response reversals. The data was also analysed according to the technique of Dixon and Mood (1948) in the form of the frequency of response distribution, giving an alternative estimate of the contrast sensitivity and the standard deviation.

4) Discrete Ascending Method of Limits (DAML)
This procedure is a novel variation on the ascending method of limits. Following an audible tone and a random delay, a series of discrete (pulsed) presentations were made, the contrast of the grating being incremented in logarithmic steps (at a rate of 0.05 log contrast units per second) for successive presentations, from a sub-contrast threshold level until the subject responded. The five spatial frequencies were presented in a random sequence and the contrast sensitivity for each spatial frequency was taken as the mean of four contrast settings at which the subject responded.

As the grating contrast was oscillated between zero and an increasing series of test contrasts the temporal envelope matched that employed for the other psychometric methods (1-3).

5) Continuous Ascending Method of Limits (CAML)
This ascending method of limits with continuous presentation of the stimulus has been called a Method of Increasing Contrast (Ginsburg and Cannon, 1983) and has been widely employed in previous studies of contrast sensitivity. CAML was identical to DAML in all respects except for the temporal envelope for presentation.

Following an audible tone and a random delay, the contrast of the grating was continuously incremented in logarithmic steps at a rate of 0.05 log contrast units per second, from a sub-contrast threshold level until the subject responded. The five spatial frequencies were presented in a random sequence and the contrast sensitivity for each spatial frequency was taken as the mean of four contrast settings at which the subject responded.

Experimental Design - general considerations

Overall order effects were minimised by employing two balanced 5 x 5 Latin squares (five psychometric procedures applied to ten subjects). Contrast sensitivity was determined for five spatial frequencies (0.3, 0.9, 2.7, 8.1, 24.3 c.p.d.) using each psychometric method.

The MOCS and APE procedures involved presenting the spatial frequencies in blocks. The order of presentation of the blocks was determined by independent Latin squares.

Spatial frequencies were randomly interleaved for the other three techniques (Staircase, DAML and CAML). To avoid problems with spatial frequency uncertainty (Davis and Graham, 1981; Cohn and Lasley, 1984), the tone which acknowledged a response was also used to indicate the spatial frequency of the next presentation. This was achieved by matching the pitch of the tone to spatial frequency (i.e. low pitch - low spatial frequency, high pitch - high spatial frequency etc.). With practice, subjects could reliably match tones to spatial frequencies. Pilot studies indicated that this simple procedure increased contrast sensitivity and improved repeatability.

The five procedures were always performed during a single session (lasting between 1½ and 2½ hours) during the afternoon. The five procedures were then repeated within a period of one week.

RESULTS

The mean duration of the five psychometric methods are shown in *Figure 1*. These values are for procedure time alone and do not include the time required to set appropriate starting contrast levels for the MOCS and APE procedures, nor rest periods between blocks for MOCS and APE procedures, nor the time required to perform an analysis of the MOCS data in order to determine the contrast sensitivity at each spatial frequency. Inclusion of this time would increase the time required to achieve a full assessment to approximately 1 hour for MOCS and 20 minutes for APE.

Contrast sensitivity functions for each subject and procedure were of the form typically described for the conditions of the test (Howell and Hess, 1978; Kelly, 1971). Mean data for the ten subjects are shown for each psychometric method in *Figure 2*. Contrast sensitivities for the staircase procedure calculated by averaging did not differ from those determined by the method of Dixon and Mood (1948) by more than 0.02 log contrast units.

Intra-test Variability

The variance of the mean contrast sensitivity for the ten subjects at each spatial frequency was similar for the five methods (*Figure 3*). Further, with all methods, the variance was greatest at the highest spatial frequency tested (24.3 c.p.d.) (*Figure 3*). Contrast sensitivity at high spatial frequencies has been shown to reduce with increasing age, and therefore the greater variance at the highest spatial frequency may be attributable to the age range of the subjects (Owsley et al, 1983; Elliott, 1987).

Estimates of the standard deviation of individual responses (i.e. a measure of the variability of the raw data) varied widely between psychometric methods. MOCS and APE returned the largest standard deviations at each spatial frequency. However, the validity of the standard deviations calculated for the other methods is questionable because a) standard deviations for CAML and DAML procedures were based on only four measurements and b) estimates of standard deviation for the Staircase method were calculated by the method described by Dixon and Mood (1948), which may not be valid for such small numbers of responses (Finney, 1952). Hence these "internally" calculated estimates of variance may be of limited value.

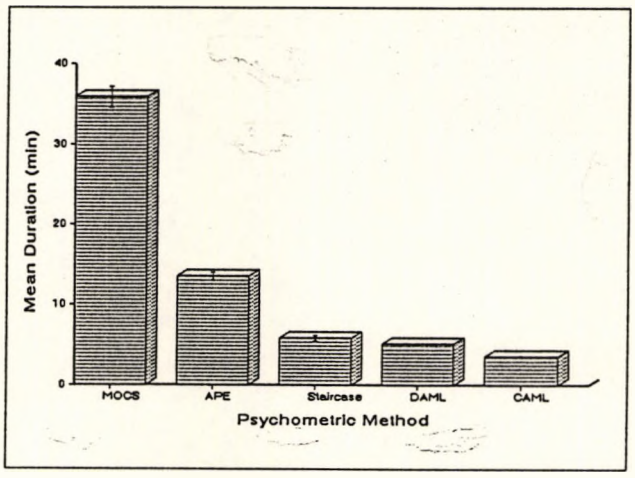

Figure 1 : Mean duration of the five psychometric methods. Bars indicate 95% confidence interval of the mean.

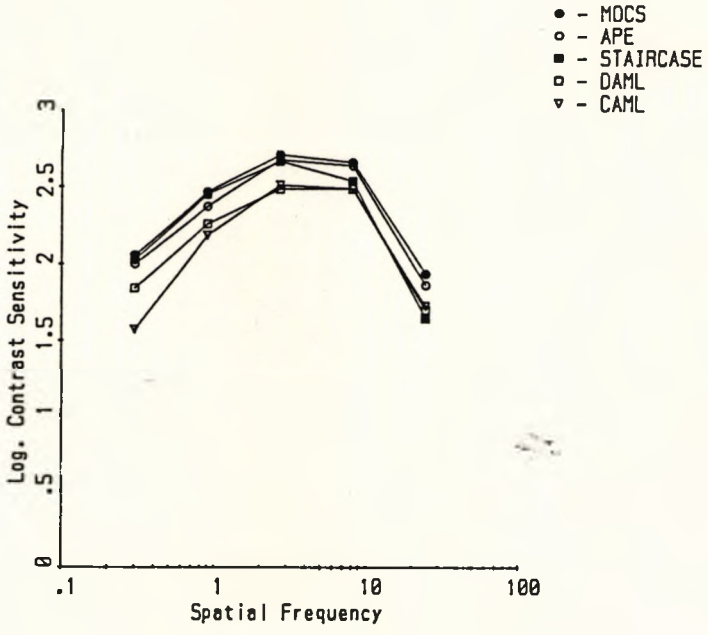

Figure 2 : Mean contrast sensitivity functions for the five psychometric methods.

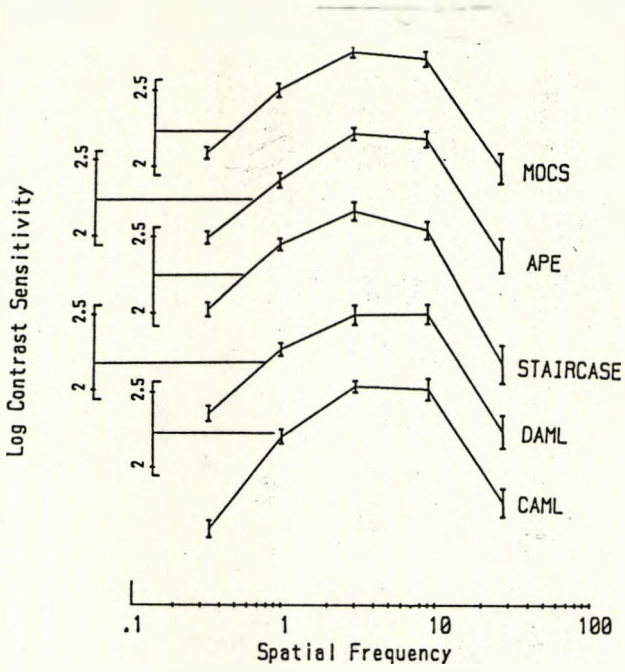

Figure 3 : Mean contrast sensitivity functions for the five psychometric methods. Bars indicate 95% confidence interval of the mean

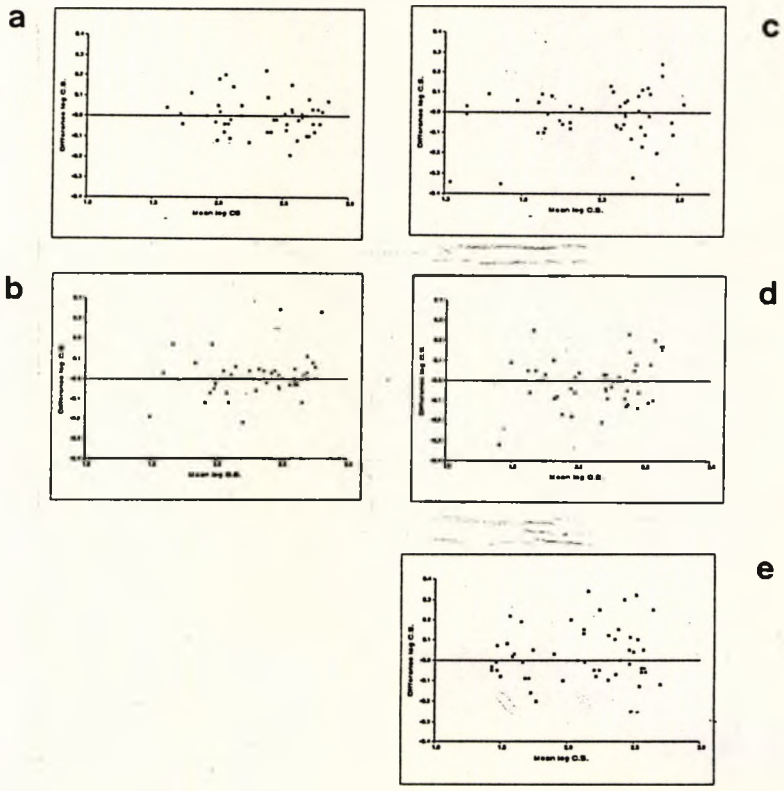

Figure 4 : The difference between test and retest versus the mean contrast sensitivity for (a) MOCS; (b) APE; (c) Staircase; (d) DAML; and (e) CAML.

Intra-test Repeatability

As the data for combined spatial frequencies were not normally distributed, Spearman rank-order correlations (Siegel and Castellan, 1988) were computed. Test-retest correlation coefficients for combined spatial frequencies were 0.97, 0.96, 0.91, 0.94, and 0.93 for MOCS, APE, Staircase, DAML and CAML respectively. Bland and Altman (1986) have noted that correlation coefficients do not necessarily provide a good index of test-retest repeatability and recommend the use of reliability coefficients (2 x s.d. of difference (test - retest): BSI 5497 part 1) to describe repeatability. The test-retest reliability coefficients for combined spatial frequencies were 0.17, 0.19, 0.27, 0.26, 0.25 log contrast units for MOCS, APE, Staircase, DAML and CAML respectively (n = 50). *Figure 4* shows the difference (test-retest) against mean contrast sensitivity (test+retest/2). The test-retest repeatability coefficients for each spatial frequency with each psychometric method are shown in *Table 2.* As these are determined for only 10 data points (from the t distribution) the significance of differences must be interpreted with caution. The mean test-retest differences (*Figure 5*) did not vary significantly from zero and a two way analysis of variance of the differences indicated that there was no effect of spatial frequency or psychometric method and no interaction.

Friedman Analysis of Variance by ranks (Siegel and Castellan, 1988) of the raw data indicated that test-retest was not a significant factor overall and therefore for the purpose of further analysis, test and retest were treated as a single replication.

Inter-test Analysis

Analyses of variance confirmed that the Latin square designs had been effective in eliminating all order effects and as there were no *a priori* reasons to suspect sequence effects, the data was then treated as a fully crossed design for psychometric method (M), subject (S) and spatial frequency (F) with test-retest data treated as a single replication (Winer, 1971). Results of the three way analysis of variance showed that all factors and interactions were highly significant (*Table 3*). Predictably, spatial frequency accounted for the largest proportion of the variance, while psychometric method and subject made significant contributions.

The shape of the contrast sensitivity function obtained was clearly dependent on psychometric Method (*Figure 1*) and this is supported by the finding of a significant interaction between psychometric method and spatial frequency (M x F: $p < 0.001$). Similarly, subjects performed differently with the various psychometric Methods (M x S: $p < 0.001$) and there were variations in the relative sensitivity of subjects to different spatial frequencies (S x F: $p < 0.001$).

Analysis by spatial frequency

Table 4 shows a matrix of Spearman correlation coefficients between spatial frequencies for all methods combined. All correlations were highly significant.

Comparison with MOCS

Inferred validity, as described by Blackwell (1952), may be assessed by investigating the robustness of a technique to external factors (e.g. changes in the observer's decision criteria). MOCS, with no subject decision criteria, might be expected to have the highest inferred validity (this is partially confirmed by having the highest test-retest correlation and smallest reliability coefficient). On this assumption, mean differences between contrast sensitivity obtained by the MOCS and each of the other methods are plotted in *Figure 6.*

Mean contrast sensitivities obtained by the APE procedure were between 0.05 and 0.1 log units lower than the mean contrast sensitivity obtained by MOCS (*Figure 6a*) and there was no apparent trend with spatial frequency.

Mean contrast sensitivities obtained by the Staircase procedure were lower than the mean contrast sensitivities obtained by the MOCS at all spatial frequencies, but the differences were greater at the higher spatial frequencies (*Figure 6b*). This was a consistent effect for all subjects.

Psychometric Method	Spatial Frequency (c.p.d.) 0.3	0.9	2.7	8.1	24.3
MOCS	0.20	0.20	0.13	0.14	0.16
APE	0.17	0.23	0.21	0.10	0.24
Staircase	0.13	0.21	0.34	0.26	0.40
DAML	0.17	0.23	0.35	0.25	0.31
CAML	0.23	0.28	0.22	0.32	0.24

Table 2 : The test-retest repeatability coefficients for each spatial frequency with each psychometric method (n = 10, t distribution).

	Sum of Squares	Deg. of freedom	Mean Square	F-Ratio	signif.
Psychometric Method (M)	4.871	4	1.218	169.214	< 0.0001
Spatial Frequency (F)	57.786	4	14.447	2007.392	< 0.0001
Subject (S)	4.181	9	0.465	20.267	< 0.0001
Interactions					
M x F	2.073	16	0.130	18.002	< 0.0001
M x S	0.506	36	0.014	1.952	< 0.0001
F x S	2.446	36	0.068	9.441	< 0.0001
M x F x S	0.879	144	0.006	0.849	0.861
Residual	1.799	250	0.007		
Total	74.541	499	0.149		

Table 3 : Analysis of variance with a single repetition (test-retest).

Spatial Freq. (c.p.d.)	0.9	2.7	8.1	24.3
0.3	0.799	0.650	0.551	0.383
0.9		0.781	0.596	0.352
2.7			0.692	0.477
8.1				0.755

Table 4 : Spearman rank-order correlation between contrast sensitivity results at five spatial frequencies with all five methods combined. All correlations were significant ($p < 0.001$).

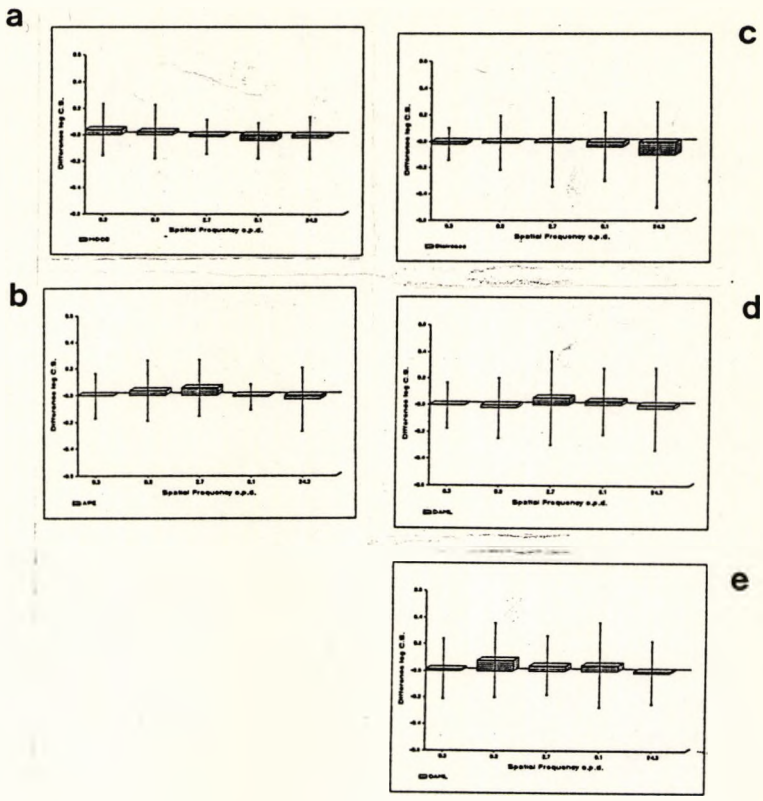

Figure 5 : Mean differences between test and retest versus spatial frequency for (a) MOCS; (b) APE; (c) Staircase; (d) DAML; and (e) CAML. Bars indicate coefficient of repeatability (2 x s.d. : BSI 5497 part 1)

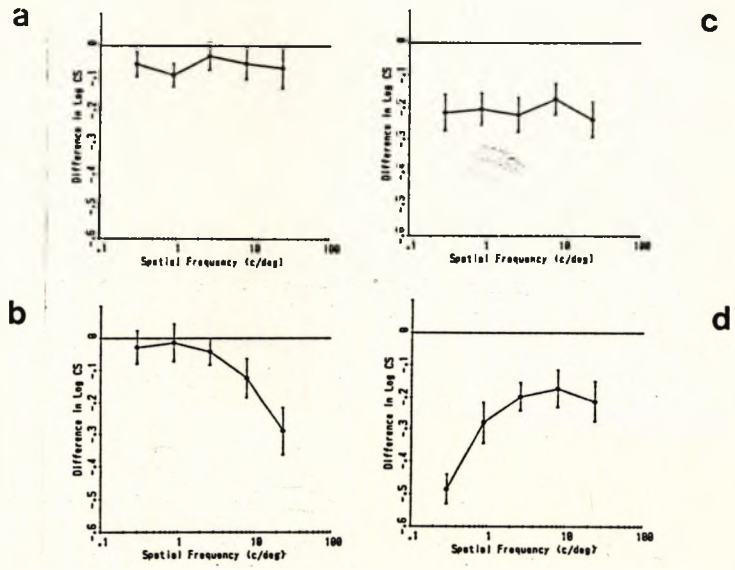

Figure 6 : Mean difference between log contrast sensitivity obtained by MOCS and (a) APE; (b) Staircase; (c) DAML; (d) CAML. Bars indicate 95% confidence interval of mean.

Mean contrast sensitivities obtained by the two implementations of the ascending method of limits were significantly lower at all spatial frequencies than the mean contrast sensitivities obtained by the MOCS ($p < 0.01$)(*Figures 6c and 6d*). Mean contrast sensitivities measured by DAML were between 0.17 and 0.24 log units lower at all spatial frequencies than contrast sensitivities obtained by the MOCS with no apparent trend with spatial frequency. Differences between mean contrast sensitivities for the MOCS and CAML, were significantly greater at the two lowest spatial frequencies ($p < 0.001$). Mean contrast sensitivities with CAML and DAML were also significantly different at the two lower spatial frequencies ($p < 0.01$).

For combined spatial frequencies, Spearman rank-order correlation coefficients between data obtained using MOCS and the other four procedures were 0.94, 0.89, 0.94 ,0.91 for APE, Staircase, DAML and CAML respectively, reflecting the differences noted above.

DISCUSSION

This study has shown that measurements of contrast sensitivity are influenced strongly by the psychometric method employed. Furthermore, the methodology has an effect on the relative contrast sensitivity at different spatial frequencies (i.e. contrast sensitivity functions are not merely displaced up or down, but the shape varies). This must be taken into account when selecting a psychometric method for an experiment and when comparing results between studies which have employed different methodologies.

The MOCS produced the highest estimates of contrast sensitivity at all spatial frequencies. This was presumably because it employed a two alternative forced choice response paradigm while the other methods required a yes/no response. This method also produced the highest test-retest correlation (0.97) and the smallest reliability coefficient (0.17 log contrast units). However, the procedure involved 500 presentations and was therefore extremely time consuming. In addition, the two alternative forced choice procedure requires a relatively complex response and would probably be less effective or even totally unsuitable for use with inexperienced observers. Blackwell (1952) described a series of conditions which improved the inferred validity and repeatability of the MOCS (footnote c). In test situations where these conditions can be met and the duration of the test is not a prime consideration, the MOCS produces highly repeatable measurements of contrast sensitivity.

The implementation of APE employed in this study produced mean contrast sensitivities lower than those obtained by MOCS, which is presumably attributable (at least in part) to the difference in response requirements (2AFC and yes/no). The overall shape of the CSF was similar to the MOCS. Test-retest correlation was 0.96, the reliability coefficient was 0.19 log contrast units and the procedure was more than twice as fast as the full MOCS.

The implementation of the Single Staircase tested in this study produced rather unexpected results. Test-retest correlation (0.91) was the lowest of the five methods tested, and the reliability coefficient was the largest (0.27 log contrast units). Furthermore, contrast sensitivity was significantly lower at the higher spatial frequencies than equivalent data obtained by MOCS ($p < 0.01$). The reason for this difference in sensitivity at high spatial frequencies is unclear but presumably reflects a difference in the decision criteria employed at high and low spatial frequencies. This was perhaps related to subject awareness of the rules governing the procedure. All subjects were aware that a negative response resulted in an increase in the contrast of the next presentation. It is possible that when subjects were unsure of a response, they responded negatively in the knowledge that the next presentation would have a higher contrast. It is unclear why this effect was greatest at the higher spatial frequencies, but it is possible that subjects experienced more ambiguity at the higher spatial frequencies and with prior knowledge of the algorithm adopted a more conservative decision criteria. If this explanation is correct, a random, double Staircase would probably reduce the differences found with the single Staircase employed here, but would involve substantially more presentations, increasing the duration of the procedure. More advanced psychometric methods such as APE which can be implemented to produce results reliably and as quickly as the single staircase may be a better choice. This will be investigated in a further report. The reduced

sensitivity at higher spatial frequencies obtained with experienced observers by this or similar implementations of the single staircase procedure must be taken into account when comparing data obtained by different methods.

Estimates of the contrast sensitivity for the staircase procedure by the procedure of Dixon and Mood (1948) were compared to those found by simply averaging the contrasts at reversal and shown to differ by less than 0.02 log contrast units. The extra complexity of the Dixon and Mood method would not seem to be justified in this context.

The implementation of the Discrete Method of Ascending Limits (DAML) employed in this study produced mean contrast sensitivities lower than the equivalent sensitivities with the MOCS. The overall shape of the CSF was similar to the MOCS. Test-retest correlation was 0.94 but the reliability coefficient (0.26 log contrast units) was large. The short duration of this novel procedure makes it an attractive implementation.

The implementation of the Continuous Method of Ascending Limits (CAML) employed in this study had a relatively high test-retest correlation (0.93) and a relatively large reliability coefficient (0.25). Mean contrast sensitivities were lower than the equivalent MOCS sensitivities. The sensitivity at the lower spatial frequencies was significantly reduced in comparison to the equivalent procedure which used discrete presentations (DAML) presumably because of the difference in the temporal envelope of the presentation (Kelly, 1971; Green, 1981). Therefore caution must be exercised when comparing contrast sensitivity measurements obtained by methods which employ different temporal envelopes for presentation.

The two implementations of the method of limits (DAML and CAML), unlike the other three methods, did not allow for breaks once the procedure had begun. Often it is advantageous for the observer to be able to stop during a procedure (e.g. to realign experimental devices). A facility to temporarily halt the method of limits presentation (e.g. another button) would overcome this problem.

It has been suggested that investigation of correlation values across the different spatial frequencies may be used to assess whether contrast sensitivity measurement is testing different underlying mechanisms. Low correlations may indicate that different mechanisms are used for detection of different spatial frequencies. Highly significant correlation was found between all spatial frequencies and was highest for adjacent spatial frequencies (*Table 4*). Sekuler and Mulvanney (1983) suggest that contrast sensitivity at spatial frequencies which differ by more than a factor of four are independent; our data support this assertion only in as much as higher correlations were found for spatial frequencies which differed by a factor of 3, than for those which varied by a factor of 9 (though all were highly significant). This agrees with other studies (Owsley et al, 1983; Long and Penn, 1987, Brown and Lovie-Kitchin, 1989).

Test-retest repeatability is a measure of the stability of a particular procedure over time. Care was taken in this study to optimize the repeatability of the psychometric procedures. All psychometric methods evaluated here produced similar test-retest repeatability. In many instances the absolute values of contrast sensitivity or even the shape of the contrast sensitivity function is of less importance than the repeatability of a procedure. In these situations, the results of this study would suggest that there is little advantage to be gained from using more complex and time consuming psychometric methods.

These findings may not be applicable to situations where inexperienced subjects are used such as the clinical situation. Kelly and Savoie (1973) and Higgins et al (1984, 1988) reported significant shifts in decision criterion with a method of adjustment but not with a forced choice procedure. Practice effects can be very variable and dependent upon methodology with inexperienced observers (Kelly and Tomlinson, 1987; Long and Penn, 1987; Long and Tuck, 1988). Furthermore, subjects suffering from certain pathological conditions have been shown to have a lower test-retest repeatability (e.g. Reeves et al, 1987, Wood et al, 1988, Rubin, 1988).

CONCLUSIONS

Care must be exercised when selecting a psychometric method for measuring contrast sensitivity and when comparing results from studies which have used different psychometric methods. This study has shown that both the absolute values and the shape of the contrast sensitivity function are influenced by the psychometric method. Where inferred validity is of paramount importance and the duration of the test is not a major consideration, there is some justification for using more complex methods such as the implementation of MOCS tested in this study. In situations where inter and intra-subject differences are of interest there would seem to be little advantage gained from using more complex psychometric methods while simpler methods which take a fraction of the time produce similar test-retest repeatability. However, this study employed experienced observers and some caution is required in extending these conclusions to situations where inexperienced observers are to be tested. Furthermore, the differences in results found by the five psychometric methods investigated in this study only apply to these particular implementations and will not necessarily apply to situations where the experimental conditions or control algorithms are not identical to those employed in this study. Similarly, these conclusions may not necessarily apply to measurements of other aspects of visual performance.

ACKNOWLEDGEMENT

RLW was sponsored by a Pilkington research studentship.

FOOTNOTES

[a] Desirable characteristics of any psychometric procedure include:
1. Validity
2. Repeatability. For the purpose of most visual functions a retest coefficient is of importance as this is a measure of the stability of the procedure (Guilford, 1954, p374).
3. Short session duration to avoid undesirable temporal effects
4. Robustness. The ability to give valid and repeatable results despite an occasional lapse by the observer

[b] Blackwell (1952) described "inferred validity" as "the extent to which variables considered irrelevant to visual functions influenced threshold data".

[c] Blackwell (1952), in a very detailed examination of methods of constant stimuli in general, concluded that repeatability and inferred validity of psychometric data is maximised by: 1) employing "forced choice" rather than a phenomenal (yes/no) response paradigms, 2) presenting the two or more alternative stimuli by temporal intervals rather than spatial location, 3) presenting stimuli in blocks rather than in a randomised sequence (to avoid adding recognition to the detection task), 4) a limited range of stimuli, 5) providing subjects with feedback on the accuracy of responses, 6) using trained subjects.

APPENDIX 4 Tables relating to the preliminary study - section 2.3

Table A4-1 ANOVA F-ratios for Monitor based CSF at 0.5, 1, 2, 4 and 8 c.p.d. with (a) one, (b) two, (c) three, and (d) four repetitions. The major interest was the interaction between Diffractive Zone Junction Height (DZJ Ht) and vergence (distance or near), and any interactions with luminance.

Note : only the F ratios and relevant significance levels have been indicated.

(a) One repetition n = 24

	CSF 0.5	CSF 1	CSF 2	CSF 4	CSF 8
DZJ Ht (H)	0.5	1.1	1.4	1.5	4.5
Luminance (L)	7.1*	9.8*	19.8****	297.7****	345.6****
Vergence (V)	1.2	2.2	2.1	2.8	4.8
H x L	0.2	0.1	0.4	1.2	0.6
H x V	0.1	0.6	0.8	6.1*	9.2*
L x V	0.1	0.0	0.1	0.2	0.4
H x L x V	0.0	0.0	0.3	1.1	0.6

(b) Two repetitions n = 48

	CSF 0.5	CSF 1	CSF 2	CSF 4	CSF 8
DZJ Ht (H)	2.1	3.8**	4.2***	0.9	4.8***
Luminance (L)	27.3****	123.5****	346.6****	268.6****	464.9****
Vergence (V)	0.2	0.3	0.2	0.4	7.7**
H x L	0.2	0.1	0.2	0.8	0.7
H x V	1.3	1.1	1.3	5.6****	11.6****
L x V	1.1	1.3	2.0	0.9	1.0
H x L x V	0.0	0.1	0.5	0.3	0.3

(c) Three repetitions n = 72

	CSF 0.5	CSF 1	CSF 2	CSF 4	CSF 8
DZJ Ht (H)	2.4**	3.6**	5.6****	2.0**	4.6****
Luminance (L)	78.2****	188.9****	472.8****	408.8****	701.2****
Vergence (V)	0.2	0.5	1.1	0.2	14.4****
H x L	0.1	0.4	0.4	0.4	0.9
H x V	1.5	2.0*	2.4*	9.4****	16.6****
L x V	0.2	0.1	0.7	0.1	0.0
H x L x V	0.3	0.2	0.3	0.3	0.3

(d) Four repetitions n = 96

	CSF 0.5	CSF 1	CSF 2	CSF 4	CSF 8
DZJ Ht (H)	1.4**	2.3***	1.9**	3.8***	4.3***
Luminance (L)	222.1****	558.1****	661.1****	608.0****	835.6****
Vergence (V)	0.4	0.4	0.7	0.5	8.8***
H x L	0.2	0.3	0.2	0.6	1.0
H x V	1.2	2.1**	3.7***	11.0****	17.6****
L x V	0.2	0.1	0.2	0.2	0.1
H x L x V	0.1	0.2	0.1	0.3	0.5

* = $p < 0.05$; ** = $p < 0.01$; *** = $p < 0.001$; **** = $p < 0.0001$

Table A4-2 ANOVA F-ratios for Vistech at 2, 4 and 8 c.p.d. with (a) one, (b) two, and (c) three repetitions. The major interest was the interaction between Diffractive Zone Junction Height (DZJ Ht) and vergence (distance or near), and any interactions with luminance.

Note : only the F ratios and relevant significance levels have been indicated.

(a) One repetition	n = 24		
	VIS 2	VIS 4	VIS 8
DZJ Ht (H)	0.8	0.7	4.2
Luminance (L)	1.4	3.3	73.6****
Vergence (V)	1.2	2.7	3.1
H x L	0.2	0.2	0.3
H x V	1.1	0.6	5.6*
L x V	0.1	0.0	1.2
H x L x V	0.1	0.3	0.5

(b) Two repetitions	n = 48		
	VIS 2	VIS 4	VIS 8
DZJ Ht (H)	1.7	0.9	5.5****
Luminance (L)	5.2*	21.6****	171.9****
Vergence (V)	0.5	7.6**	3.4
H x L	0.5	0.4	0.3
H x V	4.0**	2.0	9.1****
L x V	0.7	0.0	0.9
H x L x V	0.5	1.0	0.3

(c) Three repetitions	n = 75	72	
	VIS 2	VIS 4	VIS 8
DZJ Ht (H)	1.5	1.2	7.1****
Luminance (L)	7.1**	38.6****	262.0****
Vergence (V)	0.7	6.5*	1.0
H x L	0.3	0.5	0.5
H x V	5.2****	3.3*	13.2****
L x V	1.2	0.1	1.0
H x L x V	0.4	0.8	0.4

* = $p < 0.05$; ** = $p < 0.01$; *** = $p < 0.001$; **** = $p < 0.0001$

Table A4-3 ANOVA F-ratios for Australian Vision Chart (VA) high and low contrast with (a) one, (b) two, and (c) three repetitions. The major interest was the interaction between Diffractive Zone Junction Height (DZJ Ht) and vergence (distance or near), and any interactions with luminance.

Note : only the F ratios and relevant significance levels have been indicated.

(a) One repetition n = 24

	VA High	VA Low
DZJ Ht (H)	5.2	3.2
Luminance (L)	33.6**	27.5**
Vergence (V)	8.7*	7.7*
H x L	0.5	0.9
H x V	3.1	3.1
L x V	2.6	0.4
H x L x V	0.2	0.1

(b) Two repetitions n = 48

	VA High	VA Low
DZJ Ht (H)	6.4****	9.8****
Luminance (L)	90.1****	174.3****
Vergence (V)	16.9****	34.2****
H x L	0.8	1.1
H x V	9.1****	19.0****
L x V	4.6*	1.3
H x L x V	1.1	1.1

(c) Three repetitions n = 72

	VA High	VA Low
DZJ Ht (H)	7.5****	10.2****
Luminance (L)	156.8****	266.5****
Vergence (V)	23.3****	38.3****
H x L	0.9	0.8
H x V	14.5****	25.5****
L x V	3.8	1.1
H x L x V	1.5	0.8

* = $p < 0.05$; ** = $p < 0.01$; *** = $p < 0.001$; **** = $p < 0.0001$)

Table A4-4 ANOVA F-ratios for Pelli-Robson charts (PRC) at 2 and 4 metres and the Melbourne Edge Test (MET) with (a) one, (b) two, and (c) three repetitions. The major interest was the interaction between Diffractive Zone Junction Height (DZJ Ht) and vergence (distance or near), and any interactions with luminance.

Note : only the F ratios and relevant significance levels have been indicated.

(a) One repetition n = 24

	MET	PRC 2	PRC 4
DZJ Ht (H)	1.9	2.0	3.5
Luminance (L)	15.5	57.1***	68.6****
Vergence (V)	0.8	0.0	0.0
H x L	0.5	0.9	2.4
H x V	0.4	7.7*	14.3*
L x V	0.1	3.6	2.0
H x L x V	0.3	3.4	5.3

(b) Two repetitions n = 48

	MET	PRC 2	PRC 4
DZJ Ht (H)	9.0****	9.8****	11.1****
Luminance (L)	60.6****	154.5****	160.2****
Vergence (V)	2.7	0.1	0.0
H x L	0.5	1.7	2.5*
H x V	1.0	16.5****	29.2****
L x V	0.4	8.3**	1.6
H x L x V	1.1	5.1****	7.3***

(c) Three repetitions n = 72

	MET	PRC 2	PRC 4
DZJ Ht (H)	4.4***	4.9****	5.5****
Luminance (L)	48.1****	151.2****	115.9****
Vergence (V)	0.8	0.0*	0.1
H x L	0.1	0.7	1.2
H x V	1.4	11.5****	15.8****
L x V	0.4	5.8*	1.6
H x L x V	0.3	2.2	2.6*

* = $p < 0.05$; ** = $p < 0.01$; *** = $p < 0.001$; **** = $p < 0.0001$)

APPENDIX 5 Tables relating to Optical Performance - section 4.2

Table A5-1 **ANOVA of Refractive BCL MTF data, with the BCL Optic (COZ or POZ), COZD (1.8, 2.2, 2.6, 3.0, 3.4 mm) and apertures (2, 3, 3.5, 4, 5, 6 mm).**

	Sum of Squares	deg. of free.	Mean Square	F ratio	signif. of F
Optic (O)	1.097	1	1.097	1002.4	<0.001
COZD (D)	1.767	4	0.442	403.5	<0.001
Aperture (P)	2.256	5	0.451	412.2	<0.001
Spatial Frequency (F)	83.313	15	5.554	5074.0	<0.001
O x D	33.362	4	8.341	7619.4	<0.001
O x P	39.24	5	7.848	7169.4	<0.001
O x F	2.123	15	0.142	129.3	<0.001
D x P	1.318	20	0.066	60.2	<0.001
D x F	0.261	60	0.004	3.98	<0.001
P x F	0.978	75	0.013	11.9	<0.001
O x D x P	6.936	20	0.347	316.8	<0.001
O x D x F	8.952	60	0.149	136.3	<0.001
O x P x F	18.386	75	0.245	223.9	<0.001
D x P x F	0.476	300	0.002	1.45	<0.001
O x D x P x F	2.991	300	0.01	9.1	<0.001
Explained	202.918	959	0.212	193.3	<0.001
Residual	4.562	4168	0.001		
Total	207.481	5127	0.04		

Table A5-2 **Multiple Regression Analysis for centred Refractive BCL, with COZD (1.8, 2.2, 2.6, 3.0, 3.4 mm) and apertures (2, 3, 3.5, 4, 5, 6 mm) and spatial frequency (sf) from 0 to 66 c.p.d..**

adjusted R^2	0.949
standard error	0.062
n	5449

ANOVA

	df	Sum Sq.	Mean Sq.	F ratio
Regression	30	387.8	12.9	3375.6
Residual	5418	20.7	0.004	

Signif F < 0.0001

Regression Terms

	COZ	POZ
constant	0.9984***	0.9984***
sf	-0.2235***	-0.3447***
sf^2	0.01231***	0.02555***
sf^{-1}	-0.6725***	-0.8914***
sf^{-3}	0.09836***	0.2997***
aperture * sf	-0.01153***	0.04528***
aperture * sf^2	0.0015***	-0.00436***
aperture * sf^{-1}	-0.2794***	0.2408***
aperture * sf^{-2}	0.1305***	
aperture * sf^{-3}	-0.00555***	-0.0630***
COZD * sf	0.02754 **	0.04948***
COZD * sf^2	-0.00269 *	-0.00443***
COZD * sf^{-1}	1.4548***	0.6297***
COZD * sf^{-2}	0.3679***	0.6512***
COZD * sf^{-3}	-0.2322***	-0.2322***
aperture * COZD * sf	0.00462***	-0.01274***
aperture * COZD * sf^2	0.00046***	0.00118***

* = p < 0.05 ; ** = p < 0.01 ; *** = p < 0.0001

Table A5-3a **ANOVA of decentred Refractive BCL MTF data, with aperture = 4mm, COZD (1.8, 2.6, 3.4 mm), and decentration (0, 0.25, 0.50, 0.75, 1.0, 1.25, 1.50, 2.0 mm).**

	Sum of Squares	df	Mean Square	F ratio	signif. of F
Optic (O)	1.997	1	1.997	2847.4	<0.001
decentration (C)	0.281	7	0.04	57.2	<0.001
COZD (D)	0.197	2	0.098	140.2	<0.001
Spatial Frequency (F)	27.909	15	1.861	2652.5	<0.001
O x C	3.519	7	0.503	716.6	<0.001
O x D	14.186	2	7.093	10112.0	<0.001
O x F	1.527	15	0.102	145.1	<0.001
C x D	0.276	14	0.02	28.2	<0.001
C x F	0.102	105	0.001	1.38	0.009
D x F	0.014	30	0	0.67	0.91
O x C x D	1.794	14	0.128	182.7	<0.001
O x C x F	1.105	105	0.011	15.0	<0.001
O x D x F	3.152	30	0.105	149.8	<0.001
C x D x F	0.124	210	0.001	0.84	0.94
O x C x D x F	0.463	210	0.074	3.14	<0.001
Explained	57.078	767	0.074	106.1	<0.001
Residual	0.718	1024	0.001		
Total	57.796	1791	0.032		

Table A5-3b **ANOVA of decentred Refractive BCL MTF data, with COZD = 2.6 mm, apertures (2, 3, 3.5, 4, 5, 6 mm), and decentration (0, 0.25, 0.50, 0.75, 1.0, 1.25, 1.50, 2.0 mm).**

	Sum of Squares	df	Mean Square	F ratio	signif. of F
Optic (O)	0.853	1	0.853	1669.4	<0.001
decentration (C)	0.166	7	0.024	46.4	<0.001
Aperture (P)	0.21	2	0.105	205.5	<0.001
Spatial Frequency (F)	26.162	15	1.744	3413.1	<0.001
O x C	3.185	7	0.455	890.3	<0.001
O x P	2.609	2	1.304	2552.3	<0.001
O x F	0.933	15	0.062	121.7	<0.001
C x P	0.22	14	0.016	30.7	<0.001
C x F	0.08	105	0.001	1.49	0.002
P x F	0.044	30	0.001	2.86	<0.001
O x C x P	2.509	14	0.179	350.7	<0.001
O x C x F	1.416	105	0.013	26.4	<0.001
O x P x F	1.057	30	0.035	68.9	<0.001
C x P x F	0.237	210	0.001	2.21	<0.001
O x C x P x F	0.955	210	0.053	8.9	<0.001
Explained	40.574	767	0.053	103.5	<0.001
Residual	0.437	856	0.001		
Total	41.011	1623	0.025		

Table A5-4 **Multiple Regression Analysis for centred and decentred Refractive BCL, with COZD (1.8, 2.2, 2.6, 3.0, 3.4 mm), apertures (2, 3, 3.5, 4, 5, 6 mm), and decentration (0, 0.25, 0.50, 0.75, 1.0, 1.25, 1.38, 1.50, 1.75, 2.0 mm).**

adjusted R^2	0.980
standard error	0.037
n	2992

ANOVA

	df	Sum Sq.	Mean Sq.	F ratio
Regression	52	194.8	3.75	2804.7
Residual	2939	3.93	0.001	

Signif. F < 0.0001

Regression Terms

	COZ	POZ
constant	0.8693***	1.1188***
aperture	-0.02279 *	
decen	-0.06377 *	
COZD	0.08523***	-0.04908***
sf	-0.1748***	-0.1748***
sf^2	0.00711***	0.01031***
sf^{-1}	-1.0717***	-2.6501***
sf^{-2}	1.8376***	1.8376***
sf^{-3}	1.8376***	-0.2784***
aperture * decen	0.07465***	-0.02962***
aperture * sf	-0.01595***	0.01620***
aperture * sf^2	0.00212***	-0.00183***
aperture * sf^{-1}	-0.1684***	0.5564***
aperture * sf^{-2}	-0.2598***	-0.2598***
aperture * sf^{-3}	0.1858***	
decen * sf	-0.06419***	0.07382***
decen * sf^2	0.00801***	-0.00859***
decen * sf^{-1}	-1.1117***	-1.1560***
decen * sf^{-2}	0.3404***	0.3404***
decen * sf^{-3}	0.1204***	-0.5032***
COZD * sf	0.03366***	-0.03194***
COZD * sf^2	-0.00343***	0.00319***
COZD * sf^{-1}	0.2459***	-0.2581***
COZD * sf^{-2}	0.08364 *	
COZD * sf^{-3}	-0.08524***	0.03681***
aperture * decen * COZD	0.02275***	0.01198***
aperture * decen * sf	0.01478***	-0.01363***
aperture * decen * sf^2	-0.00181***	0.00156***
aperture * decen * sf^{-1}	0.1367***	-0.2853***
aperture * decen * sf^{-2}	0.09343 **	
aperture * decen * sf^{-3}	-0.09501***	0.07826***

* = p < 0.05 ; ** = p < 0.01 ; *** = p < 0.0001

Table A5-5 **ANOVA of variability of manufacture of rigid diffractive BCL MTF data at 548 nm, with two batches of BCL each with 2.2 μm and 2.6 μm DZJ height.**

	Sum of Squares	df	Mean Square	F ratio	signif. of F
Batch (B)	0.521	1	0.521	133.966	<0.001
DZJ height (H)	0	1	0	.016	0.901
Vergence (V)	2.849	1	2.849	732.65	<0.001
Spatial Frequency (F)	51.363	15	3.424	880.691	<0.001
B x H	0.011	1	0.011	2.944	0.086
B x V	1.401	1	1.401	360.3	<0.001
B x F	0.2073	15	0.014	3.54	<0.001
H x V	1.026	1	1.026	264.0	<0.001
H x F	0.015	15	0.001	0.25	1.0
V x F	0.803	15	0.054	13.8	<0.001
B x H x V	0.98	1	0.027	7.05	0.008
B x H x F	0.016	15	0.001	0.28	1.0
B x V x F	0.384	15	0.026	6.6	<0.001
H x V x F	0.222	15	0.015	3.8	<0.001
B x H x V x F	0.029	15	0.002	0.50	0.94
Explained	58.781	127	0.463	119.0	<0.001
Residual	3.799	977	0.004		
Total	62.58	1104	0.057		

Table A5-6a **ANOVA of difference between experimental rigid Diffractive BCL and Pilkington Diffrax, both with 2.0 μm DZJ height. MTF data at 548 nm**

	Sum of Squares	df	Mean Square	F ratio	signif. of F
Batch (B)	0.118	1	0.118	51.9	<0.001
Vergence (V)	0.172	1	0.172	75.8	<0.001
Spatial Frequency (F)	50.727	15	3.382	1489.3	<0.001
B x V	0.151	1	0.151	66.4	<0.001
B x F	0.029	15	0.002	0.87	0.61
V x F	0.035	15	0.002	1.02	0.43
B x V x F	0.046	15	0.003	1.35	0.17
Explained	51.272	63	0.814	358.4	<0.001
Residual	2.652	1168	0.002		
Total	53.924	1231	0.044		

Table A5-6b **ANOVA of difference between experimental rigid Diffractive BCL and Pilkington Diffrax, both with 2.0 μm DZJ height. MTF data at 573 nm**

	Sum of Squares	df	Mean Square	F ratio	signif. of F
Batch (B)	0.027	1	0.027	18.798	<0.001
Vergence (V)	1.210	1	1.210	855.034	<0.001
Spatial Frequency (F)	6.470	15	0.462	326.639	<0.001
B x V	0.009	1	0.009	6.678	0.01
B x F	0.005	15	0.0003	0.258	0.997
V x F	0.183	15	0.013	9.253	<0.001
B x V x F	0.007	15	0.001	0.367	0.983
Explained	7.898	63	0.134	94.617	<0.001
Residual	0.870	615	0.001		
Total	8.768	674	0.013		

Table A5-7a **ANOVA of rigid diffractive BCL MTF data at 548 nm, with DZJ height (1.8, 2.0, 2.2, 2.5, 2.6) and tool shape (250 μm, 100 μm, flatted).**

	Sum of Squares	df	Mean Square	F ratio	signif. of F
Vergence (V)	5.545	1	5.545	1996.235	<0.001
DZJ height (H)	2.975	4	0.595	214.186	<0.001
Tool Shape (S)	1.15	2	0.575	206.985	<0.001
Spatial Frequency (F)	50.809	15	3.387	1219.38	<0.001
V x H	23.086	5	4.617	1662.12	<0.001
V x S	2.397	2	1.199	431.453	<0.001
V x F	1.283	15	0.086	30.79	<0.001
H x S	0.498	10	0.05	17.945	<0.001
H x F	0.65	75	0.009	3.118	<0.001
S x F	0.367	30	0.012	4.4	<0.001
V x H x S	0.98	10	0.098	35.285	<0.001
V x H x F	4.506	75	0.06	21.626	<0.001
V x S x F	0.421	30	0.014	5.048	<0.001
H x S x F	0.156	150	0.001	0.375	1
V x H x S x F	0.212	150	0.001	0.509	1
Explained	95.849	575	0.167	60.008	<0.001
Residual	14.156	5096	0.003		
Total	110.005	5671	0.04		

Table A5-7b **ANOVA of rigid diffractive BCL MTF data at 573 nm, with DZJ height (1.8, 2.0, 2.2, 2.5, 2.6) and tool shape (250 μm, 100 μm, flatted).**

	Sum of Squares	df	Mean Square	F ratio	signif. of F
Vergence (V)	0.186	1	0.186	88.3	<0.001
DZJ height (H)	1.311	4	0.328	155.5	<0.001
Tool Shape (S)	0.799	2	0.4	189.6	<0.001
Spatial Frequency (F)	33.505	15	2.234	1059.7	<0.001
V x H	4.909	4	1.227	582.3	<0.001
V x S	2.304	2	1.152	546.5	<0.001
V x F	0.079	15	0.005	2.50	0.001
H x S	0.337	8	0.042	20.0	<0.001
H x F	0.373	60	0.006	2.95	<0.001
S x F	0.3	30	0.01	4.7	<0.001
V x H x S	0.895	8	0.112	53.1	<0.001
V x H x F	0.957	60	0.016	7.6	<0.001
V x S x F	0.404	30	0.013	6.38	<0.001
H x S x F	0.18	120	0.002	0.71	1.0
V x H x S x F	0.165	120	0.001	0.65	1.0
Explained	46.978	479	0.098	46.5	<0.001
Residual	7.605	3608	0.002		
Total	54.583	4087	0.013		

Table A5-8a **ANOVA of difference between rigid diffractive BCL with 2.0 μm DZJ height made with different tools (250 μm, 100 μm, 50 μm, and flatted). MTF data at 548 nm.**

	Sum of Squares	df	Mean Square	F ratio	signif. of F
Tool (T)	0.148	3	0.049	24.7	<0.001
Vergence (V)	0.167	1	0.167	83.5	<0.001
Spatial Frequency (F)	16.413	15	1.094	548.2	<0.001
T x V	0.133	3	0.044	22.3	<0.001
T x F	0.087	45	0.002	0.97	0.53
V x F	0.022	15	0.001	0.74	0.75
T x V x F	0.034	45	0.001	0.38	1.0
Explained	17.011	127	0.134	67.1	<0.001
Residual	3.353	1680	0.002		
Total	20.364	1807	0.044		

Table A5-8b **ANOVA of difference between rigid diffractive BCL with 2.0 μm DZJ height made with different tools (250 μm, 100 μm, 50 μm, and flatted). MTF data at 573 nm.**

	Sum of Squares	df	Mean Square	F ratio	signif. of F
Tool (T)	0.023	3	0.008	8.22	<0.001
Vergence (V)	1.560	1	1.560	1647.8	<0.001
Spatial Frequency (F)	12.220	15	0.815	860.4	<0.001
T x V	0.171	3	0.057	60.2	<0.001
T x F	0.073	45	0.002	1.72	0.002
V x F	0.257	15	0.017	18.1	<0.001
T x V x F	0.038	45	0.001	0.88	0.70
Explained	14.363	127	0.113	119.4	<0.001
Residual	1.106	1168	0.001		
Total	15.469	1295	0.013		

Table A5-9 Multiple Regression Equation Values for rigid diffractive BCL with DZJ heights from 1.4 μm to 4.0 μm for tools and wavelengths as shown.

All terms significant at $p < 0.0001$ except as marked

Wavelength	548 nm		548 nm	
Tool Shape	100 μm		flatted	
adjusted R^2	0.898		0.979	
standard error	0.071		0.033	
n	1369		1156	
	Distance	Near	Distance	Near
constant	0.9984	0.9984	0.9989	0.9989
sf	-0.1663 2	-0.1778	0.00215	-0.1831
sf^2	0.00986	0.00986	0.00648	0.01081
sf^{-1}	-1.5284	-2.4736	-0.6156	-1.9979
sf^{-2}	1.9680	1.9680	1.3535	1.3535
sf^{-3}	-0.7399	-0.5649	-0.5977	-0.3226
DZJ ht * sf	0.01092 2	0.01542 3	-0.02109	0.02497
DZJ ht * sf^2	-0.00123	-0.00132 2	0.00196	-0.00251
DZJ ht * sf^{-1}	-0.1239	0.3234	-0.5641	0.3303
DZJ ht * sf^{-2}	0.1374 4	0.3343		
DZJ ht * sf^{-3}	-0.04893	-0.04893	-0.06474	-0.06474

Wavelength	548 nm		573 nm	
Tool Shape	250 μm		100 μm	
adjusted R^2	0.916		0.847	
standard error	0.068		0.051	
n	3969		1328	
	Distance	Near	Distance	Near
constant	0.9989	0.9989	0.0791	-0.3302
sf	-0.09317	-0.2209	0.03054	0.03054
sf^2	0.00218	0.00143	-0.00273	
sf^{-1}	-0.6312	-2.4186	1.6017	
sf^{-2}	1.7341	1.7341	-0.6492	
sf^{-3}	-0.8010	-0.4304		
DZJ ht	-0.8010	-0.4304	-0.05622	0.2663
DZJ ht * sf	-0.01847	0.04043	-0.00482	-0.02816
DZJ ht * sf^2	0.00171	-0.00394	0.00057	0.00057 2
DZJ ht * sf^{-1}	-0.5204	0.4215	-0.2687	0.05224 3
DZJ ht * sf^{-2}	0.1717 3			
DZJ ht * sf^{-3}	0.01673 4	-0.08447	0.06287	-0.00991 2

All terms significant at $p < 0.0001$ except as marked

1 = $p < 0.1$; 2 = $p < 0.05$; 3 = $p < 0.01$; 4 = $p < 0.001$

Table A5-9 (cont) **Multiple Regression Equation Values for Rigid Diffractive BCL with DZJ heights from 1.4 μm to 4.0 μm for tools and wavelengths as shown.**

All terms significant at $p < 0.0001$ except as marked

Wavelength	573 nm		573 nm	
Tool Shape	flatted		250 μm	
adjusted R^2	0.950		0.781	
standard error	0.031		0.067	
n	1120		2376	
	Distance	Near	Distance	Near
constant	0.3830	-0.1313	0.5105	-0.06378 [2]
sf	0.01352	0.01352	-0.02064 [3]	-0.02064 [3]
sf^2	-0.00376	-0.00182	0.00261	
sf^{-1}	1.0721	0.7768	-0.1679	
sf^{-2}	-0.3641			
sf^{-3}	-0.03421	-0.03421	-0.1725	
DZJ ht	-0.1243	0.2487	-0.1152	0.1442
DZJ ht * sf	-0.0045	-0.02375		
DZJ ht * sf^2	0.00121 [2]	0.00033 [2]	0.00087	0.00116
DZJ ht * sf^{-1}	-0.2458	0.04379	-0.2272	0.1776
DZJ ht * sf^{-3}	0.04552	0.04777	-0.0256	

All terms significant at $p < 0.0001$ except as marked

1 = $p < 0.1$; 2 = $p < 0.05$; 3 = $p < 0.01$; 4 = $p < 0.001$

Table A5-10 **ANOVA of difference between batches of three nominally identical soft diffractive BCL (DZJ height = 3.0; tool = 100 μm round; moulded). MTF data at 548 nm.**

	Sum of Squares	df	Mean Square	F ratio	signif. of F
Batch (B)	0.101	2	0.050	18.718	<0.001
Vergence (V)	1.385	1	1.385	499.629	<0.001
Spatial Frequency (F)	3.824	15	0.255	92.0	<0.001
B x V	0.021	2	0.010	3.8	<0.001
B x F	0.010	30	0.0003	0.12	1.0
V x F	0.293	15	0.020	7.2	<0.001
B x V x F	0.013	30	0.0004	0.16	0.79
Explained	5.647	95	0.059	94.6	<0.001
Residual	0.754	272	0.003		
Total	6.401	367	0.013		

Table A5-11a **ANOVA of soft diffractive BCL (tool = 250 μm round; lathed) MTF data at 548 nm with DZJ heights 2.7, 3.0, 4.0 μm.**

	Sum of Squares	df	Mean Square	F ratio	signif. of F
DZJ height (H)	0.009	2	0.004	42.360	<0.001
Vergence (V)	0.785	1	0.785	7674.576	<0.001
Spatial Frequency (F)	2.229	15	0.149	1452.6	<0.001
H x V	1.024	2	0.512	5005.7	<0.001
H x F	0.008	30	0.0003	2.6	<0.001
V x F	0.168	15	0.011	109.3	<0.001
H x V x F	0.172	30	0.006	56.1	<0.001
Explained	4.394	95	0.046	452.2	<0.001
Residual	0.016	160	0.0001		
Total	4.410	255	0.017		

Table A5-11b **ANOVA of soft diffractive BCL (tool = 100 μm round; lathed) MTF data at 548 nm with DZJ heights 3.0, 3.3, 3.6 μm.**

	Sum of Squares	df	Mean Square	F ratio	signif. of F
DZJ height (H)	0.079	2	0.039	11.7	<0.001
Vergence (V)	3.473	1	3.473	1032.9	<0.001
Spatial Frequency (F)	14.779	15	0.985	293.0	<0.001
H x V	1.828	2	0.914	271.8	<0.001
H x F	0.249	30	0.008	2.5	<0.001
V x F	0.876	15	0.058	17.4	<0.001
H x V x F	0.531	30	0.018	5.3	<0.001
Explained	22.162	95	0.233	69.4	<0.001
Residual	4.520	1344	0.003		
Total	26.682	1439	0.019		

Table A5-11c **ANOVA of soft diffractive BCL (tool = 100 μm round; moulded) MTF data at 548 nm with DZJ heights 2.5, 2.6, 3.0, 3.3 μm.**

	Sum of Squares	df	Mean Square	F ratio	signif. of F
DZJ height (H)	0.694	3	0.231	81.6	<0.001
Vergence (V)	0.951	1	0.951	335.1	<0.001
Spatial Frequency (F)	5.619	15	0.375	132.1	<0.001
H x V	0.454	3	0.151	53.3	<0.001
H x F	0.188	45	0.004	1.48	0.027
V x F	0.222	15	0.015	5.22	<0.001
H x V x F	0.122	45	0.003	0.96	0.55
Explained	8.327	127	0.066	23.1	<0.001
Residual	1.407	496	0.003		
Total	9.734	623	0.016		

Table A5-12 **ANOVA of soft Diffractive BCL MTF data at 548 nm with DZJ heights of 3.0 and 3.3 μm comparing moulded and lathed BCL.**

	Sum of Squares	df	Mean Square	F ratio	signif. of F
Manufacture (M)	0.003	1	0.003	2.104	0.148
DZJ height (H)	0.786	1	0.786	575.567	<0.001
Vergence (V)	2.940	1	2.940	2152.658	<0.001
Spatial Frequency (F)	5.935	15	0.396	289.7	<0.001
M x H	0.051	1	0.051	37.4	<0.001
M x V	0.000	1	0.000	0.002	0.97
M x F	0.021	15	0.001	1.04	0.42
H x V	0.021	1	0.021	15.4	<0.001
H x F	0.157	15	0.010	7.7	<0.001
V x F	0.666	15	0.044	32.5	<0.001
M x H x V	0.004	1	0.004	2.90	0.089
M x H x F	0.027	15	0.002	1.32	0.19
M x V x F	0.010	15	0.001	0.49	0.95
H x V x F	0.019	15	0.001	0.94	0.52
M x H x V x F	0.019	15	0.001	0.94	0.52
Explained	10.843	127	0.085	62.5	<0.001
Residual	0.721	528	0.001		
Total	11.564	655	0.018		

Table A5-13 **ANOVA compares "reverse" add soft diffractive BCL to nominally identical conventional add BCL (tool = 100 μm round; moulded). MTF data at 548 nm**

	Sum of Squares	df	Mean Square	F ratio	signif. of F
Add (A)	0.019	1	0.019	28.642	<0.001
Vergence (V)	0.858	1	0.858	1307.931	<0.001
Spatial Frequency (F)	3.553	15	0.237	361.132	<0.001
A x V	0.679	1	0.679	1034.494	<0.001
A x F	0.005	15	0.0003	0.467	0.956
V x F	0.191	15	0.013	19.398	<0.001
A x V x F	0.132	15	0.009	13.365	<0.001
Explained	5.441	63	0.086	131.664	<0.001
Residual	0.220	336	0.001		
Total	5.662	399	0.014		

APPENDIX 6 The development of a model for changes in optical performance with refractive BCL

A6-1 CENTRED REFRACTIVE BIFOCAL CONTACT LENSES

As a first stage, a MRA model of 2.6 mm COZD refractive BCL over a 4 mm aperture was found in terms of spatial frequency (sf: c.p.mm.). The equations were :

for central optic (CD at distance; CN at near) :
$$\text{mod} = 1 - 0.2\,sf + 0.007\,sf^{2} - 1.3\,sf^{-1} - 1.2\,sf^{-2} - 0.3\,sf^{-3}$$

for peripheral optic (CD at near; CN at distance) :
$$\text{mod} = 1 - 0.2\,sf + 0.009\,sf^{2} - 1.9\,sf^{-1} + 2.4\,sf^{-2} - 0.9\,sf^{-3}$$

(adjusted $R^2 = 0.992$; s.e. = 0.0209; n = 204; $p < 0.0001$)

The large number of spatial frequency terms were required to adequately describe the MTF and to obtain a relatively unbiased spread of residuals. All terms were significant ($p < 0.001$). Though simpler MRA equations were possible, as the equations were to be used for prediction of optical performance the large number of terms was retained.

This model was expanded to include variations in the MTF due to changes in aperture by consideration of the ANOVA results. The MRA for a 2.6 mm COZD BCL over apertures from 2 mm to 6 mm was found. The equations were :

for central optic zone :
$$\text{mod} = 1 - 0.2\,sf + 0.009\,sf^{2} + 1.3\,sf^{-1} - 1.5\,sf^{-2} + 0.5\,sf^{-3} + \text{aperture} \times (0.006\,sf - 0.0002\,sf^{2} - 0.6\,sf^{-1} + 0.6\,sf^{-2} - 0.2\,sf^{-3})$$

for peripheral optic zone :
$$\text{mod} = 0.9 - 0.2\,sf + 0.009\,sf^{2} - 3.0\,sf^{-1} + 2.2\,sf^{-2} - 0.5\,sf^{-3} + \text{aperture} \times (-0.0002\,sf^{2} + 0.3\,sf^{-1} - 0.08\,sf^{-3})$$

(adjusted $R^2 = 0.967$; s.e. = 0.0479; n = 1080; $p < 0.0001$)

This model was further expanded to include variations in the MTF with all five available COZD over apertures from 2 mm to 6 mm. The equations were :

for central optic zone :
$$\text{mod} = 1 - 0.2\,sf + 0.01\,sf^{2} - 0.7\,sf^{-1} + 0.1\,sf^{-3} + \text{aperture} \times (0.06\,sf + 0.002\,sf^{2} - 0.3\,sf^{-1} - 0.3\,sf^{-2} - 0.006\,sf^{-3}) + \text{COZD} \times (0.03\,sf - 0.003\,sf^{2} + 0.2\,sf^{-1} + 0.4\,sf^{-2} - 0.2\,sf^{-3}) + \text{COZD} \times \text{aperture} \times (0.005\,sf - 0.0005\,sf^{2})$$

for peripheral optic zone :
$$\text{mod} = 1 - 0.3\,sf + 0.03\,sf^{2} - 0.9\,sf^{-1} + 0.3\,sf^{-3} + \text{aperture} \times (0.05\,sf - 0.004\,sf^{2} + 0.2\,sf^{-1} - 0.06\,sf^{-3}) + \text{COZD} \times (0.05\,sf - 0.004\,sf^{2} - 0.6\,sf^{-1} + 0.7\,sf^{-2} - 0.2\,sf^{-3}) + \text{COZD} \times \text{aperture} \times (-0.01\,sf + 0.001\,sf^{2})$$

(adjusted $R^2 = 0.949$; s.e. = 0.062; n = 5449; $p < 0.0001$)

Full details of the MRA are given in Appendix 5 (A5-2).

A6-2 RIGID DIFFRACTIVE BIFOCAL CONTACT LENSES

Initially the results obtained for five repetitions at distance and near with a single (2.0 μm DZJ height; 250 μm tool diameter; 548 nm wavelength) rigid diffractive BCL (*Figure 4.2-5*) were described by the equations:

for distance :
$$mod = 1.0 - 0.1\ sf + 0.005\ sf^{2} - 1.9\ sf^{-1} + 2.1\ sf^{-2} - 0.8\ sf^{-3}$$

for near :
$$mod = 1.0 - 0.1\ sf + 0.004\ sf^{2} - 1.3\ sf^{-1} + 1.7\ sf^{-2} - 0.6\ sf^{-3}$$

(adjusted $R^2 = 0.995$; s.e. = 0.015; n = 170; $p < 0.0001$)

As with refractive BCL, the large number of spatial frequency terms were required to obtain an unbiased spread of residuals. This MRA was expanded to include all 2.0 μm DZJ height, 250 μm tool diameter rigid diffractive BCL (548 nm wavelength). Equations at distance and near were found :

for distance :
$$mod = 1.0 - 0.1\ sf + 0.005\ sf^{2} - 1.9\ sf^{-1} + 2.1\ sf^{-2} - 0.8\ sf^{-3}$$

for near :
$$mod = 1.0 - 0.1\ sf + 0.004\ sf^{2} - 1.3\ sf^{-1} + 1.7\ sf^{-2} - 0.6\ sf^{-3}$$

(adjusted $R^2 = 0.946$ (se = 0.049; n = 1309; $p < 0.0001$)

The MRA was further expanded to include all rigid diffractive BCL with each diamond tool. For example the equation with 548 nm wavelength and the 250 μm tool is :

for distance :
$$mod = 1.0 - 0.1\ sf + 0.006\ sf^{2} - 0.8\ sf^{-1} + 2.4\ sf^{-2} - 1.2\ sf^{-3} + DZJHt \times (-0.005\ sf - 0.5\ sf^{-1} - 0.08\ sf^{-2} + 0.2\ sf^{-3}$$

for near :
$$mod = 1.0 - 0.1\ sf + 0.006\ sf^{2} - 3.6\ sf^{-1} + 3.6\ sf^{-2} - 1.2\ sf^{-3} + DZJHt \times (sf^{-1} - 0.9\ sf^{-2} + 0.3\ sf^{-3}$$

($R^2 = 0.915$; s.e. = 0.068; n = 3969; $p < 0.0001$)

Details of the MRA of the other tools are given in Appendix 5 (A5-9).

APPENDIX 7 Tables relating to Visual Performance - section 4.3

Table A7-1 a ANOVA of Contrast Sensitivity results (2, 4, 8, 16 c.p.d.) for CD and CN Refractive BCL with COZD (1.8, 2.2, 2.6, 3.0, 3.4 mm) and BCL decentration and pupil size as covariates.

	Sum of Squares	df	Mean Square	F ratio	signif. of F
decentration	1.753	1	1.753	32.1	<0.001
pupil size	23.460	1	23.460	430.0	<0.001
COZD (D)	0.551	4	0.138	2.53	0.04
Lens Design (L)	0.479	1	0.479	8.8	0.003
Vergence (V)	0.847	1	0.847	15.5	< 0.001
Spatial Frequency (F)	6.399	3	2.133	39.1	< 0.001
D x L	1.361	4	0.340	6.2	< 0.001
D x V	1.138	4	0.285	5.2	< 0.001
D x F	0.315	12	0.026	0.48	0.9
L x V	1.123	1	1.123	20.6	< 0.001
L x F	1.120	3	0.373	6.8	< 0.001
V x F	0.342	3	0.114	2.1	0.1
D x L x V	11.630	4	2.907	52.3	< 0.001
D x L x F	0.229	12	0.019	0.35	0.98
D x V x F	0.313	12	0.026	0.48	0.93
L x V x F	1.627	3	0.542	9.9	< 0.001
D x L x V x F	0.987	12	0.82	1.51	0.12
Explained	52.682	81	0.65	11.9	< 0.001
Residual	51.065	936	0.055		
Total	103.747	1017			

Table A7-1b **ANOVA of Pelli-Robson chart results for CD and CN Refractive BCL with COZD (1.8, 2.2, 2.6, 3.0, 3.4 mm) and BCL decentration and pupil size as covariates.**

	Sum of Squares	df	Mean Square	F ratio	signif. of F
decentration	0.001	1	0.001	0.07	0.8
pupil size	0.675	1	0.675	33.5	<0.001
COZD (D)	0.152	4	0.038	1.9	0.11
Lens Design (L)	0.006	1	0.006	0.3	0.6
Vergence (V)	0.06	1	0.060	3.0	0.09
D x L	0.067	4	0.017	0.8	0.5
D x V	0.164	4	0.41	2.0	0.09
L x V	1.669	1	1.669	82.7	< 0.001
D x L x V	2.586	4	0.646	32.0	< 0.001
Explained	5.534	21	0.264	13.1	< 0.001
Residual	4.701	233	0.20		
Total	10.235	254			

Table A7-1c **ANOVA of Visual Acuity results (10% and 90% contrast) for CD and CN Refractive BCL with COZD (1.8, 2.2, 2.6, 3.0, 3.4 mm) and BCL decentration and pupil size as covariates.**

	Sum of Squares	df	Mean Square	F ratio	signif. of F
decentration	7.464	1	7.464	5.9	0.016
pupil size	78.749	1	78.749	62.1	<0.001
COZD (D)	6.130	4	1.533	1.2	0.3
Lens Design (L)	12.116	1	12.116	9.5	0.002
Vergence (V)	0.829	1	0.829	0.6	< 0.001
Letter Contrast (C)	196.244	1	196.244	154.7	< 0.001
D x L	14.492	4	3.623	2.9	0.02
D x V	36.259	4	9.065	7.1	< 0.001
D x C	7.774	4	1.944	1.5	0.19
L x V	5.955	1	5.955	4.7	0.03
L x C	1.051	1	1.051	0.83	0.36
V x C	0.359	1	0.359	0.283	0.60
D x L x V	285.752	4	71.438	56.3	< 0.001
D x L x C	1.867	4	0.467	0.4	0.83
D x V x C	1.384	4	0.346	0.3	0.90
L x V x C	9.231	1	9.231	7.3	< 0.001
D x L x V x C	20.831	4	5.208	4.1	0.003
Explained	686.382	41	16.741	13.2	< 0.001
Residual	583.690	460	1.269		
Total	1270.071	501			

Table A7-2 **MRA for visual performance measures with refractive BCL of COZD 1.8, 2.2, 2.6, 3.0, and 3.4 mm considered for the COZ and the POZ in focus.**

	CS at 2 c.p.d.		CS at 4 c.p.d.	
adjusted R2		0.490		0.436
standard error		0.173		0.197
n =		259		259
	COZ	POZ	COZ	POZ
constant	0.2153****	0.7575****	-0.5574****	0.5053**
pupil (P)	-0.2490****	-0.2490****		
COZD (C)	0.1521****	-0.0712**	0.1421****	-0.3100****
decen. (D)			0.3481*	0.3481*
P x D	-0.0678****		-0.2720**	-0.2191****
C x D			0.0952*	0.0952*

	CS at 8 c.p.d.		CS at 16 c.p.d.	
adjusted R2		0.444		0.441
standard error		0.245		0.284
n =		259		259
	COZ	POZ	COZ	POZ
constant	0.1167****	0.1167	0.8150*	0.8150*
pupil (P)	-0.1101*		-0.2199****	-0.2199****
COZD (C)	0.0453***	-0.1957****	-0.1127****	-0.2307****
decen. (D)	0.2064****	0.9319****	-0.3371*	0.7313*
P x D	-0.3366****	-0.3366****	-0.2506*	-0.2506*
C x D	0.1797**		0.3080****	

	PRC at 4 m	
adjusted R2		0.551
standard error		0.134
n =		256
	COZ	POZ
constant	-0.3455****	0.3876****
pupil (P)	-0.0632*	
COZD (C)	0.1043****	-0.2639****
decen. (D)		
P x D	-0.1299***	-0.0755***
C x D	0.1040****	0.1040****

	VA low contrast		VA high contrast	
adjusted R2		0.521		0.300
standard error		1.19		0.957
n =		256		256
	COZ	POZ	COZ	POZ
constant	0.1076***	4.9037****	-1.7624****	3.3999****
pupil (P)	-0.9530**			
COZD (C)	0.7293****	-2.8064****	0.4796****	-1.8919****
decen. (D)	-1.6574****			
P x D	-0.9707****	-0.9707****	-0.4792****	
C x D	1.1602****	1.1602****	0.3228**	0.6272****

* - p < 0.1; ** - p < 0.01; *** - p < 0.001; **** p < 0.0001

Table A7-3a **ANOVA of Contrast Sensitivity (2, 4, 8, 16 c.p.d.) investigates the variability of manufacture of rigid Diffractive BCL of two batches of BCL with 2.2 and 2.6 μm DZJ height.**

	Sum of Squares	df	Mean Square	F ratio	signif. of F
Batch (B)	0.006	1	0.006	0.20	0.65
DZJ height (H)	0.035	1	0.035	1.21	0.27
Vergence (V)	0.280	1	0.280	9.73	0.002
Spatial Frequency (F)	2.424	3	0.808	28.1	<0.001
B x H	0.025	1	0.025	0.86	0.36
B x V	0.237	1	0.237	8.26	0.004
B x F	0.086	3	0.029	1.00	0.39
H x V	1.686	1	1.686	58.6	<0.001
H x F	0.073	3	0.024	0.85	0.47
V x F	0.148	3	0.049	1.72	0.16
B x H x V	0.081	1	0.081	2.81	0.09
B x H x F	0.182	3	0.061	2.11	0.10
B x V x F	0.033	3	0.011	0.39	0.76
H x V x F	0.140	3	0.047	1.63	0.18
B x H x V x F	0.034	3	0.011	0.39	0.76
Explained	5.516	31	0.178	6.19	<0.001
Residual	21.052	732	0.029		
Total	26.568	763			

Table A7-3b **ANOVA of Pelli-Robson results investigates the variability of manufacture of rigid Diffractive BCL of two batches of BCL with 2.2 and 2.6 μm DZJ height.**

	Sum of Squares	df	Mean Square	F ratio	signif. of F
Batch (B)	0.092	1	0.092	6.16	0.01
DZJ height (H)	0.004	1	0.004	0.30	0.59
Vergence (V)	0.001	1	0.001	0.07	0.80
B x H	0	1	0	0.015	0.90
B x V	0.116	1	0.116	7.73	0.006
H x V	0.293	1	0.293	19.6	<0.001
B x H x V	0.002	1	0.002	0.16	0.69
Explained	0.525	7	0.525	5.02	<0.001
Residual	2.704	181	0.015		
Total	3.230	188			

Table A7-3c **ANOVA of Visual Acuity (10% and 90% contrast) investigates the variability of manufacture of rigid Diffractive BCL of two batches of BCL with 2.2 and 2.6 μm DZJ height.**

	Sum of Squares	df	Mean Square	F ratio	signif. of F
Batch (B)	0.049	1	0.049	0.04	0.84
DZJ height (H)	6.646	1	6.646	5.75	0.02
Vergence (V)	8.365	1	8.365	7.24	0.007
Contrast (C)	161.203	1	161.203	139.6	<0.001
B x H	3.669	1	3.669	3.18	0.08
B x V	2.423	1	2.423	2.10	0.15
B x C	0.811	1	0.811	0.70	0.40
H x V	60.914	1	60.914	52.7	<0.001
H x C	4.534	1	4.534	3.93	0.05
V x C	0.328	1	0.328	0.28	0.60
B x H x V	0.563	1	0.563	0.49	0.49
B x H x C	0.160	1	0.160	0.14	0.71
B x V x C	0.298	1	0.298	0.26	0.61
H x V x C	0.083	1	0.093	0.94	0.33
B x H x V x C	0.009	1	0.009	0.01	0.93
Explained	252.122	15	16.808	14.6	<0.001
Residual	418.078	362	1.155		
Total	670.200	377			

Table A7-4a **ANOVA of Contrast Sensitivity (2, 4, 8, 16 c.p.d.) investigates differences between experimental rigid Diffractive BCL and Pilkington Diffrax, both with 2.0 μm DZJ height.**

	Sum of Squares	df	Mean Square	F ratio	signif. of F
Batch (B)	0.022	1	0.022	0.80	0.38
Vergence (V)	1.359	1	1.359	48.5	<0.001
Spatial Frequency (F)	0.516	3	0.172	6.13	<0.001
B x V	0.813	1	0.813	29.0	<0.001
B x F	0.087	3	0.029	1.03	0.38
V x F	0.333	3	0.111	3.95	0.009
B x V x F	0.019	3	0.006	0.23	0.88
Explained	3.133	15	0.209	7.45	<0.001
Residual	7.181	256	0.028		
Total	10.314	271			

Table A7-4b **ANOVA of Pelli-Robson results investigates differences between experimental rigid Diffractive BCL and Pilkington Diffrax, both with 2.0 μm DZJ height.**

	Sum of Squares	df	Mean Square	F ratio	signif. of F
Batch (B)	0.002	1	0.002	0.27	0.61
Vergence (V)	0.494	1	0.494	54.8	<0.001
B x V	0.014	1	0.014	1.56	0.22
Explained	0.511	3	0.170	18.9	<0.001
Residual	0.541	60	0.009		
Total	1.052	63			

Table A7-4c **ANOVA of Visual Acuity (10% and 90% contrast) investigates differences between experimental rigid Diffractive BCL and Pilkington Diffrax, both with 2.0 μm DZJ height.**

	Sum of Squares	df	Mean Square	F ratio	signif. of F
Batch (B)	0.294	1	0.294	0.57	0.45
Vergence (V)	46.561	1	46.561	89.9	<0.001
Contrast (C)	42.573	1	42.573	82.2	<0.001
B x V	1.027	1	1.027	1.98	0.16
B x C	1.614	1	1.614	3.12	0.08
V x C	0.813	1	0.813	1.57	0.21
B x V x C	0.032	1	0.032	0.061	0.81
Explained	92.913	7	13.273	94.617	<0.001
Residual	62.146	120	0.518		
Total	155.059	127			

Table A7-5a **ANOVA of Contrast Sensitivity Results (2, 4, 8, 16 c.p.d.) with rigid diffractive BCL with DZJ height (1.8, 2.0, 2.2, 2.5, 2.6, 3.0 μm) and tool (250 μm, 100 μm, flatted).**

	Sum of Squares	df	Mean Square	F ratio	signif. of F
DZJ Height (H)	1.558	5	0.312	10.7	< 0.001
Tool (T)	0.391	2	0.195	6.69	0.001
Vergence (V)	0.038	1	0.038	1.29	0.26
Spatial Frequency (F)	5.315	3	1.772	60.6	< 0.001
H x T	0.914	10	0.091	3.13	0.001
H x V	10.331	5	2.066	70.7	< 0.001
H x F	0.418	15	0.028	0.95	0.50
T x V	1.270	2	0.635	21.7	< 0.001
T x F	0.162	6	0.027	0.92	0.48
V x F	0.254	3	0.085	2.90	0.03
H x T x V	1.375	10	0.137	4.70	< 0.001
H x T x F	0.678	30	0.023	0.77	0.81
H x V x F	1.285	15	0.086	2.93	< 0.001
T x V x F	0.194	6	0.032	1.10	0.36
H x T x V x F	0.502	30	0.017	0.57	0.97
Explained	24.494	143	0.171	5.86	< 0.001
Residual	56.247	1924	0.029		
Total	80.741	2067			

Table A7-5b **ANOVA of Pelli-Robson chart results with Rigid Diffractive BCL with DZJ height (1.8, 2.0, 2.2, 2.5, 2.6, 3.0 μm) and tool (250 μm, 100 μm, flatted).**

	Sum of Squares	df	Mean Square	F ratio	signif. of F
DZJHt (H)	0.135	5	0.027	2.2	0.051
Tool (T)	0.164	2	0.082	6.7	0.001
Vergence (V)	0.200	1	0.200	16.4	< 0.001
H x T	0.058	10	0.006	0.48	0.91
H x V	2.527	5	0.505	41.5	< 0.001
T x V	0.236	2	0.118	9.7	< 0.001
H x T x V	0.248	10	0.025	2.04	0.028
Explained	3.499	35	0.100	8.2	< 0.001
Residual	5.760	473	0.20		
Total	9.259	508			

Table A7-5c **ANOVA of Visual Acuity results (10% and 90% contrast) with Rigid Diffractive BCL with DZJ height (1.8, 2.0, 2.2, 2.5, 2.6, 3.0 μm) and tool (250 μm, 100 μm, flatted).**

	Sum of Squares	df	Mean Square	F ratio	signif. of F
DZJHt (H)	65.789	5	13.158	15.6	< 0.001
Tool (T)	1.909	2	0.955	1.13	0.32
Vergence (V)	26.928	1	26.928	32.0	< 0.001
Letter Contrast (H)	433.165	1	433.165	514.4	< 0.001
H x T	25.578	10	2.558	3.04	0.001
H x V	336.768	5	67.354	80.0	< 0.001
H x H	10.762	5	2.152	2.6	0.026
T x V	66.918	2	33.459	39.7	< 0.001
T x H	0.351	2	0.176	0.21	0.81
V x H	0.077	1	0.077	0.09	0.76
H x T x V	35.304	10	3.530	4.2	< 0.001
H x T x C	3.261	10	0.326	0.39	0.95
H x V x C	19.343	5	3.869	4.6	< 0.001
T x V x C	1.062	2	0.531	0.63	0.53
H x T x V x C	8.292	10	0.829	0.985	0.46
Explained	1018.013	71	14.338	17.0	< 0.001
Residual	796.693	946	0.842		
Total	1814.706	1017			

Table A7-6a **ANOVA of Contrast Sensitivity Results (2, 4, 8, 16 c.p.d.) with rigid diffractive BCL (DZJ height = 2.0 μm) compares four different tools (250 μm, 100 μm, 50 μm, flatted).**

	Sum of Squares	df	Mean Square	F ratio	signif. of F
Tool (T)	0.523	3	0.174	6.90	< 0.001
Vergence (V)	2.016	1	2.016	79.7	< 0.001
Spatial Frequency (F)	0.923	3	0.308	12.2	< 0.001
T x V	0.500	3	0.167	6.59	< 0.001
T x F	0.068	9	0.008	0.30	0.98
V x F	0.383	3	0.128	5.05	0.002
T x V x F	0.135	9	0.015	0.59	0.80
Explained	4.548	31	0.147	5.80	< 0.001
Residual	13.761	544	0.025		
Total	18.309	575			

Table A7-6b **ANOVA of Pelli-Robson chart results with Rigid Diffractive BCL (DZJ height = 2.0 μm) compares four different tools (250 μm, 100 μm, 50 μm, flatted).**

	Sum of Squares	df	Mean Square	F ratio	signif. of F
Tool (T)	0.164	2	0.082	6.7	0.001
Vergence (V)	0.200	1	0.200	16.4	< 0.001
T x V	0.236	2	0.118	9.7	< 0.001
Explained	3.499	35	0.100	8.2	< 0.001
Residual	5.760	473	0.20		
Total	9.259	508			

Table A7-6c **ANOVA of Visual Acuity results (10% and 90% contrast) with Rigid Diffractive BCL (DZJ height = 2.0 μm) compares four different tools (250 μm, 100 μm, 50 μm, flatted).**

	Sum of Squares	df	Mean Square	F ratio	signif. of F
Tool (T)	4.845	3	1.615	3.18	0.025
Vergence (V)	78.334	1	78.334	154.0	< 0.001
Letter Contrast (C)	82.949	1	82.949	163.1	< 0.001
T x V	6.625	3	2.208	4.34	0.005
T x C	0.650	3	0.217	0.43	0.73
V x C	0.814	1	0.814	1.60	0.21
T x V x C	0.189	3	0.063	0.12	0.95
Explained	174.407	15	11.627	22.9	< 0.001
Residual	134.247	264	0.509		
Total	308.654	279			

Table A7-7a **MRA for visual performance measures with rigid diffractive BCL made with the 250 μm tool.**

CS at 2 c.p.d.		adjusted R^2	0.108
standard error	0.117	n =	278
	Constant		DZJ height
Distance	-0.0887		-0.1111
Near	-0.3866		0.0260
CS at 4 c.p.d.		adjusted R^2	0.272
standard error	0.170	n =	278
	Constant		DZJ height
Distance	0.1416		-0.2350
Near	-0.7892		0.1645
CS at 8 c.p.d.		adjusted R^2	0.250
standard error	0.201	n =	278
	Constant		DZJ height
Distance	0.1470		-0.2431
Near	-0.9179		0.2028
CS at 16 c.p.d.		adjusted R^2	0.264
standard error	0.223	n =	278
	Constant		DZJ height
Distance	0.2291		-0.2939
Near	-0.9670		0.1936
PRC at 4 m		adjusted R^2	0.383
standard error	0.117	n =	270
	Constant		DZJ height
Distance	0.1366		-0.2103
Near	-0.6773		0.1198
VA low contrast		adjusted R^2	0.464
standard error	1.104	n =	270
	Constant		DZJ height
Distance	2.3908		-2.1007
Near	-6.8158		1.6033
VA high contrast		adjusted R^2	0.410
standard error	0.891	n =	270
	Constant		DZJ height
Distance	1.8977		-1.3309
Near	-4.7146		1.2723

all terms significant $p < 0.0001$

Table A7-7b **MRA for visual performance measures with rigid diffractive BCL made with the 100 μm tool.**

CS at 2 c.p.d.		adjusted R^2	0.042
standard error	0.124	n =	149
	Constant		DZJ height
Distance	-0.1721		-0.0608
Near	-0.4566		0.0669
CS at 4 c.p.d.		adjusted R^2	0.300
standard error	0.137	n =	149
	Constant		DZJ height
Distance	0.0637		-0.1777
Near	-0.8023		0.1909
CS at 8 c.p.d.		adjusted R^2	0.228
standard error	0.172	n =	149
	Constant		DZJ height
Distance	0.0156		-0.1583
Near	-0.9029		0.1998
CS at 16 c.p.d.		adjusted R^2	0.170
standard error	0.199	n =	149
	Constant		DZJ height
Distance	-0.0708		-0.1639
Near	-0.9926		0.2154
PRC at 4 m		adjusted R^2	0.380
standard error	0.102	n =	147
	Constant		DZJ height
Distance	0.1568		-0.2015
Near	-0.6192		0.1119
VA low contrast		adjusted R^2	0.358
standard error	1.063	n =	147
	Constant		DZJ height
Distance	2.0993		-1.9270
Near	-5.6194		1.1540
VA high contrast		adjusted R^2	0.358
standard error	0.884	n =	147
	Constant		DZJ height
Distance	2.7472		-1.6819
Near	-3.3522		0.7093

all terms significant $p < 0.0001$

Table A7-7c **MRA for visual performance measures with rigid diffractive BCL made with the Flatted tool.**

CS at 2 c.p.d.		adjusted R^2	0.085
standard error	0.125	n =	131
	Constant		DZJ height
Distance	-0.2941		-0.0384
Near	-0.5201		0.0818
CS at 4 c.p.d.		adjusted R^2	0.427
standard error	0.157	n =	131
	Constant		DZJ height
Distance	0.0884		-0.2310
Near	-0.9454		0.2623
CS at 8 c.p.d.		adjusted R^2	0.240
standard error	0.195	n =	131
	Constant		DZJ height
Distance	-0.0151		-0.1875
Near	-0.9112		0.2310
CS at 16 c.p.d.		adjusted R^2	0.273
standard error	0.189	n =	131
	Constant		DZJ height
Distance	-0.0717		-0.1925
Near	-0.9665		0.2340
PRC at 4 m		adjusted R^2	0.338
standard error	0.119	n =	131
	Constant		DZJ height
Distance	0.0717		-0.1850
Near	-0.6859		0.1544
VA low contrast		adjusted R^2	0.444
standard error	1.150	n =	131
	Constant		DZJ height
Distance	2.8339		-2.4917
Near	-4.7278		1.0806
VA high contrast		adjusted R^2	0.407
standard error	1.008	n =	131
	Constant		DZJ height
Distance	3.5444		-2.1861
Near	-2.5547		0.6500

all terms significant $p < 0.0001$

Table A7-8a **ANOVA of Contrast Sensitivity Results (2, 4, 8, 16 c.p.d.) with soft diffractive BCL (DZJ height = 3.0 μm, 100 μm tool) compares "reverse" add to conventional add BCL.**

	Sum of Squares	df	Mean Square	F ratio	signif. of F
Lens Type (T)	0.099	1	0.099	2.81	0.10
Vergence (V)	0.006	1	0.006	0.18	0.67
Spatial Frequency (F)	1.824	3	0.608	17.3	< 0.001
T x V	1.364	1	1.364	38.7	< 0.001
T x F	0.047	3	0.016	0.44	0.72
V x F	0.019	3	0.006	0.18	0.91
T x V x F	0.038	3	0.013	0.36	0.78
Explained	3.398	15	0.227	6.43	< 0.001
Residual	7.326	208	0.035		
Total	10.724	223			

Table A7-8b **ANOVA of Pelli-Robson chart results with soft diffractive BCL (DZJ height = 3.0 μm, 100 μm tool) compares "reverse" add to conventional add BCL.**

	Sum of Squares	df	Mean Square	F ratio	signif. of F
Lens Type (T)	0.004	1	0.004	0.17	0.69
Vergence (V)	0.001	1	0.001	0.05	0.83
T x V	0.309	1	0.309	14.4	< 0.001
Explained	0.314	3	0.105	4.86	0.005
Residual	1.184	55	0.022		
Total	1.497	58			

Table A7-8c **ANOVA of Visual Acuity results (10% and 90% contrast) with soft diffractive BCL (DZJ height = 3.0 μm, 100 μm tool) compares "reverse" add to conventional add BCL.**

	Sum of Squares	df	Mean Square	F ratio	signif. of F
Lens Type (T)	8.771	1	8.771	4.57	0.035
Vergence (V)	0.002	1	0.002	0.001	0.98
Letter Contrast (C)	85.554	1	85.554	44.5	< 0.001
T x V	11.103	1	11.103	5.78	0.018
T x C	0.672	1	0.672	0.35	0.56
V x C	0.038	1	0.038	0.02	0.89
T x V x C	1.575	1	1.575	0.82	0.37
Explained	107.701	7	15.386	8.01	< 0.001
Residual	211.376	110	1.922		
Total	319.076	117			

APPENDIX 8 Tables relating to the prediction of Optical and Visual Performance from surface profile measurements of rigid diffractive bifocal contact lenses - section 4.5

Table A8-1a **MRA which described optical performance (average modulation) with rigid diffractive BCL at 548 nm and 573 nm in terms of the measured DZJ height of the third DZJ. All terms were highly significant (p < 0.0001).**

Wavelength: 548 nm		adjusted R^2	0.784
standard error	0.047	n =	46
	Constant		DZJ height
Distance	0.5728		-0.1717
Near	-0.1969		0.2146

Wavelength: 573 nm		adjusted R^2	0.751
standard error	0.047	n =	43
	Constant		DZJ height
Distance	0.5466		-0.1574
Near	-0.1885		0.1972

Table A8-1b **MRA which described optical performance (average modulation) with rigid diffractive BCL at 548 nm and 573 nm in terms of the average measured DZJ height. All terms were highly significant (p < 0.0001).**

Wavelength: 548 nm		adjusted R^2	0.807
standard error	0.044	n =	46
	Constant		DZJ height
Distance	0.6043		-0.1877
Near	-0.2366		0.2347

Wavelength: 573 nm		adjusted R^2	0.782
standard error	0.044	n =	43
	Constant		DZJ height
Distance	0.5800		-0.1740
Near	-0.2232		0.2146

Table A8-2 **MRA which described the visual performance with rigid diffractive BCL in terms of the average measured DZJ height. All terms were highly significant ($p < 0.0001$).**

CS at 2 c.p.d.		adjusted R^2	0.394
standard error	0.080	n =	48
	Constant		DZJ height
Distance	0.1051		-0.2181
Near	-0.3326		
CS at 4 c.p.d.		adjusted R^2	0.425
standard error	0.129	n =	48
	Constant		DZJ height
Distance	0.3647		-0.3749
Near	-0.4157		
CS at 8 c.p.d.		adjusted R^2	0.414
standard error	0.172	n =	48
	Constant		DZJ height
Distance	0.4275		-0.4153
Near	-0.9610		0.2246
CS at 16 c.p.d.		adjusted R^2	0.438
standard error	0.190	n =	48
	Constant		DZJ height
Distance	0.4424		-0.2477
Near	-1.1361		0.1586
PRC at 4 m		adjusted R^2	0.517
standard error	0.092	n =	48
	Constant		DZJ height
Distance	0.1598		-0.2477
Near	-0.7442		0.1586
VA low contrast		adjusted R^2	0.635
standard error	0.990	n =	48
	Constant		DZJ height
Distance	3.9218		-3.0884
Near	-8.4645		2.4565
VA high contrast		adjusted R^2	0.559
standard error	0.766	n =	48
	Constant		DZJ height
Distance	1.9175		-1.5036
Near	-5.8004		1.7812

APPENDIX 9 Tables relating to the prediction of Visual Performance from Optical Performance measurements - section 4.6

Table A9-1a **MRA which described visual performance with refractive BCL in terms of the log relative MTF measured at 4, 12, 25 and 66 c.p.d. with the BCL over a 3 mm aperture stop.**

	CS at 2 c.p.d.		CS at 4 c.p.d.	
Adjusted R^2	0.394		0.737	
s.e.	0.112		0.083	
n =	36		36	
p	= 0.0001		< 0.0001	
constant	-0.3218	****	-0.3062	****
4 c.p.d.	0.4659	****	0.5348	****
12 c.p.d.			-0.4230	****
25 c.p.d.	-0.4005	****		
66 c.p.d.			0.0902	*

	CS at 8 c.p.d.		CS at 16 c.p.d.	
Adjusted R^2	0.518		0.446	
s.e.	0.121		0.140	
n =	36		36	
p	< 0.0001		< 0.0001	
constant	-0.4171	****	-0.4239	****
4 c.p.d.	0.6139	****	0.5685	****
12 c.p.d.	-0.5612	***	-0.3083	**
25 c.p.d.	0.1775			
66 c.p.d.			0.0902	*

	PRC at 4m	
Adjusted R^2	0.610	
s.e.	0.098	
n =	36	
p	< 0.0001	
constant	-0.3279	****
4 c.p.d.	0.6479	****
12 c.p.d.	-0.5125	****
25 c.p.d.		
66 c.p.d.		

	low contrast VA		high contrast VA	
Adjusted R^2	0.643		0.511	
s.e.	0.741		0.689	
n =	36		36	
p	< 0.0001		< 0.0001	
constant	-1.5696	****	-0.0820	
4 c.p.d.	3.2481	**		
12 c.p.d.	-2.7276	****	-0.5639	*
25 c.p.d.				
66 c.p.d.	0.8732	*	1.3050	****

Table A9-1b MRA which described visual performance with refractive BCL in terms of the log relative MTF measured at 4, 12, 25 and 66 c.p.d. with the BCL over a 3.5 mm aperture stop.

	CS at 2 c.p.d.		CS at 4 c.p.d.	
Adjusted R^2	0.371		0.569	
s.e.	0.116		0.099	
n =	34		34	
p	= 0.0003		< 0.0001	
constant	-0.2237	****	-0.2614	****
4 c.p.d.			0.2245	**
12 c.p.d.			-0.1674	**
25 c.p.d.	-0.1970	****		
66 c.p.d.			0.1153	*

	CS at 8 c.p.d.		CS at 16 c.p.d.	
Adjusted R^2	0.366		0.329	
s.e.	0.141		0.158	
n =	34		34	
p	= 0.0001		= 0.0002	
constant	-0.4001	****	-0.3980	****
4 c.p.d.	0.2143	****	0.2233	****
12 c.p.d.				
25 c.p.d.				
66 c.p.d.				

	PRC at 4m	
Adjusted R^2	0.540	
s.e.	0.107	
n =	34	
p	< 0.0001	
constant	-0.2183	****
4 c.p.d.	0.1727	*
12 c.p.d.		
25 c.p.d.	-0.2327	****
66 c.p.d.	0.1835	**

	low contrast VA		high contrast VA	
Adjusted R^2	0.721		0.543	
s.e.	0.652		0.546	
n =	34		34	
p	< 0.0001		< 0.0001	
constant	-1.4400	****	-0.5924	****
4 c.p.d.	2.7969	****	1.1804	****
12 c.p.d.	-1.8809	****		
25 c.p.d.				
66 c.p.d.	0.6318	*		

* = p < 0.1; ** = p < 0.01; *** p < 0.001; **** = p < 0.0001

Table A9-1c MRA which described visual performance with refractive BCL in terms of the log relative MTF measured at 4, 12, 25 and 66 c.p.d. with the BCL over a 4 mm aperture stop.

	CS at 2 c.p.d.		CS at 4 c.p.d.	
Adjusted R^2	0.467		0.778	
s.e.	0.105		0.077	
n =	36		36	
p	< 0.0001		< 0.0001	
constant	-0.2490	****	-0.2336	****
4 c.p.d.				
12 c.p.d.	1.4096	****	1.4004	****
25 c.p.d.	-0.9920	****	-0.7673	****
66 c.p.d.				

	CS at 8 c.p.d.		CS at 16 c.p.d.	
Adjusted R^2	0.554		0.461	
s.e.	0.116		0.138	
n =	36		36	
p	< 0.0001		< 0.0001	
constant	-0.3108	****	-0.3097	****
4 c.p.d.	-0.2401	*	-0.3349	*
12 c.p.d.	1.5015	**	1.6806	**
25 c.p.d.	-0.6157	*	-0.6734	*
66 c.p.d.				

	PRC at 4m	
Adjusted R^2	0.803	
s.e.	0.069	
n =	36	
p	< 0.0001	
constant	-0.2012	****
4 c.p.d.		
12 c.p.d.	1.7661	****
25 c.p.d.	-1.1410	****
66 c.p.d.		

	low contrast VA		high contrast VA	
Adjusted R^2	0.643		0.469	
s.e.	0.741		0.718	
n =	36		36	
p	< 0.0001		< 0.0001	
constant	-1.5696	****	-0.2047	
4 c.p.d.				
12 c.p.d.	10.1367	****	1.1940	*
25 c.p.d.	-5.4268	****		
66 c.p.d.			0.6292	*

* = p < 0.1; ** = p < 0.01; *** p < 0.001; **** = p < 0.0001

Table A9-1d MRA which described visual performance with refractive BCL in terms of the log relative MTF measured at 4, 12, 25 and 66 c.p.d. with the BCL over a 5 mm aperture stop.

	CS at 2 c.p.d.		CS at 4 c.p.d.	
Adjusted R^2	0.365		0.751	
s.e.	0.114		0.081	
n =	36		36	
p	= 0.0001		< 0.0001	
constant	-0.1663	****	-0.1623	****
4 c.p.d.	0.3102	****	-0.3919	*
12 c.p.d.				
25 c.p.d.			0.7531	****
66 c.p.d.				

	CS at 8 c.p.d.		CS at 16 c.p.d.	
Adjusted R^2	0.505		0.415	
s.e.	0.122		0.144	
n =	36		36	
p	< 0.0001		= 0.0001	
constant	-0.2926	****	-0.3277	****
4 c.p.d.	-0.4987	*		
12 c.p.d.				
25 c.p.d.	1.0650	****	0.8676	****
66 c.p.d.	-0.1673	*	0.2899	***

	PRC at 4m	
Adjusted R^2	0.792	
s.e.	0.071	
n =	36	
p	< 0.0001	
constant	-0.1178	****
4 c.p.d.		
12 c.p.d.	0.4875	****
25 c.p.d.		
66 c.p.d.		

	low contrast VA		high contrast VA	
Adjusted R^2	0.797		0.422	
s.e.	0.560		0.750	
n =	36		36	
p	< 0.0001		< 0.0001	
constant	-0.6344	**	-2.4078	****
4 c.p.d.				
12 c.p.d.				
25 c.p.d.	-1.8809	****	4.3200	****
66 c.p.d.	-0.6853	*		

* = p < 0.1; ** = p < 0.01; *** p < 0.001; **** = p < 0.0001

Table A9-2a MRA which described visual performance with rigid diffractive BCL in terms of the log relative MTF measured at 4, 12, 25 and 66 c.p.d. using the 548 nm interference filter.

	CS at 2 c.p.d.		CS at 4 c.p.d.	
Adjusted R^2	0.478		0.785	
s.e.	0.061		0.078	
n =	46		46	
p	< 0.0001		< 0.0001	
constant	-0.2287	****	-0.1377	****
4 c.p.d.				
12 c.p.d.	0.2395	****	0.6070	****
25 c.p.d.				
66 c.p.d.				

	CS at 8 c.p.d.		CS at 16 c.p.d.	
Adjusted R^2	0.641		0.598	
s.e.	0.096		0.117	
n =	46		46	
p	< 0.0001		< 0.0001	
constant	-0.2135	****	-0.2143	****
4 c.p.d.				
12 c.p.d.				
25 c.p.d.			0.5229	****
66 c.p.d.	0.5345	****		

	PRC at 4m	
Adjusted R^2	0.691	
s.e.	0.061	
n =	46	
p	< 0.0001	
constant	-0.2281	****
4 c.p.d.		
12 c.p.d.	0.3975	*
25 c.p.d.	-0.3926	*
66 c.p.d.	0.4199	*

	low contrast VA		high contrast VA	
Adjusted R^2	0.707		0.695	
s.e.	0.645		0.500	
n =	46		46	
p	< 0.0001		< 0.0001	
constant	-1.2076	****	-0.5397	***
4 c.p.d.			-1.6763	**
12 c.p.d.				
25 c.p.d.				
66 c.p.d.	4.5230	****	4.9089	****

* = p < 0.1; ** = p < 0.01; *** p < 0.001; **** = p < 0.0001

Table A9-2b MRA which described visual performance with rigid diffractive BCL in terms of the log relative MTF measured at 4, 12, 25 and 66 c.p.d. using the 573 nm interference filter.

	CS at 2 c.p.d.		CS at 4 c.p.d.	
Adjusted R^2	0.402		0.819	
s.e.	0.056		0.063	
n =	42		42	
p	< 0.0001		< 0.0001	
constant	-0.2499	****	-0.1539	****
4 c.p.d.				
12 c.p.d.	0.2216	****	0.6452	****
25 c.p.d.				
66 c.p.d.				

	CS at 8 c.p.d.		CS at 16 c.p.d.	
Adjusted R^2	0.731		0.684	
s.e.	0.076		0.092	
n =	42		42	
p	< 0.0001		= 0.0001	
constant	-0.1937	****	-0.2089	****
4 c.p.d.				
12 c.p.d.	0.6006	****		
25 c.p.d.			0.6014	****
66 c.p.d.				

	PRC at 4m	
Adjusted R^2	0.801	
s.e.	0.044	
n =	42	
p	< 0.0001	
constant	-0.2469	****
4 c.p.d.		
12 c.p.d.	0.3525	*
25 c.p.d.	-0.3826	*
66 c.p.d.	0.4863	**

	low contrast VA		high contrast VA	
Adjusted R^2	0.880		0.765	
s.e.	0.430		0.449	
n =	42		42	
p	< 0.0001		< 0.0001	
constant	-0.9045	****	-0.2462	*
4 c.p.d.				
12 c.p.d.	2.9911	*		
25 c.p.d.				
66 c.p.d.	2.6652	*	3.9457	****

* = p < 0.1; ** = p < 0.01; *** p < 0.001; **** = p < 0.0001

BIBLIOGRAPHY AND REFERENCES

Adams, A.J., Wong, L.S., Wong, L. and Gould, B. (1988) Visual acuity changes with age: some new perspectives. *Am. J. Optom. Physiol. Opt.*, 65(5) : 403-406

Allen, M.J. and Vos, J.J. (1967) Ocular scattered light and visual performance as a function of age. *Am. J. Optom. Arch. Am. Acad. Optom.*, 44 : 717-727

Arden, G.B. and Jacobson, J. (1978) A simple grating test for contrast sensitivity. *Invest. Ophthalmol. Vis. Sci.*, 17 : 23-32

Atebara, N.H. and Miller, D. (1990) An optical model to describe image contrast with bifocal intraocular lenses. *Am. J. Ophthalmol.*, 110 : 172-177

Back, A.P., Holden, B.A. and Hine, N.A. (1989) Correction of presbyopia with contact lenses: Comparative success rates with three systems. *Optom. Vision Sci.*, 66(8) : 518-525

Back, A.P., Holden, B.A. and Hine, N.A. (1990) Author's response. *Optom. Vis. Sci.*, 67(3) : 235-236

Back, A. and Sayer, G. (1985) The value of near stereopsis in predicting the performance of bifocal contact lenses. (abstract) *Am. J. Optom. Physiol. Opt.*, 62(10): 6P

Back, A.P., Woods, R.L. and Holden, B.A. (1986) The comparative visual performance of monovision and various concentric bifocals. (abstract) *Am. J. Optom. Physiol. Opt.*, 63(12s) : 104P

Back, A.P., Woods, R.L. and Holden, B.A. (1987) The comparative visual performance of monovision and various concentric bifocals. *Trans Br. Contact Lens Assoc. Ann. Clinical Conf. 1987.* : 46-47

Bailey, I.L. and Lovie, J.E. (1976) New design principles for visual acuity letter charts. *Am. J. Optom. Physiol. Opt.*, 53(11) : 740-745

Barbur, J.L., Thomson, W.D. and Forsyth, P.M. (1987) A new system for the simultaneous measurement of pupil size and two dimensional eye movements. *Clin. Vision Sci.*, 2(2) : 131-142

Baude, D. and Miege, C. (1992) Presbyopia compensation with contact lenses - A new aspherical progressive lens. *J. Br. Contact Lens Assoc.*, 15(1) : 7-15

Beard, B.L., Neufeld, S. and Yager, D. (1990) Age-related reductions in sensitivity are not evident at suprathreshold contrast levels. (abstract) *Invest. Ophthalmol. Vis. Sci.* 31(4) : 51

Beddow, R.D., Martin, J.S., and Pheiffer, C.H. (1966) Presbyopic patients and single vision contact lenses. *Southern J. Optom.*, 8 : 9-11

Bedford, R.E., and Wyszecki, G. (1957) Axial chromatic aberration of the human eye. *J. Opt. Soc. Am.*, 47(6) : 564-565

Benjamin, W.J. (1990) Wet cells, back-surface bifocals, and the "lacrimal lens theory". *Int. Contact Lens Clin.*, 17(5) : 157-158

Bennett, A.G., and Rabbetts, R.B. (1984) *Clinical Visual Optics.* Butterworths, London

Bier, N. (1967) Prescribing for presbyopia with contact lenses. *Am. J. Optom. Arch. Am. Acad. Optom.*, 44(11) : 687-710

Bier, N. and Lowther, G.E. (1977) *Contact Lens Correction.* Butterworths, London

Birren, J.E., Casperson, R.C., and Botwinick, J. (1950) Age changes in pupil size. *J. Gerontol.*, **5** : 216-225

Black, G. and Linfoot, E.H. (1957) Spherical aberration and the information content of optical images. *Proc. Roy. Soc.*, **A239** : 522-540

Blackwell, H.R. (1952) Studies of psychophysical methods for measuring visual thresholds. *J. Opt. Soc. Am.*, **42**(9) : 606-616

Blackwell, O.M. and Blackwell, H.R. (1971) Visual performance data for 156 normal observers of various ages. *J. Illum. Eng. Soc.*, **1** : 3-13

Bland, J.M. and Altman, D.G. (1986) Statistical methods for assessing agreement between two methods of clinical measurement. *Lancet*, **8476** : 307-310

Borish, I.M. (1988) Pupil dependency of bifocal contact lenses. *Am. J. Optom. Physiol. Opt.*, **65**(5) : 417-423

Borish, I.M. and Perrigan, D. (1987) Relative movement of lower lid and line of sight from distant to near fixation. *Am. J. Optom. Physiol. Opt.*, **64**(12) : 881-887

Borish, I.M. and Soni, S. (1982) Bifocal contact lenses. *J. Am. Optom. Assoc.*, **53**(3) : 219-229

Born, M. and Wolf, E. (1980) *Principles of Optics. Electromagnetic theory of propagation, interference and diffraction of light.* Pergamon Press, Oxford, 6th Edition

Bouma, H. (1971) Visual recognition of isolated lower-case letters. *Vision Res.*, **11**: 459-474

Bradley, A., Rhaman, H., Soni, S. and Zhang, X. (1991a) Through-focus measures of vision with 2-zone and diffractive bifocal contact lenses. (abstract) *Optom. Vision Sci.*, **68**(12s) : 136

Bradley, A., Thomas, T., Kalaher, M. and Hoerres, M. (1991b) Effects of spherical and astigmatic defocus on acuity and contrast sensitivity: A comparison of three clinical charts. *Optom. Vision Sci.*, **68**(6) : 418-426

Breger, J.L. (1983) New design elements for a gas permeable bifocal. *Contacto*, **27**: 31-32

British Standards Institution (1968) *Specification for test charts for determining distance visual acuity.* BS 4274, HMSO, London

British Standards Institution (1971/ 1982) *Recommendations for measurement of the optical transfer function of optical devices.* BS 4779, HMSO, London

British Standards Institution (1979) *Glossary of terms relating to contact lenses.* BS 5321, HMSO, London

British Standards Institution (1979) *Precision of test methods 1: Guide for the determination and reproducibility for a standard test method.* BS 5749, part 1, HMSO, London

Brown, B., Bowman, K.J. and Collins, M.J. (1987) Visual performance with multifocal contact lenses and spectacles. Report to Department of Transport and Communications, Australia

Brown, B., Collins, M.J., and Bowman, K.J. (1988) Reaction times in a complex task by presbyopic observers with spectacle and contact lens corrections. *Clin. Exp. Optom.*, **71**(3) : 94-99

Brown, B. and Lovie-Kitchin, J.E. (1989) High and low contrast acuity and clinical contrast sensitivity tested in a normal population. *Optom. Vision Sci.*, **66**(7) : 467-473

Burnett Hodd, N.F. (1991) Bifocal contact lenses. How successful are they ? *Optom. Today*, 6 May : 14-17

Campbell, F.W. and Green, D.G. (1965a) Optical and retinal factors affecting visual resolution. *J. Physiol.*, **181** : 576-593

Campbell, F.W. and Green, D.G. (1965b) Monocular versus binocular visual acuity. *Nature*, **208** : 191-192

Campbell, F.W. and Gregory, A.H. (1960) Effect of pupil size on visual acuity. *Nature*, **187** : 1121-1123

Campbell, F.W. and Gubisch, R.W. (1966) Optical quality of the human eye. *J. Physiol.*, **186** : 558-578

Campbell, F.W. and Robson, J.G. (1964) Application of Fourier analysis to the modulation response of the eye. (abstract) *J. Opt. Soc. Am.*, **54** : 581

Campbell, F.W. and Robson, J.G. (1968) Application of Fourier analysis to the visibility of gratings. *J. Physiol.*, **197** : 551-566

Campbell, M.C.W., Harrison, E.M. and Simonet, P. (1990) Psychophysical measurement of the blur on the retina due to optical aberrations of the eye. *Vision Res.*, 30(11) : 1587-1602

Canas, R.G. and Smith, R.W. (1989) Measurements on surface relief diffractive optical elements. *I.E.R.E. publication*, **311** : 160-163

Carmichael, C.A. (1986) personal communication

Carmichael, C.A. (1987) The alges bifocal : patient selection and fitting. *Contact Lens J.*, **15**(2) : 9

Charman, W.N. (1983a) Power variation across concentric, multifocal contact lenses. *Int. Contact Lens Clinic*, **10**(5) : 301-304

Charman, W.N. (1983b) The retinal image in the human eye. in *Progress in Retinal Research* Ed. Osborne, N.N. and Chader, G.J., Pergamon, Oxford : 1-49

Charman, W.N. (1984) Optical characteristics of Bausch and Lomb Soflens (PA1) bifocals. *Int. Contact Lens Clin.*, **11**, 564-575

Charman, W.N. (1986) Diffractive bifocal contact lenses. *Contax*, 1 (May) : 11-17

Charman, W.N. and Saunders, B. (1990) Theoretical and practical factors influencing the optical performance of contact lenses for the presbyope. *J. Br. Contact Lens Assoc.*, **13**(1) : 67-75

Charman, W.N. and Walsh, G. (1986a) Properties of conicoidal surfaces and the Bausch & Lomb PA1 soflens bifocal. *Optometry Today*, 26(17) : 573-580

Charman, W.N. and Walsh, G. (1986b) Retinal image quality with different designs of bifocal contact lens. *Trans. Br. Contact Lens Assoc. Ann. Clinical Conf. 1986.* : 13-19

Charman, W.N. and Walsh, G. (1988) Retinal images with centred, aspheric varifocal contact lenses. *Int. Contact Lens Clin.*, **15**(3) : 87-93

Churms, P.W., Freeman, M.H., Melling, J., Stone, J., and Walker, P.J.C. (1987) The development and clinical performance of a new diffractive bifocal contact lens. *Optometry Today*, 27(22) : 721-724

Cohen, A.L. (1979) Zonal bifocal contact lens. United States Patent, 4,162,122

Cohen, A.L. (1980) Multifocal zone plate. United States Patent, 4,210,391

Cohen, A.L. (1982a) Multifocal phase plate. United States Patent, 4,338,005

Cohen, A.L. (1982b) Phase shift multifocal zone plate. United States Patent, 4,340,283

Cohen, A.L. (1984) An improved bifocal lens design. *Contact Lens Forum*, 9(11) : 21-33

Collins, M.J., Brown, B. and Bowman, K.J. (1989) Contrast sensitivity with contact lens corrections for presbyopia. *Ophthal. Physiol. Opt.*, 9(2) : 133-138

Cornsweet, T.N. (1962) The staircase method in psychophysics. *Am. J. Psychol.*, **75** : 485-491

Cornsweet, T.N. (1970) *Visual Perception.* Academic Press, New York

Courteney, R.C., Tarantino, N., Nelson, N.E., Mackey, A.M. and Komorowski, J. (1991a) Clinical evaluation of the Hydron Echelon bifocal hydrophilic contact lens. Part 1: Success rates. *Contact Lens Spectrum*, 7(7) : 29-38

Courteney, R.C., Tarantino, N., Nelson, N.E., Mackey, A.M. and Komorowski, J. (1991b) Clinical evaluation of the Hydron Echelon bifocal hydrophilic contact lens. Part 2: The successful patient profile. *Contact Lens Spectrum*, 7(8) : 29-35

Cox, I.G. (1985) The visual compromise with bifocal soft contact lenses. (abstract) *Am. J. Optom. Physiol. Opt.*, 62(12s)

Cox, I.G. (1986) Power variation across the surfaces of soft contact lenses and its effect on vision. Ph.D. thesis, University of New South Wales, Sydney

Crawford, B.H. (1972) The Stiles-Crawford effects and their significance in vision. in *Visual Psychphysics, Handbook of Sensory Physiology.* Vol VII/4 Eds. Jameson, D. and Hurvich, L.M., Springer-Verlag, Berlin : 470-483

Cunningham, P.J., Johnston, A.W. and Howell, E.R. (1980) Edge detection as a measure of functional visual performance of low vision patients. Proc. ANZAAS Congress, May

Davis, E.T. and Graham, N. (1981) Spatial frequency uncertainty effects in the detection of sinusiodal gratings. *Vision Res.*, 21(5) : 705-712

de Carle, J.T. (1957) Improvements in or relating to lenses. G.B. Patent 831,546

de Carle, J.T. (1984) Bifocal contact lenses. UK Patent Application GB 2 129 155 A

de Carle, J. (1989a) A refractive multizone bifocal. *Trans. Br. Contact Lens Assoc. Ann. Clinical Conf. 1989.* : 66-70

de Carle, J.T. (1989b) Bifocal and multifocal contact lenses. in *Contact Lenses*, Eds Phillips, A.J. and Stone, J., Butterworths, London, 3rd Edition : 595-624

Ditchburn, R.W. (1976) *Light*, Volume 1, Academic Press, 3rd Edition : 321-326

Ealing Electro-Optics (1989) *Solid state EROS applications manual 28-9777.*

Ealing Electro-Optics (1990) *Solid state EROS software 28-9769 version 4.50. Instruction manual.*

Edwards, A. and Freeman, M.H. (1989) personal communication ("Diffsys" calculations)

Elliott, D.B. (1987) Contrast sensitivity decline with ageing: a neural or optical phenomenon ? *Ophthal. Physiol. Opt.*, 7(4) : 415-419

Elliott, D.B. and Sheridan, M. (1988) The use of accurate visual acuity measurements in clinical anti-cataract formulation trials. *Ophthal. Physiol. Opt.*, 8(4) : 397-401

Elliott, D.B., Sanderson, K., and Conkey, A. (1990a) The reliability of the Pelli-Robson contrast sensitivity chart. *Ophthal. Physiol. Opt.*, 10(1) : 21-24

Elliott, D.B., Whitaker, D. and Bonette, L. (1990b) Differences in the legibility of letters at contrast threshold using the Pelli-Robson chart. *Ophthal. Physiol. Opt.*, 10(4) : 323-326

Elliott, D., Whitaker, D. and MacVeigh, D. (1990c) Neural contribution to spatiotemporal contrast sensitivity in healthy ageing eyes. *Vision Res.*, 30(4) : 541-547

Emerton, N. (1986) Design and fabrication techniques for surface relief diffractive optical elements. Ph.D. Thesis, University of London, London

Emerton, N., Smith, R.W., and Canas, R.G. (1987) Blazed surface relief diffractive optical elements. *I.E.R.E. publication*, 76 : 99-104

Emsley, H.H. (1939) *Visual Optics*, Hatton Press, London, 2nd Edition

Erickson, P. and Robboy, M. (1985) Performance characteristics of a hydrophilic concentric bifocal contact lens. *Am. J. Optom. Physiol. Opt.*, 62(10) : 702-708

Erickson, P., Robboy, M., Appollonio, A., and Jones, W.F. (1988) Optical design considerations for contact lens bifocals. *J. Am. Optom. Assoc.*, 59(3) : 198-202

Erickson, P. and Schor, C. (1990) Visual function with presbyopic contact lens correction. *Optom. Vision Sci.*, 67(1) : 22-28

Feinbloom, W. (1938) Contact lens. U.S. Patent 2,129,305

Finney, D.J. (1952) *Probit Analysis: A statistical treatment of the sigmoid response curve*. Cambridge University Press, London, 2nd Edition

Francon, M. (1966) *Optical Interferometry*. Academic Press, New York

Freeman, M.H. (1984) Improvements in or relating to artificial eye lenses. U.K. Patent GB 2,101,764 B

Freeman, M.H. (1986a) An ophthalmic lens having diffractive power. U.K. Patent GB 2,127,988 B

Freeman, M.H. (1986b) Bifocal contact lens having diffractive power. U.K. Patent GB 2,129,157 B

Freeman, M.H. (1986c) The optics of bifocal contact lenses. (abstract) *Am. J. Optom Physiol. Opt.*, 63(12s) : 34P

Freeman, M.H. (1987) Multifocal contact lenses utilizing diffraction and refraction. U.S. Patent 4,637,697

Freeman, M.H. (1989) unpublished report to Pilkington Plc.

Freeman, M.H. (1990) *Optics*. Butterworths, London, 10th Edition

Freeman, M.H. (1992) personal communication

Freeman, M.H. and Stone, J. (1987) A new diffractive bifocal contact lens. *Trans. Br. Contact Lens Assoc. Ann. Clinical Conf. 1987.* : 15-22

Ginsburg, A.P. (1981) Spatial filtering and vision: implications for normal and abnormal vision, in *Clinical Applications of Visual Psychophysics*. ed. Proenza, L.M., Enoch, L.M. and Jampolsky, A., Cambridge Univ. Press, London

Ginsburg, A.P. (1984) A new contrast sensitivity vision test chart. *Am. J. Optom. Physiol. Opt.*, 61(6) : 403-407

Gordon, J. (1986) Experiences with soft bifocal contact lenses. presented at Contact Lens Assoc. Ophthalmol. Ann. Conf., Jan

Green, D.G. and Campbell, F.W. (1965) Effect of focus on the visual response to a sinusoidally modulated spatial stimulus. *J. Opt. Soc. Am.*, 55(9) : 1154-1157

Greeves, A.L., Cole, B.L. and Jacobs, R.J. (1987) Reliability and validity of simple plate tests of contrast sensitivity. *Am. J. Optom. Physiol. Opt.*, 64(11) : 832-841

Greeves, A.L., Cole, B.L. and Jacobs, R.J. (1988) Assessment of contrast sensitivity of patients with macular disease using reduced contrast near visual acuity charts. *Ophth. Physiol. Opt.*, 8(4) : 371-377

Grey, C.P. and Sheridan, M. (1988) The modulation transfer function of contact lenses. *J. Br. Contact Lens Assoc.*, 11(1) : 9-17

Grey, C.P. and Yap, M. (1987) Edge contrast sensitivity in optometric practice: An assessment of its efficiency in detecting visual dysfunction. *Am. J. Optom. Physiol. Opt.*, 64(12) : 925-928

Guilford, J.P. (1954) *Psychometric Methods*. McGraw-Hill, New York, 2nd Edition

Guillon, M., Lydon, D.P.M., and Solman, R.T. (1988) Effect of target contrast and luminance on soft contact lens and spectacle visual performance. *Curr. Eye Res.*, 7(7) : 635-647

Guillon, M. and Sayer, G. (1988) Critical assessment of visual performance in contact lens practice. *Contax*, 3 (May) : 8-13

Guillon, M. and Schock, S.E. (1990) Soft contact lens visual performance: A multicenter study. *Optom. Vision Sci.*, 68(2) : 96-103

Harris, M.G. and Classe, J.G. (1988) Clinicolegal considerations of monovision. *J. Am. Optom. Assoc.*, 59(6) : 491-495

Hemenger, R.P. and Tomlinson, A. (1990) Diffractive bifocals: Confusion of design. *Contact Lens Forum*, March : 27-30

Hill, A.R., Reeves, B.C., and Wood, J.M. (1988) Contrast sensitivity screening in optometric practice. presented at Advances in the Assessment of Visual Function and Structure, London, July

Ho, A. and Bilton, S.M. (1986) Low contrast charts effectively differentiate between types of blur. *Am. J. Optom. Physiol. Opt.*, 63(3) : 202-208

Hodd, F.A.B. (1969) A design study of bifocal contact lenses. *The Ophthalmic Optician*, 9(9) : 450-469; 9(11) : 588-600; 9(12) : 644-653

Holden, B.A. (1986) personal communication ("Biflex" clinical trial)

Holden, B.A., Sweeney, D.F., Southgate, D.C. and Wong, R. (1989) Contact lens practice in Australia 1987-88. *Clin. Exp. Optom.*, 72(4) : 113-122

Hopkins, H.H. (1955) The frequency response of a defocused optical system. *Proc. Roy. Soc.*, A231 : 91-103

Hopkins, H.H. (1956) The frequency response of optical systems. *Proc. Phys. Soc.* (London), B69 : 452

Hopkins, H.H. (1962) The application of frequency response techniques in optics. *Proc. Phys. Soc.* (London), B79 : 889-919

Hopkins, H.H. (1988) personal communication

Hotchkiss, R.N., Washer, F.E. and Rosberry, F.W. (1951) Spurious resolution of photographic lenses. *J. Opt. Soc. Am.*, **41** : 600

Howell, E.R. (1978) Visual mechanisms for the detection and perception of the contrast of large objects. Ph.D. Thesis, University of Melbourne, Melbourne

Howell, E.R. and Hess, R.F. (1978) The functional area for summation to threshold for sinusoidal gratings. *Vision Res.*, **18**(4) : 369-374

Howland, B. and Howland, H.C. (1976) Subjective measurement of high-order aberrations of the eye. *Science*, **193**(4253) : 580-582

Howland, B. and Howland, H.C. (1977) A subjective method for the measurement of monochromatic aberrations of the eye. *J. Opt. Soc. Am.*, **67**(11) : 1508-1518

Indebetouw, G. and Bai, H. (1984) Imaging with Fresnel zone pupil masks: Extended depth of field. *Appl. Opt.*, **23**(23) : 4299-4302

Jenkins, F.A. and White, H.E. (1976) *Fundamentals of Optics*. McGraw-Hill, New York, 4th Edition

Jenkins, T.C.A. (1963) Aberrations of the eye and their effects on vision: Part II. *Br. J. Physiol. Opt.*, **20**(4): 161-201

Jones, B. and Lowther, G.E. (1989) The effect of near zone size of a center-near zone hydrogel contact lens bifocal on visual acuity. *Int. Contact Lens Clin.*, **16**(3) : 87-93

Josephson, J.E. (1989) The monovision controversy. *Trans. Br. Contact Lens Assoc. Ann. Clinical Conf. 1989.* : 60-65

Josephson, J.E. and Caffery, B. (1986) Bifocal hydrogel lenses: An overview. *J. Am. Optom. Assoc.*, **57**(3) : 190-195

Josephson, J.E. and Caffery, B.E. (1989) Clinical experience with the Tangent streak RGP bifocal contact lens. *J. Am. Optom. Assoc.*, **60**(3) : 166-170

Josephson, J., Erickson, P., Back, A., Holden, B., Harris, M., Tomlinson, A., Caffrey, B, Finnemore, V. and Silbert, J. (1990) Monovision: A proposed position paper. *J. Am. Optom. Assoc.*, **61**(11): 820-826, reprinted in *The Optician*, **201**(5295) : 18-23

Kadlecova, V., Peleska, M., and Vasko, A. (1958) Dependence on age of the diameter of the pupil in the dark. *Nature*, **182** : 1520-1521

Kay, C.D. and Morrison, J.D. (1987) A quantitative investigation into the effects of pupil diameter and defocus on contrast sensitivity. *Ophthal. Physiol. Opt.*, **7**(1) : 21-30

Kelly, D.H. (1971a) Adaptation effects on spatio-temporal sine-wave thresholds. *Vision Res.*, **12** : 89-101

Kelly, D.H. (1971b) Transient effects on the visibility of low spatial frequencies. (abstract) *J. Opt. Soc. Am.*, **61**(11) : 1576

Kelly, S.A. and Tomlinson, A. (1987) Effect of repeated testing on contrast sensitivity. *Am. J. Optom. Physiol. Opt.*, **64**(4) : 241-245

King, P. (1986) Multifocal low aperture diffractive optical elements for use in white light. Ph.D. thesis, Univ. London, London

Klein, M. (1970) *Optics*. John Wiley & Sons, New York

Klein, S.A. (1986) Image quality of concentric bifocal contact lenses. (abstract) *Am. J. Optom. Physiol. Opt.*, **63**(12s) : 105P

Klein, S.A. and Ho, Z.Y. (1986) Multizone bifocal contact lens design. *Current Developments in Optical Engineering and Diffraction Phenomena, SPIE*, **679** : 25-35

Korczyn, A.D., Laor, N. and Nemet, P. (1976) Sympathetic pupillary tone in old age. *Arch. Ophthalmol.*, **94**(11) : 1905-1906

Kornzweig, A.L., Feldstein, M. and Schneider, J. (1957) The eye in old age: Ocular survey of over one thousand aged persons with special reference to normal and disturned visual functions. *Am. J. Ophthalmol.*, **44** : 29-37 cited in Pitts, D.G. (1982b)

Kumnick, L.S. (1956) Aging and the latency and duration of pupil constriction in response to light and sound stimuli. *J. Gerontol.*, **11**(4) : 391-396

Lebow, K.A. and Goldberg, J.B. (1975) Characteristics of binocular vision for presbyopic patients wearing single vision contact lenses. *J. Am. Optom. Assoc.*, **46**(11) : 1116-1123

Lesem, L.B., Hirsh, P.M. and Jordan, J.A.Jr (1969) The kinoform: A new wavefront reconstruction device. *IBM J. Res. Develop.*, **13** : 150-155

Lindsay, R.G. (1990) Image quality of diffractive bifocal contact lenses. presented at 7th International Contact Lens Congress, Gold Coast, Australia

Linfoot, E.H. (1955) Transmission factors and optical design. *J. Opt. Soc. Am.*, **46**(9) : 740-752

Lloyd, M. (1984) Presbyopic contact lens correction - Old and new. *J. Br. Contact Lens Assoc.*, 7(3) : 131-136

Loewenfeld, I.E. (1979) Pupillary changes related to age. in *Topics in Neuro-Ophthalmology.*, Ed. Thompson, H.S. et al, Williams & Wilkins, Baltimore : 124-150

Long, G.M. and Tuck, J.P. (1988) Reliabilities of alternate measures of contrast sensitivity functions. *Am. J. Optom. Physiol. Opt.*, **65**(1) : 37-48

Loshin, D. and Hug, T. (1986) Image quality of single vision and bifocal contact lenses. (abstract) *Am. J. Optom. Physiol. Opt.*, **63**(12s) : 132P

Loshin, D.S. (1989) The holographic/diffractive bifocal contact lens. *Int. Contact Lens Clin.*, **16**(3) : 77-86

Lovie-Kichin, J.E. (1988) Validity and reliability of visual acuity measurements. *Ophthal. Physiol. Opt.*, **8**(4) : 363-370

Lowther, G.E. (1982) Clinical evaluation of a hydrogel bifocal contact lens. *Int. Contact Lens Clinic*, **9**(4) : 218-226

Lowther, G.E. (1985) personal communication

Maltzman, B.A., Harris, M., and Espy, J. (1985) Experience with soft bifocal contact lenses. *Contact Lens Assoc. Ophthalmol. J.*, **11**(1) : 73-77

Mandell, R.B. (1974) *Contact Lens Practice.*, Charles Thomas, Springfield, Illinois, 2nd Edition : 649-678

Marr, D. and Hildreth, E. (1980) Theory of edge detection. *Proc. R. Soc. Lond.*, **B207** : 187-207

McGeehon, M. (1988) Survey: Practitioners unhappy with current bifocal lenses. *Contact Lens Forum* **13**(6) : 22-25

McGill, E., Ames, K., Erickson, P. and Robboy, M. (1987) Quality of vision with hydrogel simultaneous vision bifocal contact lenses. *Int. Contact Lens Clin.*, 14(12) : 476-481

McGill, E., Robboy, M., Ames, K. and Erickson, P. (1986) A clinical comparison of simultaneous vision hydrophilic bifocal contact lenses. (abstract) *Am. J. Optom. Physiol. Opt.*, 63(12s) : 133P

McGrath, C. and Morrison, J.D. (1981) The effects of age on spatial frequency perception in human subjects. *Q. J. Exp. Physiol.*, 66 : 253-261

McMonnies, C.W. (1974) Monocular fogging in contact lens practice. *Aust. J. Optom.*, 57(1) : 28-32

Meier, A.M. and Lowther, G.E. (1983) Measured power distribution across the Bausch & Lomb soflens (PA1) bifocal. *J. Am. Optom. Assoc.*, 54(3) : 263-265

Meslin, D. and Obrecht, G. (1988) Effect of chromatic dispersion of a lens on visual acuity. *Am. J. Optom. Physiol. Opt.*, 65(1) : 25-28

Molinari, J.F. (1988) A clinical comparison of subjective effectiveness of monovision, aperture dependent and independent hydrogel bifocal contact lens fitting. *Trans. Br. Contact Lens Assoc. Int. Contact Lens Cent. Conf.* : 58-59

Molinari, J.F. and Caplan, L. (1984) A new soft contact lens annular bifocal. *J. Br. Contact Lens Assoc.*, 7(1) : 8-12

Molinari, J.F. and Caplan, L. (1986) Clinical evaluation of two soft lens bifocals. *J. Am. Optom. Assoc.*, 57(9) : 684-686

Morrison, J.D. and McGrath, C. (1985) Assessment of the optical contributions to the age-related deterioration in vision. *J. Exp. Physiol.*, 70 : 249-269

Nolan, J.A. and Nolan, J.J. (1984) Driving with monovision. *Optom. Monthly*, August : 308-313

Optical Services Audit Committee Report (1990) Chapter 5: Future developments of optical services.

O'Neill, E.L. (1956) Transfer functions for an annular aperture. *J. Opt. Soc. Am.*, 46(4) : 285-288

Owsley, C., Sekuler, R. and Siemsen, D. (1983) Contrast sensitivity throughout adulthood. *Vision Res.*, 23(7) : 689-699

Papas, E.B. (1991) The presbyope and the contact lens: A fatal attraction. *Trans. Br. Contact Lens Assoc.*, 14(2) : 51-54

Papas, E., Young, G. and Grey, C. (1988) Visual performance with soft diffractive bifocal contact lenses. presented at Br. Contact Lens Assoc. Int. Contact Lens Cent. Conf., May

Papas, E., Young, G. and Hearn, K. (1989) Monovision vs diffractive bifocals: a clinical comparison. *Trans. Br. Contact Lens Assoc. Ann. Clinical Conf.* : 75-76

Papas, E., Young, G. and Hearn, K. (1990) Monovision vs. soft diffractive bifocal contact lenses: A crossover study. *Int. Contact Lens Clin.*, 17 : 181-186

Pelli, D.G., Robson, J.G. and Wilkins, A.J. (1988) The design of a new letter chart for measuring contrast sensitivity. *Clin. Vision Sci.*, 2(3) : 187-199

Phillips, A.J. (1988) Results of a clinical trial of the "Diffrax" diffractive bifocal RGP lens. *Trans. Br. Contact Lens Assoc. Int. Contact Lens Cent. Conf.* : 89-94

Phillips, A.J. and Stone, J. (Eds.) (1989) *Contact Lenses*. Butterworths, London. 3rd Edition

Pitts, D.G. (1982a) The effects of aging on selected visual functions: dark adaptation, visual acuity, stereopsis, and brightness contrast. in *Aging and Human Visual Function.*, Ed. Sekuler, R., Kline, D. and Dismukes, K., Alan R. Liss, New York : 131-159

Pitts, D.G. (1982b) Visual acuity as a function of age. *J. Am. Optom. Assoc.*, **53**(2) : 117-124

Pressman, M.R., DiPhillipo, M.A. and Fry, J.M. (1986) Senile miosis: The possible contribution of disordered sleep and daytime sleepiness. *J. Gerontol.*, **41**(5) : 619-634

Ray, W.A. and O'Day, D.M. (1985) Statistical analysis of multi-eye data in ophthalmic research. *Invest. Ophthalmol. Vis. Sci.*, **26**(8) : 1186-1188

Reeves, B.C. and Hill, A.R. (1987) Practical problems in measuring contrast sensitivity. *Optician*, **193**(5085) : 29-34

Reeves, B.C., Wood, J.M. and Hill, A.R. (1991) Vistech VCTS 6500 charts - within- and between-session reliability. *Optom. Vis. Sci.*, **68**(9) : 728-737

Regan, D. (1988) Low-contrast letter charts and sinewave grating tests in ophthalmological and neurological disorders. *Clin. Vision Sci.*, **2**(3) : 235-250

Regan, D. and Neima, D. (1983) Low-Contrast letter charts as a test of visual function. *Ophthalmol.*, **90**(10) : 1192-1200

Reichart, Wien (1961) Polarization Interferometer after Nomarski for the Universal Camera-Microscope "MeF". (manufacturer's instructions)

Remole, A. (1974) Relation between border enhancement extent and retinal image blur. *Vision Res.*, **14** : 989-995

Remole, A. (1982) Spatial frequency thresholds versus border enhancement: sensitivity to retinal defocus. *Am. J. Optom. Physiol. Opt.*, **59**(2) : 135-145

Richards, O.W. (1977) Effects of luminance and contrast on visual acuity, ages 16 to 90 years. *Am. J. Optom. Physiol. Opt.*, **54**(3) : 178-184

Robboy, M.W. (1985) Performance comparison of various alternating vision hydrophilic bifocal contact lens designs. *Int. Eyecare*, **1**(6) : 445-449

Robboy, M.W. and Cox, I. (1988) Factors influencing downgaze translation in alternating vision soft bifocal contact lenses. *Int. Contact Lens Clinic*, **15**(6) : 185-187

Robboy, M. and Erickson, P. (1987) Performance comparison of current hydrophilic alternating vision bifocal contact lenses. *Int. Contact Lens Clinic*, **14**(6) : 237-243

Robirds, S.R. (1987) Central zone size requirements for simultaneous viewing bifocal contact lenses. (abstract) *Am. J. Optom. Physiol. Opt.*, **64**(10) : 100P

Ross, J.E., Bron, A.J. and Clarke, D.D. (1984) Contrast sensitivity and visual disability in chronic simple glaucoma. *Br. J. Ophthalmol.*, **68** : 821-827

Ross, J.E., Clarke, D.D. and Bron, A.J. (1985) Effect of age on contrast sensitivity function: uniocular and binocular findings. *Br. J. Ophthalmol.*, **69** : 51-56

Rubin, G.S. (1988) Reliability and sensitivity of clinical contrast sensitivity tests. *Clin. Vision Sci.*, **2**(3) : 169-177

Ruddock, K.H. (1965) The effect of age upon colour vision - II. Changes with age in light transmission of the ocular media. *Vision Res.*, **5** : 47-58

Santamaria, J., Artel, R. and Bescos, J. (1987) Determination of the point spread function of human eyes using a hybrid optical-digital method. *J. Opt. Soc. Am.*, A4(6), 1109-1114

Saunders, B.D. (1989) The optical performance of bifocal contact lenses *in vivo*. *Trans. Br. Contact Lens Assoc. Ann. Clinical Conf. 1989* : 71-74

Saunders, B.D. (1990) The optical performance of bifocal contact lenses. Ph.D. Thesis, UMIST, Manchester

Schafer, W.D. and Weale, R.A. (1970) The influence of age and retinal illumination on the pupillary near reflex. *Vision Res.*, 10 : 179-191

Scialfa, C.T., Adams, E.M. and Giovanetto, M. (1991) Reliability of the Vistech contrast test system in a life-span adult sample. *Optom. Vis. Sci.*, 68(4) : 270-274

Seitz, R. (1957) Die altersabhangigkeit der pupillenerweiterung bei dunkeladaptation. *Klin. Mbl. Augenheilk*, 131 : 48-56

Sekuler, R. and Mulvanny, P. (1983) Acuity and contrast sensitivity. (letter) *Br. J. Ophthalmol.* 67 : 134

Sekuler, R., Wilson, H.R. and Owsley, C. (1984) Structural modelling of spatial vision. *Vision Res.*, 24 : 689-700

Shapley, R.M. and Tolhurst, D.J. (1973) Edge detectors in human vision. *J. Physiol.*, 229 : 165-183

Sheedy, J.E., Harris, M.G., Bronge, M.R., Joe, S.M. and Mook, M.A. (1991) Task and visual performance with concentric bifocal contact lenses. *Optom. Vision Sci.*, 68(7) : 537-541

Sheedy, J.E., Harris, M.G., Busby, L., Chan, E. and Koga, I. (1988) Monovision contact lens wear and occupational task performance. *Am. J. Optom. Physiol. Opt.*, 65(1) : 14-18

Simpson, M.J. and Michette, A.G. (1984) Imaging properties of modified Fresnel zone plates. *Optica Acta*, 31(4) : 403-413

Smith, R.W., Canas, R.G., and West, A.A. (1989) Electron beam writing of binary and optical writing of blazed diffractive optical elements. *Proc. S.P.I.E.*, 1052 : 77-84

Southall, J.P.C. (1946) *Mirrors, Prisms and Lenses*, Dover Publications, New York, 3rd Edition : 420-423

Steward, G.C. (1928) *The symmetrical optical system.* cited in O'Neill, E.L. *Introduction to statistical optics.* Addison-Wesley, Reading, Massachussetts : 99

Stone, J. (1988) Experience with the Diffrax lens. *Optician*, 195(5138) : 21-36

Sturr, J.F., Church, K.L., and Taub, H.A. (1988) Temporal summation functions for detection of sine-wave gratings in young and older adults. *Vision Res.*, 28(11) : 1247-1253

Swarbrick, H., Pye, D. and Holden, B.A. (1985) Current Australian contact lens practice. *Aust. J. Optom.*, 68(1) : 2-7

Sweeney, D.F., Sansey, N. Lycho, T., Wong, R. and Holden, B.A. (1991) Contact lens practice in Australia 1988-1989. *Clin. Exp. Optom.*, 74(2) : 54-61

Tabachnick, B.G. and Fidell, L.S. (1983) *Using multivariate statistics.* Harper & Row, New York

Taub, H.A. and Sturr, J.F. (1991) The effects of age and ocular health on letter contrast sensitivity and high and medium contrast acuity as a function of. luminance, *Clin. Vision Sci.*, 6(3) : 181-189

Taylor, J.R. (1982) *An introduction to error analysis.* University Science Books (Oxford University Press), Mill Valley, CA

Thorpe Davis, E., Sherman, J., Bass, S.J. and Schnider, C.M. (1991) Pre-surgical prediction of post-surgical visual function in cataract patients: Multivariate statistical analyses of test measures. *Clin. Vision Sci.*, 6(3) : 191-207

Tomlinson, A. and Ridder, III, W.H. (1992) Effect of lens movement on vision with RGP contact lenses. *J. Br. Contact Lens Assoc.*, 15(1) 25-29

Trendelenberg, W. (1943) *Der Gesichtsinn*, Berlin, cited in Kadlecova, Peleska and Vasko (1958)

Tulunay-Keesey, U., Ver Hoeve, J.N. and Terkla-McGrane, C. (1988) Threshold and suprathreshold spatiotemporal response throughout adulthood. *J. Opt. Soc. Am.*, A5(12) : 2191-2219

van Meeteren, A. (1974) Calculations on the optical modulation transfer function of the human eye for white light. *Optica Acta*, 21(5) : 395-412

van Nes, F.L. and Bouman, M.A. (1967) Spatial modulation transfer in the human eye. *J. Opt. Soc. Am.*, 57(3) : 401-406

Verbaken, J.H. (1987a) Standardization of contrast sensitivity measurements. *Clin. Exp. Optom.*, 70(1) : 19

Verbaken, J. (1987b) Contrast sensitivity testing with low contrast acuity charts. Australian Vision Charts. (manufacturer's guide)

Verbaken, J. (1989) The Melbourne Edge Test: Procedure Guide for Clinical CS Testing. (manufacturer's guide)

Verbaken, J.H. and Jacobs, R.J. (1985) The technical problems of producing photographic prints for the measurement of human contrast sensitivity. *Ophthal. Physiol. Optics*, 5(4) : 459-465

Verbaken, J.H. and Johnston, A.W. (1986) Population norms for edge contrast sensitivity. *Am. J. Optom. Physiol. Opt.*, 63(9) : 724-732

Vola, J.L., Cornu, L., Carruel, C., Gastaud, P. and Leid, J. (1983) High and low luminance visual acuity in relation to age. *J. Fr. Ophthalmol.*, 6(5) : 473-479

Waiss, B. and Cohen, J.M. (1991) A comparison of peak contrast as measured by three different contrast tests on normal and low vision populations. (abstract) *Optom. Vision Sci.*, 68(12s) : 78

Walsh, G. (1988) The effect of mydriasis on the pupillary centration of the human eye. *Ophthal. Physiol. Opt.*, 8(2) : 178-182

Walsh, G. and Charman, W.N. (1985) Measurement of the axial wavefront aberration of the human eye. *Ophthal. Physiol. Opt.*, 5(1) : 23-31

Walsh, G. and Charman, W.N. (1989) The effect of defocus on the contrast and phase of the retinal image of a sinusoidal grating. *Ophthal. Physiol. Opt.*, 9(4) : 398-404

Watt, R.J. and Andrews, D.P. (1981) APE : Adaptive Probit Estimation of Psychometric Functions. *Curr. Psych. Rev.*, 1 : 205-214

Weale, R.A. (1961) Retinal illumination and age. *Trans. Illum. Eng. Soc. (London)*, 26(2) : 95-100

Weale, R.A. (1963) *The Aging Eye.* H.K. Lewis, London

Weale, R.A. (1982) *A Biography of the Eye.* H.K. Lewis, London

Weissgold, D.J., Jackowski, M.M., Weisenthal, R.W. and Sturr, J.F. (1990) Assessment of the clinical utility of contrast sensitivity: Establishment of testing procedures and normative standards for the Pelli-Robson contrast sensitivity chart. (abstract) *Invest. Ophthalmol. Vis. Sci.* 31(4) : 355

Werner, J.S., Peterzell, D.H., and Scheetz, A.J. (1990) Light, vision and aging. *Optom. Vis. Sci*, 67(3) : 214-229

Wesley, N.K. (1971) Analysis of bifocal contact lenses. *Am. J. Optom. Arch. Am. Acad. Optom.*, 48(11) : 926-931

Westheimer, G. (1979) Scaling of visual acuity measurements. *Arch. Ophthalmol.*, 97(2) : 327-330

Williamson-Noble, F.A. (1951) Contact Lenses - What of the future ? *Br. J. Physiol. Opt.*, 8 : 244-246

Wilson, M.A. and Campbell, M.C.W. (1991) Repeatability of pupil centre location with change of pupil size. (abstract) *Optom. Vis. Sci.*, 68(12s): 186

Wilson, M.A., Campbell, M.C.W. and Simonet, P. (1992) Change of pupil centration with change of illumination and pupil size. *Optom. Vis. Sci.*, 69(2) : 129-136

Winer, B.J. (1971) *Statistical principles in experimental design.* McGraw-Hill, New York, 2nd Edition

Wittenberg, S. (1988) The Badal optometer paradox. *Am. J. Optom. Physiol. Opt.*, 65(4) : 285-291

Wood, J.M., Hill, A.R. and Reeves, B.C. (1988a) The reliability and validity of high and low contrast optotypes. presented at Advances in the Assessment of Visual Function and Structure, London, July

Wood, J.M., Hill, A.R. and Reeves, B.C. (1988b) The Vistech contrast sensitivity charts - clinical evaluation of reliability and validity. (abstract) *Ophthal. Physiol. Opt.* 9(1) : 101

Wood, R.W. (1923) *Physical Optics*, Macmillan, London (revised edition) : 40

Woodhouse, J.M. (1975) The effect of pupil size on grating detection at various contrast levels. *Vision Res.*, 15 : 645-648

Woods, R.L. (1986) Stereopsis with monovision and two concentric bifocal contact lens systems. (abstract) *Ophthal. Physiol. Opt.* 7(1) : 96

Woods, R.L. (1991a) Visual and optical performance with concentric bifocal contact lenses. (abstract) *Ophthal. Physiol. Opt.*, 11(3): 280

Woods, R.L. (1991b) Choosing the correct bifocal segment diameter: an optical and visual assessment, presented at Br. Contact Lens Assoc. Ann. Clinical Conf., Brighton, May

Woods, R.L. (1991c) The aging eye and contact lenses - A review of ocular characteristics. *J. Br. Contact Lens Assoc.*, 14(3): 115-127

Woods, R.L. (1991d) Visual assessment of rigid concentric-design bifocal contact lenses. (abstract) *Optom. Vision Sci.*, 68(12s) : 144

Woods R.L. (1992) The aging eye and contact lenses - A review of visual characteristics. *J. Br. Contact Lens Assoc.*, 15(1) : 31-43

Woods, R.L., Port, M.J.A. and Saunders, J.E. (1992a) Concentric-design rigid bifocals. Part II Visual performance. *J. Br. Contact Lens Assoc.* in press

Woods, R.L., Saunders, J.E. and Port M.J.A. (1992b) Concentric-design rigid bifocals. Part I Optical performance. *J. Br. Contact Lens Assoc.* in press

Woods, R.L. and Thomson, W.D. (1989a) Psychometric methods of contrast threshold estimation with experienced observers. (abstract) *Ophthal. Physiol. Opt.*, 10(1) : 100

Woods, R.L. and Thomson, W.D. (1989b) A comparison of psychometric methods for estimation of contrast sensitivity. (abstract) *Perception*, 18(4) : 546

Woods, R.L. and Thomson, W.D. (1992) A comparison of psychometric methods for measuring the contrast sensitivity of experienced observers. submitted to *Clin. Vision Sci.*

Wright, C.E. and Drasdo, N. (1985) The influence of age on the spatial and temporal contrast sensitivity function. *Doc. Ophthalmol.*, 59 : 385-395

Young, G. and Papas, E. (1987) Clinical evaluation of a soft diffractive bifocal contact lens. (abstract) *Am. J. Optom. Physiol. Opt.*, 64(12s) : 122P

Young, G., Grey, C.P., and Papas, E.B. (1990) Simultaneous vision bifocal contact lenses: A comparative assessment of the in vitro optical performance. *Optom. Vision Sci.*, 67(5) : 339-345